CIB W062
Maribor 2026

Proceedings of the

51st International Symposium
CIB W062

WATER SUPPLY AND DRAINAGE FOR BUILDINGS

August 2026

University of Maribor

Maribor, Slovenia

ZBORNIK 51. MEDNARODNEGA SIMPOZIJA CIB W062/PROCEEDINGS of the 51st International Symposium CIB W062
Water Supply and Drainage for Buildings : Maribor, 18–20 August 2026 / Univerza v Mariboru, Slovenija

Urednikl / Editors

Bart Bleys
Buildwise, Belgium · Coordinator of CIB W062

Matjaž Nekrep Perc
Univerza v Mariboru, Fakulteta za gradbeništvo, prometno inženirstvo in arhitekturo, Slovenija

Hana Nekrep
Fakulteta za dizajn, Slovenija

Mednarodni znanstveni odbor / International Scientific Committee

Bart Bleys, Buildwise, Belgium (CIB W062 Coordinator)
Cheng-Li Cheng, National Taiwan University of Science and Technology, Taiwan
Daniel Cole, IAPMO, USA
Hiroyuki Kose, Toyo University, Japan
M. C. Jeffrey Lee, National Taichung University of Science and Technology, Taiwan
Matjaž Nekrep Perc, University of Maribor, Slovenia
Lúcia Helena de Oliveira, University of São Paulo, Brazil
Masayuki Otsuka, Kanto Gakuin University, Japan
Armando Silva-Afonso, ANQIP / University of Aveiro, Portugal
Zuzana Vranayová, Technical University of Košice, Slovakia
Ling-Tim Wong, The Hong Kong Polytechnic University, China

Izdajatelj / Issued by

Univerza v Mariboru, Fakulteta za gradbeništvo, prometno inženirstvo in arhitekturo
Smetanova ulica 17, 2000 Maribor, Slovenia · fgpa.um.si

Organizator simpozija / Symposium organiser

FGPA UM, v sodelovanju s komisijo CIB W062 (International Council for Research and Innovation in Building and Construction)

Recenzija Mednarodni znanstveni odbor CIB W062 2026 (double-blind / peer review)

Jezik angleški / English

Vrsta publikacije Zbornik mednarodnega znanstvenega simpozija / Conference proceedings

Kraj in leto Maribor, 2026

Obseg 518 strani

Tehnični urednik Hana Nekrep

Lektoriranje avtorji prispevkov (angl.) / authors

Oblikovanje platnic Hana Nekrep

Sponzorji simpozija / Symposium sponsors

Geberit · International Code Council (ICC) · Aliaxis · IAPMO

Kontakt

cibw062@um.si · https://www.fgpa.um.si/en/cibw062/

Dear colleagues and professionals,

The 51st International Symposium on Water Supply and Drainage for Buildings, CIB W062, is organised by the University of Maribor, Faculty of Civil Engineering, Transportation Engineering and Architecture, with the support of the International Council for Research and Innovation in Buildings and Construction (CIB) and the CIB W062 Commission, coordinated by Bart Bleys of Buildwise, Belgium.

This Symposium will take place in Maribor, Slovenia, from 18th to 20th of August 2026.

For more than half a century, the CIB W062 Symposium has brought together researchers, engineers, practitioners, and industry experts dedicated to advancing knowledge and innovation in water supply and drainage for buildings. It is therefore a particular privilege for the University of Maribor to host the 51st edition of this long-standing international event.

It is a special honour to host you in a country shaped by water, from the peaceful River Mura in the east to the Adriatic Sea in the west. Here in Maribor, the River Drava has shaped the city's history, identity, and development for centuries. During your stay and throughout our programme, you will have the opportunity to experience this remarkable river firsthand.

This close relationship with water and the environment is deeply reflected in the University of Maribor's values, where academic excellence goes hand in hand with environmental responsibility, sustainable development, and respect for natural resources.

These principles have also guided the organisation of this Symposium. We have made every effort to organise it as a plastic-free event, and our social programme reflects our commitment to sustainability through carefully selected venues, including Green Key-certified establishments and local cuisine prepared from fresh, locally sourced ingredients.

As water experts, you will certainly appreciate one of Slovenia's greatest natural assets: our exceptionally high-quality drinking water. Fresh, safe, and available directly from the tap, we warmly invite you to enjoy it throughout your stay.

This Symposium aims to disseminate the latest international research and innovation in building water supply and drainage while strengthening collaboration across our global community. Throughout the programme, participants will explore a broad range of topics, from sustainable water management, water conservation and reuse, and building system performance to digitalisation, public health, and resilient infrastructure. Together, these themes reflect both the diversity of our discipline and the challenges shaping its future.

We are delighted to welcome participants from around the world and sincerely thank all authors, members of the International Scientific Committee, and our sponsors for making this Symposium possible.

We hope this symposium will inspire new ideas, encourage meaningful discussions, and strengthen the international collaborations that make CIB W062 such a valued community.

Thank you for joining us in Maribor. I wish you an inspiring symposium, an enjoyable stay, and many memorable moments over the coming days. I look forward to meeting you all.

Matjaž Nekrep Perc

51st CIB W062 Organising Chairman

University of Maribor, Slovenia

KAZALO / TABLE OF CONTENTS

Proceedings of the 51st International Symposium CIB W062

Sustainable Water Systems and Net-Zero Buildings

Avtorji / Authors	Naslov / Title	Str.
Takahiko Suzuki, Masayuki Otsuka	Development of Urban Biodiversity through Water-Based Biotope Creation in a Building Site	**7**
T. Nishikawa	Investigation of Water Balance in Alternative Water Use Buildings	**11**
H. Yamaguchi	Residential Resilience to Flood Disasters: Continuity of Living Functions and Building Services	**17**
Ryuki Koike et al.	A Study on the Expansion of Non-Potable Water Use in Buildings	**21**
Satoshi Matsumoto et al.	Study on Design Methods for ZWB in Urban Mid-Sized Office Building – Part 1: Measurement of Water Balance for Achieving ZWB	**25**
Masaaki Hashimoto et al.	Development of Water Circulation System Supplying Both Potable and Non-Potable Water for ZWB	**29**
Sei Yoshioka et al.	Study on Design Methods for ZWB in Urban Mid-Sized Office Building – Part 2: Water Quality Survey and Water Balance Case Studies	**33**
Gabriela Cristina Ribeiro Pacheco et al.	Analyzing Urban Water Demand under Different Rainwater Tank Volumes	**37**
M. Zeleňáková, M. Godžáková, M. Ovčiarka	Benefits and risks associated with the design and implementation of vegetated roofs	**47**

Water Conservation, Reuse and Net-Zero Water

Avtorji / Authors	Naslov / Title	Str.
Daniel Cole	Potable Water Reuse in the USA: Regulations and Treatment Technologies	**54**
K. L. Williams	A City's Relief: A Study on the Optimization and Reallocation of Municipal Demand through Probabilistic Adoption Modeling of Conservation Measures	**66**
Cheng-Li Cheng, Hui-Chien Chang	Study on BIM and Dynamo-based Automated Life Cycle Carbon Assessment of Unit Bathrooms	**77**
Takeshi Aoi, Masayuki Otsuka, Anna Fujita	Planning Case Study and Verification of a Research Facility Aimed at Achieving a Net-Zero Water Building	**89**
Tim Bartrand	Water Management during Construction	**101**
Kosuke Osako et al.	Method for Calculating Underground Infiltration Based on Actual Water Level Measurements in Rainwater Storage and Infiltration Tanks	**114**
Shi-Feng Huang, Cheng-Li Cheng	Simulation Research on Patterns Optimization Strategies of Building Rainwater Harvesting System	**125**

Water Demand and Distribution Systems

Avtorji / Authors	Naslov / Title	Str.
C. Jacques et al.	Comparative evaluation of simplified pipe sizing methods for non-looped domestic water distribution systems in a Belgian context	**137**
M. Bilal, B. M. Josey, J. Gong	Assessment of Water Demand and Pressure Performance in an Australian Residential Building	**149**
Toju Omaghomi	An Analysis of Water Use Data in Healthcare Buildings	**159**
E. J. M. Blokker	Updated review of applications for SIMDEUM, a stochastic drinking water demand model with a small temporal and spatial scale	**171**
B. M. Josey, M. Bilal, J. Gong	Pressure Monitoring in Australian Residential Water Service Systems	**183**
C. Pimentel-Rodrigues, A. Silva-Afonso	Flush cisterns: water conservation versus drainage performance	**195**

Domestic Hot Water Systems and Legionella

Avtorji / Authors	Naslov / Title	Str.
M. van Bruggen, W. G. van der Schee	The proportional deviation of thermostatic balancing valves in hot water circulation systems	**206**
Andreas Moerman et al.	Development and validation of a Legionella test setup for low temperature domestic hot water (DHW)	**214**
Rolf Weiss, Arnd Gildemeister	Temperature-dependent Legionella growth for water changes in drinking water systems	**226**
O. F. Leever	Stagnation in Drinking Water Installations: The Role of Cold Water Circulation in Robust Hydraulic Design	**238**
Joris Van Herreweghe et al.	Towards Legionella-safe low temperature DHW production and distribution: potential of physical techniques in a contaminated system	**255**
Christoph Lohr et al.	Optimizing Thermostatic Balancing Valve Placement in Domestic Hot Water Recirculation Systems: Product Ratio Method Analysis	**268**

Building Services Performance and Energy

Avtorji / Authors	Naslov / Title	Str.
Natascha Milesi Ferretti, Lingnan Lin	Measuring Pressure Loss in Modern Plumbing Fittings	**279**
Takeru Tamiya, Takehiko Mitsunaga	Study on Hot Water Supply Systems for Reducing Energy Consumption in Japanese Hospitals	**284**
Misuzu Shima, Takehiko Mitsunaga	Optimal Operation of Hybrid Water Heating Systems in Non-Residential Buildings	**288**
Hana Nekrep	Digital Water Load: Integrating the Hidden Water Footprint of Generative AI into Building Water Assessments	**292**
Ryo Fujimoto, Shizuo Iwamoto	Calculation of energy consumption in large public baths – Part 1: CFD analysis of evaporative heat loss at the bathtub surface	**296**
Kazuki Yuki et al.	Study on simulation of building drainage systems by CFD – Part 5: Investigation of CFD analysis accuracy for siphonic drainage systems	**300**
D. Rich, T. Roberts	Integrating Head Loss Calculations into Network-Based Simulation of Water Supply Systems	**304**

Drainage Performance and Components

Avtorji / Authors	Naslov / Title	Str.
Steve Wright et al.	Compensating for Reduced Flush Volumes: Restoring Solid Transport in Sanitary Drainage Systems Through Increased Pipe Gradient	**309**
Tsuyoshi Suruki et al.	Performance Evaluation Method of Self-sealing Trap Part 2: Characteristics of a Compact Umbrella-shaped Self-sealing Trap	**321**
Hibiki Hasemi et al.	Pressure Resistance Performance and Allowable Drainage Capacity of Multi-Inlet Floor Gullies	**333**
T. W. Tsang, M. W. Chan, L. T. Wong	Impact of kitchen food waste grinders on blockage risk and water use in high-rise drainage systems	**345**
Wan-Ju Liao et al.	Hydrodynamic Characteristics Analysis of the T-CORE Special Fitting Drainage and Venting System	**357**
Tomoya Kono et al.	Improved Renovation Method for Drainage Stack Systems in High-Rise Residential Buildings	**369**
J. D. Cuellar Sedie et al.	Advances in benchmark HRB DWV system testing at the National Lift Tower	**381**

Drainage Design, Modelling and Monitoring

Avtorji / Authors	Naslov / Title	Str.
D. A. Kelly, M. Gormley	Experimental quantification of evaporation rates in water trap seals within building drainage systems	**388**
M. Gormley	Modelling approaches to produce design guidance – TM70: Tall building Drainage Design	**400**
N. Post	Drainage roof vent distance from fresh air ventilation inlet in the Netherlands	**412**
T. Waniganettige, M. Gormley, D. Kelly	Measurement of Real Wastewater Flows in Building Drainage Systems	**419**
John Lansing	An examination of the influence of 19th century disease theory on the design of sanitary drainage systems – Sewer intercepting traps	**431**
J. Bavin, M. Gormley, D. A. Kelly	Near Source Monitoring of pathogens in building drainage systems	**440**

Public Health, Water Quality and Urban Resilience

Avtorji / Authors	Naslov / Title	Str.
Matjaž Nekrep Perc, Janja Kramer Stajnko et al.	Evaluating Urban Fire Water Supply Resilience with Hydrant Networks and Mobile Supply Strategies	**450**
Z. Vranayova, D. Kosicanova, D. Kaposztasova	Integrated Risk Assessment of Legionella Proliferation in Cold Drinking Water Systems: A Hospital Case Study	**462**
Ayaka Kimura, Masayuki Otsuka, Riki Tanaka	Comparison of Droplet Dispersal in Three Types of Hand Dryers	**474**
M. C. Jeffrey Lee et al.	Investigation and Strategic Analysis of Odor Emissions and Biological Contamination Sources in Public Toilets	**486**
A. Koyama, H. Kose	Study on the Required Number of Sanitary Fixtures to Improve Conditions in Women's Restrooms	**498**
L. Wilson, M. Gormley, D. A. Kelly	Impact of Shower Drains on Infection, Prevention & Control Strategies through Design & Operation	**510**

Development of Urban Biodiversity through Water-Based Biotope Creation in a Building Site

Takahiko Suzuki (1), Masayuki Otsuka (2)

(1) takahiko.suzuki@toda.co.jp
(2) dmotsuka@kanto-gakuin.ac.jp

(1) Doctoral Student, Graduate School of Engineering, Kanto Gakuin University, Japan; Manager, Facility Management Department,Technology Research Institute, TODA CORPORATION, Tsukuba Japan

(2) Prof. Dr. Eng, Department of Architecture and Environmental Design, College of Architecture and Environmental Design, Kanto Gakuin University, Yokohama Japan

Abstract

This study examines biodiversity development during the staged creation of a biotope within a research institute site in Japan. The study area evolved through three phases: (1) a grassland area of approximately 200 m² monitored in 2015, (2) an initial biotope with a pond (200 m²) constructed in 2018 and monitored until 2021, and (3) a completed biotope expanded to approximately 300 m² and monitored from 2021 to 2025.

Biological monitoring focused mainly on insects and birds. Insects belonging to several orders including Orthoptera, Mantodea, Hemiptera, Coleoptera, Lepidoptera, and Hymenoptera were recorded. The number of insect species increased from 32 species in the grassland stage to 76 species in the initial biotope and 83 species in the completed biotope. Bird observations also showed a clear increase, from no confirmed species in the grassland stage to 16 species in the initial biotope and 23 species in the completed biotope. The results indicate that the introduction and expansion of water-based habitats in building sites significantly enhance urban biodiversity.

The staged development of the biotope and the introduction of water environments created diverse ecological niches that supported both insect and bird communities.

Keywords

Biotope, Urban biodiversity, Water environment, Rainwater, Nature-based solutions

1. Introduction

With the progress of urbanization, many cities have experienced significant alterations to natural ecosystems and a decline in biodiversity. To address these challenges, studies on the maintenance and management of green infrastructure[1)2)] and the application of Nature-based Solutions (NbS) for restoring ecological functions in urban areas have recently attracted increasing attention. Furthermore, the health value and well-being benefits provided to people through these approaches have also been discussed[3)].

Among various approaches, the creation of water environments such as ponds and wetlands is considered particularly effective for enhancing urban biodiversity. Water bodies provide habitats for insects, birds, amphibians, and plants, and can function as ecological nodes within urban landscapes.
In building sites, rainwater utilization and small water bodies can create micro-habitats that support various species. However, the ecological development process that occurs when such water environments are introduced and expanded has not been sufficiently documented, particularly in building-scale environments.
This study aims to examine the staged development of biodiversity in a biotope constructed within a research institute site. By comparing three stages of land use—grassland, an initial biotope, and a completed biotope—this research investigates how the introduction and expansion of water environments influence biodiversity in urban building landscapes.

2. Study Site and Biotope Development

The study was conducted at a research institute site in Japan where a biotope was developed as part of environmental initiatives. The target area evolved through three stages of ecological development.
The first stage was a grassland area of approximately 200 m² monitored in 2015. The vegetation mainly consisted of herbaceous species such as Miscanthus and clover, and no permanent water environment existed in this stage.
The second stage was an initial biotope constructed in 2018 with an area of approximately 200 m². A small pond was introduced to create a water environment. Monitoring was conducted from 2018 to 2021.
The third stage was the completed biotope, which was expanded to approximately 300 m² in 2021. Additional habitat features and vegetation were introduced, and monitoring was conducted from 2021 to 2025.
These three stages represent the ecological transition from a simple grassland environment to a water-based urban biotope.

		2015-	2019- Regional Native Plant Biotope		
		Grassland	Waterside	Grassland	Forest
Target Environment		Dominated by Zoysia grass. Low grassland in early summer and tall Miscanthus grassland in autumn.	Low wet grassland with Juncus and Oenanthe.	Grassland dominated by Zoysia and Miscanthus.	Mixed forest mainly composed of Quercus myrsinifolia, Quercus glauca, and Quercus serrata.
Indicator Species	Vegetation	Imperata cylindrica, Athyrium yokoscense, Deutzia crenata	Juncus, Oenanthe	Pinus densiflora, Imperata cylindrica	Myrica rubra, Callicarpa japonica
	Insects	Acrida cinerea, Atractomorpha lata	Orthetrum albistylum, Crocothemis servilia, Sympetrum frequens, Dryophytes japonicus	Atractomorpha lata, Batocera lineolata, Parnara guttata, Lycaena phlaeas	Graphium sarpedon, Graptopsaltria nigrofuscata, Prosopocoilus inclinatus, Anomala cuprea

Figure 1— Target Area and Target Environment

3 Monitoring Methods

Biological monitoring focused primarily on insects and birds, which are considered important indicators of biodiversity in urban ecosystems.
Insect surveys were conducted to record species belonging to major insect orders, including Orthoptera, Mantodea, Hemiptera, Coleoptera, Lepidoptera, and Hymenoptera. Bird observations were conducted through visual surveys within the study site. Monitoring was conducted twice in 2015, in June and October. From 2019 onwards, monitoring was carried out five times a year, in April, June, August, October, and December.
Surveys of insects and birds were conducted mainly through direct observation. During each survey, the study area was traversed as thoroughly as possible. Species were identified in the field whenever feasible, and unidentified species were photographed and later examined for identification.
Since birds tend to flee in the presence of observers, Unmanned infrared cameras were installed at bathing sites from 2019 onwards to supplement visual observations.
The number of confirmed species was used as a basic indicator to evaluate biodiversity changes across the three stages.

4 Results

The monitoring results show a clear increase in biodiversity as the biotope developed. For insects, 32 species were recorded in the grassland stage in 2015. After the construction of the initial biotope with a pond, the number of insect species increased to 76 species during the monitoring period from 2018 to 2021. In the completed biotope stage monitored from 2021 to 2025, 83 insect species were confirmed.

Table1－Changes in the number of insect and bird species over time

Year		2015	2019	2020	2021	2022	2023	2024	2025
Biotope type		Grassland	Regional Native Plant Biotope						
Area		200 m²	200 m²			510 m²			
Insect Species	Dragonflies	3	12	9	13	10	13	14	10
	Mantises	1	2	2	2	3	2	2	2
	Grasshoppers	9	17	20	9	14	17	13	12
	Hemiptera	16	4	2	7	9	6	10	11
	Butterflies	8	14	11	17	16	21	18	15
	Flies	2	2	0	1	2	1	2	4
	Beetles	8	8	6	1	10	19	17	16
	Hymenoptera	3	5	1	11	12	14	18	15
	Total	50	64	51	61	76	93	94	85
Bird Species	Observed within site	0	9	8	12	5	12	10	20
	Observed flying over/outside site	3	3	8	4	10	6	10	3
	Total	3	12	16	16	15	18	20	23

Bird observations also showed significant changes. No bird species were confirmed in the grassland stage. In the initial biotope stage, 16 bird species were recorded. In the completed biotope stage, the number of bird species increased further to 23.
These results indicate that biodiversity increased markedly following the introduction and expansion of the water environment.

5. Conclusion

The results suggest that the introduction of water environments plays an important role in enhancing biodiversity in urban building sites.
Water bodies create various ecological niches and attract insects that depend on aquatic or semi-aquatic environments. These insects also serve as food resources for birds, which may explain the increase in bird species observed during the later stages of biotope development.
The expansion of the biotope area and the diversification of vegetation likely contributed to increased habitat complexity, thereby supporting greater species diversity.
These findings demonstrate that even relatively small-scale biotopes within building sites can contribute to biodiversity enhancement when water environments are incorporated.
Although the increase in species richness was strongly associated with the introduction of water environments, other factors, including vegetation development, habitat expansion, and differences in observation methods, may also have contributed to these changes.
Future studies should quantitatively evaluate the relative contributions of these factors to biodiversity enhancement.

6. References

1) Shirou WAKUI；Special Feature: "Toward the Implementation of Green Infrastructure"Keynote Speech: "A New Era Expanded by Green Infrastructure", J. Jpn. Soc. Reveget. Tech., 45（3）, 373—374, （2020）
https://doi.org/10.7211/jjsrt.45.373_1

2)Bohyum KIM et al.;Research on maintenance management methods for green infrastructure,Technical Reports of Landscape Architecture Vol.3, 2024,
https://doi.org/10.60235/jilatech.3.0_68

3) McKinney ML, VerBerkmoes A. Beneficial health outcomes of natural green infrastructure in cities. Curr Landsc Ecol Rep 2020;5:35–44.
https://doi.org/ 10.1007/s40823-020-00051-y.

7. Presentation of Authors

Takahiko Suzuki is a researcher at the Technical Research Institute of TODA CORPORATION. His work focuses on plumbing systems, biodiversity, and green infrastructure. He is a member of AIJ, JSPE, and SHASE.

Investigation of Water Balance in Alternative Water Use Buildings

T. Nishikawa (1)
1. t-nskw@cc.kogakuin.ac.jp
(1) Prof., School of Architecture, Kogakuin Univ., Dr. Eng., Japan

Abstract

This study aims to quantitatively understand the dynamic water balance trends of alternative water use and rainwater runoff control facilities at the city block level, encompassing urban public spaces and other building complexes. It seeks to clarify water cycle efficiency, including daily environmental impact, and self-sufficiency performance during infrastructure disruptions caused by disasters. This paper presents some of the results of our investigation into the water balance of alternative water use buildings.

Keywords

Water supply and drainage system, Precipitation characteristics, Water demand, Water balance, Net zero water

1. Introduction

Considering that approximately 2 billion people worldwide still lack access to safe drinking water, Japan's water and sewage infrastructure appears to be mature from an international perspective. However, changes in precipitation characteristics caused by global warming are leading to increasingly frequent torrential rains exceeding the capacity of water and sewage systems, and coupled with the aging of these systems, urgent countermeasures are needed. This research aims to quantitatively understand the dynamic water balance trends of alternative water use and rainwater runoff control facilities at the block level, including urban public spaces and other building complexes. It seeks to clarify the water cycle efficiency, including daily environmental burdens, and the self-sufficiency performance in the event of infrastructure disruption due to disasters. This paper evaluates a single-building university campus (A), a medium-sized office building (B), and a university campus consisting of multiple buildings(C)[1]. It investigates the water cycle and water balance in each case and describes the progress of the research toward an evaluation including public spaces. Further details of this paper are included in the SHASE Annual Conference abstracts [2]-[3], please refer to those for more information.

2. Investigation of Water Balance Related to Buildings

This study evaluates several buildings in the Tokyo metropolitan area that have functions for alternative water use and rainwater runoff control. Water balances will be estimated from management records and meteorological data to serve as basic data for evaluating the water cycle across a wider area. The evaluation targets are single buildings or groups of buildings on the same site that have reclaimed water facilities using well water, rainwater, or recycled water as water sources in addition to the public water supply. While it is preferable to calculate water balances using a cumulative method based on management and meteorological data, the state of the data used for calculation (measurement items, measurement intervals, data storage status, etc.) often differs from building to building. Furthermore, there are few examples of actual buildings that clearly show water balances including rainwater trends after precipitation.
Therefore, the study will focus on three buildings: two universities with different scales and shapes (one campus consisting of a single skyscraper and the other of a group of mid-to-high-rise buildings), and an office building equipped with rainwater and drainage facilities. Annual water balance calculations, including the site, will be performed, and studies will be conducted on alternative water use and rainwater runoff control to promote zero water.

Table 1. Overview of each building

	A	B	C
Site area	4,400 ㎡	800 ㎡	195,900 ㎡
Total floor area	49,900 ㎡	1,300 ㎡	71,300 ㎡
Building use	University Campus	Office	University Campus
Alternative water use	Reclaimed Water	Rainwater, Wastewater	Well Water
Rainwater runoff coefficient	0.86	0.65	0.58
Overview of the water supply system	The area is supplied with both tap water (public water supply) and recycled water (used for toilet flushing) through a wide-area circulation system. The water supply system is gravity-fed and is divided into three zones.	Drinking water is supplied via a pressurized water supply system. Alternative water (sourced from rainwater and treated wastewater) is used for toilet flushing and is supplied via gravity from an elevated water tank for non-potable water.	The main water source is well water on the premises. After treatment, the well water is stored in a receiving tank and then distributed to each building through a pressurized water supply system and a gravity water supply system.

3. Comparison of Water Usage and Reclaimed Water Amount for Each Evaluation Target

Using hourly data on precipitation and water supply, we calculated daily cumulative values and examined the annual trend of water balance for each building, referencing the calculation method for LEED Zero Water certification [4]. The water balance (WB) for buildings (A) through (C) was calculated as follows.

$$WB_A = WU(cw+rc+rw) - WR(ev+tr+if) \quad \cdots \text{Eq.1}$$

$$WB_B = WU(cw+rc+rw) - \{ AW(rw+rc) + WR(ev+tr+if) \} \quad \cdots \text{Eq.2}$$

※Wurw（precipitation）≠Awrw（Rainwater usage）, WUrc=Awrc

$$WB_C = WU(cw+ww+rw) - WR(ev+tr+if) \quad \cdots \text{Eq3}$$

Symbol : AW (Alternative Water Use), WR (Water Returned), WU (Total Water Use), cw（city water）, rw (rainwater), ww(well water), rc（reclaimed water）, ev (evaporation),tr (Transpiration), if (infiltration), a(BuildingA), b(BuildingB), c（BuildingC）

In Building A, recycled water from a wide-area circulation system is used for toilet flushing. However, in order to make a simple comparison between buildings, recycled water was counted as water usage (WU) rather than alternative water (AW). Building A is a high-rise structure with a floor-area ratio exceeding 1,000%, and the volume of water returned to the ground (e.g., via rainwater infiltration) is negligible; consequently, with the exception of occasional closures for maintenance, the annual water balance consistently remains positive (Figure 1).

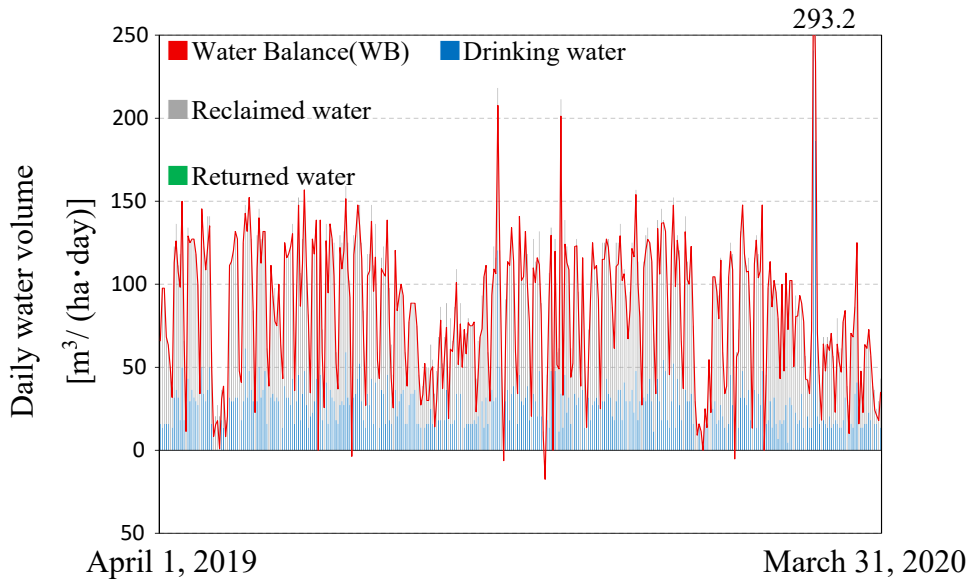

Figure 1. Annual trends in water usage and reduced water volume (A)

Next, regarding Building B—which features surrounding planting zones but consists predominantly of impervious surfaces—the volume of water returned to the ground is minimal; however, because rainwater and reclaimed water are utilized as alternative water

sources, the water balance remains negative throughout the year (Figure 2).Furthermore, Building C—which consists of a complex of multiple structures—occupies a site that is relatively large compared to its floor area; consequently, it exhibits high rates of water return (via rainwater infiltration and evapotranspiration). This results in a significant annual water balance deficit, with trends largely driven by precipitation levels (Figure 3). Although the facility relies on an on-site deep well as its water source—meaning well water constitutes the total water usage (WU)—the volume of extracted groundwater generally remains below the rate of rainwater infiltration on a cumulative daily basis, and no adverse impacts on groundwater (such as changes in water levels or quality) have been observed.

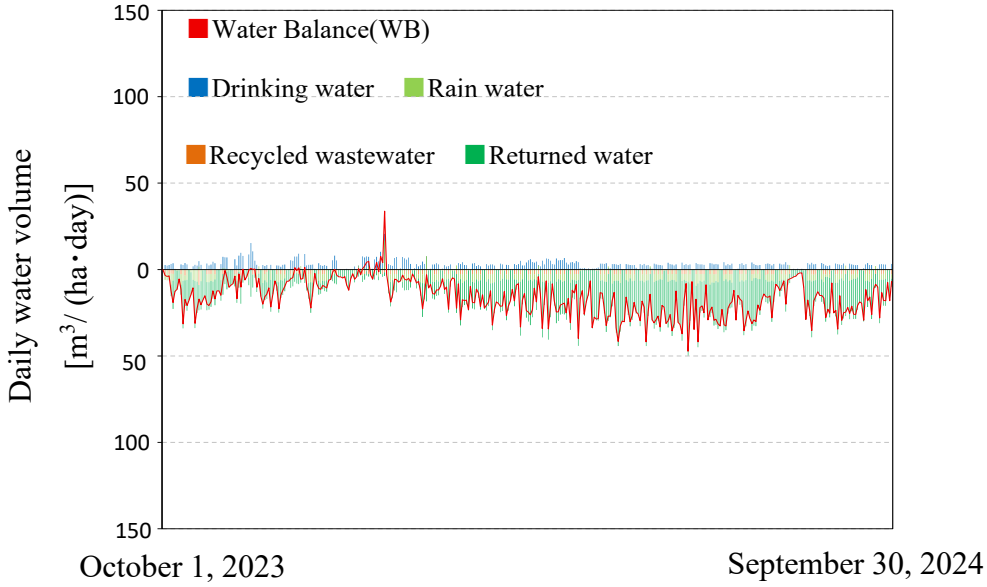

Figure 2. Annual trends in water usage and reduced water volume (B)

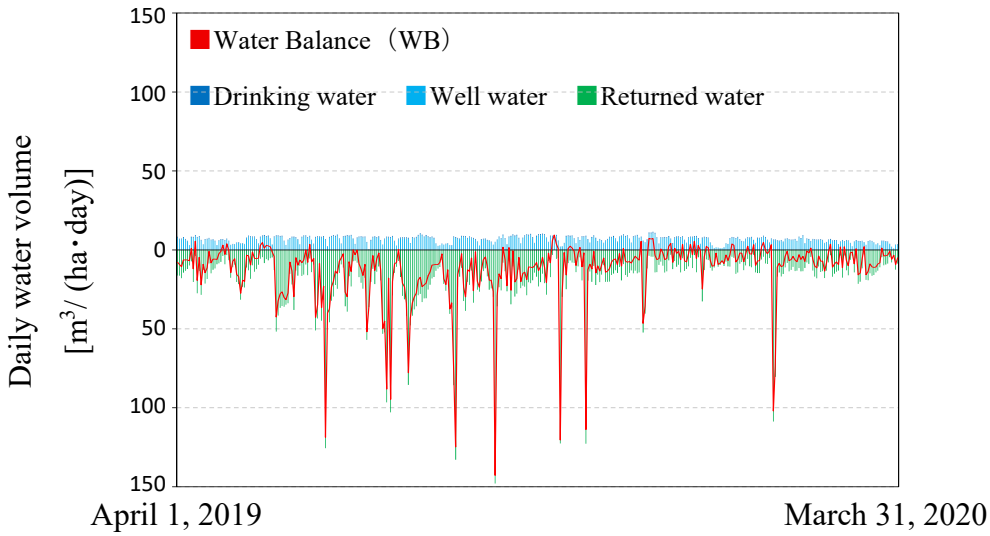

Figure 3. Annual trends in water usage and reduced water volume (C)

Figure 4 compares the results of these annual trends for each evaluation target using annual cumulative calculations. In evaluating the water balance, the recycled water in A is drawn in through a wide-area circulation system, and as mentioned above, it was counted as water usage. However, if we consider it on a specific district basis rather than on a building basis, it is conceivable that some or all of it could be interpreted as alternative water based on the trends in the wide-area water cycle.Furthermore, in cases B and C, the volume of water returned can be attributed to precipitation; however, the assessment of impacts on post-infiltration groundwater recharge and the broader water cycle requires further consideration, and these aspects will be addressed in future studies.

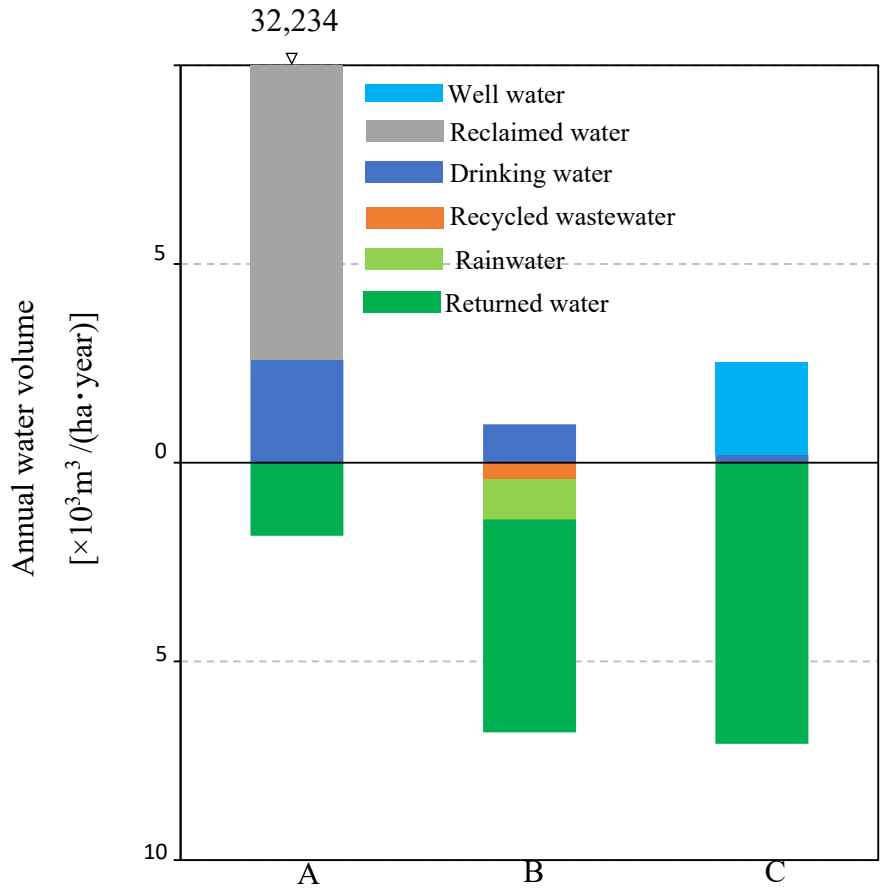

Figure 4. Comparison of water usage and returned water

4. Conclusion

In this paper, we selected three evaluation subjects that employ different alternative water uses, compiled their water balances on an annual basis, and compared them from the perspectives of building use, site, and building scale. Achieving carbon neutrality by 2050 is a common global goal, and discussions are progressing toward reducing carbon dioxide emissions throughout the entire lifecycle of buildings. In addition to addressing water shortages and reducing the burden on water and sewage infrastructure, promoting water-recycling and alternative water-use buildings requires rapid and effective measures not

only for new construction but also for existing buildings. In the future, we plan to broadly and dynamically evaluate water balances, including those in public spaces, and advance this research topic.

5.Acknowledgment

This work was supported by JSPS KAKENHI Grant Number JP26K07782. Furthermore, part of this research was conducted as a joint research project between Kogakuin University and Taisei Corporation.We would like to thank all parties concerned for their cooperation in providing materials and data on the target buildings that were evaluated.

8.References

[1] Toyohiro NISHIKAWA: Water Balance and Zero-Water Rating on University Campuses Using Alternative Water, 50th Annual CIB W062 Conference,2024.8, Northampton, UK

[2]Toyohiro NISHIKAWA et al.: Evaluating alternative water uses and stormwater runoff control to promote zero water use in public spaces and buildings （Part1）Water balance and net zero water in the evaluation area, SHASE Annual Conference 2026

[3] Kazuya AKIYAMA et al.: Evaluating alternative water uses and stormwater runoff control to promote zero water use in public spaces and buildings (Part 2) Changes in alternative water use and return water volume based on water balance using hourly water supply data, SHASE Annual Conference 2026

[4] U.S. Green Building Council ：LEED tools,https://www.usgbc.org/leed-tools, (accessed May 7, 2026)

9.Presentation of Author

Toyohiro NISHIKAWA is the Professor at School of Architecture, Kogakuin Univercity,Dr. Eng.

He is a member of AIJ (Architectural Institute of Japan) and SHASE (The Society of Heating, Air-Conditioning and Sanitary Engineers of Japan). His current research interests are Performance verification of next generation air-conditioning systems, Development of high-performance outer wall, and Analysis of water environment in urban buildings.

Residential Resilience to Flood Disasters: Continuity of Living Functions and Building Services

H.Yamaguchi (1)

(1) haruy@kanto-gakuin.ac.jp
(1) College of Architecture and Environmental Design, Kanto Gakuin University, JAPAN

Abstract

This study examines residential resilience to flood disasters in Japan, focusing on the continuity of living functions. It analyzes the impact of lifeline disruptions on daily activities and classifies strategies into prevention, functionality maintenance, and recovery. A conceptual framework is proposed to support integrated architectural and building services design.

Keywords

Flood resilience; Continuity of living functions; Building services; Residential buildings

1 Introduction

In recent years, the frequency and intensity of flood disasters have increased due to the effects of climate change. Conventional disaster mitigation strategies in Japan have primarily focused on the structural safety of buildings. In recent years, the concept of distributed evacuation during disasters has led to sheltering at home becoming one of the available evacuation options. Therefore, residential buildings are required not only to prevent physical damage but also to maintain living functions from the onset of a disaster through the recovery process.
This study reviews recent flood disasters and post-disaster living difficulties in Japan, and discusses disaster mitigation strategies and concepts for resilience evaluation from the perspective of continuity of living functions in residential buildings, focusing on both architectural and building service approaches.

2 Impact of Flood Disasters on Living Conditions

The number of natural disasters occurring between 2000 and June 2022 was investigated based on reports from the Cabinet Office and related organizations (Ref. 1) (Fig. 1). Among the 390 recorded cases, landslides were the most frequent, followed by flood-related disasters, which accounted for approximately 33% of the total.

In Japan, the seismic design standards for wooden houses have evolved through experiences of major earthquakes, and the current standards established in 2000 generally ensure an adequate level of structural safety. On the other hand, the restoration of lifeline systems, particularly water supply and sewerage systems, often requires a long period. As a result, residents may experience serious difficulties in maintaining hygiene, using toilets, and accessing information during disasters (Fig. 2) (Ref. 2).

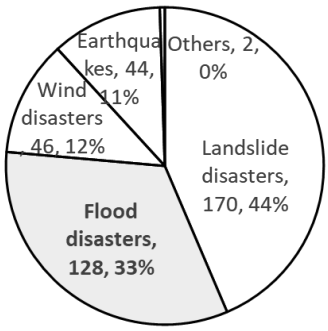

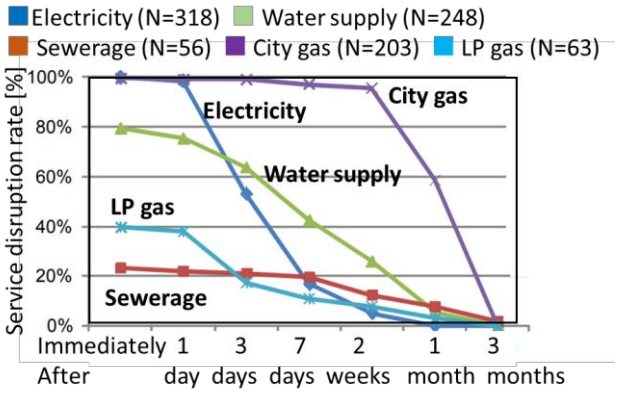

Fig.1 Distribution of natural disasters in Japan **Fig.2 Restoration period of lifeline systems**

3 Residential Flood Mitigation Strategies in Japan

Flood disaster risks in Japan vary by region and include floods, tsunamis, and landslides. Therefore, hazard maps should be utilized during site selection in order to identify potential disaster locations and the frequency of damage occurrence (Fig. 3). In addition, architectural measures such as surrounding sites with block walls, and installing alcoves, water barriers, and backflow prevention valves are effective for reducing inundation damage (Fig. 4). Furthermore, to ensure the continuity of living functions during disasters, disaster-response systems such as emergency water storage, battery storage systems, and water supply systems utilizing residential water heaters have been introduced. In addition, EV-linked systems, which utilize electric vehicles (EVs) as power sources for residential buildings, are also being utilized (Fig. 5). In recent years, flood-resilient housing has been developed in Japan. Building service equipment is installed at higher locations, and materials are selected to facilitate rapid recovery after flooding (Ref. 3).

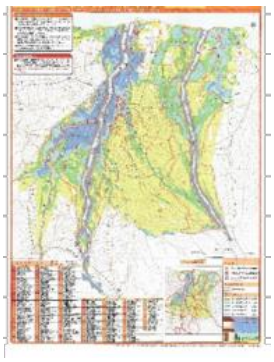

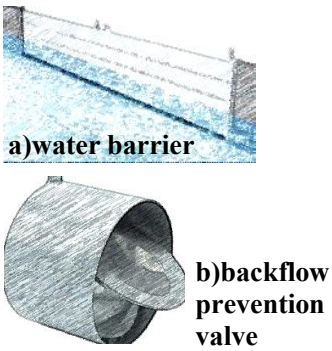

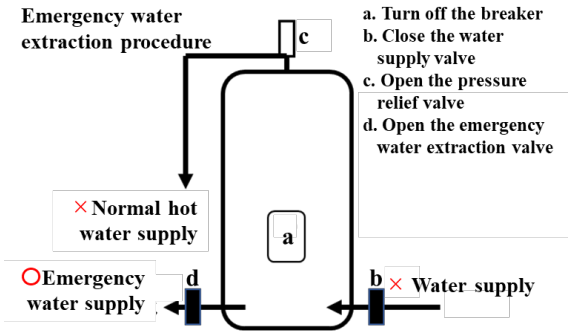

Fig.3 Flood hazard map **Fig.4 Architectural flood mitigation measures** **Fig.5 Building service strategies for emergency water supply**

4 Concept of Residential Resilience and Evaluation Framework

A conceptual framework of residential resilience was developed based on representative flood disaster cases and published reports on post-disaster lifeline recovery in Japan, together with perspectives from architectural planning and building services (Fig. 6). As a conceptual evaluation method, it assumes recovery conditions, while actual recovery processes may vary depending on disaster characteristics and regional conditions.

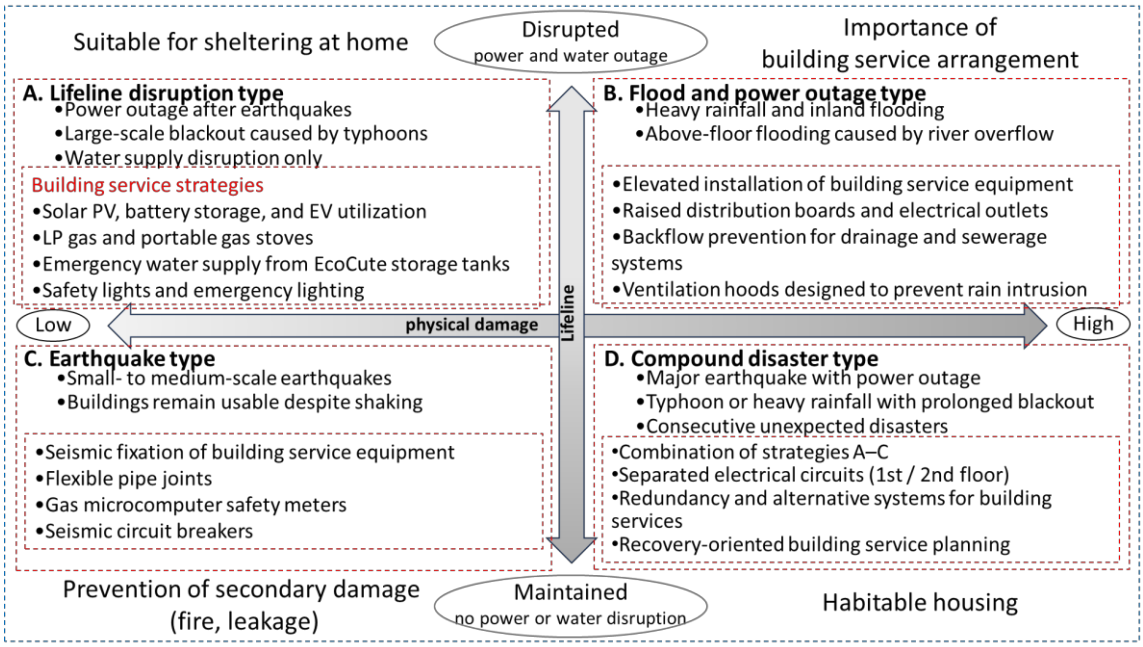

Fig.6 Conceptual framework of residential resilience

In this study, the continuity of living functions is regarded as an important indicator of residential resilience. Daily activities depend on multiple building service functions such as electricity, water supply, and drainage, and if any one of these functions becomes unavailable, the corresponding activity cannot be performed. Therefore, with reference to a previous study (Ref.4), the availability of each activity was defined as the minimum availability of the required building services, as expressed in Equation (1).

$$y_a(t) = \min_{i \in R_a} x_i(t) \quad \cdots \quad (1)$$

The overall continuity of living functions was evaluated by integrating the availability of individual daily activities, as expressed in Equation (2). Here, $x_i(t)$ represents the availability of building service functions, $y_a(t)$ represents the availability of daily activities, and $L(t)$ represents the continuity of living functions. The weighting factor $\propto_a$ represents the relative importance of each daily activity, which may be determined according to its contribution to hygiene, health, and daily living (e.g., toilet use).

$$L(y) = \frac{\sum_a \alpha_a y_a(t)}{\sum_a \alpha_a} \quad \cdots \quad (2)$$

Figure 7 shows an evaluation example focusing on toilet use. In this example, toilet use cannot be restored until all related building service functions are recovered. Although

$L(t)$ was not calculated, toilet use is considered one of the most critical daily activities.

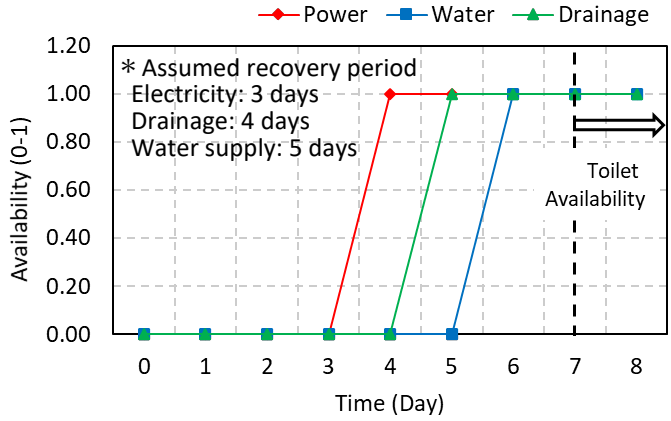

Fig.7 Time variation of toilet-use availability

5 Conclusions

In this study, a quantitative evaluation method for the continuity of living functions was proposed based on the relationship between daily activities and building service functions. Using this framework, the relationship between the recovery process of lifeline systems and living functions was quantitatively clarified.

The evaluation example of toilet use demonstrated that the failure of a single building service can significantly affect overall living functions. The proposed framework may contribute to the planning and evaluation of flood-resilient housing and building service systems by supporting the continuity of living functions during disasters.

6 References

1) Cabinet Office, Government of Japan, Disaster Prevention Information Page, available at: https://www.bousai.go.jp/updates/index.html (accessed June 15, 2022).
2) Architectural Institute of Japan, Report on the Great East Japan Earthquake: Building V olume 8 – Building Services and Environmental Engineering, p.100, 2015.
3) Endo, Y. and Yasue, T., Safety Evaluation of an RC Structure with Multiple Openings under High Water Depth Inundations, Applied Sciences, Vol. 11, No. 9, 4297, 2021.
4) Architectural Institute of Japan, Report of the Special Committee on Building Resilienc e and BCP Level Indicators: Toward the Proposal of Performance Evaluation Indicator s for Building Maintenance and Recovery in Earthquake Disasters, pp.48–49, 2020.

7 Presentation of Author

Haru Yamaguchi is a professor at the Faculty of Architecture and Environmental Design, Kanto Gakuin University. She holds a Ph.D. in environmental design from Showa Women's University and is a licensed First-Class Architect in Japan. She is also an active member of the Architect Institute of Japan's association (AIJ) and The Society of Heating, Air-Conditioning and Sanitary Engineers of Japan (SHASE).

A Study on the Expansion of Non-Potable Water Use in Buildings

Ryuki Koike (1), Takehiko Mitsunaga (2), Tomoo Inada (3), Yoshiaki Matsumura (4), Yoshinori Honma (5)

(1) ce253027@meiji.ac.jp, Meiji University, Japan
(2) mitsunaga@meiji.ac.jp, Meiji University, Japan
(3) to-inada@suga-kogyo.co.jp, SUGA Co., Ltd., Japan
(4) matsumura-y@yamashitasekkei.co.jp, Yamashita Sekkei Inc., Japan
(5) honma.y.aa@niph.go.jp, National Institute of Public Health, Japan

Abstract

In the building sector, wider use of non-potable water is expected; however, in Japan, its applications are limited, and stored non-potable water may overflow without full use. This study examined its applicability to new uses in Japan. Domestic and international water quality standards were compared to clarify the characteristics of Japan's framework. Cooling tower make-up water was then selected as a candidate use, and related operational problems and health impact cases were reviewed. The results suggest that, in assessing this application, maintenance deficiencies, as well as water quality standards, are strongly associated with Legionella proliferation and health impacts.

Keywords

Non-potable water, Water quality, Cooling tower, Legionnaires' disease, Rainwater

1 Introduction

In Japan, promoting water conservation and rainwater use is important, and wider use of non-potable water is expected in the building sector. However, the Building Sanitation Act limits non-potable water applications to toilet flushing, irrigation for greenery, landscape water, and related uses, so stored non-potable water may overflow without full use. This study examines the feasibility and requirements of using non-potable water, including rainwater-derived water, as cooling tower make-up water. Cooling towers were selected because they are outdoor facilities compatible with rainwater use and require large volumes of make-up water.

1.1 Methodology

This study reviews official laws, standards, guidelines, and government reports identified between September 2025 and May 2026. Japan, the EU, the United States, and China serve as major regulatory and standardisation frameworks for comparison, while Queensland and Singapore are included because they explicitly specify criteria for reclaimed water use in cooling towers. For Table 1, irrigation and toilet flushing are used as comparable building applications, and four representative parameters are selected to cover microbial safety, basic physicochemical quality, treatment performance, and disinfection control. For Table 2, comparable parameters are extracted, and units are standardised where necessary.

2 Position of Japanese Water Quality Standards for Non-potable Water

Table 1 compares representative criteria for irrigation and toilet flushing in Japan, the EU, China, and the United States. Uses are more finely classified outside Japan, whereas Japan has only two broad categories: toilet flushing, and water for sprinkling, landscaping, and cleaning. Because the criteria address different source waters, treatment levels, and end uses, their numerical values are not directly equivalent.

Table 1 Water Quality Criteria in Japan and Other Countries/Regions, Selected

Country/Region	Japan[1,2]	EU[3,4]		United States[5]		China[6]	
Use	Irrigation/ Toilet flushing	Agricultural Irrigation	Toilet flushing	Irrigation	Toilet flushing	Irrigation	Toilet flushing
E.coli	Not detected	≤ 10,000 [CFU/100 mL]	< 250 [CFU/100 mL]	≤ 2.2 (200) [MPN/100 mL]	≤ 2.2 (200) [MPN/100 mL]	Not detected	Not detected
pH	5.8–8.6	-	5.0–9.5	6.0–9.0	6.0–9.0	6.0–9.0	6.0–9.0
Effluent characteristics [mg/L]	-	BOD_5 and TSS: according to Directive 91/271/EEC	-	$CBOD_5$: ≤ 10 (25) *TSS*: ≤ 10 (30)	$CBOD_5$: ≤ 10 (25) *TSS*: ≤ 10 (30)	BOD_5: ≤ 10	BOD_5: ≤ 10
Disinfection control indicators [mg/L]	*Free residual chlorine*: ≥ 0.1 *Combined residual chlorine*: ≥ 0.4	-	*residual chlorine*: < 2.0 *Residual bromine*: < 5.0	-	-	*Total chlorine* ≥ 1.0 (outlet)	*Total chlorine* ≥ 1.0 (outlet)

Note: For the United States, values without parentheses indicate test averages, and values in parentheses indicate single-sample maxima.

Note: Within the scope of this review, no criteria directly addressing the use of non-potable water as cooling tower make-up water were identified for the EU, the United States, or China.

3 Feasibility of Applying Non-Potable Water to Cooling Tower Make-up Water

In Japan, applicable laws and regulations require cooling-tower make-up water to meet drinking-water quality standards [7]. By contrast, Queensland and Singapore permit reclaimed water use in cooling towers and specify water quality criteria [9, 10] (Table 2). Compared with Japan, Queensland and Singapore specify Legionella limits and stricter heterotrophic plate count limits.

Table 2 Water Quality Criteria for Non-potable Water Used as Cooling Tower Make-up Water in Queensland, Australia, and Singapore

Water Quality Parameter	Japan (Reference Values for Supply Water) [8]	Queensland [9]	Singapore [10]
Coliform bacteria [CFU/100 mL]	-	-	< 10
E. coli [CFU/100 mL]	Not detected	Not detected	Not detected
Legionella bacteria [CFU/100 mL]	-	Not detected	Not detected
pH	5.8-8.6	6.0-8.5	6.0-9.0
Odor	No abnormality	-	Not offensive
Turbidity [NTU]	≦ 2.0	< 2.0	< 2.0
Color [TCU]	≦ 5.0	-	< 15
BOD_5 [mg/L]	-	< 5.0	< 5.0
Residual chlorine [mg/L]	≦ 1.0 (target)	> 0.5 (free residual chlorine)	0.5 - 2.0 (total residual chlorine)
Heterotrophic plate count [CFU/100 mL]	≦ 2.0×10^5 (target)	< 500	≦ 5.0×10^4

"-" indicates that no limit value is specified.

Cooling water commonly circulates at 10–40 °C [11], favouring biofilm formation and aerosol generation. A national survey found that, in 2006, approximately 26% of samples contained Legionella spp. at 10 CFU/100 mL or higher [11]. Japanese investigations identified inadequate cleaning, absent chemical treatment, and residual biofilm or scale [12–15]. ASHRAE Guideline 12-2020 similarly identifies temperature, deposits, water age, disinfectant residual, and biofilm as key factors [16]. Thus, water-quality and maintenance requirements must be considered together. Scaling, corrosion, cycles of concentration, blowdown, and monitoring remain issues for further study.

4 Conclusion

This study suggests that, when considering the use of non-potable water as cooling tower make-up water, maintenance requirements—including cleaning, chemical cleaning, chemical treatment, and water quality testing—should be organized together with additional water quality parameters.

These findings provide useful insights for balancing water conservation and hygienic safety in expanding non-potable water applications in Japan.

Future work will examine these issues using a small-scale cooling-tower model under different source-water and maintenance conditions.

5 References

[1] Ministry of Health, Labour and Welfare, Building Environmental Sanitation Management Standards (in Japanese).

[2] Sewerage and Wastewater Research Department, National Institute for Land and Infrastructure Management, Ministry of Land, Infrastructure, Transport and Tourism, Report on Water Quality Standards for Miscellaneous Water Use, April 2005 (in Japanese).

[3] Regulation (EU) 2020/741, https://eur-lex.europa.eu/eli/reg/2020/741/oj/eng, accessed 28 March 2026.
[4] European Committee for Standardization, EN 16941-2:2021 On-site Non-potable Water Systems – Part 2: Systems for the Use of Treated Greywater.
[5] NSF International, NSF/ANSI 350-2023: Onsite Residential and Commercial Water Reuse Treatment Systems, 2023.
[6] Standardization Administration of China, GB/T 18920-2020.
[7] Ministry of Health, Labour and Welfare, Enforcement Regulations of the Act on Maintenance of Sanitation in Buildings, Article 3-18 (in Japanese).
[8] Ministry of the Environment, Water Quality Standard Items and Standard Values (in Japanese).
[9] Requirements for the supply of recycled greywater for cooling tower treatment plants, https://www.housing.qld.gov.au/__data/assets/pdf_file/0028/33697/requirements-supply-recycled-greywater-cooling-towers.pdf, accessed 3 February 2026.
[10] PUB, Singapore's National Water Agency, Guidelines for Treated Greywater Quality for Recycling of Greywater for Toilet Flushing, General Washing, Irrigation and Cooling Tower Make-up Water, https://www.pub.gov.sg/-/media/PUB/PDF/greywaterRequirements.pdf, accessed 3 February 2026.
[11] Japan Building Maintenance Education Centre, Guidelines for Prevention of Legionellosis, 5th Edition (in Japanese).
[12] H-CRISIS, Outbreak of Pontiac Fever Caused by Legionella pneumophila Serogroup 7, https://h-crisis.niph.go.jp/archives/83043/, accessed 3 February 2026.
[13] Japan Institute for Health Security, Suspected Legionella Infection from a Hospital Cooling Tower, Fukuoka(in Japanese), https://id-info.jihs.go.jp/niid/ja/legionella-m/legionella-iasrd/5325-kj4191.html, accessed 3 February 2026.
[14] Japan Institute for Health Security, Legionellosis Cluster Associated with a Hospital Cooling Tower (in Japanese), https://id-info.jihs.go.jp/surveillance/iasr/pathogens/vol45/533/533r03.html, accessed 3 February 2026.
[15] National Council of Environmental Hygiene Officials, Proceedings of the Case Study Presentation Meeting 2025 (in Japanese).
[16] ASHRAE, ASHRAE Guideline 12-2020: Managing the Risk of Legionellosis Associated with Building Water Systems, Atlanta, GA, 2020.

6 Acknowledgement

This study was conducted as part of a Health and Labour Sciences Research Grant (Project No. 25LA1004), "Comprehensive Study for the Verification of Building Environmental Sanitation Management Standards and the Establishment of Future Sanitation Management" (Principal Investigator: Yoshinori Honma).

7 Presentation of author

Ryuki Koike is a graduate student at the Mitsunaga Laboratory, Meiji University, Japan. His research focuses on environmentally conscious building systems.

Study on Design Methods for ZWB in Urban Mid-Sized Office Building - Part 1: Measurement of Water Balance for Achieving ZWB

Satoshi Matsumoto(1), Sei Yoshioka(2), Tomoo Inada(3), Kiichi Takeda(4), Shota Satake(5), and Takehiko Mitsunaga(6)

(1) sa-matsumoto@suga-kogyo.co.jp
(2) se-yoshioka@suga-kogyo.co.jp
(3) to-inada@suga-kogyo.co.jp
(4) ki-takeda@suga-kogyo.co.jp
(5) syo-satake@suga-kogyo.co.jp
(6) mitsunaga@meiji.ac.jp

(1) (2) (3) (4) (5) SUGA Co.,Ltd., Japan
(6) Assoc. Prof., Dep. of Architecture, School of Science & Technology, Meiji University, Japan

Abstract

While the concept of ZWB (Zero Water Building) has been gaining recognition in Japan, practical methods for achieving this goal remain uncertain. This study aims to contribute to the development of ZWB implementation by analyzing water flows in an urban mid-sized office building. The analysis revealed the occurrence of overflow during the water utilization process, indicating inefficiencies in the current system. These findings confirmed that the capacity of rainwater storage tanks significantly influences water utilization efficiency.

Keywords

Zero Water Building; Alternative water; Rainwater storage tank; Chiller spray system

1 Introduction

The concept of ZWB has recently emerged in Japan as an approach to promoting the sustainable use of water resources. The objective of ZWB is to achieve a net-zero water

balance within a building and its premises through efficient water use and reuse [2], [3]. However, there are currently no standardized methods for achieving ZWB in Japan [1]. This study aims to identify main challenges in the development of such methods by examining the water balance of a medium-sized urban office building.

2 Methodology

2.1 Building Overview

This study examines a medium-sized office building located in Koto City, Tokyo. The building consists of nine stories above the ground and one below, with a total floor area of 3,781m^2. Approximately 150 employees occupy the building on weekdays.

The building was designed to minimize overall water consumption through a dual water supply system composed of potable and non-potable water networks. The potable water system is entirely reliant on public water supplies and is primarily used for handwashing. The non-potable water system is supplied by alternative water sources and is primarily used for toilet flushing. These alternative water sources include rainwater and drain water generated by air conditioning machinery, such as air handling units and chillers.

To collect and manage alternative water, the building is equipped with a rainwater storage tank (RST) located in the basement. Rainwater and drain water flow into the RST by gravity and are stored as alternative water. This water is transferred from the RST to the non-potable water tank as needed. When the RST has insufficient water to transfer, the public water is directly supplied to the non-potable water tank to meet demand [4].

2.2 Methodology

To evaluate the annual water balance of the building, data on water flows were collected and analyzed. Records of potable and non-potable water consumption were obtained from the Building Energy Management System (BEMS). In addition, inflow and outflow volumes associated with the RST were calculated based on the relevant operational data.

Figure 1 illustrates the water flow structure related to the RST. Inflows consist of three components of alternative water: (1) rainwater collected from the building rooftop, (2) drain water from the chiller spray system (CSS), which sprays water onto air-cooled chillers to improve heat source efficiency, and (3) condensate drain water from air handling units. Outflows consist of two components: (4) supply to the non-potable water tank, and (5) overflow.

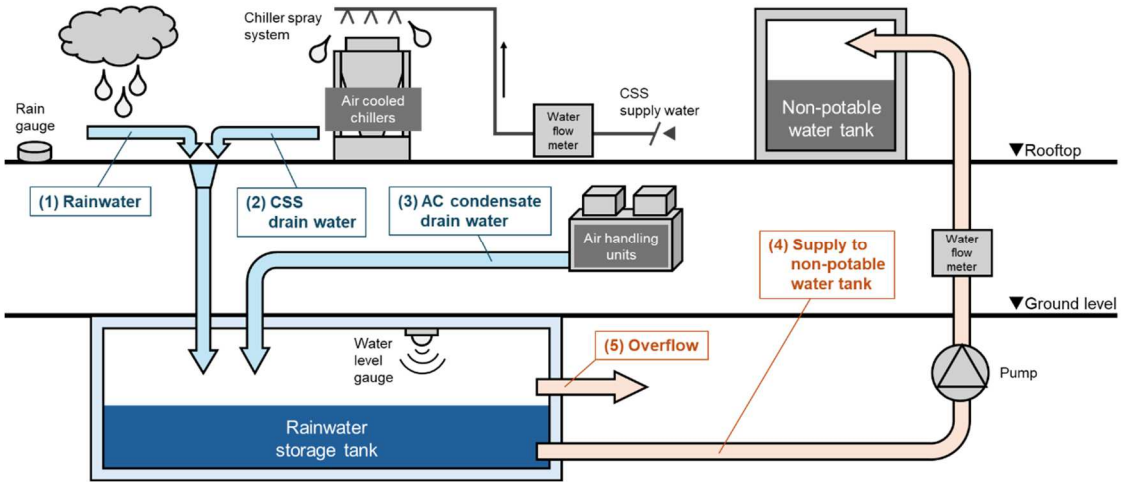

Figure 1 - Water flows concerning rainwater storage tank (RST)

3 Results

Figure 2 shows the water utilization process. The annual volume of water supplied to the CSS was 466m^3, accounting for more than half of the total potable water consumption of 797m^3. The quantity of evaporated water during the CSS process was estimated to be 112m^3 by calculating the difference between the volumes of the CSS supply and drain water. In addition, 231m^3 of water overflowed from the RST without being utilized. This overflow occurred exclusively during a specific period in the summer.

Figure 3 shows the temporal variations in the RST water level and inflow volumes. The results indicate that the CSS continuously supplied drain water to the RST through the period, while large volumes of rainwater inflow occasionally occurred. In contrast, the contribution of the AC condensate drain water was minimal. Due to the constant inflow from the CSS, the RST water level reached its maximum height of 6m, equivalent to its full capacity of 80m^3, between July 31 and September 19, resulting in overflow.

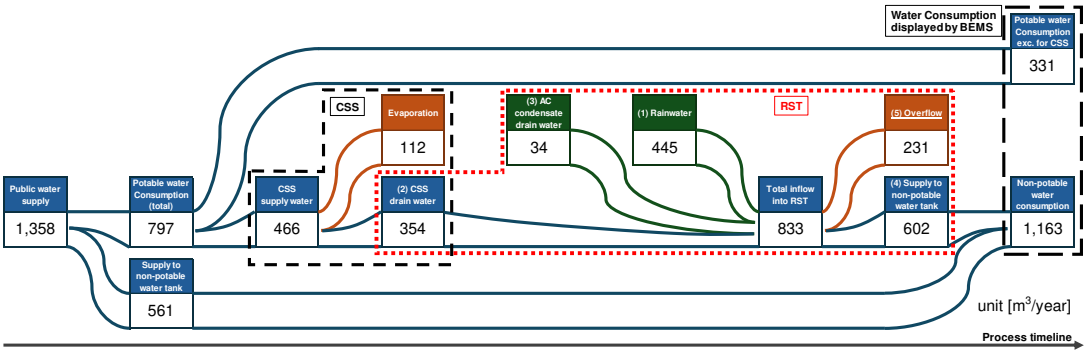

Figure 2 - Water utilization process

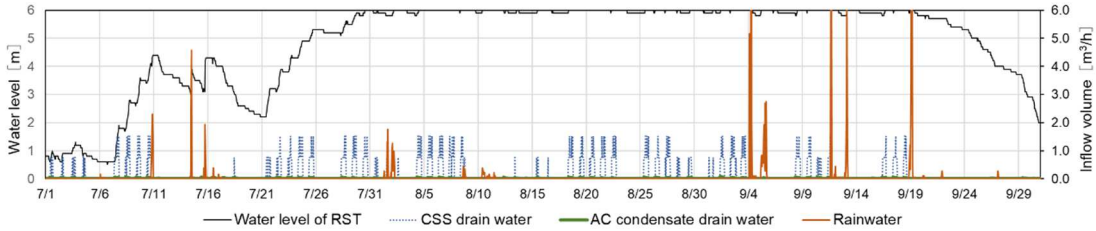

Figure 3 - Water level and inflows of RST

4 Conclusion

This study confirmed that the existing RST capacity inevitably leads to overflow, which hinders effective alternative water utilization. The results show that appropriate determination of RST capacity plays a critical role in achieving ZWB, for which alternative water losses must be minimized. Further study is required to establish effective methods for optimizing the water utilization process, taking into account influencing factors such as the inflow of CSS drain water. Part 2 of this study examines practical methodologies for building more successful water flow systems [5].

5 References

[1] Aoi T. et al, Research and investigation water circulation of laboratory by utilizing water treatment technology (Part3) Environmental assessment at the time of zero water building introduction, Technical papers of annual meeting, the Society of Heating, Air-Conditioning and Sanitary Engineers of Japan, 2023, (pp. 425-428). (in Japanese)

[2] U.S. Green Building Council: LEED Zero Program Guide, 2020.4

[3] IGBC Net Zero Water Rating for Buildings and Built Environment: IGBC Net Zero Water Rating System, 2020.10

[4] Sekine R. et al, Study on ZEB / Wellness in Urban Medium-sized Office Building (Part11) Achievement in the second year, comparison with first year / Water, Electric, ZEB, Technical papers of annual meeting, the Society of Heating, Air-Conditioning and Sanitary Engineers of Japan, 2024, (pp. 97-100). (in Japanese)

[5] S. Yoshioka et al., Study on methods for ZWB in Urban Mid-Sized Office Building - Part 2: Water Quality Survey and Water Balance Case Studies, Proceedings of CIB W062 Symposium, 2026

6 Presentation of Author

Satoshi Matsumoto is a researcher at SUGA Co., Ltd. He researches Zero Water Building, aquaponics, and CO_2 reduction. He is a member of SHASE (The Society of Heating, Air-Conditioning and Sanitary Engineers of Japan).

Development of Water Circulation System Supplying Both Potable and Non-Potable Water for ZWB

Masaaki Hashimoto (1), Takehiko Mitsunaga(2), Yoshiaki Taishi (3), Hiroshi Iizuka (4), Kyosuke Sakaue (5)

(1) masaaki@hat.co.jp, Hashimoto Sogyo Holdings Co. Ltd., Japan

(2) mitsunaga@meiji.ac.jp, Meiji University, Japan

(3) ce263056@meiji.ac.jp, Meiji University, Japan

(4) iizukah@nikken.jp, Nikken Sekkei Construction Management, Inc., Japan

(5) sakaue@carrot.ocn.ne.jp, Meiji University, Japan

Abstract

The authors have previously proposed a movable Aqua Container House (ACH) equipped with an integrated water supply and drainage system with purification functions [1,2]. However, conventional systems typically supply either potable or non-potable water, limiting flexibility in water use. In this study, based on the expertise gained from ACH development, we have developed a low-cost, and self-buildable water circulation system. This system utilizes rainwater as a raw source and is capable of supplying both potable and non-potable water lines. This study is expected to lead to the realization of Zero Water Buildings (ZWB) in these areas.

Keywords

Water supply circulation；Potable water；Non-potable water；ZWB; Self-build

1 Introduction

Japan’s water infrastructure faces vulnerability from frequent large-scale disasters and aging in remote or mountainous areas, driving the demand for decentralized water

circulation systems like the previously proposed ACH [1,2]. However, conventional systems lack operational flexibility, usually supplying either potable or non-potable water exclusively. Providing only potable water leads to over-designed filtration equipment and higher costs for low-quality needs like toilet flushing. Furthermore, dispatching technicians during disasters or to remote regions is challenging. Existing high-performance wastewater recycling systems remain prohibitively expensive and rely heavily on professional maintenance, highlighting the need for user-maintainable solutions.

In this study, based on the expertise gained from ACH development, we have developed a low-cost and self-buildable water circulation system. This system utilizes rainwater as the water source and is capable of supplying both potable and non-potable water lines. In addition, the water quality performance of the system was evaluated through water quality testing, and a smartphone application was developed to simplify system operations and manage water quality.

2 Water circulation system supplying both potable & non-potable water

Figure 1 shows an overview of the newly developed compact water circulation system, designed to be low-cost, self-buildable and capable of dual-line supply for potable and non-potable water. In this system, rainwater is utilized as the water source. The process begins by collecting rainwater in a storage tank (Rainwater tank) after the initial rainwater which typically contains high concentrations of dust, passes through the initial rainwater filtration device. Relatively large impurities are removed through two strainers, followed by chlorine disinfection.

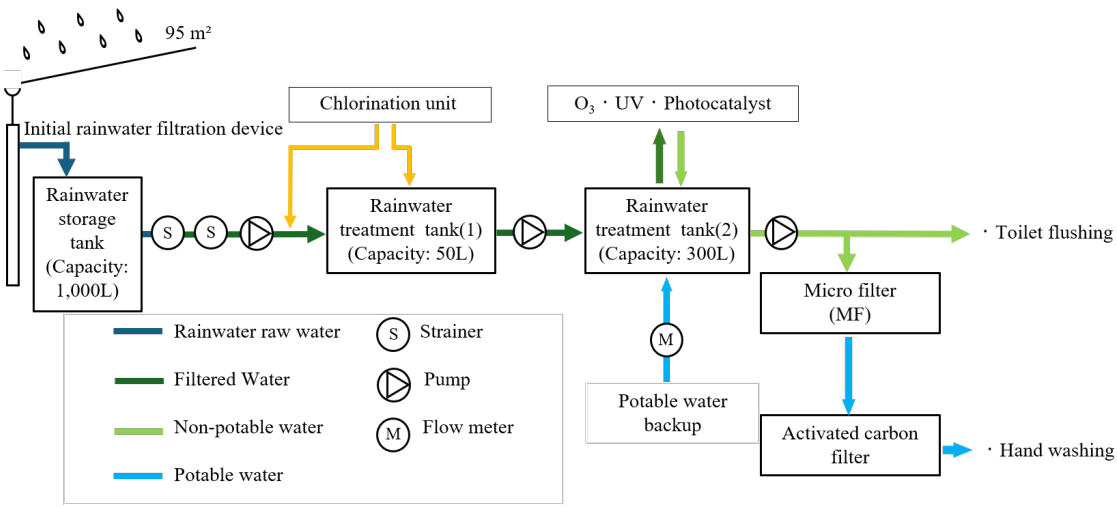

Figure 1 - Water circulation system supplying potable and non-potable water

Furthermore, the system efficiently generates highly reactive oxidants through a combination of ozone (O_3), ultraviolet (UV) light, and photocatalysis. This process rapidly decomposes and detoxifies organic compounds as well as bacteria. The water treated to this level is designated as non-potable water and is supplied for toilet flushing.

For applications involving direct skin contact, such as hand washing, the water undergoes further purification. This includes microfiltration (MF) to remove fine suspended solids that pass through the strainers, followed by an activated carbon filter for deodorization and final polishing to achieve potable water quality.

3 Water quality via the water circulation system

Table 1 presents the water quality analysis results for *E. coli* and *general bacteria* within the system. *E. coli* was not detected even in the initial rainwater storage tank stage. While the *general bacteria* count was 400 CFU/mL in the rainwater storage tank, it was significantly reduced in the rainwater treatment tank (2)—which employs highly reactive oxidants from O_3, UV, and photocatalysis—falling well below the maximum water quality standard of 100 CFU/mL. Although *E. coli* may be introduced in the future through sources such as bird droppings on the roof, the rainwater treatment tank (2) is expected to provide similar purification performance. Furthermore, a chlorine dosing system is implemented to prevent bacterial regrowth in stagnant water within the piping. In addition, the water quality analysis for *pH*, *turbidity,* and *heavy metals* will be conducted in future studies.

Table-1 Water quality within the system

Item	Rainwater tank	Rainwater treatment tank(2)	After Activated Carbon Filter	Water quality standards
E. coli	Not detected	Not detected	Not detected	Not detected
General Bacteria	400 CFU/mL	2 CFU/mL	6 CFU/mL	≤100 CFU/mL

4 Mobile application-based monitoring

A smartphone application is developed to simplify system operations and manage water quality. The remaining volume in the rainwater storage tank (RST) can be monitored through an 11-level display in 10% increments, utilizing the ten float sensors shown in Figure 2. To nudge users toward water conservation, the interface—as illustrated in Figure 3—features not only the water level but also the remaining number of available cycles for specific water-use activities. Additionally, it incorporates color-coded status changes, graphical trends of the water level (WL), and mail notification settings.

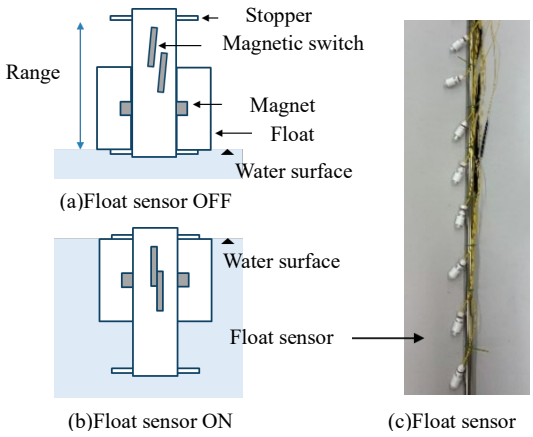

Figure 2 - Simple water level sensor

(a)WL10~30% (b)WL31~50% (c)WL51~100%

Figure 3 - Application interface

5 Conclusions

In this study, we have successfully developed a new, low-cost, and self-buildable water circulation system capable of dual-line supply for both potable and non-potable water using rainwater as the source. The analysis confirmed that the system achieves high-quality water results. In the future, we plan to implement this system in actual buildings and conduct a performance verification through real-world operation, including the utilization of the developed smartphone application. This development is expected to promote rainwater utilization in small-scale buildings, contributing significantly to the realization of ZWB.

6 Reference

[1] Masaki Hashimoto, Hiroshi Iizuka, Kyosuke Sakaue: Concept and Configuration of Aqua Container House for Disaster Response, Proceedings of CIB W062, (2022)
[2] Masaaki Hashimoto, Hiroshi Iizuka, Kyosuke Sakaue, Takehiko Mitsunaga: Aqua Container House for natural disasters Part 2 Suitability evaluation by water use experiment, Proceedings of CIB W062, (2023)

7 Presentation of Author

Masaaki Hashimoto serves as the chairman of Hashimoto Sogyo Co. Ltd., which is a general trading company with a building service. and is a doctoral student at Meiji University. His fields of specialization include the management and the development of plumbing systems.

Study on Design Methods for ZWB in Urban Mid-Sized Office Building - Part 2: Water Quality Survey and Water Balance Case Studies

Sei Yoshioka (1), Satoshi Matsumoto (2), Tomoo Inada (3), Kiichi Takeda (4), Shota Satake (5), and Takehiro Mitsunaga (6)

(1) se-yoshioka@suga-kogyo.co.jp
(2) sa-matsumoto@suga-kogyo.co.jp
(3) to-inada@suga-kogyo.co.jp
(4) ki-takeda@suga-kogyo.co.jp
(5) syo-satake@suga-kogyo.co.jp
(6) mitsunaga@meiji.ac.jp
(1)(2)(3)(4)(5) SUGA Co., Ltd., Japan
(6) Assoc. Prof, Dep. of Architecture, School of Science & Technology, Meiji University, Japan

Abstract

Our previous report [1] showed that the rainwater storage tank (RST) in a mid-sized office building overflowed, which limited the effective use of rainwater. This study proposes planning methods for achieving Zero Water Building (ZWB) in urban office buildings through a water-quality survey and case studies of rainwater reuse systems. Survey results indicate that rainwater and chiller spray drain water can be reused in the chiller spray system (CSS) after simple treatment. The case studies showed that using rainwater as the CSS supply effectively reduces the required RST capacity and prevents overflow, compared with systems where rainwater is not used for the CSS. Using rainwater in the CSS is an effective approach for ZWB in mid-sized urban office buildings with limited installation space.

Keywords

Zero Water Building; Rainwater Storage Tank; Chiller Spray System

1 Introduction

The concept of ZWB has emerged in Japan as a means of ensuring the sustainable use of water resources. However, methods for achieving ZWB have not yet been established. Our previous report [1] showed that the RST at a mid-sized office building overflowed, thereby limiting the effective use of rainwater. Since CSS drain water is a major cause of RST overflow, the objective of this study is to propose a planning method for achieving ZWB by using alternative water such as rainwater and CSS drain water for the CSS. A water quality survey was conducted to evaluate whether rainwater and CSS drain water

could be reused as the CSS supply. In addition, case studies were conducted on increasing the RST capacity, the use of rainwater for chiller spraying, and the recirculation of chiller spray water.

2 Methodology

In the target office building [1], a substantial portion of rainwater could not be fully reused during the summer months and was discharged as overflow. To address this, first, a single water quality survey was conducted to evaluate the potential for efficient use of water resources. Specifically, the survey focused on evaluating the feasibility of using reused water, such as rainwater, to supplement the water used in the CSS during the summer.

Subsequently, water balance case studies were conducted as outlined in Table 1. In Case 1, the RST capacity was increased to prevent overflow. In Case 2, rainwater was used in the CSS, and the RST capacity was increased to the level at which overflow would have occurred if rainwater had not been used in the CSS. In Case 3, a small tank was installed for the CSS to collect and recycle CSS drain water. In this case, only the water lost through evaporation during chiller spraying was supplied with potable water.

Table 1 – Overview of the water balance case studies

No.	System overview	Usable water storage capacity
Existing system	Refer to Reference [1].	80 m³ (RST: 80 m³)
Case 1	Increased RST	310 m³ (RST: 80 m³ + added RST: 230 m³)
Case 2	Increased RST + Use of rainwater in the CSS	180 m³ (RST: 60 m³ + added RST: 120 m³)
Case 3	Recirculation of chiller spray water	81 m³ (RST: 80 m³ + added tank for the CSS: 1 m³)

3 Results

3.1 Water Quality Survey Results

The results of the water quality survey are shown in Table 2. Raw rainwater did not meet the potable water quality standard [2] for general bacteria and odor. The high general bacteria count (64,000 CFU/mL) was likely due to the introduction of airborne microorganisms during rainfall. The non-potable water also did not meet the odor standard, and earthy or musty odors were detected. Similarly, the chiller spray drain water did not meet the standard for general bacteria (6,000 CFU/mL) and odor. The exceedance of the general bacteria standard is considered to be due to the introduction of microorganisms during the spraying and drainage process. A chemical odor was detected, likely due to residual chlorine in the CSS supply water. For all other parameters, these types of water satisfied the potable water quality standards.

3.2 Case Study Results

Figure 1 shows the results of the case studies, including increased RST capacity and the use of reused water, such as rainwater and chiller spray drain water, in the CSS.

Table 2 – Water quality survey results

Measurement items	Unit	Raw rainwater	Non-potable water	Chiller spray drain water	Standard value
General bacteria	CFU/mL	*64,000	0	*6,000	≤ 100
E. coli	–	Not detected	Not detected	Not detected	No detection
Lead and its compounds	mg/L	0.003	< 0.001	< 0.001	≤ 0.01
Nitrite nitrogen	mg/L	0.014	< 0.004	< 0.004	≤ 0.04
Nitrate nitrogen and nitrite nitrogen	mg/L	0.32	1.47	1.27	≤ 10
Zinc and its compounds	mg/L	0.37	< 0.005	< 0.005	≤ 1.0
Iron and its compounds	mg/L	< 0.03	< 0.03	< 0.03	≤ 0.3
Copper and its compounds	mg/L	< 0.01	< 0.01	< 0.01	≤ 1.0
Chloride ion	mg/L	0.4	35.0	25.3	≤ 200
Evaporation residue	mg/L	12	214	200	≤ 500
Organic matter (total organic carbon)	mg/L	0.7	0.9	1.0	≤ 3
pH	–	6.3	8.0	8.1	5.8–8.6
Odor	–	*Earthy or musty	*Earthy or musty	*Chemical	Not abnormal
Chroma	degree	< 0.5	< 0.5	< 0.5	≤ 5
Turbidity	degree	0.7	< 0.1	0.2	≤ 2

Items that do not meet the standard are marked with an asterisk (*).

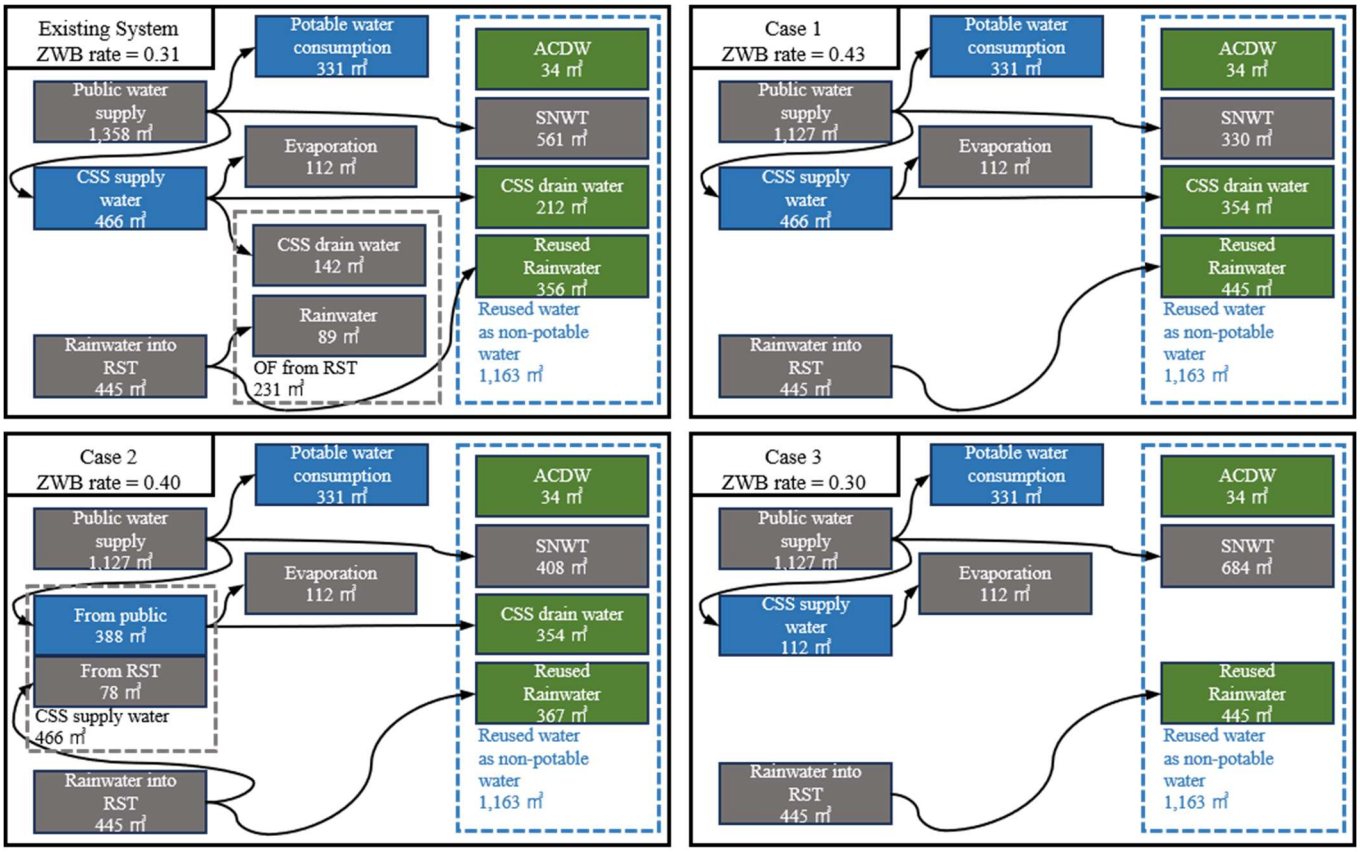

Abbreviations: ACDW = AC condensate drain water; SNWT = Supply to non-potable water tank.
ZWB rate = alternative water use / total water use [3].
Annual alternative water use items are shown in green, and annual total water use items are shown in blue.
The values of Rainwater into RST, Potable water consumption, Reused water as non-potable water, Evaporation and ACDW are fixed based on the measured data

Figure 1 – Annual water balance in each case

Case 1: By eliminating overflow, total water use was reduced by the volume that would otherwise have overflowed. The ZWB rate was 0.43, which was 0.12 higher than in the existing system.

Case 2: Using rainwater in the CSS prevented overflow even with a smaller RST capacity than in Case 1. Alternative water use was higher than that of the existing system and lower

than that of Case 1. The ZWB rate was 0.40, which was 0.09 higher than in the existing system.

Case 3: Recycling chiller spray water reduced the amount of potable water supplied to the CSS. However, because CSS drain water did not flow into the RST but into the added tank for the CSS, RST overflow did not occur, resulting in increased potable water use to replenish the non-potable water supply. The ZWB rate was 0.30, which was 0.01 lower than in the existing system.

4 Conclusion

The water quality survey showed that rainwater and CSS drain water can be used after simple water treatment, such as chlorination for disinfection to prevent the growth of Legionella bacteria. The case studies indicated that increasing the RST capacity can prevent overflow and increase the use of alternative water. Furthermore, as an alternative to adding more RST capacity, it was shown that using rainwater in the CSS and recirculating chiller supply water can reduce the RST capacity required to prevent overflow compared with simply increasing the RST capacity. In particular, as shown in Case 2, the use of rainwater in the CSS can improve the ZWB rate while reducing the RST capacity required to prevent overflow. These results confirm that using rainwater in the CSS of mid-sized urban office buildings with limited installation space is an effective planning method for achieving ZWB.

5 References

[1] S. Matsumoto et al., Study on methods for ZWB in Urban Mid-Sized Office Building -Part 1: Measurement of Water Balance for Achieving ZWB, Proceedings of CIB W062 Symposium, 2026
[2] Ministry of the Environment, Government of Japan, Water Quality Standard Items and Standard Values (52 items), accessed May 1, 2026
[3] U.S. Department of Energy, Low or Zero Water Building Strategies, https://www.energy.gov/cmei/femp/low-or-zero-water-building-strategies
[4] Aoi T. et al., Research and investigation water circulation of laboratory by utilizing water treatment technology (Part 3) Environmental assessment at the time of zero water building introduction, Technical papers of annual meeting, the Society of Heating, Air-Conditioning and Sanitary Engineers of Japan, 2023, (pp. 425-428). (in Japanese)
[5] U.S. Green Building Council: LEED Zero Program Guide, 2020.4
[6] IGBC Net Zero Water Rating for Buildings and Built Environment: IGBC Net Zero Water Rating System, 2020.10

6 Presentation of Author

Sei Yoshioka is an engineer in the Design Department at SUGA Co., Ltd., a contractor specializing in HVAC, plumbing, and sanitary systems. He is a member of SHASE (the Society of Heating, Air-Conditioning and Sanitary Engineering of Japan).

Analyzing Urban Water Demand under Different Rainwater Tank Volumes

Gabriela Cristina Ribeiro Pacheco (1), Conceição de Maria Albuquerque Alves (2)

(1) gabrielacrpacheco@gmail.com

(2) cmaalves@gmail.com

(1) Federal Institute of Goiás (IFG), Brazil

(2) University of Brasília (UnB), Brazil

Abstract

Considering the growing adoption of rainwater harvesting systems as a water conservation measure, this study aims to compare urban water savings resulting from different rainwater storage volumes to identify the most suitable storages for distinct residential users. To estimate urban water consumption, it was assumed that all residential users are equipped with rainwater harvesting systems. A daily water balance was performed and four different tank volumes were analyzed using multiple rainfall scenarios. Results indicate that users in lower consumption brackets account for the majority of urban residential demand and present substantially higher rainwater consumption. However, limitations in catchment area and water use restrict the benefits of increasing storage volume. Nevertheless, for an individual high-demand user, rainwater use results in greater potable water savings, and larger storage volumes can increase user independence from the public water supply system, which may be advantageous in areas facing water supply constraints. Additionally, rainfall patterns impose a limit on potable water substitution, with non-potable demand being met at levels below 50% across almost all scenarios. Therefore, in locations with similar consumption and rainfall patterns, rainwater harvesting systems should target low-demand users, with storage volumes defined according to building characteristics.

Keywords

Rainwater harvesting; urban water consumption; rainwater tank sizing.

2 Introduction

Water conservation has become increasingly necessary due to current water scarcity conditions, which are intensified by growing water demand and insufficient infrastructure for water supply in many locations. In many cases, measures aimed at reducing water consumption are primarily designed for large cities and users with high water demand. However, in Brazil, small cities generally present lower levels of access to sanitation services. Therefore, the implementation of water conservation techniques should also be evaluated in these locations as a strategy to support the universalization of water supply services.

Several techniques can be adopted for this purpose, including rainwater harvesting. In Brazil, this technique became widespread in the semi-arid region of the country as a water supply alternative for both potable and non-potable uses. In urban areas, however, rainwater use is restricted to non-potable demands, and the available volume depends on rainfall patterns and roof catchment areas, while the required storage volume is related to the building's non-potable water demand. Due to the dependence on multiple variables, several sizing methods have been proposed (Ilha and Campos, 2014; Ghisi and Cordova, 2014; Sampaio, 2017), many of which adopt economic criteria to determine the most efficient storage volume.

Nevertheless, considering the increasing search for water conservation measures and incentives for techniques aimed at reducing potable water demand, it is also necessary to evaluate the effects of rainwater tank volumes at the urban scale. Public policies promoting the implementation of Rainwater Harvesting Systems (RWHS) should consider not only the benefits for individual users, but also the impacts on urban water consumption and the influence of local characteristics. Previous studies have indicated that the urban water-saving potential associated with RWHS implementation may vary significantly depending on local conditions from 20% to 70% (Custódio and Ghisi, 2019; Hofman-Caris et al., 2019; Ennenbach et al., 2017; Lúcio et al., 2020; Villar-Navascués et al., 2020).

Therefore, the objective of this study was to evaluate the influence of different rainwater storage volumes for distinct residential users on urban water consumption in a small Brazilian city.

3 Method

This study evaluated rainwater harvesting potential for domestic water consumption in a city located in the central region of Brazil, based on the urban water demand simulation framework proposed by Pacheco and Alves (2025). A daily water balance was performed to estimate the volume of rainwater available, the volume effectively consumed, and its influence on urban water demand. The simulations adopted the Yield After Spillage (YAS) operating rule, assuming an initially empty storage tank. Overflow was discharged to the stormwater drainage system.

To account for variability among users, residential units (originally classified into eight consumption ranges by the local water utility) were grouped into two categories: low-demand (LD) and high-demand (HD) users. For each group, rainwater consumption was estimated considering the implementation of rainwater harvesting systems with four different storage volumes, based on Pacheco and Alves (2023), as shown in Figure 1.

The analysis was conducted for 500 scenarios generated from the combination of rainfall data and annual growth in the number of residential connections, used as an indicator of population growth in the city. Rainfall series were generated through bootstrap resampling of a 30-year historical daily rainfall series, while growth rates were defined using Latin Hypercube Sampling (LHS) based on historical minimum and maximum values.

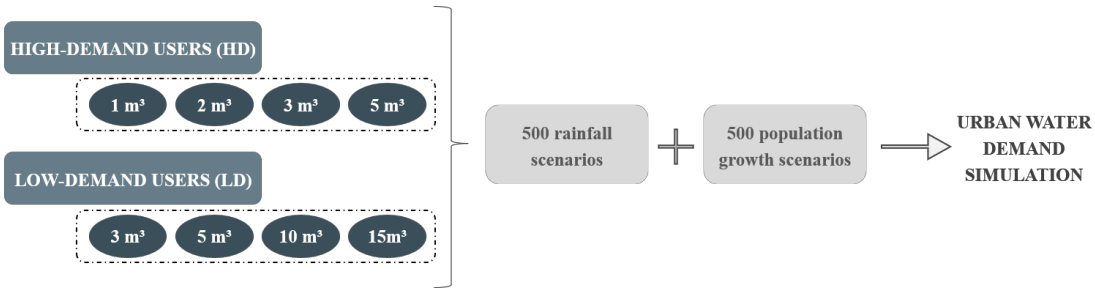

Figure 1 - Method.

Daily rainwater consumption was calculated for each storage volume using representative buildings for each consumption range, defined based on average consumption data provided by the local water utility. This approach allowed the identification of suitable storage volumes for each user group and the evaluation of their effects on urban water demand. Water quality and treatment requirements were not considered.

4 Results

The analysis was conducted for the city of Porangatu, located in northern Goiás State, Brazil. The city had 44,317 inhabitants in 2022 (IBGE, 2022). According to the local water utility, the city had 15,702 residential water connections (users). These connections are subdivided into eight consumption ranges by the utility, and most connections are concentrated in the lowest consumption ranges, as shown in Table 1. For each consumption range, a representative building was defined based on roof catchment areas estimated from an analysis of building sizes within the city. As Brazilian regulations restrict rainwater use to non-potable purposes, rainwater demand was assumed as 53% of the total water consumption presented in Table 1 (Sant'Ana, 2011), representing the non-potable fraction of water consumption.

Table 1 - Characteristics of residential water consumption users in Porangatu

Consumption ranges intervals (m^3)	**1**	**2**	**3**	**4**	**5**	**6**	**7**	**8**
	0-10	10-15	15-20	20-25	25-30	30-40	40-50	>50
Users (water connections)	8,132	3,022	1,765	958	449	303	80	41
Area (m^2)	60	60	100	150	200	300	350	350
Consumption (m^3/month)	4.871	12.848	17.739	22.719	27.733	34.426	44.375	69.390

(Saneago, 2023)

The annual growth rate of residential connections was defined based on the minimum and maximum values of 0.96 and 1.10 established by Pacheco (2025). Regarding rainfall variability, the 500 rainfall series considered did not present significant variation, with all scenarios resulting in average annual precipitation between 1,220 mm and 1,620 mm, while the historical average annual precipitation was 1,433 mm. For each rainwater harvesting system configuration (user groups and tank volumes), a daily water balance was performed considering the volume of rainfall over the roof catchment area and an initial runoff discard coefficient of 2 mm.

The results obtained for rainwater consumption under the different RWHS configurations are presented in Figure 2. Each line in the graphs represents one scenario, and all configurations were evaluated using the same 500 scenarios. The first column shows rainwater consumption by consumption range, while the second column presents monthly rainwater consumption. Results indicate that rainwater consumption is substantially higher for low-demand users. This outcome is explained by the concentration of residential connections within the lowest consumption ranges, which represent the majority of consumers in the city. Consequently, both urban water consumption and rainwater consumption are higher in the first four consumption ranges. In contrast, rainwater consumption among high-demand users remains relatively low, even with increasing tank volumes.

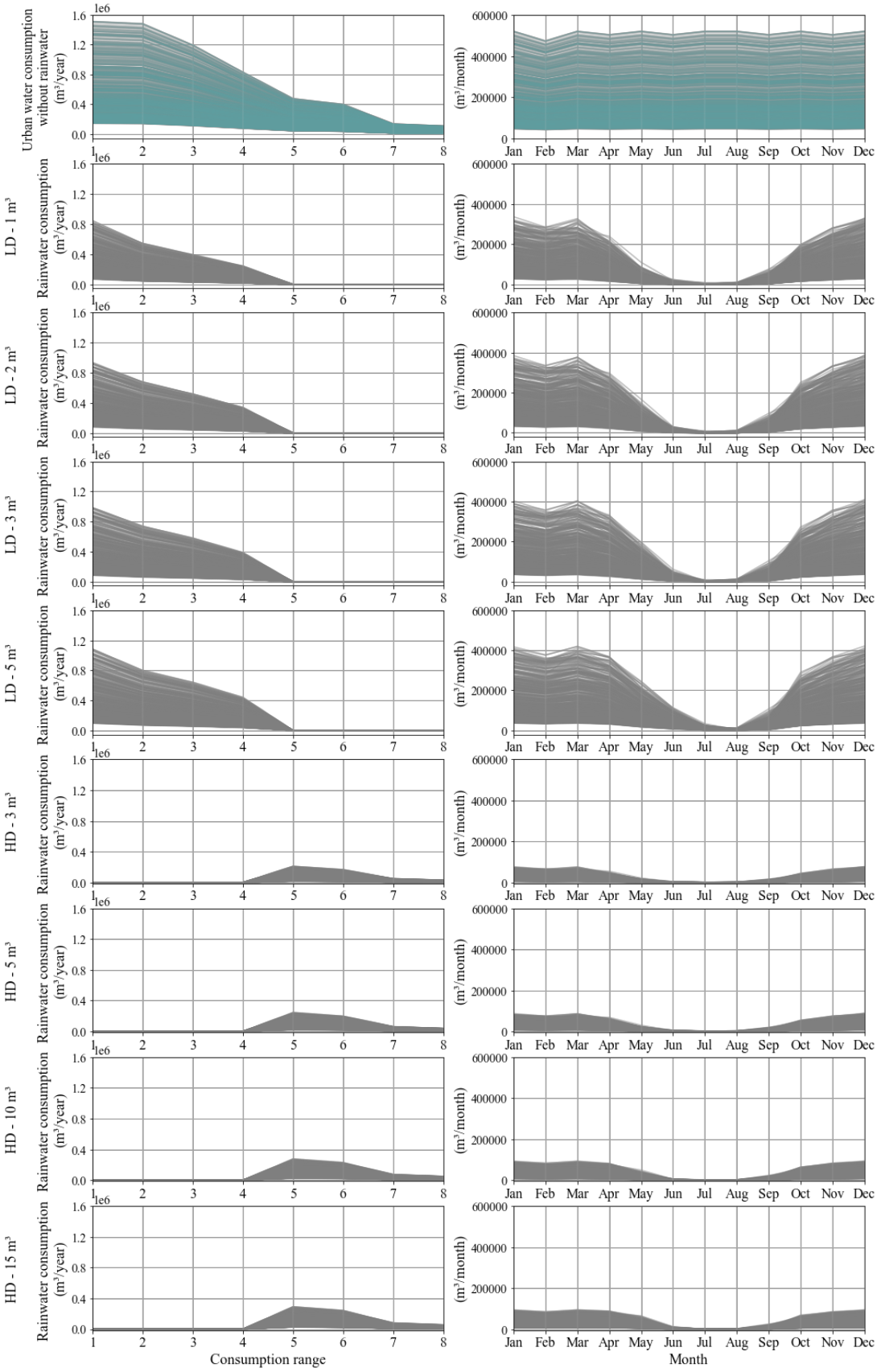

Figure 2 - Urban rainwater consumption.

Results also indicate that, due to the dry season, rainwater consumption is minimal from May to September. The use of larger storage tanks increases rainwater consumption in May, since water stored during the rainy season can still be used during this month.

The results presented in Figure 3 indicate the effects of rainwater consumption on urban water demand in the same 500 scenarios. The first row of Figure 3 illustrates urban water consumption in Porangatu considering the local water utility as the only water supply source. Due to the concentration of users within the lower consumption ranges, the effects of rainwater harvesting are greater when systems are implemented for low-demand users, even with reduced storage volumes. In contrast, the implementation of RWHS for high-demand users results in only minor changes in the urban water consumption pattern.

The percentage of urban potable water savings resulting from the substitution of non-potable demand by rainwater was also evaluated, as shown in Figure 4. Results indicate that implementing RWHS for low-demand users reduces non-potable water consumption by 25% to 53%, whereas implementation for high-demand users results in water savings below 15%.

Therefore, although individual systems may provide greater water savings for a single high-demand user, the aggregated result is more significant for low-demand users in cities with similar consumption patterns, where low-demand users account for more than 60% of urban water consumption. Consequently, incentives and public policies promoting RWHS should not focus exclusively on high-demand users, despite the greater economic feasibility of these systems for such consumers.

At the urban scale, significant reductions in potable water demand from the local water utility would only be achieved through the implementation of RWHS for low-demand users, even with small storage volumes. Since these systems tend to be less economically feasible for these users, public policies should seek mechanisms to support and enable such investments.

Finally, the potable water savings from the water utility are significant. Especially considering the implementation of RWHS for all users, the combination of LD - 5 m^3 and HD - 15 m^3 configurations, for example would result in savings higher than 50%. Nevertheless, even with rainwater harvesting, complete water supply from the public utility would still be required during the dry season in cities with similar rainfall patterns.

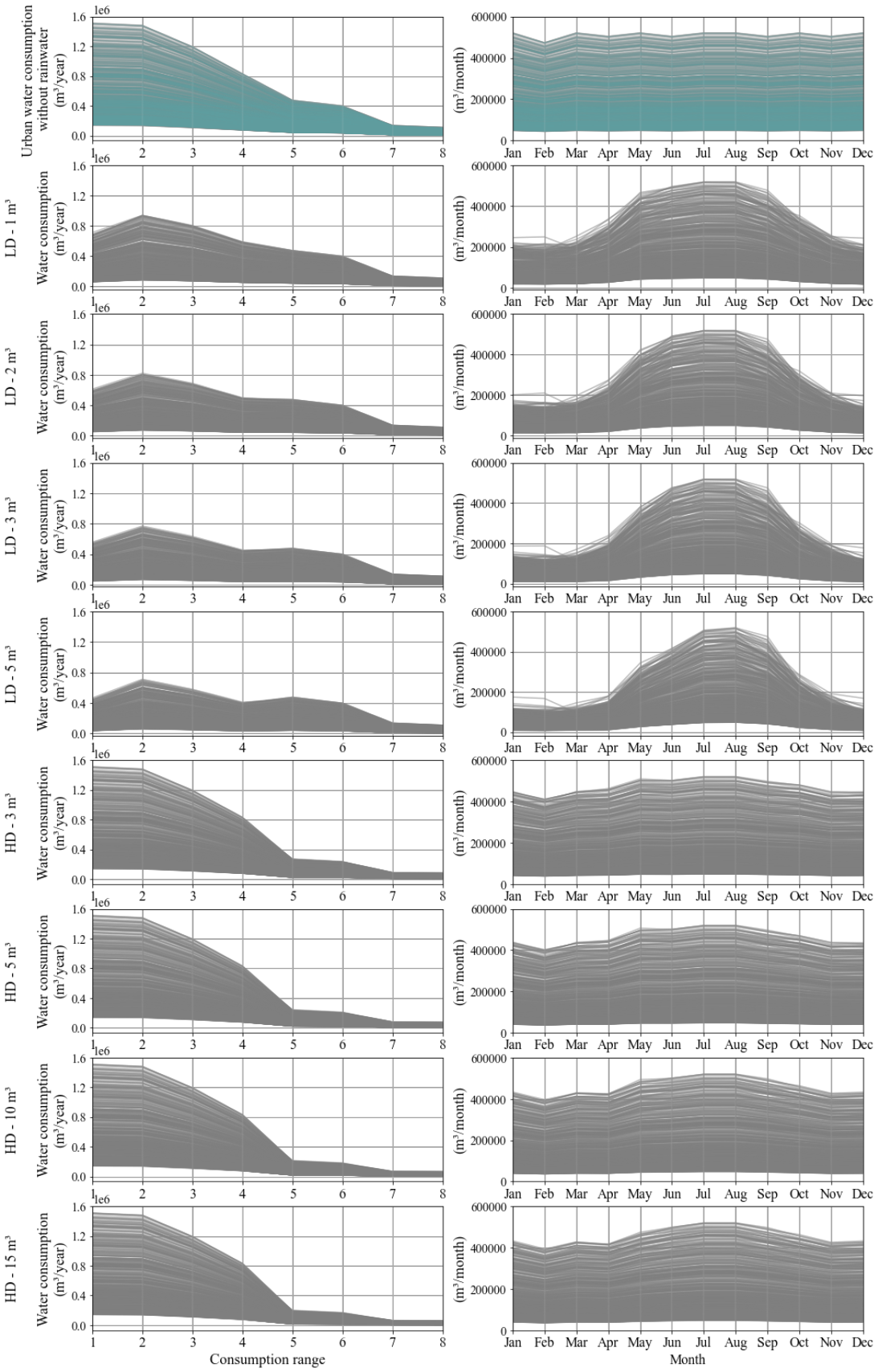

Figure 3 - Urban potable water consumption with rainwater harvesting.

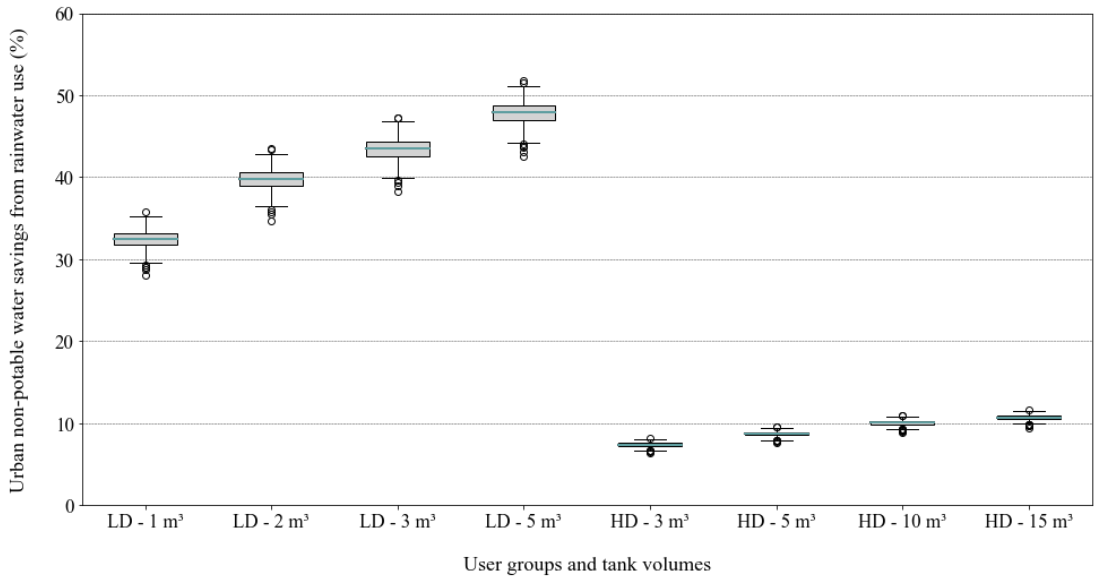

LD: Low-Demand-Users HD: High-Demand Users

Figure 4 - Urban non-potable water savings from rainwater use.

5 Conclusions

The analysis demonstrated that increasing storage volume does not necessarily result in proportional increases in potable water savings, highlighting the importance of economic assessments to determine optimal tank sizes.

For the evaluated city, whose consumption pattern is characteristic of small cities, most users are concentrated in the lower consumption ranges, which account for more than 60% of urban water consumption. Due to this pattern, rainwater use and other water conservation measures should target low-demand users in order to achieve significant results at the urban scale, even though individual benefits are greater for high-demand users.

Therefore, incentive policies for low-demand users should include economic assessments to ensure the feasibility of implementing such techniques, including the provision of financial incentives. Further studies are also required to evaluate the efficiency of these systems and the resulting water savings under different local conditions.

Acknowledgments

The authors acknowledge the support provided by IFG and the UnB for the development of this research.

4 References

Custódio DA, Ghisi E - Assessing the Potential for Potable Water Savings in the Residential Sector of a City: A Case Study of Joinville City. Water, v. 11, 1-18, 2019. https://doi.org/10.3390/w11102074

Ennenbach MW, Larrauri PC, Lall U - County-Scale Rainwater Harvesting Feasibility in the United States: Climate, Collection Area, Density, and Reuse Considerations. Journal of the American Water Resources Association (JAWRA), 54(1), 255-274, 2017. https://doi.org/10.1111/1752-1688.12607

Ghisi E, Cordova MM - Netuno 4 - Manual de usuário, Universidade Federal de Santa Catarina - UFSC, Florianópolis, Brasil, 2014.

Hofman-Caris R, Bertelkamp C, Waal L, Brand TVD, Hofman J, Aa RVD, Hoek JPV. Rainwater Harvesting for Drinking Water Production: A Sustainable and Cost-Effective Solution in The Netherlands?Water, 11, 511, 2019. https://doi.org/10.3390/w11030511

IBGE (2022). Censo Demográfico.

Ilha MSO, Campos MAS - Quality of investments in rainwater harvesting systems: Particles Swarm Optimization for maximization of net present value. Engenharia Sanitária e Ambiental, 19(4), 389–398, 2014. https://doi.org/10.1590/S1413-41522014019000001026

Lúcio C, Silva CM, Souza V - A scale-adaptive method for urban rainwater harvesting simulation. Environmental Science and Pollution Research, 27, 4557-4570, 2020. https://doi.org/10.1007/s11356-019-04889-6

Pacheco GCR - Aproveitamento de Águas Pluviais Urbanas Considerando Incertezas Profundas. Tese de Doutorado em Tecnologia Ambiental e Recursos Hídricos, , Departamento de Engenharia Civil e Ambiental, University of Brasília, Brasília, DF, 147 p, 2025.

Pacheco GCR, Alves CMA - A Framework to Evaluate the Performance of Urban Rainwater Harvesting Systems Considering Water and Sanitation Utility Perspectives under Deep Uncertainties. Water Resour Manage 39, 6823–6840 (2025). https://doi.org/10.1007/s11269-025-04278-4

Pacheco GCR, Alves CMA - The Influence of Deep Uncertainties in the Design and Performance of Residential Rainwater Harvesting Systems Water Resour Manage 37, 1499-1517 (2023). https://doi.org/10.1007/s11269-023-03436-w

Sampaio FEDOV, Alves CMA - A procedure to analyze the viability of rainwater harvesting systems in urban areas based on pre-defined diagrams. In: Revista Brasileira de Recursos Hídricos, 22, 2017. https://doi.org/10.1590/2318-0331.0217160012

Saneago. Informações de economias e volumes consumidos por faixa de consumo para os municípios de Goiás, 2023.

Sant'ana D.R. (2011). *A socio-technical study of water consumption and water conservation in Brazilian dwellings*. Thesis, Oxford Brookes University.

Villar-Navascués R, Pérez-Morales A, Gil-Guirado S. Assessment of Rainwater Harvesting Potential from Roof Catchments through Clustering Analysis. Water, 12(9), 2623, 2623, 2020. https://doi.org/10.3390/W12092623

5 Presentation of Authors

Gabriela Pacheco is Civil Engineering and PhD in Environmental Technology and Water Resources. She is a professor and researcher in the field of urban water supply.

Conceição Alves is Civil Engineering and PhD in Environmental Systems and Water Resources. She is professor and researcher in adaptive planning and management of urban water systems, water resources and the environment.

Benefits and risks associated with the design and implementation of vegetated roofs

M. Zeleňáková (1), M. Godžáková (2), M. Ovčiarka (3)

(1) martina.zelenakova@tuke.sk

(2) martina.godzakova@student.tuke.sk

(3) matej.ovciarka@student.tuke.sk

(1) Faculty of Civil Engineering, Technical University of Košice, Slovakia

(2) Faculty of Civil Engineering, Technical University of Košice, Slovakia

(2) Faculty of Civil Engineering, Technical University of Košice, Slovakia

Abstract

Vegetated roofs are increasingly considered an important part of sustainable development in urban environments. This approach explores their significance, functioning and potential for use in modern construction. It focuses on technical solutions, functional properties and benefits that vegetated roofs can bring to the environment and quality of life in cities. It also takes into account a number of factors that may influence the wider deployment of these systems. The results indicate the relevance of this topic and show the direction of further development in the field of sustainable architecture.

Keywords

Green roofs, Advantages of green roofs, Disadvantages of green roofs, Vegetation systems, Living roofs

1 Introduction

The rapid growth of urban populations driven by industrialization has significantly worsened the level of pollution in cities and caused serious environmental phenomena that pose significant threats to human health and the environment [1]. Green roofs, as vegetation systems or otherwise called living roofs, are ideal especially for dense urban areas and can provide various ecosystem services that support biodiversity, improve health and increase the well-being of residents [2].

The possibilities of building vegetation due to lack of space are often severely limited, and therefore green roofs represent an important solution to support the development of greenery. Although their contribution in the provision of ecosystem services may be relatively smaller compared to large green areas or large trees on the streets, they still provide key ecosystem services. These services can contribute to increasing the quality of life of urban residents, in particular by mitigating the urban heat island effect, improving air quality and efficiently managing stormwater [3]. Sustainable development regulations place great emphasis on implementing adaptive measures in residential areas to mitigate the effects of climate change. These measures include, in particular, nature-inspired solutions, also known as bio-inspired approaches. These approaches seek to mimic natural processes and systems, which allows for the creation of efficient and sustainable environments. By applying these principles, we can achieve long-term resilience to climate change and ensure the sustainable development of urban areas [4].

The aim of the work is to comprehensively evaluate the benefits and risks associated with the design and implementation of green roofs. The work focuses on the analysis of their structural solution, typological division, functional layers and environmental, economic and social benefits. At the same time, it points out potential problems that may arise during their application in practice. An important part is the design of specific compositions of green roofs and the implementation of these systems on various types of buildings. At the same time, the aim is to identify the perception of vegetated roofs by the public and experts and thus evaluate their overall potential to contribute to sustainable construction.

2 Advantages and disadvantages of green roofs

2.1 Advantages of green roofs

Green roofs, which are mainly built on the roofs of buildings in urban areas, bring a wide range of environmental, economic, energy and social benefits. They contribute to the sustainability of cities and improve the quality of life of residents. Their key benefits include the removal of atmospheric pollutants such as carbon dioxide and the production of oxygen, thereby improving air quality. Green roofs also help to mitigate the urban heat island effect, thereby contributing to reducing temperatures in cities. In addition, they reduce the energy consumption of buildings thanks to their insulating function, improve rainwater management and thus contribute to reducing flooding or sewer congestion. In addition to environmental benefits, green roofs also have a positive impact on the social and economic sphere. They support the development of urban agriculture and increase the amount of greenery in urban areas, thereby improving the quality of life and access to nature for residents. The benefits of green roofs are therefore evident not only for the buildings themselves, but also for the wider community. In many countries, green roof projects are financially supported due to their multiple positive effects. In times of climate change and the pursuit of sustainable development, green roofs play an important role in cities. Therefore, local governments and authorities should actively promote their construction on public and private buildings, which would lead to wider environmental, social and economic benefits for the urban population [5].

The main advantages of green roofs are:

- Environmental benefits
- Improved air quality
- Heat island
- Rainwater retention
- Biodiversity
- Improved water quality
- Protective and economic function
- Health
- Urban aesthetics

2.2 Disadvantages of green roofs

The installation of green roofs presents several challenges that can complicate their practical use. One of the main problems is that there is often a lack of detailed design and clear guidelines on how to properly implement these roofs. This can lead to incorrect arrangement of individual layers or selection of unsuitable plants, which can compromise their durability and functionality. If such errors occur, they can lead to unexpected repair and maintenance costs over time. [6].

The main disadvantages of green roofs are:

- Source of pollutants
- Increased costs of green roof construction
- Potential damage to roof structure
- Roof statics

As part of an analysis of the perception of the benefits and potential of green roofs, a questionnaire survey was conducted at TUKE and the next chapter presents the results.

3 Survey of perceptions of green roofs and their advantages and disadvantages

This survey aims to determine the attitudes and experiences of the professional and lay public on the issue of green roofs. The aim is to identify factors that influence their implementation in practice and at the same time contribute to the design of solutions that could support the wider application of these innovative systems in Slovakia. The main objective of the survey was to obtain the opinions and experiences of both experts and the general public on the advantages and disadvantages associated with the design and implementation of green roofs in the Slovak context. The survey was intended for various groups of the population, especially those living in apartment buildings, regardless of age or place of residence. Respondents had the opportunity to express their opinions via an online form that was published on social networks and other relevant platforms, thus ensuring a high level of participation and wider accessibility for the public. The form was open for three weeks. The overall survey consisted of 34 questions, which were carefully

arranged to allow for a gradual examination of basic information about the respondents, their knowledge of green roofs, and then addressed the issues of perception of the advantages and disadvantages of these solutions. In addition, the survey also included questions regarding the participants' attitudes towards various aspects of the implementation of green roofs in Slovak cities and municipalities. The survey aimed to determine the personal opinions of the participants, but also their view of the environmental, economic and aesthetic benefits of these technologies. Respondents expressed their views on the factors that, in their opinion, most influence the implementation of green roofs. The survey results provided valuable information on the role of green infrastructure in the urban environment and what obstacles prevent its wider expansion and implementation in practice. The questionnaire was divided into four main parts, each of which focused on a different aspect of the research issue. The first part of the questionnaire consisted of five introductory questions aimed at obtaining basic demographic data about the respondents. The aim of this part was to obtain an overview of the respondents' gender, age, region of residence, highest level of education and position in relation to the topic of green roofs. This information made it possible to identify the basic characteristics of the survey participants that could influence their opinions and experiences with green roofs. The second part of the questionnaire was aimed at determining the level of knowledge of the respondents about green roofs and their attitudes towards their use in practice. The aim was to examine to what extent the respondents are familiar with different types of green roofs and what their interest is in implementing them in their surroundings or on their own properties. The third part of the questionnaire focused on the perception of the advantages of green roofs and the assessment of their benefits from the respondents' perspective. The aim of this part was to determine to what extent the public perceives the ecological, economic and social benefits associated with the implementation of green roofs. Other questions focused on the perception of functional and economic benefits, such as the ability of green roofs to reduce noise in the urban environment, increase property value, or extend the life of the roof structure. This part of the survey provided important insights into which benefits of green roofs are considered most significant by the public and to what extent these ecological solutions are perceived as beneficial for the urban environment and individuals. The third part of the questionnaire focused on the main obstacles preventing the expansion of green roofs. Respondents assessed factors such as lack of information, low interest from building owners, absence of legislative support, and high additional costs. Technical barriers were also examined, such as the need to increase the load-bearing capacity of the structure, possible construction complications, and the lack of qualified companies. The results of this part of the survey provide an overview of the key factors that need to be addressed to support the wider implementation of green roofs in practice. The last part of the questionnaire focused on respondents' attitudes towards the support and future development of green roofs in Slovakia. The questions focused on opinions regarding legislative measures, mandatory inclusion of green roofs in new buildings, and financial support from the state. Respondents expressed their position on the need to expand the construction of green roofs, their feasibility on existing buildings, and the possibility of introducing a mandatory share of greenery on roofs with a larger area. This section provided important information on how the public perceives the need for legislative changes and their willingness to actively participate in supporting green roofs in practice. 105 respondents participated in the survey.

The respondents in the survey represented different groups with different attitudes towards the issue of green roofs. The largest proportion was made up of members of the general public (79 respondents), which allows for the acquisition of perspectives from

people outside the professional sector. Professionals in the construction industry were represented (21 respondents), which indicates a high level of participation by respondents with professional knowledge. Specific professions also appeared among the responses, such as an administrative worker in a plumbing company (1 respondent), or respondents with a previous interest in green walls (1 respondent). One respondent described himself as an admirer of the issue and another stated that he had no relationship to the topic. This diversity of responses provides valuable insight into the perception of green roofs not only among professionals, but also among the general public.

4 Results of the questionnaire survey

Based on the results of the questionnaire survey, it can be stated that the public is showing a growing interest in the issue of vegetated (green) roofs and at the same time perceives their potential as a significant element of sustainable development of the urban environment. The survey results indicate a predominantly positive attitude of respondents towards green roofs – up to 62.8% stated that they would be interested in implementing them on their own property, while an even higher proportion (over 80%) would welcome their expansion in public spaces or on other objects in their surroundings. These findings indicate that the public is beginning to perceive green roofs not only as an architectural or aesthetic element, but above all as a multifunctional tool for improving the quality of life in an urban environment. Respondents in the questionnaire repeatedly mentioned the benefits of green roofs, especially in relation to ecological and environmental benefits – the most frequently mentioned were the ability to retain rainwater, mitigating the urban heat island effect, improving air quality, and supporting biodiversity. In this context, it is positive that the public is aware of their complex impact on the urban ecosystem and climate adaptation. On the other hand, the survey also revealed certain shortcomings in the area of information. Despite the general positive perception and basic awareness of the existence of extensive and intensive types of green roofs, several respondents declared that they do not consider themselves sufficiently informed on the issue. This fact points to the need for systematic education of the public, not only in the area of technical aspects of vegetated roofs, but also in the area of their maintenance, costs, legislative framework and potential benefits. The main barriers preventing the wider spread of green roofs were cited by respondents as high initial costs, concerns about design limitations, lack of technical information and the absence of significant legislative or economic support from the state and local governments. These factors have a significant impact on the decision-making of both investors and ordinary citizens and point to the need for comprehensive support for the development of this type of measures - whether through subsidies, tax breaks, expert advice or the creation of binding regulations for new buildings and reconstructions. From the perspective of the further development of sustainable urban structures, it is crucial that green roofs become part of a systematic environmental policy. Based on the findings, it can be recommended to intensify information campaigns, incorporate green roofs into spatial planning documentation, as well as legislative and financial support from public institutions. A positive response from the public creates a

suitable prerequisite for vegetated roofs to become a standard in sustainable construction and an integral part of the adaptation of cities to climate change.

5 Conclusion

Green roofs, as part of green infrastructure, represent one of the most effective tools for adapting the urban environment to the negative consequences of climate change and deteriorating ecological conditions in cities. They enable the use of unused roof areas and create space for vegetation, which fulfills a number of ecological, economic and social functions. From the point of view of the functionality and efficiency of green roofs, the technical solution of individual layers, the appropriately selected type of roof, as well as the quality of the materials used are decisive. A comprehensive assessment of the conditions of a specific object, including climatic, static and structural specifics, is necessary. The classification of green roofs, their technical composition, design and implementation methods were analyzed, with special emphasis on the advantages and disadvantages from an ecological and operational point of view. Green roofs can retain a significant part of rainwater, mitigate overheating of buildings and the surrounding environment, improve air quality and support biodiversity. In addition, they increase acoustic and thermal comfort, extend the life of the roof covering and reduce the costs of energy operation of buildings, thereby contributing to the sustainable development of cities. However, the implementation of vegetated roofs requires higher initial costs, a professional approach and consistent maintenance. In the practical part, specific green roof designs were developed for various types of buildings and roof slopes, which showed how theoretical knowledge can be used in real conditions. The survey confirmed that awareness of the advantages of green roofs is still low in Slovakia. These roofs bring a number of environmental, economic and other benefits. Risks include higher investment costs, the technical complexity of the design and the need for maintenance, which require a professional approach and knowledge of local conditions. To improve the situation, it is important to focus on raising awareness among the public, designers and local governments. Educational activities, professional seminars or practical demonstrations could contribute to a better understanding of the benefits of these solutions. It is also necessary to strengthen legislative and financial support from the state, for example through subsidies, tax breaks or a mandatory share of vegetation areas in new buildings. An effective form would be to incorporate them into spatial plans as part of climate change adaptation strategies. Universities, research institutions and non-profit organizations can also support the development of sustainable solutions adapted to local conditions. By combining information, professional cooperation and political will, the potential of green roofs can be fully realized for the benefit of cities and their residents.

6 Acknowledgements

Thanks to support to VEGA project 1/0588/24.

7 References

[1] Haseeb M, Kot S, Hussain HI, Jermsittiparsert K – Impact of Economic Growth, Environmental Pollution, and Energy Consumption on Health Expenditure and R&D Expenditure of ASEAN Countries. Energies 2019, 12(19), 3598; https://doi.org/10.3390/en12193598

[2] Joshi MY, Teller J – Urban Integration of Green Roofs: Current Challenges and Perspectives. Sustainability 2021, 13(22), 12378; https://doi.org/10.3390/su132212378

[3] Oberndorfer E, Lundholm J, Bass B, Coffman RR, Doshi H – Dunnett, N.; Gaffin, S.; Kohler, M.; Liu, K.K.Y.; Rowe, B.: Green Roofs as Urban Ecosystems: Ecological Structures, Functions, and Services. BioScience, Vol 57, Issue 10, November 2007, Pages 823–833, https://doi.org/10.1641/B571005

[4] Nature-based solutions in Europe: Policy, knowledge and practice for climate change adaptation and disaster risk reduction. Report. Luxembourg: Publications Office of the European Union, 2021 https://www.eea.europa.eu/en/analysis/publications/nature-based-solutions-in-europe

[5] Vourdoubas J – Review of the Benefits of Green Roofs. International Journal of Current Science Research and Review. Vol 07 Issue 09 September 2024 DOI: 10.47191/ijcsrr/V7-i9-48

[6] Hamid HNA, Romali NS, Rahman RA – Key Barriers and Feasibility of Implementing Green Roofs on Buildings in Malaysia Buildings 2023, 13(9), 2233; https://doi.org/10.3390/buildings13092233

8 Presentation of Author(s)

Prof. Martina Zelenakova is involved in scientific research and teaching activities at the Technical University of Košice, Faculty of Civil Engineering. Her professional interest is oriented toward the sustainable water management. She belongs to significant scientific experts in the field of green buildings and their water management and actively participates in international conferences.

Potable Water Reuse in the USA: Regulations and Treatment Technologies

Daniel Cole
dan.cole@iapmo.org
Sr. Director of Research, IAPMO, USA

Abstract

Varying scales of potable water reuse from wastewater recycling and treatment approaches in the USA are discussed under two broad categories of direct and indirect potable water reuse. Direct potable water reuse at a centralized municipal scale is the most advanced form of wastewater recycling, where treated wastewater is purified to drinking water standards and then immediately reintroduced into the drinking water distribution system. Indirect potable water reuse introduces the advanced treated wastewater to an environmental buffer before being introduced to surface or groundwater.

The regulatory landscape in the USA for potable water reuse is not uniform or standardized throughout the individual states. Seventeen state regulations for potable water reuse are therefore surveyed for treatment parameters, reuse applications, and implementation. The diversity of regulations is shown in a summary table and treatment parameters and implementations of potable water reuse are discussed.

Advanced water treatment technologies for potable water reuse exceed those used for non-potable water reuse. Innovative technologies implemented to reduce both pathogen and chemicals for direct potable water reuse are discussed.

Keywords
Enhanced Source Control Program, ozonation, granular activated carbon (GAC), biological activated carbon (BAC), UV advanced oxidation process (UV AOP)

1 Introduction

The Safe Drinking Water Act (SDWA) is the US federal regulation for the public drinking water supply (40 C.F.R. § 141, 2026) that protects drinking water and its sources

– rivers, lakes, reservoirs, springs, and ground water wells. SDWA authorizes the United States Environmental Protection Agency (US EPA) to set national health-based standards for drinking water to protect against both naturally occurring and man-made contaminants that may be found in drinking water. US EPA, states, and water systems then work together to make sure that these standards are met.

There are no federal regulations specifically governing potable water reuse in the United States, but it is permissible to produce reuse drinking water, provided all applicable SDWA, Clean Water Act (CWA), and state requirements are met. Regulations specific to potable water reuse exist only at the state level and are by no means uniform or standardized.

2 Methodology

The research methodology uses data from a survey of all 50 states in the United States by the US EPA REUSExplorer Tool (REUSExplorer, 2024). The data collection was confined to potable water reuse that narrowed the selection of states surveyed. Since the REUSExplorer Tool was current only to February 2024, a further survey was conducted to collect regulatory data current to May 2026.

The data was collocated in a table to better analyze the differences across state regulations. Due to the page limitation, only a selection of the data could be displayed, focusing on treatment parameters and implementation. The goal of this research was to evaluate the potential for developing an American national consensus standard for potable water reuse and to serve as preliminary documentation. A consensus standard will accelerate the implementation of potable water resuse systems and allow manufacturers to install system products uniformly across all states reducing the variation of costs.

3 Terminology

Terminology is important in the discusson of potable water reuse (Rich, et al., 2023). State regulations have defined such terms independently of standardization and therefore differ in legal expression. The following words used in potable water reuse regulations are given their explicit meaning without trying to replicate all the ways they have been uniquely defined in state regulations.

Potable water reuse involves the use of highly treated municipal wastewater as a municipal drinking water source. The treated wastewater originates from a wastewater treatment plant that has treatment processes to achieve a defined source water quality for additional treatment by a supplier utilizing potable water reuse. This highly treated wastewater is also called *reclaimed* or *recycled* wastewater, having specific regulated treatment levels based on its intended application whether for potable or non-potable water use.

Advanced water treatment (AWT) is the water produced from wastewater for potable water applications. It involves a process train to remove chemical, pathogenic, and emerging contaminants. Similar terms in state regulations are Advanced Water Purification, Advanced Purified Water, and Advanced Treatment Water. For consistency, this paper uses AWT.

The intended implementation of potable water reuse falls in two broad categories, indirect and direct potable water reuse. *Indirect potable water reuse* (IPR) introduces the advanced treated wastewater to an environmental buffer such as surface water or groundwater augmentation. Surface water augmentation includes streams, rivers, reservoirs, and lakes. Groundwater augmentation includes surface infiltration, subsurface injection (vadose zone), and direct injection to a potable water aquifer. *Direct potable water reuse* (DPR) delivers advanced treated purified water from an advanced wastewater treatment facility directly into a potable water supply distribution system without an environmental buffer.

Some states have implemented an *Enhanced Source Control Program* for advanced wastewater treatment before delivery to an advanced potable water treatment facility. This program prevents constituents of concern (COCs, also called contaminants of emerging concern CECs) that include target chemicals from negatively impacting the advanced water treatment facility, or the water it produces, by controlling the COCs at their source. The program identifies and limits contaminants in wastewater, assesses the fate of chemicals in the wastewater treatment system prior to treatment, and investigates chemical sources and chemicals detected in monitoring.

4 Survey of regulatory and implementation landscape in USA

The regulations for potable water reuse vary throughout the country, depending on the source water quality, the level of treatment required, and the type of potable reuse implemented. Selecting the appropriate treatment technology for potable reuse can be a complex decision. The number of states with potable water reuse regulations, regulatory guidelines, or in the regulatory development phase is shown in Figure 1. Most states surveyed have implemented IPR over the past 60 years (EPA, 2017). States that have recently approved DPR regulations or regulatory guidance are Arizona (2025), California (2024), Colorado (2023), Texas (2021), Washington (2018), and Florida (2025).

Arizona currently has a demonstration facility for DPR with a prospect of commissioning an advanced water treatment facility that will produce 2.5 million gallons per day (MGD; 9.5 million liters per day MLD) of potable water in the year 2031.

California's Pure Water program is a partnership between The Metropolitan Water District of Southern California and the Los Angeles County Sanitation Districts to reuse wastewater that is currently discharged to the Pacific Ocean. This would entail a new advanced water treatment facility to treat this water to produce 150 MGD (568 MLD) of purified water. Construction of the AWT facility is expected to start in 2027 to be completed by 2040 for implementation of IPR with a portion of the purified water directed for DPR (Pure Water, 2026). Other programs in California for potable water reuse are the

Orange County Groundwater Replenishment System (IPR), the Chino Basin Program (IPR), and Pure Water San Diego (DPR) that will be operational in 2035. The Hyperion Water Reclamation Plant in the City of Los Angeles constructed a pilot facility for AWT as a proof-of-concept to produce 230 MGD (870 MLD) for future IPR and DPR reuse. Santa Monica Sustainable Water Infrastructure Project (SWIP) is an underground AWT facility collecting a blend of domestic wastewater and stormwater, producing 1 MGD (3.8 MLD) of IPR for direct injection aquifer recharge. This facility has future plans to expand to DPR.

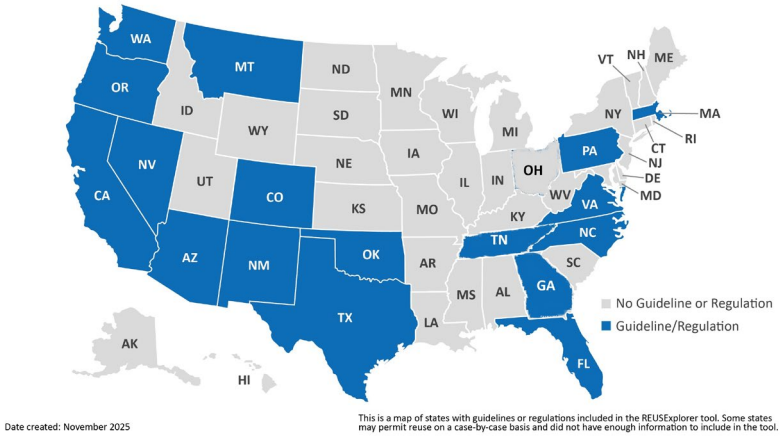

Figure 1 States with potable water reuse regulations or guidelines (Adapted from USEPA Maps, 2025)

Colorado and Washington have regulations for DPR but neither state has implemented AWT facilities. Texas has regulatory guidance for the use of DPR for case-by-case projects. Texas currently has a raw water production test facility in Big Spring and the Pure Water Center in El Paso is under construction for 2029 to produce 10 MGD (38 MLD) of DPR. Florida's recent rule making allows AWT for DPR and IPR. Two AWT facilities are under development in Florida; H2.0 Purification Center producing 1MGD (3.8 MLD) for aquifer augmentation and RECAP producing 2 MGD (7.5 MLD) for groundwater augmentation. The former Center will be operational in 2026 and the latter in 2027. Florida also has a demonstration facility as a pilot project for DPR in Plant City in hopes of a full-scale supply facility.

The treatment parameters for potable water reuse are complex and differ from state to state. Table 1 is a summary overview of seventeen states highlighting the diversity of regulations or regulatory guidelines for wastewater treatment for potable water reuse. A more detailed analysis can be studied using the US EPA REUSExplorer Tool (REUSExplorer, 2024). This tool links to state reuse regulations or guidelines and is searchable by source water and implementation. Table 1 reflects state regulations current to date (May 2026).

Five states using AWT for potable water reuse require the water treatment criteria for pathogen removal based on the quantitative microbial risk assessment (QMRA) framework that defines pathogen log reduction targets (LRTs) for pathogenic viruses, protozoa, and bacteria (USEPA, 2025). However, each state differs from the required

levels to be achieved. AWT facilities also incorporate an Enhanced Source Control Program to control constituents of concern (COCs) such as chemical contaminants that include disinfection byproducts (DBPs), pharmaceuticals, pesticides, and herbicides (Thompson, et al., 2025; NWRI, 2013).

Three states require Class A+ standards for indirect potable water reuse. Class A+ is a high-grade standard for reclaimed water and safe for high exposure and non-potable water use or IPR. Washington allows Class A+ for DPR if it further meets potable water performance criteria. However, Washington does not currently produce Class A+ reclaimed water.

Treatment parameters for IPR vary depending on implementation and location of augmentation to a potable water source. Potable aquifer recharge or injection requires effluent monitoring and sampling limiting the levels of TSS, TDS, Total Organic Halides, Turbidity, TOC, Fecal Coliform, BOD, Nitrogen, and Nitrate nitrogen.

Table 1 Survey of treatment parameters and potable water reuse implementation

State	Treatment Parameters [a]	Reuse Application	Implementation
Arizona	Pathogen LRTs – 13/10/10 QMRA – Infection (10^{-4}) Continuous monitoring Chemical Control: Tier 1 – SDWA Max Contaminant Levels Tier 2 – AWT Specific contaminants Tier 3 – Performance based indicators Enhanced Source Control Program	AWT - DPR	2025 – Regulations for DPR 2026 – Demonstration Facility 2031 – Commissioning of AWT Facility 2.5 MGD (9.5 MLD)
California	Pathogen LRTs: 20/14/15 90% of time 16/10/11 continuously QMRA – Infection (10^{-4}) Continuous monitoring Chemical Control Wastewater Source Control Program	AWT – IPR and DPR	2022 – Santa Monica Sustainable Water Infrastructure Project (SWIP) IPR aquifer recharge 2024 – Regulations for DPR 2024 – City of Los Angeles Hyperion AWT Demonstration Facility 2032 – Pure Water S. CA 50 MGD (189 MLD) 2035 – North City Pure Water Facility, San Diego 30 MGD (114 MLD)
Colorado	Pathogen LRTs: 12/10/10 unknown pathogen concentration	AWT - DPR	2023 – Regulations for DPR No treatment facilities

State	Treatment Parameters [a]	Reuse Application	Implementation
	8/6/5.5 known sampled pathogen concentration QMRA – Infection (10^{-4}) Continuous monitoring Chemical Control Enhanced Source Water Control Program		
Florida	Pathogen LRTs – 14/12/12 QMRA – Infection (10^{-4}) Monitoring and sampling Chemical Control Source Control Program	AWT – IPR and DPR	2025 – Regulations for Potable Reuse 2025 – Plant City One Water Demonstration Facility for DPR 2026 – H2.O Purification Center IPR aquifer augmentation 1 MGD (3.8 MLD) 2027 – RECAP Groundwater augmentation 2 MGD (7.5 MLD)
Georgia	Federal Regulations for secondary wastewater treatment plus State requirements when augmenting source water for potable use. Monitoring/Sampling	IPR	IPR Federal and State Regulations Surface water augmentation followed by an environmental buffer (reservoirs, rivers, streams)
Massachusetts	State Regulations for effluent limitations for TSS, Turbidity, TOC, Fecal Coliform, BOD, Nitrogen, Nitrate nitrogen Monitoring/Sampling	IPR	Aquifer recharge
Montana	State Regulations for effluent limitations for TSS, Turbidity, Total Coliform, BOD, Total Nitrogen Monitoring/Sampling	IPR	Aquifer recharge/injection Reservoir augmentation Surface water augmentation
Nevada	Class A+ Standards Pathogen LRTs – 12/10/10 State Regulations for effluent limitations for TSS, Turbidity, Total Coliform, BOD, TDS Wastewater source control	IPR	2016 – Class A+ regulations for IPR: • Injection wells • Spreading basins • Aquifer Augmentation followed by an environmental buffer

State	Treatment Parameters [a]	Reuse Application	Implementation
		AWT	(reservoirs, rivers, streams) 2028 – One Water Nevada, Advanced Purified Water Facility 2 MGD (7.5 MLD) Groundwater injection
New Mexico	Ground water quality standards	N/A	Reclaimed water for basins used to replenish water in an aquifer (not considered IPR) Allows Feasibility study for IPR and DPR 50-year Water Action Plan for IPR and DPR
North Carolina	Water reuse policy and rulemaking (no explicit rulemaking other than prohibiting reclaimed water for DPR)	IPR	Allow reclaimed water to combine with other raw water sources in a pretreatment mixing basin and pumped to a water treatment plant.
Oklahoma	Pathogen Log Removal – 5/5/3/3[b] Other pollutant benchmarks Effluent sampling/monitoring	IPR	Surface water (lake, streams, rivers) augmentation Aquifer storage and recovery 2023 - Started the Oklahoma Water Reuse Action Plan with 2060 Goal that does not exceed 2012 fresh water use by implementing IPR and DPR
Oregon	Class A standards Monitoring Total Coliform and Turbidity	IPR	Basin surface infiltration Subsurface injection (vadose zone) Direct injection to groundwater is not allowed.
Pennsylvania	Class A+ and A standards State Regulations for effluent limitations for Total Organic Halides, Turbidity, TOC, Fecal Coliform, BOD, Total Nitrogen	IPR	Groundwater recharge Surface water augmentation Direct injection augmentation to potable water aquifers Swimming pools (public and private)

State	Treatment Parameters [a]	Reuse Application	Implementation
			DPR Prohibited
Tennessee	Potable Water Reuse Program Development	IPR	2024 – Task Force started research for regulatory development DPR is not within the scope of regulation development
Texas	Pathogen LRTs – 8/6/5.5 QMRA – Infection (10^{-4}) Chemical Control and monitoring	IPR AWT DPR	IPR surface water or groundwater 2021 – Regulatory guidance for DPR (case-by-case projects) • Public water system • Raw water supply entering a treatment plant 2016 – Raw Water Production Test Facility, Big Spring 2029 – Pure Water Center, El Paso 10 MGD (38 MLD)
Virginia	State Regulations for effluent limitations for Bacteria, Total Residual Chlorine, pH, BOD, Turbidity, TSS Effluent sampling/monitoring	IPR	Surface Water augmentation Direct injection of reclaimed water into aquifer DPR Prohibited
Washington	Class A+ reclaimed water – DPR Performance standard case-by-case basis Class A and B reclaimed water – IPR Performance standards for BOD, TSS, pH, Turbidity, Total Coliform, Total Nitrogen, and Virus removal	IPR DPR	2018 – Regulations for Reclaimed Water IPR • Surface water augmentation • Groundwater recharge • Aquifer storage and recovery DPR – No facilities currently produce Class A+ reclaimed water

[a] The order of log reduction targets (LRTs) is enteric viruses/giardia/cryptosporidium. Viruses are either norovirus or adenovirus.

[b] Oklahoma – the order of pathogen log removal is Adenovirus/ Salmonella/ giardia/ cryptosporidium

5 Advanced water treatment technologies

The technology used in the treatment train for non-potable water reuse to achieve LRTs has been successfully implemented in the US (Cole, 2024; Cole, Nokhoudian, 2025). Advanced water treatment for IPR and DPR use the base technologies for non-potable treatment trains, namely, membrane bioreactor (MBR), reverse osmosis (RO), ultraviolet (UV) disinfection, and chlorine. To achieve greater levels of LRTs and chemical and organic removal needed for potable water reuse, more technologies are introduced: ozonation, granular activated carbon (GAC), biological activated carbon (BAC), and UV advanced oxidation process (UV AOP).

California regulations for DPR explicitly detail the treatment technologies required. For pathogen removal, the treatment train needs four separate treatment processes for each pathogen and at least three diverse treatment mechanisms. Such mechanisms must include one membrane physical separation, one chemical inactivation, and one UV inactivation. For chemical control, the treatment train must also consist of at least three separate treatment processes and three diverse treatment mechanisms. The sequence of processes required are ozone/BAC followed by RO membrane followed by advanced oxidation. Example of the treatment process required by California DPR regulations to meet LRTs is shown in Figure 2. Figure 3 shows a treatment train demonstration facility for DPR.

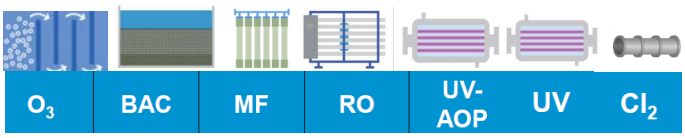

Figure 2 Example of DPR treatment process

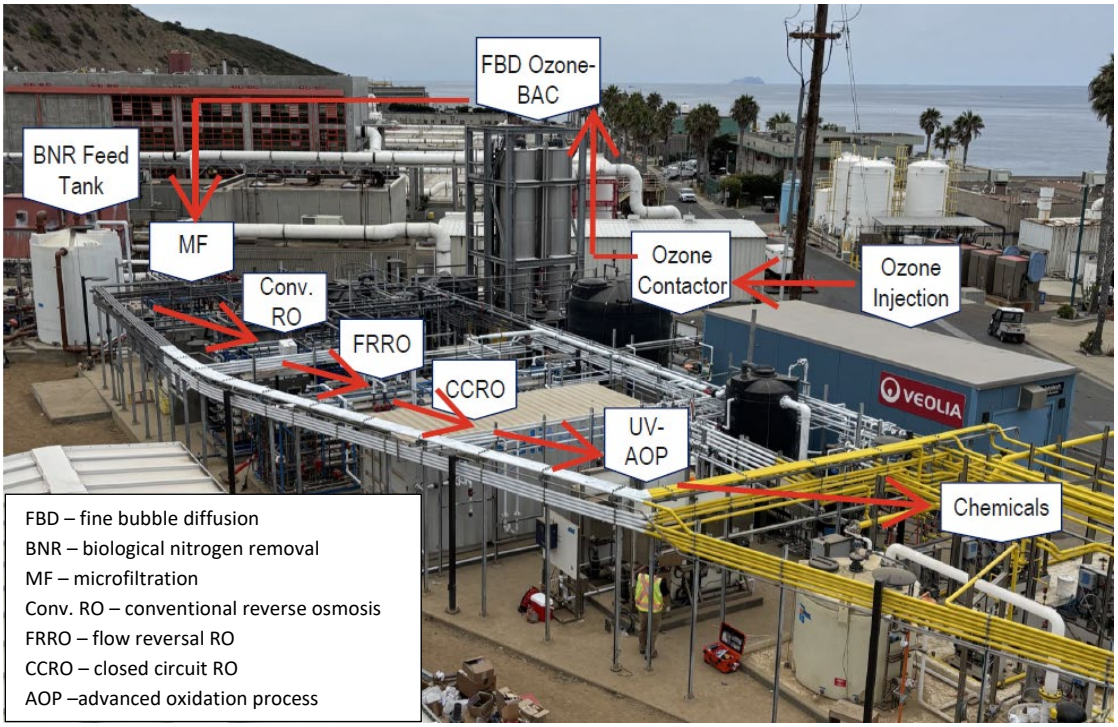

Figure 3 Pure Water San Diego Demonstration Facility – DPR train (courtesy of City of San Diego Pure Water Program)

Arizona has similar technological requirements: biological nitrogen removal (BNR), membrane bioreactor, and UV advanced oxidation process (AOP). Additional technologies are undergoing cost analysis for three pathways: 1) Ozone-BAC for injection well potable reuse, 2) Ozone-BAC with side-stream RO for injection well potable reuse where some salinity must be controlled, and 3) Full-stream RO for injection well potable reuse where comprehensive removal of salts and other dissolved solids is necessary.

Figure 4 is an example of a treatment train that would comply with Colorado's regulations for pathogen and chemical removal for DPR. DPR projects in Colorado will require non-RO treatment because of the difficulty and prohibitive cost in disposing RO concentrate in Colorado (NWRI, 2019).

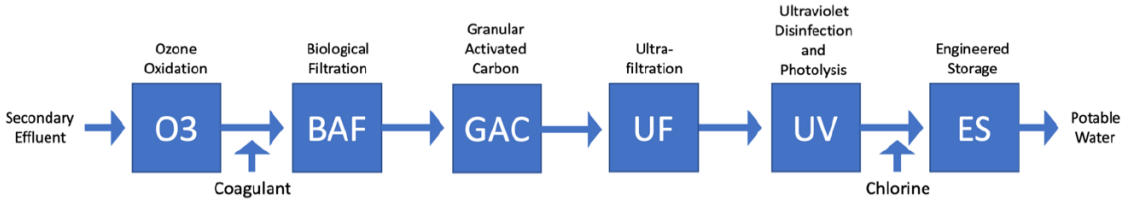

Figure 4 Colorado example DPR treatment train (NWRI, 2019)

The system design for Florida's H2.O Purification Center for IPR aquifer augmentation is shown in Figure 5. Water treatment processes depend on properly operating filtration and disinfection technologies. Membrane filtration systems may include microfiltration, ultrafiltration, nanofiltration, reverse osmosis, or alternative membrane technologies. Granular activated carbon (GAC) may also be placed before UV AOP as in Figure 4. Disinfection is by UV AOP and chlorine. The use of ozone/BAF treatment is allowed upon validation that achieves 75 percent minimum removal of selected indicator compounds under full-scale operating conditions and would be placed ahead of microfiltration. Before augmenting the aquifer, dissolved oxygen (DO) in the finished purified water is reduced to a level that corresponds to the concentration of the aquifer.

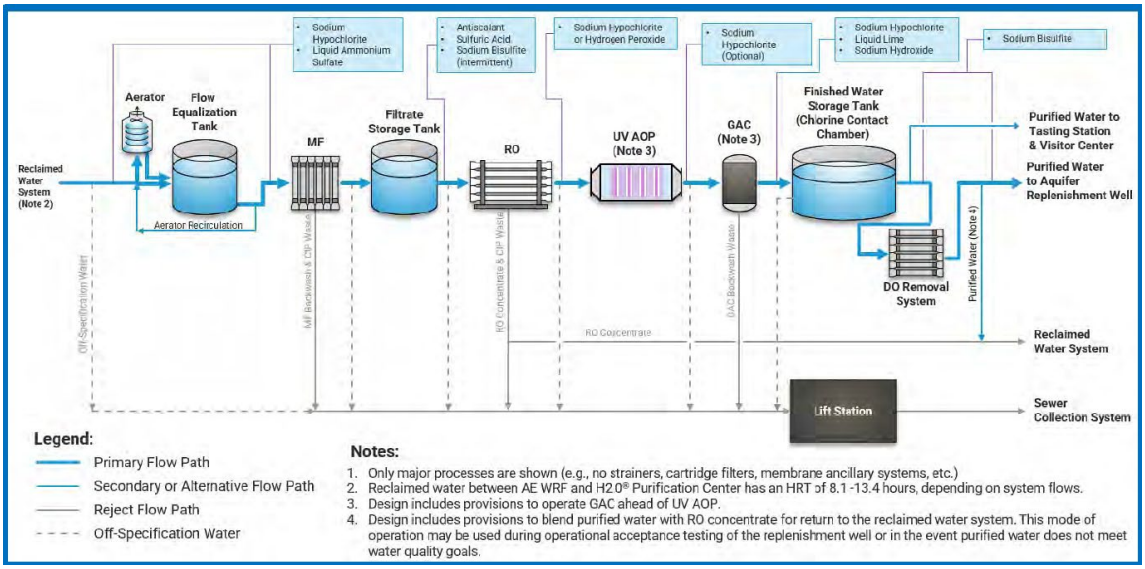

Figure 5 Florida H2.0 purification process for IPR

Texas regulatory guidelines provide several treatment schemes for DPR with technology options that are effective for full scale applications (Texas Water Development Board, 2015). The technologies include micro- and ultra-filtration, membrane bioreactors, RO, UV AOP, ozone, BAC, and chlorine. One example is shown in Figure 6.

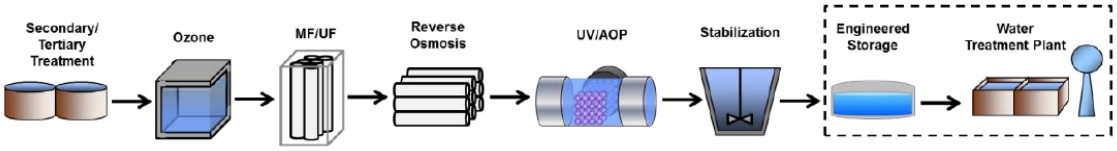

Figure 6 Example Texas treatment scheme (Texas Water Development Board, 2015)

6 Conclusion

Although the treatment parameters for potable water reuse are complex and differ from state to state, the regulatory data in this study shows good potential for developing an American national consensus standard for direct potable water reuse across three categories. First, states implementing DPR agree on the water treatment criteria for pathogen removal based on the quantitative microbial risk assessment (QMRA) framework that defines pathogen log reduction targets (LRTs). Further consensus is needed on the target levels to be achieved. Second, states that are implementing DPR incorporate an Enhanced Source Control Program to identify and limit contaminants in wastewater prior to the AWT facility. These programs already have a good common benchmark toward a consensus program. Third, states implementing DPR require common treatment technologies for AWT. Further research is needed to validate log reduction credits for pathogen removal by the technologies used in the treatment train.

The regulatory data for IPR presents more challenges for developing a consensus standard due to the diversity of environmental buffers that are used for potable use. The distance from the IPR augmentation to the source of potable water use also affects the level of treatment required. There is a common benchmark for monitoring and limiting the effluent TSS, Turbidity, TOC, Fecal Coliform, BOD, Nitrogen, Nitrate nitrogen. These challenges are not insurmountable but require inclusion of environmental conditions.

A national consensus standard alone will not overcome the public reluctance to what is called the “yuck” factor in drinking treated wastewater. The AWT facilities will also serve as educational facilities for the public and offering taste venues. The BILD collaborative global community also serves to accelerate the implementation and acceptance of water reuse systems (BILD, 2026).

7 References

40 C.F.R. § 141, National Primary Drinking Water Regulations. (2026). https://www.ecfr.gov/current/title-40/chapter-I/subchapter-D/part-141

Building Infrastructure Locally for Decentralized Water Systems (BILD). (2026). Decentralized Water Systems: Action Plan for Global Acceleration. https://www.watereuse.org/bild

Cole, Daniel. (2024). Treatment Methods for Onsite Alternate Water Treatment Systems: Part One. Proceedings of the 49th International Symposium CIB W062 on Water and Drainage for Buildings.

Cole, Daniel; Nokhoudian, Taylor. (2025). San Francisco Accelerates Implementation of Onsite Water Reuse in USA. Proceedings of the 50th International Symposium CIB W062 on Water and Drainage for Buildings.

NWRI Independent Advisory Panel, Examining the Criteria for Direct Potable Reuse. (2013). Water Research Foundation Project 11-02.

NWRI Independent Advisory Panel, Guidelines for Direct Potable Reuse in Colorado. (2019). NWRI-2019-03.

Pure Water Southern California, Final Environmental Impact Report. (2026). Metropolitan Report No. ER 1715-1 EIR Report

Rich, Drew; Andiroglu, Esber; Gallo, Kathryn; Ramanathan, Sivakumar. (2023). A review of water reuse applications and effluent standards in response to water scarcity. Water Security, Vol. 20.

Texas Water Development Board. (2015) Final Report Direct Potable Reuse Resource Document. TWDB Contract No. 12483215 Vol 2.

Thompson, Kyle; Steigerwald, Jessica; Ray, Hannah; Branch, Amos; Assi, Talia; Salveson, Andrew; Nading, Tyler; Dickenson, Eric. (2025). Review of industrial chemicals impacting potable reuse: Hazards, removal, and recommendations for enhanced source control programs. Total Environment Engineering. https://doi.org/10.1016/j.teengi.2025.100027

U.S. Environmental Protection Agency (EPA). Potable Reuse Compendium. (2017). https://www.epa.gov/ground-water-and-drinking-water/2017-potable-reuse-compendium

U.S. Environmental Protection Agency (EPA). REUSExplorer, Regulations and End-Use Specifications Explorer. (Last updated 2024). https://www.epa.gov/waterreuse/regulations-and-end-use-specifications-explorer-reusexplorer

U.S. Environmental Protection Agency. Risk-Based Framework for Developing Microbial Treatment Targets for Water Reuse. (2025). U.S. Environmental Protection Agency, Office of Research and Development, EPA/600/R-25/009. https://watereuse.org/wp-content/uploads/2025/01/Updated-Risk-Based-Framework-for-Developing-Microbial-Treatment-Targets-for-Reuse.pdf

8 Presentation of Author

Daniel Cole is Sr. Director of Research at the IAPMO. He was a licensed journeyman plumber, contractor, and inspector in the state of Illinois. He is a member of the American Society of Plumbing Engineers (ASPE) and received the ASPE Scientific Achievement Award in 2018. He has also served on the ASPE Main Standards Committee since 2015. He served as Secretariat for the American National Water Efficiency and Sanitation Standard for the built environment.

A City's Relief: A Study on the Optimization and Reallocation of Municipal Demand through Probabilistic Adoption Modeling of Conservation Measures

K. L. Williams (1)

(1) k.williams19@umiami.edu

(1) College of Engineering, Civil and Architectural Engineering Department, University of Miami, Coral Gables, Florida

Abstract

The built environment operates from the utilization of one water source. Unfortunately, due to the increasing demand from population growth and emerging sectors, the world's only water supply source is dwindling. Cities alike are withdrawing from this source and forced to maintain the status quo of meeting the potable and non-potable demands of their municipalities. In addition, geographical locations are affected by varying climate alongside unique external factors relevant to their area. In an effort to alleviate stress on municipalities and the existing water supply, this study evaluated the implementation of water conservation practices and their corresponding treatment tiers utilizing the city of Houston, Texas as a case study to identify the quantified volume of conserved water that contributes towards resource allocation through the construction of a probabilistic model. Using multiple techniques, such as stochastic modeling and Monte Carlo simulation specifically, scenarios were generated for treatment tier adoption rates ranging from 1% to 100% of existing building typologies and new construction as well as taking into account climate variability and socioeconomic factors. Preliminary results demonstrate that the implementation of water conservation measures along with the corresponding treatment tiers can provide demand offset for any city's existing water source by subsidizing the current residential demand. The goal of these findings is to emphasize the significance of long-term infrastructure planning, incentivization, and policy design as well as provide a transferable modeling architecture for municipalities in various geographical locations and climatic conditions to utilize.

Keywords

Monte Carlo simulation; stochastic modeling; harvesting; municipal water reclamation; reallocation

1 Introduction

Across the world, countries are projected to experience extreme levels of water scarcity by 2050. Currently, the United Nations has estimated that severe stages of water scarcity have been experienced by approximately 10 percent of the world's population (United Nations - UN Water, 2021). Unfortunately, a toll has been taken on the world's only water source as the growth of the urban landscape is steadily increasing. Such matters prompt the inclusion of water conservation measures as an inverse relationship between the globe's water supply and increasing demand has emerged.

Within this context, cities within the United States, such as Houston, Texas, are experiencing climate variability and stress due to the uncertain water demand stemming from external and emerging economic sectors. Today, the industrial sector has bloomed due to the increase in Artificial Intelligence (AI) usage and the need for the building of data centers as well as the cooling methodologies for the generative chips that occupy them (Turner Lee & West, n.d.). Due to the popularization of data centers, municipalities and rural areas are experiencing a lack of resources to support their current infrastructure (Turner Lee & West, n.d.). Although limited in nature, researchers have estimated that the smallest data centers can consume as much as 500,000 gallons per day whereas the largest centers may consume as much as 9 million gallons per day (Turner Lee & West, n.d.). With conditions projected to become more stringent in the next four years, the withdrawal from existing water sources has become a pertinent issue that needs to be addressed.

Moreover, the discussion regarding freshwater withdrawal from various sectors has prompted the suggestion of end-users playing a more vivid role in reducing their consumption (Arden et al., 2021; Cooley & Gleick, 2007; Gilbertson et al., 2011; Maddaus et al., 2014; Mini et al., 2015; Moglia et al., 2018; Sant'Ana & Mazzega, 2018; Tsai et al., 2011; Willis et al., 2013). According to the United States Geological Survey's 2015 report, the domestic sector equates to approximately 8 percent of the 12 percent of public supply (Dieter, 2018). With external pressures stemming from climate change and the built environment, dependence on groundwater and surface water resources has become significant as water in the region is suspected to decrease in time. With consumers making up the majority of this sector, the possibility behind end-users assisting in this task has developed.

Furthermore, freshwater withdrawal is not solely affected by one sector versus another. As the residential sector contributes to this phenomenon, the role of the end-user is critical in order to achieve sustainable water management practices (Arden et al., 2021; House-Peters & Chang, 2011; Knight et al., 2015; Mannan & Khan, 2022; Mayer, 2016; Moncur, 1987; Tong et al., 2017). Literature has established that the acceptance of households adopting and enforcing water conservation practices is based on the awareness and

perception of the end-user (Ahmed et al., 2022; Fan et al., 2014). As a result, aggregate savings can be attainable with implementation, enforceability through policy, and support from other entities. Although this potential has started to become realized, the discussion of reallocated, conserved water is limited in nature.

To address this gap, this study developed a modeling framework to focus on the redistribution of reclaimed water within the residential sector. The analysis focuses on the city of Houston, Texas within the ASHRAE Zone 2A as the case study. The impact from this study can be considered vast; however, the main contributing points discovered are: (i) the development of a stochastic modeling framework that estimates city-wide savings of treated reclaimed water; (ii) the integration of water conservation measures that evaluates their impact through implementation simultaneously; and (iii) a comparative and descriptive analysis of Houston's existing water source and the impact climate, location, and socioeconomic factors plays in the process of water reclamation.

Though certain aspects of this study have been reported in literature and previous studies, the novelty of this work lies in the multi-scenario evaluation of reclaimed water adoption using a stochastic modeling framework. Tools such as FAWCET, IRIPT, and NEWR are limited in scope as they address certain aspects of conservation such as retrofitting through fixture efficiency, optimization of centralized systems, and singular building typology evaluations, respectively (Castaneda et al., 2014; Lee et al., 2018; Arden et al., 2021). Each tool works deterministically and does not account for uncertainty. This study demonstrates the quantifiable benefits of institutionalizing water conservation measures into a city-wide initiative that lessens consumption but minimizes freshwater withdrawal, decreases municipal demand, and contributes to the needs of other sectors based on the varied climatic, geographical, regulatory, and socioeconomic conditions of a city.

2 Methodology

For this study, several key factors were selected to serve as a control for the creation of this stochastic model. The International Code Council's International Plumbing (IPC) Water Reuse Code and the International Water Conservation Code and Provisions (IWCCP) were selected as the code and policy framework for implementation; The city of Houston that resides in ASHRAE Climate zone 2A was selected as the city for evaluation (ASHRAE Standard 169); and Rainwater Harvesting, Condensate Harvesting, and Greywater Harvesting were the selected conservation measures that would align with the specified code and treatment tiers. The evaluation of the treatment of blackwater was also included within this study (ASHRAE, 2021)(International Code Council, 2024b)(International Code Council, 2021).

The creation of the stochastic model involved several components: (i) interpretation of building typology usage; (ii) the formation of synthetic household data; (iii) climate sampling; (iv) probabilistic adoption for treatment tiers; (v) water conservation technology sampling; and (vi) the aggregation of the Monte Carlo simulations. Each component is housed in a base configuration file that prompts reproducibility.

2.1 Study Context: Houston, Texas

As previously mentioned, the city of Houston was selected as the focus of this study. The following variables were utilized from previous research studies and developed deterministic modeling to establish the stochastic parameters for this study: household, climate, building stock, and socioeconomic factors. The average household encompassed approximately 2.52 people. Positioned in what's considered a "hot-humid" region, Houston's climate profile was derived as recording an average rainfall of approximately 46.12 inches per year as per the National Oceanic and Atmospheric Administration (NOAA) 5-year historical data from 2019-2023; and an average of 3,829 for annual cooling degree days at a temperature of 65 degrees. Houston's building stock was estimated to be approximately 1.3 million occupied units across five building typologies as derived from interpolation between the United States Census 5-year American Community Survey (ACS) estimates, Zillow and CoStar real estate platforms, and data obtained from the Houston Cost of Service Study. The five building typologies analyzed were single-family residences, townhouses/duplex units, garden-style/low-rise properties, mid-rise properties, and high-rise properties. The makeup of a unit was defined as three bedrooms and two and a half bathrooms with in-unit necessities such as a washer, dryer, and dishwasher (Williams et al., 2026).

2.2 Building Typology Designation

For this stochastic model, building typologies were designated as variables in order to establish the pathway of synthetic households. Because each building typology varies in nature, a building typology determined the roof area per unit, the adoption probability of specific treatment tiers, and how the baseline consumption is manipulated. With such importance, building typologies govern the means and ability of obtaining on-site systems. Furthermore, each typology received a code and probability weight based on the proportion of the building stock from the datasets listed above.

Table 1: Building typology distribution and characteristics.

Building Typology	Code	P(weight)	Avg Units/Property
Single Family	SF	0.289	1
Townhouse	TWH	0.032	12
Multifamily - Garden-Style Property	MF-G	0.436	198
Multifamily - Mid-Rise Property	MF-M	0.080	120
Multifamily - High-Rise Property	MF-H	0.162	300

2.3 Synthetic Population/ Household Generation

After assigning a building typology, each household's unique characteristic was drawn from specified distributions. Fixture-level data was not utilized within this model. The following attributes were selected: household size, baseline indoor water use, outdoor use fraction, roof areas for each building typology, annual rainfall, and household income.

2.4 Climate Sampling

For each Monte Carlo iteration, the annual rainfall is drawn to display the variability within the historical cadence. The monthly rainfall is separated into empirical historical

fractions in order to maintain the seasonal covariance that occurs in May and September. Regarding the condensation generated by each unit, the scalar derived in the deterministic model is scaled to adjust to the selected building typology's roof area. This formulation encapsulates the variation between selected equipment and the relationship between the unit's square footage and the accumulated condensate volume.

2.5 Tier Adoption Model

Aligning with the 2027 International Plumbing Code's newly adopted non-potable water reuse provisions (originally introduced as Code Change Proposal P157-24), four treatment tiers correspond with water conservation measures that aid in the reclamation of water on a city scale (International Code Council, 2024a). Similar to the deterministic model, the following water conservation measures were selected: rainwater harvesting, condensate harvesting, and greywater harvesting. The following descriptions for each tier and corresponding conservation measure to be adopted are listed below.

2.5.1 Tier 1: Municipal Reuse (reclaimed municipal wastewater)

Tier 1 consists of the least amount of intervention by homeowners as this tier is independent from the others as the collection of wastewater from homes is treated by municipalities. This tier, however, requires infrastructure to be in place, such as purple piping systems, to return to the home or select areas for its intended purpose of offsetting non-potable demand such as outdoor uses and external sector needs. Rebates, incentives, and code mandates complement this tiered level. Permitted use consists of residential landscape irrigation, golf courses, and cooling equipment for data centers, for instance. As per the IPC, tier one is considered "LC" as to be described as water that should have limited contact with humans and to not be consumed.

2.5.2 Tier 2: Rainwater Harvesting and HVAC Condensate Recovery

Tier 2 involves the capturing of two alternative water sources that can also offset non-potable uses for residents such as toilet flushing and landscape irrigation without needing to be treated to the standards of potable water. Tier 2 is hyper dependent on climate variability as the collection for both of these measures can change. Further, there's a summation of both contributions from each harvested source in order to meet the household's non-potable demand from toilet flushing and outdoor irrigation. As per the IPC, tier two is considered "IC" as to be described as water that may have indirect contact with humans and might possibly be consumed.

2.5.3 Tier 3: Greywater Harvesting

Tier 3 involves the collection of specific fixtures as designated by the NSF/ANSI 350 standard within a household to be treated for non-potable uses such as toilet flushing and irrigation. A 75% collection efficiency obtained from showers, lavatories, bathtubs, and utility sinks from select areas within the architectural footprint of a unit is assumed as every fixture cannot be collected from. The savings from this tier are attributed to the outstanding non-potable demand that was not satisfied by Tier 2. As per the IPC, tier three is considered "AC" as to be described as water that may have accidental or limited consumption by humans or consists of aerosolization.

2.5.4 Tier 4: Blackwater Reclamation

Tier 4 encapsulates the most expensive protocol for full on-site treatment and reuse of blackwater. Blackwater is defined as wastewater containing fecal matter and urine from toilets and kitchen sinks. This treatment tier cannot only meet non-potable demand, but with additional treatment, it can meet potable demand as well. As previously mentioned, this tier requires an extensive amount of funding resources as well as undergoing the most stringent standards according to the IPC. Due to costs, this treatment is projected to be low in adoption. Moreover, as per the IPC, tier four is considered "DC" as to be described as water that will have direct contact with humans and can be consumed.

2.5.5 Adoption

The adoption process for each household is twofold in nature as the adoption probability stems from the population variation in obtaining conservation systems and infrastructure as well as the logistic function that captures the relationship between a household's income and the decision to invest. Due to the variation in household income, the chances of tier adoption vary. Hence, the introduction of a conditional multiplier that suggests that each household's ability to adopt a higher tier is dependent on whether or not the previous tier(s) may have been committed to. As a result, this multiplier works independently at each level. Also, in addition to the multiplier, an option to adopt city code mandates is outlined as well. With new construction adding to the building stock of a city, the implementation of code-mandate infrastructure can add to the savings generated per building typology and overall aggregate potential.

2.6 Monte Carlo Engine

The preliminary run of this simulation is executed as a nested loop over N_iterations as well as seven adoption scenarios corresponding to a discrete distribution of 1%, 5%, 10%, 25%, 50%, 75%, and 100% of the eligible household pool. For each iteration, a synthetic population was generated, climate parameters were sampled, and tier adoption was determined independently for each household. For each adopted tier, savings were computed and aggregated based on designed constraints and totaled for the city/municipal level. The combined savings across each tier are designed to be capped in order to not have over-counting of savings. A full, completed loop generates a distribution of 10,000 total annual municipal savings estimates (converted to billion gallons per year) for each scenario based on an 80% confidence interval. Variance decomposition using Sobol first-order and total-order indices was also calculated.

2.7 Graphical User Interface

Combining all of the components outlined above, a coded graphical user interface was developed by the author to translate data into visual, comprehensible outputs that municipalities can use to infer the best scenarios and treatment tier combination for implementation. At a general level, users shall be able to input the number of iterations desired to be performed and the number of households per iterations; select desired adoption scenarios to evaluate; and select whether or not code mandates should be active when determining tier adoption.

3 Discussion and Results

While additional scenario testing remains ongoing, the methodology outlined above produced the iteration of the stochastic model shown below, displaying the intended workflow and resulting outputs. As previously described, the intent is to generate an easy-to-use model to reduce municipal demand utilizing potential savings from the residential sector.

In Figure 1, the initiated display of the user interface is shown in a simplistic manner to receive input from the user.

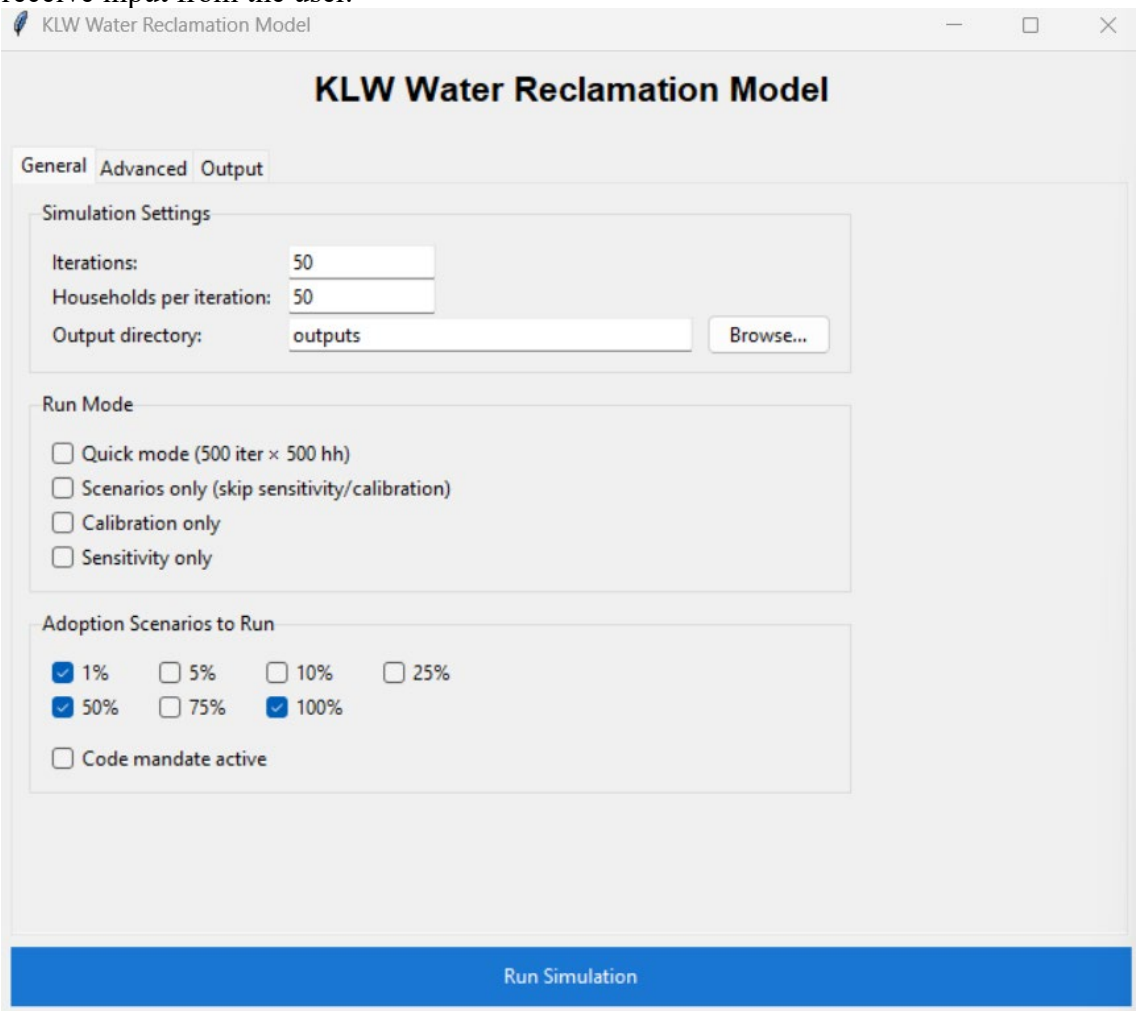

Figure 1 – Example of GUI for reclamation model for municipalities.

After key selections, the following outputs are to be produced after the "run simulation" in the form of charts: Baseline Demand vs. Reclamation Potential; Percentage of Demand Offset by Treatment Tier Adoption; Water Savings per Reclamation Tier; and Potential Reduction in Water Source Demand. In addition, detailed csv files with numerical data to support the visualization are produced as well.

Results at the 25% adoption scenario indicate a median household savings of 13,200 GPY, corresponding to an approximate 17.3% offset of baseline residential demand across Houston's modeled building stock. Among the decentralized tiers, Tier 4 (blackwater reclamation) emerged as the leading contributor, followed by Tier 2 (rainwater and

condensate harvesting) and Tier 3 (greywater harvesting), suggesting that as adoption scales, higher-investment treatment measures may yield disproportionate returns despite their lower expected utilization. With the model now validated against Houston's residential water demand data across all seven adoption scenarios, these early findings offer a promising indication that even moderate adoption rates can meaningfully contribute to municipal-scale demand reduction.

Based off obtained literature and previous research, this study presents the first probabilistic, multi-tier adoption model for residential water conservation for a given city. The intent of this model is to be modular in nature to expand to other cities and regions across the U.S. and globally. Aims of this study are threefold: (i) to explicitly represent household heterogeneity through empirically calibrated distributions; (ii) to produce confidence bands rather than point estimates for aggregate municipal savings; and (iii) to identify uncertain drivers through variance-based sensitivity analysis.

4 Conclusion

The stochastic Monte Carlo adoption model outlined in this paper provides a novel approach to municipal-scaled aggregate savings potential across four treatment tiers and water conservation practices within the city of Houston based on demand and consumption from the residential sector. Addressing the gaps left by existing tools, this modeling framework focuses on decentralization at the building-scale that evaluates multiple measures and scales to municipal-wide impact through multi-scenario evaluation and classification based on adoption rates. Such procedures permit transferability across cities allowing for the framework to be adapted based on a city's demographics, code enforcement, and state of water. Results stemming from the reduction savings can permit the reallocation of conserved water to external and emerging sectors, specifically data centers. With evaluations of stochastic variables such as population and climate, the evolving nature of a city can be studied and analyzed appropriately. Based on the model architecture, this model can be reproduced for other cities and regions through the recalibration of parameters from local datasets or resources.

5 Disclaimer

This paper was condensed in order to meet the requested format and guidelines. The framework for the model outlined within this study shall be considered as intellectual property and will be submitted to the appropriate party for such designation.

6 References

Ahmed, T., Sipra, H., Zahir, M., Ahmad, A., & Ahmed, M. (2022). Consumer Perception and Behavior Toward Water Supply, Demand, Water Tariff, Water

Quality, and Willingness-To-Pay: A Cross Sectional Study. *Water Resources Management*, *36*(4), 1339–1354. https://doi.org/10.1007/s11269-022-03085-5

Arden, S., Morelli, B., Cashman, S., Ma, X. (Cissy) C., Jahne, M., & Garland, J. (2021). Onsite Non-potable Reuse for Large Buildings: Environmental and Economic Suitability as a Function of Building Characteristics and Location. *Water Research*, *191*. https://doi.org/10.1016/j.watres.2020.116635

ASHRAE. (2021). *Standard 169-2021, Climatic Data for Building Design Standards*. https://ashrae-meteo.info/v2.0/

Castaneda, M. A., Mason, A., & Geursen, V. (2014). *Florida Automated Water Conservation Estimation Tool Overview*.

Cooley, H., & Gleick, P. H. (2007). Water Conservation and Efficiency. In *Encyclopedia of Life Sciences*. Wiley. https://doi.org/10.1002/9780470015902.a0003296

Dieter, C. (2018). *Water Availability and Use Science Program Estimated Use of Water in the United States in 2015*.

Fan, L., Wang, F., Liu, G., Yang, X., & Qin, W. (2014). Public perception of water consumption and its effects on water conservation behavior. *Water (Switzerland)*, *6*(6), 1771–1784. https://doi.org/10.3390/W6061771

Gilbertson, M., Hurlimann, A., & Dolnicar, S. (2011). Does water context influence behaviour and attitudes to water conservation? *Australasian Journal of Environmental Management*, *18*(1), 47–60. https://doi.org/10.1080/14486563.2011.566160

House-Peters, L. A., & Chang, H. (2011). Urban water demand modeling: Review of concepts, methods, and organizing principles. *Water Resources Research*, *47*(5). https://doi.org/10.1029/2010WR009624

International Code Council. (2021). *2021 International Water Conservation Code Provisions (IWCCP)*. I-Codes. https://codes.iccsafe.org/content/IWCCP2021P1

International Code Council. (2024a). *P157-24 Part I - Proposed Water Reuse Changes - International Plumbing Code*. https://www.iccsafe.org/products-and-services/i-codes/water-reuse/

International Code Council, Inc. (2024b). *2024 International Plumbing Code (IPC)*. https://codes.iccsafe.org/content/IPC2024V2.0

Knight, S. L., Heaney, J. P., & Morales, M. A. (2015). Flat-rate reclaimed use and savings in single-family homes. *Journal - American Water Works Association*, *107*(5), E263–E273. https://doi.org/10.5942/jawwa.2015.107.0054

Lee, E. J., Criddle, C. S., Geza, M., Cath, T. Y., & Freyberg, D. L. (2018). Decision support toolkit for integrated analysis and design of reclaimed water infrastructure. *Water Research*, *134*, 234–252. https://doi.org/10.1016/j.watres.2018.01.037

Maddaus, L. A., Maddaus, M. L., Maddaus, W. O., & Matyas, C. A. (2014). Pursuing more efficient water use: The history and future of water conservation in the United States. *Journal (American Water Works Association)*, *106*(8), 150–163. https://doi.org/10.2307/jamewatworass.106.8.150

Mannan, M., & Khan, S. A. (2022). Water Consumption and Environmental Impact of Multifamily Residential Buildings: A Life Cycle Assessment Study. *Buildings*. https://doi.org/10.3390/BUILDINGS12010048

Mayer, P. W. (2016). Water research foundation study documents water conservation potential and more efficiency in households. *Journal - American Water Works Association*, *108*(10), 31–40. https://doi.org/10.5942/jawwa.2016.108.0160

Mini, C., Hogue, T. S., & Pincetl, S. (2015). The effectiveness of water conservation measures on summer residential water use in Los Angeles, California. *Resources, Conservation and Recycling*, *94*, 136–145. https://doi.org/10.1016/j.resconrec.2014.10.005

Moglia, M., Cook, S., & Tapsuwan, S. (2018). Promoting water conservation: Where to from here? In *Water (Switzerland)* (Vol. 10, Number 11). MDPI AG. https://doi.org/10.3390/w10111510

Moncur, J. E. T. (1987). Urban water pricing and drought management. *Water Resources Research*, *23*(3), 393–398. https://doi.org/10.1029/WR023i003p00393

Sant'Ana, D., & Mazzega, P. (2018). Socioeconomic analysis of domestic water end-use consumption in the Federal District, Brazil. *Sustainable Water Resources Management*, *4*(4), 921–936. https://doi.org/10.1007/s40899-017-0186-4

Tong, Y., Fan, L., & Niu, H. (2017). Water conservation awareness and practices in households receiving improved water supply: A gender-based analysis. *Journal of Cleaner Production*, *141*, 947–955. https://doi.org/10.1016/j.jclepro.2016.09.169

Tsai, Y., Cohen, S., & Vogel, R. M. (2011). The impacts of water conservation strategies on water use: Four case studies. *Journal of the American Water Resources Association*, *47*(4), 687–701. https://doi.org/10.1111/j.1752-1688.2011.00534.x

Turner Lee, N., & West, D. M. (n.d.). *The future of data centers*. The Brookings Institution. Retrieved May 5, 2026, from https://www.brookings.edu/articles/the-future-of-data-centers/

United Nations - UN Water. (2021). *Water Scarcity*. https://www.unwater.org/water-facts/water-scarcity

Williams, K. L., Andiroglu, E., & Erkoc, M. (2026). Integrated Water Conservation Measures for Single-Family Homes: A Multi-City Assessment. *Water (Switzerland)*, *18*(8). https://doi.org/10.3390/w18080942

Willis, R. M., Stewart, R. A., Giurco, D. P., Talebpour, M. R., & Mousavinejad, A. (2013). End use water consumption in households: Impact of socio-demographic factors and efficient devices. *Journal of Cleaner Production*, *60*, 107–115. https://doi.org/10.1016/j.jclepro.2011.08.006

7 Presentation of Authors

Kyrah L. Williams is a PhD candidate at the University of Miami. Her commitment to create an equitable, sustainable future for all communities drives her focus for her studies. With a vast background covering all Architecture, Engineering, and Construction industries, Kyrah intends to continue using her skillset to create knowledge, curate experiences, and cultivate growth within the built environment.

Study on BIM and Dynamo-based Automated Life Cycle Carbon Assessment of Unit Bathrooms

Cheng-Li Cheng (1), Hui-Chien Chang (2)

(1) CCL@mail.ntust.edu.tw

(2) M11413029@mail.ntust.edu.tw

(1)(2) National Taiwan University of Science and Technology, Department of Architecture, Taiwan, R.O.C.

Abstract

In response to 2050 Net-Zero targets and Taiwan's 2025 Manual for Low-Carbon Building Assessment, this study quantifies the carbon reduction potential of Unit Bathrooms (UB) versus traditional RC methods. While traditional methods are carbon-intensive and hard to manage, this research proposes an automated evaluation model to support early-stage low-carbon decision-making. The research utilizes Dynamo to automatically extract component data from Revit models, integrating it with maintenance databases and embodied carbon coefficients. A dynamic LCA analysis prototype is established, encompassing stages from raw material production and construction transport to operational maintenance and end-of-life recycling. The study focuses on quantifying the carbon reduction achieved by UB through industrial prefabrication and material lightweighting. The results demonstrate that UB holds a distinct advantage in embodied carbon intensity, providing developers with concrete data during the early design phase to support decision-making for low-carbon building certifications.

Keywords

Unit Bathroom, Life Cycle Carbon, BIM, Dynamo

1. Introduction

Currently, the adoption and market penetration of UB in Taiwan remain significantly lower compared to international markets such as Japan. In both new construction and renovation projects, industrial inertia still favors traditional wet-trade RC construction methods, in which reinforced concrete structures and mortar-based waterproofing and tiling are cast and applied on site, as opposed to the dry-assembly approach of UB, which relies on factory-prefabricated panel components installed by bolting or clipping without on-site curing.[1] However, with the comprehensive promotion of same-floor drainage policies [2], there is a growing market focus on Building Life Cycle (BLC) benefits and maintenance performance. This trend is prompting the industry to re-evaluate bathroom system selection, particularly regarding its potential to reduce construction waste and leakage risks. The adoption rate is expected to increase further if the information gap regarding the Life Cycle Assessment (LCA) of UB can be bridged through systematic integration. This study aims to overcome the current challenges of fragmented and difficult-to-quantify carbon data. By establishing a Building Information Modeling (BIM) framework, this research digitizes and aggregates the life cycle carbon data of UB components, such as wall panels, waterproof pans, and fixtures. Utilizing Dynamo as a visual programming tool for automated information extraction, the study achieves a seamless data bridge from Revit models to carbon assessment outputs, consistent with similar Dynamo-based embodied carbon workflows reported elsewhere.[3] This dynamic evaluation model enables carbon calculation across all life cycle stages, from raw material extraction and manufacturing to transportation and end-of-life recycling.[4]

2. Material and Methods

This study focuses on the specific UB models most widely utilized in Taiwan's social housing projects.[5][6] Based on empirical data from the LCA of bathroom systems, a dedicated digital database has been established. Leveraging quantitative calculation and automated data detection technologies, this research conducts an in-depth carbon emission comparison between UB and traditional wet-trade RC construction. The focus is on analyzing the life cycle carbon intensity of both systems within identical floor areas, encompassing stages from material production and construction to operation and end-of-life.[7]

In response to digital transformation trends in the AEC (Architecture, Engineering, and Construction) industry, this study integrates BIM to develop a UB carbon emission model

with visualized parametric information, incorporating both geometric data and embedded dynamic environmental performance parameters. Dynamo visual programming scripts establish an auxiliary calculation system that streamlines data extraction, reducing the errors and time costs of traditional manual measurement or itemized entry, toward a preliminary "Automated Carbon Assessment Module."[8]

The Total Embodied Carbon (TEC) results presented were generated using this BIM-Dynamo framework; manual, spreadsheet-based calculations were performed in parallel to establish and validate the underlying carbon accounting framework, coefficients, and system boundaries.

3. Research Scope and Preliminary Assessment

The preliminary stage of this study conducted a comparative LCA assessment between UB and traditional wet-trade RC construction, as shown in Figure 1.[9]

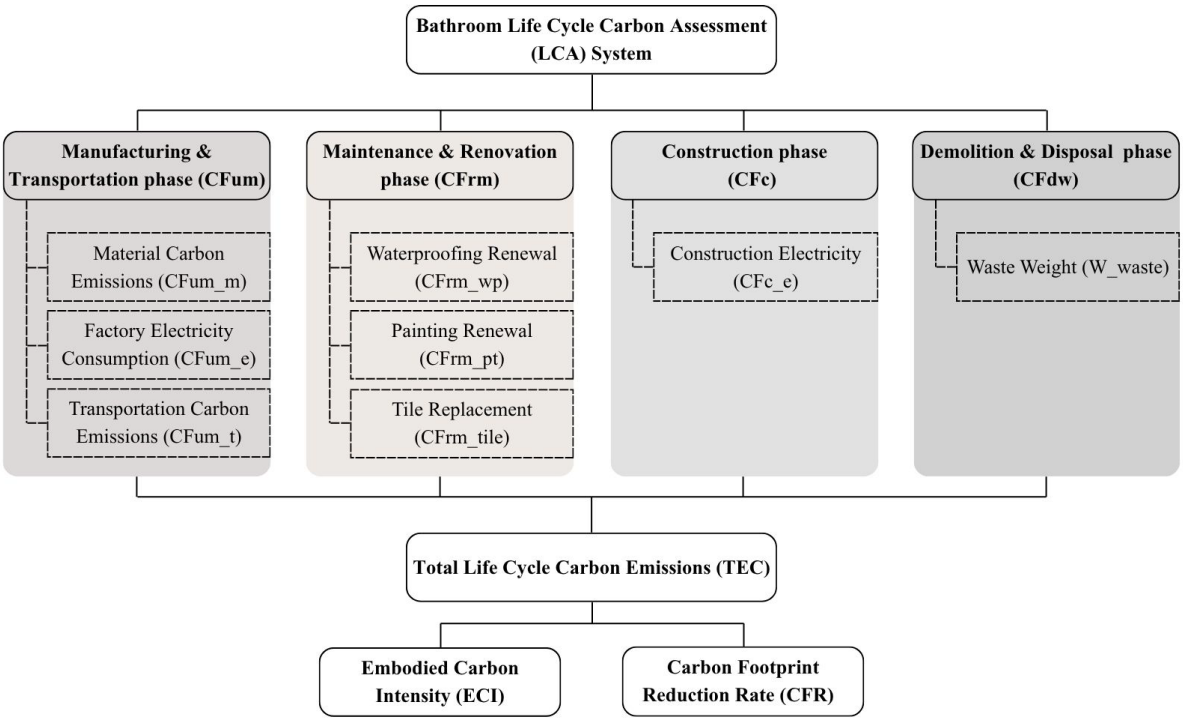

Figure 1 Preliminary Life Cycle Carbon Assessment System for Bathroom Spaces

3.1 Preliminary Carbon Emission Comparison between UB and Traditional RC Construction

The system boundaries for the calculation were primarily defined as follows: First, in the Maintenance & Renovation phase (CFrm phase), it was assumed that the industrial

prefabricated wall panels of the UB exhibit exceptional durability and modular serviceability; therefore, the model assumes no full replacement is required within a 60-year life cycle (RT_panel = 0, Replacement Times for the panel). Furthermore, the inventory focused on primary components—including wall panels, floor trays, and ceilings—estimating that the generated construction waste is only 23% of that produced by traditional bathrooms. Consequently, an ideal peak TEC reduction rate of 48.2% was achieved. This phase of research successfully validated the high potential of transitioning from 'wet-trade demolition' to 'dry-assembly' within a circular economy framework, establishing a robust academic baseline for subsequent detailed inventories of specific drainage construction methods.

3.2 Life Cycle Carbon Calculation

3.2.1 Comparison of Carbon Emissions Across Stages

Table 1 presents a comparison of the four carbon emission stages. The Manufacturing & Transportation phase (CFum phase) represents the largest gap in carbon emissions between the two construction methods. Specifically, the traditional RC bathroom accounts for 1,550.75 $kgCO_2e$, while the UB accounts for 1,020.71 $kgCO_2e$, achieving a reduction rate of 34.2%. This reflects the significant advantage of lightweight Fiber-Reinforced Plastic/Polyurethane (FRP/PU) materials over traditional brick and concrete structures in terms of manufacturing carbon emissions.

In the CFrm phase, the UB emits only 52.09 $kgCO_2e$, which is substantially lower than the 512.87 $kgCO_2e$ produced by the RC method. This disparity is attributed to the corrosion-resistant properties of UB wall panel materials and the assumption that the entire unit does not require replacement within a 60-year life cycle. While the absolute values for the Demolition & Disposal phase (CFdw phase) are relatively small for both systems, the proportional differences remain significant.

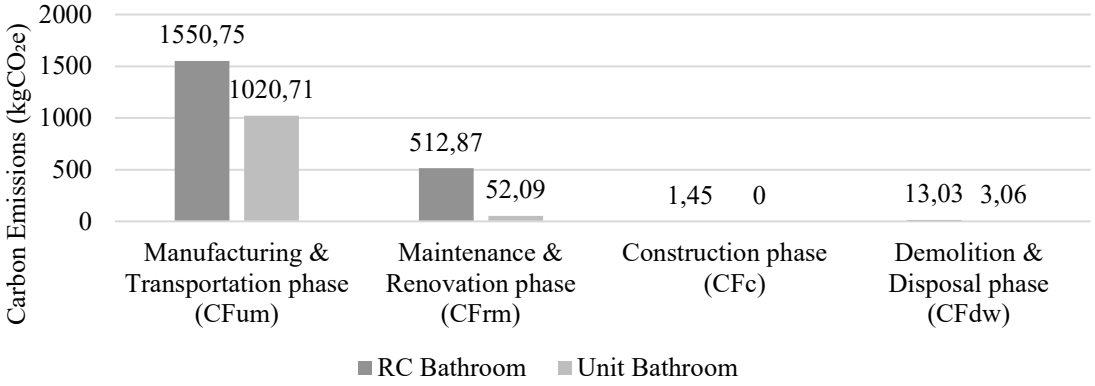

Table 1 Comparison of carbon emissions at different stages: Traditional vs. Unit Bathrooms

3.2.2 Life Cycle Carbon Emission Composition

Table 2 presents the proportional TEC composition by stage. The RC bathroom's TEC (2,078.10 $kgCO_2e$) is nearly double that of the UB (1,075.88 $kgCO_2e$), a 48.2% reduction. RC emissions concentrate heavily in the CFum phase (74.6%), reflecting the dominant burden of material manufacturing for traditional brickwork and concrete. In contrast, the UB's CFrm accounts for only 4.8%—far below RC's 24.7%—underscoring the UB's carbon advantage during operation and maintenance and yielding a more balanced life cycle emission structure.

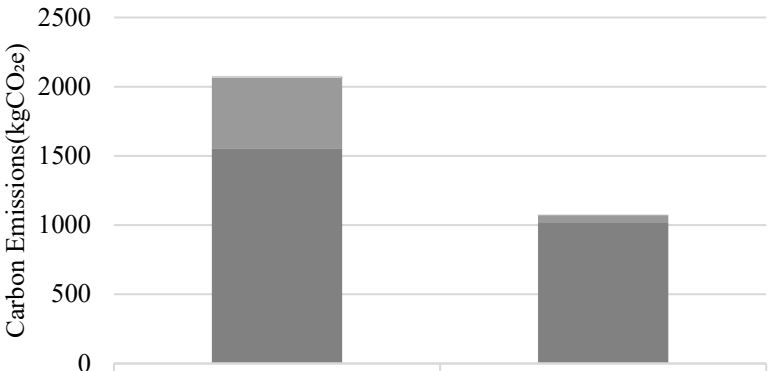

	RC Bathroom	Unit Bathroom
CFdw	13,03	3,06
CFc	1,45	0
CFrm	512,87	52,09
CFum	1550,75	1020,71

Table 2 Comparison of Life Cycle Carbon Emission Composition: Traditional vs. Unit Bathrooms

3.2.3 Analysis of Carbon Reduction Rates Across Stages

Table 3 presents the carbon reduction rates of UB relative to RC for each stage. The Construction phase (CFc phase) exhibits the highest reduction rate at 100%, as the electricity consumed during UB factory manufacturing is categorized under the A3 Manufacturing stage, leaving only on-site hoisting, resulting in CFc tends to 0.

The CFrm phase achieves a reduction rate of 89.8%, primarily because the UB wall panels do not require full replacement within a 60-year life cycle. For the CFdw phase, the reduction rate is 76.5%, reflecting that the waste weight of lightweight FRP/PU components (318 kg) is only 23% of that generated by traditional brickwork (1,358 kg).

The CFum phase shows a reduction rate of 34.2%. Synthesizing all four stages, the TEC achieves an overall reduction rate of 48.2%, demonstrating that Unit Bathrooms possess a consistent carbon emission advantage across all stages of the life cycle.

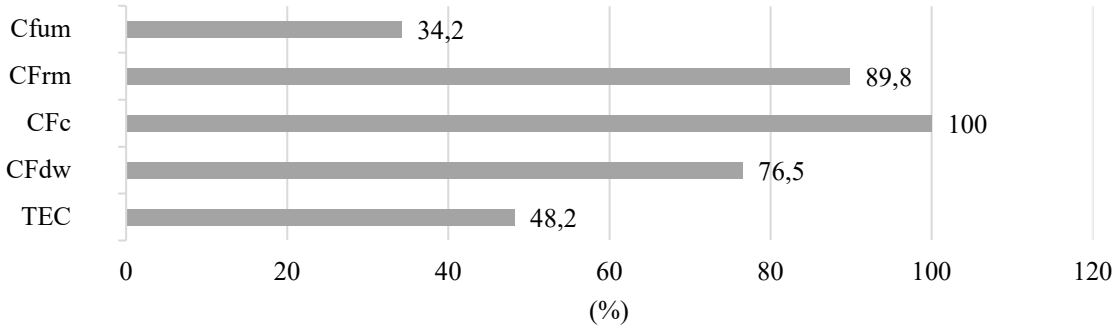

Table 3 Analysis of carbon reduction rates at each stage of UB

4. Optimized LCA Model and Automated Framework

To better reflect the current state of construction practice and enhance data precision, this stage of the research continues to apply the BIM-Dynamo automated framework to an optimized LCA model, introducing significant refinements to the system boundaries.

4.1 Refinement of Calculation Boundaries and Granular Construction Classification

In contrast to the idealized assumptions made in the preliminary study (see Section 3.1), the following adjustments have been implemented:

- Integration of Sanitary Fixtures and Piping: Rather than treating fixtures as common constants, this model fully incorporates various grades of toilets, washbasins, and water supply/drainage piping into the inventory to ensure the integrity and closure of the TEC values.

- Granular Classification of Drainage Methods: The research further categorizes the assembly into five detailed construction types: Elevated System, Elevated Dry Construction, Sunken Slab Method, Sunken Slab with Dry Construction, and Prewall System.

Through these boundary expansions and weighting refinements, this study aims to provide developers and engineers with a more reliable, quantitative basis for low-carbon decision-making when selecting between different drainage strategies.

4.2 Comparative Analysis of Carbon Emission Intensity for Various Material Combinations and Construction Methods

Based on the 1624 configuration (denoting a UB module with net clear-space plan dimensions of 1600 mm × 2400 mm, following the industry's four-digit sizing convention) results, Table 4 illustrates Embodied Carbon Intensity (ECI) trends across five drainage methods. The Prewall method consistently yields the lowest carbon intensity, achieving a minimum of 195 $kgCO_2e/m^2$ when paired with pre-painted steel and microcrystalline stone panels. Conversely, Precast High-strength Concrete (PHC) composite panels combined with the Sunken Slab Method result in the highest ECI (750 $kgCO_2e/m^2$), underscoring the heavy environmental burden of high-mass components and structural backfilling. The linear trend indicates a steady emission increase as materials shift from lightweight steel to heavy concrete, providing designers with essential quantitative evidence for low-carbon material selection during early project stages.

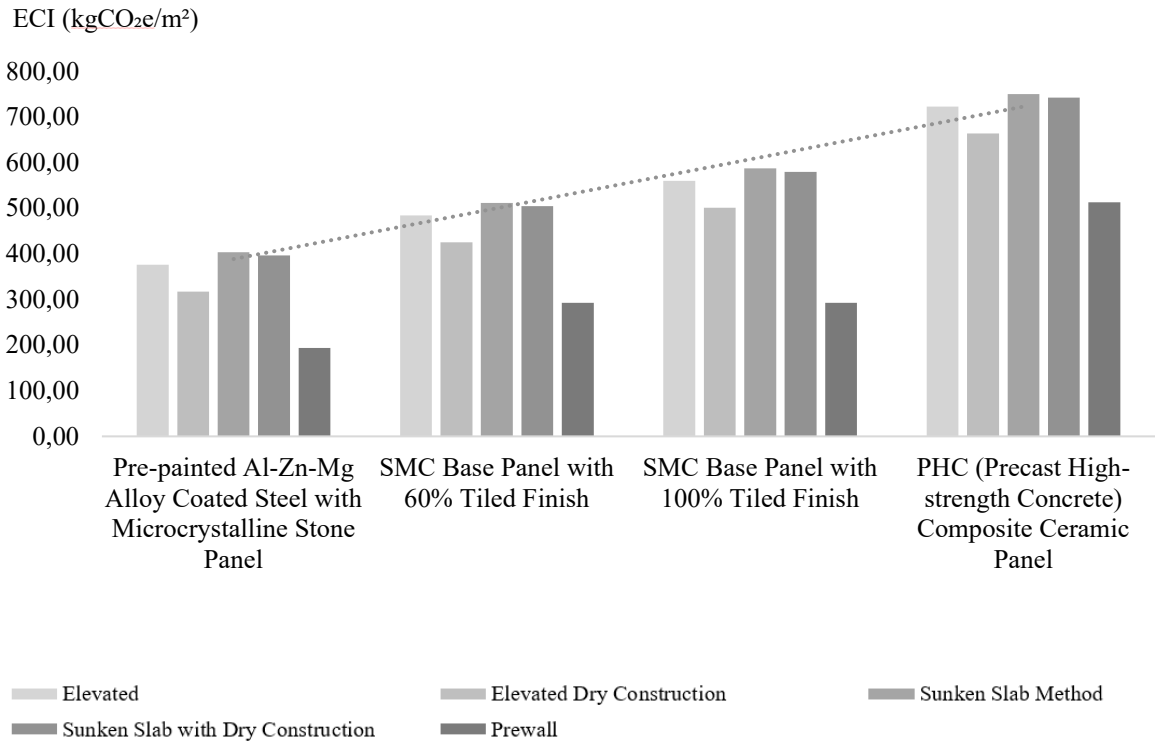

Table 4 Comparison of ECI for Various UB Material Combinations and Construction Methods

(Size Configurations:1624)

4.3 Detailed Analysis of Carbon Emission Composition for Various Drainage Methods

Regarding the 1421 configuration (denoting a UB module with net clear-space plan dimensions of 1400 mm × 2100 mm), Table 5 details the relationship between life cycle stages and TEC. The Prewall method achieves the lowest TEC (1,240.69 kgCO_2e), representing a 36% reduction compared to the Sunken Slab Method (1,942.51 kgCO_2e). Across all methods, the CFum phase is the primary emission source. Notably, Dry Construction—in both elevated and sunken configurations—results in near-zero CFc emissions, validating the efficiency of dry assembly. Furthermore, the Prewall method excels in the CFrm phase with only 314.41 kgCO_2e, outperforming other methods due to superior pipeline accessibility and higher component modularization.

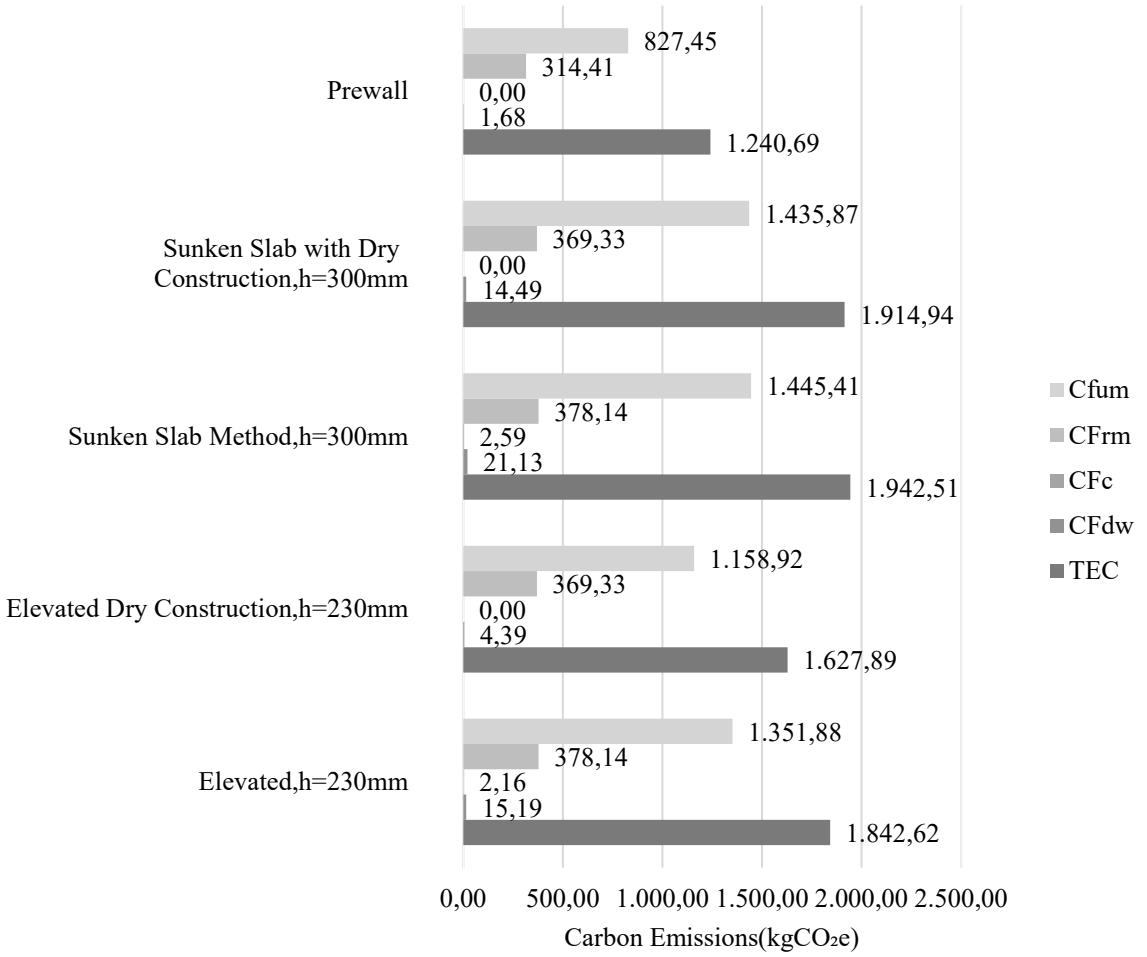

Table 5 Carbon Emission Composition Analysis of Various Construction Methods (Size Configurations:1421)

5. Carbon Emission Comparison of Bathroom Systems and BIM Integration

5.1 Life Cycle Carbon Calculation System for Bathroom Spaces

This section details the automated workflow used to generate the above results (Figure 2). Integrating BIM with Dynamo, the system performs real-time carbon assessments, replacing the manual measurement and itemized entry described in Section 2, via a dynamic database of emission factors, component life cycles, and replacement frequencies that lets calculation boundaries be flexibly adjusted per research setting.

Using Dynamo and Python, this study builds a single-platform tool for real-time carbon calculation. Geometric data—wall, ceiling, and floor areas—are extracted from Revit 2024 models to compute emissions across four life cycle stages. Resulting TEC, ECI, and Carbon Footprint Reduction Ratio (CFR) values are written back into Revit room parameters for immediate inspection and rapid analysis.

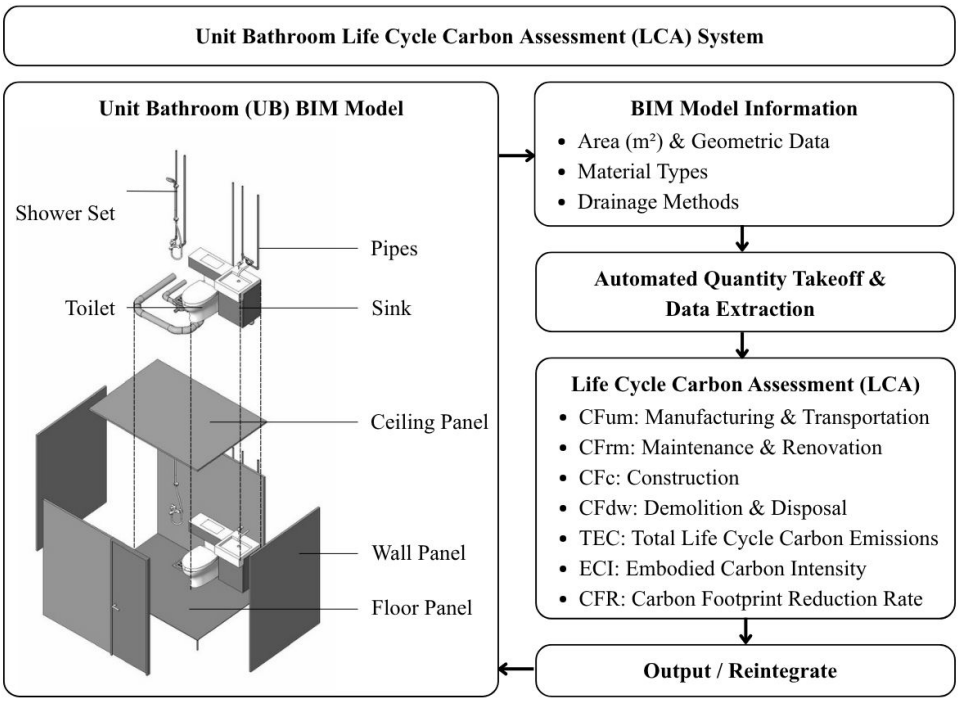

Figure 2 Relates to the Simulation value and the Actual value

5.2 BIM and Dynamo Operational Workflow

The workflow integrates BIM and Dynamo visual programming across five distinct stages: Information Gathering, Modeling, Parameter Setting, Automated Calculation, and Visualized Output, as illustrated in Figure 3.

- **Information Gathering Phase**: Consolidates material compositions, construction sequences, and energy data for UB and RC methods as the emission database basis.
- **Modeling Phase**: Revit 2024 models are built for both methods, with geometry matched to actual floor plans for accurate area extraction.
- **Parameter Setting Phase**: Carbon output fields link PLCC_Database coefficients and replacement parameters to family/room components.

- **Automated Calculation Phase**: Dynamo Python nodes read geometric areas to execute weight conversions and four-stage calculations without manual input.
- **Visualized Output Phase**: Results export to Excel and write back to Revit parameters for immediate review and fewer errors.

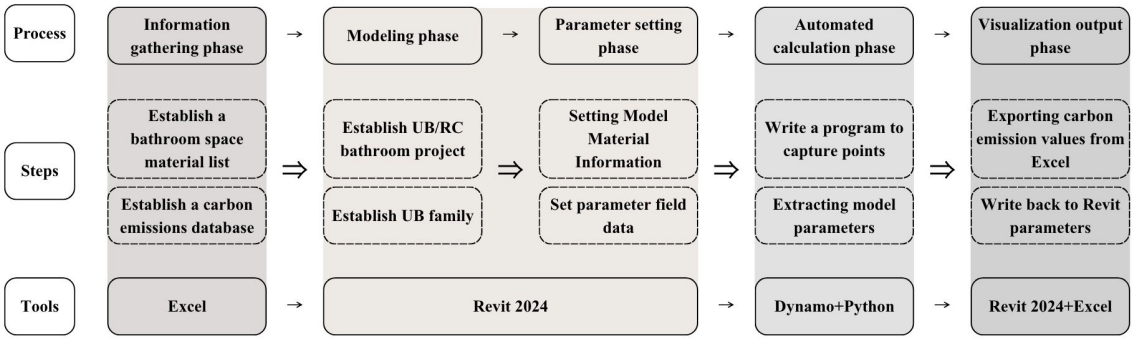

Figure 3 Relates to the Simulation value and the Actual value

6. Conclusion

This study integrates BIM with Dynamo visual programming to establish an automated Life Cycle Carbon Assessment (LCA) framework. By extracting geometric information from Revit models and linking it to a dynamic database for real-time calculation, the system overcomes the time-consuming, error-prone nature of manual methods, offering an efficient early-design decision-making tool. Results show UB achieves significant carbon reduction over traditional RC methods, up to 48.2% overall. CFc phase emissions for dry construction are nearly zero, and the Prewall system performs best across all life cycle stages, cutting total emissions by 36% versus the Sunken Slab method—validating the critical role of industrial prefabrication and lightweight materials. These quantitative models directly support Taiwan's 2050 Net-Zero roadmap and the Manual for Low-Carbon Building Assessment, letting developers and architects precisely evaluate drainage methods and material combinations at the early design stage, optimizing low-carbon decisions and advancing the industry toward a sustainable circular economy.

7. References

[1] Taiwan Association for Industry of Unit Bathroom. White Paper on Taiwan’s Unit Bathroom Industry. Taiwan Association for Industry of Unit Bathroom, TW, 2025

[2] Cheng-Li Cheng et al. Study on the Standardization and Technical Specification Revision of Same Floor Drainage Method in Collective Housing. Architecture and Building Research Institute, Ministry of the Interior, TW, 2020

[3] Chia-Chun Chang. Study on the Optimization and Evaluation of Drainage System Planning in Residential Building Integrated with BIM. Unpublished master's thesis, NTUST, TW, 2025

[4] Hsien-Te Lin et al. Manual of Low Embodied-carbon Building Rating System. Architecture and Building Research Institute, Ministry of the Interior, TW, 2025

[5] Shyh-Meng Huang et al. Investigation on Key Technologies and Construction Methods of Unit Bathrooms in Residential Buildings. Architecture and Building Research Institute, Ministry of the Interior, TW, 2022

[6] Chen-Yuan Lo. Study on the Performance Evaluation System of Unit Bathrooms for Residential Building. Unpublished master's thesis, NTUST, TW, 2024

[7] Kung-Jen Tu et al. Survey and analysis of maintenance performance of residential bathroom systems. Architecture and Building Research Institute, Ministry of the Interior, TW, 2004

[8] Chiung-Jui Chen. Study on the Application and Feasibility of Same Floor Drain System in Residential Buildings. Unpublished master's thesis, NTUST, TW, 2019

[9] Chih-Yung Huang. Study on the Comparison of Greenhouse Gas Emissions between the Prefabricated Bathroom Unit and the Traditional Bathroom during the Construction and Remodeling Phase. Unpublished master's thesis, NKUST, TW, 2018

8. Presentation of Authors

Cheng, Cheng-Li is a Professor at National Taiwan University of Science and Technology, Department of Architecture. He is a research scholar for water supply and drainage in building. He has published extensively on a range of sustainable issues, including water and energy conservation for green buildings.

Chang, Hui-Chien holds a master's in the Department of Architecture from NTUST. Her recent research is focused on BIM-based automated life cycle carbon assessment for bathroom spaces.

Planning Case Study and Verification of a Research Facility Aimed at Achieving a Net-Zero Water Building

Takeshi Aoi (1), Masayuki Otsuka (2), Anna Fujita (3)

(1) takeshi.aoi@nikken.jp
(2) dmotsuka@kanto-gakuin.ac.jp
(3) fujita.anna@nikken.jp

(1) Associate, Mechanical Engineer Group, Nikken Sekkei Ltd.
(2) Prof. Dr. Eng., Department of Architecture and Environmental Design,
College of Architecture and Environmental Design, Kanto Gakuin University, Japan
(3) Staff, Sustainable Design Group, Nikken Sekkei Ltd.

Abstract

Global concerns over access to water have been intensifying, with the situation particularly acute in Asia and Africa. According to the United Nations World Water Development Report (2018), more than half of the world's population (57%) is expected to face water scarcity and water insecurity by 2050. Against this backdrop, global interest in achieving Net-zero water buildings (NZWB) is increasing. The authors presented, at the CIBW062 International Symposium (held in the United Kingdom in 2024), an investigation into NZWB trends and evaluation methods in various countries, together with a portion of the survey results from a research facility project pursuing NZWB. [1)]
This paper focuses on the same research facility project and describes two distinctive initiatives adopted to achieve NZWB: cascade treatment of wastewater to substantially improve the water circulation rate, and architectural planning approaches designed to promote infiltration and recharge of rainwater into the soil. In addition, to verify the achievement status of NZWB, we report the results of field measurements conducted over a three-year period after completion, as well as the NZWB evaluation method.

Keywords

Net-Zero Water Building (NZWB); reclaimed water use; stormwater infiltration and groundwater recharge; cascade wastewater treatment

1. Introduction

Kurita Water Industries Ltd., the owner of the target research facility, is one of Japan's leading companies in water-related businesses, including water treatment systems and ultrapure water supply. With the aim of reorganizing its major sites and promoting open innovation, Kurita constructed the Kurita Innovation Hub (KIH), which consolidates research functions and technical training functions. This facility represents a case in which effective water use was pursued alongside energy conservation, with the overall objective of minimizing environmental impacts.

As detailed measures to improve the efficiency of water treatment systems, the facility was planned and equipped with a piping and drainage system that enables wastewater segregation according to pollutant load. In addition, external rainwater conveyance piping and a large-scale infiltration tank were installed to promote stormwater infiltration and groundwater recharge. Water sources and wastewater streams associated with utility systems (e.g., heat-source systems) were also planned as integral components of the on-site water cycle. This paper presents the measured evaluation results of the reductions in water use and energy consumption achieved through these measures.

2. Building Overview

The project site was selected in Akishima City, Tokyo, which is well known as a "water-circulation city." In Akishima, a municipal water supply system based on groundwater as the source water has been developed. In addition, the city has established guidelines requiring that rainfall be infiltrated and returned to the water source, and it is actively engaged in protecting water resources and restoring biodiversity. Furthermore, by combining Kurita Water Industries' water treatment technologies with Nikken Sekkei's design expertise, a research facility that contributes to the regional water cycle was realized. Figure 1 presents an overall aerial view of the facility, and Figure 2 shows the building configuration.

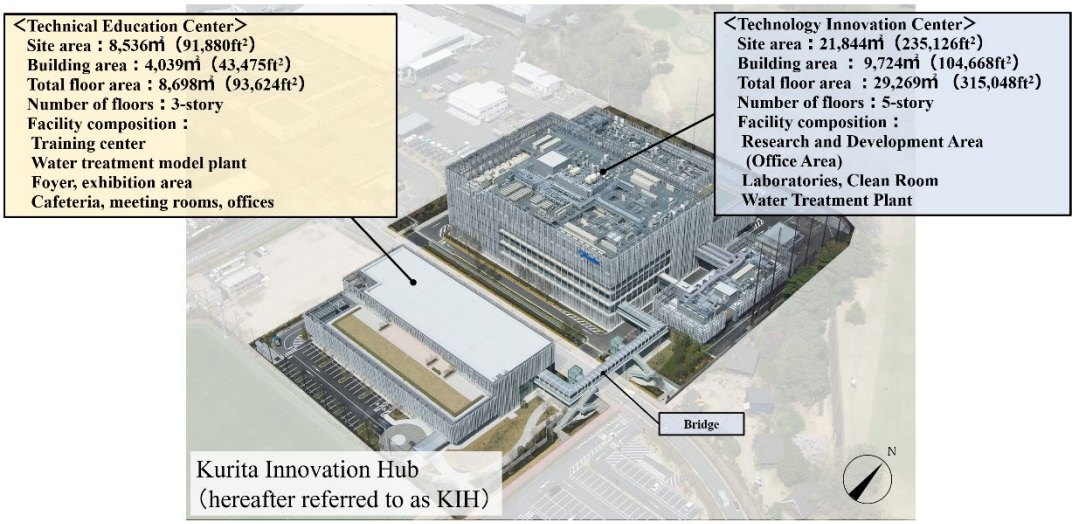

Figure 1 - Facility Overview and Architectural Summary

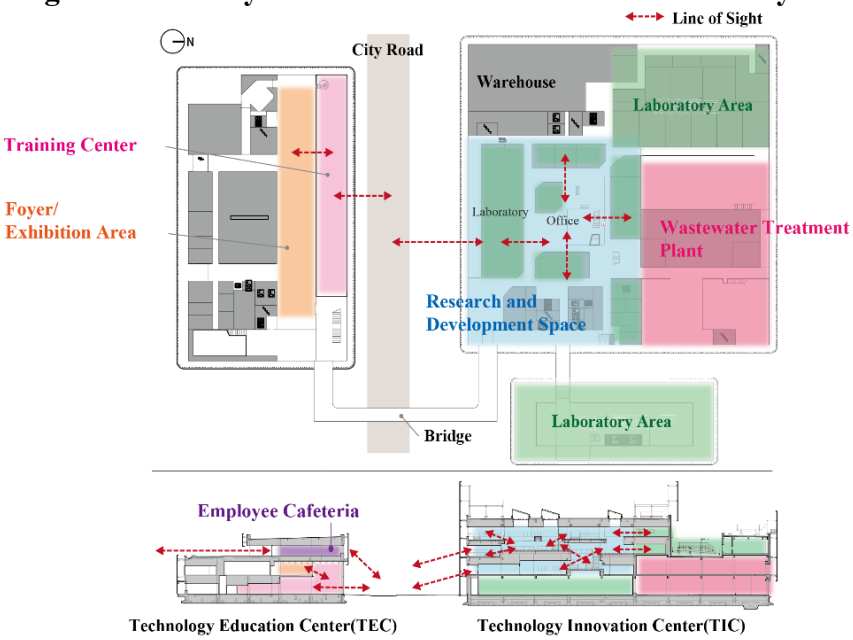

Figure 2 - Building configuration (elevation and section)

3. Measures to Improve the Water Circulation Rate and Energy Efficiency

3.1 Spatial Configuration and Adopted Environmental Technologies

Based on two core concepts—(i) “a water circulation system that contributes to the local community” and (ii) “a system that achieves energy saving and carbon neutrality while maintaining safety”—the project implemented the environmental technologies shown in Figure 3. As part of the energy-saving and carbon-neutral strategy, the facility was planned to cover 100% of its electricity consumption with green electricity generated from renewable energy sources, thereby achieving net-zero emissions for purchased electricity. In addition, assuming that safety requirements for a research facility must be ensured, new energy-saving measures were introduced.

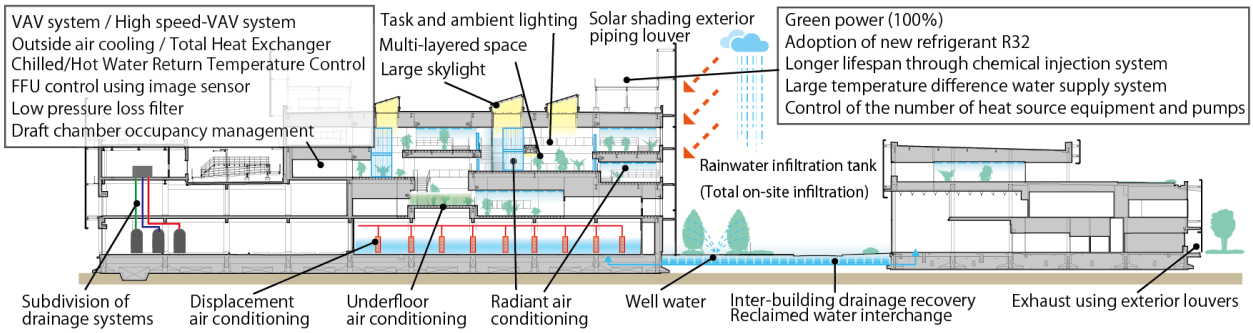

Figure 3 - Overview of Adopted Environmental Technologies

3.2 Water Circulation System Contributing to the Local Community

To realize an NZWB, the facility referenced two evaluation frameworks: (i) the approach proposed by the U.S. Department of Energy (USDE; hereafter USDE)[2] and (ii) LEED Zero Water in the LEED Zero Program Guide proposed by the U.S. Green Building Council (USGBC) (hereafter LEED-ZW).[3] Based on these references, three measures were implemented.

3.2.1 Water conservation through high-efficiency sanitary fixtures

To reduce indoor water use, the project adopted water-saving fixtures that are available as domestic products, including water closets with a flush volume of 5.5 L/flush, urinals with a flush volume of 1.0–2.0 L/flush, and washbasins equipped with automatic faucets.

3.2.2 Installation of a Large-Scale Infiltration Tank

To infiltrate all rainfall falling within the site, a large-scale infiltration tank with a capacity of approximately 1,617 m³ was installed on the premises. Together with newly developed green areas, the system was designed to infiltrate rainfall with an intensity of 78 mm/h within the site (Figure 4). The large-scale infiltration tank is composed of infiltration sheets and stacked plastic structural units, which increase the void ratio and enable a large volume of rainwater to be infiltrated with a relatively small footprint (Figure 5). In addition, for the rain gutters, part of the metal piping adopted for the building exterior—intended to evoke the corporate identity as a water-related company—was repurposed by adding gutter functionality (Figure 6). Through these measures, the system suppresses discharge to the public sewer and also contributes to reducing the treatment load at wastewater treatment plants.

3.2.3 Water Treatment and Reuse

A plant for producing ultrapure water for research purposes was installed in this facility. The plant was configured by improving the conventional system and adopting a cascade

treatment scheme in which treatment processes are differentiated according to wastewater pollutant load, thereby reducing both energy and water consumption (Figure 7).

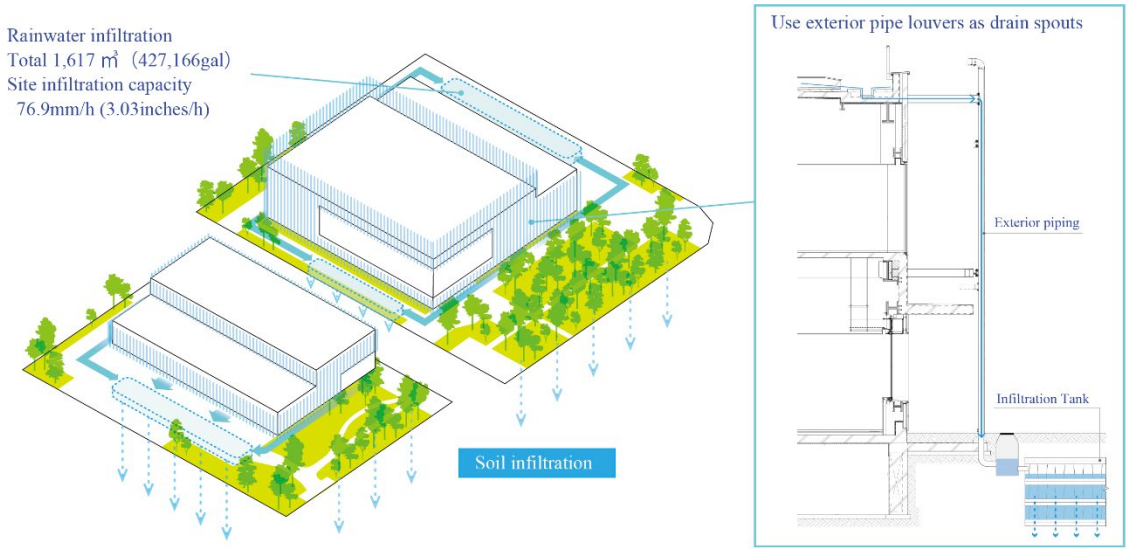

Figure 4 - Replenishing Groundwater via Rainwater Retention

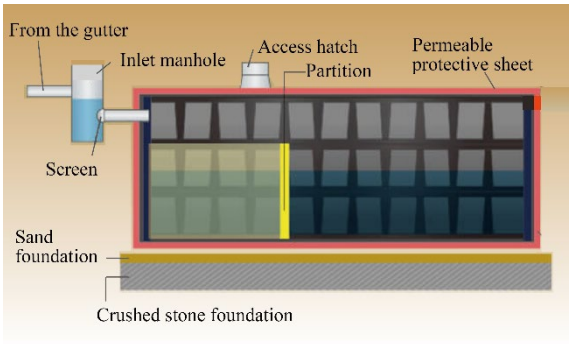

Figure 5 - Infiltration Tank

Figure 6 - Using Exterior Piping as Rain Gutters

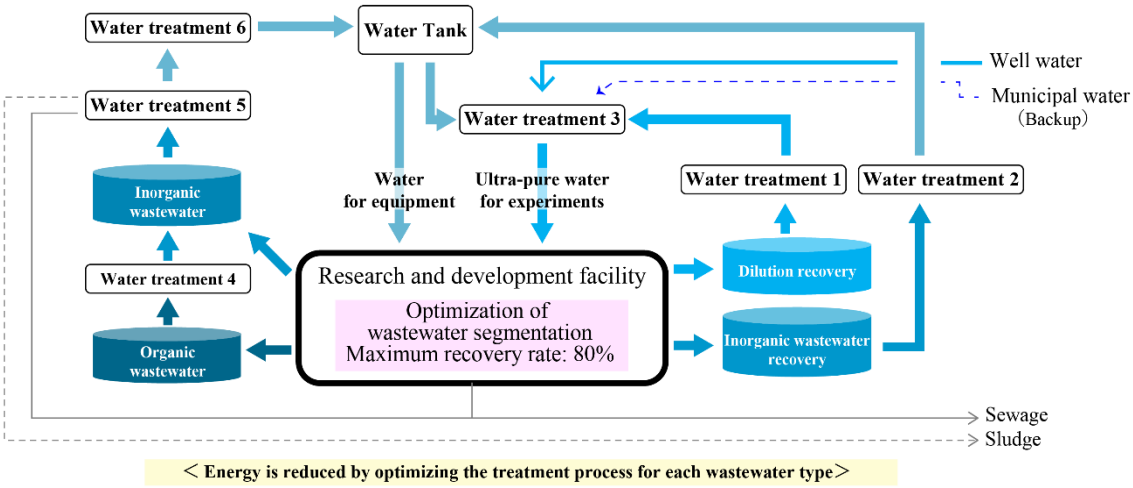

Figure 7 - Optimizing Treatment Processes Based on Wastewater Types

On the building side, six dedicated wastewater piping networks were provided for each treatment process to accommodate the cascade treatment scheme (Figure 8). In addition, reverse-osmosis (RO) permeate—which had previously been surplus during the ultrapure water production process—was effectively reused, with water quality compliant with Japanese standards, as water for toilet flushing, utility/process water for building services, and a source water for humidification.

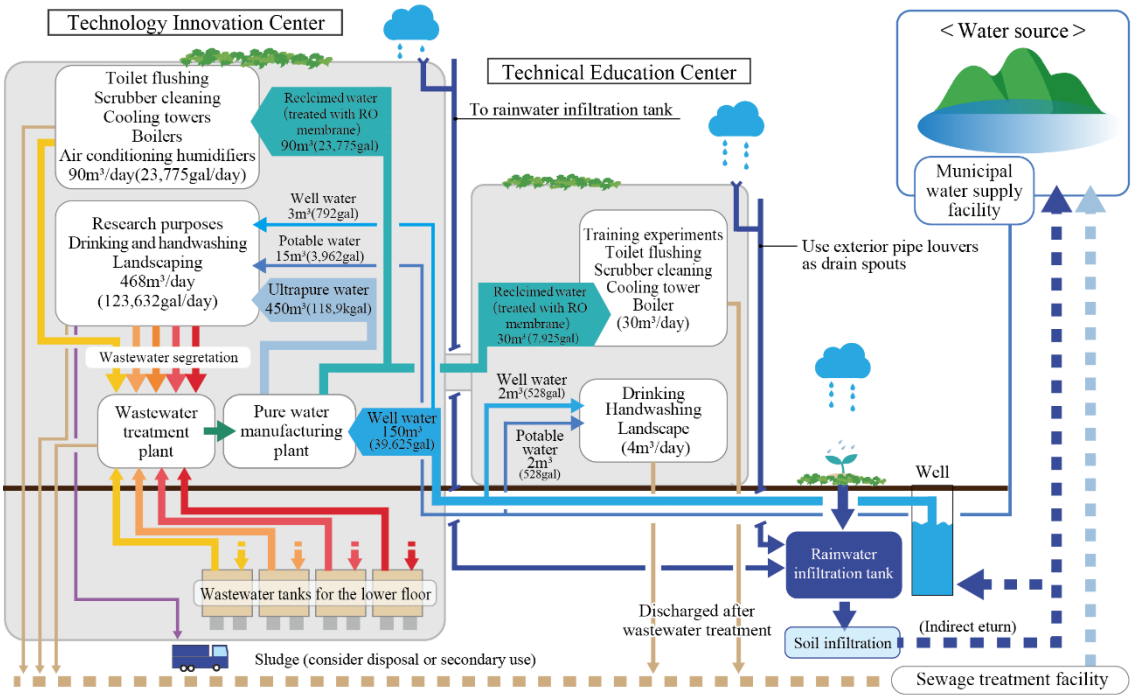

Figure 8 - The Water Circulation Flow in the Site and Building

3.3 Heat-Source System and Condensate / Wastewater Recovery Measures

To actively utilize green electricity, the heat-source system was designed as a predominantly electric system combining air-cooled heat-pump chillers and turbo chillers. All make-up water for the heat-source equipment was supplied using reclaimed water, and all generated condensate and wastewater streams—including condensate and cooling tower blowdown—were recovered and reused (Figure 9).

For wastewater recovery, laboratory sinks were designated according to wastewater quality categories to ensure correct segregation. To prevent user carelessness and enable error-free collection, color-coded labels were provided on the side panels of each laboratory sink (Figure 10). In the event of human error in which wastewater is discharged to an incorrect destination, the plant's primary treatment line is planned to detect wastewater cleanliness and, based on automatic detection, route the flow to the appropriate treatment process.

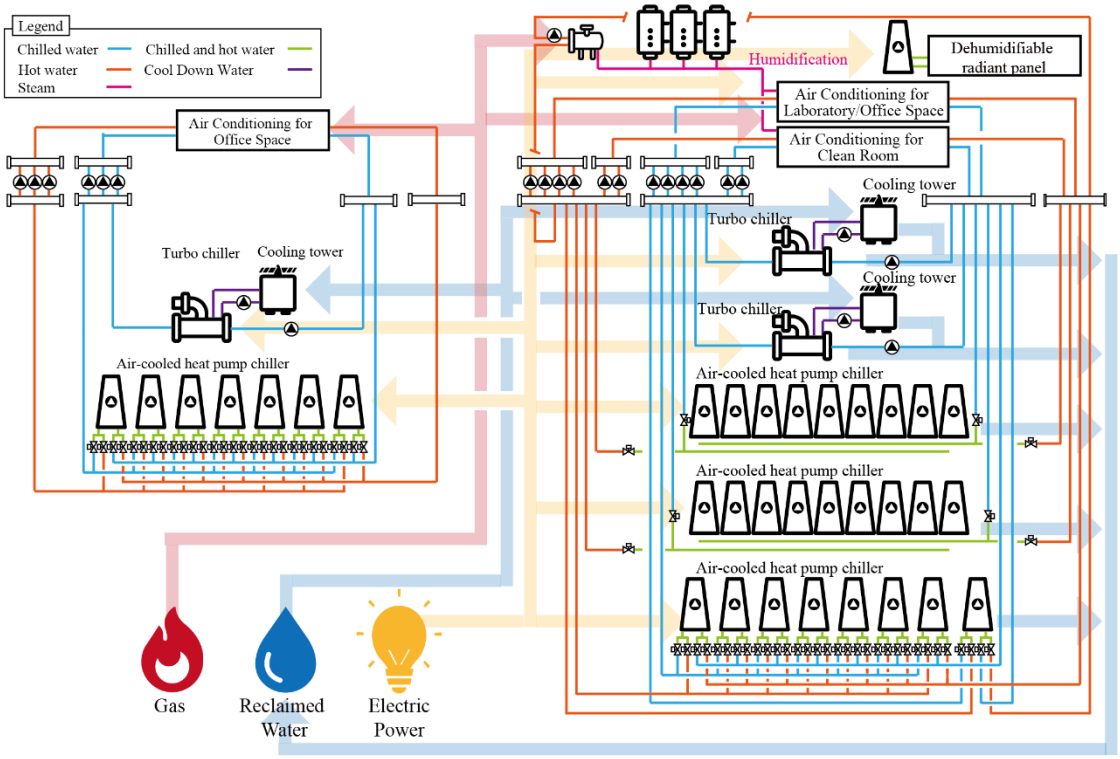

Figure 9 - Heat Source Configuration

Figure 10 - Experimental Operation and Measures to Mitigate Human Error

3.4 Metering and Monitoring System

Figure 11 shows the conceptual diagram of the monitoring system. Water use is planned to be metered at 126 locations on the building side, including supply points from the infrastructure and discharge points. In addition, dedicated flow meters will be installed in the water treatment plant to manage and monitor the system, and measurements will be conducted separately for the building and the plant.

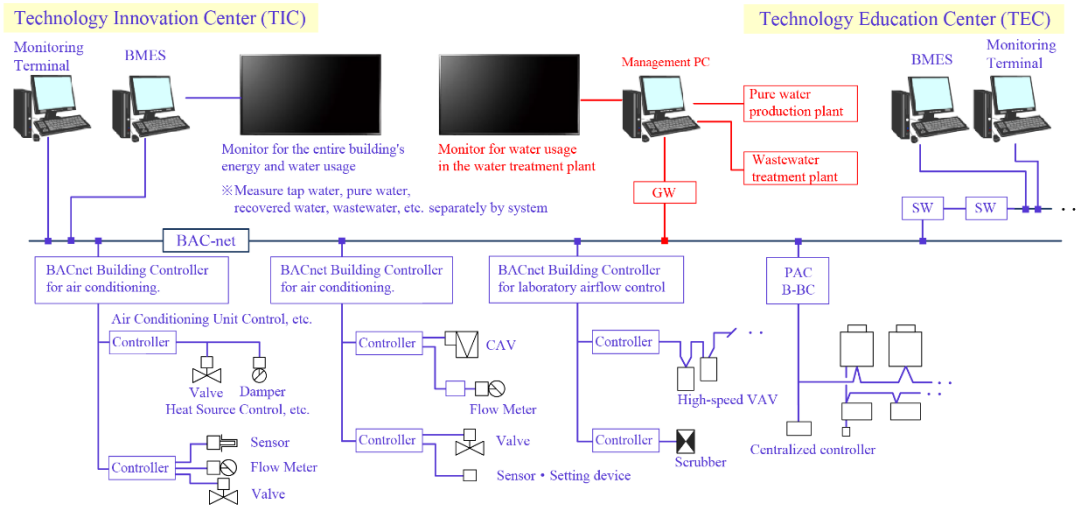

Figure 11 - Outline of the Building and Water Treatment Plant Monitoring System

4. Calculation Methods and Measurement Periods for Each Evaluation Metric

As in the previous report,[1]) the NZWB achievement rate is calculated using two evaluation equations—those of LEED-ZW and USDE—as shown in Table 1. For estimating the amount of returned water used in the NZWB evaluation, monthly precipitation data published by the Japan Meteorological Agency (JMA) were used, adopting the station closest to the facility site (Hachioji).[4)] In addition, the potable water substitution rate was measured, and the results were compared with water-use intensity benchmarks for research laboratory facilities of a similar scale in Japan.

Table 1 - Formulae for calculating NZWB evaluation

	Item	USDE	LEED Zero
Formula	NZWB rating formula	Formula(1): $\left(\frac{(③+④)+⑤}{①+②+③+④}\right)\times 100$	Formula(2): $\left(\frac{(③+④)+⑤}{①+②}\right)\times 100$
	Portable water replacement rate	Formula(3): $\left(1-\frac{①}{①+②+③+④}\right)\times 100$	$\left(1-\frac{①}{①+②}\right)\times 100$

Annotation: ① Potable water; ② Well water; ③ Reclaimed water (i.e., recycled water); ④ Ultrapure water; ⑤ Returned water

5. Measured Results and Discussion

5.1 Monthly Trends in Each Evaluation Metric

As shown in Figure 12, the values exceeded 100% in every month, indicating that the NZWB target was achieved. In addition, the potable water substitution rate was 93.4% ± 1.1%, while the discharge rate to the public sewer system was 28.8% ± 2.0%. These

results confirm that dependence on municipal water supply and sewerage was substantially reduced and that on-site water circulation was enhanced.

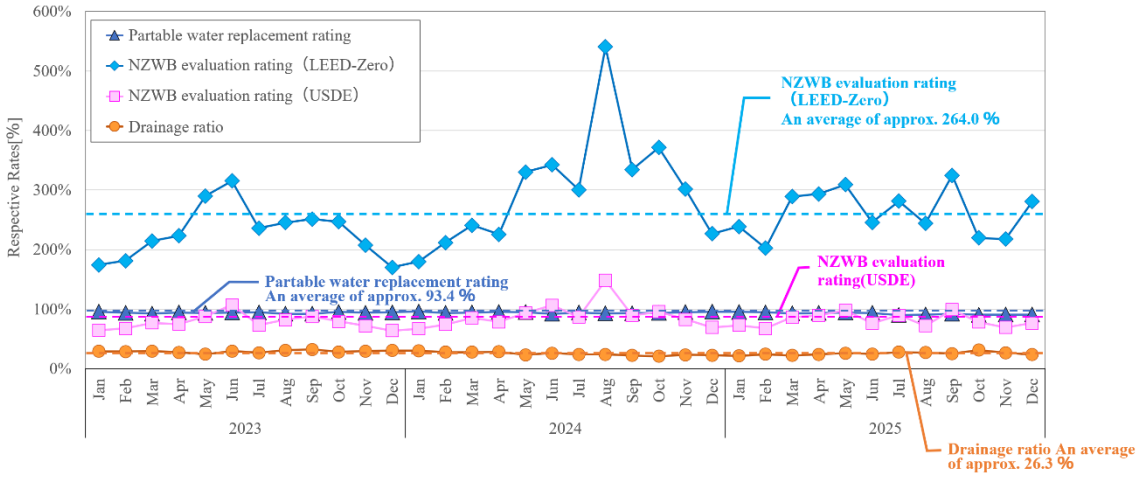

Figure 12 - Monthly changes in water substitution rate, NZWB score, and drainage rate from 2023 to 2025

5.2 Comparison of Potable Water Use Intensity

Because the target research facility is more specialized in water use than typical research facilities, Figure 13 presents potable water use per unit floor area to enable comparison with other facilities. In the same figure, potable water use data for other research institutions were extracted from the publicly available database published by DECC [5)]. Based on these data, the maximum potable water use intensity was approximately 130 $m^3/(m^2 \cdot year)$, the average was approximately 1.1 $m^3/(m^2 \cdot year)$, and the minimum was approximately 0.02 $m^3/(m^2 \cdot year)$. Excluding the maximum value, approximately 99.8% of research institutions were below 3.5 $m^3/(m^2 \cdot year)$.

For reference, although it is a different building use, the average potable water use intensity for office buildings was approximately 0.70 $m^3/(m^2 \cdot year)$, which is lower than the average for research facilities. This is presumably because research institutions use a larger amount of water for research activities than offices. However, the 2023 measured value for the target research facility was approximately 0.46 $m^3/(m^2 \cdot year)$, which is lower than both the average for research institutions and that for offices. Therefore, potable water use in the target facility is considered to be low, and the use of substitute water and returned water is presumed to contribute to improving the NZWB achievement rate.

5.3 Annual Energy Consumption and Annual Water Savings

Annual energy consumption was 4,160 $MJ/(m^2 \cdot year)$, compared with the baseline

primary energy consumption of 5,250 MJ/(m²·year) (a value derived using the simulation method specified under Japan's Energy Conservation Act), representing an energy reduction of approximately 20% (Figure 14). The absolute amount of energy reduced exceeded 590 MJ/(m²·year), which is the reduction target for office buildings aiming to achieve ZEB, confirming that the measures implemented in this facility were more effective.

With respect to water consumption, NZWB-related measures resulted in an estimated reduction of 43,500 m³ in annual water consumption compared with a typical research laboratory facility (Figure 15). When combined with the volume of rainwater returned to the ground through soil infiltration, it was confirmed that the facility achieved NZWB (LEED-ZW) also in the annual evaluation.

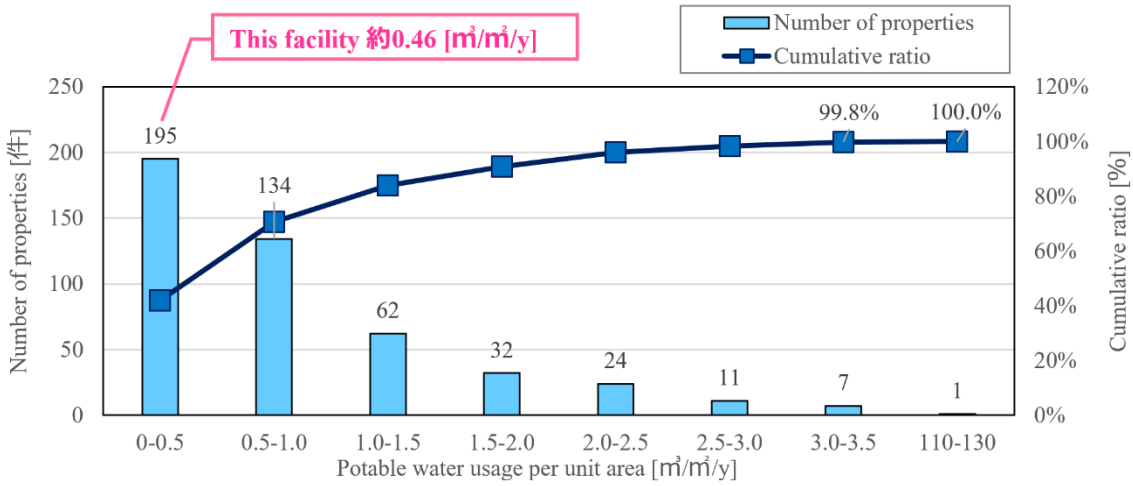

Figure 13 - Comparison with Water Use Intensity Benchmarks for Research Facilities

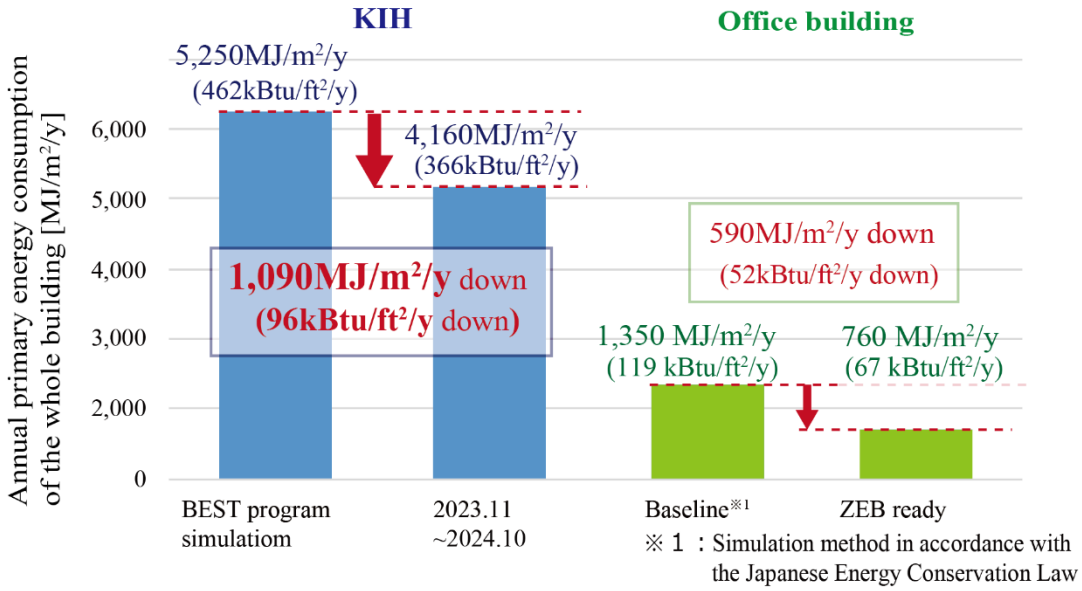

Figure 14 - Comparison of Annual Energy Consumption

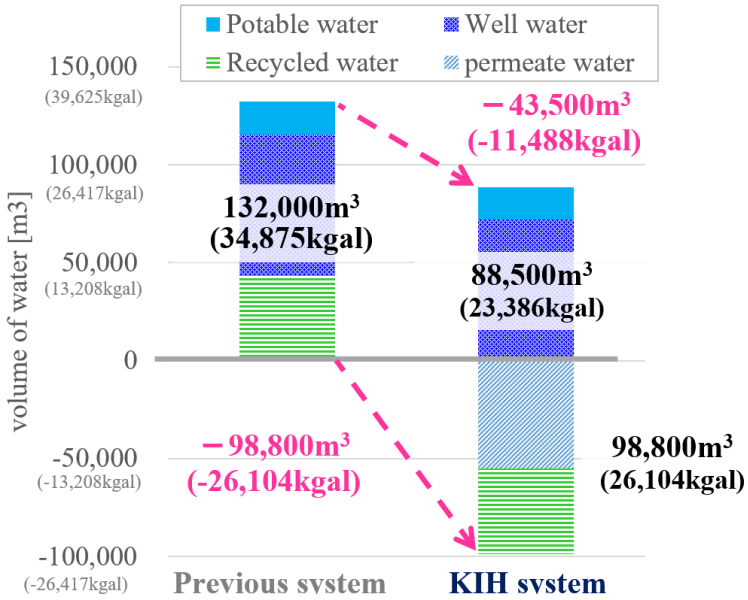

Figure 15 - Water Savings from Achieving NZWB

6. Cost-Effectiveness and Contribution to Decarbonization

The incremental investment cost for implementing energy-saving technologies and water resource-saving technologies was JPY 1,500 million (USD 10,000,000), while the reduction in running costs was 115,676 thousand JPY (USD 771,177). Accordingly, the simple payback period was approximately 10.4 years.

Regarding water resource savings, it was confirmed that the annual running cost can be reduced by 28,996 thousand JPY/year by effectively reusing, within the building, RO permeate from the water treatment plant that had previously been disposed of as surplus. In addition, when comparing CO_2 emissions including those associated with potable water supply and sewerage infrastructure, it was confirmed that the measures contribute to an annual reduction of 30.5 t-CO_2/year.

7. Conclusion

In this project, we challenged the NZWB target by developing a water-circulation-oriented building that leverages local conditions, and post-occupancy investigations of water use confirmed that NZWB performance has been achieved. In addition, with consideration for carbon neutrality, the facility adopted energy-saving technologies and a metering/monitoring system tailored to the requirements of a research laboratory, realizing a research facility that achieves substantial reductions in both energy consumption and water use.

8. Acknowledgement

The authors of this report wish to thank the staff of Kurita Water Industries Ltd. for their involvement and generous support in conducting this study, including providing information regarding the “Kurita Innovation Hub”.

9. References

1) Anna Fujita, Masayuki Otsuka, Takeshi Aoi, Global Net-zero Water Building Trends and Examination of Case Study of Research Facility in Japan, Proceedings of 2024 Symposium CIB W062 – Northampton, UK, 22, 2024.
2) United States Department of Energy, Energy Efficiency and Renewable energy, Net Zero Water Strategies, https://www.energy.gov/eere/femp/net-zero-water-building-strategies (viewed on 2026/4/28)
3) U.S. GREEN BUILDING COUNCIL, LEED Zero Program Guide, April 2020, last updated: January 2020
4) Japan Meteorological Agency: Historical Weather Data Search https://www.data.jma.go.jp/obd/stats/etrn/index.php?prec_no=44&block_no=0366&year=2023&month=&day=&view=(viewed 4/28/2026)
5) Japan Sustainable Building Consortium (JSBC), General Incorporated Association: DECC Public Database, “Public Data: Regional Classification ALL” (in Japanese), accessed 28 April 2025.

10. Presentations of authors

Takeshi Aoi works for Nikken Sekkei and is primarily engaged in mechanical equipment design. He is a member of both ASHRAE (the American Society of Heating, Refrigerating and Air-Conditioning Engineers) and AIJ (the Architectural Institute of Japan). He is a member of AIJ's Zero Water Building Modeling Subcommittee.

Masayuki Otsuka is a professor in the School of Architecture and Environment at Kanto Gakuin University, where he conducts research on water supply, drainage, and sanitation systems, and served as president of SHASE (the Society of Heating, Air-Conditioning and Sanitary Engineers of Japan).

Anna Fujita works for Nikken Sekkei and primarily conducts research on Zero Water Buildings. She is a member of AIJ (the Architectural Institute of Japan) and SHASE (the Society of Heating, Air-Conditioning and Sanitary Engineers of Japan).

Water Management during Construction

Tim Bartrand
tim.bartrand@iapmo.org
Director of Water Research, The IAPMO Group, USA

Abstract

Deliberate and effective water management during construction or major renovations can make the difference between turning over a building ready for occupancy and a system that starts its service life contaminated and requiring costly remediation. This study reviews published and unpublished reports of the consequences of lax water management during construction, the water quality hazards that require management during construction, and best practices for water management during construction. Best practices are drawn from a recent guidance on water management during construction.

Much of water management during construction and major renovation is similar to water management during beneficial occupancy: water is turned over regularly, temperatures are maintained outside the ideal growth range of *Legionella pneumophila* and other harmful organisms, and routine monitoring allows assessment of how consistently the controls are applied and whether they achieve their objective (typically, *Legionella* control). Particular aspects of construction and installation require measures beyond those after beneficial occupancy. The key additional measures include staging installation and filling to minimize the time between filling the building and final disinfection, sanitary handling of plumbing materials prior to installation, flushing after first filling the system to remove construction residuals, oversight of construction water uses, and final disinfection prior to beneficial occupancy. This paper describes these additional measures and their rationale. While managing water as described in the guidance and in this paper cannot guarantee a *Legionella*-free system at hand-over, it does reduce the likelihood of contamination and demonstrate that the highest standard of care was used during construction.

Keywords

Water management program, water safety planning, *Legionella*, water quality, construction

1 Introduction

Illnesses associated with building water systems (BWSs) are the cumulative outcome of the BWS design, installation, operation and water supply (Figure 1). Risk management is possible in all the processes depicted in Figure 1 and robust risk management requires management of risk in all of the processes. This document focuses on microbial risks and risk management associated with construction and installation of building water systems. As demonstrated in reports reviewed herein, insufficient water management during construction and installation can result in BWSs contaminated at the beginning of beneficial occupancy.

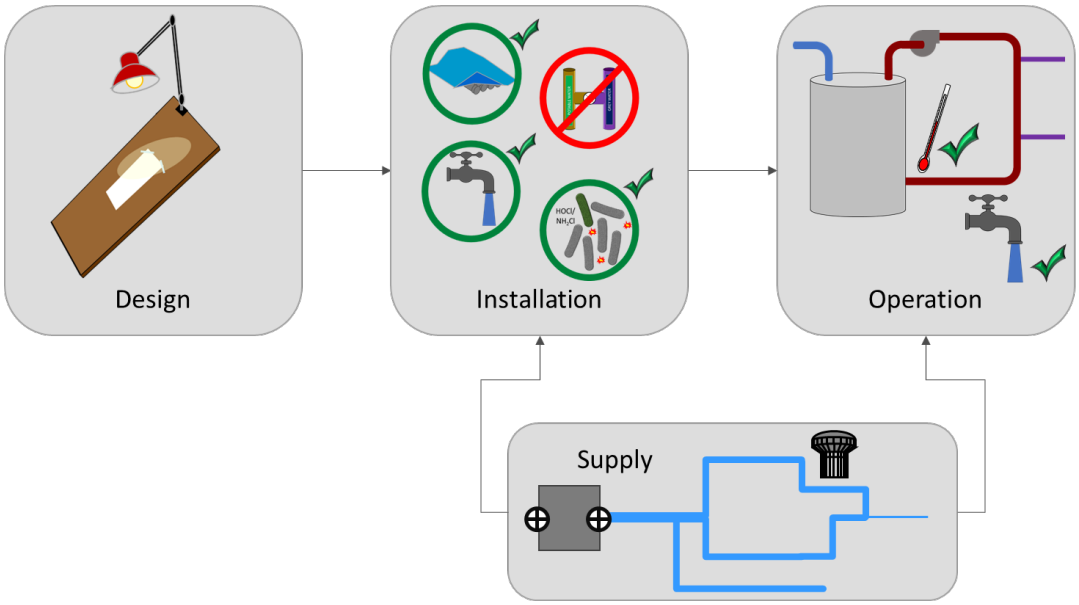

Figure 1. Engineering Processes that Determine the Risk of Legionellosis from Potable Water Systems over the Building Water System Life Cycle

Figure 2 shows a generic timeline for building water system installation during construction. Building water system installation and construction activities vary widely from site to site and the activities depicted in Figure 2 may overlap or occur in a different sequence on a given construction site. Although most of the activities in Figure 2 provide opportunities for water quality degradation as well as for water quality management, current requirements and standards in the US [1], the UK [2] and focus on the water system commissioning process (the final step in new system installation) and not on other water system activities prior to commissioning.

Some BWSs are excessively colonized by *Legionella pneumophila* and other opportunistic premise plumbing pathogens (OPPPs) from the start of beneficial occupancy and others are not. Costs and public health impacts for BWSs that begin their service life contaminated can be significant and, as noted in European Technical Guidelines for the Prevention and Control of *Legionella* [3], "From a microbiological perspective, the period between filling the system and bringing it into normal use is potentially the most hazardous and if not carried out to limit the potential for colonisation

the building is likely to be problematic for the rest of the system's life and be more costly to manage both economically and environmentally."

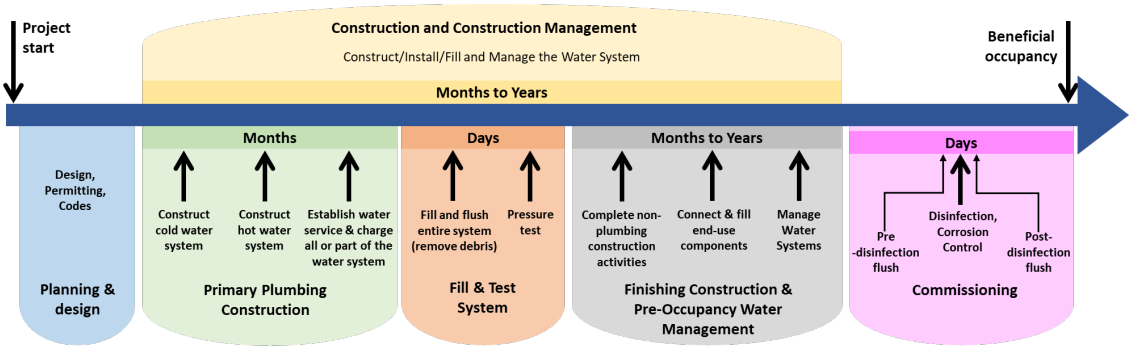

Figure 2. Overview of Building Water System Construction/Installation

In most reported cases, etiological agents of illnesses associated with building water systems are opportunistic premise plumbing pathogens (OPPPs) – environmental organisms that can survive and grow under conditions typical of BWSs and that are more likely to infect vulnerable susceptible populations. BWS design impacts the ecology for operational BWSs and determines some activities during installation. BWS construction can cause acute exposures to pathogenic organisms as well as latent exposures occurring after construction, when conditions cause a bloom of organisms that were introduced into the BWS during construction. The building water supply can have both positive and negative impacts on OPPPs control both during and after installation. To date, BWS operation has been the focus of OPPPs risk management efforts and guidances such as the WHO's Water Safety in Buildings focus on systematic operation and surveillance of BWSs to reduce the risk of waterborne illness.

No data exist to estimate the proportion of new BWSs that begin their service life excessively contaminated, much less science-based benchmarks for assessing whether BWSs are excessively contaminated. Anecdotal evidence [4–15] shows that some buildings are excessively contaminated at the outset of their service life despite getting water from a regulated, safe water supply and despite flushing, disinfection and other commissioning activities prior to beneficial occupancy. It is also known that BWSs contaminated at the beginning of their service life pose a public health risk and can be very expensive to maintain or remediate.

2 Objectives and Methods

This paper (i) uses a review of published studies and guidances to identify water quality risks and hazardous conditions that may be present during construction and major plumbing system renovations and (ii) presents practices described in a recent guidance for avoiding or mitigating water quality degradation during construction. Published studies reviewed for this paper were identified via Google scholar search using the search terms ("Water quality") AND ("Construction" OR "Installation") AND ("Plumbing System" OR "Building Water System"). Articles citing those meeting the search criteria were also reviewed for inclusion in the review.

3 Overview of Water Management Opportunities during Construction

Construction presents both water quality hazards and opportunities. As shown in Figure 3, hazards can enter plumbing systems during construction if materials are not stored under sanitary conditions prior to installation, if water of insufficient quality is used to fill the plumbing system, and via cross connections once systems are filled.

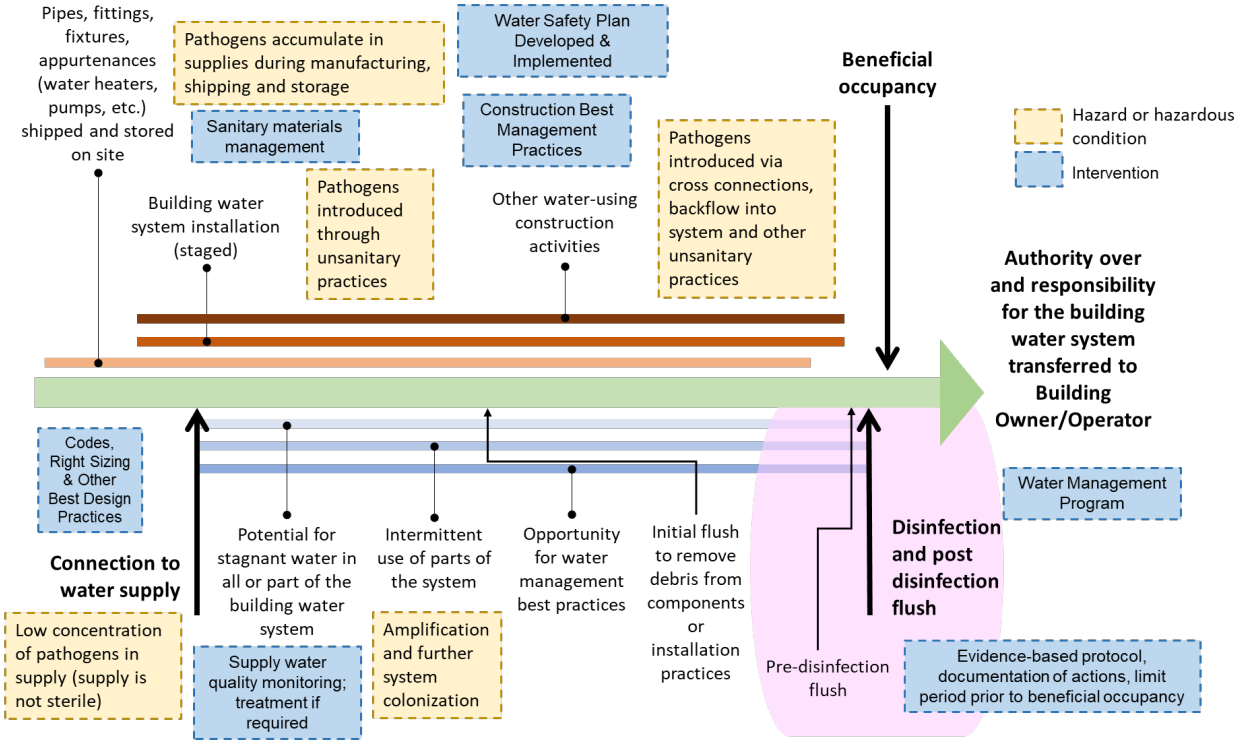

Figure 3. Water Quality Hazards and Interventions during Construction

Interventions that can prevent contaminant intrusion should be applied during construction and can include sanitary storage of plumbing materials prior to installation (e.g., end caps on pipes), water testing for confirmation that the quality of water used to fill the system is sufficient, a high-velocity flush after the system is filled to remove debris and contaminants, and implementation of a cross-connection control program. Oftentimes a potable water system is used as supply for water during construction and care must be taken to avoid backflow of water from construction offtakes into the potable water system.

Once a system is filled, water management needs to be similar to water management in an occupied building and should align with standards and guidances for water management programs or water safety planning [16–18]. Stagnation is the single most important hazardous condition promoting OPPPs amplification and water should be turned over regularly in what has been termed "simulated occupancy flushing" [19]. Simulated occupancy flushing removes loose biofilm that accumulates during stagnancy and replaces old water with lower-temperature water that may have disinfectant, if disinfectant is present in the building supply. Water management after the system is filled

should include regular monitoring of water quality, as described in section 3 of this manuscript. The staging of filling the system is critical. Delaying filling the system until necessary delays the potential for water quality degradation while reducing the effort required to manage water between filling the building system and commissioning.

Depending on the building size, type and occupancy, final disinfection may be required prior to beneficial occupancy. In some United States jurisdictions, plumbing code specifies that final disinfection is conducted following AWWA Standard C651. That standard was developed for disinfecting new and replaced distribution system mains for municipal systems. The very high levels and contact times for disinfectant in C651 were not established for disinfecting building systems and, although the extent remains unknown, may damage plumbing system components. An alternative approach is provided in a guidance in preparation by the AWWA. The revised approach recommends much lower disinfectant CTs (product of concentration and contact time) than C651 and is more appropriate for building systems and their potential hazards

4 Water Management from Design through Occupancy

In 2024, IAPMO published a manual of recommended practice for water management during construction [20]. The manual's purpose is "to establish a process of water management during construction for new buildings, additions, and renovation of existing buildings. A process for water management during construction is necessary to control the unique hazardous conditions associated with the construction phase of work." In this section of the paper, an overview of the manual is provided and key elements are highlighted

4.1 Preconstruction Activities

The manual recognizes that pre-construction activities set the stage for successful water management during construction. Perhaps the two most important pre-construction activities entail coordination between contractors, design engineers and the water management team: developing a project timeline for water management activities and design coordination. As noted in section 2 of this paper, water quality challenges and water management activities begin as soon as the system is filled and continue for the duration of construction. Thus, making sure that water management activities are planned and staged optimally yields water quality benefits and can reduce the time and expense associated with managing water during construction. Water management during construction requires coordination with design engineers to ensure that flushing and sampling ports used for water management during construction (and probably after occupancy) are included in designs (Figure 4). As noted below, an initial flush is recommended when the system is first filled to clear construction residuals from the system. Large diameter plumbing requires high volumetric flow rates to achieve velocities high enough to scour pipes and transport debris. High volumetric flow rates require flushing points designed to pass the required flow and with sufficient drainage. Injection point(s) are required for charging the system with disinfectant in final

disinfection and can be useful during beneficial operation if remedial disinfection is required.

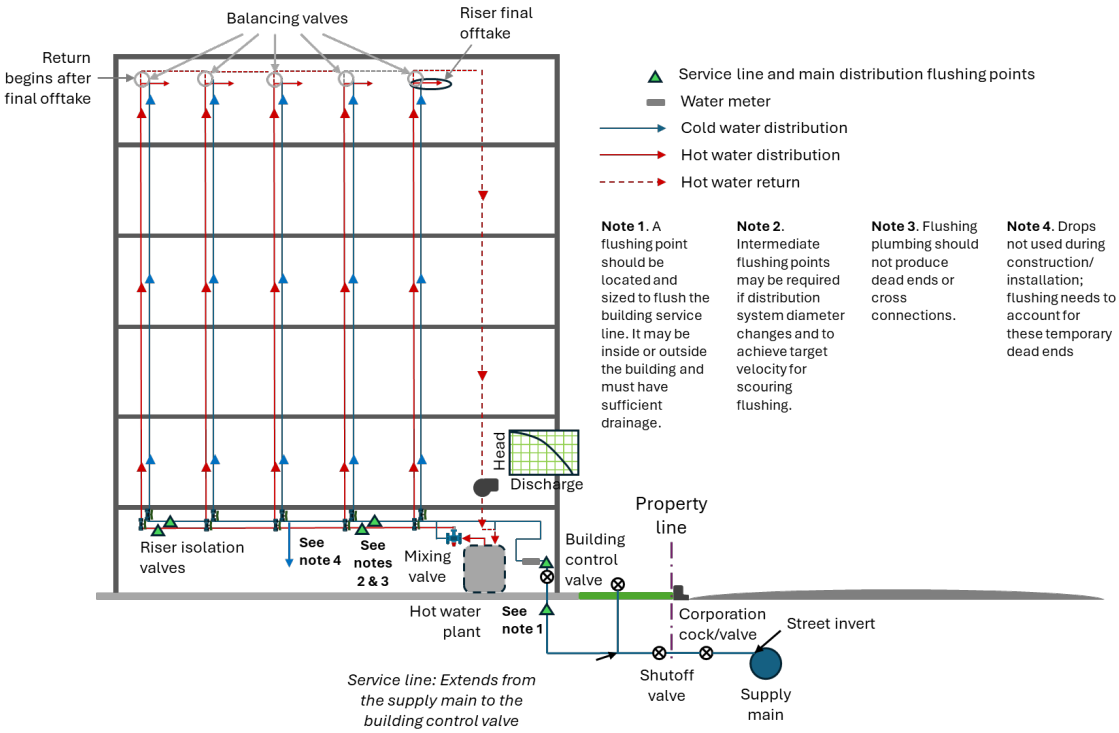

Figure 4. Illustration of Key Flushing Points for Inclusion in System Design

Water management during construction differs according to the building's intended use and size. The manual assigns four categories of building type with increasingly more stringent water management requirements for construction (Table 1). Activities such as sanitary storage of plumbing materials, minimizing the time between filling the water system and occupancy, and preventing intrusion of contaminants into the system are common sense and applicable to all building types. Other activities such as daily simulated occupancy flushing and intensive water quality monitoring are most appropriate for buildings with high likelihood of exposure of sensitive populations to aerosols. Comprehensive Water Management Programs (WMPs) or Water Safety Plans (WSPs) should be developed prior to construction for buildings systems in categories C and D.

Both design engineers and the water management team should have a detailed understanding of the water supply (typically a municipal water supplier) before construction. This ensures only appropriate water is used to fill the system and can inform system design features such as softening and supplemental disinfection. Key supply characteristics to review prior to installation include:

- **General water quality information from the water supplier**. In the United States, basic information is provided in Consumer Confidence Reports (CCRs). Important parameters include pH, temperature, hardness, alkalinity.

- **Type and level of disinfectant at the building service connection**. In rare cases, the water supplier may have these data. If not, the water management team should collect these data at the building entry point.
- **Corrosion control chemicals added to the water**. These data come from the water supplier and can be used for developing a building system corrosion assessment and control system.
- **Supplier distribution system maintenance, main breaks, or other significant disruptions of the supplier distribution system near the building service connection(s) during the prior three months**. This information is helpful in assessing water quality during system filling.

Table 1. Building Risk Categories

CATEGORY	DESCRIPTION
A	Buildings with low likelihood of human exposure to aerosols such as: • Single-family residences, duplexes, town homes and other small residential buildings
B	Buildings with *low/moderate* likelihood of human exposure to aerosols such as: • Commercial buildings without showering facilities • Retail buildings • Warehouses, data centers and other low occupancy buildings with low incidence of occupant exposure to aerosolized potable water
C	Buildings with *moderate* likelihood of human exposure to aerosols with sensitive occupants/users (excludes healthcare) such as: • Institutions, schools, and childcare facilities • Hotels and resorts • Gyms and Recreational facilities • Large office buildings • Medical office buildings • High-rise residential
D	Buildings with *high* likelihood of human exposure to aerosols including healthcare facilities with sensitive occupants/users such as: • Hospitals, critical access hospitals, and skilled nursing facilities (i.e., over 24-hour stay) • Senior facilities (e.g., assisted living) • Nursing and rehabilitation facilities • All other health care facilities including outpatient surgical centers and other outpatient care

4.2 Water Management during Construction Activities

Water system milestones during construction activities are outlined line Table 2, along with details and requirements outlined in the manual of best practices. Many of the activities must be coordinated with the Authority Having Jurisdiction (AHJ) and conducted as required by locally-adopted code. Ideally, at the conclusion of construction and commissioning, WMPs/WSPs developed during construction are delivered to the building owner along with documentation such as sample/monitoring results and remedial actions taken in response to events and water quality test results.

Table 2. Water System Milestones during Construction

KEY EVENT OR MILESTONE	DETAILS AND REQUIREMENTS
Service connection to water supply	(1) Water provider to determine schedule for connections in coordination with the construction project schedule and shall ensure adequate flushing in accordance with the Authority Having Jurisdiction. (2) Document the following dates: Taps and connections, shutdowns and lockouts, flushing prior to connection, service interruptions.
Construction start date	(1) Document temporary water connection requirements and or permits in WMP/WSP (e.g., hydrant connections, or temporary water lines). (2) Document permanent water connection requirements and or permits in the WMP.
Cold water activation start date	(1) Document first time the BWS is filled or charged (a) Partial system activation dates (2) Document adequate flushing (a) Partial system flushing dates (3) Document cross connection device testing reports (4) Environmental Testing
Hot water system activation start date	(1) Document permanent start date (activation) (2) Document temporary start date (activation) (3) Document temperature and ranges (4) Equipment maintenance schedules
Piping system installation (cold, hot, sanitary, storm)	(1) Determine methods to minimize contractor or building occupant exposures (2) Drainage scheduling for flushing availability (3) Insulation (4) AHJ inspections
Equipment installation (ice machines, etc.)	(1) All equipment start-up documentation (e.g., medical equipment, equipment with filters) (2) Procedures for health and safety
System purging (sediment & debris)	(1) Dry Nitrogen (2) Strainers/equip
Flushing protocols (start and duration)	Protocols in place for initial system flush, simulated occupancy flushing and flushing as part of final disinfection
Installation testing	(1) Pressure testing
Water quality monitoring and testing	(1) Water quality monitoring (e.g., temperature, residual disinfectant, water age) (2) Analytical water testing (e.g., HPC, *Legionella*, or other pathogens) (a) Dates (b) Level/results
Disinfection	(1) Procedure/method and testing results documented
Beneficial occupancy (substantial completion)	(1) AHJ final inspections/certificate of occupancy (2) Building owner's staff is the primary building occupant prior to first day of public operations (3) Determine hand-off of building water system from contractor to building owner
Building owner transition to on-going operations	(1) Utilities on and commissioned (2) Transfer of WMC from construction/commissioning to WMP for on-going operations
First day of business operations to public	(1) Public occupancy of the building for designated use (2) Healthcare providers have obtained a license to operate and admit patients for treatment

4.3 Water Management Means and Methods

Specific recommendations for conducting activities required for water management during construction are provided in the manual of practice's final section. Those recommendations supplement other water quality management guidances such as ASHRAE 188 and the WHO Guidance on Water Safety in Buildings by providing more specific information and highlighting activities that are related to construction. Recommendations are provided for pressure testing, filling the system (initially). flushing, and water quality monitoring. Recommendations for filling the system, flushing the system and water quality monitoring are highlighted in this section.

Water quality of the supply should be tested and confirmed prior to initially filling the system. Recommended actions to take prior to filling the system are:

- Communicate with the water purveyor to coordinate the connection and to verify that BWS water quality meets target goals and specifications specified in the construction WMP/WSP
- Ensure only potable water from a suitable supply is used for filling the system.
- Draw samples and test the water just upstream of building entry point to meet the following potable water requirements:
    - Sample is clear via visual inspection with no sediment OR turbidity of less than 1.0 NTU
    - Sample is free of color via visual inspection
    - Sample disinfectant residual meets water purveyor regulatory requirement.

Flushing is conducted for multiple purposes during construction, as outlined in Table 3. Because each type of flushing is conducted with a different purpose, flushing should be conducted to meet the characteristics associated with the desired outcome. When high-velocity flushing is required, ports must be available to achieve required flows and drainage must accommodate flushed water. Frequent and high-volume flushing may waste significant volumes of water and flushing water losses should be considered within wider water conservation plans for construction projects [21–23]. Because flushing is only conducted after the system is filled, water conservation is an additional motivation for staging construction to delay filling the system until necessary.

Water testing should be conducted periodically for building types C and D. Water should be tested to ensure controls are implemented as intended (verification monitoring) and, ideally, to confirm that controls are limiting biological growth and other adverse outcomes (validation monitoring). Recommendations for verification monitoring and validation monitoring are provided in Table 4 and Table 5, respectively.

Table 3. Flushing Purposes and Characteristics

FLUSHING TYPE	PURPOSES	CHARACTERISTICS
Initial flushing (Prior to system filling and before disinfection)	• Removes debris, construction residuals, and environmental contaminants introduced into plumbing components during storage and installation	Velocity high enough to mobilize sediment; flushing from near point of entry outward to distal locations to avoid entrainment of contaminants deeper into the system; flushing duration required to turnover the supply line at least five times the volume of the pipe.
Routine flushing (water turn-over) (After the system is filled and before disinfection)	• Simulate occupancy by flushing water to maintain adequate disinfectant residual and maintain hot and cold water temperatures outside the growth range of OPPPs • Remove loose biofilm and organisms that accumulated during stagnation	Flushing conducted daily (building type D) or once per three days (building type C); when feasible, flow started impulsively (not gradual) with aerators and other flow-restricting components removed; flushing can be conducted via fixtures or flushing locations at distal outlets at the end of the branches.
Final disinfection flushing	• Remove water with high disinfectant concentration • Remove detached and degraded biofilm and other materials generated during disinfection	Flushing conducted per standards specified in code. Flushing may be conducted before disinfection to remove debris and reduce disinfectant demand. Flushing must be conducted after disinfection to purge the system of high disinfection concentration water that can damage plumbing materials and that can be higher than the US EPA maximum disinfectant residual level (MDRL) or above other limits on disinfectant concentration.
Adverse events or hazardous conditions flushing	The purpose of this type of flushing differs with the adverse event or hazardous condition that triggers the flushing. Examples: • Purging nonpotable water introduced into the potable water plumbing inadvertently • Proactive response to upsets in the building water supply..	Velocity high enough to mobilize sediment; flushing from near point of entry outward to distal locations to avoid entrainment of contaminants deeper into the system; flushing duration required to turnover the supply line at least five times the volume of the pipe. If the triggering event was high Legionella level detections or a suspected Legionnaire's disease case, flushing should be conducted as part of a remediation and disinfection process.

5 Conclusion

Relatively simple measures can be taken during construction of BWSs to avoid systems starting their service lives contaminated. Water management during construction requires coordination between all stakeholders – the building owner, general contractors, plumbing design engineers, plumbers, and water quality contractors. Together, the stakeholders can ensure that systems are designed with all of the features required for effective water management, using project timelines that minimize negative water quality

impacts, and with practices that maintain water quality after the system is filled and verify and validate that water quality at beneficial occupancy is not impaired. This paper provided highlights of the IAPMO manual of practice for managing water during construction. Additional details may be found in the full report [20].

Table 4. Verification Monitoring Parameters and Target Levels

PARAMETER	METHOD & FREQUENCY	TARGET LEVELS
Water age	Flushing protocol. Begin after initial flush; twice weekly thereafter	Less than 96 hours (document flushing protocol with frequency and duration)
Disinfectant residual after flushing[1]	Digital colorimeter instrument with proper reagents. On first filling, after initial flush, and weekly thereafter	≥ 0.2 ppm (mg/L) or the minimum residual concentration for the water supplier (set by state regulatory agencies when water is not self-supplied)
		Prior to water heating, the greater of 0.2 ppm (mg/L) or 80% of the entry point disinfectant residual
		The greater of 0.2 ppm (mg/L) or 80% of the entry point disinfectant residual
		The greater of 0.2 mg/L or 80% of the entry point disinfectant residual
Temperature after flushing[2]	Digital thermometer. Monthly after initial flush until heating is initiated; weekly thereafter heating system activation	< 77°F (cold, prior to heating) and ≥ 131°F (after heating initiated)
Sediment after flushing	Visual inspection. On first filling and weekly thereafter	Water is clear, no visible discoloration, no visible sediment
pH after flushing	Digital instrument. On first filling, after initial flush, and monthly thereafter	6.5-8.5 pH units based on pH scale 0 -14 [5]
		Within 0.2 pH units of the entry point pH
		Within 0.2 pH units of the entry point pH

Table 5. Validation Monitoring Parameters and Target Levels.

PARAMETER	METHOD & FREQUENCY	TARGET LEVELS
Heterotrophic plate count (HPC) or, alternatively, approved test by AHJ	Certified analytical laboratory sample method. On first filling and monthly thereafter	≤ 500 CFU/mL HPC
		Note: for HPC assure results are within 1 log of the concentration in the prior measurement for the same location and no more than 0.5 logs above the geometric mean of all measurements for the location
Culturable *Legionella species* or *L. pneumophila*	Samples shall be analyzed by a certified analytical laboratory; alternative methods from an accredited laboratory. Quarterly sampling after water activation	As required by the Authority Having Jurisdiction

6 References

(1) IAPMO. *Uniform Plumbing Code*; 2021; Vol. Section 609.

(2) WaterRegs UK. *Commissioning Plumbing Systems - Advisory Leaflet*; No. 9-05-01; WaterRegs UK: Crumlin in Gwent, Wales, UK, 2021. https://www.waterregsuk.co.uk/downloads/public_area/guidance/publications/april_2021/9-05-01_commissioning-2021-v3web-_apr2021_.pdf.
(3) European Guidelines Working Group. *European Technical Guidelines for the Prevention, Control and Investigation, of Infections Caused by Legionella Species*; 2017. https://ecdc.europa.eu/sites/portal/files/documents/Legionella%20GuidelinesFinal%20updated%20for%20ECDC%20corrections.pdf (accessed 2017-08-10).
(4) Bartley, J.; Bjerke, N. B. Infection Control Considerations in Critical Care Unit Design and Construction: A Systematic Risk Assessment. *Critical care nursing quarterly* **2001**, *24* (3), 43–58.
(5) Bartley, J. M. APIC State-of-the-Art Report: The Role of Infection Control during Construction in Health Care Facilities. *American journal of infection control* **2000**, *28* (2), 156–169.
(6) Chinn, R. Y.; Sehulster, L. Guidelines for Environmental Infection Control in Health-Care Facilities; Recommendations of CDC and Healthcare Infection Control Practices Advisory Committee (HICPAC). **2003**.
(7) Collinge, W. H. Infection Control in Design and Construction Work. *HERD: Health Environments Research & Design Journal* **2015**, *8* (3), 68–79.
(8) Edwards, P.; Durand, M. A.; Hollister, M.; Green, J.; Lutchmun, S.; Kessel, A.; Roberts, I. Scald Risk in Social Housing Can Be Reduced through Thermostatic Control System without Increasing Legionella Risk: A Cluster Randomised Trial. *Archives of disease in childhood* **2011**, *96* (12), 1097–1102.
(9) Gamage, S. D.; Ambrose, M.; Kralovic, S. M.; Roselle, G. A. Water Safety and *Legionella* in Health Care: Priorities, Policy, and Practice. *Infectious Disease Clinics* **2016**, *30* (3), 689–712.
(10) Mermel, L. A.; Josephson, S. L.; Giorgio, C. H.; Dempsey, J.; Parenteau, S. Association of Legionnaires Disease with Construction: Contamination of Potable Water? *Infection Control & Hospital Epidemiology* **1995**, *16* (2), 76–81.
(11) Nakamura, I.; Miura, Y.; Umeda, A.; Imura, R.; Watanabe, Y.; Watanabe, H. The *Legionella* Contamination of Tap Water in a Brand-New Hospital in Japan before Patients Move In. *Infection Control & Hospital Epidemiology* **2020**, *41* (8), 998–999.
(12) Olmsted, R. N. Prevention by Design: Construction and Renovation of Health Care Facilities for Patient Safety and Infection Prevention. *Infectious Disease Clinics* **2016**, *30* (3), 713–728.
(13) Ryu, S.; Yang, K.; Chun, B. C. Community-Acquired Legionnaires' Disease in a Newly Constructed Apartment Building. *Journal of Preventive Medicine and Public Health* **2017**, *50* (4), 274.
(14) Scanlon, M. M.; Gordon, J. L.; McCoy, W. F.; Cain, M. F. Water Management for Construction: Evidence for Risk Characterization in Community and Healthcare Settings: A Systematic Review. *International journal of environmental research and public health* **2020**, *17* (6), 2168.
(15) Voss, L.; Button, K. S.; Lorenz, R. C.; Tuovinen, O. H. *Legionella* Contamination of a Preoperational Treatment Plant. *Journal-American Water Works Association* **1986**, *78* (1), 70–75.
(16) ASHRAE. ASHRAE 514. Risk Management for Building Water Systems: Physical, Chemical and Microbial Hazards, 2023.
(17) ASHRAE. *ASHRAE 188 Legionellosis: Risk Management for Building Water Systems*; ASHRAE: Atlanta, GA, 2018. www.techstreet.com/ashrae/products/1897561.
(18) WHO. *Water Safety in Buildings*; World Health Organization: Geneva, Switzerland, 2011. http://apps.who.int/iris/bitstream/10665/76145/1/9789241548106_eng.pdf.
(19) Scanlon, M. M. Personal Correspondence, 2024.
(20) International Association of Plumbing and Mechanical Officials. *Manual of Practice: Construction Practices for Potable Building Water Systems*; IAPMO: Ontario, CA, USA, 2024. https://iapmo.org/research/manuals/construction-practices-for-potable-water-manual.
(21) Liu, Z.; Zhang, C.; Guo, Y.; Osmani, M.; Demian, P. A Building Information Modelling (BIM) Based Water Efficiency (BWe) Framework for Sustainable Building Design and Construction Management. *Electronics* **2019**, *8* (6), 599.
(22) Rahman, M. M.; Rahman, M. A.; Haque, M. M.; Rahman, A. Sustainable Water Use in Construction. In *Sustainable construction technologies*; Elsevier, 2019; pp 211–235.
(23) Waidyasekara, K.; De Silva, L.; Rameezdeen, R. Water Use Efficiency and Conservation during Construction: Drivers, Barriers and Practices. *Built Environment Project and Asset Management* **2016**, *6* (5), 553–566.

7 Presentation of Author

Tim Bartrand is Director of Water Quality Research at the International Association of Plumbing and Mechanical Officials (IAPMO). Tim joined IAPMO in 2025 when IAPMO acquired ESPRI – the Environmental Science, Policy and Research Institute, a nonprofit organization and group of scientists and engineers dedicated to safe water from sources all the way to fixtures. Over his career, Tim has specialized in microbial risk management, most recently focusing on better management of *Legionella* bacteria in both public water systems and building water systems. Tim holds a doctoral degree from Drexel University and is an active member of AWWA, ASHRAE, and ASPE.

Method for Calculating Underground Infiltration Based on Actual Water Level Measurements in Rainwater Storage and Infiltration Tanks

Kosuke Osako (1), Kenta Tanaka (2), Masayuki Otsuka (3)

(1) kosuke_osako@tte-net.com
(2) Kenta.Tanaka@kumesekkei.co.jp
(3) dmotsuka@kanto-gakuin.ac.jp
(1) Takasago Thermal Engineering Co., Ltd., Japan
(2) Kume Sekkei Co., Ltd., Japan
(3) Prof. Dr.Eng, Department of Architecture and Environmental Design, College of Architecture and Environmental Design, Kanto Gakuin University, Japan

Abstract

In zero-water buildings (ZWB), the infiltration of rainwater into the ground is a key parameter, often assessed as water returned. In this study, we modified an existing rainwater storage and infiltration tank to evaluate its infiltration performance and to explore improved methods for calculating infiltration volumes. Conventionally, infiltration volumes are estimated using rainfall intensity, catchment area, and runoff coefficient. However, discrepancies frequently occur between the calculated and measured water levels owing to losses during collection and overflow events in the rainwater storage and infiltration tank. To address these issues, we developed a novel approach that directly calculates infiltration volumes based solely on actual tank water level measurements, in addition to the conventional method that uses on-site rainfall and tank water level data. Comparative analysis demonstrated that the proposed method, which relies on measured water levels, provides a more accurate representation of actual storage and infiltration dynamics. This approach offers a more realistic assessment of rainwater infiltration volumes and is anticipated to be applicable to ZWB evaluations.

Keywords
Net-zero-water building (ZWB); Water Returned; Rainwater infiltration

1 Introduction

Interest in zero-water buildings (ZWBs) has increased significantly in recent years, driven by the need for more effective utilization of water resources. ZWBs go beyond conventional water conservation and reuse strategies by also aiming to reduce the burden on water supply and sewage infrastructure. At our innovation center (hereinafter "this building"), we are actively evaluating a range of technologies that support the advancement of ZWB performance, with the aim of achieving ZWB certification in accordance with the LEED definition of zero water [1, 2]. Among these technologies, the infiltration of rainwater into the ground is crucial in ZWB assessment, as infiltrated rainwater can be credited as reduced water demand. Accordingly, we modified the existing rainwater storage and infiltration tank in this building and conducted validation tests utilizing its infiltration function. The direct measurement of infiltration volume is generally challenging; therefore, it is commonly estimated using rainfall volume, catchment area, and runoff coefficients. In this study, we utilized actual measurement data from on-site rain and water level gauges installed in the infiltration tank to determine the runoff coefficient and infiltration capacity coefficient. We then explored a calculation method for the infiltration volume that incorporates water level data [2]. However, our analysis revealed discrepancies between water levels calculated from rainfall data and those actually measured in the tank. These differences are attributed to losses during the collection process and the effects of overflow from the infiltration tank. Therefore, this study proposed a novel method for calculating infiltration volumes based on actual water level measurements within the infiltration tank. The objective was to establish a calculation approach grounded in empirical data, thereby enabling a more accurate and realistic assessment of infiltration volume in rainwater storage and infiltration tanks. This report details the modifications implemented on an existing infiltration tank and presents the results of a comparative analysis of infiltration volume calculations using both the conventional and proposed methods.

2 Overview of the rainwater storage and infiltration tank, and comparison cases

2.1 Rainwater storage and infiltration tank for this building

2.1.1 Location of the rainwater storage and infiltration tank

This building [3] is located in Tsukubamirai City, Ibaraki Prefecture. As shown in Figure

1, the site is equipped with two rainwater storage and infiltration tanks, which serve as rainwater runoff control facilities. Rainwater Storage and Infiltration Tank A (referred to as Tank A hereinafter) collects rainwater from Area A, whereas Rainwater Storage and Infiltration Tank B (referred to as Tank B hereinafter) collected rainwater from Area B.

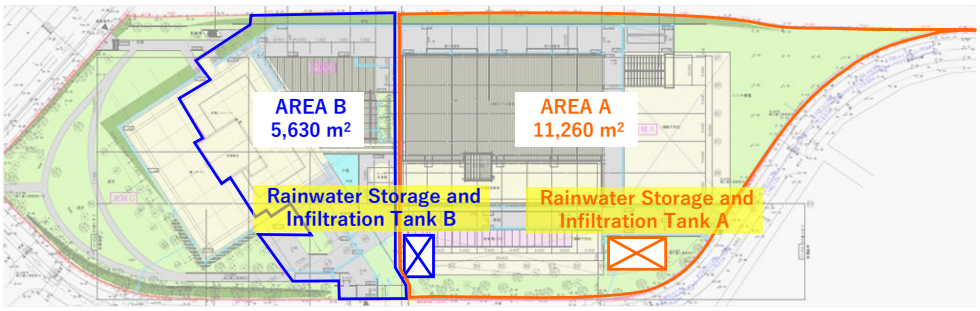

Figure 1 Location of the rainwater storage and infiltration tanks and catchment areas

2.1.2 Structure of the Rainwater Storage and Infiltration Tanks

Although these tanks were originally designed with underground infiltration capabilities, their primary function was to control rainwater runoff, resulting in underutilization of their infiltration potential. To enhance the effectiveness of the infiltration capabilities of the tanks, the discharge sections of both Tank A and Tank B were modified by us. An overview of the modifications implemented in Tank B is shown in Figure 2. Specifically, the discharge pipe at the outlet of the tank was raised by 900 mm, enabling the tank to retain a greater volume of rainwater and promote active infiltration into the ground. Water levels within each infiltration tank were monitored at two locations, and rainfall data were collected using an on-site rain gauge. Based on the measurement data, the infiltration volumes of Tanks A and B after modification were calculated.

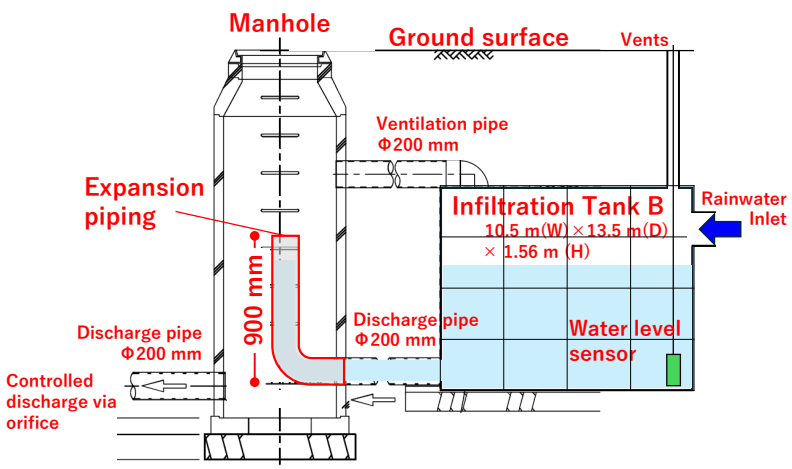

Figure 2 Modification of the discharge pipe

2.2 Calculation of the infiltration volume in rainwater storage and infiltration tanks

The process from the onset of rainfall to the final discharge of rainwater off-site is shown in Figure 3. ①Rainfall is collected through gutters or side ditches, ② then conveyed to the rainwater storage and infiltration tank, where it either ③ infiltrates into the ground or ④ is discharged.

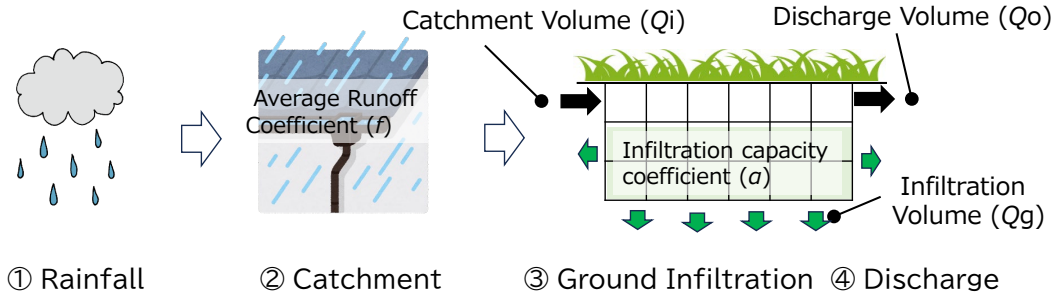

Figure 3 Process flow from the onset of rainfall to rainwater discharge

2.3 Comparison cases for calculating infiltration volume

In this study, three scenarios were established to evaluate different methods for calculating the infiltration volume in rainwater storage and infiltration tanks. Case 1 represents the conventional calculation method widely used to date. In Case 2, the infiltration volume is calculated by revising the catchment coefficient from Case 1, determining the catchment volume, and subsequently estimating the water level within the rainwater storage and infiltration tank. However, discrepancies were observed between the water level estimated in Case 2 and the actual measured water level. Therefore, Case 3 was introduced, in which the infiltration volume is calculated directly using the measured water level within the tank. For ZWB evaluations, the volume of rainwater infiltrating the ground is considered as reduced water and is generally calculated based on cumulative rainfall, catchment area, and the average runoff coefficient (as in Case 1). In such cases, rainfall data from the nearest Japan Meteorological Agency weather station are often utilized, which may introduce variability owing to regional differences and other factors. In contrast, Case 2 employs actual measurement data from on-site rain and water level gauges to determine the average runoff and infiltration capacity coefficients, allowing for a more accurate calculation of the infiltration volume by accounting for fluctuations in water level within the rainwater storage and infiltration tank. In contrast, Case 3 employs a methodology that does not incorporate rainfall data; instead, it determines the infiltration volume directly from actual water level measurements within the tank. A distinguishing feature of this approach is that it relies solely on measured water levels to calculate infiltration

volumes, thereby eliminating the need for rainfall data. Consequently, the volume of water collected in the rainwater storage and infiltration tank cannot be determined; however, as discussed later, the discharge volume can be calculated. In summary, while Case 2 employs a calculation method based on rainfall data and modeling, Case 3 adopts a calculation method that directly utilizes measured water levels. The input parameters and calculation flow characteristics for each case are listed in Table 1.

Table 1 Characteristics of each case

Case	Input Values (Measured Values)	Calculation Flow	Characteristics
1	Rainfall	Runoff ⇒ Infiltration	Calculated using rainfall data only
2	Rainfall	⇒Collected water volume, inflow ⇒ Water level in the tank ⇒ Infiltration volume, discharge volume	Reflects infiltration characteristics through fitting with measured water levels
3	Water level in the tank	⇒ Infiltration volume, discharge volume	Tank water levels are measured to reflect actual infiltration conditions

2.4 Rainfall data for the period during which infiltration volume was calculated

For Cases 1 and 2, rainfall data were obtained from a rain gauge installed on the premises of the building, covering the period from September 1, 2024, to August 31, 2025. The monthly rainfall trends during this period are shown in Figure 4. Rainfall peaked in May and June and remained relatively low throughout winter. The total annual rainfall recorded was 1,097 mm.

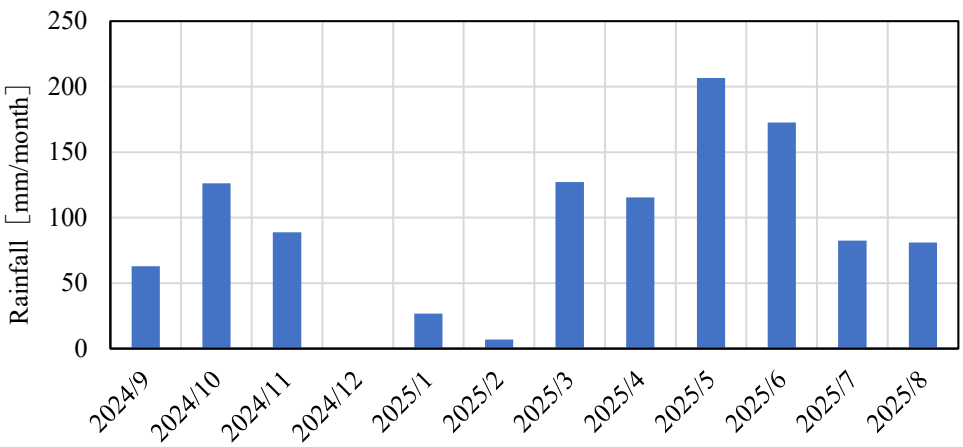

Figure 4 Monthly rainfall (September 2024–August 2025)

3 Results of infiltration calculations

3.1 Results for Case 1

In Case 1, the infiltration volume Qg was calculated as the product of the measured rainfall P, runoff coefficient f, and catchment area A, assuming that Qg is equivalent to the catchment volume Qi (Equation 1). The average runoff coefficient f was obtained from the values used in the building design. Based on Equation 1, the infiltration volume was 9,018 m³/year for Tank A and 5,060 m³/year for Tank B, resulting in a combined total of 14,078 m³/year. This is the theoretical maximum value when losses due to overflow and evapotranspiration are ignored.

$$Q_{\mathrm{g}} = Q_{\mathrm{i}} = P \times f \times A \times 10^{-3} \qquad \text{(Equation 1)}$$

where Qg represents the infiltration volume [m³/year], Qi represents the catchment volume [m³/year], P, represents the annual rainfall [mm/year], f represents the average runoff coefficient from the catchment area to the rainwater storage and infiltration tank [-] (Tank A: 0.73, Tank B: 0.82), and A represents the catchment area [m²].

3.2 Results for Case 2

In Case 2, the inflow rate Qi to the rainwater storage and infiltration tank was determined using Equation 3, outflow rate Qo using Equation 4, and infiltration volume Qg using Equation 5. The calculation method assumes the water level H(t) in the rainwater storage and infiltration tank varies dynamically in response to these temporal changes (Equation 2). The cumulative rainfall R(t), obtained from actual rainfall measurements, was used as the input value.

$$\frac{dH}{dt}(t) = \frac{Q_{\mathrm{i}}(t) - Q_{\mathrm{o}}(t) - Q_{\mathrm{g}}(t)}{\lambda W L} \qquad \text{(Equation 2)}$$

$$Q_{\mathrm{i}}(t) = \frac{fA}{360}\left[\frac{R(t) - R(t - 60t_c)}{t_c/60}\right] \qquad \text{(Equation 3)}$$

$$Q_{\mathrm{o}}(t) = \begin{cases} C\frac{\pi D^2}{4}\sqrt{2g(H(t) - H_{\mathrm{o}})} & (H(t) > H_{\mathrm{o}}) \\ 0 & (H(t) \leq H_{\mathrm{o}}) \end{cases} \qquad \text{(Equation 4)}$$

$$Q_{\mathrm{g}}(t) = \alpha \lambda W L H(t) \qquad \text{(Equation 5)}$$

where H represents the water depth [m], t represents the time [s], Qi represents the inflow rate [m³/s], Qo represents the outflow rate [m³/s], Qg represents the infiltration volume [m³/s], λ represents the void ratio of the storage and infiltration tank, W represents the short side length of the storage and infiltration tank [m], L represents the long side length

of the storage and infiltration tank [m], *WL* represents the base area of the storage and infiltration tank [m^2], *f* represents the average runoff coefficient, *A* represents the catchment area [ha], t_c represents the travel time (10 in this calculation) [min], *R* represents the cumulative rainfall [mm], *D* represents the diameter of the discharge connection pipe [m], *C* represents the flow coefficient of the discharge connection pipe (0.6344), *g* represents the acceleration owing to gravity (= 9.8) [m/s^2], *H*o represents the head of the discharge connection pipe [m], and α represents the infiltration capacity coefficient [s^{-1}]. Because Equation 2 is a nonlinear differential equation, unlike Equation 4, which involves square root operations, an approximate solution was obtained through numerical calculations. Equation 3, which calculates the inflow volume *Q*i, utilizes the rational formula synthesis method [4], a widely adopted approach for modeling rainwater inflow in small watersheds. Equation 4, used to determine the outflow volume, *Q*o, is derived from the standard orifice flow rate equation. The infiltration capacity coefficient α in Equation 5, representing the infiltration volume *Q*g, was calculated using actual water level data recorded within the tank during specific periods. The infiltration capacity coefficient α [s^{-1}] is defined as a parameter representing the rate of water level decrease due to infiltration, obtained from observed water level variations in the storage tank. This coefficient α serves as an indicator of the infiltration efficiency of the rainwater storage and infiltration tank. The discharge coefficient f was refined by fitting the calculated water level inside the tank to the actual measured water level, using the cumulative rainfall *R* as the input parameter. For Case 2, the calculated annual infiltration volumes were 5,091 m^3 for Tank A and 2,710 m^3 for Tank B, resulting in a combined total of 7,801 m^3/year. The corresponding rainwater discharge volumes were 399 m^3 for Tank A and 77 m^3 for Tank B, totaling 476 m^3/year.

3.3 Results for Case 3

In Case 3, the infiltration volume was determined using Equation 5, based on the measured water level data *H*(t) from the rainwater storage and infiltration tank. The discharge rate can also be calculated using Equation 4. As the measured water level served as the input, rainfall data were not required, and the inflow volume *Q*i was not computed. The calculation results indicated that the annual infiltration volumes were 4,778 m^3 for Tank A and 2,750 m^3 for Tank B, yielding a total of 7,528 m^3/year. Meanwhile, the annual discharge volume was 612 m^3 for Tank A and 133 m^3 for Tank B, totaling 745 m^3/year.

4 Discussion of the infiltration calculation results

4.1 Differences in average runoff coefficients

The average runoff coefficients used to calculate the infiltration volume in Cases 1 and 2 are listed in Table 2. In Case 1, the coefficients correspond to those used in the original design of each basin. In Case 2, the coefficients were obtained by fitting cumulative rainfall data over a specific period to observed water levels within the basins, providing a more empirical basis for comparison. For Tank A, the average runoff coefficients were 0.725 for Case 1 and 0.441 for Case 2. For Tank B, the coefficients were 0.817 for Case 1 and 0.440 for Case 2.

Table 2 Average runoff coefficients for Cases 1 and 2

	Average runoff coefficient [-]	
	Case 1	Case 2
Rainwater Storage and Infiltration Tank A	0.725	0.441
Rainwater Storage and Infiltration Tank B	0.817	0.440

Although the average runoff coefficients in Case 2 were lower for both tanks compared with those of Case 1, the values obtained in Case 2 were considered to reflect actual conditions more accurately. This is attributable to the increased influence of infiltration and evapotranspiration during light or intermittent rainfall events, which reduces the volume of runoff reaching the infiltration tanks and consequently lowers the average runoff coefficient. In summary, although the use of the average runoff coefficient from Case 1—commonly adopted in the design of rainwater storage and infiltration basins—offers a straightforward approach for calculating reduced water volume in ZWB evaluations, it may not accurately represent actual infiltration volumes.

4.2 Differences in calculated infiltration volumes

The infiltration volumes calculated for Cases 1 through 3 are listed in Table 3. A comparison of these results highlights notable differences between Case 1 and Cases 2 and 3. The higher infiltration volume in Case 1 stems from the assumption that all collected water infiltrates, whereas Cases 2 and 3 incorporate the water level within the tank into the calculation process. This adjustment yields infiltration volumes that more closely reflect actual site conditions.

Table 3 Infiltration volumes for each case (Unit: m^3/year)

Case	Case 1	Case 2	Case 3
Rainwater Storage and Infiltration Tank A	9,018	5,091	4,778
Rainwater Storage and Infiltration Tank B	5,060	2,710	2,750
Total	14,078	7,801	7,528

A detailed comparison of Case 2 and Case 3 reveals a discrepancy between the water levels calculated in Case 2, which relies solely on rainfall data, and the water levels measured in Case 3. A comparison of the water level calculated in Case 2 and that measured in Case 3 for Tank A, is shown in Figure 5. In Case 2, when a water level peak occurs, the peak in the measured water level in Case 3 may be smaller than that in Case 2. This difference is likely attributable to inflow blockages at the infiltration tank, as shown in Figure 6, underscoring the importance of regular maintenance. Given these findings, calculating the infiltration volume based on the measured values of Case 3 is considered more accurate, as it accounts for the effects of the inflow blockage and actual storage behavior.

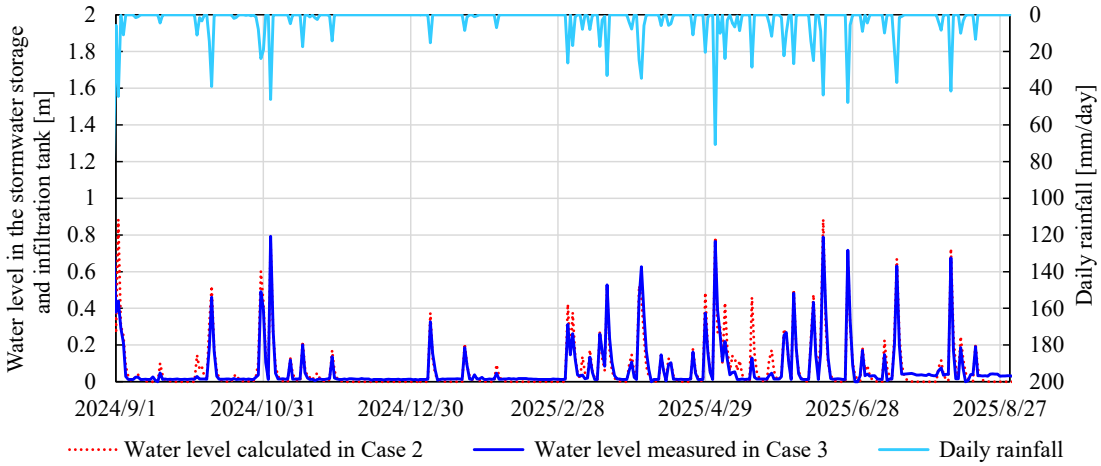

Figure 5 Water levels in tank A for Case 2 and Case 3

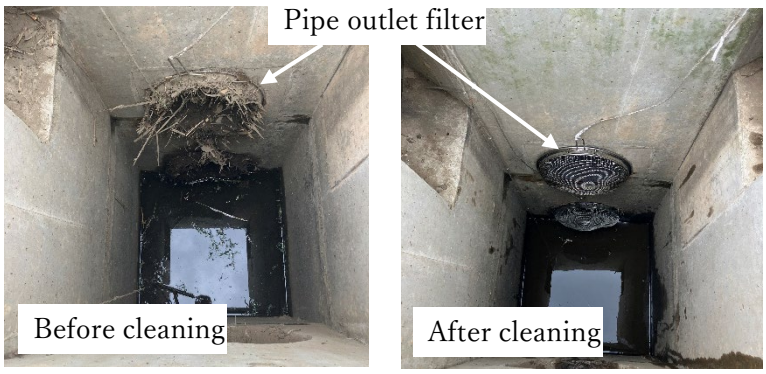

Figure 6 Inlet of rainwater storage and infiltration tank A

5 Conclusion

As part of the ZWB measures for this building, particular emphasis was placed on increasing the volume of reduced water critical factors in ZWB evaluation. Accordingly, we sought to enhance the infiltration capacity of the existing rainwater storage and infiltration tank, and a comparative analysis of infiltration volume calculation methods was conducted. The results demonstrate that the method of calculating infiltration volume based on actual water level measurements within the tank (Case 3) can reflect the effects of inflow blockage and actual storage behavior in the calculation of infiltration volume for ZWB evaluation, thereby enabling a more realistic assessment of infiltration volume. This method is expected to improve the accuracy of ZWB assessments. Furthermore, this study revealed that the infiltration capacity coefficients used in both Cases 2 and 3 were identified based on actual water level data collected within the tank over specific periods, suggesting the potential for further improvement in the future.

Acknowledgments
We extend our sincere gratitude to all members of the Association of Rainwater Storage and Infiltration Technology for their invaluable cooperation in analyzing the measured data utilized in this study.

6 References

[1] Kosuke Osako, Katsuhiko Shibata, Naoki Aizawa, Anna Fujita, Masayuki Otsuka, Feasibility study for ZWB on a sustainable office, 2024 Symposium CIB W062 – Northampton, UK, 22, 2024.
[2] Kosuke Osako, Katsuhiko Shibata, Kenta Tanaka, Masayuki Otsuka, Approaches and Verification of Net-Zero-Water Building Conversion in Sustainable Office, 2025 Symposium CIB W062 – Miami, USA, 19, 2025.
[3] Kosuke Osako, Uwais Roslan, Katsuhiko Shibata, Naoki Aizawa, Masayuki Otsuka, Advanced building facilities embodying the transition to carbon neutrality, 2023 Symposium CIB W062 – Leuven, Belgium, pp. 269-280, 2023.
[4] Emil Kuichling, The relation between rainfall and the discharge of sewers in populous districts, Transactions of the American Society of Civil Engineers, vol. 20, pp. 1-60, 1889.

7 Presentation of authors

Kosuke Osako is the chief research engineer at the HVAC Environment Office at the R&D Center of Takasago Thermal Engineering Co., Ltd., Japan. His research focuses on zero-water buildings and the efficient utilization of water resources. He is a member of the Architecture Institute of Japan (AIJ) and the Society of Heating, Air-Conditioning, and Sanitary Engineers of Japan (SHASE).

Kenta Tanaka is a mechanical equipment designer at Kume Sekkei Co., Ltd., While a graduate student at Kanto Gakuin University, he was a member of the Otsuka Laboratory, where he was primarily involved in research regarding zero water buildings. He is a member of the Architectural Institute of Japan (AIJ) and SHASE.in Japan.

Masayuki Otsuka is a professor in the Faculty of Architecture and Environment at Kanto Gakuin University, Japan. He has conducted extensive research on water supply, drainage, and sanitary equipment. Professor Otsuka is a member of the Architecture Institute of Japan (AIJ) and is a former president of the Society of Heating, Air-Conditioning and Sanitary Engineers of Japan (SHASE).

Simulation Research on Patterns Optimization Strategies of Building Rainwater Harvesting System

Shi-Feng. Huang (1), Cheng-Li. Cheng (2)
(1) M11313019@mail.ntust.edu.tw
(2) CCL@mail.ntust.edu.tw
(1)(2) National Taiwan University of Science and Technology, Department of Architecture, Taiwan, R.O.C.

Abstract

Taiwan has long been affected by climatic variability and uneven rainfall, frequently experiencing water shortages during the dry season and flooding during the wet season. Accordingly, water storage and reuse have become critical issues. Rainwater is a renewable and relatively clean resource; when collected from sites and rooftops, it can be treated through disinfection and filtration and then reused within buildings. In practice, rainwater reuse remains largely limited to irrigation due to regulatory constraints, resulting in low utilization efficiency. This study selects 416 green-building cases in northern Taiwan and investigates the operational status and equipment variations of their rainwater harvesting systems. Adopting a designer-centered perspective, the typologies are examined in terms of configuration requirements, use scenarios, and cost considerations, and optimization recommendations are proposed to address identified deficiencies. A rainwater harvesting cycle model is then developed to simulate daily flow dynamics across cases under daily rainfall conditions. By modeling storage, utilization, make-up water supply, and overflow processes, the study evaluates the efficiency of storage capacity and rainwater use among different typologies. The results (1) identify prevailing typologies of building rainwater harvesting systems under current practice, (2) assess operating modes and utilization efficiency and summarize performance patterns across typologies, and (3) establish typology-specific optimization strategies to improve efficiency and remedy equipment limitations. Overall, the proposed typologies and actionable recommendations aim to enhance rainwater substitution and better satisfy water demand, thereby supporting sustainable water resources management.

Keywords

Green building, Rainwater harvesting system, Rainwater utilization, Water resources

1. Introduction

Taiwan is in the subtropical zone and is strongly influenced each year by typhoons and the plum rain season. Although annual precipitation is high, topographic constraints limit effective retention, and less than 10% of rainfall is practically captured and utilized for daily life, making water resources a critical issue for national development. According to domestic water-use statistics compiled by Taiwan's Water Resources Agency, the average per-capita daily domestic tap water consumption increased from 274 L/person/day to 289 L/person/day between 2015 and 2024, representing a 5.54% rise and indicating a continuing upward trend in per-capita water demand.

Moreover, the utilization of building rainwater harvesting systems remains suboptimal. In the present sample, 92.31% of harvested rainwater is used exclusively for watering plants, with limited application to cleaning and toilet flushing. Existing rainwater-harvesting configurations exhibit substantial diversity, yet there are few additional constraints or standards governing equipment selection and operational practices. This research analyzes the operational status of rainwater harvesting systems across Taiwanese green-building cases and systematically classifies the diverse system patterns. Furthermore, a rainwater cycle modeling framework is employed to simulate typology-specific utilization efficiency and to propose optimization and improvement strategies, with the overarching aim of advancing sustainable water resource circulation.

2. Scope and methodology

2.1 Research Process

This research adopts a research logic of "current practice inventory → typology synthesis → performance quantification → strategy formulation," aiming to establish an evaluation framework that can be adopted by professionals and referenced by institutional governance. Based on field investigations, four key issues are identified, and the research objectives are as follows:

(1) Current practice investigation of rainwater harvesting systems

This research conducts a current practice survey of green-building cases in northern Taiwan that are equipped with rainwater harvesting systems, covering three major climatic zones and five primary building categories. Using empirical case data, the study systematically documents and explains the practical challenges encountered in implementing rainwater harvesting systems and the gaps between real-world

planning/design practices and the provisions of existing evaluation manuals and guidelines.

(2) Patterns analysis and integration of building rainwater harvesting systems
Drawing on 416 rainwater harvesting cases, the study examines system heterogeneity and synthesizes typological differences across key components and processes, including collection, filtration, conveyance/flow routing, storage tanks, equipment configurations, make-up water supply, and end-use reuse. Representative configuration typologies are identified for in-depth analysis, followed by a discussion of their advantages, limitations, and potentially applicable scenarios.

(3) Development of a rainwater cycle simulation model for efficiency calculation
Daily rainfall records over the past decade from the three major climatic zones in northern Taiwan are compiled to develop an Excel-based simulation model that quantifies operational performance across typologies. By incorporating building-specific parameters—such as total gross floor area, total catchment area, total irrigation area, and storage tank capacity (Vs)the model outputs key indicators including tank utilization rate, make-up water rate, overflow rate, and municipal water substitution rate, which serve as the basis for subsequent evaluation.

(4) Formulation of optimization strategies and improvement recommendations based on simulation outcomes
Using the simulated efficiency results, the study evaluates system operational performance across cases and proposes optimization-oriented assessment perspectives. In addition, reuse end-uses are incorporated into further simulation analyses to support the development of objective and defensible optimization recommendations aligned with improvement targets.

Ultimately, this study conducts an in-depth analysis of rainwater harvesting systems in current practice, establishes standardized representative typologies, and performs simulation-based evaluation. With the goals of enhancing rainwater utilization and advancing typology optimization, the study provides an important foundation for improving the long-term benefits of water resource management.

2.1 Rainwater Havesting and Reuse

Figure 1 illustrates five main rainwater harvesting surfaces commonly used in current building engineering, as well as five common rainwater storage spaces. Currently, rainwater harvesting in the industry includes roofs, building facades, terraces, balconies,

and ground surfaces. Corresponding water storage spaces include raft foundations, underground water tanks, reservoirs, flood control ponds, and ecological ponds.

Figure 2 illustrates the conceptual components of a typical rainwater harvesting and reuse system, which mainly consists of six key devices and operational processes, incorporating a reuse objective. A brief overview of each component is as follows:

(1) **Rainfall Catchment Facilities:** Surfaces in direct contact with rainfall, including rooftops, façades, terraces, balconies, and site ground areas.
(2) **Conveyance Facilities:** Piping systems that transport collected rainwater.
(3) **Filtration Facilities:** the filtration process is divided into three stages—preliminary filtration, depth filtration, and disinfection/aeration/dichlorination/ chemical dosing—to purify water quality.
(4) **Storage Facilities:** Infrastructure for storing rainwater, such as Silt Basin/Detention Pond/ Rainwater Recycling Pool/ Water Purification Pool
(5) **Monitoring Facilities:** Equipment for controlling and monitoring water quality and inflow volume.
(6) **Power Facilities:** Pumps and related components necessary for water transport.
(7) **Utilization Targets:** End uses of treated rainwater, including irrigation, toilet flushing, supplemental water supply, and cleaning.

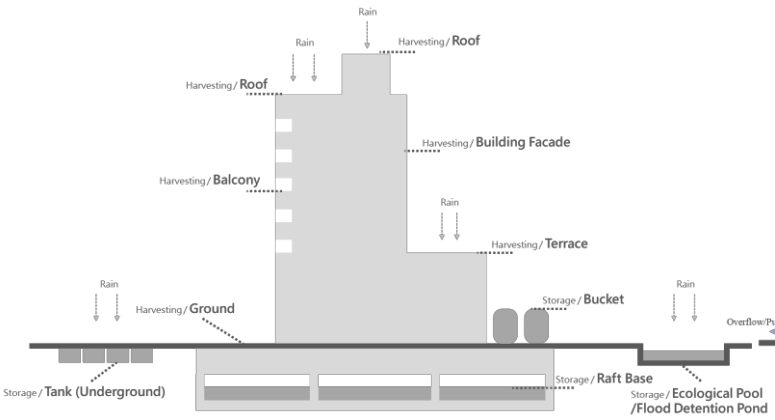

Figure 1. Rainwater Havesting and Storage

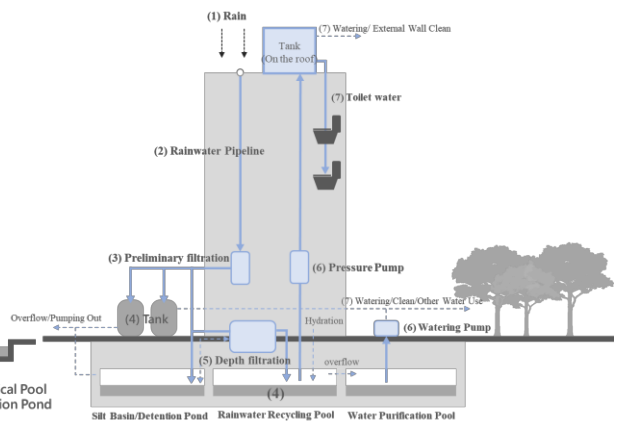

Figure 2. Rainwater Recycling Process

3. Current survey and pattern analysis of building rainwater harvesting systems

3.1 Current status of building rainwater harvesting systems

This study compiled data from 416 buildings with rainwater harvesting systems. *Figure 3*, the most common method of rainwater harvesting was the roof, with 100% of the cases involving rooftop collection. Specifically, 93.99% of the cases used the roof as the sole rainwater harvesting method. Currently, *Figure 4* rainwater reuse is highly concentrated in irrigation, with 92.31% of the cases using irrigation as their primary purpose. Furthermore, reuse for toilet flushing accounts for only 2.88%, indicating a low proportion of rainwater used for this purpose. One case was even disqualified, revealing a significant flaw in the water consumption rating section of the *Green Building Assessment Handbook*, highlighting the need for immediate improvement of existing regulations. The study results reflect that rainwater harvesting in practical applications tends towards low-water-quality, low-risk strategies. Further research is needed to explore technologies and address bottlenecks in other uses, aiming to substantially improve efficiency.

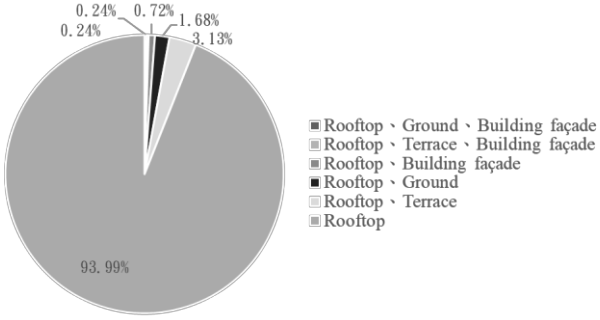

Figure 3 Rainwater harvesting methods

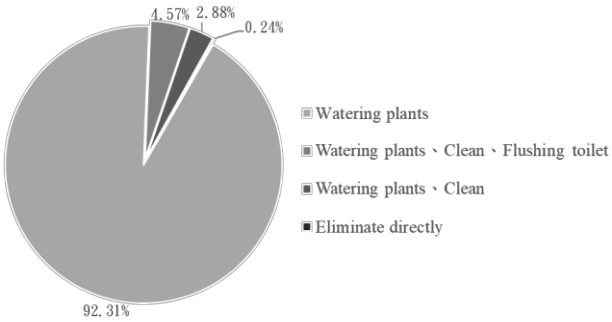

Figure 4 Rainwater reuse status

As shown in *Figure 5*, the main of cases (87.98%) used raft foundations for storage, followed by raft foundations combined with water tanks (9.62%), while water tanks alone accounted for the lowest proportion at only 2.40%. Overall, the storage method is highly concentrated in the single form of "raft foundation." As shown in *Figure 6*, This discussion primarily focuses on the ratio of rainwater harvesting ponds and stormwater retention ponds to the raft foundation area, examining five building types. The light-colored area represents the ratio of rainwater harvesting ponds to the raft foundation area, showing that current building examples average 9.54% of the rainwater capacity. Next, the stormwater retention pond is added to the rainwater harvesting pond (black-colored area), clearly showing an increased utilization rate of the raft foundation, averaging 18.92%. However, approximately 80% of the raft foundation space remains unused, indicating significant wasted space. Therefore, the raft foundation space, as a rainwater storage space, still has shallow potential and room for development.

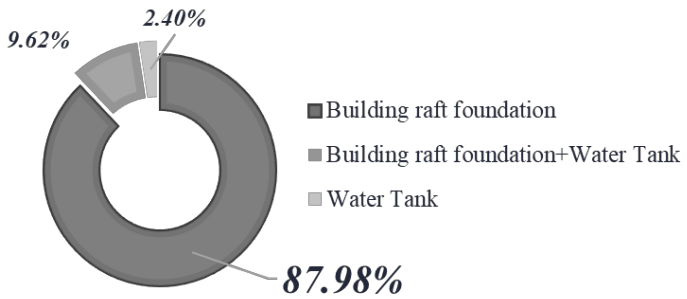

Figure 5 Rainwater storage methods

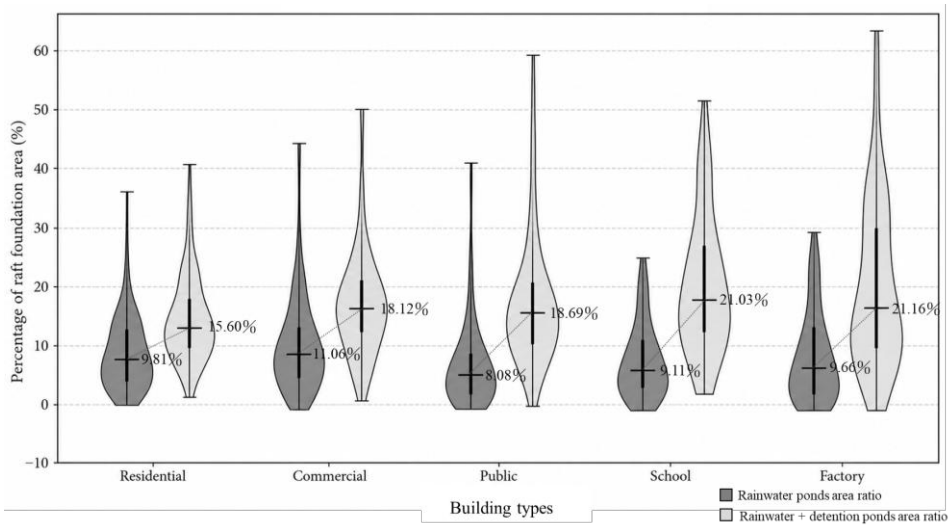

Figure 6 Rainwater harvesting plus rainwater detention ponds as a percentage of raft foundation area

3.2 Rainwater harvesting system patterns classification logic

This research collected 416 new green building projects from seven counties and cities in northern Taiwan between 2013 and 2024 as samples. Rainwater runoff level maps and detailed design drawings of rainwater harvesting systems were extracted from water resource indicators for discussion. Information was gathered on water storage space, equipment types, system operation processes, overflow methods, and reuse patterns. The purpose of the raft foundation and the area, depth, and volume of the corresponding pool were determined through raft foundation plans. Based on *Figure 7*, common filtration equipment and differences in rainwater flow were analyzed, and the patterns were combined and summarized into five patterns (A to E) for further discussion. Furthermore, combining the pattern flow diagrams clearly identifies the differences and operation processes of the patterns, facilitating subsequent discussion and analysis. As

shown in *Figure 8*, according to Taiwanese laws and regulations, filtered rainwater must not come into contact with humans. Therefore, high-filtration patterns must be used for promotion. This study recommends patterns B and D as the optimal configuration choices for promoting rainwater harvesting and reuse.

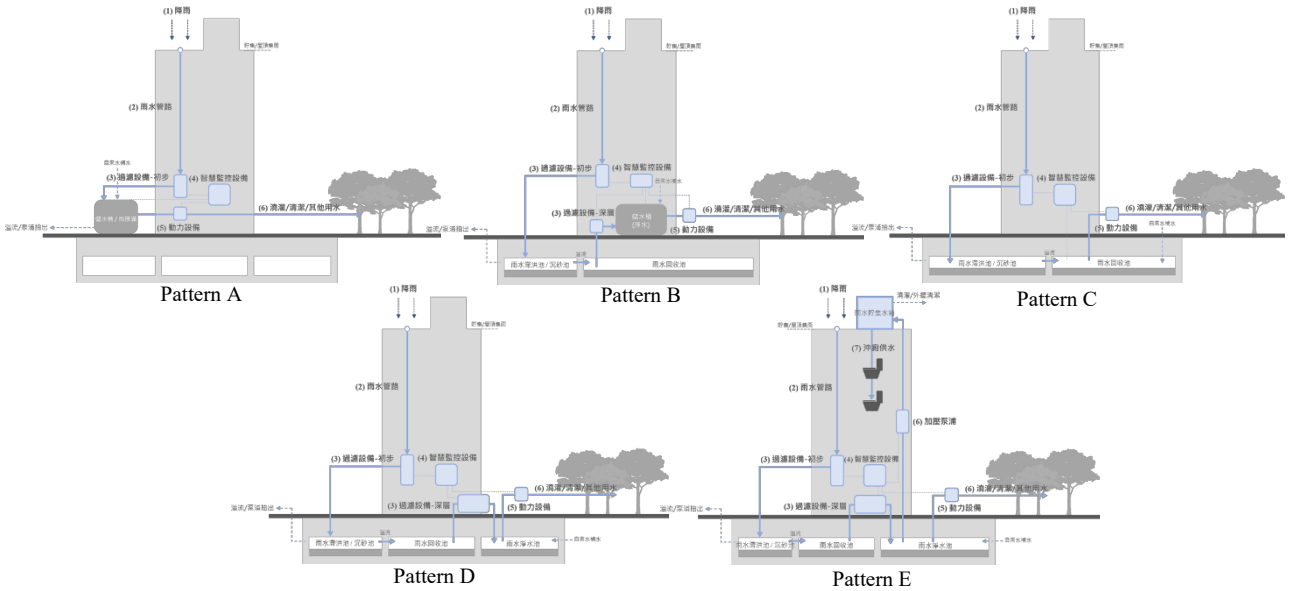

Figure 7 Representative patterns of building rainwater harvesting systems

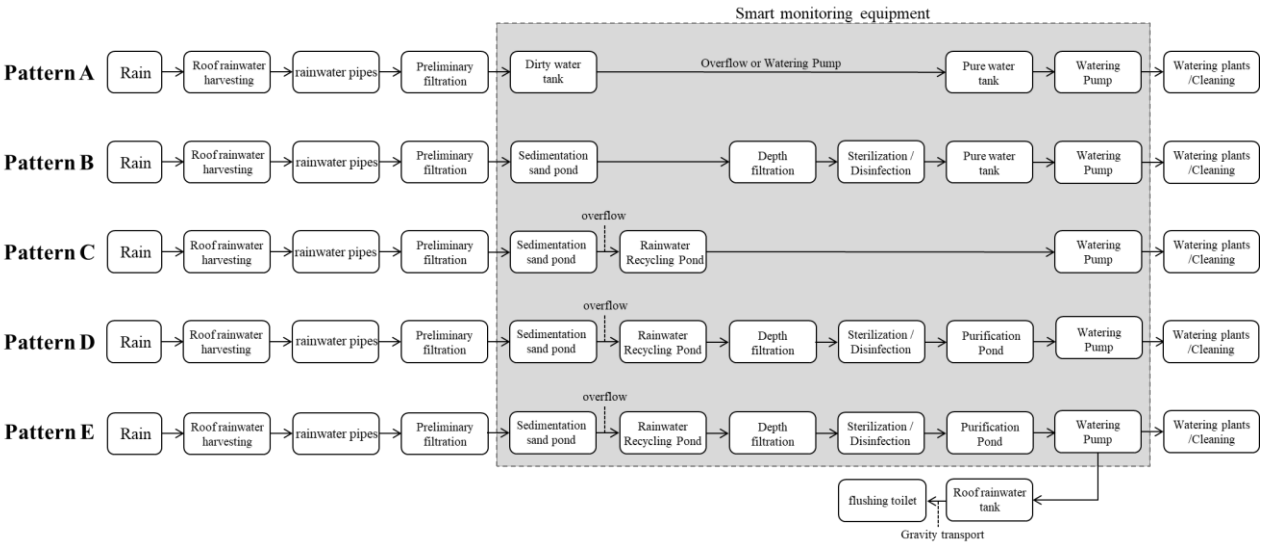

Figure 8 Rainwater harvesting system operation process

3.3 Rainwater harvesting system pattern analysis and evaluation

Figure 9 further discusses rainwater harvesting schemes in this study. Currently, Pattern C and Pattern D have the highest adoption rates, at 35.34% and 48.56% respectively. Pattern A, which uses water storage tanks, has 9 cases, accounting for 2.16%. Pattern E,

which includes a flushing toilet system, has 19 cases, accounting for 4.57%. Furthermore, the choice of scheme types is generally consistent across building types, concentrated in Pattern C and Pattern D. Pattern A has the lowest overall percentage, likely because tank volume and capacity limitations are not a priority.

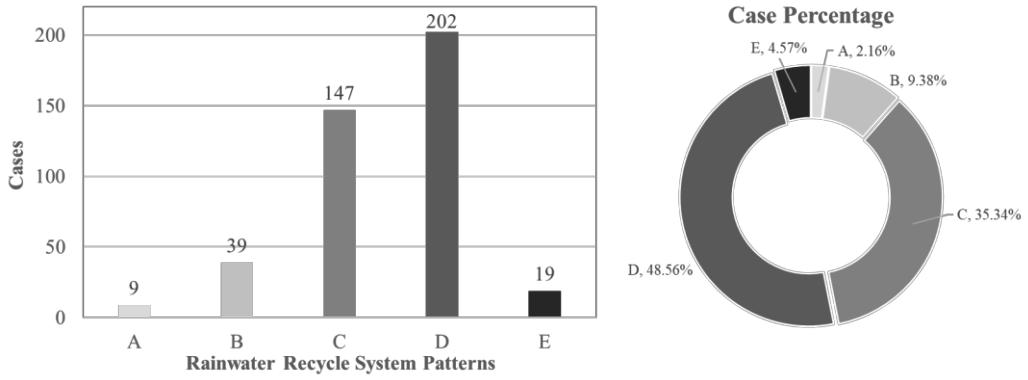

Figure 9 The case percentage of different architectural types used

According to *Figure 10,* commercial and office buildings have the highest adoption rate for Pattern D, and none use Pattern A; residential buildings do not use Pattern E, indicating that current residential buildings do not incorporate flushing toilets. Public and school buildings show a lower adoption rate in Pattern B compared to other building types, but the highest adoption rate in Pattern E, which includes flush toilet systems, indicating a higher prevalence of flush toilet systems in public and school buildings. Factory buildings show relatively even adoption rates in Patterns C and D, but the adoption rate in Pattern D is significantly lower than other building types, which can be understood as factory buildings not having particularly high requirements for water quality. Factory buildings also show a relatively high proportion of Pattern E, which includes flush toilets, indicating a higher acceptance rate for this feature.

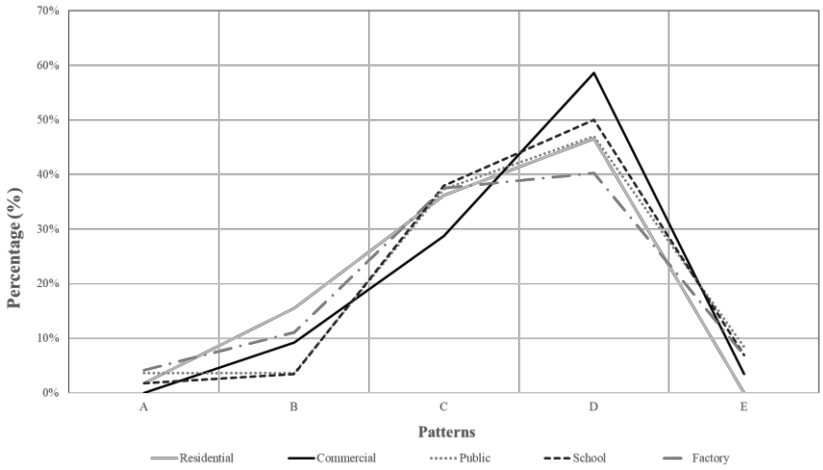

Figure 10 Architectural types and Pattern types of ratios

4. Pattern simulation and Optimization Strategy

4.1 Establish a rainwater harvesting simulation model

This study uses Excel as the simulation software to construct a rainwater cycle model. This model is based on the three major rainfall zones in northern Taiwan and the average daily rainfall over the past ten years. Necessary data, such as total building area, total rainwater harvesting area, total area irrigated by vegetation, and rainwater collection volume, were obtained through case studies. This study aims to improve rainwater reuse and uses simulations to predict the **replacement rate of tap water**. This indicator allows for understanding the operational efficiency of the case studies. Including other reuse needs allows for the identification of changes in system utilization. Finally, insights and expectations can be derived from the simulation results.

$$Rc = Ws \div Wt \quad (1)$$

$$Wt = Wf \times Af \quad (2)$$

$$Wr = R \times Ar \quad (3)$$

$$Wd = \Sigma Ri \quad (4)$$

Rc：tap water replacement rate

Ws：replacement water of tap water (L/day)

Wt：building water consumption (L/day)

Wf：unit area water consumption (L/day)

Wd：rainwater utilization design capacity (L/day)

Af：total floor area (m^2)

Ar：rainwater collection area (m^2)

Ri：rainwater reuse consumption (L/day)

4.2 Pattern efficiency simulation analysis

This study collected 416 green building case studies, conducting data collection and simulation research. *Figure 11,* from five different rainwater harvesting patterns (A-E), the rainwater utilization status of buildings can be determined. It was found that buildings A-D, which did not employ flushing systems, showed a trend towards lower rainwater utilization, averaging 2.35%. This confirms the findings in Chapter Three, where most cases only utilized plant watering as a reuse item. Pattern D had some outliers and higher tap water usage, indicating an excellent rainwater system

configuration. Pattern E, which included flushing toilet systems, showed an overall average higher than other patterns, averaging 15.27%. Therefore, incorporating flushing toilet systems can improve rainwater utilization and reduce resource waste.

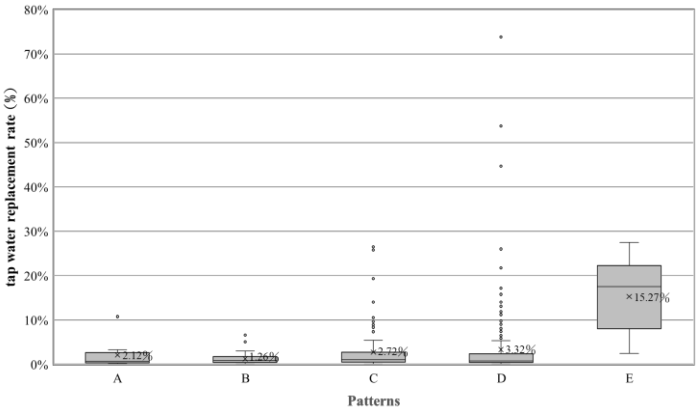

Figure 11 tap water replacement rate simulation results

4.3 Efficiency Optimization Analysis

Figure 11 clearly shows that simply adding a flushing system without adjusting other parameters can effectively improve rainwater utilization and tap water replacement rate. *Figure 12* shows that after adding the flushing system, the overall average increased from 2.35% to 7.06%, an increase of 4.57%. In the sample, 11.50% saw an increase of over 10% in tap water replacement rate, with a few samples even reaching an increase of 40%. However, the increase in most cases remains relatively low. Overall, the addition of a flushing system can improve the tap water replacement rate, but it is still insufficient for some buildings and warrants further discussion.

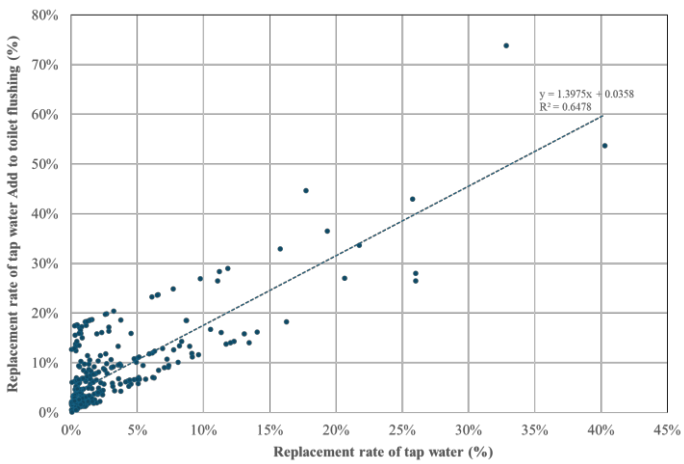

Figure 12 tap water replacement rate into a toilet flushing system

When the toilet flushing system was added to the cases, there were significant changes in the utilization efficiency of the storage space and the replacement of tap water. The simulation results will provide a significant breakthrough for the future promotion of rainwater harvesting systems in Taiwan. Additionally, this research will serve as an important reference for future policy formulation and design planning.

5. Conclusion

This study investigates **416 newly constructed green-building projects** equipped with rainwater harvesting systems in seven cities/counties in northern Taiwan, covering five major building categories. Key variables include rainwater collection approaches, reuse patterns, and the raft-foundation storage-to-area ratio. The results indicate that **rooftops** are the primary collection surface, **watering plant** is the dominant end use, and the rainwater harvesting area accounts for an average of **9.54%** of the raft-foundation area. The utilization rate of raft foundations increased by an average of **18.92%** after the addition of a flood detention basin. Based on the case dataset, system components—including storage design, equipment configurations, rainwater flow paths, and reuse end uses—were decomposed and re-integrated to define f**ive representative patterns (A–E)**.To test improvement potential, toilet flushing was incorporated as an additional reuse end use for patterns A–D, followed by re-simulation. The enhanced scenarios produce an average increase of **4.57%** in **tap-water replacement rate**. In the sample, **11.50%** of cases achieve an improvement of at least **10%**, suggesting that expanding reuse beyond irrigation can meaningfully enhance rainwater utilization. Finally, the study based on both empirical configuration analysis and simulation outcomes proposes typology-specific optimization recommendations, offering a practical direction for advancing rainwater reuse in Taiwan.

References

1. D.Bermudez,R.Gomes,A.Silva-Afonso,C.Pimentle-Rodrigues,J.Gurierrez (2018). *Water Efficency in Collective Non-Residental Building (Hotels)*.2018 Symposisum CIB W062
2. M. Fernandes Caetano, H. Tavares da Silva(2018). *R. Ribeiro ,Systems for the use of rainwater in buildings*; the European standard EN16941-1.2018 Symposium CIB W062
3. Tamio NAKANO(2019). *The Construction Design Using Rain Water and Potential Effective Use of Rain Water*. 2019 Symposium CIB W062

4. S. Kuo , S. Ho, C. Liu, 2006, Estimation irrigation water requirements with derived crop coefficients for upland and paddy crops in ChiaNan Irrigation Association, Taiwan, *Agricultural Water Management*, vol. 82, p. 433-451
5. T. Wung, S. Lin, S. Huang, 2006, Rainwater reuse supply and demand response in urban elementary school of different districts in Taipei, *Resources, Conservation and Recycling*, vol. 46, p. 149-167
6. Lin Yingjun, 2021, Research on the water supply and demand balance assessment model of thin-layer green roofs, Master's thesis, Institute of Architecture, National Taiwan University of Science and Technology
7. Ye Xinfu, Wang Shiming, Li Zhewei, Li Zhengao, 2014, Research on using limited meteorological parameters to evaluate evapotranspiration, *Crop Environment and Biological Information*, vol.11 p.203-218
8. Construction and Planning Agency, Ministry of the Interior, 2012, *Technical specifications for the design of rainwater storage and utilization in buildings*

Presentation of Authors

Huang, Shi-Feng is the Master Student at National Taiwan University of Science and Technology, Department of Architecture. His research is focus on building rainwater recycling system.

Cheng, Cheng-Li is the Professor at National Taiwan University of Science and Technology, Department of Architecture. He is a research scholar for water supply and drainage in building. He has published extensively on a range of sustainable issues, including the water and energy conservation for green building.

Comparative evaluation of simplified pipe sizing methods for non-looped domestic water distribution systems in a Belgian context

C. Jacques (1), B. Poncelet (2)

(1) colin.jacques@buildwise.be

(2) benoit.poncelet@buildwise.be

(1) (2) Buildwise, Belgium

Abstract

Domestic water distribution systems must be properly sized to ensure adequate hydraulic performance, water quality, comfort and energy efficiency. Oversizing may cause stagnation and bacterial growth (e.g. *Legionella*), while undersizing can lead to insufficient flow rates. Additionally, inappropriate sizing increases water waste and energy losses, especially in hot water systems.

In Belgium, the only normative approach currently available for pipe sizing is the simplified method defined in EN 806-3:2006. However, this method presents several limitations, notably a lack of clarity regarding its application domain and underlying assumptions, which may explain its limited use. As a result, designers often rely on alternative methods developed in neighbouring countries.

This study analyses and compares several simplified pipe sizing methods in order to assess their behaviour and identify their strengths and limitations. The analysed methods were selected from a broader review of international approaches, based on their relevance for practical application in Belgium. The analysis focuses on simplified methods intended for practical design use, in contrast to more detailed hydraulic calculation methods.

The analysed methods include EN 806-3:2006, DTU 60.11:2013, ISSO 55:2023 and SSIGE W3:2013. The methods are applied to representative residential building configurations, focusing on non-looped (tree-shaped) systems. DIN 1988-300:2012 is included as a detailed hydraulic reference to support the interpretation of results.

The results reveal significant discrepancies between methods, particularly for distribution pipes. Systematic trends are observed, with some methods tending to recommend larger diameters, while others recommend smaller diameters. Methods based on pressure constraints generally result in larger diameters under low-pressure conditions compared to velocity-based approaches.

Within the scope of the analysed cases, none of the analysed simplified methods achieved a satisfactory balance between simplicity, applicability and hydraulic reliability, highlighting the need for an improved simplified sizing approach.

Keywords

Pipe sizing; domestic water distribution; simplified methods; residential buildings; comparative analysis

1 Introduction

Proper sizing of domestic water distribution systems is essential to ensure hydraulic performance, water quality, comfort and energy efficiency [1,2]. Oversized pipes increase water residence time, stagnation risk, heat losses and water waste, especially in hot water systems, whereas undersized pipes may lead to insufficient flow rates and reduced comfort [1–4].

In Belgium, EN 806-3:2006 [5] is the main normative simplified method for sizing non-looped domestic water distribution systems. However, previous work identified limitations regarding its field of application and underlying assumptions [6]. Belgian designers therefore often refer to methods from neighbouring countries, such as DTU 60.11:2013 [7], ISSO 55:2023 [8] or DIN 1988-300:2012 [9]. At the time of writing, EN 806-3 was listed by CEN as being under revision [10], reinforcing the relevance of reassessing simplified sizing approaches.

Previous Buildwise studies based on Belgian measurement campaigns identified DIN 1988-300 as the best available basis for sanitary pipe sizing and reported good agreement between measured peak flow rates and values calculated using this method [1–3]. However, DIN 1988-300 remains relatively complex for routine design because it requires a more detailed hydraulic assessment than table-based approaches.

The present study compares simplified pipe sizing methods relevant to Belgian practice under identical boundary conditions. The objective is to assess their behaviour and determine whether one of them could reasonably be recommended to practitioners, using DIN 1988-300 as a detailed hydraulic reference to support the interpretation.

2 Methodology

2.1 Preliminary bibliographic review and analytical framework

A broad, but non-exhaustive, international bibliographic review was conducted to identify existing sizing methods for non-looped domestic water distribution systems and to select the methods retained for detailed comparison. The reviewed approaches covered European, Swiss, Nordic and North American references [5,7–9,11–22] and were grouped into three categories: (i) simplified table-based methods, in which a demand indicator, such as loading units or fixture units, is converted into pipe diameters using charts or tables; (ii) iterative hydraulic methods, where a preliminary diameter is selected and then verified against velocity and pressure-loss criteria; and (iii) methods based on allowable pressure loss per unit length, where the most hydraulically unfavourable path

governs the sizing procedure. This classification was used as the analytical framework for the subsequent comparison.

2.2 Selection of methods for detailed comparison

The detailed comparison focused on methods considered relevant to Belgian practice and to the objective of identifying, or supporting the development of, a simplified sizing approach for non-looped domestic water systems. The analysed simplified methods were EN 806-3:2006 [5], DTU 60.11:2013 [7], ISSO 55:2023 [8] and SSIGE W3:2013 [11].

EN 806-3 was included because it is the current simplified normative method applicable in Belgium, although previous Buildwise work identified limitations regarding its field of application and assumptions [6]. DTU 60.11 and ISSO 55 were selected because they originate from neighbouring countries and are commonly referred to by Belgian practitioners.

SSIGE W3 was included because it is recommended by several manufacturers active on the Belgian market [17,23] and combines a simplified table-based procedure with explicit applicability criteria and a more detailed calculation method when these criteria are not met [11]. Since the simplified method relies on manufacturer-specific tables, the Geberit Mepla multilayer pipe tables [16,23] were used, considering both direction changes using fittings and direction changes by pipe bending.

DIN 1988-300 was included as a detailed hydraulic reference, based on previous Buildwise studies identifying it as a reliable basis for pipe sizing [1–3]. The DIN framework was assessed using both its original velocity limits and Belgian common-practice velocity limits, namely 2.0 m/s in basements and technical rooms, 1.5 m/s in vertical shafts, and 1.0 m/s in occupied rooms [24].

2.3 Case studies, selected pipe sections and common boundary conditions

The selected methods were applied to four representative Belgian residential case studies, all corresponding to *non-looped* domestic water distribution systems. In this study, *non-looped* systems include both tee-based distribution layouts and manifold-based layouts, as opposed to looped distribution systems. The four analysed case studies correspond to typical Belgian residential configurations, illustrated in Figure 1. These include: (Case A) a terraced worker-type house with two storeys and a basement, using tee-based branching on the ground floor and manifold-based on the first floor ; (Case B) a terraced townhouse with three storeys and a basement, using manifold-based distribution on each level; (Case C) a detached villa with two storeys, using manifold-based distribution; and (Case D) a single-level apartment with manifold-based distribution. These cases were selected to represent common variations in building height, internal layout and distribution principles of Belgian residential buildings.

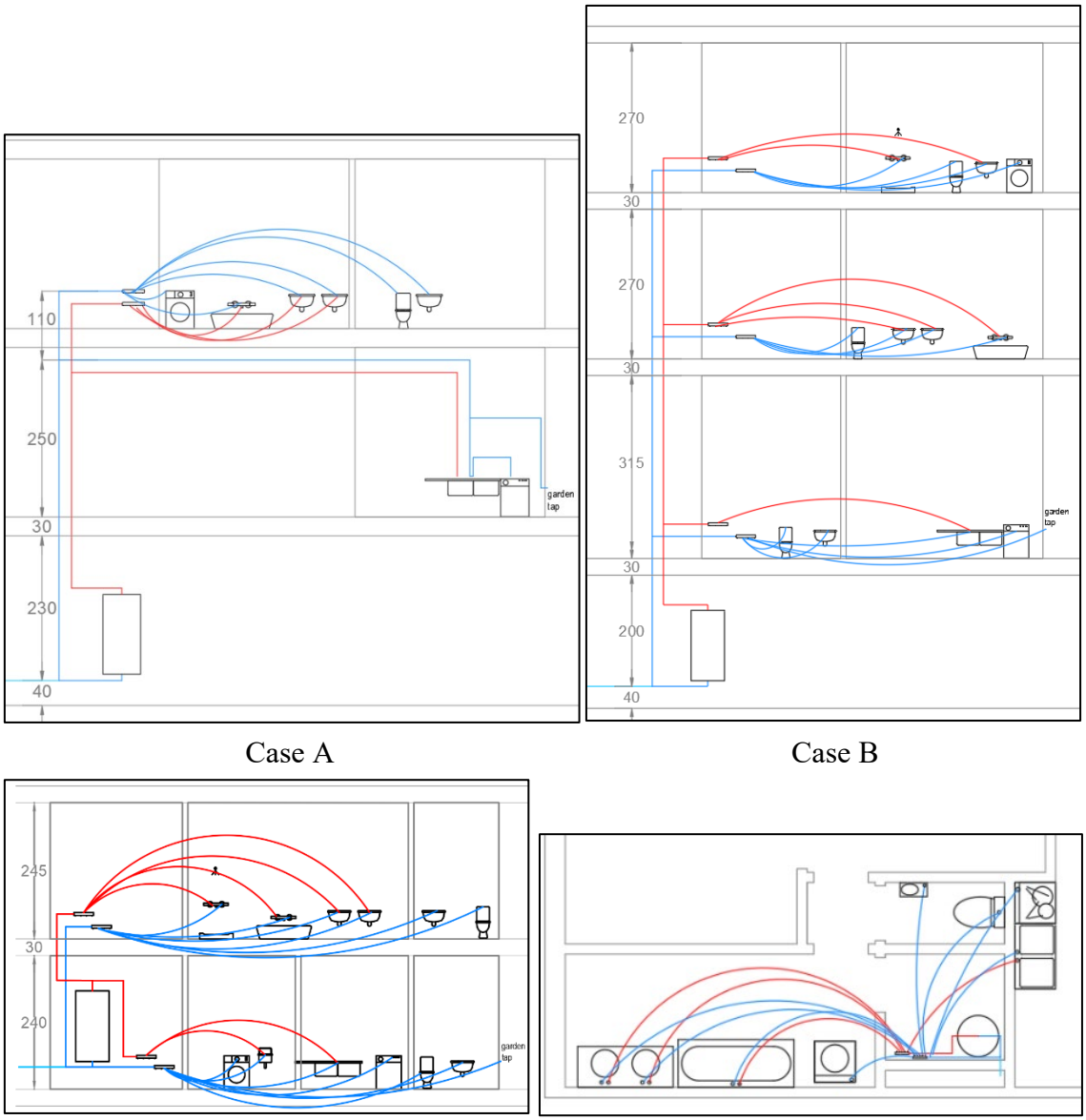

Case A Case B

Case C Case D

Figure 1 - layouts of the four typical Belgian dwellings studied

A limited set of representative and critical pipe sections was selected, including the main distribution pipe, the first cold-water and hot-water distribution pipes, and terminal pipes supplying the shower, bathtub, kitchen sink and outdoor tap. The median-based comparison and the interpretation relative to DIN 1988-300 were carried out on this subset. In this study, *distribution pipes* refer to pipes supplying one or several wet rooms, *storey pipes* to downstream sections located between the first and last draw-off points of a given path, and *terminal pipes* to pipes supplying a single appliance.

To ensure comparability, a common set of assumptions was adopted for all case studies unless a method explicitly required otherwise. The available service pressure was set at *3 bar*. All diameters considered in the comparison were internal pipe diameters. The calculations were carried out assuming multilayer pipes. Bathtubs were considered

hydraulically equivalent to showers, both to facilitate comparisons between buildings containing slightly different sanitary layouts and because DIN 1988-300 does not distinguish between these two fixtures in the demand assumptions used for sizing. In addition, when some methods imposed a minimum internal diameter of 11.5 mm and others 12 mm, these values were treated as equivalent for comparison purposes.

2.4 Comparative procedure

Each selected method was applied to the same case study layouts and to the selected subset of pipe sections defined above. The comparison covered both *distribution pipes* and *terminal pipes* in the cold and hot water branches. For each case study and each pipe category, the internal diameter recommended by each method was determined according to the rules, tables, charts or formulae prescribed by the considered method.

The comparison was then performed on the basis of the recommended internal diameters. For each case study and each pipe category, the median of the diameters obtained from all analysed methods was used as a comparative reference value. The deviation between the diameter recommended by a given method and this median value was then calculated in order to identify tendencies to recommend larger or smaller diameters relative to the general trend observed across the set of methods. The median was preferred to the arithmetic mean because it is less sensitive to extreme values and therefore provides a more robust comparative indicator when methods diverge significantly. In this study, however, the median was not considered as an absolute hydraulic truth, but as a practical comparative reference allowing each method to be positioned relative to the others.

In addition to the median-based comparison, the results were interpreted, where applicable, relative to DIN 1988-300 as a detailed hydraulic reference. This comparison was used to support the interpretation of the simplified methods, not as an exhaustive validation of each method against DIN 1988-300.

A dimensionless comparative index was developed to position each sizing method according to its relative tendency to recommend larger or smaller pipe diameters. For each method, deviations from the median diameter of all compared methods were calculated separately for distribution and terminal pipes. The sum of these deviations was used to capture the overall magnitude and direction of the tendency, while the median deviation was used to represent its recurrent behaviour with reduced sensitivity to isolated extreme values. Both indicators were normalised on a −10 to +10 scale and averaged to obtain the final graphical index. Positive values indicate a tendency towards larger diameters, negative values a tendency towards smaller diameters. The index should therefore be interpreted as a relative comparison tool rather than as a hydraulic validation criterion.

3 Results

3.1 Overall trends across methods

The comparison revealed significant discrepancies between the analysed methods, particularly for distribution pipes. By contrast, terminal pipes showed greater convergence, with several methods producing identical or very similar diameters for the

same fixtures. This indicates that the main methodological differences do not affect all parts of the network equally, but are concentrated in the pipe sections where simultaneity, available pressure and cumulative demand have the strongest influence.

A first global result is that the methods did not depart from the central trend in the same way. EN 806-3 and DTU 60.11 generally occupied a central position. ISSO 55 tended to recommend smaller diameters, especially for distribution pipes. SSIGE W3 showed the opposite tendency and often recommended larger diameters than the other simplified methods. DIN 1988-300 generally led to larger diameters when pressure constraints became governing, particularly under low-pressure conditions.

The comparison with DIN 1988-300 confirms that these tendencies are not only visible relative to the median, but also relative to a more detailed hydraulic calculation framework. The strongest deviations from DIN 1988-300 were observed for distribution pipes, whereas agreement was generally higher for terminal pipes.

Figure 2 shows the aggregated comparative index defined in Section 2.4, with the x- and y-axes representing distribution and terminal pipe sizing tendencies, respectively.

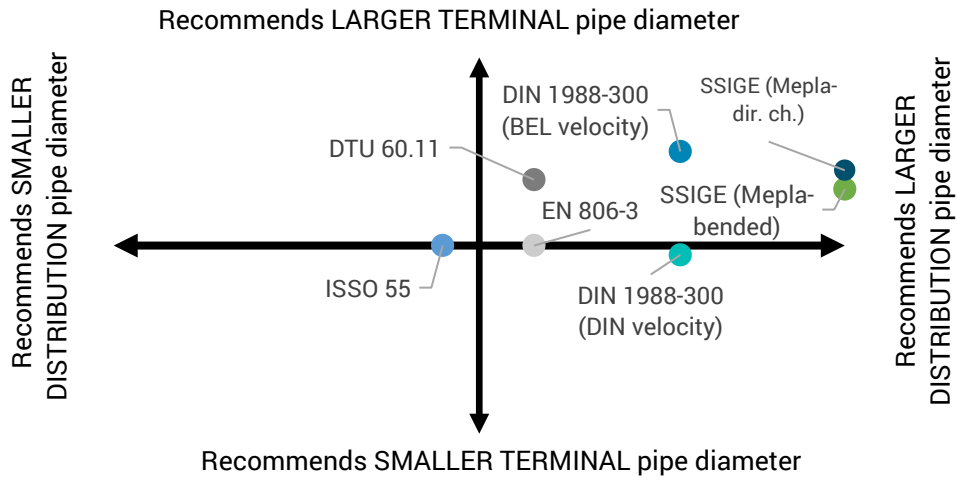

Figure 2 - Aggregated comparative index of relative sizing tendencies

3.2 EN 806-3:2006 and DTU 60.11

EN 806-3:2006 and DTU 60.11 provided identical results in the large majority of the analysed cases. The differences were limited to specific low-flow situations, notably the garden tap, where DTU 60.11 recommended larger diameters. This behaviour can be explained by the additional fixture-weight criterion included in DTU 60.11, which gives greater importance to cases where a single fixture contributes a large share of the total demand.

Relative to DIN 1988-300 with its original velocity limits, EN 806-3:2006 and DTU 60.11 remained in an intermediate position for distribution pipes. They produced the same diameters as DIN in 49% and 46% of the analysed distribution-pipe cases, respectively, and smaller diameters than DIN in 43% of cases for both methods. These results confirm their intermediate behaviour: they do not systematically remain aligned with the DIN

1988-300 calculation framework, but they also do not show a systematic tendency to recommend the largest diameters.

Therefore, EN 806-3:2006 and DTU 60.11 should not be interpreted as automatically validated methods. Their central position relative to the set of compared methods indicates a compromise between more conservative and less conservative approaches.

3.3 ISSO 55: sizing tendencies

ISSO 55 frequently recommended the smallest diameter among the analysed methods. When it differed from the median, this occurred exclusively for distribution pipes, indicating a systematic tendency towards lower diameters in those pipe sections. Furthermore, ISSO 55 tended to recommend smaller diameters for distribution pipes while generally matching the median for terminal pipes.

This tendency was confirmed by the comparison with DIN 1988-300. For distribution pipes, ISSO 55 produced smaller diameters than DIN 1988-300 with original velocity limits in 74% of the analysed cases. When the Belgian common-practice velocity limits were applied within the DIN 1988-300 framework, this proportion increased to 83%. These results reinforce the interpretation that ISSO 55 tends to provide less conservative sizing for distribution pipes.

3.4 SSIGE W3

SSIGE W3 represented the conservative end of the analysed methods. Compared with the intermediate behaviour observed for EN 806-3:2006 and DTU 60.11, it tended to recommend larger diameters, especially for distribution pipes. Whenever it differed from the median, it recommended equal or larger diameters, and no systematic tendency towards smaller diameters relative to the median was observed. However, its practical applicability is limited by its reliance on manufacturer-specific tables and by applicability criteria related to maximum pipe lengths and minimum available pressure.

The comparison with DIN 1988-300 supports this interpretation. For distribution pipes, SSIGE W3 resulted in larger diameters than DIN 1988-300 with original velocity limits in 71–74% of the analysed cases, depending on the table configuration considered. Even when the Belgian common-practice velocity limits were applied within the DIN 1988-300 framework, SSIGE W3 still remained above DIN 1988-300 in 66–69% of the analysed distribution-pipe cases. This confirms that the conservative character of SSIGE W3 is robust and not only an artefact of the median-based comparison.

The differences between the two SSIGE W3 implementation variants considered in the study remained limited. This indicates that, within the scope of the analysed cases, the conservative character of the method is more strongly linked to its overall sizing logic than to the specific multilayer-pipe table configuration.

3.5 Applicability limits of SSIGE W3

The simplified SSIGE W3 method includes an applicability criterion requiring a minimum available pressure of 1.5 bar [11]. Under the common boundary condition of 3

bar at the building entry, here referred to as the minimum service pressure available (MSPA), this requirement was not satisfied for any of the analysed cases. Additional calculations were therefore performed for inlet pressures of 4 and 5 bar. With the tested 1 bar pressure increments, only the 5 bar condition allowed all analysed cases to satisfy the criterion for both cold and hot water branches.

When this criterion is not satisfied, the simplified procedure is no longer applicable and the designer must rely on the more detailed calculation method provided in SSIGE W3 or on another detailed hydraulic sizing approach [11]. Under the common 3 bar inlet-pressure condition used in this study, the minimum available-pressure criterion made the simplified SSIGE W3 method inapplicable to all analysed cases. Only when the inlet pressure was increased to 5 bar, using 1 bar pressure increments, did all analysed cases satisfy the criterion.

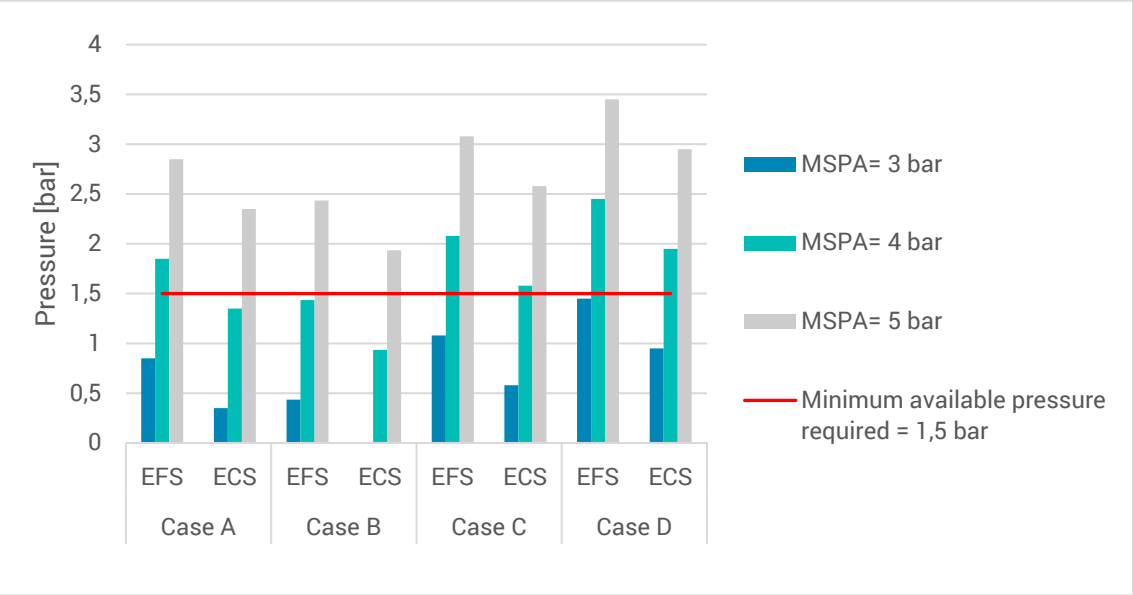

Figure 3 - Comparison of the MSPA with the 1.5 bar minimum available-pressure criterion, by case

3.6 DIN 1988-300, pressure constraints and Belgian common-practice velocity limits

DIN 1988-300 behaved differently from the simplified methods because the available pressure loss per metre may become the governing sizing criterion. In the analysed cases, deviations from the median increased as this available pressure decreased; below approximately 0.016 bar/m, DIN 1988-300 generally recommended larger diameters. This effect was particularly visible in cases with greater elevation differences or additional pressure losses in the hot water branch.

The comparison between the original DIN velocity limits and the Belgian common-practice velocity limits showed that the stricter Belgian practice limits shifted the DIN-based calculation towards larger diameters when velocity was the governing criterion. By contrast, no difference was observed when available pressure loss governed the sizing.

This comparison was therefore treated as a sensitivity analysis of the DIN framework rather than as a separate simplified method.

4 Discussion

4.1 Main drivers of divergence between methods

The comparison clearly shows that the analysed simplified methods cannot be considered interchangeable. Significant discrepancies were observed between methods, especially for distribution pipes, whereas terminal pipes were generally less affected. This confirms that the choice of sizing method may substantially influence the resulting hydraulic design, even when the same building layout and boundary conditions are considered.

A first major source of divergence lies in the hydraulic criterion that governs the sizing process. In DIN 1988-300, the available pressure loss per metre of pipe plays a central role and may become the governing criterion when the available pressure is low. In the analysed cases, this led to systematically larger diameters when the available pressure per metre (Rv) dropped below a critical range of approximately 0.016 bar/m. Under such conditions, DIN 1988-300 departed markedly from the other methods, which rely more strongly on simplified flow tables, velocity criteria or embedded safety margins.

A second source of divergence is the way simultaneity and pipe function are handled. Some methods differentiate between pipe categories, while others apply the same sizing logic to both terminal and distribution pipes. This distinction proved to be particularly important in the present analysis. Methods such as ISSO 55, which do not sufficiently distinguish between distribution and terminal branches in their simplified formulation, tended to recommend smaller diameters for distribution pipes. By contrast, SSIGE W3 showed the opposite tendency and generally remained on the conservative side, especially for distribution pipes.

4.2 Contribution of the DIN 1988-300 interpretation

The DIN-based comparison provides a complementary interpretation of the median-based analysis. While the median helps position each method relative to the set of compared methods, DIN 1988-300 provides a more physically grounded reference, particularly regarding pressure constraints. The comparison confirms that the main uncertainty concerns distribution pipes: methods that appeared less conservative relative to the median also tended to give smaller diameters than DIN 1988-300, whereas SSIGE W3 remained on the conservative side. The use of Belgian common-practice velocity limits acted as a sensitivity analysis, shifting the DIN-based calculation towards larger diameters without changing the overall interpretation.

4.3 Implications for Belgian design practice

Within the scope of the analysed case studies, the results did not identify any simplified method that could be recommended without reservation for Belgian practice. DIN 1988-300 remains the most robust detailed method in the comparison, but its practical implementation is too complex for routine simplified design work. SSIGE W3 is particularly informative because it combines a simplified table-based procedure with

explicit applicability criteria. However, this apparent advantage is accompanied by practical limitations: the method relies on manufacturer-specific tables, tends to recommend larger diameters than the other simplified methods, especially for distribution pipes, and includes a minimum available-pressure criterion.

In the analysed cases, this pressure criterion was not satisfied under the common 3 bar inlet-pressure condition. With the tested 1 bar pressure increments, all cases satisfied the criterion only at 5 bar. This represents a practical limitation, since 5 bar is close to the threshold above which NBN EN 806-2 recommends a pressure-reducing valve [25]. The simplified SSIGE W3 procedure may therefore have limited applicability in residential buildings with moderate available inlet pressure, requiring designers to switch to a more detailed calculation method.

A further limitation of SSIGE W3 is its dependence on manufacturer-specific sizing tables. The simplified procedure can only be applied when such tables are available for the considered pipe system and installation configuration. This limits its direct transferability to Belgian practice and may favour manufacturers whose tables already exist.

This raises a broader question for simplified sizing methods. Pressure-based applicability limits are intended to improve hydraulic reliability, but they may also reduce the range of cases in which the simplified method can actually be used. EN 806-3 and DTU 60.11 remain operationally simple but insufficiently explicit, ISSO 55 tends to produce smaller diameters for distribution pipes, and SSIGE W3 remains conservative but constrained by applicability limits. These findings support the development of an improved simplified approach for Belgian practice, combining table-based usability with explicit but practically applicable pressure criteria and a clearer distinction between terminal, downstream/storey and distribution pipes. The ongoing revision of EN 806-3 reinforces the relevance of this need, as it indicates that the current simplified sizing framework is being reconsidered.

4.4 Methodological limitations

The study has several limitations. It was designed as a comparative, non-experimental assessment under identical boundary conditions and should not be interpreted as validation against field measurements. The bibliographic review was broad but non-exhaustive. The median-based comparison identifies relative trends but does not establish hydraulic correctness, and the DIN-based comparison was limited to selected representative pipe sections. The four case studies do not cover all building typologies, pressure conditions, pipe materials or operating conditions. Finally, the SSIGE W3 results are based on selected Geberit Mepla multilayer pipe tables and should not be interpreted as covering all manufacturer-specific SSIGE W3 implementations.

5 Conclusion

This study compared several simplified pipe sizing methods relevant to Belgian practice for non-looped domestic water distribution systems under identical boundary conditions. The objective was to assess their behaviour and determine whether one of the analysed methods could reasonably be recommended to practitioners.

The results showed that the methods are not interchangeable. The largest discrepancies were observed for distribution pipes, whereas terminal pipes showed greater agreement in the median-based analysis. The DIN-based comparison confirmed that the main uncertainties concern the distribution part of the network.

ISSO 55 tended to recommend smaller diameters, especially for distribution pipes, while SSIGE W3 remained on the conservative side and generally recommended larger diameters when its applicability criteria were satisfied. EN 806-3 and DTU 60.11 occupied an intermediate position, but this should not be interpreted as proof of hydraulic adequacy. DIN 1988-300 remains the most robust detailed method in the comparison, but its practical implementation is too complex for routine simplified design work.

Within the scope of the analysed cases, none of the simplified methods could be recommended without reservation for Belgian practice. The results support the development of an improved simplified approach combining practical usability, explicit pressure criteria and a clearer distinction between terminal, downstream/storey and distribution pipes. The ongoing revision of EN 806-3 provides an opportunity to address these limitations in the current simplified sizing framework [10].

6 References

[1] Bleys B, Poncelet B, Van den Bossche P. Production d'eau chaude sanitaire dans les logements unifamiliaux. Méthode de dimensionnement 2025.

[2] Bleys B. Comment dimensionner une installation de production d'eau chaude sanitaire ? CSTC Contact 2019.

[3] Gerin O, Bleys B. Dimensionnement des conduites de distribution d'eau selon la norme DIN 1988-300. CSTC Contact 2015.

[4] Gerin O, Bleys B, De Cuyper K. Domestic hot water consumption in apartment buildings, Beijing, China: 2015.

[5] NBN EN 806-3:2006. Specifications for installations inside buildings conveying water for human consumption — Part 3: Pipe sizing — Simplified method 2006.

[6] Optimisation du dimensionnement de la production d'eau chaude sanitaire - OPTIDIM. Buildwise n.d. https://www.buildwise.be/fr/recherche-innovation/showroom-des-projets/optimisation-du-dimensionnement-de-la-production-d-eau-chaude-sanitaire-optidim/ (accessed May 7, 2026).

[7] NF DTU 60.11 P1-1:2013. Building works — Calculation rules for sanitary installations and rainwater draining off — Part 1-1: Cold and warm sanitary networks 2013.

[8] ISSO-publicatie 55:2023. Leidingwaterinstallaties voor woon- en utiliteitsgebouwen 2023.

[9] DIN 1988-300:2012-05. Codes of practice for drinking water installations — Part 300: Pipe sizing; DVGW code of practice 2012.

[10] Technical Work-CEN Technical Bodies-Work Program-Project prEN 806-3-rev n.d. https://standards.cencenelec.eu/ords/f?cs=12E6AC5B1558BEDB72460A9A7A145B546&p=CEN%3A110%3A%3A%3A%3A%3AFSP_PROJECT%3A67328 (accessed May 7, 2026).

[11] SSIGE. W3 f: Directive pour installations d'eau potable. Édition 2013. 2013.

[12] DS 439:2009. Code of Practice for domestic water supply installations 2009.

[13] International Association of Plumbing and Mechanical Officials. Uniform Plumbing Code 2024: An American National Standard. Ontario: IAPMO; 2023.
[14] International Association of Plumbing and Mechanical Officials. 2024 National Standard Plumbing Code Illustrated. IAPMO; 2023.
[15] Canadian Commission on Building and Fire Codes. National Plumbing Code of Canada 2020. 11th ed. Ottawa: CCBFC; 2020.
[16] Détermination du diamètre des conduites d'eau. Jona: Geberit Distribution SA; 2023.
[17] Détermination du diamètre des conduites d'eau potable selon la directive W3 de la SSIGE, édition 2013. Lonay: Georg Fischer Piping Systems; 2015.
[18] Kiinteistöjen vesi- ja viemärilaitteistot. Määräykset ja ohjeet 2007 - Liite 2: Vesilaitteiston mitoitusohjeet. Helsinki: Ympäristöministeriö; 2007.
[19] NEN 1006+A1:2018. General requirements for water supply installations 2018.
[20] Plumbing engineering design handbook: A plumbing engineer's guide to system design and specifications. Volume 2, Plumbing systems. Chicago, IL: ASPE; 2010.
[21] ASHRAE. 2017 ASHRAE Handbook: Fundamentals (SI Edition). ASHRAE; 2017.
[22] International Code Council, editor. IPC: International Plumbing Code 2021. Country Club Hills, Illinois: International Code Council, Inc; 2020.
[23] Détermination des diamètres de conduites d'eau et gaz. Geberit.ch n.d. https://www.geberit.ch/service-et-support/prestations/determination-des-diametres-de-conduites-d-eau-et-de-gaz/ (accessed May 7, 2026).
[24] De Geetere L. Directives visant à réduire le bruit dans les installations de distribution d'eau. CT Acoustique 2015.
[25] NBN EN 806-2:2005. Specifications for installations inside buildings conveying water for human consumption — Part 2: Design 2005.

7 Presentation of authors

Colin Jacques is an industrial building engineer from ECAM Brussels Engineering School. He is an R&D scientist at Buildwise in the Building Technologies unit, where he previously completed his thesis on greywater reuse systems. His work mainly focuses on domestic hot water production and distribution systems.

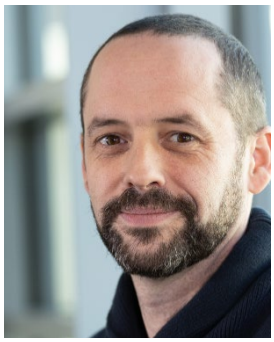

Benoit Poncelet is an architectural engineer from UCLouvain. He is R&D programme leader for water-related topics at Buildwise and coordinator of the Technical Committee on Sanitary Installations within the Building Technologies unit.

Assessment of Water Demand and Pressure Performance in an Australian Residential Building

M. Bilal (1), B.M. Josey (2), J. Gong (3)

(1) m.bilal@deakin.edu.au

(2) b.josey@deakin.edu.au

(3) james.gong@deakin.edu.au

(1) School of Engineering, Deakin University, Waurn Ponds, Australia

(2) School of Engineering, Deakin University, Waurn Ponds, Australia

(3) School of Engineering, Deakin University, Waurn Ponds, Australia

Abstract

This study presents a data-driven assessment of water demand and pressure performance in a multi-storey residential building in Australia where occupants on levels 1-5 reported low pressures and intermittent flow fluctuations at fixture points. The hydraulic consultants engaged by building management suspected the issue might be caused by undersized risers and insufficient pressure from the water main, proposing a costly solution to upsize building pipework and add an additional pump set. After building management learnt of conflicting research that generally pipework is oversized in Australian residential buildings, they engaged the research team for flow and pressure monitoring to investigate the issue further. The research team installed ultrasonic flow meters on cold, heated and recycled water pipes between August and November 2025, together with apartment-level pressure monitoring. Results indicate that the size of the 50 mm (2 inch) diameter riser supplying levels 1-5 is more than sufficient, given the observed absolute maximum flow as 0.67 L/s (10.6 GPM) and the 99th percentile flow Q99 as 0.56 L/s (8.87 GPM). The measured Q99 corresponds to a flow velocity of approximately 0.29 m/s within the 50 mm riser, and an estimated friction loss of only 0.025 kPa per metre of pipe length. This indicates that the existing pipework is operating within its hydraulic carrying capacity. Pressure monitoring in an apartment on level 5 revealed unstable cold-water pressures (100-600 kPa, or 14.5-87 PSI) and excessive heated-water pressures (~800 kPa, or 116 PSI). These conditions exceed recommended limits stipulated in Australian plumbing codes and standards and surpass the ±10% allowable pressure differential specified by manufacturer for tempering valves, believed to be a contributing factor to unstable pressures at fixture points. The findings confirm

that the observed issue is not due to undersized plumbing systems, and most likely caused by the significant pressure difference between the cold- and heated-water systems.

Keywords

Pipe sizing; premise plumbing; pressure management; residential buildings

1 Introduction

Premise plumbing systems (PPS) comprise interconnected pipes, valves, pumps, water heaters, and fixtures that convey water from the point of entry to end-use outlets within buildings. In multi-storey residential buildings, PPS are commonly designed using probabilistic approaches to estimate the 99th percentile demand (Q99) (also commonly termed as the peak demand) and ensure adequate hydraulic performance under peak conditions. In practice, peak demand is typically derived using fixture-unit or loading-unit methods embedded in plumbing standards, many of which originate from Hunter's work on simultaneous fixture use [1]. Numerous studies have demonstrated that conventional fixture-unit or loading-unit based design approaches systematically overestimate actual water demand in residential buildings [2–8]. This overestimation frequently results in oversized plumbing systems, increasing construction costs, energy use, water age, and the likelihood of operational problems [3].

In multi-storey residential buildings, improperly configured pressure-zoning strategies may introduce additional performance issues. Cold- and heated-water services are often supplied from different pressure zones. If pressure management between these services is not adequately coordinated, large pressure differentials may occur at fixtures, leading to unstable operation of mixing and tempering valves and consequent pressure and temperature fluctuations [9].

Despite extensive evidence of peak-demand overestimation, limited studies integrate high-resolution demand monitoring with in-situ pressure measurements when diagnosing performance issues in existing buildings. This study begins to address this gap by undertaking a data-driven investigation of a multi-storey residential building in Australia using combined high-resolution flow and pressure monitoring. Occupants on levels 1 to 5 (cold-water pressure provided by water main) reported poor fixture operation in terms of low pressure in general with intermittent flow fluctuations. The objective of this research is to evaluate whether observed fixture-level performance issues are associated with demand conditions and incorrectly sized pipe work or arise from pressure behaviour within the system. By linking measured demand patterns with pressure conditions at the apartment level, the study provides a systematic assessment of system performance and supports more targeted identification of the underlying cause of pressure instability.

2 System Configuration and Data monitoring

Figure 1 presents a schematic overview of the monitored building's cold and heated water supply configuration and monitoring locations. The building has two levels of basement for parking, a ground level with a small gym and no residents, and 12 levels for apartments. Ultrasonic flow meters were installed on all three cold-water pipes serving a) levels 1-5, b) levels 6 and above and the heated-water plant for the whole building, and c) recycled (storm) water serving toilets on levels 1-3. An additional ultrasonic flow meter was installed on the outlet of the rooftop heated-water plant to determine total heated water circulatory flow for the building. All flow sensors recorded flow data at a temporal resolution of 1s, enabling capture of short-duration peak demands and intra-day variability. A high-frequency (900 Hz sampling frequency) dual-channel pressure data logger was installed under the laundry sink to measure cold- and heated-water pressure in an apartment on level 5. An additional pressure logger was installed at the backflow prevention device located at the cold-water inlet to the building to measure street pressures serving the building. Monitoring durations included both weekdays and weekends. According to the building manager and representatives of the residents, the occupancy rate was estimated over 90% for levels 1 to 5.

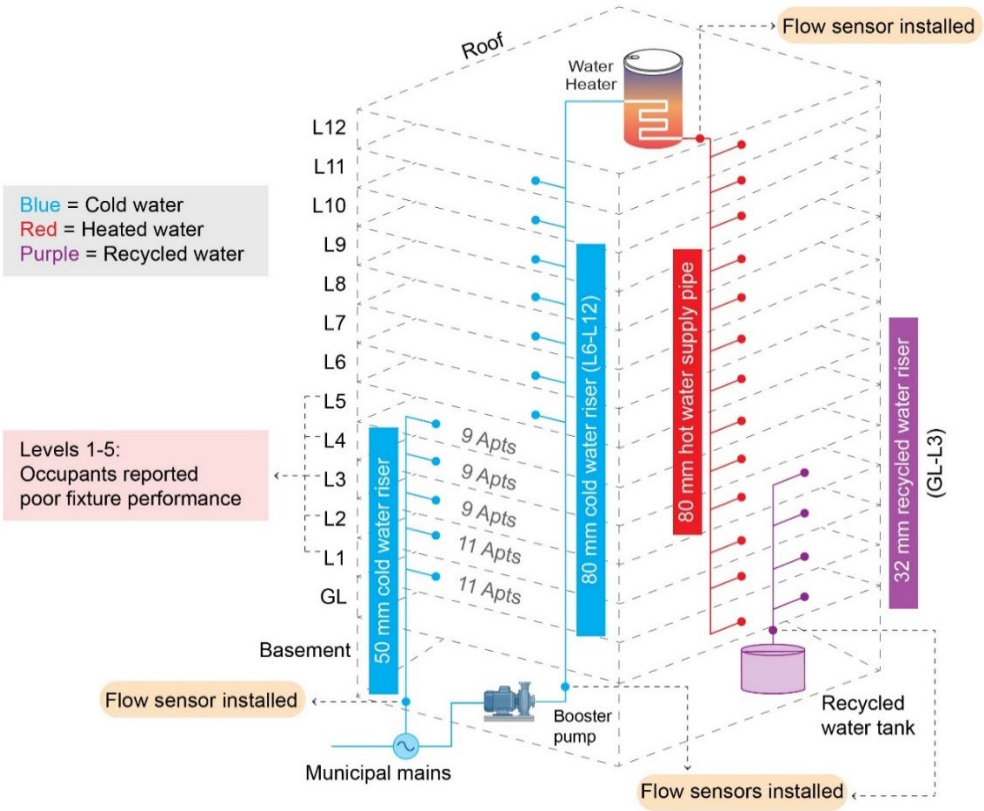

Figure 1 - Schematic representation of the building water supply configuration and monitoring locations.

3 Key Findings

3.1 Water demand and system sizing

Measured flow data from the 50 mm (2 inch, DN50) cold-water riser serving levels 1-5 showed consistently low demand even on the peak day (Figure 2a). The observed flow rates for each hour of the day for the 50 mm riser (Figure 2b) further indicates that demand within the lower-floor riser remained relatively low and stable throughout the monitoring period.

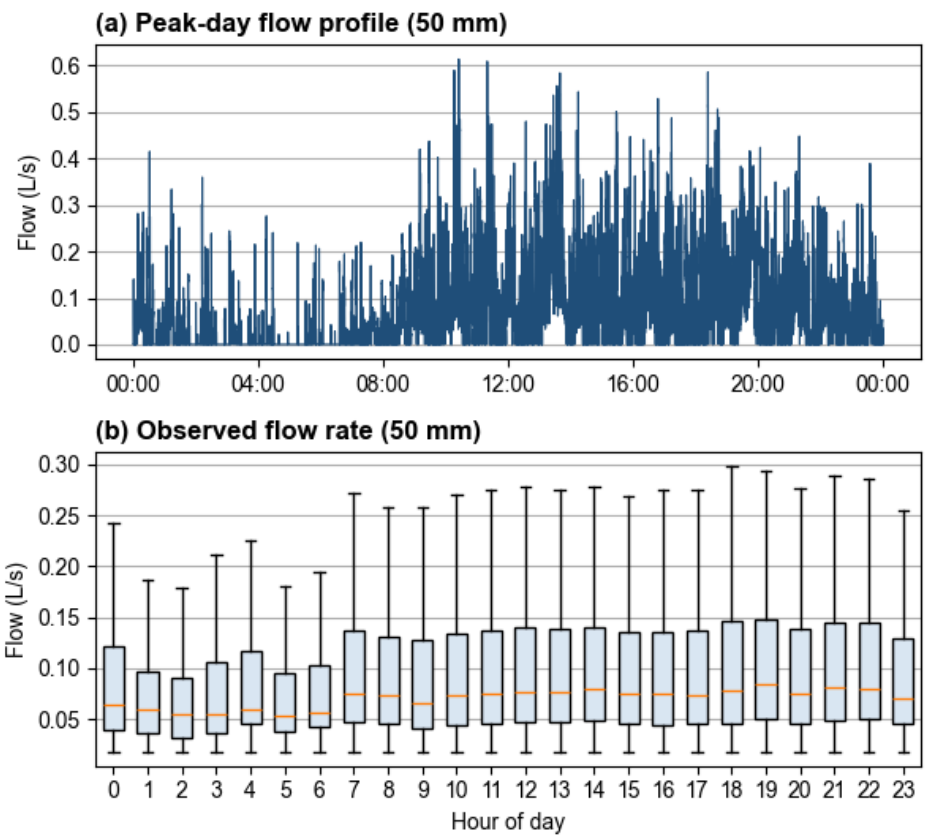

Figure 2 - a) Measured peak-day flow profile and b) Observed flow rates for each hour of the day for the 50 mm cold-water riser servicing 49 apartments on levels 1 to 5 for the entire monitoring period (83 days).

The absolute maximum flow rate recorded within the monitoring period was 0.67 L/s, while the corresponding Q99 flow rate was 0.56 L/s (Figure 3). The Q99 flow was determined by the following steps: 1) determine the busiest hour of each monitoring day based on the hourly water consumption; 2) determine the 99th percentile value based on the non-zero flow rate values recorded in the busiest hour for each day; 3) select the largest 99th percentile value across all the monitoring days.

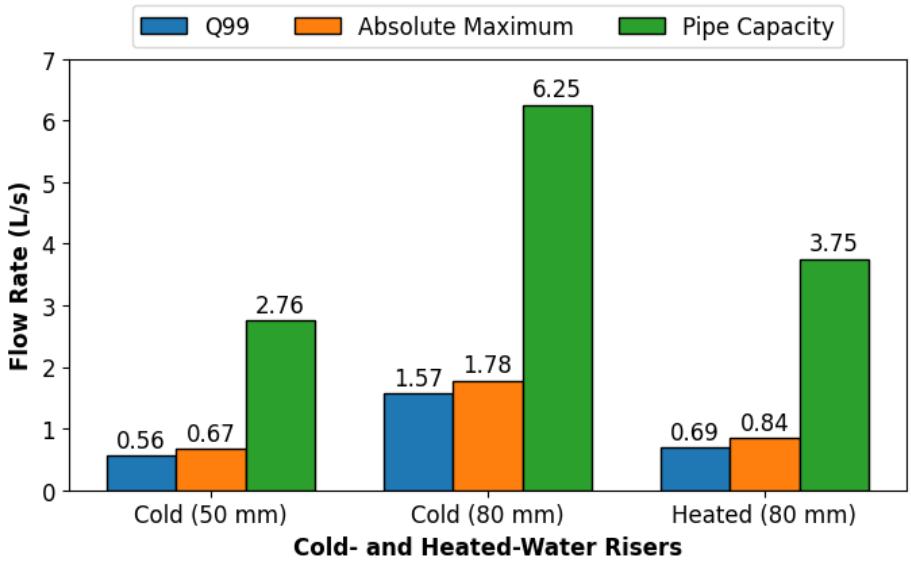

Figure 3 - Comparison of measured Q99, absolute maximum flow rates, and estimated pipe flow capacities for the monitored cold- and heated-water risers. Pipe flow capacity is estimated using the pipe size and a design velocity of 1.5 m/s for cold-water pipe and 0.9 m/s for heated-water pipes.

Figure 3 also compares the measured Q99 and absolute maximum flow rates against the estimated carrying capacity of the existing pipework based on intended design velocities commonly adopted in plumbing practice. For the cold-water risers, an intended design velocity of 1.5 m/s (maximum allowable velocity is 3 m/s in AS/NZS 3500.1 [10]) was adopted. For the 50 mm cold-water riser, this design velocity corresponds to an estimated pipe capacity of approximately 2.76 L/s, which is substantially greater than both the measured Q99 (0.56 L/s) and absolute maximum demand (0.67 L/s) conditions. Similarly, the 80 mm cold- and heated-water risers also showed that the measured demands substantially lower than their estimated pipe capacities. These results indicate that the monitored pipework is operating well below its practical hydraulic carrying capacity.

The measured Q99 flow rate of 0.56 L/s within the 50 mm riser corresponds to a flow velocity of approximately 0.29 m/s. Assuming a Darcy friction factor of 0.03, the corresponding frictional loss is approximately 0.025 kPa/m. Assuming a 20 m pipe length (from the ground level to level 5), this corresponds to a total friction loss of 0.5 kPa under the Q99 flow condition. Even under the absolute maximum measured flow of 0.67 L/s, the corresponding flow velocity and friction losses remain low. These results indicate that frictional losses within the existing 50 mm riser are minimal and insufficient to explain the fixture performance issues reported by occupants.

The measured demand characteristics therefore suggest that the existing pipe infrastructure serving levels 1-5 is already hydraulically oversized and not capacity limited. Consequently, the proposed pipe upsizing intervention is unlikely to improve fixture performance and may represent an unnecessary capital expenditure. Further

upsizing of the pipework may also introduce additional operational issues, including increased water age and associated water quality risks associated with lower flow velocities and prolonged residence times within the plumbing system.

3.2 Pressure differences

To investigate the reported fixture performance issues within the lower floors of the building, high-frequency pressure monitoring was undertaken simultaneously on the cold- and heated-water pipes at the laundry trough in an apartment on level 5. Figure 4 presents a simplified schematic of the apartment plumbing layout and the monitoring location used for the pressure investigation. The monitored apartment is representative of the lower-floor pressure zone supplied directly from the municipal mains through the 50 mm cold-water riser.

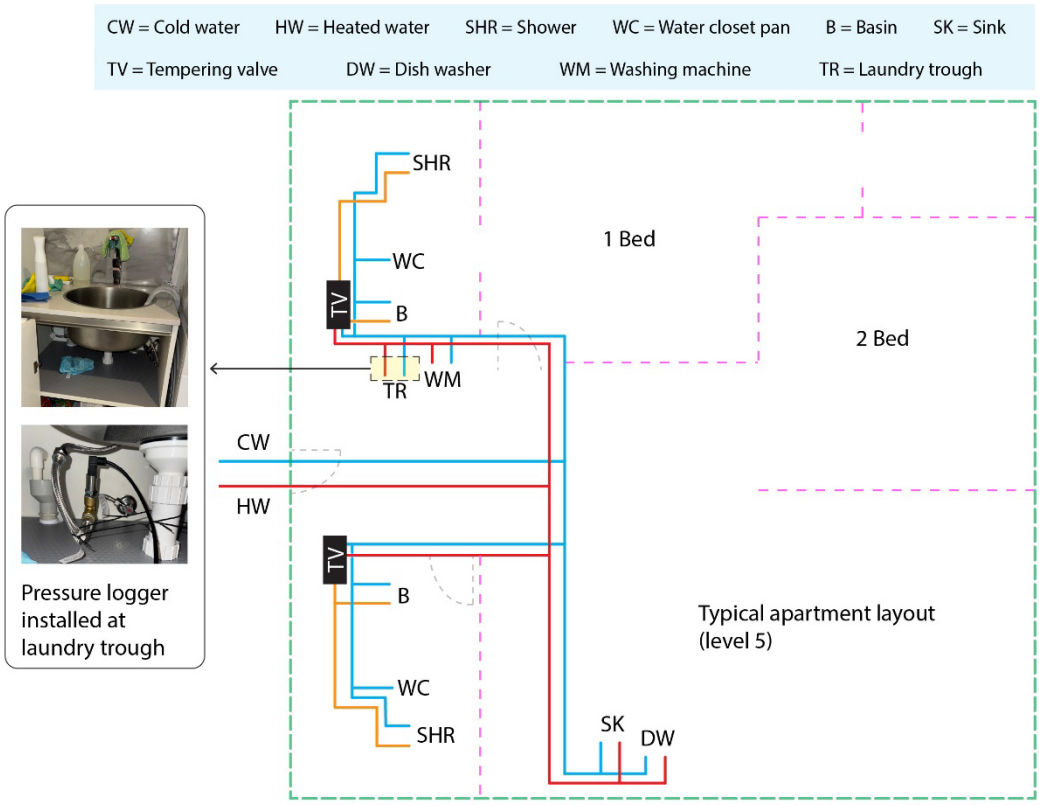

Figure 4 - Typical apartment plumbing layout and pressure logger location.

The pressure measured at the cold-water inlet to the building at ground level was 380-400 kPa, which was consistent with the pressure condition supplied by the local water authority. However, simultaneous monitoring of cold- and heated-water pressures within the apartment on level 5 revealed a substantial and persistent pressure imbalance between the two services. As shown in Figure 5a, the baseline cold-water pressure within the apartment was generally around 150-200 kPa (which is expected given the elevation),

while the heated-water system operated at a relatively stable pressure of approximately 800 kPa throughout the monitoring period. These results indicate that the lower-floor apartments were subjected to significantly different pressure conditions between the cold- and heated-water systems during normal operation. Short-duration transient pressure behaviour was also observed within the cold-water system. As shown in Figure 5b, cold-water pressures occasionally increased rapidly, with transient pressures ranging between approximately 100 and 600 kPa over short time periods. The observed behaviour was not characterised by abrupt instantaneous spikes, but rather by gradual pressure increases and decays occurring over several seconds. Similar transient patterns were repeatedly observed during fixture operation events and are indicative of pressure-trapping or pressure-balancing phenomena within the plumbing system. Although the precise mechanism responsible for these phenomena could not be fully resolved within the scope of this investigation, the results suggest that the large pressure differential between the cold- and heated-water systems contributes significantly to the observed instability.

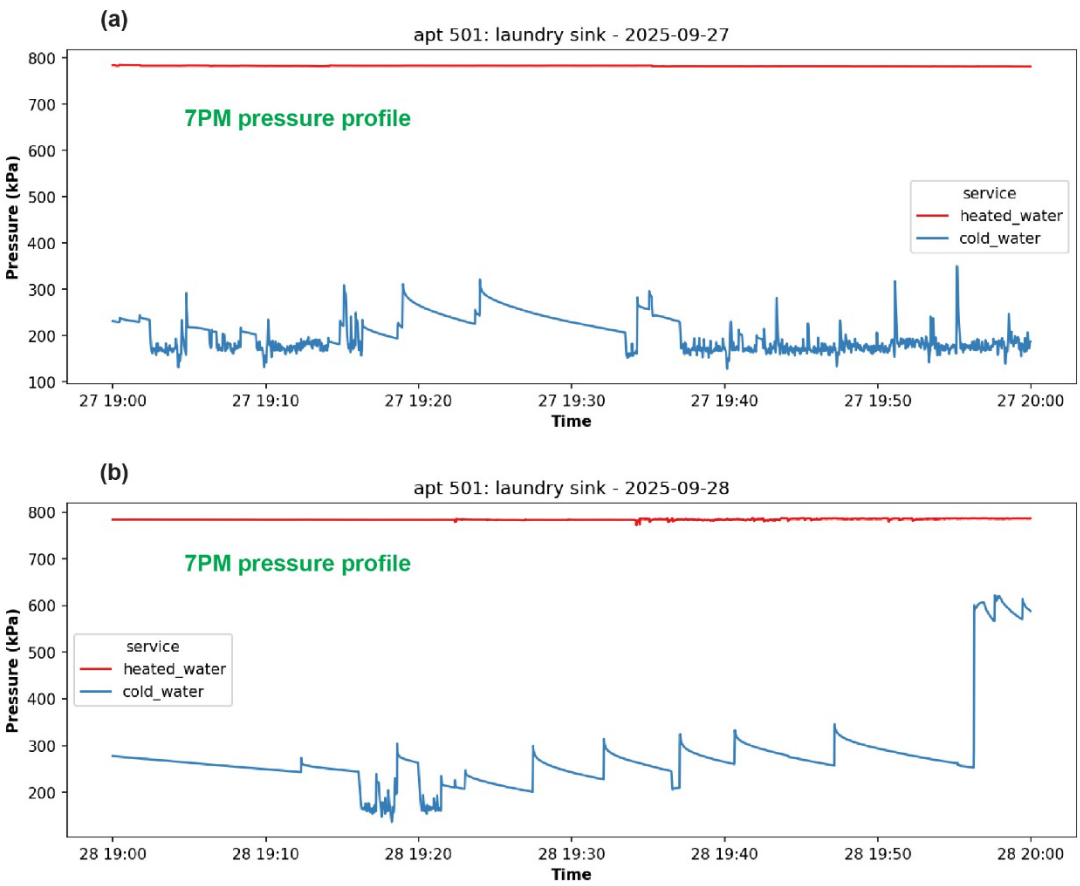

Figure 5 - Simultaneous cold- and heated-water pressure measurements (1-second resolution) in an apartment on level 5 showing baseline pressure differences and transient behaviour in the cold-water pipe: a) pressure between 7 and 8 pm on 27 Sep 2025, and b) pressure between 7 and 8 pm on 28 Sep 2025.

Each apartment contains two tempering valves (TVs) positioned within the internal plumbing distribution system adjacent to the bathroom and laundry fixture groups. These TVs are connected to both the cold- and heated-water services and regulate fixture outlet temperature by blending heated and cold water to a safe delivery temperature. Stable TV operation requires relatively balanced inlet pressures between the cold- and heated-water supplies. Manufacturer specifications for the installed TVs indicate that stable operation requires the inlet pressure differential to remain within approximately ±10%. For example, at a cold-water pressure of 500 kPa, the corresponding heated-water pressure should typically remain within the range of 450-550 kPa.

The monitored pressure data demonstrates that these allowable pressure differentials were consistently exceeded. Under such conditions, the internal TV components may become unstable and flutter between open and closed positions, resulting in fluctuating flow conditions, unstable mixed-water delivery, and poor fixture performance. The elevated heated-water pressure may also contribute to transient interactions within the cold-water service, particularly during fixture operation events. In addition to the excessive pressure differential, the measured heated-water pressure of approximately 800 kPa exceeds the maximum allowable pressure limit of 500 kPa specified in Australian plumbing standard AS/NZS 3500.4 [10] for heated-water services. Sustained operation under these conditions may increase the likelihood of valve wear, leakage, unstable fixture operation, and long-term system deterioration.

A review of the as-built hydraulic drawings indicates that pressure reducing valves (PRVs) should be installed upstream of individual apartments to regulate incoming heated-water pressure. However, the presence and operational settings of these PRVs could not be confirmed during the site investigation. Importantly, the observed pressure fluctuations and fixture instability occurred during normal low-flow operating conditions rather than during periods of high-water demand. Combined with the low measured flow rates presented in Section 3.1, these findings demonstrate that the reported fixture performance issues are unlikely to be related to insufficient pipe capacity or excessive friction losses within the 50 mm riser. Instead, the results indicate that the primary cause is most likely associated with pressure-zone interaction and inadequate pressure regulation between the cold- and heated-water systems within the building.

4 Conclusions

The current study investigates whether the reported water fixture performance issues in a multi-storey residential building are driven by supply limitations or pressure-related deficiencies. High-resolution monitoring of water demand confirms that the existing plumbing system is oversized rather than undersized. For the 50 mm riser that serves levels 1-5, the monitored absolute maximum flow rate is 0.67 L/s and the Q99 flow is

0.56 L/s, both well below the flow capacity of the pipe assuming a flow velocity of 1.5 m/s.

Pressure monitoring within an apartment on level 5 has identified a substantial and persistent pressure imbalance between the cold- and heated-water systems. Baseline cold-water pressures within the apartment were generally around 150-200 kPa, while the heated-water system operated at approximately 800 kPa. The pressure in the heated-water system also exceeds the allowable pressure limits of 500 kPa specified in Australian plumbing standard AS/NZS 3500.4. Transient pressure behaviour was also observed within the cold-water system, with pressure increasing to approximately 600 kPa. The monitored pressure differentials substantially exceeded the allowable operating range recommended for stable TV performance, providing a likely explanation for the unstable fixture behaviour and flow fluctuations reported by occupants.

The findings presented in this study demonstrate that the observed operational issues are primarily associated with pressure imbalance and pressure-zone interaction rather than insufficient pipe capacity. Consequently, retrofit solutions focused solely on increasing pipe diameters or installing additional booster pumps are unlikely to address the underlying cause of the problem. Instead, improved pressure regulation and balancing between the cold- and heated-water systems are required to achieve stable fixture operation within the lower floors of the building.

5 Acknowledgments

The authors acknowledge the building management and residents for their cooperation and support in facilitating site access and data collection for this study.

6 References

[1] Hunter RB. Methods of estimating loads in plumbing systems. US Government Printing Office; 1940.
[2] Bleys B, Van den Bossche P, Kuborn X. Measurements of water consumption in apartment buildings, 2012.
[3] Douglas C, Buchberger S, Mayer P. Systematic oversizing of service lines and water meters. AWWA Water Science 2019;1:e1165. https://doi.org/https://doi.org/10.1002/aws2.1165.
[4] Jack L, Whorlow B. An assessment of the validity of the loading units method for sizing domestic hot and cold water services. London: 2017.
[5] Mayer P, Davis SE, Buchberger S, Douglas C. Assessing water demand patterns to improve sizing of water meters and service lines 2019.
[6] Tindall J, Pendle J. Are we significantly oversizing domestic water systems? 2015.

[7] Josey BM, Buchberger SG, Gong J. Comparing actual and designed water demand in Australian multilevel residential buildings. Journal of Water Resources Planning and Management 2023;149:05022013.
[8] Josey BM, Gong J. Determination of Fixture-Use Probability for Peak Water Demand Design Using High-Level Water End-Use Statistics and Stochastic Simulation. Journal of Water Resources Planning and Management 2023;149:05023015.
[9] E. van der Blom, J. van den Brink, W.G. van der Schee, W.J.H. Scheffer. Temperature Fluctuations in Shower Mixing Valves. CIB W062 Symposium 2015, 2015.
[10] Standards Australia. AS/NZS 3500 Plumbing and Drainage Set 2025. 2025.

7 Presentation of Author(s)

Muhammad Bilal is a PhD researcher at Deakin University, Australia. His research focuses on modelling and analysis of water demand and premise plumbing system performance in multi-storey residential buildings.

Brendan Josey is an Associate Research Fellow at Deakin University, Australia. His research focusses on the improved peak demand estimates and how a “model informed” approach can improve the design of premise plumbing systems.

James Gong is a Senior Lecturer Deakin University, Australia. His research expertise and interests include smart water and wastewater network design and data analytics, condition assessment and leak management of water networks, and optimal design and operation of premise plumbing systems.

An Analysis of Water Use Data in Healthcare Buildings

Toju Omaghomi (1)

(1) Toju.Omaghomi@iapmo.org

(1) Industry Research Manager, Technical Services and Research, IAPMO, USA

Abstract

There is consensus in the plumbing industry that design peak water demands in buildings are overestimated and therefore indoor water distribution systems are oversized. To address this challenge, the Water Demand Calculator® (WDC) was developed. However, its application is currently limited to residential buildings. The WDC was first incorporated into the 2018 Uniform Plumbing Code and has since been adopted by several states and municipalities across the United States. In order to expand the use of the WDC to nonresidential buildings, such as offices, hotels, and hospitals etc., it is essential to collect and analyze water use data specific to these types of buildings.

Within the healthcare sector, water use can vary significantly due to the unique functions of different facility types. Healthcare buildings may include medical office buildings, outpatient care clinics, inpatient behavioral clinics, and full hospitals etc. These facilities may also contain various departments such as pharmacies, imaging centers, surgical units, doctors' offices, and laundries, each with distinct water use profiles.
This paper presents an analysis of water use data collected at the meter in 26 healthcare buildings. The collected data is examined to identify patterns, similarities, and differences that arise from specific building uses within the healthcare category. Preliminary findings reveal a reduction in design peak demand ranging from 15% to 91% when compared to the average daily maximum peak flows measured in these buildings. Additionally, elevated water consumption was observed, primarily due to routine flushing activities implemented as part of water management programs in some buildings.

Further analysis of the collected data will estimate the probability of fixture use by employing a building utilization approach. This step is critical in updating the WDC for application in healthcare buildings, ensuring that peak water demand calculations more accurately reflect actual usage patterns in these environments.

Keywords

Water Demand Calculator®, WDC, Healthcare buildings, peak water demand, fixture probability of use

1 Introduction

Water consumption in healthcare buildings is characterized by diverse end uses associated with clinical care, sanitation and building operations. Healthcare buildings can come in varying sizes and provide specific or multiple services. These services can be inpatient or outpatient clinic, triage, emergency and ambulatory services, optometry, pharmacy, behavioral clinic, radiology, surgery center, dialysis, Intensive Care Unit (ICU), cafeteria and laundry services etc. These services can be categorized as full-service building, palliative care, assisted living, medical office, long term care, urgent care and surgical center. Hospitals also rely heavily on water for patient hygiene, sterilization, laundry, food services, and mechanical systems such as HVAC and cooling towers, making them among the most water-intensive commercial building types (González *et al*., 2016; Chen-Xu *et al*., 2024). Specialized clinical activities further amplify demand, and specific hospital departments disproportionately influence overall consumption (Haddad et al., 2024). Therefore, understanding water use in healthcare buildings is a necessary and complex process required to accurately predict peak water demand for pipe sizing and possibly water management plan.

The specific activities in a building do affect how the indoor water distribution is designed and how water is consumed. Designing water supply in healthcare buildings requires redundancy as per code requirements such as two water service pipes to minimize the potential for interruption. Also, hand washing sinks are required in each patient area and other specific water using equipment for disinfection etc., thus increasing the fixture count and number of dead ends if not fully utilized. These high fixture count impact the peak design flow estimate, usually resulting in an oversized water distribution system and introducing the need for water management plan that requires regular flushing to maintain water quality in the building. In order to improve the prediction of peak water demand, data sources and analysis are necessary to understand water use behavior in healthcare buildings. There is a need to evaluate data from multiple healthcare buildings to estimate fixture probability of use for peak water demand prediction and right pipe sizing.

The International Association of Plumbing and Mechanical Officials (IAPMO) is actively collecting water use data for analysis to expand the capabilities of its Water Demand Calculator® (WDC) to non-residential buildings. Healthcare buildings are one of the major classifications of non-residential buildings. Current water monitoring practices in non-residential buildings are usually for leak detection or volumetric total or hot water consumption patterns or to determine if water management plans are required based on water residency time/turnover. Point-of-use data collection is cost-prohibitive and is an uncommon practice. Available data is usually in private hands and mostly out of reach. As such, the necessary water use data is either widely unavailable, or the available data is collected at higher intervals (*i.e.,* low resolution) in a format unsuitable for the right pipe sizing research or inaccessible due to privacy concerns.

In the United States, healthcare facilities account for roughly 7% of water use in commercial buildings. Right-sizing domestic water systems in healthcare buildings

offers substantial benefits beyond cost savings. Reducing pipe diameters not only decreases installation costs and system complexity but also significantly lowers the volume of water that remains static during low-use periods—a key factor in the proliferation of waterborne pathogens such as *Legionella pneumophila* (ASPE, 2022, and CDC, 2024). In addition, smaller, rightly sized systems facilitate faster hot water delivery, which improves user satisfaction and further minimizes water waste (Omaghomi and Buchberger 2018 and Klien, G. 2013).

So far, data from 26 healthcare buildings have been collected and analyzed. This paper presents a summary review of the findings and preliminary fixture *p*-values derived using the building utilization factor approach.

2 Healthcare Buildings

An important aspect of water use in healthcare buildings is the effect of low water turnover and stagnation within complex plumbing systems, these have important implications for both efficiency and infection control. Low flow conditions due to increased fixture efficiency, oversized plumbing systems and intermittent occupancy can promote microbial growth. Biofilm formation and the persistence of opportunistic pathogens such as Pseudomonas aeruginosa and Legionella in hospital water systems (Wilson, 2024). Water management plans can be instituted to limit these identified risks however, they can influence peak water demand and water use patterns in healthcare buildings.

Apart from finding a building, getting permission to monitor the building and finding the location of the meter in the building, there are several challenges of sourcing water use data in healthcare buildings. Examples of challenges are the acquisition of the demographics of plumbing fixtures i.e. the accurate counting of fixture type and count. Also, depending on the building size and specific use, there is a need to monitor two meters supplying water to the same building. Having the building plan is helpful, however, they are usually the built-as-is plumbing plan which does not have the recent renovations that resulted in additions or removal of fixtures, therefore, a physical walkthrough to count fixtures in the entire building is required.

After meeting the aforementioned challenges, supplying ultrasonic water meters and allocating personal and labor to assist in the water monitoring exercise, instantaneous flow rates measured at the main water meter at specific intervals from all the fixtures in 26 healthcare buildings were obtianed and analyzed.

2.1 Building Details

The healthcare buildings monitored varied in size and function, ranging from medical office buildings used for only outpatient visits on weekdays, to full hospital buildings with in-house pharmacy, accident and emergency, surgery unit, inpatient unit etc. Some of the buildings were used for a mixture of healthcare related activities. Table 1 is a summary of the specific building use for the healthcare buildings monitored.

Table 1- Summary of Types of Healthcare Buildings Monitored

S/N	Building Use	S/N	Building Use
B1	Medical Office Building	B14	Hospital
B2	Outpatient, Primary care, lab , imaging	B15	Hospital
B3	Hospital	B16	Behavioral Clinic
B4	Outpatient, Sports Medicine, orthopedics, Occupational therapy, Spine Center and Imaging	B17	Outpatient Clinic, Outpatient Surgery, Laboratory, Imaging, Infusion
B5	Outpatient clinic, office, café, sleep medicine	B18	Outpatient Clinic, Lab, Pharmacy, Optics, Imaging, Café and offices
B6	Hospital	B19	Medical Office Building
B7	Hospital	B20	Emergency Room, Observation room, Clinic
B8	Hospital	B21	19 Bed Hospital
B9	Outpatient Clinic, Lab, Imaging, Offices, infusion, Occupational Medicine, Cardiac Rehab	B22	Hospital
B10	Hospital	B23	Hospital
B11	Behavioral Clinic	B24	Hospital
B12	Behavioral Clinic	B25	Hospital
B13	Hospital	B26	Hospital

2.2 Data Analysis

Instantaneous flow rates were monitored at the main meter and logged at 5, 10, 50 and in one case 900-seconds intervals over 4 -77 days. Table 2 is a summary of the building data collected. All buildings but one had design flowrate 1.2 -10.8 times greater than what was measured. This follows the general consensus that buildings, especially large buildings are currently been oversized using the fixture unit method and Hunter's curve. Building B8 had an incomplete fixture count and thus a wrong estimate of the design flow rate. It is worth noting that all buildings had their 50th percentile non-zero flow below 10 gpm (0.631 l/s). Meaning when all the recorded flows are ranked, and zero flows deleted, 50% of the recorded flows are below 10 gpm (0.631 l/s). There is a dominance of low flow in the buildings monitored.

The number of times with zero flow in the pipes is the percentage of time water was not flowing during the study period. The higher the stagnation period, the higher the residency time of water in the pipes, thus impacting water quality. There were 5 buildings with average stagnation periods greater than 80%, these buildings had limited or single specific activities like medical office building, etc. There were 11 buildings with average stagnation periods less than 10%, these were buildings with full hospital activities and had water management plans that required regular flushing of the water in the pipe to maintain water quality. Buildings with consistent daily stagnation of 0% had the possibility of low flow leaks.

Table 2- Summary of Data in 26 Healthcare Buildings

S/N	Total Number of Fixtures	Monitoring Period (Days)	Logging Interval (Seconds	Average Daily Volume Consumed - Gallons (Liters)	Times with Zero Flow	Design Peak Flow Rate - GPM (l/s)	Average Daily Maximum Flow Rate - GPM (l/s)	50th Percentile (non zero) Flow Rate - GPM (l/s)	Design Relative to Study Maximum
B1	17	37	5	310 (1,173)	96.8%	41.6 (2.62)	31.9 (2.01)	3.33 (0.21)	1.3x
B2	82	20	50	1,045 (3,956)	54.5%	85.1 (5.37)	7.9 (0.50)	2.00 (0.13)	**10.8x**
B3	82	39	10	3,453 (13,071)	0.1%	49.8 (3.14)	17.8 (1.12)	1.43 (0.09)	2.8x
B4	94	20	50	620 (2,347)	85.3%	93.3 (5.89)	29.4 (1.86)	0.76 (0.05)	3.2x
B5	129	20	50	774 (2,930)	53.6%	106.3 (6.71)	20.3 (1.28)	0.35 (0.02)	5.2x
B6	143	27	10	20,399 (77,219)	0.7%	132.0 (8.33)	111.7 (7.05)	7.27 (0.46)	1.2x
B7	150	4	10	6,945 (26,290)	0.0%	124.0 (7.82)	81.7 (5.15)	1.53 (0.10)	1.5x
B8	152	18	10	20,936 (79,252)	21.2%	133.2 (8.40)	284.8 (17.97)	1.32 (0.08)	**0.5x**
B9	201	20	50	777 (2,941)	73.7%	138.2 (8.72)	18.9 (1.19)	0.81 (0.05)	7.3x
B10	224	25	10	5,729 (21,686)	13.9%	157.0 (9.91)	101.8 (6.42)	1.47 (0.09)	1.5x
B11	237	24	5	1,133 (4,289)	88.8%	170.5 (10.76)	20.9 (1.32)	5.92 (0.37)	8.2x
B12	268	19	5	9,788 (37,052)	38.5%	173.5 (10.95)	58.7 (3.70)	8.25 (0.52)	3.0x
B13	287	40	10	20,872 (79,007)	0.0%	192.1 (12.12)	112.9 (7.12)	9.85 (0.62)	1.7x
B14	287	40	10	5,955 (22,542)	0.0%	192.1 (12.12)	22.3 (1.41)	2.24 (0.14)	8.6x
B15	302	34	10	16,226 (61,421)	0.0%	182.6 (11.52)	68.7 (4.33)	9.59 (0.61)	2.7x
B16	307	15	5	8,979 (33,989)	9.3%	188.0 (11.86)	50.4 (3.18)	4.94 (0.31)	3.7x
B17	323	28	50	20,267 (76,719)	83.7%	135.6 (8.56)	32.3 (2.04)	7.52 (0.47)	4.2x
B18	380	20	50	2,022 (7,654)	41.0%	194.1 (12.25)	41.1 (2.59)	1.07 (0.07)	4.7x
B19	400	18	5	2,854 (10,805)	74.5%	165.4 (10.44)	40.6 (2.56)	5.83 (0.37)	4.1x
B20	424	13	50	1,427 (5,402)	87.5%	204.2 (12.88)	31.9 (2.01)	5.94 (0.37)	6.4x
B21	445	77	900	- -	39.1%	214.3 (13.52)	39.0 (2.46)	0.94 (0.06)	5.5x
B22	476	28	10	5,729 (21,687)	5.8%	247.5 (15.61)	169.2 (10.67)	3.21 (0.20)	1.5x
B23	506	29	10	2,221 (8,407)	38.0%	294.0 (18.55)	62.0 (3.91)	0.73 (0.05)	4.7x
B24	1101	39	10	20,732 (78,479)	2.0%	376.6 (23.76)	172.8 (10.90)	8.76 (0.55)	2.2x
B25	1188	34	10	11,521 (43,612)	3.6%	427.0 (26.94)	110.0 (6.94)	3.38 (0.21)	3.9x
B26	1207	29	10	33,350 (126,243)	0.9%	430.4 (27.15)	330.0 (20.82)	3.23 (0.20)	1.3x

As shown in Figures 1 (a, c, e), some buildings were in operation only on weekdays while others {Figures 1 (b, d, f)}, were fully operational all through the week, including on weekends. Buildings with mostly weekday water use and significantly reduced water use on the weekends cut across the different sizes and uses of the healthcare buildings monitored. In general, Figure 2 shows water is consumed mostly between 8AM in the morning and 6PM in the evenings.

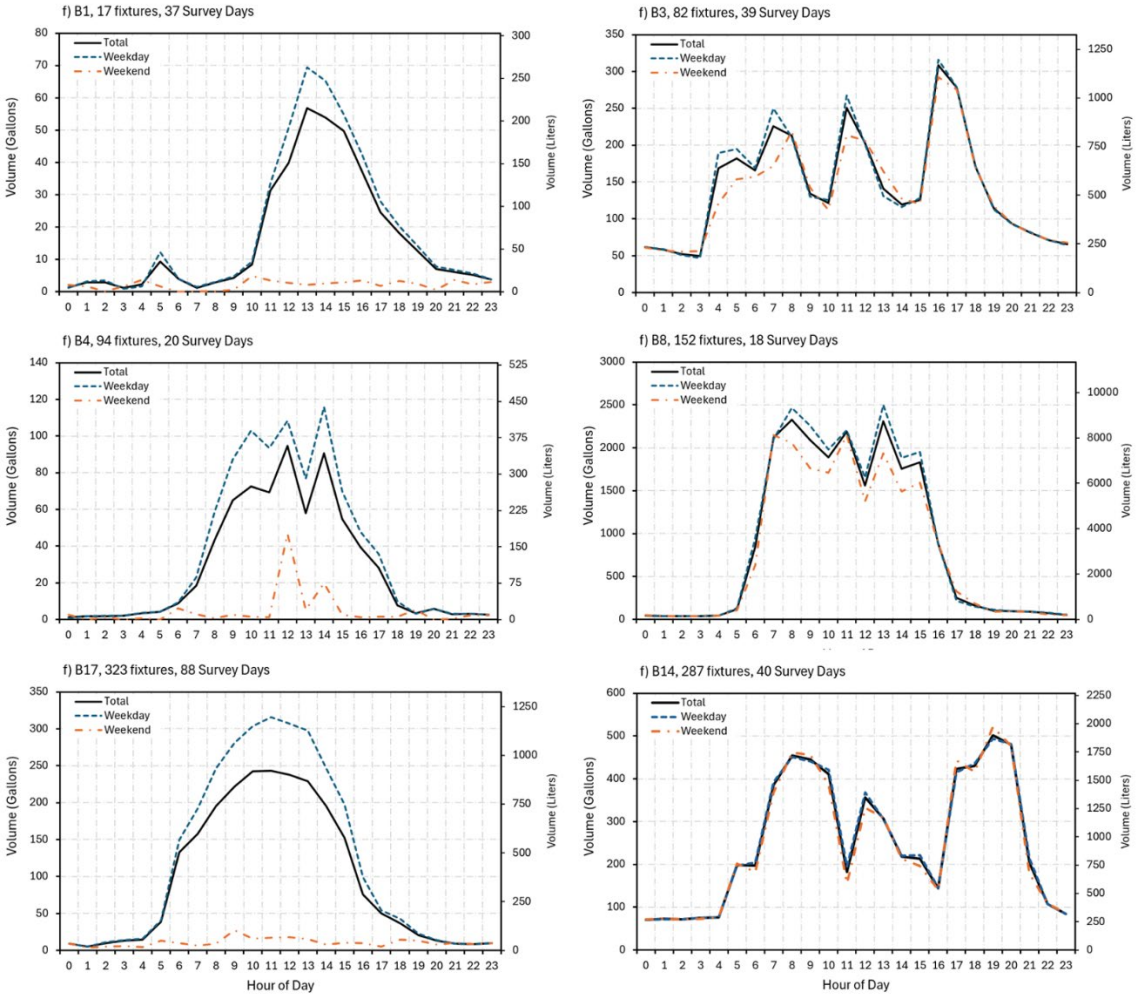

Figure 1- Volumetric Flow Profile of Some Healthcare Buildings Comparing their Weekday to Weekend Water Use Profiles

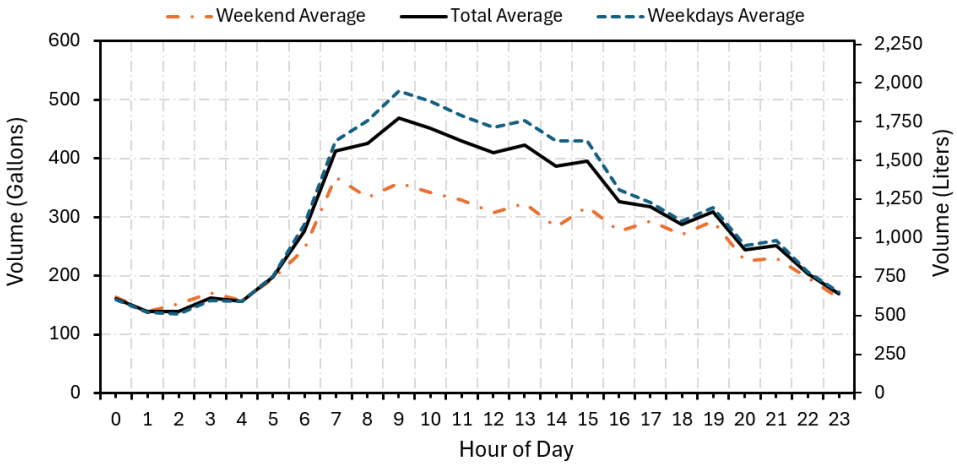

Figure 2-Summary of Total Weekday and Weekend Volumetric Flow Profile of 25 Healthcare Buildings

3 Results and Discussion

3.1 Summary

Since the details of building size and occupancy during the study period were not readily available for all the buildings, fixture count can be assumed as measure of the building size, as in a building with more square footage will have more fixtures compared to buildings with less square footage. As shown in Figure 3, as the fixture counts increased, the design demand increased. The volume of water consumed did not increase with fixture count [building size].

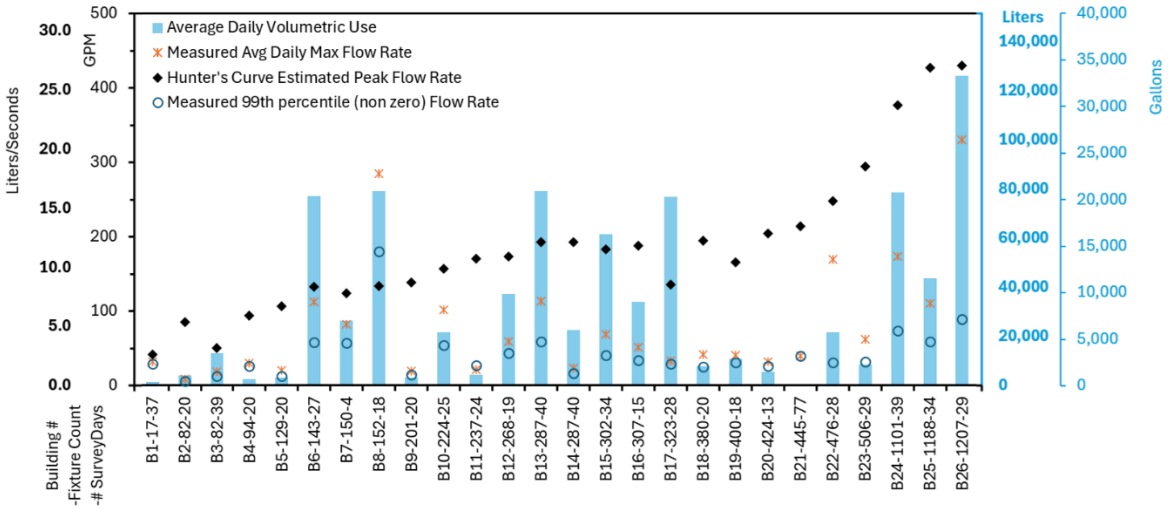

Figure 3-Summary of Water Use Data in 26 Healthcare Buildings

A review of the volume of water consumed relative to fixture count [building size] did not show a positive correlation. This is due to the various and specific types of activities in the buildings not related to their size. Figure 4 illustrates the relationship between periods with zero water use (stagnation) and the daily volume of water consumed. Buildings with low water consumption had higher probability stagnation, both daily and even during the peak hour of water use. Three out of the 26 buildings had greater than 10,000 gallons of water consumed per day and daily stagnation at 20%, 40% and greater than 80%.

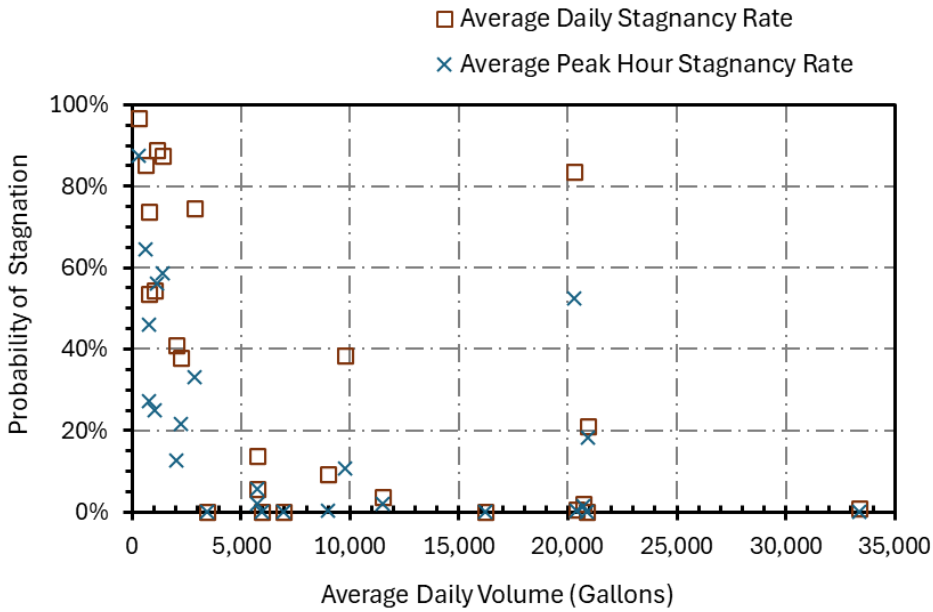

Figure 4- Scattered Plot of Stagnation Probability Versus Average Daily Volume of Water Consumed.

3.2 Building Utilization Factor

After identifying the daily peak demand flow rate, the fixture probability of use can be back calculated using the building utilization factor. Buchberger *et al*., (2024) introduce the utilization factor as a demand-to-supply ratio. When demand (arrivals to use a fixture) equals supply (number of fixtures available), and all the fixtures are occupied, a maximum fixture *p*-value, i.e., probability at congestion (p_c), can be calculated based on the fixture characteristics. Table 3 summarizes the assumptions for worst-case fixture use and the corresponding fixture probability of congestion.

Table 3- Worst-Case Assumptions for Probability of Congestion for Some Fixtures

Fixture	p_c	Worst Case Hourly Consumption Assumption	GPM (l/s)
Bottle Filler | Drinking Fountain	0.1250	30 events/hour to fill a 32 oz bottle flowing at 1.0 gpm (0.063 l/s)	1.0 (0.063)
Shower only	0.2667	2 shower events/hour; 8 minutes/shower event	2.2 (0.139)
Sink, Lavatory	0.0833	30 events/hour; 10 seconds of flow/event	1.5 (0.095)
Sink, Service sink| Mop Sink	0.0333	2 events/hour; 1 minute of flow/event	3.5 (0.221)
Urinal, Flush Valve	0.0500	30 events/hour; 1 gallon flowing at 10 gpm (0.631 l/s)	10 (0.631)
Toilet, Flush Valve	0.0320	30 events/hour; 1.6 gallons flowing at 25 gpm (1.577 l/s)	25.0 (1.577)
Toilet, Tank	0.2286	30 events/hour; 1.6 gallons flowing at 3.5 gpm (0.221 l/s)	3.5 (0.221)

The probability of congestion for the fixtures in Table 3 were applied in Equation 1 to determine the probability of fixture use for a known building utilization factor, ρ. As illustrated by Omaghomi and Cole (2024), the building utilization factor is solved by adjusting the p-value in Equation 1 until the models in the WDC accurately predict the observed maximum daily peak flow rate.

$$\rho . p_c = p \qquad [1]$$

Figure 5 is a distribution of the utilization factors solved for using the congestion fixture p-values and the maximum daily peak flow rate observed. Peak data from 18 buildings were suitable to use in determining the Utilizations factor, the other building data were not suitable for the Wistort's model or its modified version. Note: there are three models in the WDC that use the same fixture parameters n, p and q to estimate peak demand. The Wistort's model or its modified version are equations and are suitable for buildings with low to zero probability of stagnation. Seven out of the eight buildings that were not suitable for the Wistort's model or its modified version had a combination of high probability of stagnation (53 – 96%) and low peak flow rates (< 32 gpm (2.08 l/s)), thus requiring the third model, which is an enumeration of all the combinations of fixture use a rather complex process. The eight building had incomplete fixture counts. There is a difference in the average and median utilization factor due to the current small sample size.

The resulting fixture p-values (for some fixtures) are summarized in Table 4. Note that the healthcare fixture p-values in Table 4 are not final; data from additional healthcare buildings is needed for a statistically sound fixture parameter. Therefore, the p-values will be updated as more data is collected.

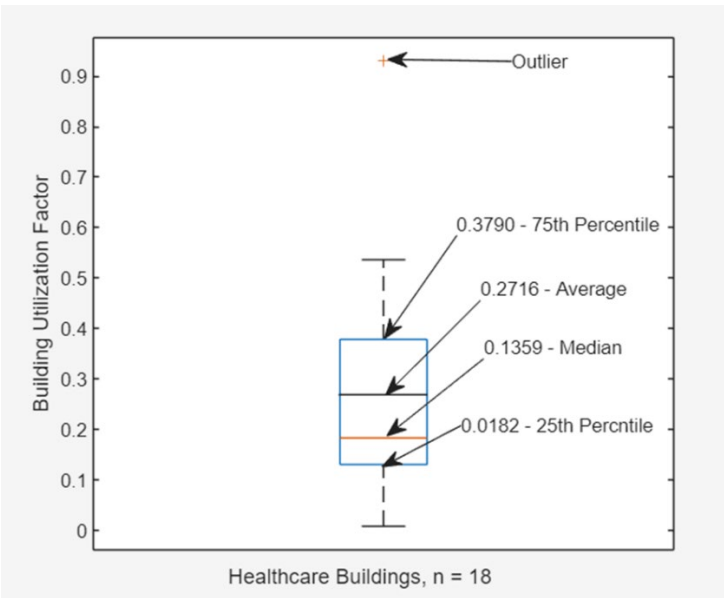

Figure 5-Boxplot of Building Utilization Factor from 18 Healthcare Buildings

Table 4- Summary of and Probability Values in Healthcare Buildings for an Average Utilization Factor of 0.27

Fixture	p_c	*p*-value
Bottle Filler | Drinking Fountain	0.1250	0.0338
Shower only	0.2667	0.0720
Sink, Lavatory Sink-Private	0.0833	0.0225
Sink, Service sink| Mop Sink	0.0333	0.0090
Urinal, Flush Valve	0.0500	0.0135
Toilet, Flush Valve	0.0320	0.0086
Toilet, Tank	0.2286	0.0617

4 Conclusion

Water use data collection and analysis will aid the shift from conservative design to an evidence-based design of rightly sized plumbing systems that will improve efficiency and reduce cost while maintaining hydraulic performance and improved water management protocols for infection control in healthcare buildings.

The water use data from 26 healthcare buildings reviewed in this paper covers a small sample from the wide range and variety of healthcare buildings available. These flow data collected at the meter represents water use from all the fixtures downstream of the meter, which sometimes includes laundry and kitchen processes if available. The data shows that measured demand is 1.2 to 10.8 times less than the design demand. Also, half of the instantaneous demand flows measured at each building is less than 10 gpm (0.631 l/s), indicating that most of the time low flows are predominant in the distribution system. The 99th percentile and maximum demand flow are instantaneous not sustained, meaning they occur very briefly, usually once in the window of measurement. Even for scenarios where high velocity flushing necessary for scouring the pipes is needed, it has to be achieved outside of the regular water use in the building.

Using the building flow data, the fixture *p*-value was estimated based on two models (i.e. Wistort's method and the modified Wistort's method) in the WDC and an assumed worst-case use of the fixture in conjunction with the utilization factor. The resulting *p*-values are from 18 data points and will be updated as more data is obtained in order to extend the application of the WDC to healthcare and other non-residential buildings.

Acknowledgments

The authors thank the International Association of Plumbing and Mechanical Officials (IAPMO) and anonymous donors of the data analyzed.

4 References

ASPE Working Group, "Engineering Methodologies to Reduce the Risk of Legionella in Premise Plumbing Systems" accessed online May 2025 at https://www.aspe.org/wp-content/uploads/Engineering_Methodologies_to_Reduce_Risk_of_Legionella_in_Premise_Plumbing_Systems_Draft_PUBLIC_REVIEW_8-19-22_updated.pdf (2022)

Buchberger S, Li T, Omaghomi T, and Gary K; "Research on Fixture Level Peak Probability of Water Use in Commercial Buildings" Grant/Contract Reports (NISTGCR), NIST, Gaithersburg, MD (2024)

UC Centers for Disease Control and Prevention (CDC), "Reopening Buildings Guidance," accessed online May 2025 at https://www.cdc.gov/control-legionella/php/guidance/building-water-system.html (2024)

Chen-Xu, J. et al. (2024) "Interventions for increasing energy efficiency in hospitals", Cochrane Database of Systematic Reviews.

González, A.G., García-Sanz-Calcedo, J., Salgado, D.R. and Mena, A. (2016) "A quantitative analysis of cold water for human consumption in hospitals in Spain", Journal of Healthcare Engineering, 2016, pp. 1–10.

Haddad, S., Kittner, N., & Flythe, J. E. (2024). Thinking globally, acting locally: Water use in a hospital hemodialysis unit. Kidney360, 5(11), 1747–1749.

Klein, G., "Efficient Hot Water Piping: Smarter Layout and Right-Sized Pipes Saved Time, Water, and Energy", Journal of Light Construction (2013)

Omaghomi T, and Buchberger S., "Residential Water and Energy Savings in Right-Sized Premise Plumbing", 1st International WDSA / CCWI 2018 Joint Conference, Kingston, Ontario, Canada, (2018)

Omaghomi T., and Cole D.; "The Challenges of Data Sourcing and Data Analysis of Non-Residential Water Use Data" 49th CIBW062 Annual International Symposium on Water Supply and Drainage for Buildings, (2024)

Wilson, A.P.R. (2024), "Will we need water in the hospitals of the future? The role of water versus waterless systems", Journal of Hospital Infection, 149, pp. 135–136.

6 Presentation of Authors

Toju Omaghomi is an Industry Research Manager at the International Association of Plumbing and Mechanical Officials (IAPMO). She developed IAPMO's Water Demand Calculator® for residential buildings as part of her Doctoral Dissertation at the University of Cincinnati and received the ASPE Scientific Achievement Award in 2018. Her research interests include water conservation, modeling, and integrated engineering of water as a resource at the building level. Her research involves predicting peak water demand in buildings to size indoor plumbing systems rightly and extending the WDC to commercial and institutional buildings.

Updated review of applications for SIMDEUM, a stochastic drinking water demand model with a small temporal and spatial scale

E.J.M. Blokker (1)

(1) mirjam.blokker@kwrwater.nl, KWR Water Research Institute, the Netherlands. TU Delft, Water Management, the Netherlands

Abstract

SIMDEUM is a stochastic end-use model for drinking water demand, at a small temporal scale (1 s) and a small spatial scale (the end use). SIMDEUM has often been applied in research and practice since it was first developed. SIMDEUM's original purpose was to calculate maximum demands to design self-cleaning networks. Yet the model has been useful in many more applications. This paper presents a quick scan review of the published applications over the last 10 years, which may have missed some important publications.

SIMDEUM has been used in modelling drinking water distribution systems, the drinking water installation, and to a limited extent in the sewer system. We see possibilities of using SIMDEUM also in hot water supply and the wastewater system inside the building. Applications can be found in water quantity (hydraulics, prognoses), water quality (temperature, solids, dissolved substances, micro-organisms), network design, scenario studies (varying regions, future demands, …), and research purposes (e.g. in operating a virtual playground). We see possibilities for more applications in the design of wastewater systems.

Some applications, such as water quality modelling in the drinking water distribution system or drinking water installation, rely on a small temporal or spatial scale. Other applications rely on the fact that SIMDEUM's input parameters have a physical meaning, which means that it is easy to use it in scenario studies or which allows for easy conversion of drinking water demand patterns into wastewater discharge patterns or water related energy demand patterns. A third group of applications relies on the stochastic nature of SIMDEUM, that allows for understanding or explicitly using the variability of outcomes. Also, realistic demand patterns are required for applications such as model validation or applications in practice. Most applications are benefitting from a combination of these unique aspects of SIMDEUM.

Keywords

SIMDEUM, demand modelling, applications.

1 Introduction

SIMDEUM was developed as a drinking water demand model (Blokker and van der Schee 2006). SIMDEUM has some unique features that allow researchers to do detailed scenario studies and to incorporate realistic demand and realistic variability in demands in their studies. For drinking water demand models with a small spatial and temporal scale the main application was assumed to be in water quality modelling (Blokker et al. 2008) and the design of self-cleaning networks. However, SIMDEUM has found many other usages, both in research and practice Blokker et al. (2017).

In 2017, ten years after the first launch of SIMDEUM, the applications that were reported were mainly from SIMDEUM's developers with limited use outside of their research group, and the applications were very much focussed on the Dutch drinking water practice. Since then, another ten years later, many researchers from around the world have used SIMDEUM and applied it in their field of research.

The purpose of this paper is to give an overview of new applications since 2017: in a new context or research field, in a new location with their specific input parameters. For each it was determined which unique aspects of SIMDEUM were essential for their study.

2 Methods and materials

2.1 Selecting references

SIMDEUM was first released in 2006 (Blokker and van der Schee 2006). Blokker et al. (2017) gave an overview of the first ten years of research done with the help of SIMDEUM. The comment from one of the reviewers was that SIMDEUM obviously had a lot of potential, but that the group of users was almost entirely comprised of KWR researchers. Since then, KWR has made SIMDEUM available to other researchers[1]. Those who signed an MOU could use the Matlab® version. A scientific literature search on these researchers' names allowed to identify 22 research publications where SIMDEUM was applied (and not just mentioned) that were selected for this review. Since 2022 there is an open access python version (pysimdeum[2]). Papers that cite the pysimdeum paper (Steffelbauer et al. 2022) were also selected for this review. After scanning the paper for applications of pysimdeum 13 papers and reports were selected. This quick scan review may have missed some important applications.

2.2 Categorizing applications

Blokker et al. (2017) distinguished six types of applications: (drinking) water quantity, (drinking) water quality, design of the drinking water distribution system (DWDS), design of the drinking water installation (DWI), prediction of future demands, research in the DWDS. In this paper we have decided to group the applications in two

[1] https://www.kwrwater.nl/en/tools-producten/simdeum/
[2] https://github.com/KWR-Water/pysimdeum

dimensions with the first dimension being the application domain from drinking water transport to waste water transport (DWDS, DWI, in-home sewer, sewer) and the second dimension being the goal of the application: water quantity, water quality, design, and other.

These goals are further specified in the results table, and include the following:

- Water quantity as the main purpose means controlling or predicting (in an operational sense) the water quantity. Applications are e.g. hydraulic modelling, pump scheduling, leak reduction, water saving, research related to digital water meter.
- Water quality as the main purpose means controlling or predicting (in an operational sense) the water quality. Applications are e.g. minimising or optimizing discolouration, water age, chlorine levels, lead, temperature, biofilm, wastewater quality.
- Design as the main purpose means ensuring water quantity and quality by design. Applications are e.g. pipe diameter selection (in DWDS, DWI, and sewer system), reservoir sizing for drinking water, hot water, grey water, rainwater, and designing (drinking water or wastewater) treatment plants.
- The "other" category entails e.g. the design of lab setups, interpretation of field data, and model development where SIMDEUM is used as a reference.

Applications were classified with their main goal. For water quality purposes, typically there is a need for water quantity modelling; for design purposes, typically there is a need for water quantity (and water quality) modelling. In these cases, water quantity is not the main purpose and therefore not indicated in the table.

Scenario studies are included in many of the applications, but they are not the main goal. Scenario studies are related to e.g. the influence of building type, population statistics, (mixed) land-use, urban planning, water conservation schemes on water quality in the DWDS, and the wastewater load to the WWTP.

2.3 Identifying indispensable aspects of SIMDEUM

The author of this paper (and developer of SIMDEUM) has had some correspondence with the researchers that signed the MOU and asked them to identify which aspects of SIMDEUM were important for their research. Based on their reactions and expert judgment, the applications were assessed on how essential the unique aspects were, and why. This approach may have introduced some selection bias.

- Model input parameters have physical meaning: the fact that all input parameters have physical meaning allows for doing scenario studies with respect to changes in household composition, diurnal patterns, water saving appliances, etc. Introducing leakage and compare results with non-leak scenarios is another application.
- The model is stochastic in nature: an ensemble of demand patterns will allow the user to determine the effect of the variability of demand on hydraulics and water quality and to design a system based on the average or maximum demands. In this paper the publications were assessed on their interest in understanding the (effect of the) variability or in the need to use high variability rather than deterministic demand patterns.

- Small spatial & temporal scale: SIMDEUM has a small spatial scale (end-use level) and a small temporal scale (1 s). It is easy to aggregate to the water meter or household level or street level. For high aggregation levels (e.g. of a DMA or supply zone) the use of SIMDEUM is less obvious. It is also easy to aggregate to a coarser resolution (1 min, 5 min). For high aggregation levels (e.g. 1 hour or 1 day) the use of SIMDEUM is less obvious. If it was easy to assess from scanning the publications, specific information on the exact aggregation level was included in the review.
- Resulting demand patterns are realistic: in this paper the publications were assessed whether they relied on realistic demand patterns because it was important to either validate their (model) results, assess the potential for use in practice, use SIMDEUM as a reference or ground truth, or use the results in a risk assessment.

Figure 1 summarises the process of selecting and assessing the relevant publications.

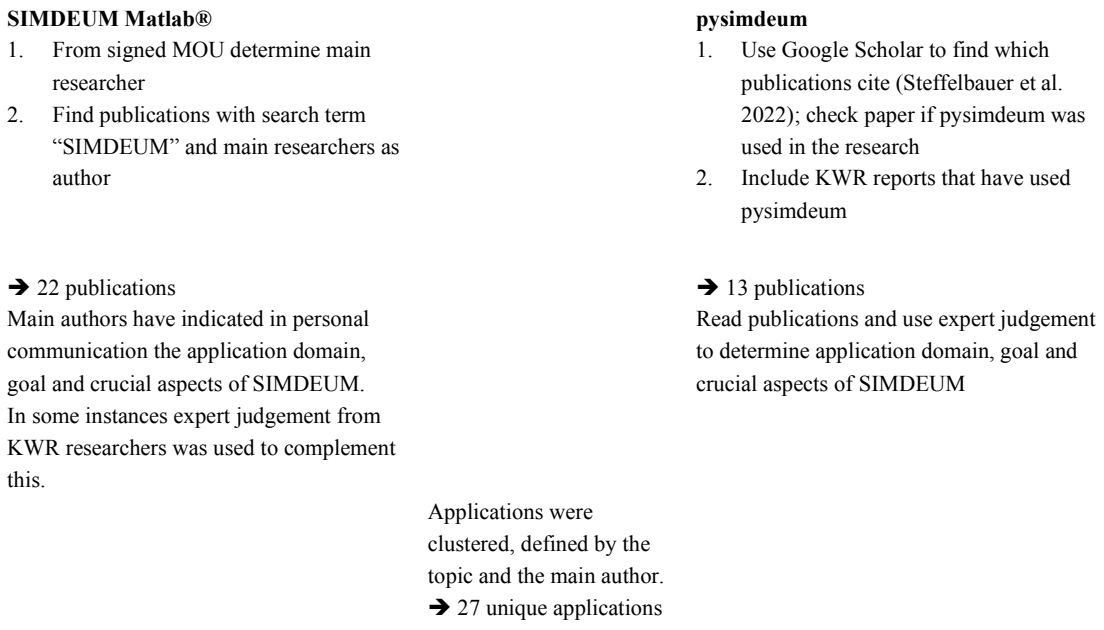

Figure 1. Flow chart of quick scan review of applications

3 Results

Table 1 shows the overview of the selected publications. The results are further discussed in the next section.

Table 1. Overview of selected applications from the literature. Application domain: DWDS (Drinking Water Distribution System), DWI (Drinking Water Installation), Sewer. Application goal: water quantity (only if this is the main goal, L = leakage, S = water saving), water quality (implicitly includes water quantity, aspect of water quality is specified), design or other (e.g. research support). Which unique SIMDEUM properties are required for the application: parameters have physical meaning (S = scenario generation incl. water saving, household composition, etc. , L = allows for cluster labelling), stochastic process (U = understand variability, N = need for high variability), small spatial scale (E = end use level, H = hot water supply, W = household level, incl. at the water meter), small temporal scale (minimum resolution given), realistic demand patterns (V = allows for validation, P = assessment of potential, R = used as a reference, Q = risk assessment).

Reference	**Application domain**			**Application goal (incl. scenario studies)**				**Unique SIMDEUM properties**				
	DWDS	**DWI**	**Sewer**	**Water quantity**	**Water quality**	**Design**	**Other**	**Parameters have physical meaning**	**Stochastic process**	**Small spatial scale**	**Small temporal scale**	**Realistic demand patterns**
Abraham et al. (2017)	X				X (discolouration)	X (valve settings)			X (U)			X (P)
Hook and Speight (2018)	X				X (water age)			X (S)	X (U)	X (W)	X (5 min)	X (P)
van Steen (2020)	X			X (L)						X (W)	X (5 min)	X (P)
Piazza et al. (2020)	X				X (dispersion)			X (S)	X (N)		X (5 min)	X (P)
Díaz and González (2020); (2021)	X						X (develop method for instantaneous mean/ variance)		X (U)		X	X (R)
Steffelbauer et al. (2021)	X			X			X (clustering analysis)	X (L)	X (U)	X (W)		X (P)
Dobson et al. (2021)			X		X (contamination)			X (S)	X (N)			X (V)
Bailey et al. (2019); (2020a; 2020b)			X	X (S)	X (nutrients)			X (S)				X (P)
König and Joksimovic (2022)			X			X (dynamic pricing)		X (allowed to determine non-potable use)				X (P for residential and non-residential)
Berlin et al. (2022)	X					X (pipe sizing)			X (N)	X (W +)	X (1 s)	X (V)
Abhijith et al. (2023)	X				X (fate and transport of emerging contaminants)				X (N)			X (P)
(2024a; 2024b); Clements et al. (2023a); (2023b)		X			X (water age, chlorine, Legionella)				X (U, N)	X (E)	X	X (Q)
van der Holst et al. (2023)		X					X (energy use for hot water)					
De Backer et al. (2023)		X			X (Legionella)		X (control in hot water systems)			X (E)	X	X (Q)

Reference	Application domain			Application goal (incl. scenario studies)				Unique SIMDEUM properties				
	DWDS	**DWI**	**Sewer**	**Water quantity**	**Water quality**	**Design**	**Other**	**Parameters have physical meaning**	**Stochastic process**	**Small spatial scale**	**Small temporal scale**	**Realistic demand patterns**
Zeidan and Hillebrand (2023)	X			X			X (weighing factors for water meter accuracy)			X (W)	X (1-10 s)	X (P)
Koop et al. (2023)		X		X (S)				X (S)		X (E)		X (P)
Oberascher et al. (2024); (2025a; 2025b)	X			X (L)						X (W)	X	X (P)
Vargas et al. (2024)		X			X (Legionella)					X (E)		X (Q)
Kleckers et al. (2024)			X		X (urine separation)			X (S)	X (U)			X (P)
Lokk et al. (2024)	X				X (discolouration)			X (S)	X (U)	X (W)	X (1-10 s)	X (Q)
Junggeburth (2024)		X				X	X (energy for hot water)		X (U)	X (H)		X (P)
Hall et al. (2025)		X		X (hot water)			X (HomeWaterLab)		X (U)	X (E)		X (Q)
Josey and Gong (2025)		X				X	X (comparing design methods)		X (U)	X (E)	X (1 s)	X (P, R)
Hatam et al. (2025)		X			X (lead)				X (U)	X (E)		X (Q)
Willet et al. (2025)	X						X (test disaggregation and labelling SW)	X (S)	X (N)	X (E)	X (1 s – 5 min)	X (R)
Jacque et al. (2026)		X		X (non-residential)				X (allows for adding information on presence of users)	X (U)	X (W)		X (V)
(Dash et al. T.B.P.)		X			X (lead)			X (S)	X (U, N)	X (E)	X (10 s)	X (Q)

4 Discussion

4.1 Application domain and goal

In total 27 unique applications were selected, defined by the topic and the main contributor. Some of these applications have been described in multiple publications. These were merged into one row in Table 1 and counted as 1. Some of these applications are new because they were done in a new context (outside of the Netherlands), others because they are focussing on a new domain or a new goal.

SIMDEUM developers' applications up to 2017 focussed very much on the drinking water side with its main application in the DWDS, and a few in the DWI. Table 1 shows that there are even more (new) applications in the DWDS (12 of 27) and DWI (11 of 27). Also, there are applications in the sewer (4 of 27), where SIMDEUM-WW is used to generate wastewater discharge patterns. However, there are no applications yet in the in-home sewer system.

Table 1 shows that water quality is most often the main goal (12 of 27), but the other applications are also important (5-7 each). Water quantity is related to (hot) water efficiency, leakage and SIMDEUM improvements for non-residential water demand. There are water quantity applications for all domains (DWDS, DWI and sewer). Water quality is related to discolouration, water age, chlorine and tracers (DWDS), lead and Legionella (DWI), nutrients and (emerging) contaminants (sewer). i.e. in all domains. Design is related to (pipe) sizing and energy use. There are design applications for all domains. Other is related to using SIMDEUM as a ground truth or reference to test other applications (e.g. the accuracy of disaggregation and labelling algorithms, research to simplify modelling by using an analytical approximation instead of a Monte Carlo approach), both in modelling applications and in lab setups. These applications were found for the DWDS and DWI, but not (yet) for the sewer.

4.2 SIMDEUM's unique aspects

4.2.1 Model input parameters have physical meaning

SIMDEUM builds on the fact that all water use events can be described as a rectangular pulse with a flow rate (L/s), a duration (s) and a starting time. The total demand pattern is the sum of all these events. The starting time is linked to the household composition and water related behaviour (age, gender, diurnal patterns with respect to sleep and presence at home).

The fact that SIMDEUM input parameters have physical meaning is typically important for scenario studies where either demographics, technical specifications or behavioural patterns change. For many of the applications that are introduced in this paper, the physical meaning of parameters is a big plus, as this means that demand or discharge patterns can be generated without the need for an extensive measurement campaign. For 11 (of 27) this aspect was important in their research.

SIMDEUM's input parameters all have a physical meaning and are typically acquired from (extensive) surveys. The number of input parameters for SIMDEUM is relatively high, ca. 40 to describe presence, frequency of use, flow rate, duration of all end-uses, ca. 30 to describe household composition and ca. 24 to describe people's diurnal

patterns. It can be quite a challenge to determine country (or case) specific input parameters. As the input parameters have physical meaning it is easily determined to what extent parameters can be transferred to other locations: technical parameters such as flow rate and user behaviour such as shower duration and number of toilet flushes per day can typically be used in a whole country, or even in, e.g., the whole of North Western Europe. Household composition and diurnal patterns of when people leave the house and go to bed may be more local. Most applications are found in the Netherlands (12 of 27), some in the UK (4) and Canada (3) and the others mainly in other European countries (Austria, Ireland, Germany, Belgium, Spain, Norway). Some researchers have adapted the input parameters to their country's specific water demand, but many also used the Dutch data.

Mazzoni et al. (2022); (2026) have done a vast literature review to determine for residential (cold and hot) water use at the end-use level information on (probability distributions of) frequency of use, flow rate and duration, as well as occupation daily profiles of water use. These are basically the input parameter to SIMDEUM, collected for various countries around the world and over a time frame of decades. This may help researchers to use input parameters that are most suitable for their cases.

4.2.2 The model is stochastic in nature

For simulating individual houses on a per second basis, SIMDEUM generates many random number to determine the specific number of water use events, the flow rate, duration and time of day. Each demand pattern that is thus generated is different. The fact that SIMDEUM is a stochastic model is important in design, where e.g. enough pressure is available for the 99-percentile water demand, or the self-cleaning velocity is reached at least once per day. Also, for processes with a high variability (e.g. residence time in the outskirts of a DWDS), it is good to consider multiple sets of demand patterns when modelling or validating the model.

The fact that SIMDEUM is a stochastic model is important in 18 (of 27) applications. Here for 13 the understanding of the effect of the variability was the reason; for 7 the model approach needed high variability that was not easy to obtain with deterministic demand models.

4.2.3 Small spatial & temporal scale

SIMDEUM has a small spatial scale and a small temporal scale. Typically, the need for a small spatial scale and small temporal scale go hand in hand, but not always. For water quantity modelling, for example, typically, the closer the application domain is towards the end user (or the tap), the more need there is for a small spatial scale and small temporal scale. A spatial scale as small as the end-use is found in the premise plumbing, aggregation to the water meter is found in research on digital water meters and pressure sensors in the smaller pipe diameters, aggregation to several buildings is done when considering DMA's and (waste) water treatment plants. A temporal scale as small as 1 s is found in the premise plumbing, aggregation to 5 min – 1 hour is found in research on digital water meters and pressure sensors in the smaller pipe diameters, aggregation to 1 hour is done when considering DMA's and to 1 day for (waste) water treatment plants.

A drinking water demand model with a small spatial and temporal scale is required for water quality modelling (Blokker et al. 2008). There are publications that have suggestions for the optimal spatial and temporal resolution depending on the

application. For example Blokker et al. (2010) showed that for water age modelling a temporal scale of 5 min or smaller is required.

The fact that SIMDEUM has a small spatial scale is important in 18 (of 27) applications. Here 9 used SIMDEUM at the end-use level, 1 at the hot water level, and 8 at the level of a single connection (at the water meter). Other studies aggregated the demand over multiple households.

The fact that SIMDEUM has a small temporal scale is important in 9 (of 27) applications. Depending on the goal the temporal resolution is 1 s (design of DWI), 1-10 s (design of DWDS), 5 min (water quality in the DWDS). For the other applications it was either not easy to determine whether the small temporal scale was important, or resolutions of 15 min or 1 h were used.

4.2.4 Resulting demand patterns are realistic

The aspect of realistic water demand patterns – i.e. realistic average values, maximum values, realistic diurnal patterns and realistic variability from minute to minute, and day to day – is important for all applications that are meant for practical implementation. Especially when models need to be validated, this aspect is very important. On the other hand, as the majority of the researchers have not undertaken validation measurements for their application, SIMDEUM's realistic results are undisputed. For scenario studies the fact that the current patterns are realistic, builds confidence in the plausibility of future scenario results.

The fact that SIMDEUM leads to realistic demand patterns is important in 26 (of 27) applications. Here 14 require this aspect as they want to determine the potential for using their applications in practice; 7 want to determine the risk (in practice); 3 are using SIMDEUM as a ground truth or reference and 3 have validated the results with measurements in practice.

4.3 Validation

For residential and non-residential drinking water demands SIMDEUM(-DW) has been extensively validated for various spatial scales (single home, street, District Metered Area), various temporal scales (per 5 s, 1 min, 5 min, 1 h), and on various aspects (mean and maximum flow rate, diurnal pattern, variability and effect on travel times and tracer pulse shape) (Blokker et al. 2017). For this, both flow measurements and tracer studies in a DWDS were used. Some of the new applications were done on previously validated Dutch case studies. Piazza et al. (2020) used the tracer study of Blokker et al. (2010), and Díaz and González (2020); (2021) used the tracer study of Blokker et al. (2011). Some of the new applications used measurements to calibrate their model, rather than validate (Lokk et al. 2024; van Steen 2020).

Bailey et al. (2020b) have validated SIMDEUM-WW, where they measured flow time series, and water quality time series (phosphate, nitrate, COD and temperature) and showed that a water quality discharge depending on the end-use (toilet, washing machine, shower, etc.) fitted measurements much better than a standard average loading model. Dobson et al. (2021) also validated the SIMDEUM-WW approach, focussing on flows and viruses.

Applications in the premise plumbing system have not yet been validated.

4.4 Future research directions

With more information on typical (residential) water use in various countries, the application of SIMDEUM outside of the Netherlands can be expanded more. This may enhance the use of SIMDEUM for applications where small temporal and spatial scales are crucial. For non-residential water use, the input parameters for SIMDEUM are not well known yet. Using SIMDEUM to better understand non-residential water demand (Pieterse-Quirijns et al. 2013) is an interesting research direction.

Based on Table 1, we see possibilities of using SIMDEUM more in hot water supply and using it in the wastewater system inside the building. We see possibilities for more applications in the design of wastewater systems.

Validation is needed for applications in the premise plumbing system.

5 Conclusions

SIMDEUM was first launched in 2006. Ten years later it was applied in a lot of water quality related research in Dutch DWDS and DWI; mainly by the research group of the developers. In the following ten years SIMDEUM has found an application in many more countries and research groups. Also, the applications have been broadened to water quantity research (water saving, leakage) in DWDS and DWI, water quality in sewer systems, design of drinking water supply and wastewater collection systems. Most researchers used SIMDEUM because of its realistic demand (or discharge) patterns, that allowed them to validate and apply their models in practice. The small spatial scale and the realistic variability were also important reasons to use SIMDEUM.

6 References

Abhijith, G. R., Steffelbauer, D. B. and Ostfeld, A. (2023). "Toward digital twins for emerging contaminants in water distribution systems." *World environmental and water resources congress 2023*, 1047-1057.

Abraham, E., Blokker, M. and Stoianov, I. (2017). "Decreasing the Discoloration Risk of Drinking Water Distribution Systems through Optimized Topological Changes and Optimal Flow Velocity Control." *Journal of Water Resources Planning and Management*, 144(2), 04017093.

Bailey, O., Arnot, T., Blokker, E., Kapelan, Z., Vreeburg, J. and Hofman, J. (2019). "Developing a stochastic sewer model to support sewer design under water conservation measures." *Journal of Hydrology*, 573, 908-917.

Bailey, O., Arnot, T. C., Blokker, E. J. M., Kapelan, Z. and Hofman, J. A. M. H. (2020a). "Predicting impacts of water conservation with a stochastic sewer model." *Water Science & Technology*, 80(11), 2148-2157.

Bailey, O., Zlatanovic, L., van der Hoek, J. P., Kapelan, Z., Blokker, M., Arnot, T. and Hofman, J. (2020b). "A Stochastic Model to Predict Flow, Nutrient and Temperature Changes in a Sewer under Water Conservation Scenarios." *Water*, 12(4), 1187.

Berlin, M. K., van Laarhoven, K. A. and Sanders, J. (2022). "Finding a relation to estimate the maximum simultaneous water demand of a number of households, using real-life and synthetic data (Master Internship Report) (OPENBAAR)." *KWR 2022.138*, KWR, Nieuwegein.

Blokker, E. J. M., Agudelo-Vera, C., Moerman, A., van Thienen, P. and Pieterse-Quirijns, E. J. (2017). "Review of applications for SIMDEUM, a stochastic drinking water demand model with a small temporal and spatial scale." *Drinking Water Engineering and Science*, 10(1), 1-12.

Blokker, E. J. M., Beverloo, H., Vogelaar, A. J., Vreeburg, J. H. G. and van Dijk, J. C. (2011). "A bottom-up approach of stochastic demand allocation in a hydraulic network model; a sensitivity

study of model parameters." *Journal of Hydroinformatics*, 13(4), 714-728, doi:10.2166/hydro.2011.067.

Blokker, E. J. M. and van der Schee, W. (2006). "Simulation of water demands provides insight." CIB W062 Symposium 2006 - water supply and drainage for buildings, Taipei, Taiwan.

Blokker, E. J. M., Vreeburg, J. H. G., Beverloo, H., Klein Arfman, M. and van Dijk, J. C. (2010). "A bottom-up approach of stochastic demand allocation in water quality modelling." *Drink. Water Eng. Sci.*, 3(1), 43-51.

Blokker, E. J. M., Vreeburg, J. H. G., Buchberger, S. G. and van Dijk, J. C. (2008). "Importance of demand modelling in network water quality models: a review." *Drink. Water Eng. Sci.*, 1(1), 27-38.

Clements, E., Bibby, K. and Nerenberg, R. (2024a). "Assessing the Impact of Stochastic Demands and Fixture Purging on Free Chlorine Residuals in Premise Plumbing Systems." *ACS ES&T Water*.

Clements, E., Crank, K., Nerenberg, R., Atkinson, A., Gerrity, D. and Hannoun, D. (2024b). "Quantitative Microbial Risk Assessment Framework Incorporating Water Ages with Legionella pneumophila Growth Rates." *Environmental Science & Technology*.

Clements, E., Irwin, C., Koestner, J., Taflanidis, A., Bibby, K. and Nerenberg, R. (2023a). "Characterizing stochastic water age in premise plumbing systems using conventional and advanced statistical tools." *Environmental Science: Water Research & Technology*.

Clements, E., Irwin, C., Taflanidis, A., Bibby, K. and Nerenberg, R. (2023b). "Impact of fixture purging on water age and excess water usage, considering stochastic water demands." *Water Research*, 245, 120643.

Dash, A., Dignum, M. and Blokker, E. J. M. (T.B.P.). "Dutch drinking water sector readiness for stricter EU lead norm." *Water*.

De Backer, L., Van Kenhove, E., Cleiren, J., Rabaey, J., De Jonge, L. and Laverge, J. (2023). "Techno-economic assessment of a model-based Legionella control measure by combining thermal shocks and UV radiation in residential hot water systems." *Building Simulation 2023*, 3736-3743.

Díaz, S. and González, J. (2020). "Analytical stochastic microcomponent modeling approach to assess network spatial scale effects in water supply systems." *Journal of Water Resources Planning and Management*, 146(8), 04020065.

Díaz, S. and González, J. (2021). "Temporal scale effect analysis for water supply systems monitoring based on a microcomponent stochastic demand model." *Journal of Water Resources Planning and Management*, 147(5), 04021023.

Dobson, B., Jovanovic, T., Chen, Y., Paschalis, A., Butler, A. and Mijic, A. (2021). "Integrated modelling to support analysis of COVID-19 impacts on London's water system and in-river water quality." *Frontiers in Water*, 3.

Hall, R., Kenway, S., Memon, F. and O'Brien, K. (2025). "Trade-offs between total and peak energy consumption due to plumbing layouts in Australian and UK domestic hot water systems." *Journal of Cleaner Production*, 518, 145941.

Hatam, F., Blokker, M. and Prevost, M. (2025). "Integrated Flushing and Corrosion Control Measures to Reduce Lead Exposure in Households with Lead Service Lines." *Water*, 17(15), 2297.

Hook, J. and Speight, V. (2018). "Patterns in the Deterioration of Water Quality in Distribution Networks with Demand Reduction Technologies:(115)." *WDSA/CCWI Joint Conference Proceedings*.

Jacque, H., Mozafari, B., Kaan Dereli, R. and Cotterill, S. (2026). "Extending SIMDEUM: Stochastic Water Demand and Wastewater Modeling in the Educational and Food Service Sectors." *Journal of Water Resources Planning and Management*, 152(2), 05025016.

Josey, B. M. and Gong, J. (2025). "Comparing the Hydraulic Performance of Cold-Water Premise Plumbing Systems Designed Based on Traditional and Modern Peak Demand Estimates." *Journal of Water Resources Planning and Management*, 151(8), 04025025.

Junggeburth, T. (2024). "Simulation-based design optimization and robustness analysis of the Crailo local energy community," TU Eindhoven.

Kleckers, J., Abadi, A., Brandherm, K. M. and Haberkamp, J. (2024). "Wastewater generation model to predict impacts of urine separation on wastewater treatment plants." *Water Science & Technology*, 89(5), 1312-1324.

König, A. W. and Joksimovic, D. (2022). "Dynamically priced stormwater discharge fees as a way to organize distributed stormwater infrastructure." *12th International Conference of Urban Drainage Modelling: UDM 2022*.

Koop, S. H. A., Brouwer, S. and Zeidan, M. (2023). "100 liter per persoon per dag – Welke waterbesparingsmaatregelen zijn nodig?" *BTO 2023.037*, KWR, Nieuwegein.

Lokk, R., Blokker, M., Boxall, J., Romano, M., Provost, A. and Husband, S. (2024). "The impact of drinking water network model spatial and temporal scale on hydraulic metrics indicating discolouration risk."

Mazzoni, F., Blokker, M., Alvisi, S. and Franchini, M. (2022). "Evaluating residential water consumption at high spatio-temporal level of detail: a Dutch case study." Copernicus Meetings.

Mazzoni, F., Marsili, V., Blokker, M. and Alvisi, S. (2026). "Investigating the Characteristics of Residential Hot-Water Consumption: a Worldwide Review." *Water Research*, 126109.

Oberascher, M., Maussner, C., Cominola, A. and Sitzenfrei, R. (2024). "Sensitivity of model-based leakage localisation in water distribution networks to water demand sampling rates and spatio-temporal data gaps." *Journal of Hydroinformatics*, 26(8), 1824-1837.

Oberascher, M., Minaei, A. and Sitzenfrei, R. (2025a). "Graph-Based genetic algorithm for localization of multiple existing leakages in water distribution networks." *Journal of Water Resources Planning and Management*, 151(1), 04024059.

Oberascher, M., Minaei, A. and Sitzenfrei, R. (2025b). "Localization of Multiple Existing Leakages in Water Distribution Networks by a Graph-Based Genetic Algorithm." *World Environmental and Water Resources Congress 2025*, 940-947.

Piazza, S., Blokker, E. M., Freni, G., Puleo, V. and Sambito, M. (2020). "Impact of diffusion and dispersion of contaminants in water distribution networks modelling and monitoring." *Water Supply*, 20(1), 46-58.

Pieterse-Quirijns, E. J., Blokker, E. J. M., van der Blom, E. and Vreeburg, J. H. G. (2013). "Non-residential water demand model validated with extensive measurements and surveys." *Drink. Water Eng. Sci.*, 6(2), 99-114, doi:10.5194/dwes-6-99-2013.

Steffelbauer, D. B., Blokker, E. J. M., Buchberger, S. G., Knobbe, A. and Abraham, E. (2021). "Dynamic Time Warping Clustering to Discover Socioeconomic Characteristics in Smart Water Meter Data." *Journal of Water Resources Planning and Management*, 147(6), 04021026.

Steffelbauer, D. B., Hillebrand, B. and Blokker, E. J. M. (2022). "pySIMDEUM - An open-source stochastic water demand end-use model." *WDSA CCWI*, Valencia, Spain.

van der Holst, B., Verhoeven, G., Nguyen, P., Kok, K., Emde, M., Nutma, J. and la Fleur, S. (2023). "A quantification method for the potential downward flexibility of full-electric heat pumps during congestion events." *2023 IEEE Belgrade PowerTech*, 01-06.

van Steen, J. (2020). "Robustness assessment of leak detection and localization in water distribution networks under stochastic water demand."

Vargas, K., Waak, M., Tscheikner-Gratl, F. and Rokstad, M. (2024). "Tool to Model the Potential Risk of Legionella Growth in Premise Plumbing Systems." *Engineering Proceedings*, 69(1), 162.

Willet, J., Hillebrand, B. and Blokker, E. J. M. (2025). "Beoordelingen van disaggregatiemethoden op synthetische digitale watermeterdata." *KWR 2025.007*, KWR, Nieuwegein.

Zeidan, M. and Hillebrand, B. (2023). "A golden standard of representative flow rate distributions. Inventory for the new inspection system for water meters." *KWR 2023.044*, KWR, Nieuwegein.

7 Presentation of Author(s)

Mirjam Blokker works at KWR Water Research Institute as a pricinpal scientist and is an associate professor at TU Delft.

Mirjam is an expert in water demand modelling and water quality modelling in the drinking water distribution network.

Pressure Monitoring in Australian Residential Water Service Systems

B. M. Josey (1), M. Bilal (2), J. Gong (3)

(1) b.josey@deakin.edu.au

(2) m.bilal@deakin.edu.au

(3) james.gong@deakin.edu.au

(1) School of Engineering, Deakin University, Waurn Ponds, Australia

(2) School of Engineering, Deakin University, Waurn Ponds, Australia

(3) School of Engineering, Deakin University, Waurn Ponds, Australia

Abstract

Researchers at Deakin University conducted pressure monitoring on the water service systems in several residential houses in Victoria, Australia. Pressure data was collected via a dual-channel high-frequency data acquisition device connected to both the cold- and headed-water pipes. Typical locations included fixtures at washing machines or underneath kitchen and bathroom sinks. Pressure data was collected at ~925Hz for each channel continuously for several weeks. The pressure data showed that some of the plumbing systems monitored were regularly subjected to "excessive pressures" greater than the maximum pressure allowable (500 kPa, 72.5 PSI) by the Australian plumbing standard (AS/NZS 3500). The findings to date specifically highlight 3 critical issues: 1) systemic over-pressure: properties without boundary pressure control are influenced the main's pressure fluctuations, often exceeding the maximum pressure limit; 2) thermal expansion: water heating cycles cause significant pressure rises in systems with heated water storages; and 3) transient pressure entrapment: check-valves within modern "mini stop taps" can trap hydraulic transients (water hammer) within the braided hose between the tap and the water fixture. This research has confirmed that the issue of excessive pressure and non-compliance to plumbing standard is not uncommon in Victorian houses.

Keywords

Hydraulic transient pressure; Residential plumbing systems; Water hammer.

1 Introduction

Most plumbing codes and standards have some requirements regarding pressure conditions in premise plumbing systems (PPS). In Australia, the plumbing standard (Standards Australia, 2025) requires that the operating pressure should be no less than 50 kPa (7.25 PSI) at any fixture under its design flow, and the maximum static pressure should be no more than 500 kPa (72.5 PSI) at any fixture (other than fire services) in both the cold- and heated-water services. Some plumbing codes, such as the International Plumbing Code (IPC) (ICC, 2021) and the Uniform Plumbing Code (UPC) (IAPMO, 2024) also have prescriptive water hammer control requirements (water hammer arresters need to be installed where quick-closing valves are used), while for others (like the Australian plumbing code and standard) water hammer control is a performance requirement but no prescriptive rules. In Australia, water hammer control devices are rarely seen in PPS.

Water hammer, also known as hydraulic transients, are temporary pressure surges caused by rapid velocity changes in liquid piping systems. When abruptly opening or closing a fixture in a plumbing system, hydraulic transients are generated. Modern fast-acting PPS fixtures and appliances can change the flow of water, on or off, within 0.1 to 0.3 seconds (Lee et al., 2009). These fast valve closures generate rapid flow velocity changes, converting the momentum of water flowing through the pipe (kinetic energy) into pressure (potential energy) against the pipe wall.

Water hammer events in PPS may result in low-pressure extremes that can lead to localized cavitation, backflow and contamination intrusions, as well as excessively high pressures that can elevate the risk of pipe burst or damage to PPS appurtenances (Lee et al., 2009; Lee et al., 2012; Lee, 2015). A recent study (Marsili et al., 2023) found the monitored transient pressures generated by user activities (fixture events) induced significant pressure variations (up to 65m relative to the steady-state pressure). That study (Marsili et al., 2023) also highlighted that the research regarding transient pressure in PPS and smaller water service lines was limited to only a handful of studies.

This research aims to better understand the steady-state and dynamic pressure conditions in the cold- and heated water services in detached houses located in Victoria, Australia. The research team have developed dual-channel pressure loggers that are capable to measure transient pressure up to 925 Hz per channel. The pressure loggers were installed in ten detached Australian houses for several weeks each, with nine of them returned valid data. Key findings indicate significant non-compliance with the pressure limit of 500 kPa, particularly in houses without pressure control at the property boundary and those with heated water storage systems. The study also identified a "trapped transient pressure" phenomenon caused by modern “mini-stop” check-valves (cistern valves), which can elevate internal system pressure beyond mains levels.

2 Methodology

2.1 Study households

Presented in Table 1 are the details regarding nine households that produced valid data in the study (Household H6 stopped their engagement soon after the start so no information). Houses were located across five Victorian regions, that represented four water utilities. Household occupancy ranged from 1-10 with an average occupancy of 4.33. Each house ranged from 2-6 bedrooms with an average of 2.5, and 1-4 bathrooms with an average of 2.5. Water heating for each household was categorised as "instantaneous" (three houses) and "storage" (seven houses) across a mixture of gas, electric element, and heat pumps water heating equipment. Plumbing system piping materials were classified as metallic (copper), plastic, or combination with four, three, and two houses respectively. Of the nine houses, none of the houses had backflow prevention devices installed at the property boundary, and only two had active pressure control devices [pressure reducing valve (PRV) or pressure limiting valve (PLV)] at the property boundary.

Table 1 – Study household details

ID	Water Utility	Year	Occ	Bed	Bath	Water Heating		Pressure Control
						Type	Category	
H1	1	1980	4	5	2	Electric	Storage	No
H2	1	1930	2	4	2.5	Gas	Instant'	No
H3	1	2023	4	3	2	Heat Pump	Storage	No
H4	2	1990	10	6	3	Heat Pump	Storage	No
H5	2	1985	4	3	2	Gas	Instant'	No
H6	*Invalid*							
H7	3	1995	1	2	1	Heat Pump	Storage	PRV
H8	4	2024	4	4	4	Electric	Storage	No
H9	4	2000	4	5	2	Gas	Instant'	PLV
H10	1	1980	3	3	3	Electric	Storage	No
		Average:	**4.33**	**3.83**	**2.50**			

2.2 Data collection

Pressure data was collected via a high-frequency data acquisition (DAQ) device (Figure 1) connected to two pressure transducers capable of reading 0 to 1000 kPa (145 PSI). Two DAQ devices were installed at two different locations (where allowed) within each house. At each location, one pressure transducer monitored the cold-water pipe and another on the heated-water pipe (Figure 1). Typical locations included fixtures at washing machines or the connectors underneath kitchen and bathroom sinks. Pressure data was collected at ~925 Hz for each channel, with each pressure transducer representing a single channel. All sensing equipment was installed by licensed plumbing contractors.

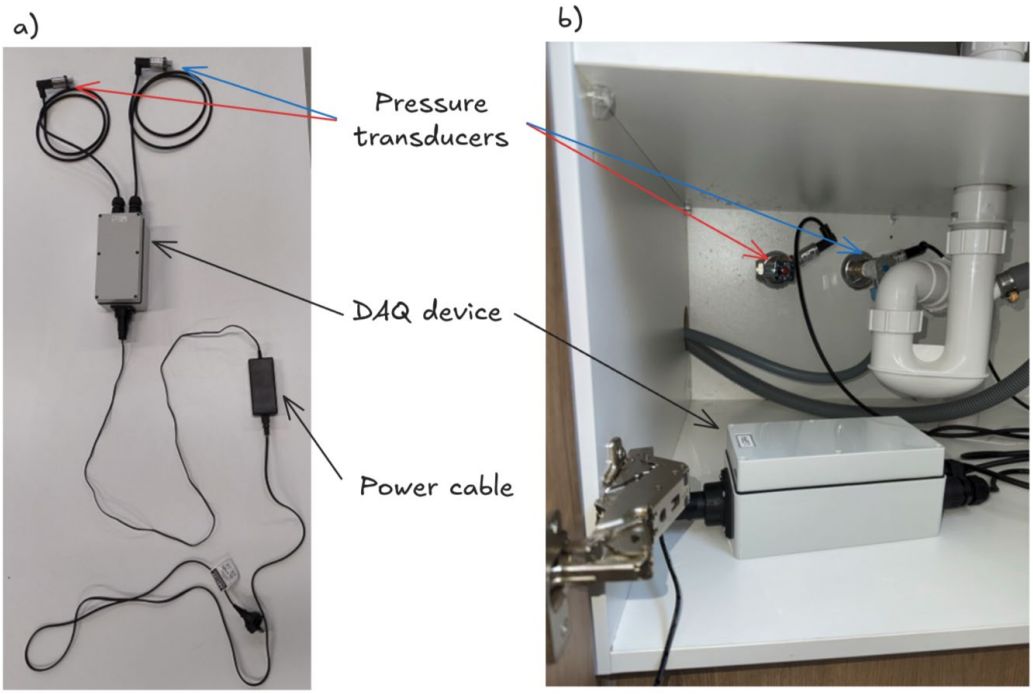

Figure 1 - a) a DAQ device connected with two pressure transducers, and b) a DAQ device installed in line with cold and heated water pipes under a sink.

Valid data include the pressure data collected from nine houses, at 15 different fixture locations (two in each house except for H1, H7 and H10). As stated previously, the study lost contact with H6 entirely. The research team has been unsuccessful in retrieving the DAQ devices installed in H6 to process data stored locally on the devices.

For Houses H1 and H7, readings from one of the DAQ devices (which was the same device used during different monitoring periods) were subject to extreme measurement noise across certain hours of the day. To ensure accuracy of the results presents, data from this device has been removed from the study dataset.

When considering H10, the household intermitted turned the device on and off, resulting in not enough data collection to extract meaningful comparisons for that house in two separate locations.

3 Results and Discussion

3.1 Diurnal pressure profile

Presented in Figure 2 and Figure 3 are the mean hourly pressure for each hour of the day, for all days monitored at each home. Data considers cold and heated water services separately. The curves presented are for nine houses at 15 different fixture locations (two in each home except for H1, H7 and H10).

For cold-water pressure data (Figure 2), mean hourly pressures ranged between 300 to 680 kPa (43.5-98.6 PSI), with 3 houses (H1, H2 and H10) above or at the 500 kPa (72.5 PSI) limit set by the Australian plumbing standard (Standards Australia, 2025) for all hours of the day. These three houses are supplied by the same water utility (utility 1), where high water pressures were observed when compared to other houses supplied by other water utilities. Pressure variations across the day ranged between 22-108 kPa (3.2-15.7 PSI) from the maximum hourly average to the minimum hourly average.

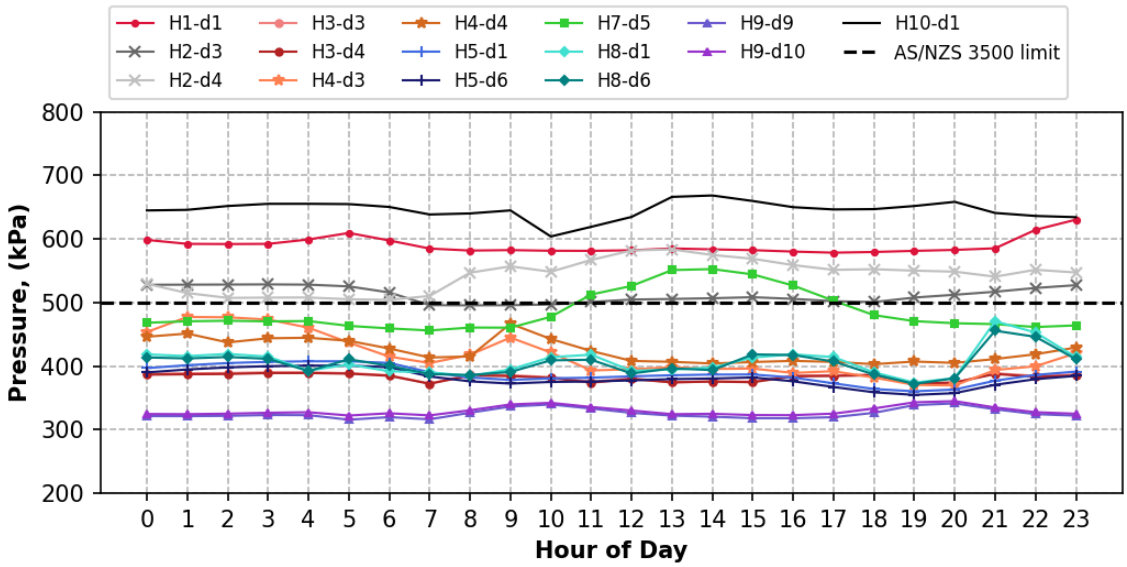

Figure 2 - Mean hourly pressure for monitored cold-water services in nine houses and at 15 different fixture locations (designation for each home H1-d1 = House id-DAQ device id).

For heated-water pressure data (Figure 3), the mean heated water pressures were between 300 and 780 kPa (43.5-113 PSI). Houses with storage water heating (solid lines, Figure 3) spent significant portions of the day above the 500 kPa (72.5 PSI) limit set by the Australian plumbing standard. This is because when water is heated, it expands, forcing an increase in pressure. This pressure is only released when a fixture is used, or when the water storage Temperature and Pressure Relief (TPR) Valve is activated. Houses with instantaneous water heating (dashed lines, Figure 3) generally followed similar pressures at or near the cold-water service.

Daily 10-second aggregated (averaged) pressures observed for two houses with heated water storage (H3, Figure 4a) and instantaneous water heating (H9, Figure 4b), respectively, are presented in Figure 4 to highlight the difference between daily heated-water pressure profiles. It appears that the heated-water storage systems stayed at the TPR valve limit for a considerable amount of time (hours), where the pressure slowly decayed, after water heating stopped, or rapidly released when a fixture was used.

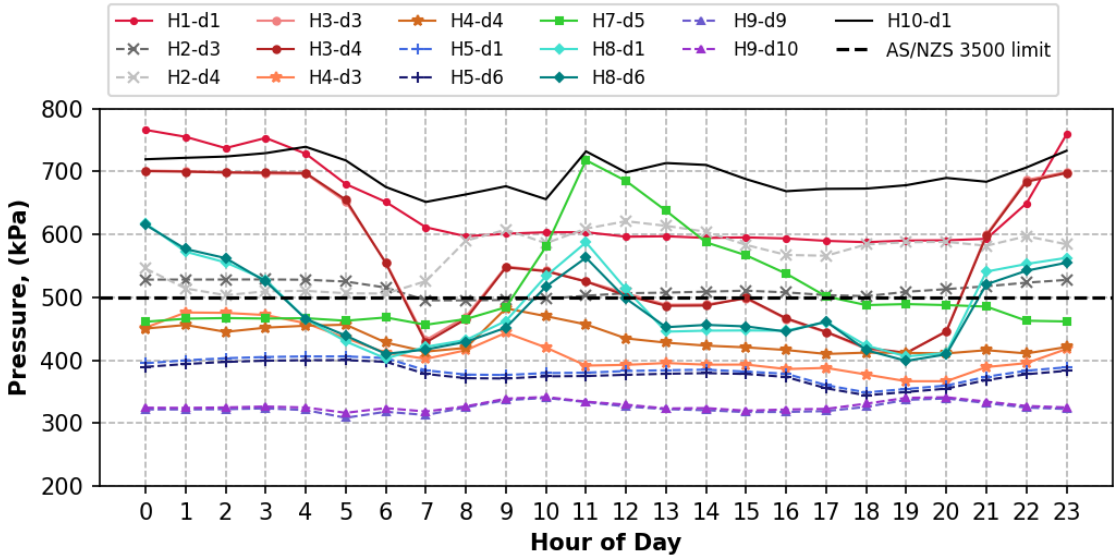

Figure 3 - Mean hourly pressure for monitored heated-water services in nine houses and at 15 different fixture locations, solid lines represent homes with storage water heating, dashed lines represent homes with instantaneous water heating (designation for each home H1-d1 = House id-DAQ device id).

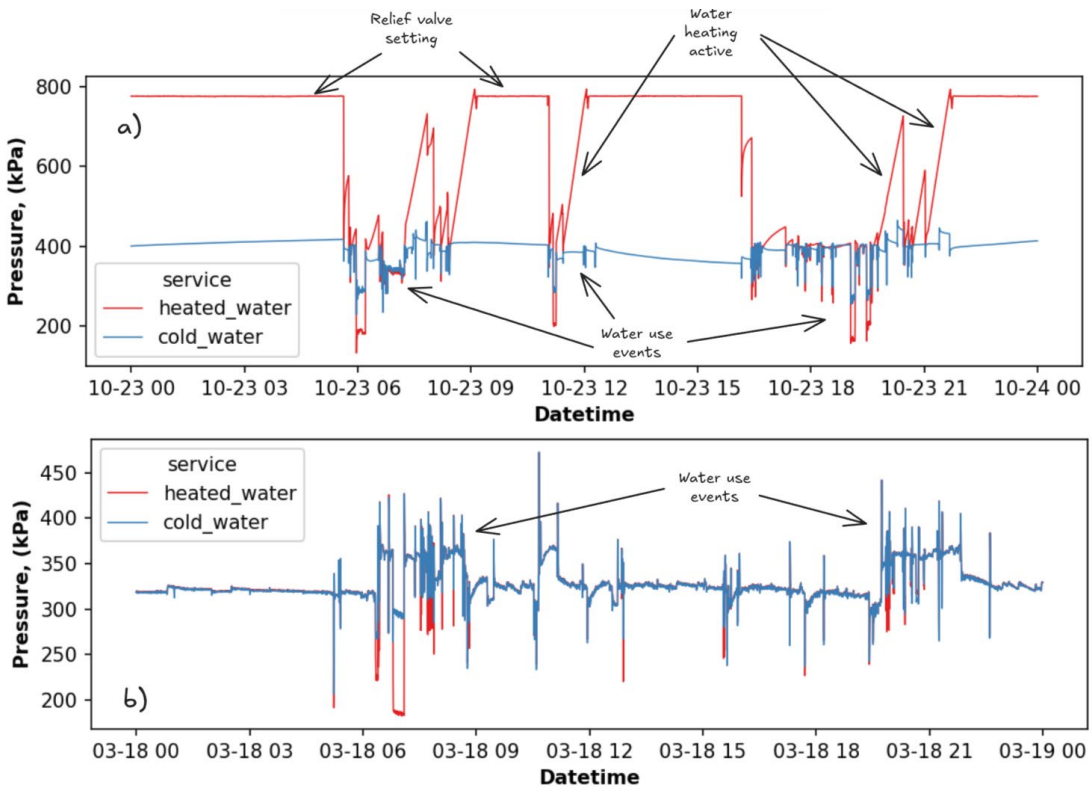

Figure 4 - Pressure profiles (10-second average) for a single day in a) H3 with heated water storage and b) H9 with instantaneous water heating.

3.2 Compliance with pressure requirements

Table 2 presents the percentage of time each DAQ device observed cold- and heated-water service pressures between the 50-500 kPa (7.25-72.5 PSI) pressure requirements set within the Australian plumbing standard (Standards Australia, 2025). Two houses (H1 and H10) supplied by the same water utility spent all their time above 500 kPa (72.5 PSI). House H2, also supplied by the same water utility, rarely met this performance requirement at 28-21% across its two DAQ devices. For H3, while it showed good compliance with cold-water pressures entering the property at 100%, the compliance was nearly halved for the heated-water network (55%), further demonstrating the impact of thermal expansion in heated-water storage on elevating the pressure for extended periods.

The remaining five houses showed better compliance, ranging from 100-67% of the time within the allowable pressure range. When reviewing the data for these five houses, the research team suspect that the incoming service pressures were fine and under the 500 kPa limit (72.5 PSI), and that certain characteristics of internal plumbing network were contributing to times spent above 500 kPa (72.5 PSI).

Table 2 - Percentage of time each house and monitoring device was observed in compliance with Australian standard pressure requirement of 50-500 kPa.

ID	Water Utility	Device 1		Device 2		Water Heating		Pressure Control
		CW %	HW %	CW %	HW %	Type	Category	
H1	1	0.3	0.0	N/A	N/A	Electric	Storage	No
H2	1	28.0	25.3	21.6	26.8	Gas	Instant'	No
H3	1	100.0	55.4	100.0	55.9	Heat Pump	Storage	No
H4	2	92.7	92.7	90.3	85.0	Heat Pump	Storage	No
H5	2	100.0	100.0	100.0	100.0	Gas	Instant'	No
H6								
H7	3	72.8	71.1	N/A	N/A	Heat Pump	Storage	PRV
H8	4	92.8	67.6	92.9	67.7	Electric	Storage	No
H9	5	100.0	100.0	100.0	100.0	Gas	Instant'	PLV
H10	1	0.0	0.0	N/A	N/A	Electric	Storage	No

3.3 Other causes of non-compliance

In addition to the two causes discussed earlier (no pressure control at the property boundary and thermal expansion in heated-water storage), the research has investigated other causes of non-compliance. When comparing data from houses H4 and H5, these two are located within a 5-minute drive from each other. A key difference between these two is that one has a heated-water storage (H4) and the other has instantaneous water heating (H5). The pressures measured at both DAQ devices in H5 were fully compliant with the plumbing standard. However, when looking at the data for H4, compliance drops to 90-92% for the cold-water service. This is because there was pressure rise in the cold-

water network that followed the heated-water network as shown in Figure 5, suggesting there was pressure creep from the heated-water network to the cold-water network. Theoretically the cold- and heated-water networks should be isolated from each other as the heated-water system has a check-valve installed before the heated-water tank to prevent reverse flow. Speculated causes of this pressure rise are either poor installation or a faulty check-valve that wasn't fully isolating the cold- and heated- water network from each other.

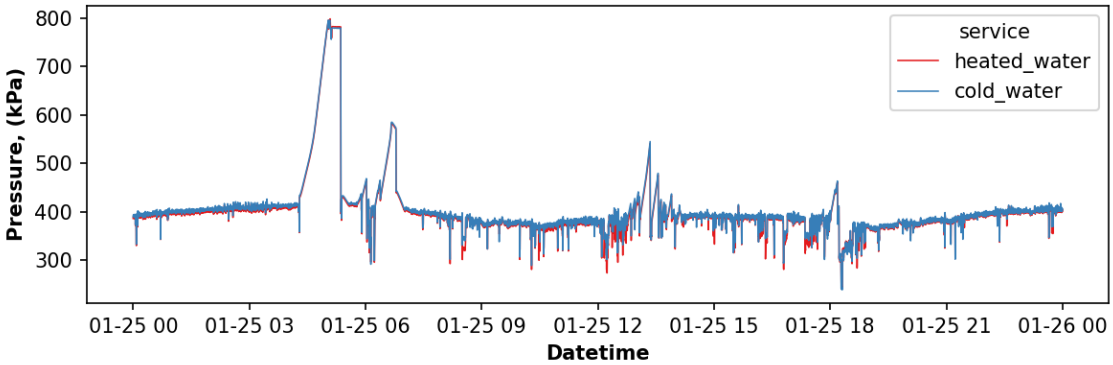

Figure 5 - Daily pressure profiles (10-seconf average) in H4 for cold- and heated-water pressure monitored at the kitchen sink.

When evaluating houses H7 and H9, both of which had pressure control devices located at the boundaries of the property, the data suggests that these pressure control devices did well at protecting the home from excessive pressure in the cold-water mains network (before the water meter), but did little to protect the plumbing system from large pressure spikes and phenomena that were generated from within the home.

Figure 7 presents 10-second aggregated (averaged) time series pressure data for H7 for a select day (MM-DD HH). H7 had a PRV installed at the boundary. In the early hours of the morning, the pressure was limited to below 500 kPa (72.5 PSI), suggesting the PRV was actively working. However, at approximately 10 am, a large series of cold-water pressure spikes were generated when the dishwasher stopped filling and the solenoid valve quickly closed, elevating the pressure well above 500 kPa (72.5 PSI). When reviewing the raw pressure signal, the transient pressure generated from dishwasher filling cycles were trapped (stored) and slowly dissipated, only releasing when a downstream fixture was opened (another filling cycle). Note that none of the houses have any water hammer arresters installed.

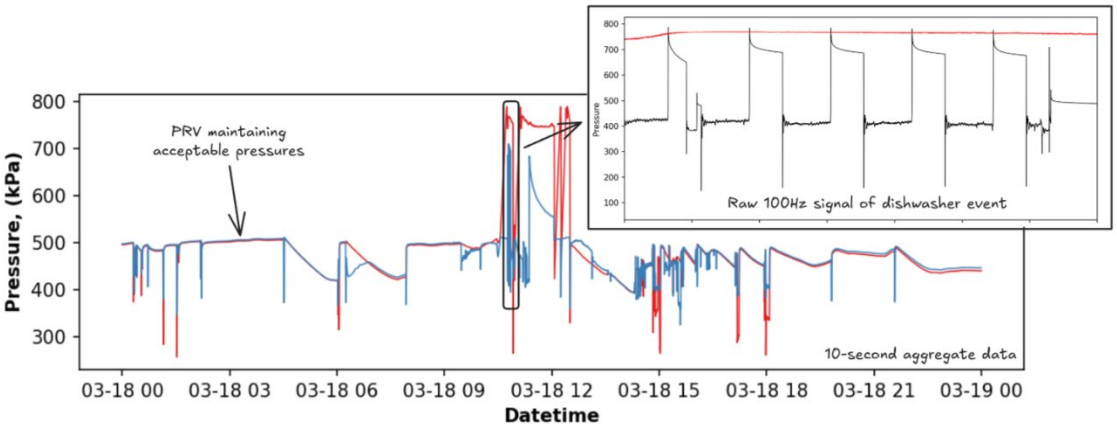

Figure 6 - Daily pressure profiles (10-second average) in H7 for cold- and heated-water pressures monitored at the kitchen sink, with 100 Hz pressure data shown in the zoomed-in window for a series of dishwasher filling cycles.

It is believed that the "trapping" of transient pressures occurs because modern "mini stop taps" (Figure 8) incorporate a check-valve mechanism that prevents reverse flow and the entry of contaminants into the plumbing system. Transient pressure (water hammer) waves have both positive and reverse flows. It is believed that the closure of the water fixture at the downstream end of the braided flexible hose (a solenoid valve in the dishwasher) stopped the flow and induced the initial spike in pressure. This increased pressure could not be balanced by the lower static pressure in the network because the check-valve mechanism prevented negative (reverse) flow.

Figure 7 - Example of internal check-valve in a mini-stop tap.

This phenomenon was also evident in H3, where pressures in an upstairs bathroom (Figure 9b) were higher than the pressures at the washing machine (Figure 9a) located on the ground floor. Transient waves generated elsewhere entered the braided flexible hose after the "mini stop tap" but was prevented from escaping because of the check-valve mechanism. Because the built-up pressure was slow to dissipate, successive transient events elevated the pressure further (Figure 9b), explaining the reduced compliance between device 1 and device 2 for H3 in Table 2.

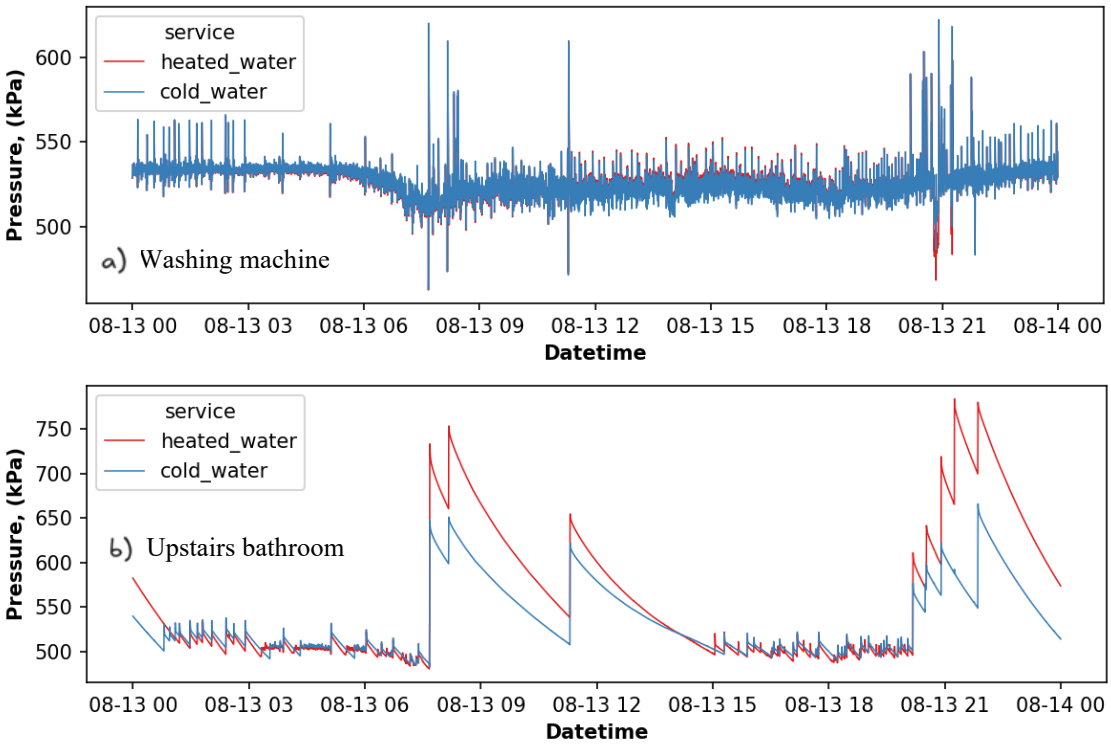

Figure 8 - Daily pressure profiles (10-second average) observed for a select day in H3 for cold- and heated- water pressure monitored at a) washing machine on the ground floor and b) basin in an upstairs bathroom.

4 Policy Considerations

Based on the findings, policy makers (especially in Australia) may want to consider the following when reviewing and updating the current plumbing standards and regulations:

1. **Pressure Control in High-Pressure Zones:** In regions where water mains' pressure consistently exceeds the maximum pressure limit (500 kPa in Australia), boundary pressure reduction is needed for all new and existing properties. This is probably more of a problem for existing properties. They might be following the regulation when commissioned, but later the regulation or the pressure in the water main changed.

2. **Pressure Management for Heated Water Storages:** Standards for pressure management of domestic water heaters with storages need to be reviewed. For houses with heated water storages, the installation of expansion control valves or expansion vessels may need to be more strictly enforced to mitigate the extreme pressure caused by thermal expansion (currently not mandatary in most states and territories in Australia). While Australian and some international plumbing standards provide mitigation guidance (e.g., sizing of expansion vessels), it typically focuses on protecting the TPR valves rather than maintaining pressures below the limit.

3. **Standards for Plumbing Components with Check Valves:** Standards for internal check-valves need to be reviewed to address the "trapped pressure" phenomenon. The review should not be limited to the “mini stop taps” as investigated in this project, but also on other plumbing components that have check-valve mechanisms. Repeated fixture operations elsewhere in the system allow pressure to accumulate in the short pipe section (typically a braided flexible hose in Australia) between the check valve and the water fixture, with only temporary relief when the affected fixture is used (often followed by a new transient event on closure).

4 Conclusions

Pressure data has been collected in nine residential houses across Victoria, Australia. Each house was monitored for several weeks, and the pressure was measured continuously at a high sampling frequency about 925 Hz. This is enabled by the development of a customised data acquisition device. Each device enables pressure to be measured at the cold- and heated-water pipes simultaneously.

The analysis of the collected pressure data has revealed a systemic problem in Australian residential plumbing to maintain water pressure below the regulatory limit of 500 kPa (72.5 PSI). In specific, the research has identified three critical issues: 1) Systemic over-pressure from the water main: Many residential properties lack effective boundary pressure control and are therefore exposed to fluctuating mains pressures that frequently exceed the regulatory pressure limit; 2) Thermal expansion in heated-water systems: Water heaters with a heated-water storage generate significant pressure increases during normal operation and expose the heated-water network in excessive pressure (up to the limit set by the TPR valve) for prolonged time; and 3) Transient pressure entrapment in modern fittings with check-valve mechanisms: Check-valves embedded in modern “mini stop taps” can trap transient pressure in the short pipe section (typically a braided flexible hose in Australia) between the check valve and the water fixture.

5 Acknowledgments

The research presented in this paper was supported by the Building and Plumbing Commission, Victoria, Australia, through their research program (project ID: PJ12434).

6 References

IAPMO. (2024). "2024 Uniform Plumbing Code." International Association of Plumbing and Mechanical Officials (IAPMO), Ontario, USA, https://iapmo.org/codes-standards-development/code-development/uniform-plumbing-code.

ICC. (2021). "International Plumbing Code." International Code Council (ICC), Washington, DC, USA, https://codes.iccsafe.org/content/IPC2021P3.

Lee, J., Lohani, V. K., Dietrich, A. M., and Loganathan, G. V. (2009). "Low Pressure Propagation at Service Lines." American Society of Civil Engineers, 10.1061/41036(342)66.

Lee, J., Lohani, V. K., Dietrich, A. M., and Loganathan, G. V. (2012). "Hydraulic transients in plumbing systems." *Water Science & Technology*, 12(5), 620–629, 10.2166/ws.2012.036.

Lee, J. (2015). "Hydraulic Transients in Service Lines." *International Journal of Hydraulic Engineering*, 4, 31–36, 10.5923/j.ijhe.20150402.02.

Marsili, V., Mazzoni, F., Alvisi, S., Maietta, F., Capponi, C., Meniconi, S., Brunone, B., and Franchini, M. (2023). "Investigation of pressure transients induced on a real water service line by user's activity." *AQUA - Water Infrastructure, Ecosystems and Society*, 72(12), 2331–2346, 10.2166/aqua.2023.276.

Standards Australia. (2025). "AS/NZS 3500 Plumbing and Drainage Set 2025." Standards Australia, Sydney, Australia.

7 Presentation of Author(s)

Brendan Josey is an Associate Research Fellow at Deakin University, Australia. His research focusses on the improved peak demand estimates and how a “model informed” approach can improve the design of premise plumbing systems.

Muhammad Bilal is a PhD researcher at Deakin University, Australia. His research focuses on modelling and analysis of water demand and premise plumbing system performance in multi-storey residential buildings.

James Gong is a Senior Lecturer at Deakin University, Australia. His research expertise and interests include smart water and wastewater network design and data analytics, condition assessment and leak management of water networks, and optimal design and operation of premise plumbing systems.

Flush cisterns: water conservation *versus* drainage performance

C. Pimentel-Rodrigues (1,2,3), A. Silva-Afonso (1,2,4)

(1) anqip@anqip.pt

(1) ANQIP (Associação Nacional para a Qualidade nas Instalações Prediais), Polo Operacional da Universidade de Aveiro

(2) RISCO, Departamento de Engenharia Civil da UA, 3810-193 Aveiro, Portugal

(3) ISCIA (Instituto Superior de Ciências da Informação e da Administração, 3810-488 Aveiro, Portugal

(4) WFEO (World Federation of Engineering Organizations), Committee on Water, Maison de l'UNESCO, 1 Rue Miollis, Paris, France

Abstract

In theory, a toilet should only receive urine, faeces, and toilet paper, which form the basis of the tests generally required by product certification standards. Starting from this premise and seeking not to compromise the effectiveness of bowl cleaning as measured by normative tests, a trend towards the progressive reduction of flush volume has been observed since the last decades of the 20th century, in response to growing concerns about sustainability and resource conservation. However, it is noted that consumer society produces an increasing number of products that are incorrectly disposed of in the toilet. Paper towels, disposable razors, baby wipes, diapers, kitchen sponges, sanitary napkins, etc., are causing increasing problems with the building's drainage system, leading to recurring blockages. Based on laboratory tests involving the disposal of various products frequently flushed down the toilet, the drainage performance of branches with different slopes was verified for multiple flush volumes. The results confirm that a growing conflict may be developing between concerns about water conservation and the proper functioning of building drainage systems. In its conclusions, this article presents some reflections aimed at mitigating this conflict, focusing on discharge conditions.

Keywords

Flush cistern volumes; water conservation; drainage performance; building drainage

1 Introduction

In principle, a toilet bowl should only receive urine, feces, or toilet paper... In reality, that's not quite what happens. Over time, our consumer society has progressively invented new products, many of which end up being flushed down the toilet.

A study conducted in Finland [1] revealed that several inappropriate objects reached sewage treatment plants via building drainage systems, including small soccer balls, mobile phones, children's toys, mattress parts, eyeglasses, dentures, clothing, and medications. Other authors [2] add cleaning and hygiene items to this list, such as cotton swabs, paper towels, cleaning cloths, baby wipes, diaper liners, dog waste bags, and cleaning wipes, in significant quantities.

In recent years, the disposal of fats, oils, and grease (FOG) through building drainage systems has intensified, leading to significant blockages in public networks [1]. The situation is worsening to such an extent that a specific term has been created for these blockages: "fatbergs" (a term even included in the Oxford English Dictionary in 2015). In January 2019, a fatberg approximately 60 meters in size – blocking the sewer – was discovered in the city of Sidmouth, in the United Kingdom [3], reporting that it was an agglomeration of fat mixed with wet wipes, sanitary napkins, and other household products that should be disposed of in the trash and not in the toilet. In early 2017, a fatberg was observed in East London, estimated at 130 tons and 250 meters long [4].

The studies by Joksimovic et al. (2020) [2] demonstrate that heavier products, such as baby wipes, cleaning cloths, hygiene wipes, cleaning wipes, diaper liners, and paper towels, often require multiple flushes to unclog pipes. Test results with cleaning cloths indicate that about 4 flushes are needed on average. Products with slightly less mass, such as dog waste bags and paper towels, often unclog the plumbing with one or two flushes.

Given this situation and the tendency for it to worsen, one conclusion seems obvious: increasing the volume of flushes can be advantageous, if not necessary. This conclusion, however, conflicts with another trend observed since the 1970s: the need to conserve fresh water in many regions of the planet for sustainability. This concern has led to a continuous reduction in the volume of toilet flushes in recent decades [5] (but often creating problems in the rehabilitation of old buildings, where existing and to-be-maintained networks were initially designed to function adequately with relatively high flush volumes). Taking Europe as a reference, there is a trend towards a significant reduction in volumes, with models featuring a full flush of only 3 or 4 L, which is common on the market. However, volumes close to 6 L are still the most common, in general with dual flush (3/6 L).

This article presents the results of a study to evaluate the functioning of a toilet drain in relation to the disposal of various common household products that are known to frequently end up in the toilet, concluding that it is necessary to reconcile these two issues: water conservation versus the performance of the building's drainage system. The study

does not analyze the functioning of toilets under usual conditions (with urine, feces, and toilet paper), but many studies that have been developed in recent decades in this context [6-16], analyzing flushing conditions with standard solids (generally set out in standards, such as EN 997 [17]), lead to similar conclusions.

2 Methods and materials

For the development of this study, an installation was constructed, equipped with a toilet bowl with an adjustable-volume cistern, connected to a branch pipe with a commercial diameter of 90 mm, made of transparent material, and 10 meters in length (Figures 1 and 2). The branch line supports allow a slope range of 0.5% to 4%, but the tests were conducted only for the most common slopes of 0.5%, 1%, and 2%. The branch line was not ventilated and had an open outlet to the atmosphere (in an open discharge receptacle).

Figure 1 – Toilet bowl with adjustable flush cistern

Figure 2 - 90 mm discharge branch with 10 meters

It is known that the results of this type of test can be influenced by the toilet design and not just by the characteristics of the branch or the volume flush cistern. Different toilet models have different flushing profiles, which can influence the initial speed at which solids are flushed and the drag flow. Therefore, the toilet selected was a very common model on the Portuguese market.

A measuring tape was attached to the branch line, allowing the direct determination of the drag distance for the various objects used in the tests at different slopes (0.5%, 1%, and 2%) and discharge volumes (Figure 3). Regarding these discharge volumes, the tests

were carried out at 6, 4, 3, and 2 litres, to simulate the use of dual flush toilets with 6/3 L and 4/2 L.

Figure 3 - Measuring tape on the branch line

The objects used in the tests were (Figure 4):

- Sponge kitchen scouring pad;
- Toilet disinfectant block
- Diapers
- Hygiene wipes
- Wet toilet paper
- Women's sanitary pads
- Lady tampon
- Disposable razor blade
- Toothbrush

For the hygiene wipes, 5 were used simultaneously, a practice considered normal.

Figure 4 - Objects used in the tests

3 Results and Discussion

The results of the various tests are summarised in Tables 1-3. These tables indicate "OK" when the object has travelled the 10 meters of the branch line without incident. It should be noted, however, that after the first experiments with the highest slope considered (2%), it was decided not to use some of the objects in the tests, as it was quickly found that they caused permanent or difficult-to-overcome blockages.

This was the case, for example, with the diapers that consistently got stuck on the curves at the toilet exit. However, it is interesting to note that, after being pushed towards the toilet outlet, they flowed without difficulty along the entire branch. The toilet disinfectant blocks also got stuck in the toilet bowl outlet, and it was particularly difficult to remove them without dismantling the installation.

The kitchen cleaning sponge was also abandoned because, even with the greatest slope (2%) and the highest discharge flow rate (6 L), five flushes were needed to complete the drag to the end of the branch. The distances travelled for the first four discharges were 4.63 m, 6.18 m, 7.69 m, and 8.22 m, respectively. With smaller slopes or lower discharge volumes, it was generally not possible to drag the sponge up to 10 meters, even with a high number of discharges.

Finally, the toothbrush was also discarded because, perhaps due to its size, it could easily get stuck in small protrusions or differences in fittings and connections between the tubes. In summary, for all possible installation variants, the complete set of tests was performed

using only hygiene wipes, wet toilet paper, women's sanitary pads, lady tampons, and disposable razor blades.

The stopping distances in the branch line (*in italic*) are indicated in relation to the number of consecutive discharges made. It should be noted that objects reached 10 meters in the discharge following those indicated. It was found that wet toilet paper and disposable razor blades always flowed without problems, regardless of the pipe slope or flush volume.

Table 1 - Distances travelled by objects (m), with a 2% slope in the branch line and for different discharge volumes. (V)

Objects	**V = 6 L**	**V = 4 L**	**V = 3 L**	**V = 2 L**
Hygiene wipes (5)	OK	OK	*9.10 m*	*4.60 m (7.00 m after a second discharge)*
Wet toilet paper	OK	OK	OK	OK
Women's sanitary pads	OK	OK	OK	OK
Lady tampon	OK	OK	OK	*8.60 m*
Disposable razor blade	OK	OK	OK	OK

Table 2 - Distances travelled by objects (m), with a 1% slope in the branch line and for different discharge volumes. (V)

Objects	**V = 6 L**	**V = 4 L**	**V = 3 L**	**V = 2 L**
Hygiene wipes (5)	*8.97 m*	*5.40 m*	*3.75 m (9.40 m after a second discharge)*	*2.50 m (5.90 m after a second discharge and 9.70 m after a third discharge)*
Wet toilet paper	OK	OK	OK	OK
Women's sanitary pads	OK	OK	*9.44 m*	*8.07 m*
Lady tampon	OK	OK	*6.28 m*	*4.69 m (9.70 m after a second discharge)*
Disposable razor blade	OK	OK	OK	OK

Table 3 - Distances travelled by objects (m), with a 0.5% slope in the branch line and for different discharge volumes. (V)

Objects	**V = 6 L**	**V = 4 L**	**V = 3 L**	**V = 2 L**
Hygiene wipes (5)	*6.35*	*4.43 m (6.70 m after a second discharge)*	*3.20 m (6.73 m after a second discharge and 9.40 after a third discharge)*	*2.18 m (5.35 m after a second discharge, 7.96 m after a third discharge and 9.50 m after a fourth discharge)*
Wet toilet paper	OK	OK	OK	OK
Women's sanitary pads	OK	OK	*5.25 m*	*5.65 m*
Lady tampon	*8.75 m*	*6.65 m*	*5.10 m (9.70 m after a second discharge)*	*4.10 m (7.20 m after a second discharge and 9.17 after a third discharge*
Disposable razor blade	OK	OK	OK	OK

Figure 5 illustrates one of the tests performed (with a lady tampon, a slope of 0.5% and a discharge of 2 L).

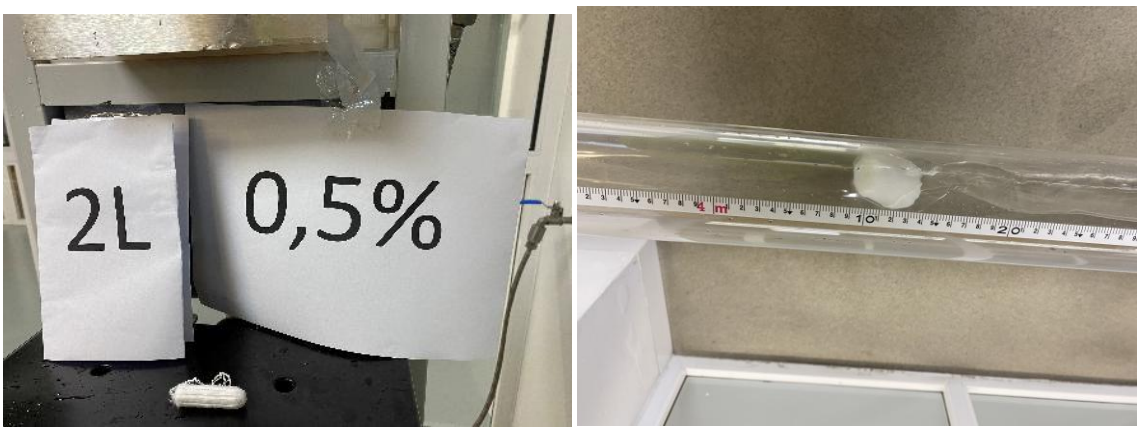

Figure 5 - Example of a test (with a lady tampon, a slope of 0.5% and a discharge of 2 L)

It is debatable whether the lack of ventilation on the branch line could affect the results. It was assumed that it did not (which will be proven in future experiments), given that the low flow from the toilets always led to flows below half the section. On the other hand, the European Standard EN 12056-2 [18] is under revision, admitting that collective branches up to 10 meters without ventilation may be accepted (in the current version, ventilation can only be dispensed with up to 4 meters). The branch line in question was not a collective one. Still, even if it were, this would not alter its characteristics, since EN 12056-2 allows a 90 mm branch line for the discharge of all sanitary appliances in a typical domestic bathroom.

Another aspect that can be discussed concerns the diameter of the branch line. A 110 mm branch line can be used in this case and would likely avoid some blockages, but previous ANQIP experiences show that the drag distance can be compromised [8].

The fact that toilet paper was not used in these experiments can also be questioned, given that the barrier effect it forms in the branch may favour the flushing of some objects [8]. Although this aspect will be the subject of future research, it was not considered that the disposal of the selected objects was generally accompanied by toilet paper, except for women's sanitary pads and lady tampons.

Therefore, without prejudice to future research, an experiment was also conducted assuming the disposal of a probable combination of a woman's sanitary pad and three hygiene wipes in the toilet bowl. The results, obtained only for flush volumes of 4 and 2 litres and a slope of 0.5% s, are presented in Table 4.

Table 4 - Distances travelled by objects, with a 0.5% slope in the branch line and for different discharge volumes. (V)

Objects	**V = 4 L**	**V = 2 L**
1 women's sanitary pad + 3 hygiene wipes	*6.10 m*	*3.40 m (5.95 m after a second discharge and 7.80 after a third discharge)*

It is foreseeable that the characteristic flush curve of the toilet bowl (which is a specific parameter of each model), may have some influence on the results in this type of test. In the present case, a commercially available toilet was used, for which the characteristic flush curve is unknown and was not provided by the manufacturer, but the authors plan to develop, in the continuation of this work, an analogous study using toilets of different brands/models, to evaluate the differences in the results (experimentally determining, if necessary, the respective flush curves).

4. Conclusions

Tests have shown that the trend of reducing toilet flush volumes, motivated by sustainability and drinking water conservation reasons, can compromise the proper functioning of the building's drainage system, particularly regarding its ability to eliminate certain solids, especially throwaway products whose disposal in the toilet bowl, although inappropriate, is becoming increasingly common. As expected, this conclusion is more relevant when the slopes of the branch lines are reduced.

In fact, consumer society is increasingly creating disposable hygiene and cleaning products and objects, and many of them usually end their useful life in the toilet bowl. In addition to these objects, many others can inadvertently fall into the toilet, such as small soccer balls, mobile phones, children's toys, mattress parts, eyeglasses, dentures, clothing, and medications, whose removal from the drainage system can be particularly difficult.

This situation, which may probably worsen in the future, shows that there can be a conflict between sustainability concerns and the need to ensure the proper functioning of building drainage. The solution will certainly involve maintaining an adequate minimum volume in the cisterns, prioritizing the use of non-potable water in this device, such as saltwater, rainwater, greywater, etc.

As mentioned in a previous paper presented at CIB W062 [5], there are already cisterns on the market suitable for use with saltwater and dual-inlet cisterns (potable/non-potable). Currently, some companies are developing products designed to work with various types of non-potable water, including those with high chlorine levels. These flushing cisterns could, for example, be used to reuse water from public swimming pools (where the water is partially replaced daily, due to legal requirements) for toilet flushing, thereby reducing significant drinking water waste in many countries.

The use of a cistern with a relatively low volume can also be important in rehabilitation contexts, when the aim is to maintain the old drainage network, which was generally designed for larger volumes than those of the current one. Several authors mention this issue.

5 Acknowledgments

The authors thank OLI World for its support in developing this research.

6 References

[1] Katko, T., Hukka, J., Juuti, P., Juuti, R., Nealer, E. (Eds.) (2025). Dispelling Myths about Water Services. IWA Publishing, London. ISBN: 9781789064162 (eBook).

[2] Joksimovic D., Khan A., Orr B. (2020). Inappropriate disposal of 'flushable' consumer products – reasons for concern. *Water Science & Technology*, 81(1), 102–108, https://doi.org/10.2166/wst.2020.087.
[3] Schaverien A. (2019). Scientists Solve a Puzzle: What's Really in a Fatberg. *New York Times*, 4 Oct 2019. https://www.nytimes.com/2019/10/04/world/europe/sidmouth-fatberg.html (accessed 29 January 2026).
[4] Taylor M. (2017). Total monster': fatberg blocks London sewage system. *Guardian*, 12 Sept 2017. https://www.theguardian.com/environment/2017/sep/12/total-monster-concrete-fatberg-blocks-london-sewage-system (accessed 30 January 2026).
[5] Pimentel-Rodrigues, C., Silva-Afonso, A., Gago, H., Teles, J. (2025). Water efficiency in buildings: A review of the role of the flush cistern over time. *In Proceedings CIB W062 2025 – Water Supply and Drainage for Buildings*, Miami, USA, 24 to 27 August 2025.
[6] Gormley. M. (2017). Assessment of the impact of low flush volume WCs on building drainage system operation. Heriot-Watt University, Mar. 2011.
[7] Silva-Afonso, A., Van der Schee, W., Scheffer, W. (2014). "4-liter closetspoeling blijft kritisch", *TVVL Magazine*, Netherlands, May 2014, pp. 2-5.
[8] Silva-Afonso, A., Bernardo, J., Pimentel-Rodrigues, C. (2013) Implications of reduced flow volumes in building drainage: An experimental study. *Proceedings CIB W062 2013 Symposium on Water Supply and Drainage for Buildings*. Nagano, Japan, 17 to 20 September 2013.
[9] Delwiche, T., Vos, L., Bleys, B. (2025). Impact of low-flush toilets on drainage design: A Belgian case study. *Proceedings of the CIB W062 2025 – Water Supply and Drainage for Buildings*. Miami, USA, 24 to 27 August 2025.
[10] Littlewood, K., Memon, F., Butler, D. (2007). Downstream implication of ultra-low flush WCs. *Water Practice & Technology*, vol. 2, no. 2, 2007.
[11] Kagami, H., Otsuka, M., Nakato, T. (2013). A Study on the Discharge Characteristics of Water-Saving Toilets using Different Amounts of Flushing Water and the Evaluation of the Carrying Performance Thereof, *Proceedings of the CIB W062 2013 Symposium on Water Supply and Drainage for Buildings*, Nagano, Japan, 17 to 20 September 2013.
[12] Otsuka, M. (2015). Carrying performance evaluation of a horizontal fixture drain branch system in relation to drainage characteristics of water-saving toilets installed therein. *Proceedings of the CIB W062 Symposium on Water Supply and Drainage for Buildings 2015,* Beijing, China, 18 to 20 August 2015.
[13] DeMarco, P., Koeller, J., Martin, S., Swatkowski, C., White, C., Burgess, M. (2013). The drainline transport of solid waste in buildings, *Proceedings of the CIB W062 2013 Symposium on Water Supply and Drainage for Buildings*, Nagano, Japan, 17 to 20 September 2013.
[14] Valencio, I., Gonçalves, O. (2016). Field evaluation of housing units with low flush toilet (4,8 l/flush) installed -water consumption monitoring and damage verification in the drainage system performance *Proceedings of the CIB W062 2013 Symposium on Water Supply and Drainage for Buildings*, Nagano, Japan, 17 to 20 September 2013.

[15] Swaffield, J., McDougall, J. (2006). The transport of deformable solids at low flush volumes within building drainage networks". *Proceedings of the CIB W062 2006 Symposium on Water Supply and Drainage for Buildings*. Sydney, Australia, 2006.
[16] Gauley, B., Koeller, J. (2005). Evaluation of water-efficient toilet technologies to carry waste in drain lines. *Final Report CMHC Project*, Canada, 2005.
[17] CEN (European Committee for Standardization). EN 997:2012 - *WC pans and WC suites with integral trap*. Brussels, 2012.
[18] CEN (European Committee for Standardization). EN 12056-2:2000 - *Gravity drainage systems inside buildings - Part 2: Sanitary pipework, layout and calculation*. Brussels, 2000.
.

6 Presentation of Authors

Carla Pimentel Rodrigues holds a PhD in Civil Engineering (Hydraulics) from the University of Aveiro (Portugal) and is a Senior Member of the Portuguese Order of Engineers. She is the Executive Director of ANQIP – the National Association for Quality in Building Installations- and has developed the Portuguese system for labelling products' water efficiency. She is also a Senior Lecturer at ISCIA (Aveiro).

Armando Silva-Afonso is a retired Full Professor at the University of Aveiro (Portugal), Department of Civil Engineering, where he continues to collaborate as a Visiting Professor. He is the current President of the Board of ANQIP - Portuguese Association for Quality in Building Installations and Vice-Chair of the Committee on Water of WFEO - World Federation of Engineering Organizations. He is also an expert at UN-Water (Expert Group on Water Scarcity).

The proportional deviation of thermostatic balancing valves in hot water circulation systems

M. van Bruggen (1)
W.G. van der Schee (2)

(1) De Energie-manager, Amsterdam, member TVVL Expert group indoor climate, The Netherlands
(2) Climate en Sanitary Consulting, Amersfoort, member TVVL Expert group Sanitary Technologies, The Netherlands

Abstract

In 2016 TVVL reported a study, "Thermostatic Balancing Valves in Hot Water Circulation Systems," on the performance of thermostatic balancing valves [1].
In large buildings with extensive hot water systems, a circulation system is required to meet the maximum allowable hot-water delivery time and to maintain microbiologically safe water temperatures. To keep the entire hot water system at the required temperature, a circulation pump provides a constant flow. Thermostatic balancing valves are used to distribute that flow correctly among the loops. But how does a thermostatic balancing valve actually perform in detail? This paper focuses on the proportional deviation of thermostatic balancing valves in hot water circulation systems.

When sizing a TBV, a calculation determines the required TBV temperature based on the required flow rate and pressure loss (K_v value). Technicians commonly adjust the TBV to that calculated hot-water temperature, but they often overlook the effect of **proportional deviation**. The actual adjusted hot-water temperature is lower than the calculated value, which adversely affects the operation of a hot-water recirculation system.

Keywords
hot water circulation system, thermostatic balancing valves, proportional deviation

1 Introduction

The proper functioning of a hot-water system requires a continuous flow through the entire system, including the recirculation loops. The required hot-water flow must be distributed across the system to maintain a minimum temperature. Thermostatic balancing valves (TBVs) are commonly used to balance flow rates among the loops. However, TBVs exhibit a phenomenon called proportional deviation, which is largely unknown in the field of hot-water circulation systems.

2 Design of domestic hot water circulation systems

The design of a domestic hot water circulation system is based on the following principles:

- The return temperature in circulation mode is at least 60 °C.
- The flow velocity in circulation pipes is a maximum of 0.7 m/s
- The domestic hot water pipes forming part of the domestic hot water system are designed for a maximum flow velocity of 1.5 m/s at the maximum instantaneous flow rate.

In addition, the design is based on a calculation of the maximum temperature drop throughout the circulation system during circulation operation. The results of the design calculation are (assuming steady-state conditions during circulation operation):

- The actual temperature drop between the supply and return.
- The diameters of the circulation pipes.
- The minimum insulation required for all pipes in the circulation system.
- The temperature profile in the system.
- The pressure drop across the balancing valves. The pressure drop is such that hydraulic balance is achieved at the desired temperature profile across the system.
- The flow rates in the circulation pipes and domestic hot water pipes that form part of the circulation system.
- The design circulation flow rate and the pressure difference to be achieved by the circulation pump at this flow rate.

Figure 1 shows a HWS with thermostatic balancing valves and several loops.

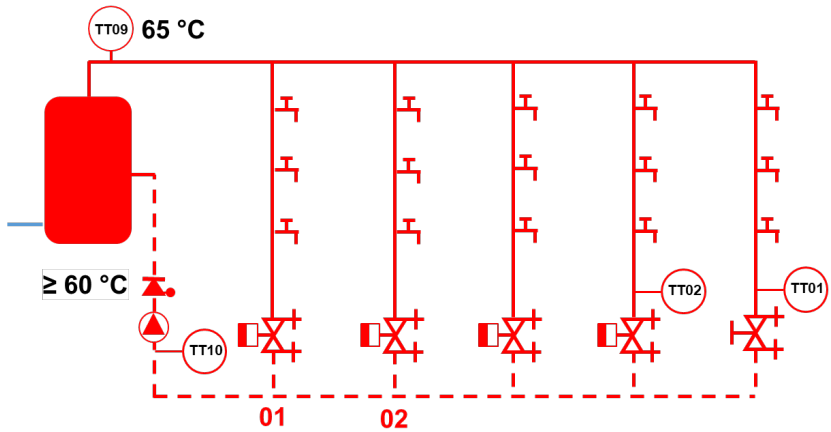

Figure 1. A Hot drinking water circulation system with thermostatic balancing valves. Temperatures according to the Dutch standard NEN 1006.

The design calculation is usually carried out using specialised software. Sometimes the calculation is performed by component suppliers. The study revealed that the Dutch calculation method (in accordance with NEN 1006 [2] and ISSO 55) is not always used in such cases. The calculation is based on a system with static balancing valves.

When commissioning a domestic hot water circulation system, the balancing valves are set so that they have the desired pressure drop at the calculated flow rate. The system is adjusted based on measurements of temperature and (sometimes) flow velocity.
Thermostatic balancing valves (IRAth) are often used in the installation of the domestic hot water system. There is no methodology for determining the set temperature; the choice of set temperature is largely arbitrary. It is then set manually, for example, to 61 °C, 62 °C or 63 °C.

3 Thermostatic balancing valves

To understand how thermostatic balancing valves (IRAth) affect hydraulic balance, it is necessary to understand how an IRAth operates. With an IRAth, pressure drop depends on water temperature. If the actual $K_{v;i}$ at a given water temperature is higher than the value on the valve's characteristic curve, the balancing valve will close further. If the actual $K_{v;i}$ is lower than the characteristic value, the valve will open further. The valve stabilises at a combination of the domestic hot-water temperature and the $K_{v;i}$ on the characteristic curve. As a result, the temperature at the valve is always lower than the setpoint temperature T_{set}. The IRAth is defined by a Temperature–K_v characteristic curve (see Figure 2). According to the manufacturers manual the TBV is preset to a temperature of e.g. 58 °C for the German situation, the valve will be in maximum open position till the temperature reaches 52 °C. Above 52 °C, the TBV starts to throttle the flow and reaches the maximum throttle position when the preset temperature of 58 °C is reached. When the hot water heater is turned to 70 °C to do a thermal disinfection, the valve starts to open at 62 °C and reaches a thermal disinfection position at 70 °C.

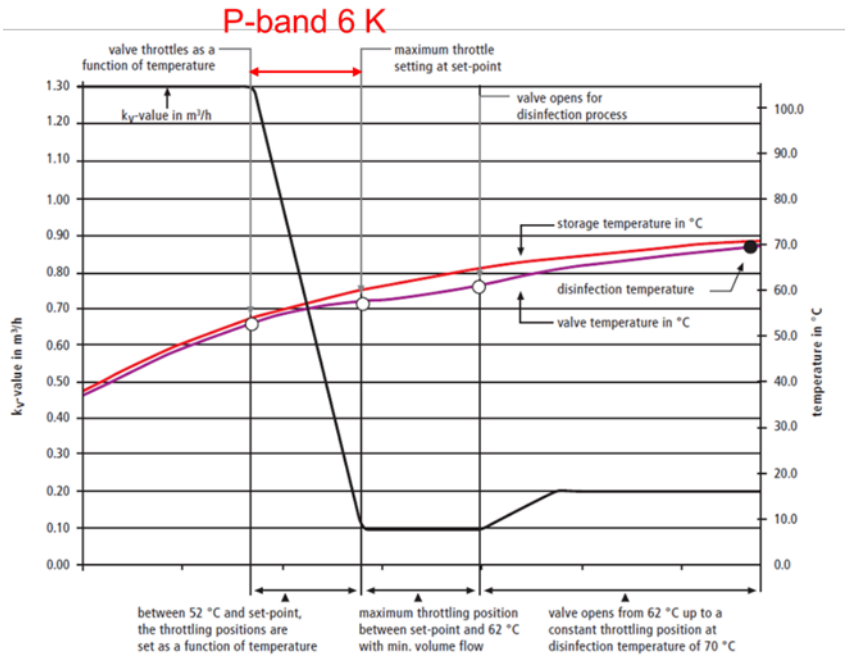

Figure 2 T-K_v characteristic of a thermostatic balancing valve with a P-band of 6 K

For proper operation, the operating point must lie on the TBV's characteristic curve: the K_v value corresponding to the required hot-water temperature in the loop. Figures 3 and 4 illustrate the TBV's behaviour more in detail. The thermostatic valve closes as the hot-water temperature rises and opens as the temperature falls. The red dot indicates the operating point.

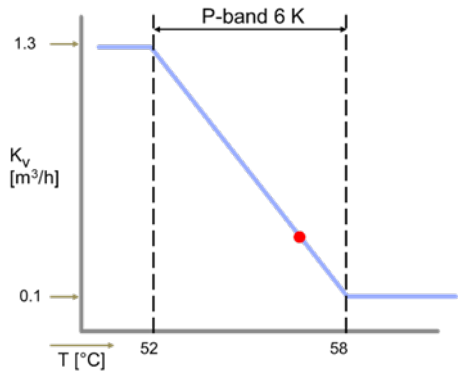

Figure 3: Detailed T-K_v characteristic of a thermostatic balancing valve.

K_v is a measure of pressure drop in relation to the flow rate under standardised conditions. A low K_v value indicates a higher pressure drop; a high K_v value indicates a lower pressure drop. In Figure 4, $K_{v;min} = 0.1$ represents the valve in a (virtually) fully closed position and $K_{v;max} = 1.3$ represents the valve fully open. $K_{v;i}$ represents a $K_{v;i}$ value set on the valve. Due to the adjusted temperature from 58 °C, the manufacturers preset, to 62.5 °C on the TBV, the characteristic shifts to the right.

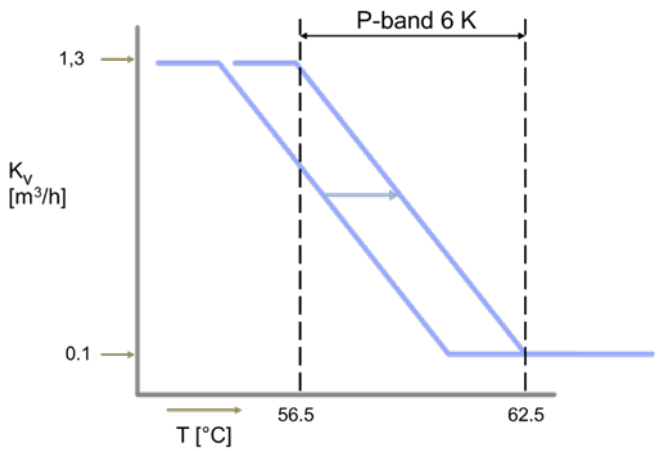

Figure 4: T-K_v characteristic shifted to the right to the desired temperature of 62.5 °C.

An IRAth does not regulate exactly to the setpoint T_{set}; it regulates to a point on its characteristic curve, which lies below the set temperature (T_{set}). The higher the K_v and the flatter the characteristic curve (i.e., the larger the proportional band), the greater the deviation from T_{set}.

To achieve the desired temperature at the calculated flow rate, T_{set} must be set such that the desired combination of temperature and K_v lies on the characteristic curve. The value to be set for T_{set} can be calculated using the formula 1:

$$T_{set} = T_i + -\frac{P - band\ .\ (K_{v;i} - K_{v;min})}{K_{v;max} - K_{v;min}} \qquad \text{Formula 1}$$

Where:

T_{set}	The temperature to be set on the balancing valve	°C
T_i	Desired temperature at the balancing valve	°C
P-band	Proportional band width	K
$K_{v;i}$	(calculated) value of $K_{v;i}$ at which the desired temperature is achieved	m³/h
$K_{v;min}$	Minimum $K_{v;i}$ value of the balancing valve	m³/h
$K_{v;max}$	Maximum $K_{v;i}$ value of the balancing valve	m³/h

A thermostatic balancing valve is selected so that the desired $K_{v;i}$ value lies within the control range and the proportional control deviation is not significant. For setting the balancing valve, a choice can be made between a simple method and a theoretical method.

With the simple method (which is common practice), the setpoint temperature of the balancing valves is set to, for example, 61 °C, 62 °C or 63 °C. Since the temperature achieved at the balancing valve is (usually) lower than the set temperature, it should be checked in advance whether the achieved temperature will not fall below 60 °C.

Standard DHW circulation calculation software does not predict the hydraulic balance that results from a chosen temperature setpoint, so the resulting volumes, flow rates and circulation temperatures are unknown. Any excessively high (or low) flow velocities or excessively low circulation temperatures can usually be corrected through readjustment in steady-state circulation operation. Due to varying inlet temperatures from the domestic hot water heater, the behaviour of the thermostatic balancing valves and their influence on flow rates and circulation water temperatures remains not entirely predictable.
In the theoretical method, the setpoint temperature is calculated based on the temperature at the end of the sub-loop, as calculated by the computer, and the characteristic curve of the IRAth, so that the calculated temperature and calculated $K_{v;i}$ lie on the characteristic curve of the thermostatic balancing valve. The formula 1 given above can be used for this purpose. Setting a setpoint temperature on the balancing valve has limited accuracy (approximately ± 1 °C), makes it difficult to set the exact desired temperature. The value of a theoretical method is therefore limited.

The thermostatic balancing valve is also characterised by hysteresis. Hysteresis means that the relationship between temperature and K_v is not straightforward, as it also depends on the direction in which the valve moves (opening or closing). From a stable state, the control valve must overcome a certain resistance before regulation begins. As a result, the actual temperature may differ from that expected based on the characteristic curve.
This hysteresis is not described in the documentation of most manufacturers.

4 Example to size a TBV

Figure 5 shows a HWS with the desired flow rate $K_{v;i}$ and hot water temperature T in loop 1.

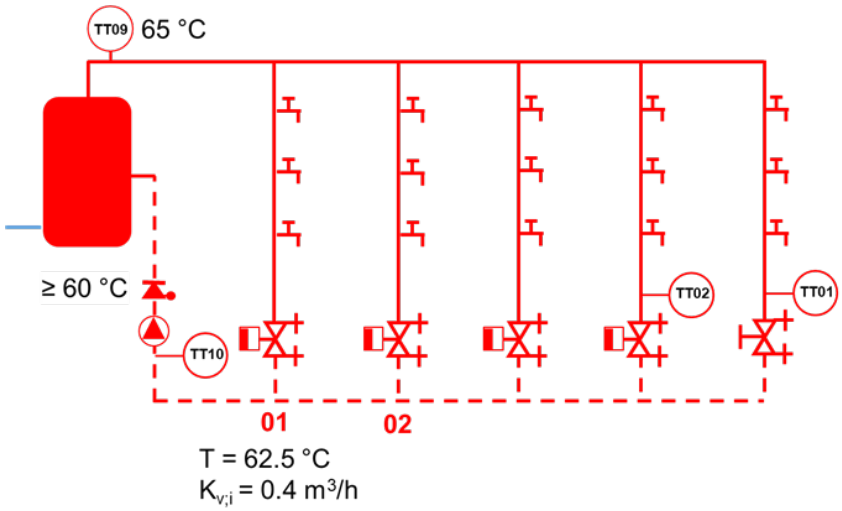

Figure 5 A Hot drinking water circulation system with thermostatic Balancing valves. Example with values for $K_{v;i}$ and temperature T.

The required $K_{v;i} = 0.4\ m^3/h$ and the required hot water temperature is 62.5 ˚C. According formula 1 the T_{set} has to be calculated:

$$T_{set} = T_i + \text{P-band}\ \frac{(K_{v;i} - K_{v;min})}{K_{v;max} - K_{v;min}}$$

$$T_{set} = 62.5 + \frac{6\ (0.4 - 0.1)}{1.3 - 0.1} = 64\ ˚C$$

Figure 6 shows the result. The characteristic curve has shifted to the right from 62.5 °C to 64 °C, and the desired operating point lies exactly on the TBV characteristic curve.

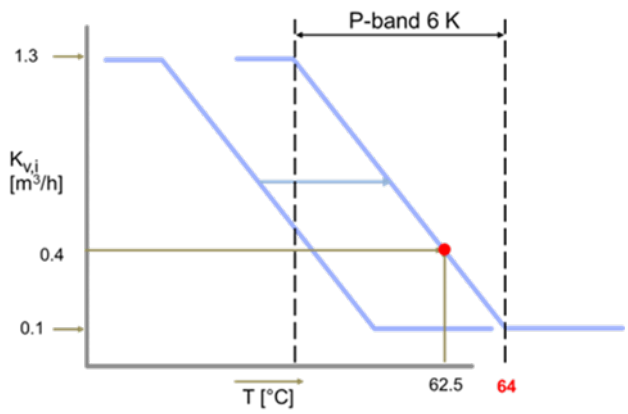

Figure 6: The characteristic of the TBV shifts to the right from 62.5 ˚C to 64 ˚C, the operating point lies exactly on the characteristic.

5 Conclusion

The best way to size a TBV is to take in account the proportional deviation. It's recommended to use the calculation according formula 1.

Application of TBV's:

- Generally, adjustment is done according to the calculated temperature. Technicians overlook the effect of the proportional deviation
- If the proportional deviation is overlooked, the real hot water temperature is lower than the calculated and required hot water temperature. This affects negative the operation of a hot water recirculation system.
- In general, the accuracy of a TBV is ± 1 K, and it might be ± 2 K.
  (In comparison: the accuracy of a static BV is 5 – 10 % of the flow rate)
- Hysteresis might be 1 K, this affects the operation of TBV's.

Recommendations:

- Although manufacturers recommend to size a TBV on the half of the maximum K_v-value, consider to size on a low K_v-value, on the bottom of the characteristic, to keep the proportional deviation low.
- Check always the hot temperatures in the loops afterwards. Realise the difference between theoretical calculation and practice.
- Manufacturers should mention the TBV's proportional deviation with a method to calculate exactly T_{set} in their manuals.

6 References

1. Report ST-46 Hot water circulation systems, Michiel van Bruggen et al, TVVL, April 2020
2. NEN 1006+A1, General requirements for water supply installations, 2018
3. Dynamic behaviour of hot water circulation systems, Michiel van Bruggen, The energy manager, September 2020

7 Presentation of authors

Michiel van Bruggen MSc is a self-employed consultant on energy matters operating under the name *De Energiemanager*. As member of the technical committee, he conducted various research projects on plumbing technology.
E-mail: m.vanBruggen@deenergiemanager.nl

Walter van der Schee BSc was an employee of Croonwolter&dros based in Amersfoort, the Netherlands. Since July 2020 he's retired and he delivers consulting and training activities.

As a member of the Dutch Technical Association for Building Installations (TVVL), he is one of the experts consulting for Plumbing technologies. For his work within the TVVL he was awarded the BJ Max Award in 2006.

For further information about the TVVL association consult the website www.tvvl.nl
E-mail Walter van der Schee: censconsulting2020@gmail.com

Development and validation of a *Legionella* test setup for low temperature domestic hot water (DHW)

Andreas Moerman (1), Frank Oesterholt (2), Amitosh Dash (3), Paul van der Wielen (4)
(1) andreas.moerman@kwrwater.nl
(2) frank.oesterholt@kwrwater.nl
(3) amitosh.dash@kwrwater.nl
(4) paul.van.der.wielen@kwrwater.nl

(1, 2, 3, 4) KWR Water Research Institute, Nieuwegein, The Netherlands

Abstract
In the energy transition, there is a growing focus on (very) low-temperature (LT) heating systems, both in district heating networks and within collective building systems ("block heating"). These systems are more sustainable, due to lower heat losses during transport. In LT heating systems, the production of safe hot water using LT water heaters is a key focus area, where the challenge is to prevent the growth of *Legionella* bacteria, among other things (legal requirements). Low-temperature hot water is a topic where two societal interests interfere: public health (due to possible *Legionella* risk) on the one hand and sustainability (energy efficiency) on the other. In the Netherlands, in accordance with the NEN 1006 standard, DHW should have a temperature of 55 °C at the tap (in homes without circulation systems). For sanitary use (showering), however, a temperature of 38 °C is sufficient. In addition, the shower is the largest consumer of hot water in an average household; 72 – 84% of all hot water used in an average Dutch household is used for showering (Moerman *et al*., 2015). When hot water can be produced at a lower temperature, substantial energy savings are possible, and peaks in electricity consumption (resulting from electric reheating) can be reduced (Moerman and Oesterholt, 2023). However, *Legionella*, and in particular the most dangerous species (*L. pneumophila*), grows optimally in drinking water systems at temperatures between 35 and 40 °C (Van der Wielen *et al*., 2021; 2023). Therefore, without proven *Legionella*-safe solutions, such a low temperature for hot water can lead to health risks. A test setup, build within the context of the "ProVe IT-LT"-project (phase I)[1] was evaluated under various conditions to determine whether it is suitable for testing the safety of low-temperature LT water heaters.

Keywords
Domestic hot water, public health, energy use, energy transition

[1]https://www.kwrwater.nl/en/projecten/prove-it-lt-proven-safe-and-innovative-hot-tap-water-at-low-temperature/

1 Background

In the energy transition, there is a growing focus on low-temperature (LT, 30-50 °C) heating systems, both in district heating networks and within collective building systems ("block heating"). These systems are more sustainable, due to lower heat losses during transport. In LT heating systems, the production of safe hot water using LT water heaters is a key focus area, where the challenge is to prevent the growth of *Legionella* bacteria, among other things (legal requirements). Low-temperature hot water is a topic where two societal interests interfere: public health (due to possible Legionella risk) on the one hand and sustainability (energy efficiency) on the other. In the Netherlands, in accordance with the NEN 1006 standard, DHW should have a temperature of 55 °C at the tap (in homes without circulation systems). For sanitary use (showering), however, a temperature of 38 °C is sufficient. In addition, the shower is the largest consumer of hot water in an average household; 72 – 84% of all hot water used in an average Dutch household is used for showering (Moerman *et al*., 2015). When hot water can be produced at a lower temperature, substantial energy savings are possible, and peaks in electricity consumption (resulting from electric reheating) can be reduced (Moerman and Oesterholt, 2023). However, *Legionella*, and in particular the most dangerous species (*L. pneumophila*), grows optimally in drinking water systems at temperatures between 35 and 40 °C (KWR & Berenschot, 2021). Therefore, without proven legionella-safe solutions, such a low temperature for hot water can lead to health risks.

2 Problem formulation

In the last years several suppliers of water heaters entered the market with new LT hot water concepts, either designed for block heating or low-temperature district heating. Local authorities hesitate to give permission for these systems since there is no clear scientific basis to guarantee the water safety of these systems. Therefore, there is a need for a protocol to determine to what extent new concepts may or may not be equivalent to the requirements of the NEN 1006 standard. In this protocol not only the hot water heater itself but also the domestic water installation (DWI) between the hot water heater and the hot water taps should be considered. Next to this, the protocol has to be as simple as possible, but still representative for DWIs.

3 Method

3.1 System layout

3.1.1 General

A test setup was developed containing both (1) a full representation of a DWI, developed by KWR called the HomeWaterLab® (hereinafter 'HWL') and (2) a simple representation to measure growth of biofilm and opportunistic pathogens, called a biofilm monitor (hereinafter 'BFM').

3.1.2 HomeWaterLab (HWL)

The HWL is a high-end representation of a real DWI, wherein all kind of water qualities and circumstances can be tested in a safe environment without negative exposure to a water user (client). The HWL contains pipes, a break tank, pump, water heater (heat exchanger), magneto-electric valves, temperature sensors and flow sensors and can be controlled with tapping patterns for the cold and hot taps (Figure 1, left). A more extensive description of the HWL can be find on the KWR website[2].

Figure 1. Front view of the HWL (left) and example of a BFM (right). The BFMs connected to the test setup are situated in the grey cabin at the right side of the HWL (marked by the yellow box). The blue container on the right picture is a casing for safe transport.

3.1.3 Biofilm monitor (BFM)

As a simple representation of the DWI biofilm monitors were used (Figure 1, right). A BFM is a small test setup mainly consisting of a glass cylinder containing rings of a specific pipe material. The rings can be taken out one by one in a certain frequency to

[2] https://www.kwrwater.nl/en/tools-producten/homewaterlab/

sample the biofilm on the material surface of the inner side of the ring. Two biofilm monitors were used to test materials often used in the DWI (multilayer pipe PE-Al-PE and copper). A third monitor (PVC-P) was used as positive reference for growth of *L. pneumophila*.

3.1.4 Full test setup

The BFMs (PE-Al-PE, copper and PVC-P) were connected to the hot water part of the HWL to be supplied with hot water every time shower use in the HWL takes place. Although the HWL represents a full DWI containing cold water and hot water pipes and taps, the scope of this research was only on the hot water part.

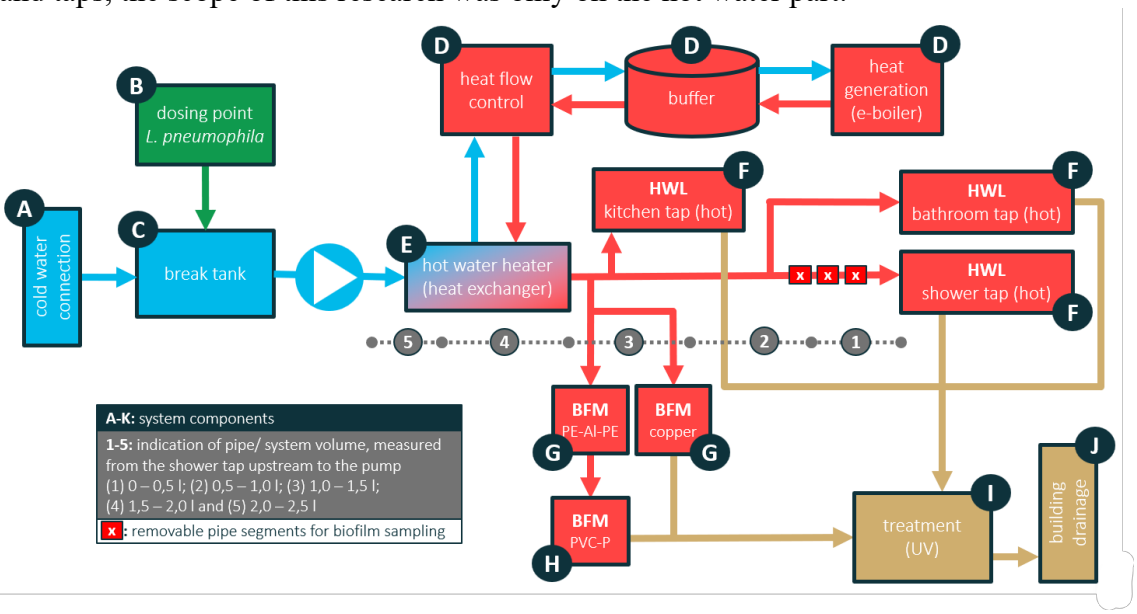

Figure 2. Schematic overview of the test setup. HWL = HomeWaterLab, BFM = biofilmmonitor

Figure 2 shows a schematic overview of the test setup, only the hot water related piping and appliances are shown. Below an explanation of the components A to K is given.

A. Drinking water connection. This is the point at which drinking water is drawn from the building's drinking water supply and fed into the break tank (C).
B. Dosing point. At this point, the precultured *L. pneumophila* is dosed into the system.
C. Break tank. As the system is contaminated, an atmospheric separation is required between the drinking water connection to the drinking water system and the test installation where the measurement protocol is applied.
D. Heat generation. The heat generation system consists of a heat generator (electric boiler), a buffer tank and a thermostatic controller. The thermostatic controller ensures that the heat exchanger receives sufficient heat at the correct temperature on the primary side.
E. Heat exchanger. The cold water is heated by a heat exchanger wherein the temperature of hot water production was maintained. Hence, the heat exchanger does not cool down after hot water use.
F. HWL hot water taps. The hot water taps are imitated using electro-magnetic valves which is controlled by the tapping pattern controller of the HWL. Water samples for analysis of adenosine triphosphate (ATP), as measure for active biomass, and *L.*

pneumophila were taken from the shower tap only. In the last pipe section between the T-junction and the shower tap three removable pipe sections (, hereinafter 'coupons') were built in for biofilm analysis in the HWL.
G. BFM PE-Al-PE and copper. These BFMs contain rings of multilayer pipe (PE-Al-PE) and copper. The multilayer pipe rings were made from the same pipe batch the hot water pipes of the HWL were made from.
H. BFM PVC-P. This BFM is filled with PVC-P rings and serves as a positive control, as PVC-P contains high concentrations of growth-promoting substances, meaning that *L. pneumophila* is expected to grow optimally when other conditions, i.e. temperature, are optimal.
I. Post-treatment (UV). All water flowing from the BFMs is treated with UV to prevent *L. pneumophila* bacteria from entering the building's drainage system (and thereafter the urban sewerage system/ wastewater treatment plant).
J. Building drainage system. This is the point where the treated water from the test installation is discharged into the building's drainage system.

3.2 Tapping pattern

To imitate a real situation the test setup was run by a tapping pattern generated by the Simdeum® water use pattern generator for a small household consisting of 1-2 inhabitants. This pattern consists of multiple moments for water use during the day both for cold and hot water (only the hot water demand is reported in this paper). Hot water use for the kitchen tap and the bathroom sink were randomly distributed over the day. At the start of the experiment (until day 120) the shower hot water demand equalled 7 l/min (hot + cold water) during a shower of 8 minutes two times a day (morning, evening), hereinafter called 'shower pattern I'. In reaction to limited growth of *L. pneumophila* (see Discussion part) the shower hot water demand was changed after day 120 to four showers with equal flow and duration in the evening with 15 min. in between (Figure 3, hereinafter called 'shower pattern II'). The flow patterns of the different hot water demands were monitored using flow meters in the HWL.

Figure 3. Hot water demand in the HWL in afternoon/ evening of a random day. The flow rates for the shower tap are based on a hot water temperature of 40 °C.

3.3 Reference tests

3.3.1 Positive reference test 40 °C

A first test was executed using a hot water production temperature of 40 °C, measured at the heat exchanger outlet (approx. 38 °C at the shower tap). The first goal of this test was to ensure *L. pneumophila* was able to grow in the HWL and BFMs using a

dynamic situation with periods of warming (during hot water use), cooling down and periods of standstill after cooling down. The heat exchanger was continuously maintained at production temperature. The second goal of this test was the comparison of the growth results in the HWL and the BFMs. The total test duration was 32 weeks, from which 8 weeks were used to cultivate a mature biofilm for potential growth of *L. pneumophila.* After 8 weeks *L. pneumophila* was dosed once to the system (see paragraph 3.4). At first instance shower pattern I was applied for a duration of 14 weeks. After this period the test was continued for 18 weeks while using shower pattern II (see paragraph 3.2 and Discussion part).

3.3.2 Negative reference test 60 °C

A second test was executed to compare the results for the HWL and BFMs using a hot water production temperature of 60 °C, measured at the heat exchanger outlet (approx. 58 °C at the shower tap). The heat exchanger was continuously maintained at production temperature. The goal of this test was the comparison of the growth results in the HWL and the BFMs. The total test duration was 20 weeks, from which 8 weeks were used to cultivate a mature biofilm for potential growth of *L. pneumophila.* In this period, the production temperature was first kept at 40 °C. Since *L. pneumophila* was already present in the system (due to dosing in the positive reference test), dosing *L. pneumophila* was not necessary. After the initial period for biofilm growth the hot water production temperature was carefully increased step by step within one week from 40 °C to 60 °C. After a production temperature of 60 °C was reached, the test was continued for 12 weeks. The shower pattern II was applied during this test.

3.4 Dosing and sampling of *Legionella*

To study *Legionella* growth in the test setup, *Legionella* was actively dosed. The dosed mix of *L. pneumophila* consisted of four strains/ types: *L. pneumophila* SG 1 ST 1, *L. pneumophila* SG 1 ST 47, *L. pneumophila* SG 1 ST 62 and *L. pneumophila* SG 3.

The total initial concentration of the dosed *L. pneumophila* was 2×10^3 cfu/l (measured at the HWL shower tap). This concentration is based on *Legionella* numbers found in practice in Dutch DWIs. Directly after dosing the tapping pattern was paused for approximately 8 hours to enable the *L. pneumophila* to enter the biofilm. After this standstill period the tapping pattern was restarted, and the system was sampled every 1-2 week(s) by taking

- water samples (5 x 500 ml) from the HWL shower tap;
- biofilm samples from PE-Al-PE, copper and PVC-P BFMs, and PE-Al-PE coupons from the HWL.

The grey line in Figure 2 gives an indication of the position of the five water samples taken at the HWL shower tap. Since less coupons ware available within the HWL (max. 3-4 per test), biofilm samples from the HWL ware taken in lower frequency equally divided over time during the experiments. All samples were analysed for ATP (conform NEN-EN-ISO 16421.2015) and cultivable *Legionella* (conform NEN-EN-ISO 11731.2017), followed by DNA-isolation/ qPCR of *Acanthamoeba* spp en *Vermamoeba vermiformis*.

4 Results

4.1.1 Positive reference test 40 °C

In Figure 4 the results for *L. pneumophila* numbers are shown measured in water samples taken from the shower tap in the HWL. The black line at day 120 marks the change from shower pattern I to pattern II. The results for *L. pneumophila* in the water samples vary quite over time, although samples were taken on the same day every week. Further analysis of the data showed that the time between moment of sampling and the last hot water demand (before sampling) was not constant during the test and varied between 2-16 hours. This difference correlates with the variation in Figure 4. The sudden increase in numbers for *L. pneumophila* at day 132 is probably caused by unintentional coincidence between the moment of sampling and actual hot water demand. As a result, all the water sampled came from the heat exchanger or from upstream of the heat exchanger, where numbers for *L. pneumophila* were higher dan downstream of the heat exchanger.

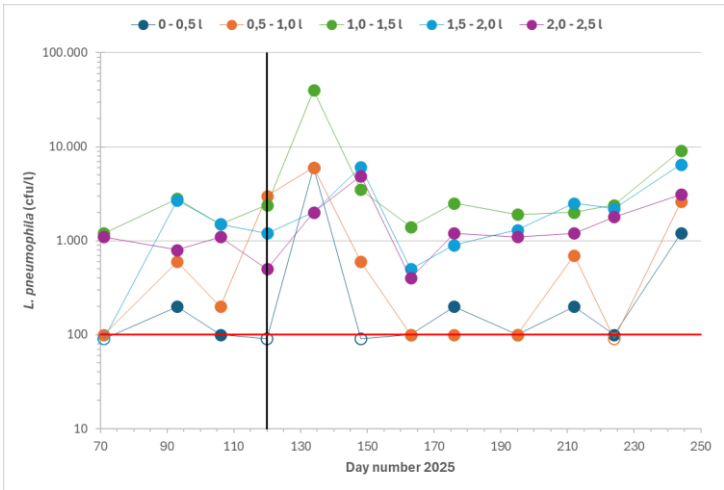

Figure 4. Concentrations of *L. pneumophila* in water samples taken from the shower tap of the HWL. The different colours show the results for the consecutive samples (5 x 500 ml). The red line shows the detection limit.

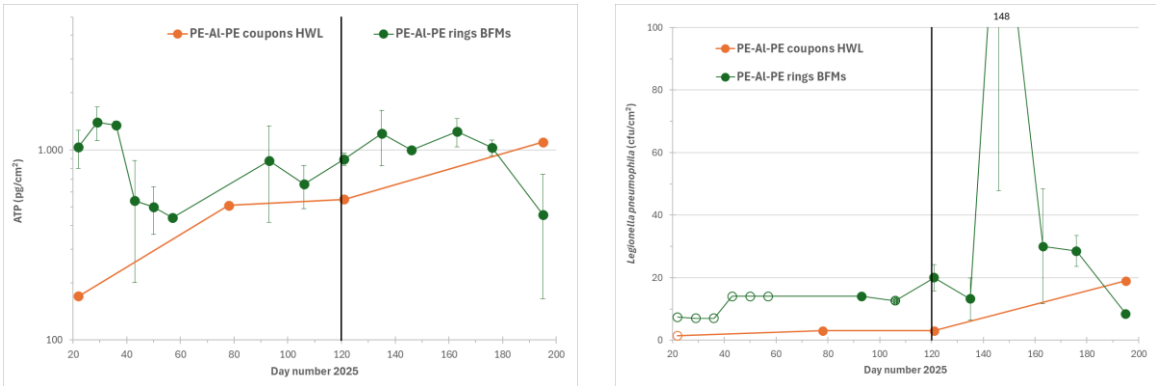

Figure 5. Left: ATP-concentration measured on PE-Al-PE coupons from the HWL (orange) and PE-Al-PE rings from the BFM (green).
Right: Concentrations of *L. pneumophila* analysed from the biofilm on PE-Al-PE coupons of the HWL (orange) and PE-Al-PE rings from the BFM (green).
Open marker = below detection limit

Figure 5 shows the ATP values and numbers for *L. pneumophila* in the PE-Al-PE rings from the BFM and the coupons from the HWL. It is likely that the higher variation in the BFM values is caused by the smaller area of the BFM rings (compared to the HWL coupons) over which the measured ATP-values and *L. pneumophila* numbers are arithmetically distributed.

4.1.2 Negative reference test 60 °C

In Figure 6 the results for *L. pneumophila* numbers are shown measured in water samples taken from the shower tap in the HWL during the 60 °C test. The grey area marks the days wherein the hot water production temperature was stepwise increased from 40 °C to 60 °C.

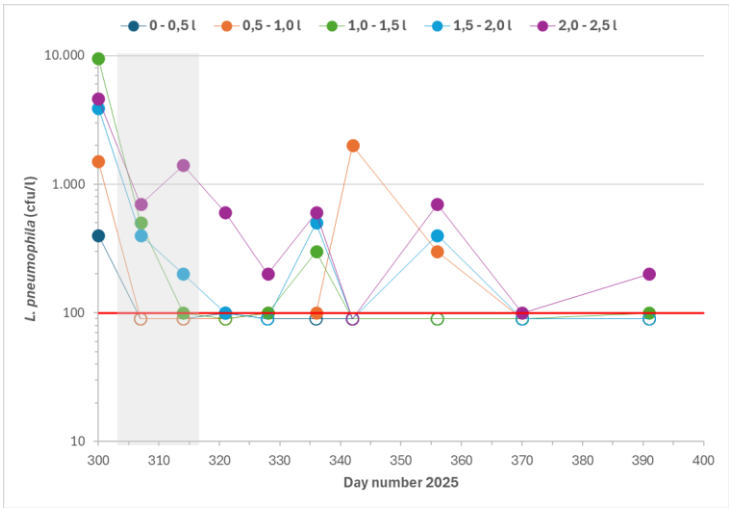

Figure 6. Concentrations of *L. pneumophila* in water samples taken from the shower tap of the HWL. The different colours show the results for the consecutive samples (5 x 500 ml). The red line shows the detection limit. The day number (x-axis) represents cumulative experimental days (spanning into 2026).

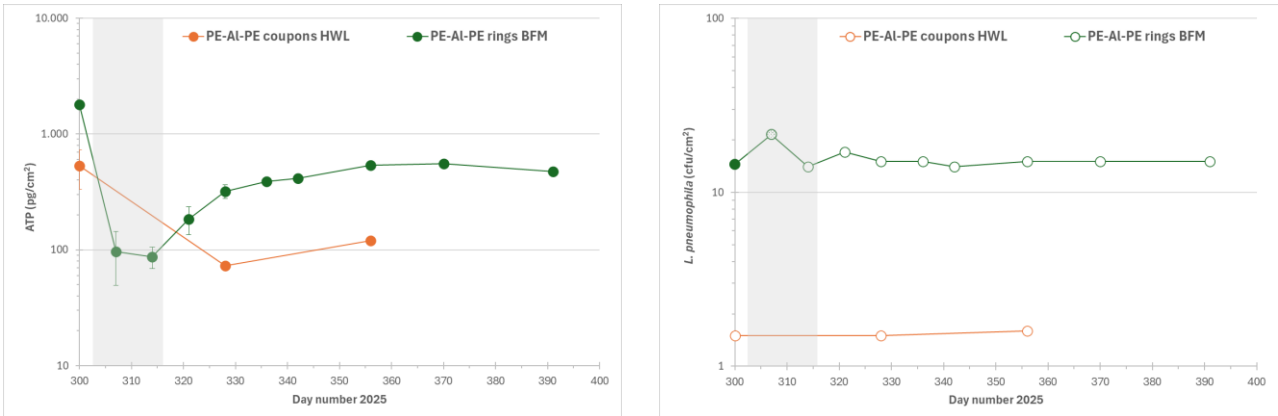

Figure 7. Left: ATP-concentration measured on PE-Al-PE coupons from the HWL (orange) and PE-Al-PE rings from the BFM (green).
Right: Concentrations of *L. pneumophila* analysed from the biofilm on PE-Al-PE coupons of the HWL (orange) and PE-Al-PE rings from the BFM (green). Open marker = below detection limit. The day number (x-axis) represents cumulative experimental days (spanning into 2026).

As expected, numbers for *L. pneumophila* decreased to numbers under detection limit. There was one exception: the fifth sample (2,0 – 2,5 l from shower tap) remained consequently positive for *L. pneumophila*. As can be seen from the test setup scheme (Figure 2), this sample comes from upstream the heat exchanger, where there is no hot water to kill the *Legionella* (see also the Discussion part).

Figure 7 shows the ATP values and numbers for *L. pneumophila* in the PE-Al-PE rings from the BFM and the coupons from the HWL. The differences in ATP-values for the HWL and BFM are higher during the 60 °C test compared to the differences during the 40 °C experiment.

5 Discussion

5.1.1 Positive reference test 40 °C

The primary objective of the study is to develop a protocol for testing LT water heaters for *Legionella* safety. This requires a system capable of simulating the hot-water component of a DWI, in which *L. pneumophila* can multiply when conditions are favorable. This initial test was therefore conducted to determine whether *L. pneumophila* can multiply in the HWL and BFMs when the hot water temperature is 40°C. When using shower pattern I (see paragraph 3.2) the numbers of *L. pneumophila* in the biofilm were very low and usually below the detection limit (Figure 5), despite the presence of a biofilm concentration above 400 pg ATP/cm² and the presence of host protozoa on the PVC-P rings (positive control) and PE-Al-PE rings in the BFMs and on the coupons of the HWL. Previous research has shown that when biofilm concentrations exceed 400 pg ATP/cm² and host protozoa are present, *L. pneumophila* is capable of multiplying if the temperature is within the growth range of *L. pneumophila* (van der Wielen et al., 2021, 2023). This means that the growth of *L. pneumophila* was inhibited by a factor other than the presence of sufficient biofilm and host protozoa. Analysis of the water samples showed that the water coming from the heat exchanger always tested positive for relatively high numbers of *L. pneumophila* (Figure 4). A key difference between the heat exchanger and the HWL/ BFMs is that the heat exchanger was constantly maintained at 40°C, an ideal temperature for *L. pneumophila* to multiply. It is therefore highly likely that *L. pneumophila* in the biofilm on the heat exchanger, which we cannot sample, is able to multiply to high numbers. However, *L. pneumophila* was unable to develop to measurable numbers in the biofilm in the HWL/ BFMs, as the period during which the temperature was within the range in which *L. pneumophila* can multiply was too short. For this reason, the shower tap pattern was adjusted halfway through the experiment, with more frequent showering (see paragraph 3.2) so that the hot water temperature in the HWL/ BFMs remained within the growth range of *L. pneumophila* for a longer period. Following the adjustment of the tap-off pattern, *L. pneumophila* numbers above the detection limit were found at all measurement times in the biofilm on the coupons in the HWL and on the PVC-P and PE-Al-PE rings of the BFMs (Figure 5). Both the HWL and the BFMs, in combination with shower pattern II, therefore provide a test setup in which the growth of *L. pneumophila* can be determined for LT water heaters.

5.1.2 Negative reference test 60 °C

To reach the primary objective of the study (test protocol) it was also necessary to assess whether *L. pneumophila* dies off when the hot water temperature reaches 60°C. A second test was therefore carried out at 60°C to determine whether *L. pneumophila* in the HWL and BFMs dies off at that temperature and is no longer detected. However, the ATP concentrations in the biofilm taken from the HWL coupons were significantly lower than those on the PE-Al-PE rings in the BFM (Figure 7). It is not clear what caused this difference, as the same batch of materials (PE-Al-PE) was used in both the HWL and the BFM). As the PE-Al-PE rings in the biofilm monitor resulted in higher ATP concentrations, the biofilm monitor can be regarded as a worst-case scenario for biofilm formation at 60°C. The advantage of this is that, at the biofilm concentrations found, *L. pneumophila* is still capable of multiplying if conditions are favourable, whereas at the low ATP concentrations of the biofilm in the HWL, *L. pneumophila* is unable to survive even when conditions are favourable. In that case, it is therefore more difficult to investigate whether a LT hot water system enables regrowth of *L. pneumophila* or whether growth is prevented because the biofilm concentration is too low. Based on the results of this second test, the biofilm monitor therefore appears to be a good alternative to the HWL for investigating biofilm growth and the growth of *L. pneumophila* when the drinking water temperature is 60°C.

A striking result of the 60°C experiment was that the water sampled from the HWL remained positive for *L. pneumophila*, particularly the fifth 500 ml sample from the shower tap (Figure 6). This water originates from upstream of the heat exchanger (Figure 2) and therefore does not come into contact with the 60°C hot water. It came out that upstream of the heat exchanger a hotspot occurred in the cold water pipe between the pump and the heat exchanger. This hotspot arose because of heat conduction through the stainless steel material of the cold water pipe. This heat was generated from the heat exchanger, because the temperature in the heat exchanger was maintained continuously at hot water production temperature. This results unavoidable in a hotspot (with favourable temperatures for growth of *L. pneumophila*) at a certain distance upstream from the heat exchanger. These *L. pneumophila* bacteria will enter the water from the biofilm and are not sufficiently killed when this water flows through the heat exchanger and the DWI during hot water use. Incidentally, the results do show that, with the shower pattern II used, a temperature of 60°C was sufficient to kill *L. pneumophila* in the distal section of the HWL. However, it also shows that if there is a hotspot within the system where temperatures are favourable for the proliferation of *L. pneumophila*, this can lead to *L. pneumophila* numbers in DWI exceeding the Dutch legal limit of 100 cfu/l.

6 Conclusion

The positive reference tests show clearly that *L. pneumophila* was able to grow in the test setup. The negative reference test show that *L. pneumophila* present in the system died off during the time that hot water with 60°C was distributed in the HWL and BFM. The results for the HWL and BFM monsters (both for water and biofilm) are in the same order of magnitude. The BFMs show slightly higher values for ATP compared with the values measured in the HWL. It was therefore concluded that the BFM could be used as a sufficient representation of the DWI-pipes between the water heater and the shower tap to enable further tests of LT hot water in the DWI (see next paragraph).

7 Future work

As part of the "ProVe IT-LT" project, a test protocol was developed to assess the *Legionella* safety of LT water heaters. The unexpected growth of *L. pneumophila* in the upstream cold water pipe is a 'lesson learned by coincidence' and points out the necessity of very accurate temperature control for LT hot water in the DWI since LT hot water systems have no capability of killing *L. pneumophila* by thermal disinfection. It is expected that *Legionella* safe LT hot water systems will only be technically feasible when the hot water section of the DWI (both production and distribution) cools down to ambient temperature (~ 20 °C) after every hot water draft. During this study several technical and practical challenges to the large-scale rollout of LT water heaters were identified. For instance, the developed test protocol assumes a situation where a residential installation meets all requirements of Dutch building norms (i.e. NEN 1006), such as the prevention of hotspots. However, practical experience shows that hotspots can still occur, posing a public health risk when implementing LT water heaters. Furthermore, the use of LT water heaters significantly reduces the mixing of cold water at (particularly) the shower tap. As a result, with LT hot water, the flow rate in some cold-water pipes within an existing DWI is lower, which can cause water quality issues (e.g., increased microbial growth, odor/taste complaints). A phase II for the ProVe IT-LT project is in development to assess two types of LT water heaters and to study the boundaries in practice for the application of LT hot water in DWI, in particular for existing buildings.

Acknowledgements

This research was funded by the Top Consortia for Knowledge and Innovation (TKI) Grant from the Dutch Ministry of Economic Affairs and financial contributions of Waternet, Eneco and Ennatuurlijk. The authors also want to thank all the contributors, in particular the participants from Eneco and Fortes Energy Systems, who supported this study by sharing their expert knowledge and field experience.

References

Blokker, E.J.M. et. al. (2017), Using a stochastic demand model to design cold and hot water installations inside buildings, CIBW062 Symposium 2017, Haarlem.

Moerman, A., *et al.* (2015), Efficiënte bereiding warm tapwater in woningen, BTO 2015.006, KWR, Nieuwegein, https://library.kwrwater.nl/publication/53699348/.

Moerman, A. and Oesterholt, F. (2023), Impact of domestic hot water safety advices on energy consumption and the energy transition in The Netherlands, CIBW062 Symposium 2023, Leuven.

NEN 1006 (2018), Algemene voorschriften voor leidingwaterinstallaties, NEN, Delft,

Van der Wielen, et. al. (2021), Met recht naar een doeltreffender legionellapreventie, Berenschot & KWR, Utrecht, https://www.rijksoverheid.nl/documenten/rapporten/2021/11/16/bijlage-1-rapport-met-recht-naar-een-doeltreffende-legionellapreventie.

Van der Wielen, P. and Oesterholt, F. (2023), Legionella legislation for drinking water in the Netherlands revisited, CIBW062 Symposium 2023, Leuven.

Presentation of Authors

Andreas Moerman MSc is a senior researcher/ project manager in the Energy & Circular Systems team at KWR Water Research. His expertise is modelling and analysis in several domains in the energy-water-nexus, like aquathermal energy, (domestic) hot water and impact of the energy transition on (drinking) water systems.

Frank Oesterholt MSc is a chemical engineer and senior researcher/ project manager in the Energy & Circular Systems team at KWR Water Research. He is expert in the field of legionella prevention, mainly focused on risk assessment and legionella management for tap water installations, cooling water systems and wastewater treatment plants.

Amitosh Dash PhD is a scientific researcher in the Water Infrastructure team at KWR Water Research Institute. His work focuses on understanding water quality transitions during drinking water supply and on assessing the condition of water distribution materials and assets.

Paul van der Wielen Prof, PhD is principal scientist, working in the field of microbial ecology in water systems and specialized in the microbial ecology and growth of *L. pneumophila* in man-made water systems.

Temperature-dependent *Legionella* growth for water changes in drinking water systems

Rolf Weiss (1), Arnd Gildemeister (2)

(1) rolf.weiss@geberit.com
(2) arnd.gildemeister@geberit.com

(1) & (2) Geberit International AG, Jona, Switzerland

Abstract

Legionella bacteria pose a significant hygiene risk in drinking water installations, especially in countries without residual chlorine in the tapping water, which is why technical guidelines typically require cold water temperatures to be kept below 25°C and hot water temperatures above 55°C. The microbiological basis for this temperature behaviour was investigated in the study "The *Legionella* Lqs-LvbR regulatory network controls temperature-dependent growth onset and bacterial cell density" by Hochstrasser and Hilbi (University of Zurich), which shows in detail how different strains of *Legionella* grow depending on temperature and nutrient availability.

This paper systematically transfers the biological findings of the scientific study into applied sanitary engineering.

Based on the doubling times determined in the study, a temperature-dependent water exchange diagram is derived that clearly illustrates how strongly *Legionella* bacteria increase their growth rate between 25°C and their preferred temperature zone. In addition, the paper links these findings with research results presented at CIB conferences, which confirm that regular water changes are an effective measure for controlling *Legionella* bacteria.

The conclusions provide a new basis for future test series, for the evaluation of existing installations, and for the development of further guidelines for the hygienically safe design of drinking water systems.

Keywords

Legionella, hygiene risk, water exchange, growth temperature, flushing interval

1 Introduction

Legionella pneumophila is considered one of the most relevant opportunistic pathogens in drinking water installations of buildings. Inhalation of aerosols containing *Legionella* can lead to Legionnaires' disease, an often severe and potentially fatal form of pneumonia. For this reason, national and international technical guidelines have defined temperature requirements as a central preventive hygiene measure for decades. Typical specifications require cold water to be kept below 25 °C at all times, while hot water systems should have temperatures above 55 °C.

These temperature limits are established in practice and are routinely applied in standards, regulations and hygiene recommendations ([1][2]). However, their microbiological justification is often based on simplified assumptions, historical empirical values or qualitative growth curves in absence of quantitative data on the growth rate of *Legionella*.

Against this background, the question of the growth of *Legionella* as a function of temperature is of central importance. In particular, the question arises as to whether existing, static limit values and fixed flushing intervals reflect the microbiological risk in a sufficiently differentiated way or whether a more temperature-dependent consideration is necessary.

Recent microbiological research at the University of Zurich [4] provides reliable quantitative data for the first time. In these studies, temperature-dependent growth rates of different *Legionella* strains were systematically investigated. This opens up the possibility of transferring microbiological findings into engineering evaluation and design concepts.

The aim of this technical paper is to systematically transfer these scientific results to applied sanitary technology. The focus is on the development of a temperature-dependent flushing interval model for drinking water systems.

2 Scientific background: temperature-dependent *Legionella* growth

The microbiological basis of this paper is the study "The *Legionella* Lqs-LvbR regulatory network controls temperature-dependent growth onset and bacterial cell density", which was conducted by Hochstrasser and Hilbi at the University of Zurich and published in 2022 [4]. In this study, the temperature-dependent growth behaviour of *Legionella pneumophila* was investigated in detail under controlled laboratory conditions.

As part of the experiments, various *Legionella* strains were analysed, including well-characterized reference strains such as JR32, as well as clinical and environmental isolates. The investigations were carried out on two different culture media:

- AYE medium, which represents nutrient-rich conditions, and
- MDM medium, which depicts nutrient-poor conditions and thus comes closer to the conditions in drinking water but still has significantly higher nutrient values.

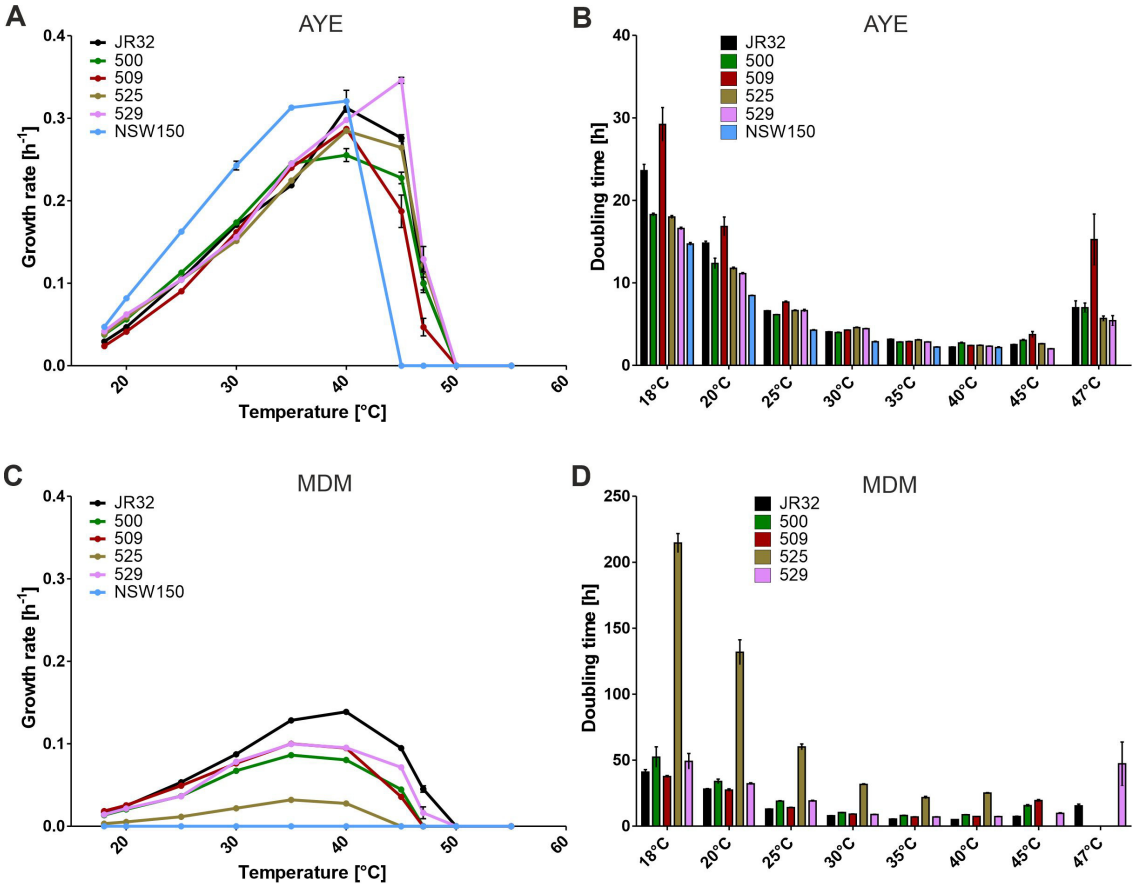

Figure 1: A) Temperature-dependent growth rate [h^{-1}] of the different Legionella strains in the AYE medium, B) Temperature-dependent doubling times [h] in the AYE medium, C) Temperature-dependent growth rate [h^{-1}] of the different Legionella strains in the MDM medium, D) Temperature-dependent doubling times [h] in the MDM medium. The source of the diagram is [4].

For each combination of strain, medium and temperature, the respective doubling time was determined (see Figure 1 B) & D)). This is the time it takes for the number of bacteria to double and thus represents a direct quantitative measure of the growth rate.

The results show that at temperatures in the range of optimal growth – typically around 37 °C – doubling times of about 3 to 6 hours occur, depending on the strain and medium. As the temperature decreases, the growth rate decreases significantly.

It is noteworthy that no measurable growth was detected at temperatures of 50 °C and above, even under nutrient-rich conditions. This temperature thus seems to represent an upper limit for the proliferation of *Legionella*.

The study conditions in the laboratory were specifically selected to be well controllable and very favourable for *Legionella* growth. These include nutrient-rich media and the

absence of competing microorganisms. In this study extracellular growth was observed, whereas in drinking water systems *Legionella* growth often occurs by parasitizing amoebae. We assume that this has no material impact on the temperature-dependence of growth rates, however. The measured growth rates can therefore be interpreted as conservative worst-case scenarios when transferred to real drinking water installations.

3 Transferability of laboratory results to drinking water systems

Laboratory tests offer the great advantage of being able to isolate and vary individual influencing factors such as temperature, nutrient availability or bacterial strain in a controlled manner. This enables reproducible measurements of growth velocity and provides quantitative results that are essential for engineering modelling. Laboratory studies are therefore of great significance.

At the same time, real drinking water systems differ from laboratory environments in several ways. The concentration of available nutrients in drinking water is usually significantly lower, hydraulic conditions are changeable, and the microbial community consists of many organisms. In addition, the starting concentration of *Legionella* after a water exchange is almost always unknown in practice.

For a technical assessment, it is therefore necessary to explicitly take these differences into account. In this article, a conservative approach is deliberately chosen: The doubling times determined in the laboratory under favourable conditions are adopted unchanged, and the resulting growth predictions are interpreted as an upper estimate. This ensures that the derived technical recommendations offer sufficient hygiene safety even under real conditions.

Another central point is the question of the comparability of different *Legionella* strains and culture media. The evaluation of the experimental data shows that although the absolute growth rates differ, the basic temperature-dependent course is very similar (see Figure 1). This allows to develop generic, temperature-dependent models that are not limited to a single strain or a specific medium or nutrient concentration.

In summary, it can be said that the transfer of laboratory results to practice is sensible, provided that the limits of comparability are made transparent and conservative assumptions are made. Under these conditions, the available microbiological data provide a reliable basis for the engineering derivation of rinsing intervals, temperature limits and operating strategies.

4 Derivation of a temperature-dependent flushing interval model

4.1 Initial situation: "Conventional" limit values and motivation

Several technical regulations and guidelines specify a critical cold water temperature of 25 °C and a maximum water stagnation or a maximum flushing interval of 72 h (3 d) as hygienic boundary conditions [1][2][3].

These two points are used for automated hygienic flushing in the drinking water sector. A programmed algorithm flushes the cold water pipes at least every 72 hours and when the temperatures of the cold water rise above 25 °C, additional flushes are triggered. The corresponding flushing pattern is shown in Figure 2 .

Several studies have shown that regular water exchange can substantially reduce *Legionella* concentrations [5][6]. However, study [5] also indicates that simply replacing the pipe contents once is not sufficient to achieve a meaningful reduction. This is consistent with an internal Computational Fluid Dynamics study carried out at Geberit, which suggests that achieving a 99.99% water exchange requires flushing approximately twice the pipe volume under turbulent flow conditions (Reynolds number > 2300). Under laminar flow, complete replacement of the pipe contents is theoretically not achievable.

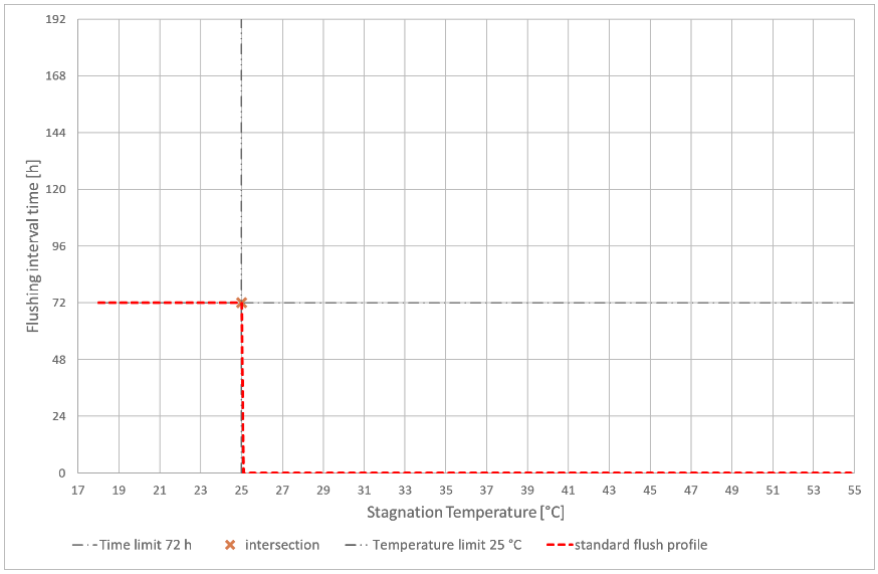

Figure 2: Standard flush profile for automated flushing devices. The automated hygienic flush is triggered after 72 hours at the latest, or if a temperature in the cold water of over 25 °C is measured.

In the absence of quantitative *Legionella* growth data, it is usually recommended to avoid temperatures between 25 °C and 55 °C by all means. Some even propose to use active cooling to achieve this. The central new idea here is to replace this static view with a temperature-dependent model based on the measurement data of the University of Zurich [4] on the growth speed (doubling time) (see Figure 3).

To do so, the key assumption is that at 25 °C flushing intervals of 72 h are sufficient to maintain low-enough *Legionella* concentrations, i.e. that current standards do offer good hygienic protection.

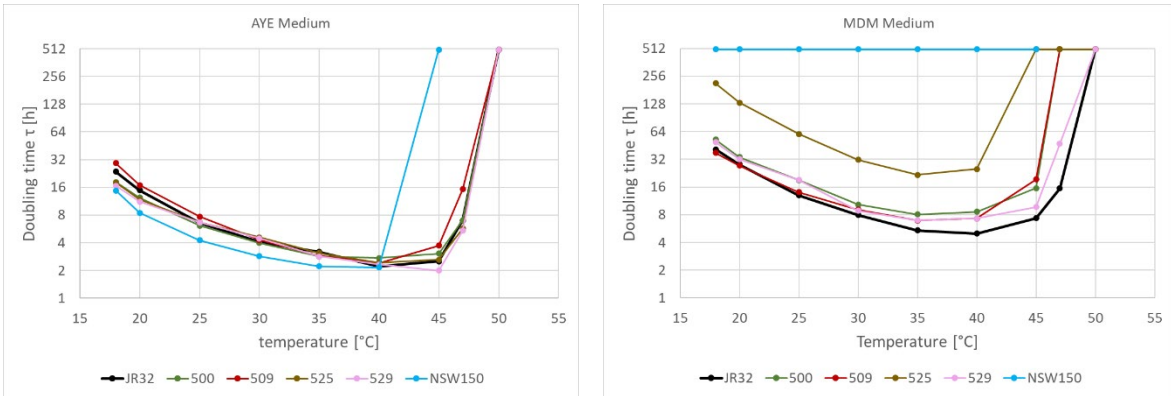

Figure 3: Doubling time as a function of temperature in a logarithmic scale for AYE and MDM medium.

4.2 Model assumption

Growth as measured in "doubling time" as a function of temperature is used to derive a flushing interval as a function of temperature.

For technical modelling, *Legionella* growth is described as exponential (doubling process) in the first approximation. In this diagram, the doubling time τ(T) as a function of temperature is used as a parameter taken directly from the measurement data.

The formula for the calculation is:

Equation 1

$$\boldsymbol{N(t) = N_0 \cdot 2^{t/\tau(T)}}$$

with

$N(t) = Legionella\ concentration\ \ at\ time\ t,$

$N_0 = starting\ concentration\ after\ water\ exchange$

$\tau(T) = doubling\ time\ at\ temperature\ T$

Whereby $\tau(T)$ is known from [4].

4.3 Calibration at the reference point 25 °C / 72 h

It can be assumed that if the boundary conditions of 25 °C and 72 h are observed, the *Legionella* concentration will reach the maximum permitted limit but will not exceed it.

By inserting the following values into Equation 1, a specific value for N_0 can be calculated.

The following general values are used:

- Maximum flushing interval: $t = 72\ h$
- "critical" temperature: $T = 25\ °C$
- Limit of *Legionella* concentration: $N_{lim} = 1000\ CFU/L$

And for each *Legionella* strain and medium examined (basis [4]):

- Doubling time (JR32, MDM): $\tau_{25°C} = 12.98\ h$

Equation 2

$$N_{0_{JR32\ MDM}} = \frac{N_{lim}}{2^{t/\tau(T)}} = \frac{1000\ CFU/L}{2^{72h/12.98h}} = 21.4\ CFU/L$$

The interpretation in the sense of modelling means: After a complete water exchange, it is conservatively assumed that the *Legionella* concentration corresponds at most to this calibrated starting concentration.

4.4 Derivation of the flush interval function t(T) and standardization

The ratio of N_{lim} and N_0 can be used in the following Equation 3, which is a conversion of Equation 1, to calculate the exchange time as a function of the temperature and the corresponding doubling time. t

Equation 3

$$t = log_2\left[\frac{N_{lim}}{N_0}\right] \cdot \tau(T)$$

If you calculate all times for the existing doubling times, you get a function $t(T)$. This is a flush interval function for JR32 in the MDM medium, which is shown in Figure 4.

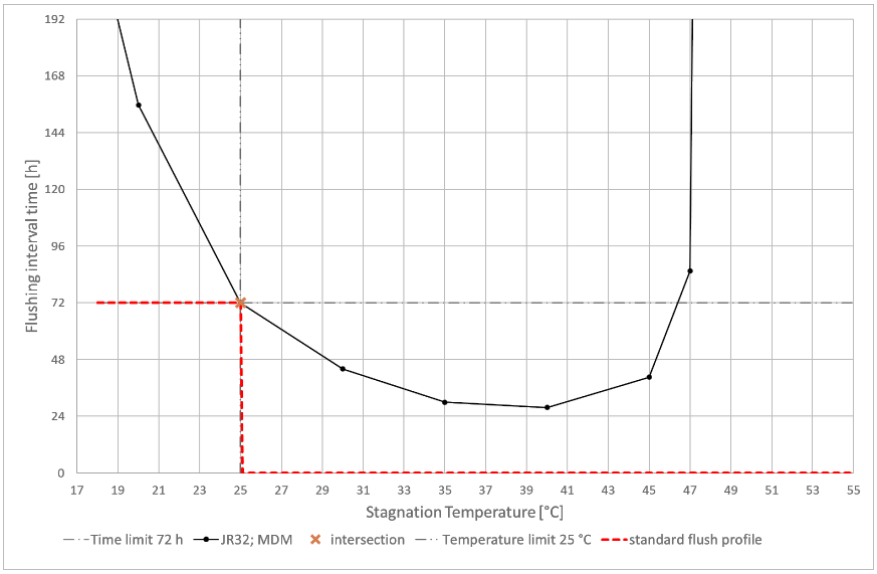

Figure 4: Flush interval curve for JR32 in MDM medium vs. standard flush interval curve.

The interpretation of this curve is that, for example, at a temperature of 30 °C, flushing is sufficient to occur every 44 hours in order to not increase the risk of *Legionella* growth compared to the 25 °C/72 h-point. This fits with one of the conclusions of the research project [5], which states that short-term temperature increases are generally tolerable.

If this procedure is now carried out and plotted for all in the publication [4] examined combinations of *Legionella* strains and media, the image in Figure 5 is obtained.

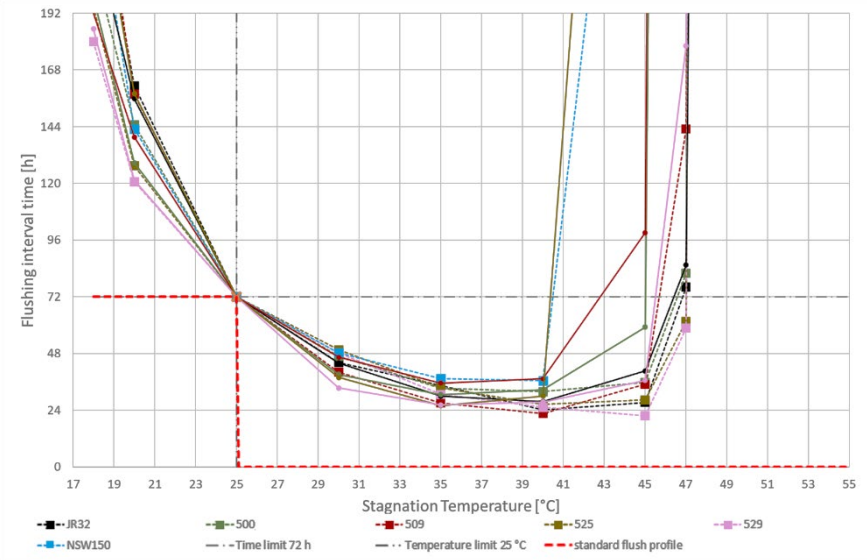

Figure 5: Flush interval curves for all Legionella strains in all media compared to the standard flush interval curve.

Figure 5 suggests that the resulting functions are similar, "almost independently" of the medium and strain.

If you then plot an envelope curve based on the lowest “flushing interval time” values, you obtain a conservative, generally applicable flushing curve for drinking water installations.

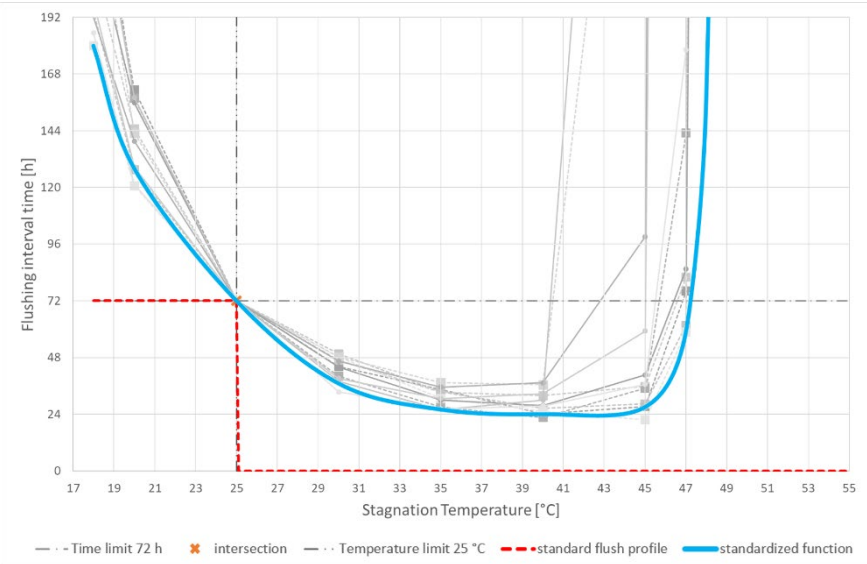

Figure 6: Generally valid standardized flushing curve (envelope curve based on lowest flushing interval times)

The standardized flush interval function shown in Figure 6 is independent of:

- *Legionella* strain
- Nutrient Medium
- *Legionella* concentration limit

The practical significance of this statement is high: it implies that a robust, transferable recommendation for flushing intervals can be derived from the temperature-dependent doubling times, independent of the initial concentrations, limit values or the exact strain of *Legionella*.

4.5 Interpretation for practice and reference to standards

As a conclusion for practice, it can be formulated that temperature-dependent flushing intervals can be calculated and that the temperature range between 25 °C and 55 °C may be less problematic than previously assumed – provided that flushing is carried out at the appropriate intervals. This means that by reducing the flushing interval by a factor of 3 (72 h to 24 h), it should be possible to keep *Legionella* growth below the limit value even in the most critical temperature range, provided that the water exchange is sufficient (≥ 2x pipe volume, in turbulent flow).

Thus, the model represents a bridge between established fixed hygiene limits (72 h flushing interval, absolute avoidance of the temperature range 25 °C and 55°C) and a physical-biological interpretation via temperature-dependent growth kinetics.

5 Observation of the 50 °C limit

The measurement results of the University of Zurich show a pronounced temperature dependence of the growth of *Legionella*. In particular, growth comes to a complete standstill at high temperatures. In the diagram of the growth rate as a function of temperature (see Figure 1 A) & C)) it can be explicitly seen that no growth could be measured above 50 °C.

This temperature threshold fits well with the regulatory requirements [1][2], which require a water temperature of 60 °C at the outlet of the hot water heater in a circulation pipe and 55 °C in the return line.

The 50 °C-limit is not an automatic reduction recommendation, but a scientifically based orientation for a possible future, more differentiated view of hot water temperatures, if one keeps system homogeneity, safety margins and monitoring in mind. These limitations are important, because the laboratory results also show that growth increases rapidly if the temperature drops below the mentioned threshold.

6 Discussion and implications for regulations and practice

6.1 Classification of the results in the context of existing limit values

In existing regulations, two operational boundary conditions are typically used side by side: a critical cold water temperature of 25 °C and a maximum water exchange/flush interval of 72 h. These two limits are explicitly combined in the presentation as "two limits described in different standards" and serve as a starting point for deriving a "conventional" flushing interval curve.

The available temperature-dependent growth data make it possible for the first time to supplement this static view with a biologically based time-temperature relationship.

6.2 Temperature-dependent flushing intervals as a further development of existing specifications

From the measurement data of the University of Zurich, a temperature-dependent flushing interval function can be derived, and as a second conclusion it can be formulated that the temperature range between 25 °C and 55 °C may be less problematic than previously assumed, provided that flushing is carried out at the correct intervals; this raises the question of whether the flushing intervals required by standards should be temperature-dependent.

As a point of discussion for standardization, this does not necessarily result in the immediate change of a limit value, but the possibility of supplementing existing specifications (25 °C and 72 h) with a model-based, temperature-dependent recommendation system, especially where temperature situations in the building cannot be ideally maintained (e.g. seasonal heat load, edge zones, low use).

6.3 Implications of the 50 °C limit for hot water temperature requirements

Another finding is that no *Legionella* growth was observed above 50 °C, even at high nutrient concentrations.

This finding should not carelessly be seen as an invitation to lower warm water temperatures, however. Two reasons to be careful stand out: Today's typical limit of 55 °C is not much higher and in practice temperatures may already be lower as they are challenging to control precisely in complex installations. And while the study shows no growth at 50 °C, this does not mean that *Legionella* immediately start to die at this temperature either and may again start to multiply if temperature falls. Another study [7] shows that only at 60 °C *Legionella* will quickly go into a state that prevents growth even upon lowering the temperature again.

6.4 Limits of transferability and need for further research

Further measurements and further research are needed, especially about additional influencing variables besides nutrient concentrations, temperature and time (e.g. oxygen, kind of nutrients offered, other environmental conditions).

This results in the following points for the scientific and technical development of the approach:

- Comparison of the model-based flushing interval functions with measurement data from real installations (temperature profiles, usage profiles, microbiological findings).
- Mapping of other growth and limitation factors: Consideration of situations in which nutrient limitation or ecological interactions can suppress growth.
- Systemic consideration: Interaction of temperature maintenance, flushing strategy, pipe routing and thermal coupling (e.g. PWH/PWC interaction) to derive robustly implementable recommendations.

7 Summary

On the basis of the summarized measurement results of Hochstrasser and Hilbi [4] and the technical interpretation derived from them, the central conclusion is a proposed temperature-dependent flushing interval instead of fixed time limits.

From the measurements, a temperature-dependent flushing interval can be calculated, which is independent of the *Legionella* strain, nutrient occurrence and limit value. This shows that the temperature range between 25 °C and 55 °C may be less problematic than previously assumed, provided that the correct (temperature-adjusted) intervals are used.

Also, above 50 °C, even at high nutrient concentrations, no growth of *Legionella* was observed.

8 Outlook

The conclusions presented provide a basis for technically refining existing recommendations; at the same time, it should be emphasized that further measurements, investigations and research are necessary in order to systematically take into account additional influencing factors beyond temperature and time and to confirm the applicability of the flushing curve.

9 References

[1] German Standard DIN 1988-200 Codes of practice for drinking water installations Part 200: Installation Type A (closed system), Berlin DE, Beuth Verlag, May 2012

[2] SVGW W3/E3 Richtlinie für Hygiene in Trinkwasserinstallationen, Zürich CH, SVGW, May 2020

[3] European Standard DIN EN 806-2 Specification for installations inside buildings conveying water for human consumption Part 2: Design. European Committee for Standardization, October 2024

[4] Hochstrasser R., Hilbi H., «The *Legionella* Lqs-LvbR Regulatory Network Controls Temperature-Dependent Growth Onset and Bacterial Cell Density", Applied and Environmental Microbiology 88(5): e0237021, March 2022

[5] DVGW, Abschlussbericht Forschungsprojekt W 201629 «Schutz des Trinkwassers: Anforderungen an den bestimmungsgemäßen Betrieb kaltgehender Trinkwasser-Installationen unter dem Gesichtspunkt der Vermehrung von Legionellen», Bonn, DVGW, July 2019

[6] Bartrand T., Guarin P., Cudahy M. «The impacts of velocity, pipe type, and use frequency on water quality», in CIB W062 International Symposium for Water Supply and Drainage for Buildings, Miami, 2025

[7] Schmid C., Hilbi H., «Rapid Icm/Dot T4SS inactivation prevents resuscitation of heat-induced VBNC *Legionella pneumophila* by amoebae", Environmental Microbiology 27(1): e70035, January 2025

10 Presentation of Authors

Rolf Weiss is the head of product development for piping systems at Geberit International AG in Jona, Switzerland, where he has been widely involved in research and development of sanitary equipment, drinking water systems, rain and wastewater drainage systems. He has expertise in hydraulics and CFD applications. One of his current research interests involves drinking water hygiene.

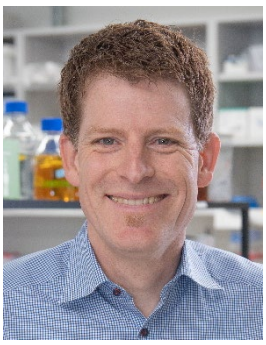

Dr. Arnd Gildemeister is the head of products for piping systems at Geberit International AG in Jona, Switzerland. Trained as a physicist, he takes a keen interest in hydraulics and drinking water hygiene, besides his managerial role.

Stagnation in Drinking Water Installations

The Role of Cold Water Circulation in Robust Hydraulic Design

O.F. Leever

onno@leever.nl

Leever installatie adviseurs B.V.

Abstract

In modern drinking water installations, stagnation is an important but often underestimated cause of reduced water quality. Increasing building insulation, higher ambient temperatures, and changing usage patterns make it more difficult to control cold water temperature. In practice, temperatures above 25 °C are regularly observed, potentially supporting microbiological growth.

Current design approaches mainly focus on temperature control and waiting times at tapping points. However, these parameters do not give enough insight into how the system really works. In particular, the amount and distribution of stagnation are rarely considered. This can lead to design problems, such as low water refresh in branch lines and poor circulation in parts of the system.

This paper introduces a system-based approach in which stagnation is treated as a key design factor. A distinction is made between stagnation in service lines, which is related to residence time and pipe volume, and stagnation at system level, which is related to flow distribution and circulation behaviour. For the system level, an assessment method is proposed based on stagnation degree and a Risk Indicator (RI). This makes it possible to evaluate how effective cold water circulation really is.

Based on practical observations and design evaluations, stagnation is shown to be a common feature in many installations, rather than an exception. Continuous circulation does not always ensure that all parts of the system are properly refreshed.

Cold water circulation can be used as a measure to reduce stagnation. However, its effectiveness strongly depends on the hydraulic design and balance of the system. This paper therefore proposes a shift towards robust design principles, in which stagnation is clearly addressed and controlled, to support future-proof drinking water installations.

This is particularly relevant in the context of climate change, where higher ambient temperatures further amplify the limitations of temperature-based control. (This does not imply that temperature control is unimportant. Temperature remains an essential operational parameter, but should be interpreted in relation to hydraulic system behavior and stagnation dynamics).

Keywords

Stagnation; Cold water circulation; Hydraulic behaviour; System performance; Legionella risk

1. Executive Summary

Drinking water systems are generally designed to comply with temperature requirements, peak demand calculations and existing design standards. Nevertheless, elevated temperatures and Legionella contamination are still regularly observed in practice. This suggests that current design methods do not fully describe the hydraulic behaviour of drinking water systems during normal operation.

This paper introduces **dynamic stagnation**, defined as insufficient hydraulic renewal caused not only by periods without water use, but also by prolonged low-flow conditions and unstable circulation during operation. The concept extends the traditional understanding of stagnation by explicitly including hydraulic conditions that may occur while a system is in use.

To evaluate these conditions, four engineering indicators are proposed:

- **Stagnation Degree (SG)**, describing the extent of hydraulic renewal;
- **Circulation Factor (CF)**, expressing the hydraulic robustness of circulation systems;
- **Risk Index (RI)**, representing the influence of environmental conditions;
- **System Score (SS)**, combining stagnation and environmental risk into a single comparative design indicator.

The methodology is demonstrated using representative building examples, including hotel rooms and marina facilities. These examples illustrate that water-saving measures may unintentionally increase stagnation unless hydraulic renewal is maintained. They also show that cold water circulation is beneficial only when it substantially reduces stagnation and remains hydraulically robust during operation.

The proposed methodology is intended as a **comparative engineering design tool**, not as a predictive microbiological model. It provides a structured framework for comparing design alternatives and identifying opportunities to improve hydraulic robustness. Further validation through field measurements and case studies is recommended.

2. Introduction

Drinking water systems are generally designed to comply with temperature requirements, hygiene regulations and peak demand calculations. Although these approaches have significantly improved drinking water safety, elevated temperatures and Legionella contamination are still observed in many compliant installations. This indicates that additional hydraulic mechanisms may influence water quality during normal operation.

Current design methods mainly evaluate temperature, water age and periods without water use. However, they often provide only limited insight into how water actually moves through a system during daily operation. In practice, drinking water systems operate under highly variable conditions, with long periods of low demand interrupted by relatively short periods of peak demand. As a result, hydraulic conditions may differ considerably from those assumed during conventional design calculations.

This paper introduces the concept of **dynamic stagnation**. Unlike traditional stagnation, which is associated with complete water standstill, dynamic stagnation also includes prolonged periods of low flow and unstable circulation during system operation. These hydraulic conditions may reduce effective water renewal while the installation is still in use.

To evaluate these effects, four engineering indicators are proposed:

- **Stagnation Degree (SG)**, describing hydraulic renewal;
- **Circulation Factor (CF)**, describing circulation robustness;
- **Risk Index (RI)**, representing environmental conditions;
- **System Score (SS)**, combining these parameters into a comparative engineering indicator.

The methodology is intended as a practical engineering design tool for comparing design alternatives and improving hydraulic robustness. It is not intended as a predictive microbiological model. The objective is to complement existing design methods by explicitly incorporating hydraulic behaviour into the assessment of drinking water installations.

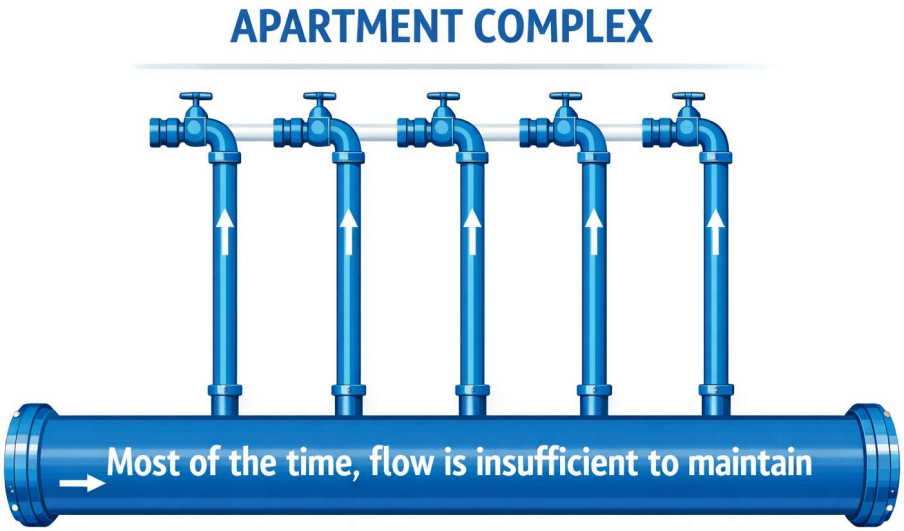

Figure 1 – Dynamic stagnation in building water systems
Under real operating conditions, flow is unevenly distributed and large parts of the system operate under prolonged low-flow conditions (< 0.2 m/s). These conditions may occur sequentially across different sections, resulting in cumulative stagnation and limited hydraulic renewal.
This illustrates a fundamental principle: the presence of flow does not guarantee effective system-wide renewal.

3. State of the Art: Design Approaches and Limitations

Current design practices for drinking water installations are primarily based on temperature control, flow rates, and waiting times at draw-off points. Existing standards and guidelines focus on limiting microbiological risks by controlling temperature and promoting water renewal, while stagnation is generally only implicitly addressed (NEN 1006, 2018; ISSO 55, 2023; ISSO 55.1, 2024; TVVL, 2020; TVVL, 2024; WHO, 2007; WHO, 2011). Within this approach, temperature is widely used as an indicator of water quality. For cold water systems, a limit value of 25 °C is commonly applied. However, research shows that this threshold is increasingly exceeded in practice due to climate change and rising ambient temperatures. Technical studies (e.g. ST46, ST51) demonstrate that circulation systems are hydraulically complex and highly dependent on flow distribution, system balance, and usage patterns. Flow conditions vary during operation, and the presence of a circulation pump does not guarantee effective flow in all parts of the system. Evaluations of Legionella prevention strategies

further indicate that measures such as flushing and thermal control do not consistently result in structural risk reduction. Their effectiveness depends strongly on overall system behaviour and is often difficult to guarantee in practice (Van der Wielen et al., 2021). At the same time, developments in modern buildings — including reduced water consumption, energy-efficient systems with limited circulation, compact pipe networks, and higher ambient temperatures — increase residence times and system sensitivity to stagnation.Despite these developments, stagnation is typically addressed only implicitly, for example through waiting time criteria or flushing recommendations, rather than being explicitly quantified as a design parameter. This reveals a fundamental gap: stagnation is recognized, but not explicitly modelled as a design parameter.

4. Objective of the Methodology

The methodology proposed in this paper introduces stagnation as an explicit and quantifiable design variable, enabling a system-based assessment of drinking water installations.

Stagnation is defined as the combined effect of:

absence of use

low-flow conditions

loss of circulation

Stagnation Degree

$SG = (t_{no_use} + t_{low} + t_{stop}) / t_{ref}$

Circulation Factor

$CF = t_{active} / t_{total}$

Corrected Stagnation

$SG_{corr} = SG / CF$

Risk Index

The risk index (RI) represents the influence of temperature and environmental conditions on microbiological risk. The Risk Index is intended as a comparative engineering indicator rather than an absolute microbiological parameter. It reflects the relative influence of ambient temperature and environmental exposure on stagnation-related risk.

System Score

$SS = SG_corr \times RI$

Effectiveness of Cold Water Circulation

$\Delta SS = (SS_without - SS_with) / SS_without$

The main variables used in the methodology are summarised in Table 1.

The methodology allows comparison between systems without circulation, with non-robust circulation, and with robust cold water circulation, based on a single integrated performance indicator.

The model is intended as a comparative design tool, not a predictive microbiological model.

Table 1: Definitions and Abbreviations

Abbreviation	Full term	Definition	Unit
SG	Stagnation Degree	Ratio between effective stagnation time and reference time.	-
CF	Circulation Factor	Fraction of time during which circulation is effectively maintained.	-
SG_corr	Corrected Stagnation Degree	Stagnation degree corrected for actual active circulation.	-
RI	Risk Index	Index representing thermal and environmental influence on microbiological risk.	-
SS	System Score	Combined indicator of stagnation and environmental risk.	-
ΔSS	Relative improvement	Relative reduction in system score due to application of cold water circulation (CWC).	%

The system score should be interpreted as a comparative indicator. Higher values indicate increased sensitivity to microbiological risk. The interpretation of the system score is given in Table 2.

Table 2: Interpretation of the System Score

SS-range	Assessment	Recommended measure
< 1	Good	No action required
1 – 3	Attention required	Monitor and verify
3 – 6	Elevated	Intervene (e.g. flushing or design improvement)
6 – 10	High	Redesign or intensive control measures
> 10	Very high	Major intervention required

The escalation in recommended measures reflects increasing system sensitivity to stagnation-related risks. The System Score is intended as a comparative engineering indicator rather than an absolute predictor of microbiological growth. Higher values indicate increased sensitivity to stagnation-related microbiological risk. The proposed System Score ranges are preliminary engineering thresholds intended for comparing design alternatives. They are not regulatory limits and require further validation through field measurements.

5. Decision Framework for the Application of CWC

Cold water circulation should only be applied when it demonstrably improves system performance.

CWC is justified only if:

- $\Delta SS > 50\%$
- $SS_with < 3$
- $CF \geq 0.8$

The decision framework is shown in Figure 2.

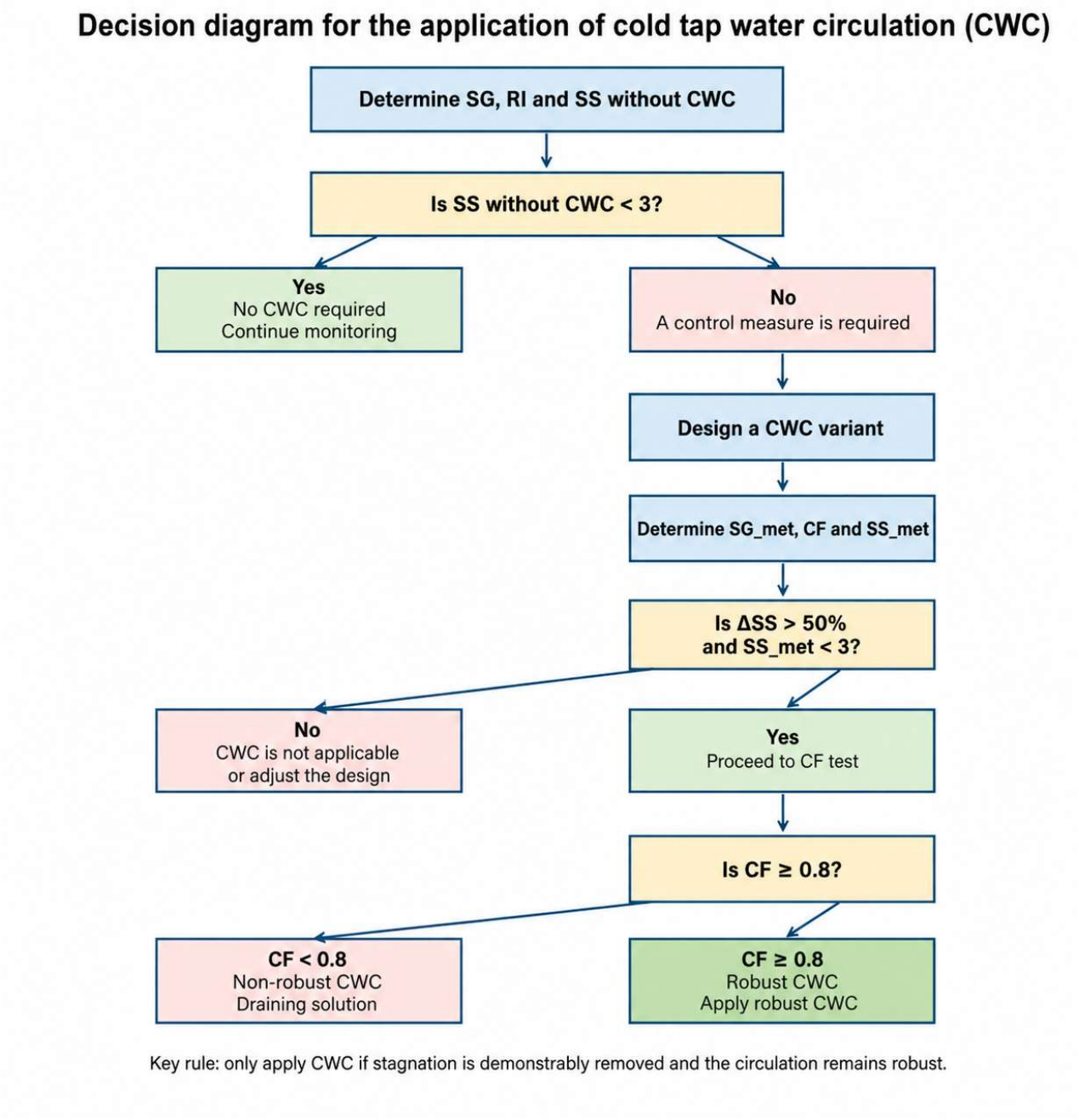

Figure 2 – Decision framework for the application of cold water circulation
Decision framework for evaluating whether cold water circulation should be applied. The framework combines relative improvement in system score (ΔSS), the remaining system score after application (SS_with), and the circulation factor (CF). Cold water circulation is only considered justified when it results in a substantial reduction in risk and the circulation remains hydraulically effective.

The presence of circulation does not guarantee effective renewal of water.

Definition of Robust Circulation

In this document, *robust circulation* is defined as:

A circulation system in which, under all operating conditions—including peak demand (Qmax)—a minimum but continuous circulation flow is maintained in all relevant parts of the system.

This implies that circulation does not cease or significantly decrease as a result of water use, but is hydraulically designed in such a way that both draw-off demand and circulation flows can operate simultaneously.

6. Dynamic Stagnation in Circulation Systems (Optimized)

During peak demand, flow distribution changes. As a result, parts of the system may experience little or no effective flow. This leads to dynamic stagnation: stagnation occurring during use. An example of unstable hydraulic behaviour is shown in Figure 3.

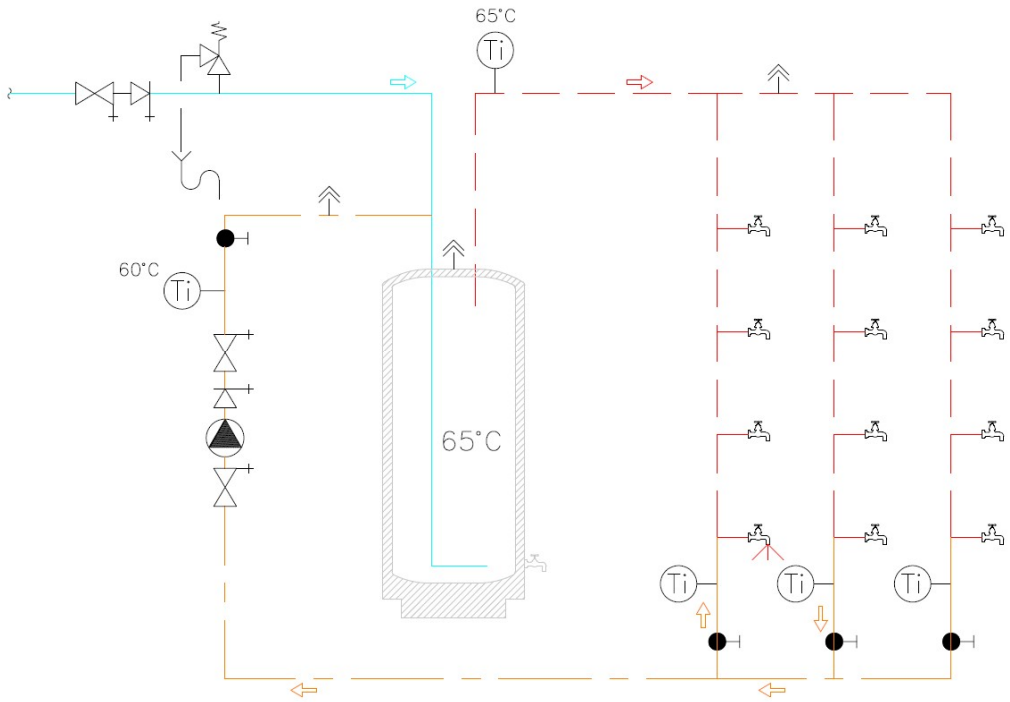

Figure 3 – Unstable hydraulic behaviour in circulation loops
In systems lacking hydraulic robustness, flow distribution becomes unstable. Circulation loops may experience low-flow conditions or local flow reversal, resulting in insufficient renewal in parts of the system.
These effects demonstrate that circulation does not ensure stable or effective hydraulic performance and are relevant for both conventional and cooled water circulation systems.

Water use does not guarantee effective renewal of water.

7. Example 1 – Hotel Room with Shower, Washbasin, and WC

- ambient temperature: 24 °C → RI = 1
- weekend or vacancy scenario: 48 hours without use
- reference time ($t_{(ref)}$) for shower, washbasin, and WC: 24 hours
- terminal pipe volumes: shower 0.7 L; washbasin 0.5 L; WC 0.6 L
- room distribution pipe: 0.9 L

The calculated system scores are presented in Table 3.

Table 3: System Score Calculation

Segment	Scenario	t_no_use (h)	t_low (h)	t_stop (h)	CF	SS
Shower pipe	Without CWC	48	0	0	1.00	2.00
Shower pipe	Non-robust CWC	0	4	6	0.70	0.60
Shower pipe	Robust CWC	0	1	1	0.95	0.09
Washbasin pipe	Without CWC	48	0	0	1.00	2.00
Washbasin pipe	Non-robust CWC	0	4	6	0.70	0.60
Washbasin pipe	Robust CWC	0	1	1	0.95	0.09
WC-pipe	Without CWC	48	0	0	1.00	2.00
WC-pipe	Non-robust CWC	0	3	4	0.75	0.39
WC-pipe	Robust CWC	0	1	1	0.95	0.09
Room distribution pipe	Without CWC	48	0	0	1.00	2.00
Room distribution pipe	Non-robust CWC	0	2	4	0.75	0.33
Room distribution pipe	Robust CWC	0	0.5	0.5	0.95	0.04

Interpretation:
Non-robust CWC reduces the system score, but only to a limited extent. A truly robust system

is only achieved when the circulation factor (CF) is high and the duration of circulation failure (t_{stop}) is low.

This example demonstrates that non-robust cold water circulation may provide an improvement compared to no circulation, but that this improvement remains limited as long as the circulation factor is low and stagnation occurs during use.

Only when circulation remains active under all operating conditions (high CF), and stagnation due to low flow and loss of circulation is minimized, can a truly robust system be achieved.

This type of installation is representative of small-scale sanitary facilities.

8. Example 2 – Marina Facility with 10 Showers, 20 WCs, and 20 Washbasins

This example illustrates how system risk increases when WCs are no longer connected to the drinking water system and therefore no longer contribute to water renewal.

- ambient temperature: 28 °C → RI = 2
- 10 showers, 20 WCs, 20 washbasins
- in the initial situation, WCs provide frequent renewal of the distribution network

without these flushing events, showers and washbasins remain as the primary contributors to water renewal. The calculated system scores and assessments are presented in Table 4.

Table 4: System Score Calculation and Assessment

Scenario	Renewal pattern	SG_corr	RI	SS	Assessment
WCs connected to drinking water	Regular and distributed	1.2	2	2.4	Attention required
WCs replaced by alternative water sources (including rainwater and wastewater reuse)	Significantly reduced renewal	2.1	2	4.2	Measures required
WCs replaced + non-robust CWC	Circulation present, but limited effectiveness	1.8	2	3.6	Questionable
WCs replaced + robust CWC	Low stagnation, high CF	0.9	2	1.8	Acceptable

Only robust circulation significantly reduces system risk.

9. Discussion

The proposed methodology extends conventional design approaches by explicitly considering hydraulic behaviour during normal operation. Current design methods primarily evaluate temperature, peak demand and periods without water use, whereas the present framework also considers prolonged low-flow conditions and circulation stability.

The proposed indicators are intended as **comparative engineering tools** rather than predictive microbiological models. Their primary purpose is to compare alternative design solutions and to identify systems that may be more sensitive to stagnation-related risks.

The case studies demonstrate that dynamic stagnation may occur even in systems that comply with existing design practices. They also show that cold water circulation is not universally beneficial. Its effectiveness depends on a significant reduction in stagnation while maintaining sufficient hydraulic robustness during water use.

The methodology further illustrates that water-saving measures may unintentionally reduce hydraulic renewal. Consequently, sustainability measures should be evaluated together with their hydraulic effects on drinking water quality.

The proposed indicators require further validation through field measurements, microbiological investigations and practical case studies. Future research should also investigate the relationship between hydraulic renewal, biofilm development and microbial growth under different operating conditions.

Overall, the proposed framework complements existing design methodologies by introducing hydraulic behaviour as an explicit engineering design parameter. Rather than replacing current standards, it provides an additional method for evaluating and comparing hydraulic robustness during the design process.

10. Limitations and Further Research

The proposed methodology should be regarded as a conceptual and design-oriented framework intended to support discussion and further development of hydraulic risk assessment in building water systems.

The presented stagnation indicators and scoring approach have not yet been validated using large-scale microbiological datasets or long-term field measurements.

In addition, the presented scenarios are illustrative and depend on assumptions regarding user behavior, hydraulic balance, temperature conditions, and circulation performance.

Further research is recommended to validate the proposed indicators using practical measurements, CFD simulations, dynamic hydraulic modelling, and microbiological monitoring.

11. Conclusions

The proposed methodology demonstrates that stagnation is not only caused by absence of use, but also by low flow conditions and dynamically failing circulation.

A key insight is that:

circulation does not guarantee effective renewal.

Cold water circulation should only be applied when it demonstrably improves system performance.

This shifts the design question from: “Is circulation present?” to: “Does the system perform robustly under all conditions?”

Final conclusion: Building water safety should not only be assessed by temperature compliance, but also by the hydraulic ability of the system to maintain effective circulation, refreshment, and flow continuity under realistic operating conditions.

12. References

Blokker, E.J.M. (2015) Influence of the public drinking water network on tap water temperature. TVVL Magazine, 03/2015, pp. 42–45.

Centers for Disease Control and Prevention (CDC) (2024) Developing a Water Management Program to Reduce Legionella Growth and Spread in Buildings. Atlanta, GA: CDC.

Cullom, A.C., Chapman, R.L. and Schwake, D.O. (2020) 'Critical review: Propensity of premise plumbing pipe materials to enhance or diminish growth of Legionella pneumophila and other opportunistic pathogens', Pathogens, 9(11), 957. https://doi.org/10.3390/pathogens9110957.

ISSO (2023) ISSO 55: Legionella prevention in drinking water installations. Rotterdam: ISSO.

ISSO (2024) ISSO 55.1: Supplement to legionella prevention. Rotterdam: ISSO.

National Academies of Sciences, Engineering, and Medicine (2020) Management of Legionella in Water Systems. Washington, DC: The National Academies Press. https://doi.org/10.17226/25474.

Neu, L. and Hammes, F. (2020) 'Feeding the building plumbing microbiome', Water, 12(6), 1774. https://doi.org/10.3390/w12061774.

NEN (2018) NEN 1006+A1: General requirements for drinking water installations. Delft: NEN.

TVVL (2020) Technical Report ST-46: Domestic hot water circulation systems. Woerden: TVVL.

TVVL (2024) Technical Report ST-51: Keeping it cold – cold water (circulation) systems. Woerden: TVVL.

Van der Wielen, P.W.J.J. et al. (2021) Towards more effective legionella prevention. Utrecht: KWR / Berenschot.

World Health Organization (WHO) (2007) Legionella and the Prevention of Legionellosis. Geneva: WHO.

World Health Organization (WHO) (2011) Guidelines for Drinking-water Quality. 4th edn. Geneva: WHO.

13. Presentation of Author

Onno Leever is director of Leever Installatie Adviseurs B.V. in the Netherlands. He specialises in hydraulic design and system behaviour of drinking water installations. His work focuses on stagnation, cold & hot water circulation, and robust system performance. He is actively involved in knowledge development and international standardisation within the field of building water systems.

Towards *Legionella*-safe low temperature DHW production and distribution: potential of physical techniques in a contaminated system

J. Van Herreweghe, B. Poncelet, C. Jacques, K. Dinne, B. Bleys (1)
F. Oesterholt, A. Moerman (2)

(1) joris.van.herreweghe@buildwise.be
(1) benoit.poncelet@buildwise.be
(1) colin.jacques@buildwise.be
(1) karla.dinne@buildwise.be
(1) bart.bleys@buildwise.be
(2) frank.oesterholt@kwrwater.nl
(2) andreas.moerman@kwrwater.nl

(1) Unit Building Technologies, Buildwise, Belgium (BE)
(2) KWR Water Research Institute, The Netherlands (NL)

Abstract

Domestic hot water (DHW) production at 60 (BE)/65°C (NL), with a temperature drop of no more than 5°C throughout the entire distribution system, is a well-established strategy for controlling *Legionella* growth in building installations, but is increasingly challenged by energy transition goals. Lower production temperatures can improve heat pump efficiency, reduce thermal distribution losses, and decrease overall energy consumption. However, ensuring *Legionella* safety at reduced temperatures remains a major barrier.

One potential approach is to combine DHW production at reduced temperatures (<60 °C) with additional physical control techniques. At Buildwise, the performance of ultrafiltration (UF) and UV-C disinfection was evaluated in collaboration with KWR Water Research Institute and the system manufacturers. The systems were installed in a domestic hot water test installation consisting of a 200 L electric storage tank, a 40 m circulation loop, and two draw-off points (kitchen and bathroom). A daily hot water consumption of 156 L was applied following a usage profile representative of a single family household (four persons). Every single system was installed in the circulation loop immediately after the storage water heater, so that the entire recirculating flow passes through the unit. The installation has been chronically contaminated with a *Legionella pneumophila* serogroup 1 wild type strain for years.

With the physical treatment not activated (UV-C) or in bypass (UF), *Legionella* concentrations were allowed to stabilise at 10^6–10^7 CFU/L at all sampling points during one week at a production temperature of 40 °C. Subsequently, the physical treatment was

activated and the production temperature was successively set to 45, 50, and 55 °C, each for an evaluation period of six weeks. *Legionella* concentrations were monitored weekly at the inlet and outlet of the circulation loop, at both draw-off points and immediately upstream and downstream of the physical treatment unit.

Both physical treatment technologies consistently reduced *Legionella* concentrations immediately downstream of the treatment unit to the detection limit (≤ 50 CFU/L). Only in combination with a production temperature of 55 °C this also resulted in significantly reduced *Legionella* concentrations (around detection limit) throughout the circulation loop and at the bathroom tap, while concentrations at the kitchen tap remained around (UV-C) or well above (UF) 10^3 CFU/L.

Keywords

Legionella, Domestic Hot Water (DHW), Low temperature production, Ultrafiltration, UV-C

1 Introduction

Legionella is a key concern in domestic hot water systems because inhalation of contaminated water aerosols (e.g. during showering) can lead to infection and, ultimately , legionellosis in building occupants. *Legionella* grows effectively at water temperatures ranging from 25°C to 45°C. Once the water temperature rises above 50°C, the legionella bacteria are gradually killed, and above 60°C they die off more quickly [1]. Therefore, maintaining DHW production at 60°C, with a minimum of 55°C throughout the entire distribution system, is a long-standing and widely applied strategy to limit *Legionella* growth in building hot water installations.

However, the energy transition increasingly challenges the conventional 60°C DHW setpoint. As buildings become more insulated and energy efficient, DHW production accounts for a larger share of the total energy use. Lowering the production temperature to 40-45°C, which still meets comfort requirements, can lower the overall energy use by cutting thermal distribution losses and improving the performance of energy efficient heat sources such as heat pumps.

However, such low production temperatures fall within the growth range of *Legionella*, making it a major constraint and technical challenge to maintain *Legionella* safety throughout the entire installation upon implementing low-temperature hot water production. Moreover, related health risks make it difficult to assess this approach, along with any necessary additional control measures, in real occupied buildings.

In earlier research, Buildwise therefore investigated the *Legionella* safety of DHW production at 45 °C combined with periodic heat shocks in a with *Legionella* contaminated domestic hot water test installation. Thermal shocks at 60°C (up to 1h), even when applied daily, did not maintain the *Legionella pneumophila* concentration below 1000 CFU/L and resulted in a regrowth to 10^5-10^6 CFU/L within days after the shock. In contrast, a weekly 24h during shock at 65°C combined with at least 150 seconds draw-offs at both tapping points, kept the system controlled (*Legionella pneumophila* < 1000 CFU/L) [2, 3]. This protocol however has some practical limitations. In practice

achieving sufficiently long draw-offs at all draw-off points during the shock, as required for effective disinfection, is rarely feasible in occupied buildings.

In this follow-up research Buildwise, in collaboration with KWR, explored low-temperature DHW production combined with UV-C (to inactivate *Legionella*) or ultrafiltration (to remove them) in/from the circulation flow as strategies to maintain *Legionella* control.

2 Research setup

2.1 DHW test installation

As shown by Figure 1 the used test installation consists of the following major components (see corresponding numbers in figures 1):

① a 200 L electric storage water heater (boiler) which is during the test phase connected to cold mains water. The desired production temperature is regulated by a temperature probe positioned at mid-height in the tank. The storage heater is equipped with a destratification loop. However, during tests this loop is not in operation. The destratification loop is only active during thermal disinfection to obtain a homogenous temperature distribution in the storage heater, as required by Flemish legislation in Belgium.

② a 40 m long hot water circulation loop consisting of a DN32 multilayer riser pipe with 20 mm insulation and a DN16 recirculation pipe with 15 mm insulation. A circulation pump provides continuous circulation in the loop at a flow rate of 2.9 L/min.

③ & ④ two non-insulated draw-off lines (L =7 & 10 m), each with one draw-off point. The first draw-off point is situated at the first floor of the building and represents kitchen usage of hot water ③. The second draw-off point is situated at the seventh floor and represents shower usage ④.The applied consumption profiles are detailed in § 2.2.

⑤ the physical *Legionella* protection technique to be evaluated is installed in the circulation loop immediately after the storage water heater, so that the entire circulation flow passes through the treatment unit an then continues its path throughout the circulation loop. More details about the evaluated techniques can be found in § 2.3.

The installation has been chronically contaminated with a *Legionella pneumophila* serogroup 1 wild type strain originating from a hospital facility for years. Whenever a treatment should succeed in eliminating *Legionella* from the test installation, a recontamination with the original wild type strain can be done by connecting the installation to the culture storage water heater (culture boiler) ⑥. This 160 L electric storage water heater contains a permanent culture of our *L. pneumophila* sg1 wt strain at a concentration of 10^5–10^6 CFU/L. This culture is maintained by daily draw-offs of 127 L of water, ensuring a sufficient supply of fresh water, and by ensuring a homogeneous 40°C production temperature distribution within the storage water heater through a destratification loop. During the tests, the culture storage water heater is physically isolated from the test installation, which is at that time exclusively supplied with clean drinking water.

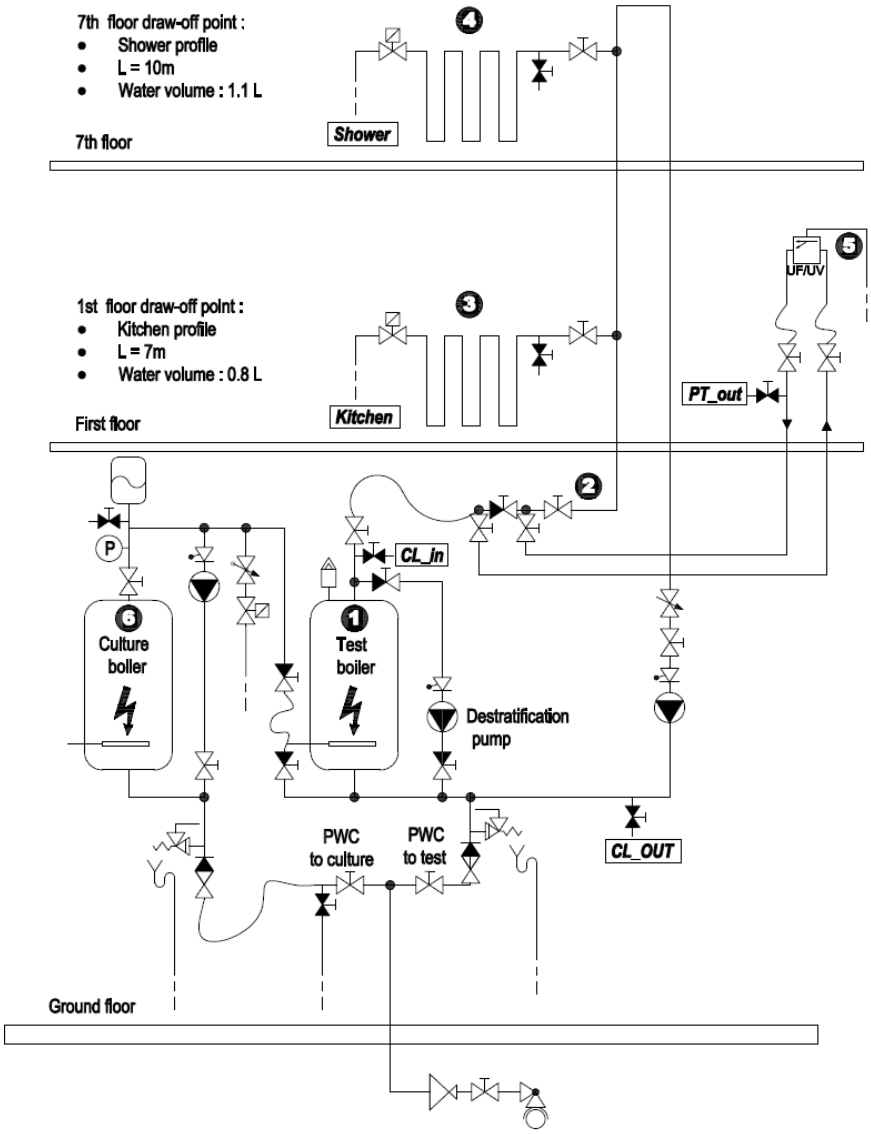

Figure 1 Hydraulic diagram of the DHW test installation with integration of the physical *Legionella* protection technique (either UV-C or ultrafiltration) to be evaluated

2.2 DHW consumption profile

A realistic daily hot water consumption was applied following a consumption profile representative of a single family household (four persons). This profile, based on monitoring data of Buildwise, is given in Table 1 below. As shown in Table 1, the total daily domestic hot water (DHW) consumption is approximately 156 L/day, with about 148 L used for showers and 7.9 L allocated to kitchen activities. The DHW flow rate for the shower has been set at 6.5 L/min, which corresponds to a mixed water flow rate of 8 L/min at 38°C, assuming a production temperature of 45°C. For the kitchen, the DHW flow rate is set at 5 L/min. The draw-offs according to the schedule below are realized using time-controlled solenoid valves on the respective draw-off lines.

Table 1 DHW Consumption profile. The real start hour refers to the time at which draw-offs were observed in monitored buildings. The indicated start hour in the test installation represents a temporal shift of the real draw-off events, allowing sampling to be carried out in the morning before the start of the draw-offs.

Start hour [test installation]	Start hour [real]	Type of draw-off	Tap duration	DHW flow rate	Tapped DHW volume
hh:mm	*hh:mm*	-	*s*	*L/min*	*L*
10:29	06:59	Shower	10	6.5	1,1
10:30	07:00	Shower	355	6.5	38,5
10:40	07:10	Shower	393	6.5	42,6
11:30	08:00	Shower	296	6.5	32,1
15:30	12:00	Kitchen	6	5.0	0,5
16:00	12:30	Kitchen	20	5.0	1,7
17:15	13:45	Kitchen	30	5.0	2,5
21:45	18:15	Shower	311	6.5	33,7
22:30	19:00	Kitchen	6	5.0	0,5
22:45	19:15	Kitchen	3	5.0	0,3
23:30	20:00	Kitchen	30	5.0	2,5
					155,8

2.3 Physical techniques

Two KIWA certified physical techniques, both commercially available, were tested separately in successive experiments in close collaboration with their manufacturers.

2.3.1 UV-C inactivation

Low pressure UV-C lamps emit light at a wavelength of 254 nm which will damage DNA from exposed microorganisms. At the effective dose tailored to the target microorganism, the resulting DNA damage is so extensive that the microorganism is no longer able to reproduce. The evaluated system consists of a reaction chamber containing a single 18 W UV-C lamp enclosed in a quartz glass tube capable of treating a water flow rate of 0.8m³/h. The water to be treated enters the reaction chamber at the bottom (IN in Figure 2), flows around the UV-C lamp, and exits the reaction chamber at the top (OUT in Figure 2). A UV sensor in the reaction chamber and a flow sensor at the entry make it possible to monitor the delivered UV-C dose (J/m²) via an online platform. Throughout the experiments, the dose consistently remained above the minimum dose of 400 J/m². Regular UV-C transmission measurements of

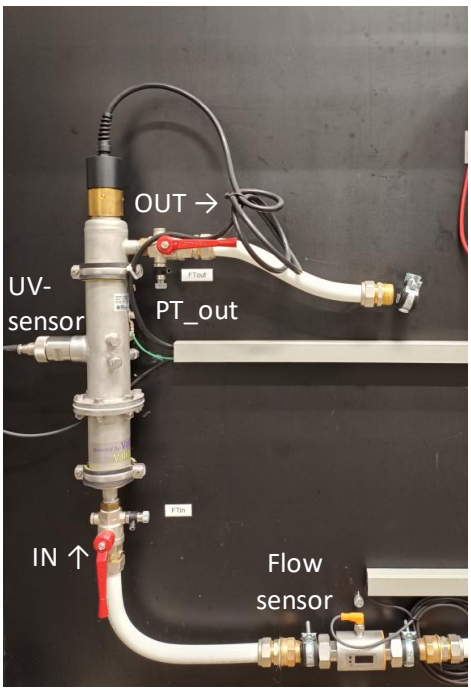

Figure 2 Picture of the tested single lamp UV-C system with UV and flow sensor monitoring.

the water showed that it consistently remained above 90 %.

2.3.2 *Ultrafiltration*

Ultrafiltration removes bacteria such as *Legionella* from the water stream by physical separation, without causing microbial inactivation. The evaluated ultrafiltration unit consists of a cylindrical module containing numerous hollow-fibre filter capillaries made of PESM multibore® membrane. The module provides a total filter surface of 4.57 m² and is designed for a maximum water flow rate of 2.5 m³/h. Water enters the capillaries at the bottom of the module and is filtered radially through the porous capillary walls (nominal pore size 0.02 µm), after which the permeate leaves the module laterally. Retained bacteria remain confined within the capillary lumen. To limit accumulation and a resulting increase in pressure drop, the system applies a short forward flush (5 s) every four hours to evacuate retained bacteria via a solenoid valve at the top of the module. During operation, the transmembrane pressure drop and flow rate were continuously monitored via an online platform to ensure proper filter operation. In the tested UF system, 100% of the circulation flow passes through the system.

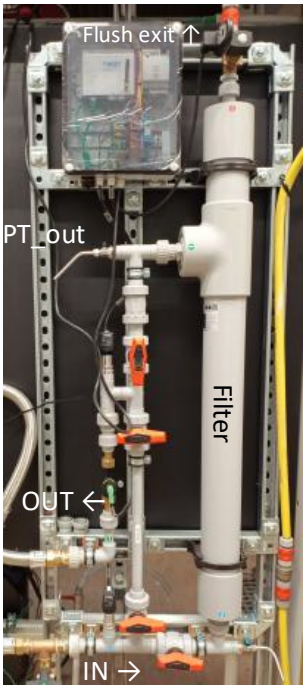

Figure 3 Picture of the tested ultrafiltration system.

2.4 Sampling and *Legionella* analysis

To enable monitoring of the *Legionella* concentration in the installation, sampling valves/points were installed at various locations throughout the system. Table 2 briefly describes each point and lists the corresponding sampling point names used in the result graphs. The sampling points are also indicated in Figure 1.

Table 2 Naming and description of the sampling points

Point name	Description
CL_In	At the outlet of the storage water heater (top), also representing the entry of the circulation loop and upstream of the physical treatment technique.
CL_Out	At the outlet of the circulation loop, immediately upstream of the storage water heater inlet (bottom)
PT_Out	Directly at the outlet of the physical technique allowing the assessment of its local effectiveness in comparison to CL_In
Kitchen	At the draw-off point of the draw-off pipe (7m) on the 1st floor with a kitchen draw-off profile
Shower	At the draw-off point of the draw-off pipe (10m) on the 7th floor with a shower draw-off profile

Sampling at the technical points (CL_In, CL_Out and PT_Out) was intended as a control of the water within the installation at that point. The sampling procedure was as follows: first, the outside and inside of the tap were disinfected with 70% ethanol. Subsequently,

a short flush of 50 mL was carried out to rinse away residual disinfectant. Finally, a 1 L water sample was collected.

Sampling at the draw-off points (kitchen and shower) was intended as an instantaneous check of the water as it would be consumed (worst-case scenario). For this purpose, the solenoid valve was manually activated and the first liter of the outflowing water was collected without prior disinfection of the sampling point.

All samples were collected in sterile plastic bottles. The analysis was performed in accordance with NBN EN ISO 11731:2017 for water samples of water matrix A, using both an unconcentrated and a concentrated fraction (after filtration through a 0.2 µm PES filter and elution), by culturing on selective media (GVPC, BCYE and BCYE + Ab). The detection limit of the applied method is 50 CFU/L.

3 Results

3.1 Low temperature production combined with UV-C inactivation

The evaluation of UV-C inactivation as a *Legionella* control strategy for low-temperature domestic hot water production was conducted in several phases. During each phase, water samples were collected (see § 2.4) at the different points in the installation (see Table 2), and the *Legionella spp.*[1] concentration was determined (see § 2.4). The graphs in Figure 4 illustrate the evolution of this concentration across the different phases at the various sampling points.

During the first phase, the hot water production temperature was set to 40 °C, and the UV-C system was included in the circulation loop but remained inactive. This phase aimed to stabilise the *L. pneumophila* concentration already present at the different points of the pre-contaminated installation. The analytical results indicate a stable concentration ranging from 6.6×10^6 to 1.4×10^7 CFU/L across the different sampling points.

During Phase 2, the production temperature was increased to 45 °C and the UV-C system was activated. In this 6-week phase, samples were collected weekly for the first four weeks and twice a week in the last two weeks; the same schedule applied to phases 3 and 4. The results show a gradual decrease in concentration at the different sampling points. In the final two weeks of this phase, the *L. pneumophila* concentration ranged between 10^4 and 10^5 CFU/L at the inlet of the circulation loop (CL_In) and at the kitchen tap, and between 10^5 and 10^6 CFU/L at the outlet of the circulation loop (CL_Out) and at the shower tap.

In the subsequent Phase 3, the production temperature was increased to 50 °C. This production temperature, in combination with UV-C treatment, resulted from the second week onward in a decrease of the *L. pneumophila* concentration to below the threshold value of 1000 CFU/L at the outlet of the circulation loop (CL_Out). Initially, the inlet of the circulation loop (CL_In), located directly downstream of the storage water heater outlet, also showed a decrease in *L. pneumophila* concentration to just above the

[1] Although the applied method allows the detection of both *Legionella pneumophila* and *Legionella* species, only *L. pneumophila* sg 1 was detected in all samples analysed.

1000 CFU/L threshold. However, during the final two weeks of this phase, the concentration at this point increased again to above 10^5 CFU/L. This is most likely due to thermal stratification in the storage water heater, resulting in zones where temperatures remain favourable for *Legionella* growth. The concentrations at both draw-off points stabilised in the order of 10^4 CFU/L, with slightly higher values observed at the draw-off point following the shower draw-off profile.

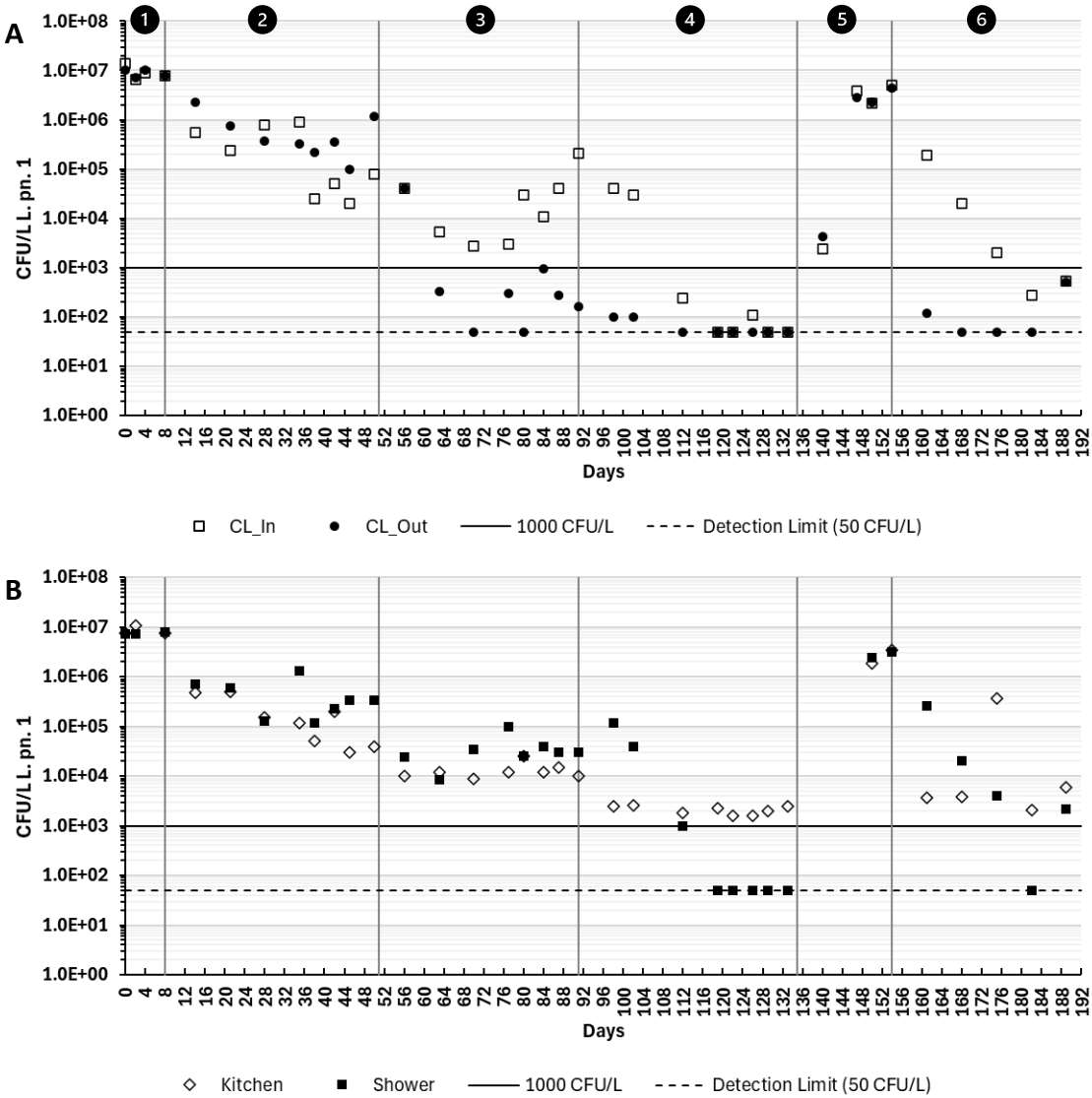

Figure 4 Results of the *Legionella pneumophila* sg 1 analyses at the inlet (CL_In) and outlet (CL_Out) of the circulation loop (graph A) and at the kitchen and shower draw-off points (graph B) throughout the different evaluation phases (1–6) of the UV-C system at low temperature DHW production. Phase 1: stabilisation at 40 °C; Phase 2: 45 °C + UV-C; Phase 3: 50 °C + UV-C; Phase 4: 55 °C + UV-C; Phase 5: stabilisation at 40 °C; Phase 6: 55 °C + UV-C (confirmation). The grey vertical lines indicate the transition to the next phase. The horizontal black line represents a threshold value of 1000 CFU/L, and the dashed line indicates the detection limit of the applied analytical method (50 CFU/L).

In Phase 4, the production temperature was further increased to 55 °C in combination with UV-C treatment. As a result, the *L. pneumophila* concentration at the outlet of the circulation loop (CL_Out) decreased to below the detection limit of 50 CFU/L from the third week onward. From the fourth week, concentrations at the inlet of the circulation

loop (CL_In) and at the draw-off point following the shower draw-off profile also dropped below the detection limit. The concentration at the kitchen outlet decreased to just above the threshold value of 1000 CFU/L.

In Phase 5, the UV-C system was switched off and the production temperature was reset to 40 °C. Within two weeks, *L. pneumophila* had recolonized the installation, with concentrations rising to 10^6–10^7 CFU/L at all sampling points.

In a final Phase 6, the production regime of 55 °C combined with UV-C inactivation was re-applied to the installation to confirm the results obtained in Phase 4. This again led to a reduction in *L. pneumophila* concentration to below the threshold value of 1000 CFU/L at the inlet of the circulation loop (CL_In) and to below the detection limit at the outlet (CL_Out). Concentrations at both draw-off points also decreased markedly to around the threshold value of 1000 CFU/L, with one measurement at the shower daw-off point falling below the detection limit confirming previous findings.

During the first four weeks of phases 2, 3, 4, and 6, samples were also collected directly at the outlet of the UV-C system (PT_Out). In all samples taken, the *L. pneumophila* concentration was below the detection limit of 50 CFU/L. This indicates good performance and local effectiveness of the UV-C system

3.2 Heat disinfection and recontamination between both tests

After completion of the UV-C system tests, the entire DHW test installation was thermally disinfected to restore the original test conditions. This was achieved by heating the storage water heater to 70 °C, resulting in 65 °C at the outlet of the circulation loop (CL_Out). The draw-off points were opened sequentially—first the shower, then the kitchen—at low flow (pencil-sized stream) for 10 min once a stable temperature of 65–70 °C was reached. Throughout the procedure, the storage water heater destratification loop was active to ensure a homogeneous temperature distribution within the storage water heater. Sampling immediately after the procedure showed that *Legionella* concentrations at all points had dropped below the detection limit. The test installation was subsequently connected for one week to the culture storage water heater to re-establish contamination with the original *L. pneumophila* sg 1 strain (see § 2.1), after which it was switched back to a connection with mains water.

3.3 Low temperature production combined with ultrafiltration

The evaluation of the ultrafiltration system was also conducted following phases 1–4, with the same duration and sampling frequency, as described in §3.1 for the UV-C system. The graphs in Figure 5 illustrate the evolution of the *L. pneumophila* concentration across the different phases at the various sampling points.

To start from a stable contamination a stabilisation phase was first initiated at a production temperature of 40 °C with the ultrafiltration system switched off (in bypass). Subsequently, in phase 2, the production temperature was increased to 45 °C and the ultrafiltration system was activated. The results show a gradual decrease in concentration at the different sampling points. In the final two weeks of this phase, the *L. pneumophila* concentration ranged between 10^4 and 10^5 CFU/L at the inlet and outlet of the circulation loop (CL_In, CL_Out) and between 10^5 and 10^6 CFU/L at the kitchen and shower draw-off points.

In Phase 3, the production temperature was increased to 50 °C. This resulted in a further decrease in *Legionella* concentrations at the different points in the installation, although concentrations remained >10^3 CFU/L at the inlet and outlet of the circulation loop and between 10^4 and 10^5 CFU/L at the kitchen and shower draw-off points.

In Phase 4, the production temperature was further increased to 55 °C. At both the inlet and outlet of the circulation loop, *L. pneumophila* concentrations rapidly declined to below 1000 CFU/L and subsequently remained at or near the detection limit. At the shower draw-off point, concentrations decreased to below 1000 CFU/L from the third week of Phase 4 onwards and reached the detection limit during the final three sampling events. In contrast, concentrations at the kitchen draw-off point remained predominantly above 1000 CFU/L throughout Phase 4. During the first four weeks of Phases 2, 3 and 4, additional samples were collected directly downstream of the UF system (PT_Out). In all samples, *L. pneumophila* concentrations were below the detection limit of 50 CFU/L, demonstrating the consistent local effectiveness of the UF system.

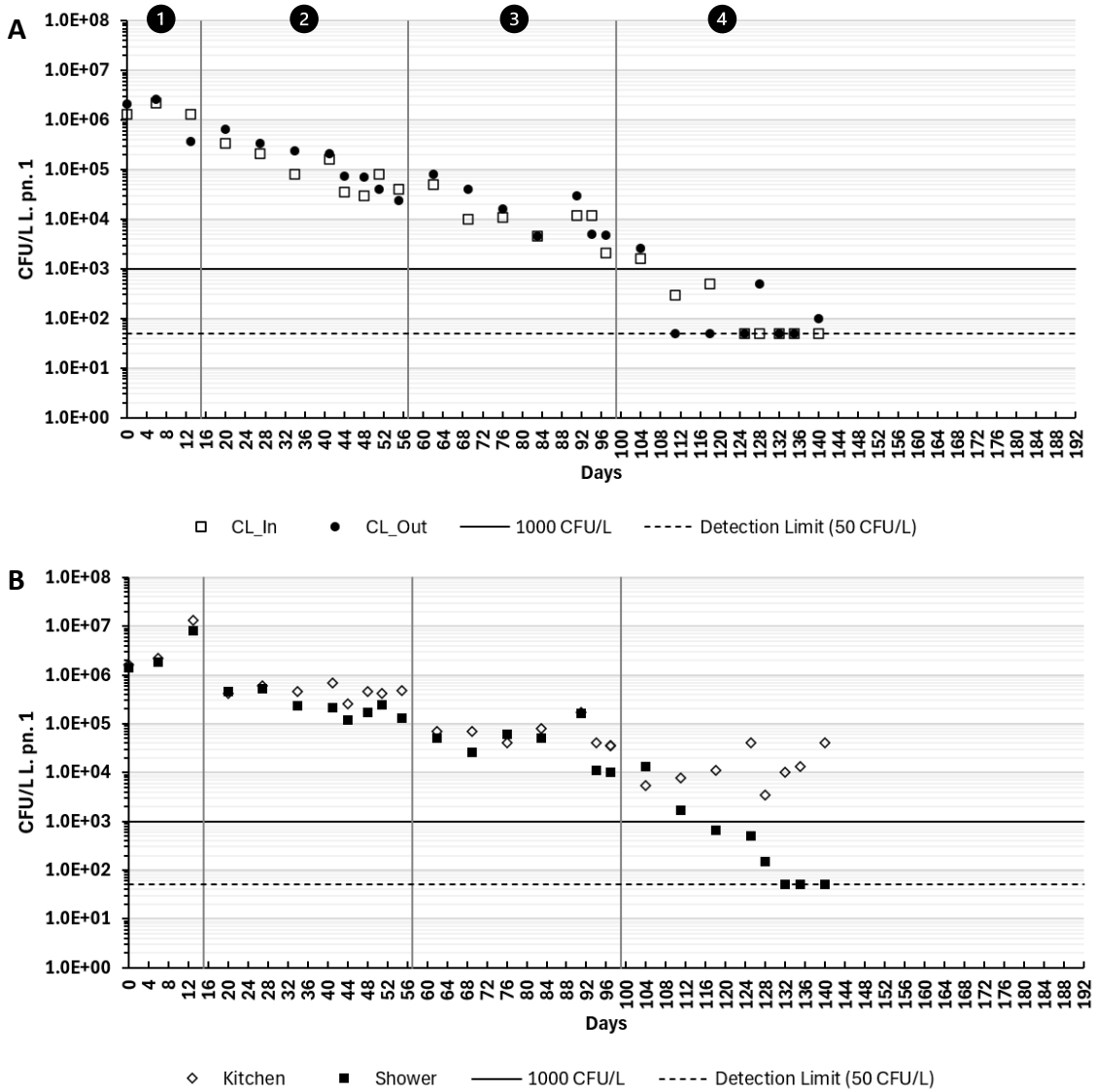

Figure 5 Results of the *Legionella pneumophila* sg 1 analyses at the inlet (CL_In) and outlet (CL_Out) of the circulation loop (graph A) and at the kitchen and shower draw-off points (graph B) throughout

the different evaluation phases (1–4) of the UF system at low temperature DHW production. Phase 1: stabilisation at 40 °C; Phase 2: 45 °C + UF; Phase 3: 50 °C + UF; Phase 4: 55 °C + UF The grey vertical lines indicate the transition to the next phase. The horizontal black line represents a threshold value of 1000 CFU/L, and the dashed line indicates the detection limit of the applied analytical method (50 CFU/L).

4 Conclusions, discussion and next steps

Flemish regulation (Belgium) considers a sanitary building installation with less than 1000 CFU/L of *Legionella pneumophila* to be under control [4]. This value is not a health-based safety limit but an operational action threshold within a risk management framework, indicating the need for increased vigilance and corrective measures when exceeded. *Note: European [5] and Dutch regulation [6] respectively use threshold values of 1000 and 100 CFU/L but for Legionella spp.*

The evaluation of physical treatment techniques for *Legionella* control in a heavily contaminated DHW test installation operating at low-temperature production showed that:

- At production temperatures of 45 °C and 50 °C, both techniques led to reduced *Legionella* concentrations at the different points within the installation. However, with the exception of the outlet of the circulation loop in the UV-C system, concentrations remained above the threshold value of 1000 CFU/L, meaning that the installation cannot be considered *Legionella* controlled under these conditions.
- When combined with a production temperature of 55 °C, both techniques led to a consistent decrease in *Legionella* concentrations to below the threshold of 1000 CFU/L (and often below the detection limit) at both the inlet and outlet of the circulation loop. This indicates that the circulation loop and storage water heater can be considered under control. At the shower draw-off point, both UV-C treatment and UF maintained concentrations below the detection limit for the majority of the time. At the kitchen draw-off point, concentrations were generally around (UV-C) or well above (UF) the threshold value of 1000 CFU/L, meaning that additional control measures are required. The consistently lower concentrations at the shower draw-off point for both techniques is likely related to the higher daily water usage at this location (shower:148L vs. kitchen:7.9 L), resulting in higher average temperatures in the draw-off pipe throughout the day resulting in less favourable conditions for regrowth.

To further substantiate the added value of combining physical techniques at a production temperature of 55 °C, a next step will be to evaluate the effect of a 55 °C production temperature without any physical treatment on *Legionella* concentrations within the installation.

In the current study, a heavily contaminated system was used as a starting point. In a subsequent experimental series, the effectiveness of both techniques in protecting a non-contaminated installation will be evaluated. In this setup, the production temperature will be gradually reduced from 55 °C to 50 °C and 45 °C, while a low dose (<100 CFU/L) of *L. pneumophila* sg1 will be continuously injected into the cold water supply.

Further research will also aim to evaluate the effectiveness of these physical treatment technologies in a more complex DHW test installation representative of larger multi-family residential buildings.

5 Acknowledgements

This article was written in the framework of the pre-normative OptiDis project at Buildwise, with financial support from the Belgian Federal Public Service Economy, and the PPS-project RELOaDH at KWR (The Netherlands). The RELOaDH project was funded by the Top Consortia for Knowledge and Innovation (TKI) Grant from the Dutch Ministry of Economic Affairs. The authors would like to thank Jan Willem Meisen (Van Remmen UV) and Arran Kassens (HollandWater) for their constructive input and the dedicated collaboration.

6 References

[1] Brundrett, G. W. (1992). *Legionella and building services*. Butterworth-Heinemann (Oxford).

[2] Dinne, K., Gerin, O., Bleys, B., & De Cuyper, K. (2017). *Evaluation of the risk of Legionella spp. development in sanitary installations.* In *Proceedings of the CIB W062 Symposium 2017* (Haarlem, The Netherlands).

[3] Dinne, K., Gerin, O. & Bleys, B. (2018). *Evaluation of the risk of Legionella spp. Development in sanitary installations (part 2).* In *Proceedings of the CIB W062 Symposium 2018* (Azores, Portugal).

[4] Vlaamse Regering (2007). Besluit van de Vlaamse Regering van 9 februari 2007 betreffende de preventie van de veteranenziekte (legionellose) in publiek toegankelijke plaatsen. *Belgisch Staatsblad*, gepubliceerd op 4 mei 2007.

[5] European Parliament and Council (2020). Directive (EU) 2020/2184 of 16 December 2020 on the quality of water intended for human consumption (recast). *Official Journal of the European Union*, L435, 23 December 2020.

[6] Nederlandse overheid. (2024). *Regeling legionellapreventie in drinkwater en warm tapwater*. Geraadpleegd via https://wetten.overheid.nl

6 Presentation of Authors

Joris Van Herreweghe is a biochemical engineer and holds a PhD in Bioscience Engineering from the KU Leuven. He is an R&D Expert in Microbiology and Microparticles in relation to water, building materials and indoor air quality at the Unit Building Technologies of Buildwise.

Benoit Poncelet is an architectural engineer from UCLouvain. He is R&D programme leader for water-related topics at Buildwise and coordinator of the Technical Committee on Sanitary Installations within the Building Technologies unit.

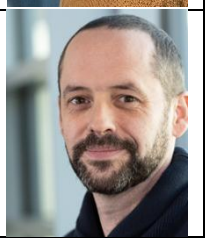

Colin Jacques is an industrial building engineer from ECAM Brussels Engineering School. He is an R&D scientist at Buildwise in the Building Technologies unit, where he previously completed his thesis on greywater reuse systems. His work mainly focuses on domestic hot water production and distribution systems	
Karla Dinne is safety expert at Buildwise. She is a biochemical engineer and a senior researcher in the field of Legionella.	
Bart Bleys is Quality, Safety, Environmental, Risk and Compliance Manager and Animator of the Technical Committee Sanitary installations at Buildwise. He is a senior researcher in the field of water supply and drainage in buildings.	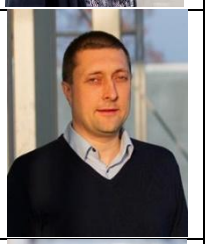
Frank Oesterholt MSc is a chemical engineer and senior researcher/ project manager in the Energy & Circular Systems team at KWR Water Research. He is expert in the field of legionella prevention, mainly focused on risk assessment and legionella management for tap water installations, cooling water systems and wastewater treatment plants.	
Andreas Moerman MSc is a senior researcher/ project manager in the Energy & Circular Systems team at KWR Water Research. His expertise is modelling and analysis in several domains in the energy-water-nexus, like aquathermal energy, (domestic) hot water and impact of the energy transition on (drinking) water systems.	

Optimizing Thermostatic Balancing Valve Placement in Domestic Hot Water Recirculation Systems: Product Ratio Method Analysis of Thermal Performance and Hydraulic Efficiency

Christoph Lohr, PE, CPD, ASSE 12080, LEED AP BD+C (1)

(1) Christoph.Lohr@iapmo.org

(1) Vice President, Technical Services and Research, IAPMO, USA

Abstract

This study examines the influence of thermostatic balancing valve (TBV) placement within domestic hot water recirculation systems using the Product Ratio Method as a modeling framework with pressure and flow calculations being completed in the Hardy Cross + Heat Loss Integration method. Two configurations are evaluated: positioning TBVs immediately downstream of plumbing fixtures where the return system connects into the supply system, and locating them at the convergence point of two hot water return branches. The analysis considers how valve location, relative to branch length and system geometry, affects temperature stability, flow distribution, and head losses within the recirculation loop. Iterative simulations employing the Product Ratio Method assess the performance across two system layouts. Findings establish design strategies that optimize TBV placement for enhanced thermal performance and hydraulic efficiency, contributing to improved best practices in plumbing system design.

Keywords

thermostatic balancing valves, TBV placement, domestic hot water recirculation, product ratio method, hydraulic efficiency, thermal performance, head loss analysis, plumbing system design, branch convergence, flow distribution, temperature stability.

1 Introduction

Thermostatic balancing valves (TBVs) are increasingly specified in domestic hot water recirculation systems as a means of achieving precise flow control without manual balancing after commissioning. Unlike fixed-orifice balancing valves, TBVs modulate flow in response to temperature, closing progressively as water temperature at the valve approaches the set point, and reopening as the loop cools. This behavior is intended to maintain a minimum supply temperature at each branch while preventing excessive circulation and energy waste [1].

Despite their growing use, current plumbing engineering practice offers limited quantitative guidance on where TBVs should be located within a hot water return loop. Typical specifications place valves either immediately after the last fixture connection on a branch—a location sometimes called the "fixture-adjacent" position—or near the point where return branches converge before entering the combined return main. These two positions expose the valve to different thermal and hydraulic conditions and, as this paper demonstrates, produce meaningfully different system-level outcomes.

The Product Ratio Method (PRM) [5], introduced in previous CIB W062 work as a complement to the Hardy Cross + Heat Loss Integration (HCHI) approach [4], provides a systematic framework for calculating flow rates at each branch based on the ratio of downstream heat losses. The PRM is well-suited to this analysis because it explicitly assigns flow based on the thermal load of each piping segment, making it sensitive to where heat-generating return piping is included in or excluded from the flow-ratio calculation.

This paper evaluates two TBV placement configurations—designated the "SHORT" configuration (TBV immediately after the last fixture) and the "LONG" configuration (TBV immediately before the return branch junction) - across a prototype two-loop recirculation system. The analysis quantifies differences in required flow rate, system pressure loss, supply temperature drop, and return temperature drop, and discusses implications for pump sizing, valve selection, and overall system efficiency.

2 Background: Product Ratio Method

2.1 Review of the Product Ratio Method

The Product Ratio Method (PRM) is an approach for determining the required flow rates through a domestic hot water recirculation system by assessing the ratio of flow at each division in circulation flow, estimating the heat loss of all downstream segments of piping at each node [1, 5].

The method uses taxonomical designations for each segment, enabling analysis of the relationships between segments without visual reference to a diagram. This allows flow rates, as regulated by balancing valves, to be determined using only the heat loss per unit length and the segment designations, once a supply temperature and minimum return temperature are selected. Key PRM equations determine the segment ratio rn and the cumulative ratio Rr at each branch point, which are then used to allocate total system flow to each loop:

$$rn = \Sigma Q_downstream_segment_n / \Sigma Q_total_system$$

$$qn = Rr \times Q_total$$

The PRM assumes a uniform temperature is to be maintained at each balancing valve and accounts for heat loss in the supply piping only; return piping heat losses inform the target supply and minimum return temperature selection but are not directly used in the flow ratio calculation. This characteristic makes the PRM particularly sensitive to how piping segments are assigned to each loop—and therefore to where the TBV is placed, since valve location determines which return pipe segments are included in the system heat loss accounting.

2.2 Heat Loss Calculation Basis

Heat loss per linear foot of insulated pipe is calculated using the cylindrical conduction equation, assuming 100% of heat transfer occurs through the insulation:

$$Q = 2\pi(k)(\Delta T) / [(40.944) \times \ln(Do/Di)]$$

Where:

k = thermal conductivity of insulation [(BTU)(in)/((ft²)(°F)(hr))] = 0.24

ΔT = temperature difference between fluid and ambient air [°F]

Do = outer insulation diameter [in]

Di = inner insulation diameter [in]

40.944 = unit conversion factor (12 in/ft × 3.412 BTU/W·hr)

Representative heat loss values used in this analysis (1.5" thick insulation, 140°F fluid, 65°F ambient) are shown in Table 1.

Table 1: BTU/hr Heat Loss Per Linear Foot — Selected Pipe Sizes, 1.5" Insulation

Pipe Size [in]	Actual OD [in]	ln(Do/Di)	120°F	130°F	140°F	150°F
3/4"	0.875	1.488	4.64	5.49	6.33	7.18
1"	1.125	1.299	5.32	6.29	7.25	8.22
1-1/4"	1.375	1.157	5.97	7.06	8.14	9.23
1-1/2"	1.625	1.046	6.61	7.81	9.01	10.22
2"	2.125	0.880	7.85	9.28	10.71	12.13

3 System Description and Configuration Definitions

3.1 Prototype System Geometry

The prototype system modeled in this analysis consists of a two-loop domestic hot water recirculation system fed from a common supply trunk. The water heater (WH) connects to a central node (A1) via a 2-inch supply main (WH-A1, 175 ft). At A1, the supply divides into two branches: Loop A, served by a 1-inch supply line to fixture PFIX-A (A1-A2, 100 ft), and Loop B, served by a 1-inch supply line to fixture PFIX-B (A1-B1, 350 ft). Both branches return to a common return main (A3) and then back to the water heater (A3-WH, 75 ft, 3/4-inch). Flow is counterclockwise through the system, as shown in Figures 1 and 2.

Design conditions are as follows: 140°F supply temperature; target maximum supply temperature drop of 3°F per loop; target maximum return temperature drop of 2°F per loop; maximum allowable velocity of 4.0 ft/sec in copper piping; 1.5-inch insulation on piping 1.5 inches in diameter and smaller; 2-inch insulation on piping larger than 1.5 inches; Hazen-Williams coefficient C = 135 for Type L copper.

3.2 Configuration SHORT: TBV Immediately After Last Fixture

In the SHORT configuration (Figure 1), each TBV is located 1 foot downstream of the last fixture connection on its respective return branch. For Loop A, TBV1 is placed 1 ft from fixture PFIX-A (segment A2-TBV1 = 1 ft return). For Loop B, TBV2 is placed 1 ft from fixture PFIX-B (segment B1-TBV2 = 1 ft return). The bulk of the return piping in each loop—50 ft for Loop A (TBV1-A3) and 300 ft for Loop B (TBV2-A3)—lies downstream of the valve, between the TBV and the return junction at A3. In this arrangement, the PRM treats only the supply piping and the 1-ft return stub as contributing to the flow ratio calculation for each loop.

Figure 1: SHORT Configuration — TBV Located Immediately After Last Fixture

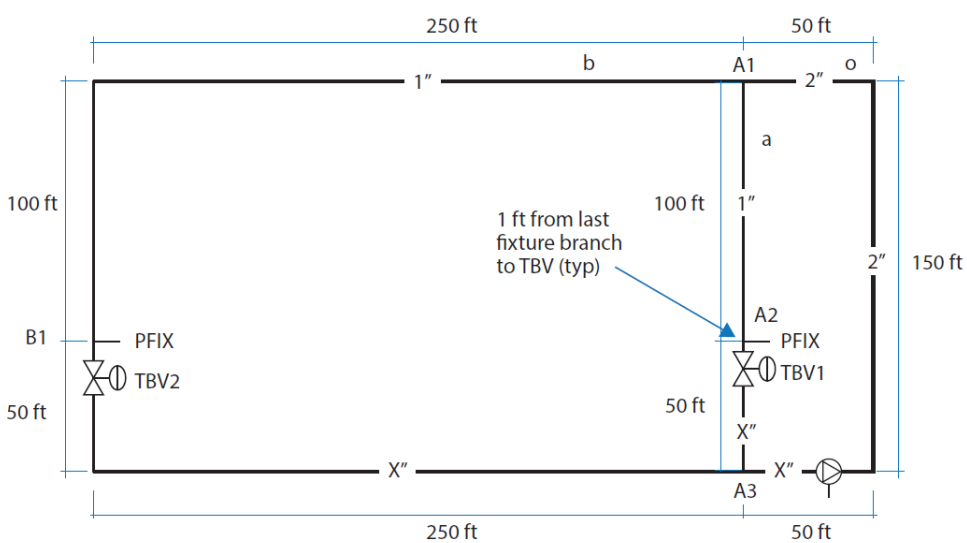

3.3 Configuration LONG: TBV Immediately Before Return Branch Junction

In the LONG configuration (Figure 2), each TBV is relocated to 1 foot upstream of the return branch junction at A3. For Loop A, TBV1 is placed at the end of a 50-ft return segment (A2-TBV1 = 50 ft). For Loop B, TBV2 is placed at the end of a 300-ft return segment (B1-TBV2 = 300 ft). The segment between the TBV and the junction (TBV-A3 = 1 ft) is minimal. In this arrangement, the full length of return piping in each branch is upstream of the valve and is therefore included in the PRM heat loss accounting for that loop.

Figure 2: LONG Configuration — TBV Located Immediately Before Return Branch Junction

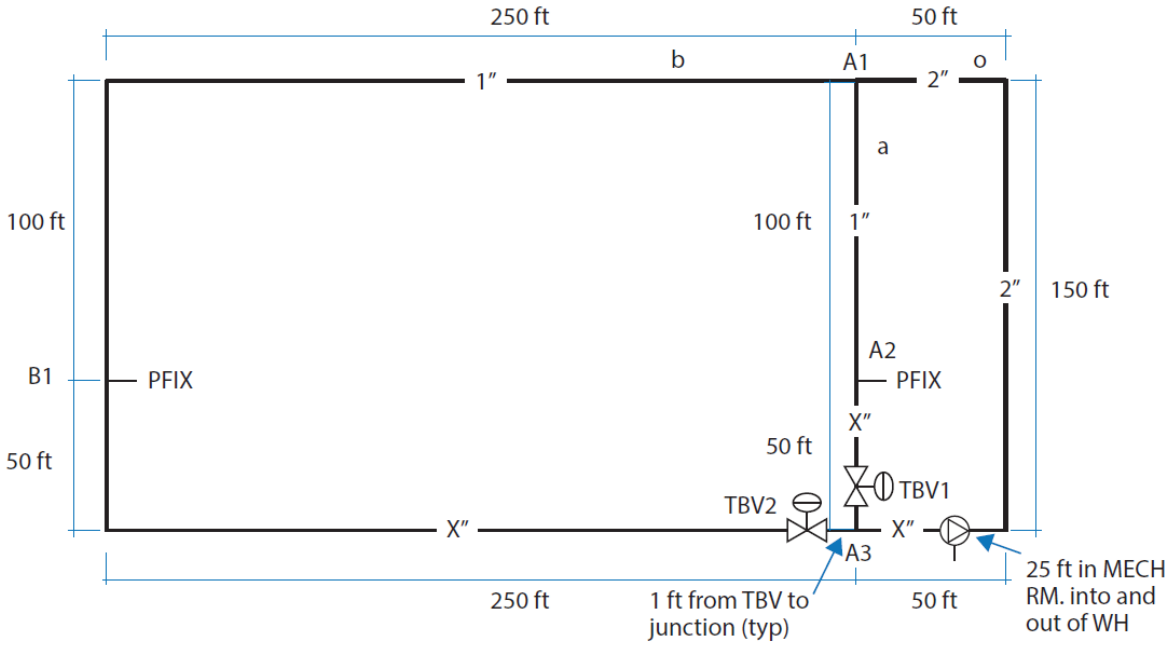

4 PRM Analysis

4.1 Pipe Segment Identification — SHORT Configuration

Table 2 presents the pipe segment labeling and associated heat losses used in the PRM for the SHORT configuration. Because both TBVs are positioned 1 ft from their respective fixtures, the return heat loss included in the PRM calculation for each loop is negligible (6.3 BTU/hr/ft each). The total heat loss accounted for in the PRM is 4,834.9 BTU/hr.

Table 2: PRM Pipe Segment Identification — SHORT Configuration

Segment	PRM Label	Type	Length [ft]	Heat Loss [BTU/hr]	Notes
WH-A1	o	Supply	175	1,558.0	Common trunk
A1-A2	a	Supply	100	725.4	Loop A branch
A2-TBV1	a	Return	1	6.3	TBV1 near fixture
A1-B1	b	Supply	350	2,538.8	Loop B branch
B1-TBV2	b	Return	1	6.3	TBV2 near fixture

4.2 PRM Flow Results — SHORT Configuration

Table 3 presents the PRM flow allocation results for the SHORT configuration, targeting a 3°F supply temperature drop. The total system flow is 3.22 GPM. Loop B (the longer branch) receives 2.50 GPM (TBV2), while Loop A (the shorter branch) receives 0.72 GPM (TBV1). The flow split ratio is approximately 78% to Loop B and 22% to Loop A, reflecting the substantially larger supply heat loss in the longer branch.

Table 3: PRM Flow Allocation Results — SHORT Configuration

Segment	Seg. BTU/hr	Sum Seg. (Supply + Return to TBV) BTU/hr	rn	Rr	qn [GPM]	TBV
-	1,558.0	4,834.9	0.00	1.00	3.22	—
b	2,545.2	2,545.2	0.777	0.777	2.50	TBV2
a	731.7	731.7	0.223	0.223	0.72	TBV1

Note: Supply temperature drop target = 5.0°F

4.3 Pipe Segment Identification — LONG Configuration

Table 4 presents the PRM segment identification for the LONG configuration. With TBVs moved to the junction end of each return branch, the full return piping length is now included upstream of each valve: 50 ft of return (316.7 BTU/hr) for Loop A and 300 ft of return (1,900.1 BTU/hr) for Loop B. Total heat loss in the PRM calculation increases to 7,039.0 BTU/hr—a 45.6% increase over the SHORT configuration—because the return piping thermal load is now fully captured in the flow ratio calculation.

Table 4: PRM Pipe Segment Identification — LONG Configuration

Segment	PRM Label	Type	Length [ft]	Heat Loss [BTU/hr]	Notes
WH-A1	0	Supply	175	1,558.0	Common trunk
A1-A2	a	Supply	100	725.4	Loop A branch
A2-TBV1	a	Return	50	316.7	TBV1 near junction
A1-B1	b	Supply	350	2,538.8	Loop B branch
B1-TBV2	b	Return	300	1,900.1	TBV2 near junction

4.4 PRM Flow Results — LONG Configuration

Table 5 presents the PRM flow allocation results for the LONG configuration. Total system flow increases to 4.69 GPM. Loop B receives 3.80 GPM and Loop A receives 0.89 GPM, reflecting the larger heat loss now attributed to the longer return branch. The flow split shifts to approximately 81% to Loop B and 19% to Loop A, driven by the inclusion of the 300-ft return segment in Loop B's heat loss ratio.

Table 5: PRM Flow Allocation Results — LONG Configuration

Segment	Seg. BTU/hr	Sum Seg. (Supply + Return to TBV Only) BTU/hr	rn	Rr	qn [GPM]	TBV
-	1,558.0	7,039.0	0.00	1.00	4.69	—
b	4,438.9	4,438.9	0.810	0.810	3.80	TBV2
a	1,042.1	1,042.1	0.190	0.190	0.89	TBV1

Note: Supply temperature drop target = 3.0°F

5 Hydraulic Performance Comparison

With PRM-derived flow rates applied to the HCHI calculation framework, full hydraulic and thermal performance for each configuration was evaluated. Table 6 presents a comprehensive comparison of the two configurations across all key performance metrics.

Table 6: Hydraulic and Thermal Performance Comparison — SHORT vs. LONG Configuration

Parameter	Config.	Loop A	Loop B	System Total	% Change (S→L)
Flow Rate [GPM]	SHORT	0.72	2.50	3.22	—
Flow Rate [GPM]	LONG	0.89	3.80	4.69	+31.3%
Max Pressure Loss [ft hd]	SHORT	8.55	18.90	18.90	—
Max Pressure Loss [ft hd]	LONG	12.01	34.64	34.64	+45.4%
Temp Drop Supply [°F]	SHORT	2.98	3.00	3.00	—
Temp Drop Supply [°F]	LONG	2.29	2.00	2.29	—
Temp Drop Return [°F]	SHORT	1.19	1.82	1.82	—
Temp Drop Return [°F]	LONG	0.93	1.21	1.21	—
Temp Drop Total [°F]	SHORT	4.17	4.82	4.82	—
Temp Drop Total [°F]	LONG	3.22	3.21	3.22	—

Notes:

All pressure losses include a 5 ft head flow control valve allowance at this time.

Temperature drop values calculated using $Q = V \times 500 \times \Delta T$.

Maximum velocity in both configurations: 3.45 ft/sec (A3-WH, 3/4" return main).

5.1 Flow Rate Impact

Moving TBVs from the fixture-adjacent position to the junction-adjacent position increases total system flow by 31.3%, from 3.22 GPM to 4.69 GPM. This increase is entirely a consequence of the PRM accounting mechanism: when the return piping heat loss is included upstream of the valve, the method calculates a higher flow requirement to offset that additional thermal load. Loop B's flow demand increases from 2.50 GPM to 3.80 GPM (+52%), while Loop A's increases more modestly from 0.72 GPM to 0.89 GPM (+24%).

It is important to note that this flow increase does not necessarily translate to improved temperature maintenance. In the SHORT configuration, the valve modulates flow based on temperature sensed immediately after the fixture—a location that is thermally representative of supply-side performance. In the LONG configuration, the valve senses temperature after a long return run, which may already have lost significant heat before reaching the valve, potentially causing the TBV to over-circulate in an attempt to compensate for return-side losses that are not efficiently addressable through increased flow.

5.2 Pressure Loss Impact

System pressure loss increases 45.4% in the LONG configuration, from 18.90 ft of head to 34.64 ft of head. This increase is disproportionately concentrated in Loop B, where the maximum pressure drop rises from 18.90 ft to 34.64 ft (+83%). The combined effect of higher flow through longer return piping at higher velocities drives substantially increased frictional losses. Loop A's pressure loss increases more moderately, from 8.55 ft to 12.01 ft (+40%).

From a pump selection standpoint, the LONG configuration requires a significantly larger and more energy-intensive pump to deliver the required head and flow. This has downstream implications for electrical infrastructure, pump operating costs, and life-cycle cost of the system.

5.3 Temperature Performance

Supply temperature drops were lower in the LONG configuration (2.29°F and 2.00°F temperature drop for supply Loops A and B, respectively) compared to the SHORT configuration (supply temperature drops of 2.98°F and 3.00°F). Both configurations maintain total temperature drops well within the 5°F design target, and neither produces conditions in the hot water system that would approach the *Legionella pneumophila* growth range [2,3]. However, the SHORT configuration achieves near-target performance of the supply temperature drop with less pump energy, making it the more energy efficient design from a whole-system perspective.

6 Discussion

6.1 Why TBV Placement Affects PRM Results

The fundamental reason TBV placement affects PRM output is that the method calculates flow based on the heat loss of all piping upstream of the valve that requires thermal maintenance. When the TBV is near the fixture (SHORT), only the supply piping and a minimal return stub are included in the heat loss ratio—the long return run downstream of the valve is not assigned to that loop's flow calculation. When the TBV is near the junction (LONG), the full return run is upstream of the valve and is included in the flow ratio. This adds substantial heat loss to Loop B in particular, since its return run is 300 ft.

This sensitivity is not a flaw in the PRM, it accurately reflects the physical reality that more piping requires more thermal maintenance. However, it raises an important design question: should the recirculation flow be sized to maintain temperature through the return piping, or should return piping temperature loss be managed through insulation selection and accepted as a design condition? The SHORT configuration implicitly takes the latter approach, relying on adequate insulation to limit return temperature drop while using the TBV primarily to balance supply-side temperature.

6.2 Thermostatic Balancing Valve Selection and Cv Impact

TBV placement is inseparable from valve selection. The flow rates derived from the PRM for each configuration determine which valve sizes and Cv ratings are applicable, and the pressure loss across the TBV at a given operating point is a direct function of both the flow rate and the valve Cv. The relationship governing pressure loss across a valve is:

$$\Delta P\ [psi] = (Q / Cv)^2$$
$$\Delta P\ [ft\ hd] = \Delta P\ [psi] \times 2.31$$

Three commercially representative TBV configurations were evaluated across all four loop/configuration combinations: Manufacturer A Adjustable, Manufacturer B Adjustable, and Manufacturer C Cartridge. For each valve, pressure loss was calculated at three Cv states: the fully closed (minimum) Cv, the fully open (maximum) Cv, and the design Cv. Tables 7 and 8 present these results for the SHORT and LONG configurations, respectively. The ΔP Range column represents the difference in pressure loss between the fully closed and fully open Cv states, indicating the hydraulic authority the TBV exercises over the loop under modulating conditions.

Table 7: TBV Pressure Loss by Manufacturer and Cv State — SHORT Configuration

Loop	Manufacturer / Type	Flow [GPM]	Size [in]	Design Cv	ΔP @ Closed Cv [ft hd]	ΔP @ Open Cv [ft hd]	ΔP @ Design Cv [ft hd]	ΔP Range [ft hd]
A	Mfr. A — Adjustable	0.72	3/4"	0.52	22.64	0.27	4.43	22.37
A	Mfr. B — Adjustable	0.72	3/4"	0.35	22.64	0.34	9.78	22.30
A	Mfr. C — Cartridge	0.72	3/4"	0.85	29.94	0.37	1.66	29.57
B	Mfr. A — Adjustable	2.50	1"	1.90	14.48	0.75	4.01	13.73
B	Mfr. B — Adjustable	2.50	1"	1.87	10.05	1.41	4.14	8.64
B	Mfr. C — Cartridge	2.50	1"	1.57	361.96	1.33	5.87	360.63

Notes:

Design Cv is the Cv at which the valve operates at the design flow rate for that loop.

Table 8: TBV Pressure Loss by Manufacturer and Cv State — LONG Configuration

Loop	Manufacturer / Type	Flow [GPM]	Size [in]	Design Cv	ΔP @ Closed Cv [ft hd]	ΔP @ Open Cv [ft hd]	ΔP @ Design Cv [ft hd]	ΔP Range [ft hd]
A	Mfr. A — Adjustable	0.89	3/4"	0.52	34.59	0.41	6.77	34.18
A	Mfr. B — Adjustable	0.89	3/4"	0.35	34.59	0.52	14.94	34.07
A	Mfr. C — Cartridge	0.89	3/4"	0.85	45.74	0.56	2.53	45.18
B	Mfr. A — Adjustable	3.80	1"	1.90	33.36	1.72	9.24	31.64
B	Mfr. B — Adjustable	3.80	1"	1.87	23.16	3.26	9.54	19.90
B	Mfr. C — Cartridge	3.80	1"	1.57	833.91	3.06	13.53	830.85

Several important findings emerge from this Cv comparison. First, the range of pressure loss across TBV operating states is extremely wide, spanning from less than 1 ft of head at fully open Cv to over 800 ft of head at fully closed Cv for a cartridge-type valve at high flow. This spread has profound implications for pump sizing: a pump sized to the design Cv pressure drop may be entirely inadequate when the valve modulates toward its closed position under high-temperature conditions, while sizing to the closed Cv condition would result in gross over-pumping when the valve is open.

Second, manufacturer selection has a disproportionate effect on system hydraulics. For the same loop and flow condition, pressure loss at design Cv varies by a factor of two to six among the three manufacturers evaluated.

This variation is amplified in the LONG configuration due to its higher flow rates. For Loop B in the LONG configuration, design Cv pressure losses range from 9.24 ft hd (Manufacturer A) to 13.53 ft hd (Manufacturer C), a 47% spread that directly impacts pump head sizing.

Third, cartridge-type TBVs exhibit particularly high closed Cv pressure losses at higher flow rates, driven by the inherently low minimum orifice area of fixed-cartridge designs. While cartridge valves offer installation simplicity and tamper resistance, their hydraulic behavior near the closed position can create severe system imbalance if not accounted for in pump selection. Adjustable-type TBVs generally demonstrate more moderate closed Cv pressure losses and a wider practical operating range at the flow rates encountered in this study.

These findings underscore that TBV placement, PRM-based flow calculation, and valve Cv selection must be treated as an integrated design process rather than sequential steps or assumed to work. The pressure loss introduced by the TBV under modulating conditions is not a fixed value but a dynamic range that the system pump must accommodate. Treating TBV selection as a post-sizing detail after the pump has already been specified is a design error that can result in inadequate circulation or excessive energy consumption. A comprehensive TBV selection methodology, incorporating Cv operating range analysis against system curve characteristics, warrants dedicated study and is proposed as the focus of a Part 2 analysis.

6.3 Design Guidance

Based on this analysis, the following design guidance is offered for TBV placement in domestic hot water recirculation systems:

1. Placing TBVs immediately after the last fixture connection (SHORT configuration) results in lower total system flow (31% less), lower pump head requirements (45% less pressure loss), and near-target supply temperature performance. This configuration is recommended for systems where energy efficiency and pump sizing are primary concerns.
2. Placing TBVs immediately before the return branch junction (LONG configuration) results in the PRM assigning flow to maintain temperature through the full return branch. This may be appropriate where long return runs pass through unconditioned or poorly insulated spaces requiring active thermal protection, but engineers should carefully evaluate the resulting pump sizing and operating cost impact. Additionally, for buildings that require design to mitigate for Legionella [2,3], improved control of the hot water return piping to reduce growth conditions indicates that TBV's should be located immediately before the return branch junction, or higher temperature TBV's may be required.
3. The PRM should be applied with explicit documentation of which piping segments are considered upstream of each TBV. This requires that valve placement be determined before or concurrently with PRM modeling, rather than as a specification detail added after system sizing is complete.

7 Conclusions

This study demonstrates that thermostatic balancing valve placement has a significant and quantifiable effect on domestic hot water recirculation system performance as determined by the Product Ratio Method and as analyzed by the Hardy Cross + Heat Integration method. Moving TBVs from the fixture-adjacent position (SHORT) to the junction-adjacent position (LONG) in a prototype two-loop system increased total system flow by 31.3% and maximum system pressure loss by 45.4%. These differences arise directly from the PRM's mechanism for assigning heat losses to flow ratios: piping upstream of each TBV is attributed to that loop's flow requirement, while piping downstream is not. Valve location therefore determines the thermal boundary of each loop in the PRM model, and must be established before or concurrently with PRM segment identification.

First, TBV location directly governs the flow rate and pressure loss that the recirculation system must deliver, and therefore governs pump sizing. In this study, moving TBVs from the fixture-adjacent to the junction-adjacent position increased required system flow by 31.3% and maximum pressure loss by 45.4%. These are not marginal differences: they translate to a materially larger pump, larger electrical service, higher operating energy cost, and increased life-cycle cost. Engineers applying the PRM must recognize that TBV placement is

a pump sizing decision, not merely a valve placement detail. The system hydraulic design and the valve placement strategy must be developed together.

Second, while the SHORT configuration is more energy efficient, there are circumstances where the LONG configuration's higher flow rates and extended thermal coverage of the return piping represent a deliberate design choice rather than an inefficiency. Where prevention of waterborne pathogen growth is a primary concern, the junction-adjacent TBV placement offers a meaningful advantage: by maintaining higher circulation flow through the full length of the return branch, it reduces return temperature drop and improves the potential to keep temperatures throughout the return piping further from the *Legionella pneumophila* growth range [2, 3]. In this study, total temperature drops for the LONG configuration (3.22°F for Loop A, 3.21°F for Loop B) were consistently lower than those for the SHORT configuration (4.17°F and 4.82°F, respectively), reflecting improved thermal maintenance throughout the return piping. For healthcare facilities, high-risk occupancy buildings, or systems with long return branches through unconditioned spaces, this benefit may justify the additional pump capacity required. The decision between configurations therefore involves a direct tradeoff between energy efficiency and infection control risk tolerance, a tradeoff that must be made explicitly by the engineer and owner, not by default.

Third, TBV selection—specifically, the Cv operating range of the chosen valve—is a vital and underexamined dimension of hot water recirculation system design that deserves dedicated study as a Part 2 analysis. The initial findings presented here reveal a wide range of pressure drop outcomes depending on both TBV location and manufacturer. Design Cv pressure losses for Loop B ranged from 4.01 to 5.87 ft hd in the SHORT configuration and from 9.24 to 13.53 ft hd in the LONG configuration across the three manufacturers evaluated. More striking, pressure losses at the fully closed Cv ranged from 10.05 to 361.96 ft hd in the SHORT configuration and from 23.16 to 833.91 ft hd in the LONG configuration for Loop B alone. These ranges far exceed the system piping pressure losses in the same loops, hinting that the TBV may have a larger influence on hydraulic conditions under modulating conditions. No single valve selection methodology currently exists in US plumbing engineering practice that integrates PRM-based flow rates, Cv operating range, system curve compatibility, and valve authority into a unified design procedure. A dedicated Part 2 study addressing these topics, including variable-speed pump interaction with modulating TBV behavior, is warranted and proposed.

In summary, TBV placement, PRM-based flow sizing, and TBV Cv selection form an interdependent design triad. No element can be responsibly addressed in isolation. The Product Ratio Method provides a rigorous and accessible framework for quantifying the flow and pressure implications of placement decisions, and its integration with Cv-based valve analysis—as demonstrated here—represents a meaningful step toward a more complete design methodology for domestic hot water recirculation systems.

Acknowledgments

The author would like to thank John Lansing for his foundational work in developing and describing the Product Ratio Method, which continues to serve as the analytical basis for this line of research, along with his continued support in the development of this paper which included concept discussions and peer review.

.

References

[1] American Society of Plumbing Engineers. "ASPE Plumbing Engineering Design Handbook – Volume 2 Plumbing Systems." Chapter 6 – Domestic Water Heating Systems. 2022–2023.

[2] American Society of Plumbing Engineers. "Engineering Methodologies to Reduce the Risk of Legionella in Premise Plumbing Systems." 2023.

[3] National Academy of Sciences Engineering and Medicine. "Management of Legionella in Water Systems." 2023.

[4] Lohr, C. "Improving Domestic Hot Water Recirculation Sizing Using Hardy-Cross and Product Ratio Methods." 2025 Symposium CIB W062. 2025.

[5] Lansing, J. The Product Ratio Method – An Approach for Determining Circuit Flow Rates in Domestic Hot Water Systems." ASPE Pipeline Website. July 19, 2021. Accessed May 11, 2026. https://aspe.org/pipeline/the-product-ratio-method-an-approach-for-determining-circuit-flow-rates-in-domestic-hot-water-circulation-systems/

Presentation of Authors

Christoph Lohr, PE is IAPMO's Vice President of Technical Services and Research. Christoph has over a decade of experience in designing plumbing systems and has a reputation as a results-oriented expert, particularly in the realm of balancing waterborne pathogen prevention and water sustainability. He is a distinguished graduate from the Virginia Military Institute with a Bachelor of Science in Mechanical Engineering.

Measuring Pressure Loss in Modern Plumbing Fittings

Natascha Milesi Ferretti (1), Lingnan Lin (2)

(1) natascha.milesi-ferretti@nist.gov

(2) lingnan.lin@umd.edu

(1) National Institute of Standards and Technology (NIST), Gaithersburg, MD 20899, USA

(2) University of Maryland, College Park, MD, USA

Abstract

The pressure loss characteristics of tube fittings are essential to plumbing system design, yet in the USA there is no standardized test method and manufacturers rarely provide pressure loss data for fittings. We present an overview of ongoing plumbing hydraulics research to develop a method for characterizing pressure losses in fittings. The method was used to investigate pressure losses across three commonly used ¾-inch elbows (glue-joint CPVC, solder-joint copper, push-to-connect brass). A custom test rig was constructed to measure static pressure upstream and downstream of each fitting across a range of flow velocities (0.3 m/s (1 ft/s) to 3 m/s (10 ft/s)), corresponding to Reynolds numbers from 6,400 to 64,000. The measured pressure loss coefficients agree with predictions from existing methods based on bend radius. These results contribute to a more accurate understanding of how different materials and internal profile configurations affect performance in plumbing systems. The goal is to lower the practical barrier to manufacturers collecting pressure-loss data to support more efficient system designs, potentially reducing construction costs, improving fixture performance, and conserving water in both new construction and retrofits.

Keywords

Flow; Head Loss; Water; Fittings; Plumbing.

1 Introduction

Characterizing pressure losses within a piping system is of primary importance because they are directly related to sizing pipes, fittings, and pumps. Incorrect sizing can hinder the achievement of desired flow rates and increase installation and operational costs [1]. Furthermore, there are water quality concerns as oversized pipes can increase water age and lower disinfectant residuals, fostering conditions favorable for the growth of pathogens such as Legionella pneumophila [6]. Existing, publicly available pressure loss data originate from outdated studies of fittings that were common in the USA in the early 20th century, manufactured with materials and geometric designs that are no longer representative of modern plumbing fittings [2]. It was also learned that, in the USA, there is no standard method in the plumbing industry to test fittings for pressure loss. Over the past 5 years, NIST researchers built the Plumbing Hydraulics Laboratory to better understand the fluid flow in modern pipes and fittings and to inform the development of a practical and reliable standard method of test to characterize pressure losses in tube fittings with different materials, geometries, and connection types, without requiring a dedicated instrumented test section for each fitting. This document is an overview of the methodology used and presents example measurements for four common plumbing fittings tested in the NIST Plumbing Hydraulics Laboratory: a glue-joint CPVC elbow, a solder-joint copper elbow, a push-to-connect brass elbow, and a PEX tube bend [5].

2 Test Facility and Methodology

The experimental setup at NIST consists of a closed water loop driven by a variable-speed centrifugal pump [3]. The test section, shown in Figure 1, includes a 1.5 m upstream tube and a 2.1 m downstream tube. Data collection captures key measurements: density and mass flow rate using 3 Coriolis flow meters, temperature using PT100 RTDs, and pressures using both absolute and differential pressure transducers. The pressure measurement stations were designed with custom piezometer rings (three upstream, seven downstream) to sequentially scan static pressures.

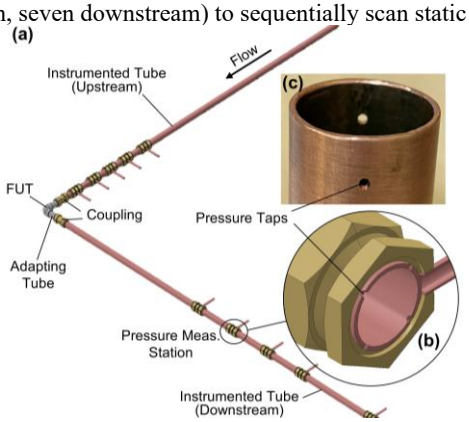

Figure 1. Illustration of the test section: (a) setup for a test elbow with adaptors; (b) cross section of a pressure measurement station; (c) photograph of the test tube with pressure taps. [5]

One practical challenge was finding a repeatable way to connect the fitting under test (FUT) to instrumented tube. We developed a streamlined, two-phase method using adaptors. Phase I involves measuring the pressure loss of the adaptor assembly (two couplings and an adapting tube) across a range of Reynolds numbers. In Phase II, the adapting tube is cut, and the FUT is inserted. The pressure loss due to the fitting is obtained by subtracting the correlated adaptor loss from the total measured assembly loss [5].

3 Results and Discussion

In 2025, NIST tested three 90° elbows (CPVC, copper, and brass) and a PEX tube bend. Measured pressure loss coefficients (K) are shown in Figure 2 to decrease with increasing Re before plateauing. The push-to-connect brass elbow produced the greatest pressure loss among all fittings tested due to sharp internal geometry [5]. Data screening based on straight-tube friction factors was used to validate fully developed flow. It was found that increasing upstream tapping locations, from three to five, reduced the expanded uncertainty by up to 75% [4,5].

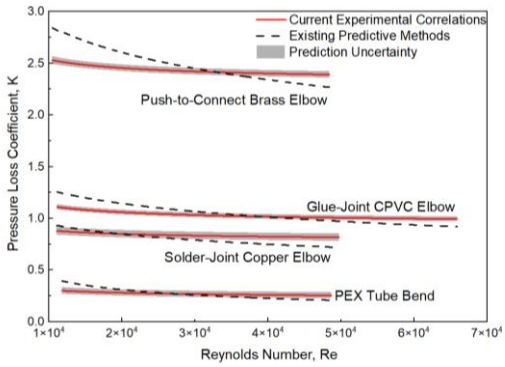

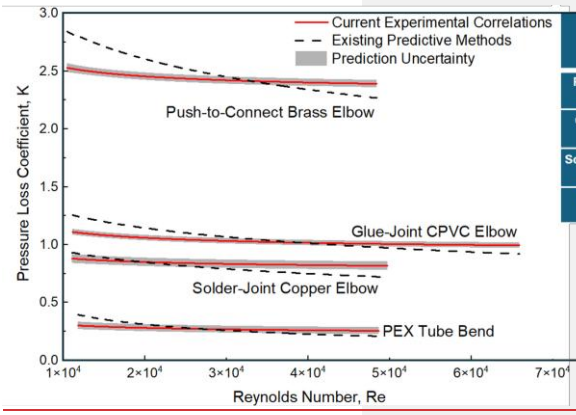

Test Fitting	Prediction uncertainty	Prediction uncertainty (%)
Push-to-connect brass elbow	0.032–0.039	1.3-1.5%
Glue-joint CPVC elbow	0.024–0.026	2.2–2.4%
Solder-joint copper elbow	0.036–0.040	4.2–4.5%
PEX tube bend	0.030–0.033	10.6–12.0%

Figure 2. Comparison of current experimental correlations with existing predictive methods for pressure loss coefficient of elbows and the associated prediction uncertainty. The prediction is primarily based on the bend radius. [5]

4 Conclusions

The NIST Plumbing Hydraulics Laboratory successfully established a practical measurement method for plumbing fittings to support the goal of 'right-sizing' premise plumbing for the US building stock, yielding improved building water quality, greater water savings, and lower operating and installation costs. [5]. Advancements include

Met opmaak: Links, Afstand Na: 12 pt, Regelafstand: Meerdere 1,15 rg

refined approaches for pressure measurement, repeatable test-fitting installation, and methods to reduce uncertainty. Future efforts will focus on standardizing terminology, expanding the method to complex branching fittings, and working with standards development organizations to establish a consensus standard for measuring pressure loss in modern plumbing fittings.

Acknowledgments

The authors acknowledge Glen Glaeser for constructing the Plumbing Hydraulics Laboratory, Victor Mathias for conducting tests, and Henry Gagliardi for assistance with method development and data analysis. University of Maryland collaborators were supported by the NIST Measurement Science and Engineering Research Grant (Award Number: 70NANB25H084), the NIST Professional Research Experience Program, and the NIST Summer Undergraduate Research Fellowship. The fittings under test were provided under a Materials Transfer Agreement with the Plastics Pipe Institute (MTA-24-063).

heeft opmaak toegepast: Lettertype: Times New Roman, 14 pt, Vet

Met opmaak: Afstand Voor: 0 pt

References

[1] ASHRAE (2021) Chapter 22 - Pipe Design. ASHRAE Handbook - Fundamentals.
[2] Lin L., et al. (2022) State-of-the-art review on pressure losses. NIST TN 2206.
[3] Lin L., et al. (2024) Test facility for pressure losses. NIST TN 2294
[4] Lin L., et al. (2025) Measurement and Uncertainty Analysis. NIST TN 2342
[5] V. Mathias, H. Gagliardi, G. Glaeser, N. Milesi-Ferretti, L. Lin, (2026) A practical method for measuring pressure loss characteristics in tube fittings. ASME Journal of Fluids Engineering, ~~(Accepted for publication).~~(Accepted for publication).
[6] NASEM (2019) Management of Legionella in Water Systems. National Academies.

5 Presentation of Authors

Natascha Milesi Ferretti is a Supervisory Research Engineer at the Engineering Laboratory of the U.S., National Institute of Standards and Technology.

Lingnan Lin is an Assistant Professor at the University of Maryland.

Study on Hot Water Supply Systems for Reducing Energy Consumption in Japanese Hospitals

Takeru Tamiya (1), Takehiko Mitsunaga (2)

(1) ce263053@meiji.ac.jp
(2) mitsunaga@meiji.ac.jp
(1)(2) Meiji University, Japan

Abstract

This study aims to obtain fundamental insights to support the development of strategies for reducing energy consumption associated with hot water supply in hospitals, which accounts for a large share of energy use. An empirical analysis was conducted using databases of building services systems in Japan. By analyzing hot water supply systems, heat sources, and the Building Energy Index (BEI) for both conventional buildings and Net Zero Energy Buildings (ZEBs), the feasibility of reducing hot water energy consumption was examined. The findings of this study are expected to contribute to the planning of energy-efficient hot water supply systems.

Keywords

Energy Consumption; Hot Water Supply; ZEB (Net Zero Energy Building); BEI (Building Energy Index)

1 Introduction

Hot water supply is one of the major energy uses in Japanese buildings. In particular, hospitals have substantial hot water demand due to activities such as handwashing, cooking, and bathing, resulting in a higher share of energy consumption for hot water supply compared to other building types. Therefore, reducing energy consumption in hot water supply systems is an urgent issue.

Although there are reports on measured hot water consumption and analyses of heat source systems in individual hospitals, these data are limited in scope. A comprehensive understanding based on statistical data is required to examine system improvements.

This study aims to obtain fundamental insights to support the development of energy reduction strategies for hot water supply. An empirical analysis was conducted using databases of building services systems in Japan.

2 Methodology

Table 1 shows the number of hospitals in each database used for the analysis. [1] contains data on conventional buildings, whereas [2] and [3] contain data on ZEBs. Regarding the data on ZEBs, [2] is for heat source analysis, and [3] is for BEI analysis. Hospital scales are categorized by total floor area as follows: Small (≥ 1,200 m^2), Medium (≥ 6,000 m^2), and Large (≥ 30,000 m^2).

ZEB is a Japanese building certification system, that evaluates based on their designed energy consumption. It refers to buildings that achieve significant energy savings while maintaining indoor environmental quality, and aim to maximize energy self-sufficiency through the use of renewable energy, ultimately targeting a net-zero annual primary energy balance. It is a relatively recent system, having been launched in late 2015, and the number of cases remains limited. Achieving ZEB status is particularly challenging for large facilities because of their substantial energy demand from equipment. Consequently, few such cases have been reported.

Table 1－Number of hospitals in each database

Database	Building type	Fiscal year	Number of hospitals	Small	Medium	Large
[1]	Conventional	1985-2023	598	138	329	131
[2]	ZEB	2017-2025	84	61	21	2
[3]	ZEB	2017-2025	23	7	15	1

*Clinics with less than 1,200m^2 were excluded due to the small number of cases.

3 Heat source for hot water system

In conventional hospitals, centralized hot water supply systems, including those combined with decentralized systems, account for more than 87% across all scales. Therefore, the analysis of heat sources in conventional buildings focuses on hospitals with centralized systems.

Figure 1 shows the adoption ratios of hot water heat sources by building scale in both conventional and ZEB hospitals. In conventional buildings, boilers account for more than 60% across all scales. One possible reason for the widespread use of boilers, is that steam boilers used for medical equipment sterilization are also utilized for hot water supply.

On the other hand, heat pump water heaters (HPs) account for more than 50% in ZEBs. This suggests that high-efficiency heat sources are introduced for hot water supply in

ZEBs, while sterilization processes may be handled either by separate steam boilers or by alternative methods, such as chemical sterilization using ethylene oxide gas.

In addition, cogeneration waste heat and solar heat are also utilized in ZEBs following HPs, suggesting that energy savings can be achieved not only through high-efficiency heat sources but also through the use of waste heat and renewable energy.

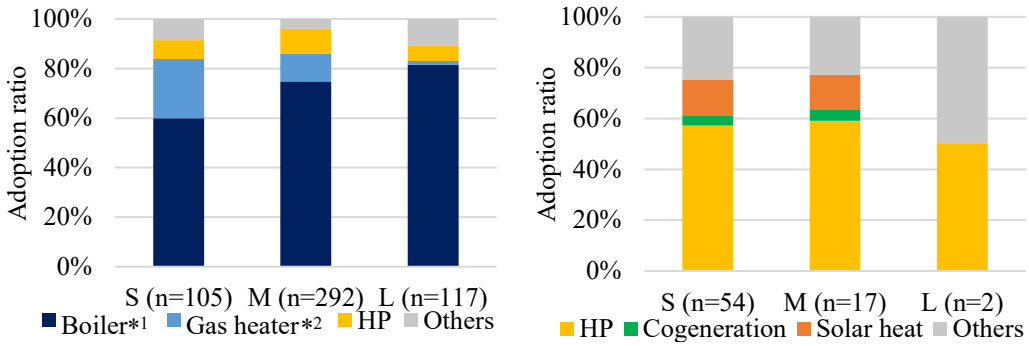

(a) Conventional facilities (b) ZEB

*Multiple answers allowed for both (a) and (b).
*1Boilers include heat exchanger–only responses.
*2Gas heaters include instantaneous water heaters with unspecified fuel.

Figure 1－Adoption ratios of hot water heat sources by building scale

4 Hot water supply BEI in ZEB

BEI is an index defined as the ratio of primary energy consumption to the reference value specified by Japanese standards. In this study, the effectiveness of improving hot water supply efficiency is evaluated by comparing the designed and actual BEI in ZEBs.

Figure 2 shows the designed and actual BEI for hot water supply in ZEBs. In 17 out of 23 buildings, the actual BEI is lower than the designed BEI. This indicates that energy-saving performance exceeding the designed values has been achieved under operational conditions, although ZEB evaluation is based on designed values.

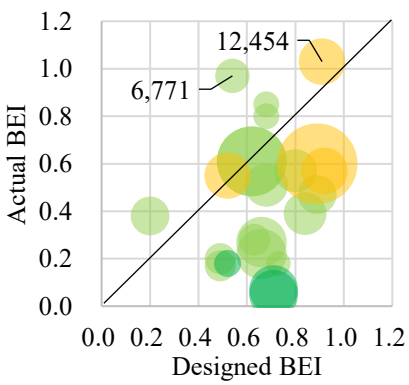

ZEB Rank	Definition
●Nearly ZEB (n=3)	More than *75%* reduction in primary energy consumption, *including* renewable energy.
●ZEB Ready (n=16)	More than *50%* reduction in primary energy consumption, *excluding* renewable energy.
●ZEB Oriented (n=4)	More than *30%* reduction in primary energy consumption, *excluding* renewable energy.

*Bubble size represents the total floor area [m^2].

Figure 2－Designed and actual BEI for hot water supply in ZEBs

The largest difference is observed in a case where the designed value is 0.71, whereas the actual value is 0.05, corresponding to a 93% reduction. Therefore, further investigation is required from the perspectives of both design assumptions and operational conditions, to achieve a more detailed understanding of methods for substantially reducing energy consumption during actual operations.

5 Conclusions

This study investigated the actual conditions of hot water supply systems in conventional and ZEB hospitals using building services databases.

In ZEBs where HPs are widely adopted, improvements in energy efficiency for hot water supply are observed based on both the designed and actual BEI. Therefore, it is suggested that HPs can contribute to reductions in energy consumption for hot water supply.

On the other hand, the majority of hospitals still employ centralized systems using boilers. To reduce energy consumption in these systems, further investigation is required into the promotion of cogeneration waste heat utilization and renewable energy sources, such as solar heat, as well as into methods for reducing heat losses and pump power consumption associated with hot water circulation.

6 References

[1] Japanese Association of Building Mechanical and Electrical Engineers, Building services annual database ELPAC 2025 (in Japanese)
[2] Sustainable open Innovation Initiative, ZEB leading owner list, https://sii.or.jp/zeb/leading_owner/search/example/, May 1 2026 (in Japanese)
[3] Sustainable open Innovation Initiative, Public data, ZEB demonstration project, https://sii.or.jp/opendata/#prj7, May 1 2026 (in Japanese)

7 Presentations of author

Takeru Tamiya is a graduate student at the Mitsunaga Laboratory of Meiji University, Japan. The main research projects include studies on hot water supply system for hospital facilities and on application of small pumping drainage system.

Optimal Operation of Hybrid Water Heating Systems in Non-Residential Buildings

Misuzu Shima (1), Takehiko Mitsunaga (2)

(1) ce253068@meiji.ac.jp
(2) mitsunaga@meiji.ac.jp
(1)(2) Meiji University, Japan

Abstract

Hybrid water heating systems use both a heat pump water heater (HP) and combustion water heater. The HP covers the base hot water demand, while the combustion water heater supplies the remaining demand.

This type of system can reduce installation costs and required pace, and it can also improve energy efficiency. However, optimal control and operation methods for these systems have not been sufficiently studied.

The purpose of this study is to examine how different operation control modes affect energy use in non-residential buildings. We analyzed three operational control modes for hospitals, hotels, central kitchens, and employee cafeterias. We compared their energy consumption and discussed the conditions for optimal operation.

Keywords

Hybrid water heater; Heat pump water heater; Combustion water heater; hot water system.

1 Introduction

In Japan, when constructing a new building, energy performance must generally be evaluated using the web-based evaluation program in accordance with the Building Energy Efficiency Act.

However, evaluation methods for hybrid water heating systems in non-residential buildings have not yet been sufficiently developed, and their energy-saving effects are not properly reflected. Therefore, the development of an evaluation method that considers actual operational conditions is required.

A hybrid water heating system combines a HP and a combustion water heater. The high-efficiency HP covers the base hot water demand, while the combustion water heater supplies the remaining load. This system is expected to achieve both high energy efficiency and reductions in installation cost and required space. On the other hand, its energy performance changes depending on operation control methods and operating conditions.

This study aims to compare and analyze the effects of different operation modes of hybrid water heating systems on energy consumption in hospital, hotel, central kitchen, and employee cafeteria.

2 Methodology

In this study, three operation modes of a hybrid water heating system and a combustion water heater only operation were compared in terms of energy consumption for four building types: hospital, hotel, central kitchen, and employee cafeteria. Table 1 shows the specifications of each system, including tank capacity, heating capacity, and hot water load. These specifications were set under identical conditions for all operation modes.

Table 1 – Specifications of Hybrid Hot Water Systems and Hot Water Demand

Building type		Hospital	Hotel	Central kitchen	Employee cafeteria
Tank capacity [L]		6,857	2,786	5,143	5,486
Heating capacity [kW]	HP (COP : 4)	44	18	33	35
	Combustion water heater (Efficiency : 0.85)	384	576	959	384
Hot water demand [MJ/Day]		4,604	5,180	3,453	3,683

Table 2 – Overview of Operating Mode

Operating mode	Mode 1	Mode 2	Mode 3
Operation strategy HP heat storage mode HP base load mode HP tank Combustion heat water	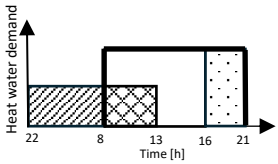	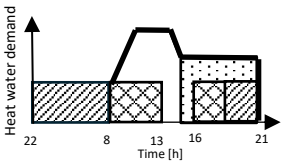	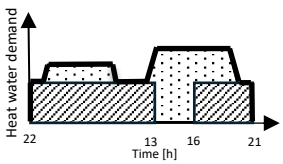
System configuration HP : Heat pump water heater C : Combustion heat water T : tank	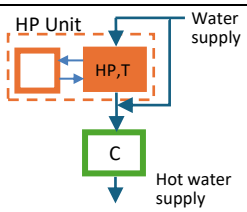	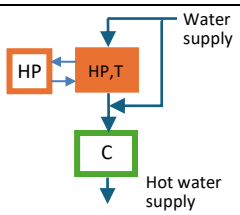	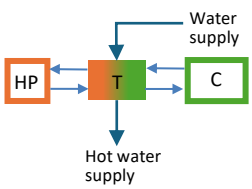
Operation details*	At night, the HP charges the storage tank, while the nighttime hot water load is covered by the combustion water heater. During the daytime, the HP follows the hot water load, but its operation is stopped after 13:00. Any remaining demand is supplied in order by the storage tank and then the combustion water heater.	At night, the HP charges the storage tank, while the hot water load is covered by the combustion water heater. During the daytime, the HP follows the hot water load. Any remaining demand is supplied in order by the storage tank and then the combustion water heater.	Both the HP and the combustion water heater charge the same storage tank. The HP continuously follows the hot water load, and any remaining demand is covered by the combustion water heater.

*In all operation modes, the HP was stopped from 13:00 to 16:00 to reduce peak electricity demand

The operation modes were defined based on the system configuration, and their details are shown in Table 2. Each mode has different operating schedules for the water heaters and the HP operates in two modes: heat storage mode and base load mode.

3 Comparison of Energy Consumption

Table 3 shows the energy consumption for each building type and operation mode. Figure 1 presents the hourly hot water load profiles for each building type, and Figure 2 shows the hourly load distribution among the water heaters for each operation mode in the hospital. When comparing each building type with hot water demand, the energy consumption ratio was found to be 69–106%. When comparing the building types, in hospital, central kitchen, and employee cafeteria. Mode 2 showed the highest reduction,

Table 3 – Energy Consumption for Each Building Type and Operating Mode

Mode	Hospital		Hotel		Central kitchen		Employee cafeteria	
	Energy consumption [MJ/Day]	Ratio* [%]	Energy consumption [MJ/Day]	Ratio* [%]	Energy consumption [MJ/Day]	Ratio* [%]	Energy consumption [MJ/Day]	Ratio* [%]
1	4,044	88	5,478	106	3,043	88	3,429	93
2	3,195	69	5,074	98	2,821	82	3,013	82
3	3,662	80	4,955	96	3,405	99	3,528	96

*These ratios show the percentage of hot water demand for each building type.

*Energy consumption was calculated assuming a COP of 4.0 for the HP and an efficiency of 0.85 for the combustion water heater.

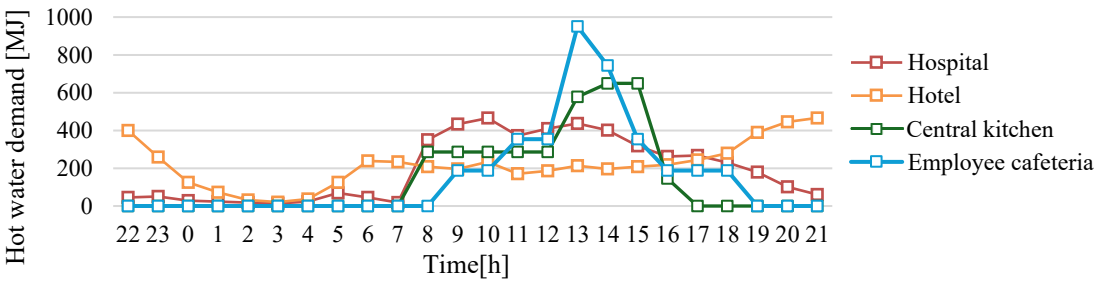

*The hourly hot water loads were calculated by applying the hourly hot water load ratios reported in Reference [1] to the daily hot water loads shown in Table 1.

Figure1 – Hourly Hot Water Demand by Building Type

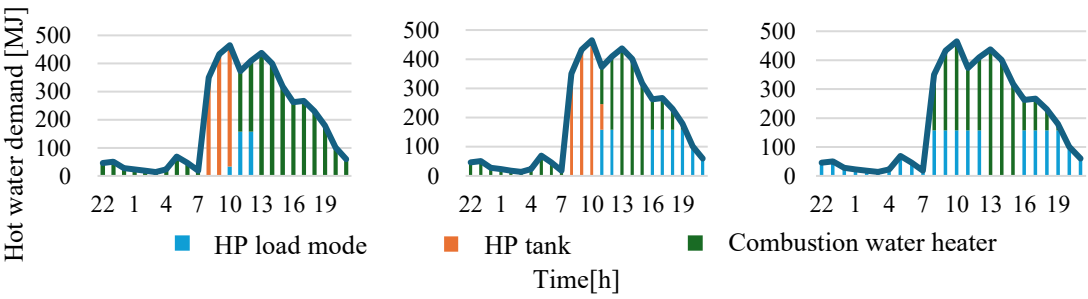

(a) Operating mode 1 (b) Operating mode 2 (c) Operating mode 3

Figure 2 – Case Studies of Hot Water Heat Source in Hospital

while in hotel, Mode 3 showed the highest reduction, because hot water demand is more distributed into nighttime hours. This is likely because the base load mode of the HP and the effective use of the storage tank reduced the operation of the combustion water heater.

As shown in Figure 1, hospitals have low nighttime hot water demand (22:00–8:00). Unlike central kitchens and employee cafeterias, their hot water load is spread throughout the day rather than concentrated in specific periods. As a result, the ratio of energy consumption to hot water load decreased by up to 69% in the hospital. This indicates that HP heat storage mode and effective tank utilization are feasible, and that hybrid water heating systems may achieve greater energy-saving effects under such conditions.

Table 4 shows the maximum hourly energy consumption of the combustion water heater for each building type and operating mode. No difference among the operating modes was observed for building types in which the peak hourly hot water load occurred during the HP shutdown period (13:00–16:00).

Table 4 – Maximum Hourly Energy Consumption of the Combustion Water Heater for Each Building Type and Operating Mode

Mode	Hospital	Hotel	Central kitchen	Employee cafeteria
1	437MJ/h	466MJ/h	649MJ/h	948MJ/h
2	437MJ/h	402MJ/h	649MJ/h	950MJ/h
3	437MJ/h	402MJ/h	649MJ/h	950MJ/h

4 Conclusion

This study compared and analyzed how different operating modes of hybrid water heating systems affect energy consumption. The results indicate that the most suitable operating mode varies depending on the timing of peak hot water demand, the hourly distribution of the load, and the characteristics of nighttime hot water demand.

5 References

[1] Hybrid Water Heating System Research Committee. Hybrid Water Heating System Design Manual, April 2009 (in Japanese)

[2] Building Research Institute (National Research and Development Agency), Hot Water Supply Section of Hybrid Systems Combining Electric Heat Pumps and Gas Instantaneous Water Heaters, https://www.kenken.go.jp/becc/documents/house/7-6_250401_v29.pdf, Accessed April 2026 (in Japanese)

6 Presentation of author

Misuzu Shima is a graduate student at the Mitsunaga Laboratory, Meiji University, Japan. Her research focuses on evaluation methods for energy consumption performance of water heating system and life cycle carbon assessment of rainwater utilization systems.

Digital Water Load: Integrating the Hidden Water Footprint of Generative AI into Building Water Assessments

Hana Nekrep, MSc Arch. (1)

1. hana.nekrep@fd.si

(1) Faculty of Design, Ljubljana, Slovenia

Abstract

Generative artificial intelligence is increasingly used in offices, universities, design studios and public buildings. Although it is commonly perceived as an immaterial service, its operation depends on data centres, electricity generation, cooling systems and specialised computing hardware. These systems consume freshwater directly at data-centre sites and indirectly through energy production, yet this demand is normally excluded from building water assessments. This study introduces digital water load as the water consumption attributable to digital and AI-supported activities initiated by building occupants. A literature-based framework connects user activity with Water Usage Effectiveness, electricity-related water intensity and an allocated share of embodied water in computing equipment. A teaching example from Artificial Intelligence in Design illustrates cumulative use: students required 6–30 image generations for one task, whereas skilled use of reference images and prompts produced a suitable result after approximately five generations. Because impacts vary with workload, hardware, cooling technology, electricity mix, location and time, the framework uses transparent ranges rather than a universal water-per-prompt value. Digital water load extends assessment beyond the building site and links occupant behaviour, AI literacy and infrastructure-scale water impacts.

Keywords

water footprint; generative artificial intelligence; data centres; Water Usage Effectiveness; digital water load.

1 Introduction

Artificial intelligence is embedded in writing, visualisation, translation, programming, administration, teaching and architectural design. From the user's perspective, these activities require only a device and an internet connection. Each interaction, however, activates a physical system of processors, servers, cooling equipment, electricity infrastructure and communication networks. The expansion of artificial intelligence is therefore not hydrologically neutral.

Water is consumed directly through cooling and humidification and indirectly through electricity generation. A wider life-cycle boundary also includes semiconductor and

server manufacturing. Data-centre operators commonly report Water Usage Effectiveness (WUE), expressed as litres of site water per kilowatt-hour of IT energy [1]. Source-based indicators may additionally include water associated with electricity production.

2 Research problem and objectives

Building water assessments mainly include fixtures, appliances, irrigation, cooling towers, process water and site metering. Remote computational services initiated by occupants are assigned to data centres or electricity producers. A building may therefore report on-site savings while increasing its dependence on water-consuming digital infrastructure. The apparent efficiency partly depends on where the assessment boundary is drawn.

Digital water load (DWL) is defined as the direct, indirect and allocated embodied water consumption associated with digital computational services initiated by building occupants or operational systems during a defined period.

The objectives are:

- to define a system boundary for building-related digital water consumption;
- to connect occupant activity with data-centre and electricity indicators;
- to complement conventional building water assessment; and
- to identify transparency requirements for implementation.

3 Methodology

The study applies a conceptual, literature-based and scenario-oriented methodology. Published research on the energy and water requirements of artificial intelligence, data-centre cooling, Water Usage Effectiveness (WUE), electricity-related water consumption and computing hardware is reviewed and translated into variables that can be related to building use.

The assessment distinguishes three components of digital water use: direct operational water consumed at data-centre facilities, mainly for cooling; indirect water associated with electricity generation; and an allocated embodied component related to the manufacture of processors, servers and other computing equipment. These components vary with model and workload, data-centre efficiency, cooling technology, electricity mix, climate, location and time of operation. Because embodied-water data are particularly uncertain, they should be reported separately where possible.
At building level, digital water load is estimated by combining the frequency and type of AI-supported activities initiated by occupants with the best available service-specific or literature-based water-intensity information. Where provider data are unavailable, transparent ranges and scenario assumptions are preferable to a single universal water-per-prompt value. Water withdrawal and water consumption should also be distinguished in reporting [2,3].

4 Illustrative scenario and preliminary findings

A practice-based example was observed in the Faculty of Design course Artificial Intelligence in Design. For one visual-material assignment, students generally needed 6–30 image generations, depending on their ability to formulate prompts and select reference images. For a group of n students, this represents approximately 6n–30n full-image generations for one assignment. With Vizcom, the most proficient students obtained a high-quality result after approximately five generations when they used appropriate references and precise instructions. Later changes were mostly minor local corrections made with generative fill rather than complete image regeneration.

Because provider-specific workload, energy and water data were unavailable, the example is an activity-based observation rather than a direct water measurement. It nevertheless shows that AI literacy and workflow design affect the number of full-image generations and therefore the computational load attributable to a building-based activity.

The preliminary findings are that cumulative use can be expressed as a building load; transparent ranges are more defensible than a single water-per-prompt value; text, image and multimodal workloads require different computation; AI literacy can reduce unnecessary repeated generations; and location is particularly important in water-stressed catchments.

5 Discussion

Digital water load reveals an impact that is absent from most building assessments. Occupants may work in buildings with low-flow fixtures, rainwater systems and detailed metering while using remote services whose water impacts are displaced and undisclosed. The building appears efficient because the assessment ends at the site boundary, not because every activity inside it has a low water footprint.

Responsibility should not be transferred entirely to users. Providers must disclose workload energy demand, PUE, site WUE, grid water intensity, location and uncertainty. However, the teaching example indicates that precise prompts, suitable reference images and local generative editing can avoid unnecessary full-image regeneration. Assessment can use three levels: a basic AI-use inventory, an intermediate calculation with peer-reviewed ranges and an advanced calculation with service-specific data.

6 Conclusions

Digital water load connects artificial-intelligence use with building water assessment. The proposed framework combines workload frequency, IT energy demand, WUE, PUE, electricity-related water intensity and an allocated embodied-water component. Its purpose is not to assign a fixed value to every prompt, but to provide a transparent structure for service-specific data or documented scenario ranges.

The teaching scenario shows that the number of generations required for a design task can vary substantially with user competence and workflow. Future work should validate the method in universities, offices and design studios; obtain service-specific data for text, image and multimodal systems; apply scarcity-weighted indicators; and examine integration with building certification and environmental reporting. Recognising digital

water load would not imply avoiding digital services. It would prevent their physical consequences from being excluded from claims of sustainable building operation.

7 References

1. The Green Grid, Water Usage Effectiveness (WUE): A Green Grid Data Center Sustainability Metric, White Paper No. 35, 2011.
2. Lei N, Lu J, Shehabi A and Masanet ER, The water use of data center workloads: A review and assessment of key determinants, Resources, Conservation and Recycling, Vol. 219, 108310, 2025.
3. Li P, Yang J, Islam MA and Ren S, Making AI Less "Thirsty": Uncovering and Addressing the Secret Water Footprint of AI Models, arXiv:2304.03271, 2023.
4. Shehabi A et al., 2024 United States Data Center Energy Usage Report, Lawrence Berkeley National Laboratory, 2024.
5. International Energy Agency, Energy and AI, Paris, 2025.
6. Alissa H et al., Using life cycle assessment to drive innovation for sustainable cool clouds, Nature, Vol. 641, pp. 331–338, 2025.

8 Presentation of author

Hana Nekrep, MSc Arch., is an interdisciplinary artist, architect and Senior Lecturer at the Faculty of Design in Ljubljana. Her research and teaching connect sustainable built environments, water systems, environmental ethics and artificial intelligence in design.

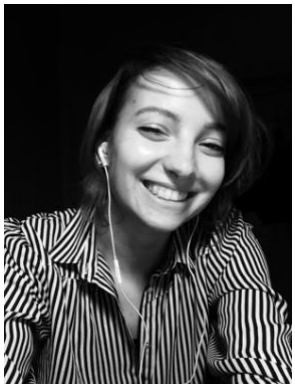

Calculation of energy consumption in large public baths

Part 1 CFD analysis of the amount of evaporative heat loss at the surface of the water in the bathtub

Ryo Fujimoto(1), Shizuo Iwamoto(2),

(1) ryo-fujimoto@kanagawa-u.ac.jp
(2) iwamotos@jindai.jp
(1) Assistant Professor, Kanagawa University, Japan
(2) Professor, Kanagawa University, Japan

Abstract

Energy consumption for large bathtubs in hotels and other lodging facilities, as well as public bathhouses, is not insignificant compared to the thermal load required for hot water supply for shampooing and body washing, making it a key issue in energy conservation related to hot water supply systems.

The energy consumption for bathtubs can be broadly categorized into the thermal load for filling the tub with hot water and the thermal load for maintaining water temperature. Regarding the thermal load for maintaining water temperature, sensible and latent heat losses from the water surface are particularly significant. While sensible heat loss is treated using the convective heat transfer coefficient and latent heat loss using the evaporation coefficient, it is difficult to set these values appropriately. The objective of this paper is to propose a valid method for determining these coefficients using computational fluid dynamics simulation.

Keywords

bathtubs; evaporative heat loss; experiments; computational fluid dynamics (CFD).

1 Introduction

Energy consumption for large bathtubs in hotels and other lodging facilities, as well as public bathhouses, is not insignificant compared to the thermal load required for hot water supply for shampooing and body washing, making it a key issue in energy conservation related to hot water supply systems.

The energy consumption for bathtubs can be broadly categorized into the thermal load for filling the tub with hot water and that for maintaining the water temperature. Regarding the thermal load for maintaining water temperature, sensible and latent heat losses from the water surface are particularly significant. Although sensible heat loss is treated using the convective heat transfer coefficient and latent heat loss using the evaporation coefficient, it is difficult to appropriately set these values.

Generally, using an evaporation coefficient is an effective method for determining the heat of evaporation from a water surface, and Akai et al. [1] proposed empirical formulas based on wind speed:

$$q_{\mathrm{evp}} = C_{\mathrm{N}} \cdot \Delta P \cdot A \cdot 0.2778\gamma \qquad [\mathrm{W}] \tag{1}$$

$$C_{\mathrm{N}} = \begin{cases} 0.114v + 0.134 & (v > 3.0\ [\mathrm{m/s}]) \\ 0.061v + 0.125 & (v \leq 3.0\ [\mathrm{m/s}]) \end{cases} \qquad [\mathrm{kg/(m^2 \cdot s \cdot kPa)}] \tag{2}$$

where ΔP is vapor pressure gap [kPa], A is water surface [m^2], and γ is evaporative latent heat [kJ/kg]. However, these formulas do not account for no-wind conditions. This paper compares the evaporation coefficients obtained from simple experiments, computational fluid dynamics (CFD) simulations, and the empirical formulas, and proposes a method for determining the evaporation coefficient.

2 Evaporation experiment

2.1 Experiments overview

A simple experiment was conducted to investigate the amount of evaporation and the evaporation speed from the water surface. As shown in Photo 1, an empty container was placed on a desktop scale and hot water was poured into it. Then, the water temperature and the room temperature and humidity were measured. At the same time, an anemometer was placed 15 cm above the edge of the container and the wind speed, temperature, and humidity were measured. The anemometer position is referred to as the "Monitor Point." A fan was placed at the position shown on the right side of Photo 1, and the experiment was conducted using three airflow patterns (high, low, and no wind) settings. Each experiment continued until the water temperature approached room temperature (approximately 28 °C). Measurements were taken at 1-s intervals.

Photo 1: The experiment in progress

2.2 Results of experiments

Since the measured weight could fluctuate due to vibrations in the water surface under both strong and weak conditions, all experimental results are presented as 10-s moving averages. This report presents only the experimental results for the strong condition in Figure 1. The wind speed was approximately 2.6 m/s, and the mass decreased from approximately 800 g to approximately 730 g. Although there were some fluctuations, the ambient temperature was generally around 28 °C. The temperature at the Monitor Point (blue line) is not visible because it overlaps with the room temperature (green line).

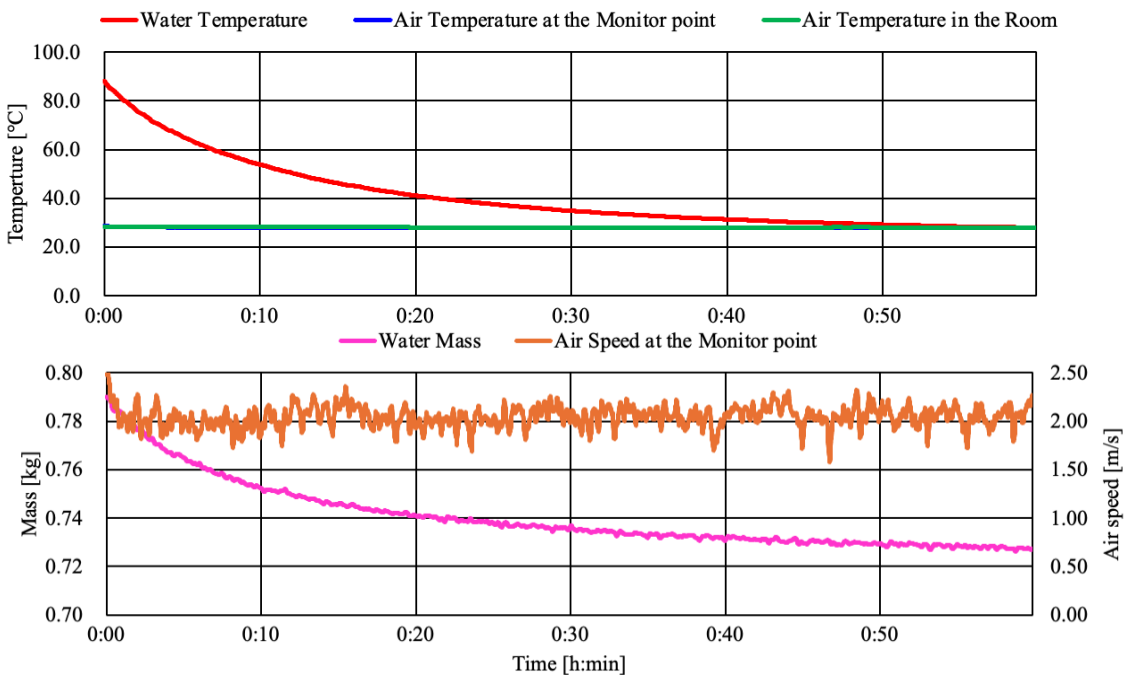

Figure 1 - Experimental data under the strong condition

3 Framework of CFD analysis

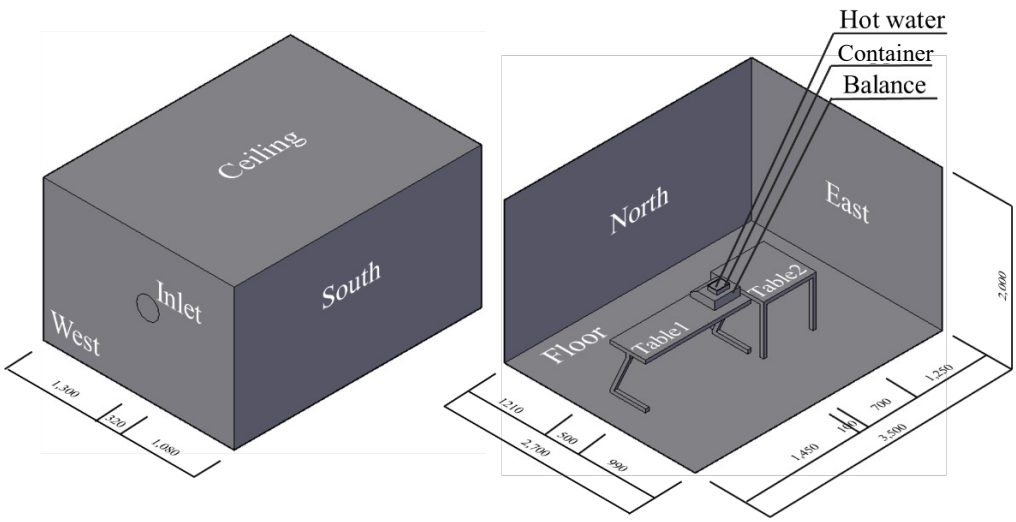

Figure 2 - A part of this laboratory

We attempted to reproduce the experiment using CFD analysis. Figure 2 shows a part of the laboratory. The calculation will be based on a part of this laboratory. To reduce computation time, the computational domain will be scaled down for the model. The turbulence model will be the low-Reynolds-number AKN k-ε model, and the boundary conditions for evaporation will use the scFLOW defaults. The heat transfer conditions will also be examined in the future.

4 Conclusion

Small-scale evaporation experiments were conducted under high-, low-, and fan-off conditions, and time-series data for water temperature, air temperature and humidity, air velocity, and water mass were obtained. Under the high-airflow condition presented in this extended abstract, the water mass decreased by approximately 70 g as the water temperature approached room temperature. These measurements provide validation data for the CFD model.

The CFD model, including the treatment of evaporation and heat transfer at the water surface, is currently being revised. The completed analysis will be used to compare the evaporation coefficients derived from the experiments, CFD simulations, and the correlation proposed by Akai et al., including the fan-off condition. The results of this comparison will be presented at the symposium.

5 References

[1] Akai H, Kamata M, Oda M, Heat loss from a large bathtub, the Society of Heating, Air-Conditioning and Sanitary Engineers of Japan, Jan. 1999

6 Presentation of Authors

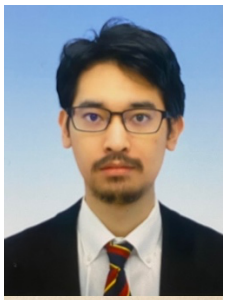

Ryo Fujimoto (M. Eng.) is a research associate at Department of Architecture and Building Engineering, Faculty of Architecture and Building Engineering, Kanagawa University. He is interested in built environment and building services such as air conditioning.

Shizuo Iwamoto (Dr. Eng.) is the presenter of this study and a professor at Department of Architecture and Building Engineering, faculty of Architecture and Building Engineering, Kanagawa University. He is interested in built environment and building services such as air conditioning and hot water supply system.

Study on simulation of building drainage systems by CFD

Part 5 Investigation of CFD analysis accuracy for siphonic drainage systems

Kazuki Yuki(1), Shizuo Iwamoto(2), Ryo Fujimoto(3), Kyosuke Sakaue(4), Takehiko Mitsunaga(5)

1. r202570120mp@jindai.jp
2. iwamotos@jindai.jp
3. ryo-fujimoto@kanagawa-u.ac.jp
4. sakaue@carrot.ocn.ne.jp
5. mitsunaga@meiji.ac.jp

(1) Graduate Student, Kanagawa University, Japan
(2) Professor, Kanagawa University, Japan
(3) Assistant Professor, Kanagawa University, Japan
(4) Emeritus Professor, Meiji University, Japan
(5) Associate Professor, Meiji University, Japan

Abstract

The flow of water and air in sanitary fixtures and drains has usually been analyzed using full-scale experiments because it is difficult to apply the laws of similarity. Further knowledge is needed for the optimal design of drainage systems, and computational fluid dynamics (CFD) simulations are expected to be used in addition to experiments.

In a previous report, we used CFD analysis to simulate drainage characteristics—such as pipe pressure, flow rate, and flow patterns—in a siphonic drainage system and compared the flow patterns with those from previous experiments. We found that the CFD results had a lower tendency for the siphon effect to occur compared to the experiments. Furthermore, under conditions of low inflow and low outflow head, differences remained in the occurrence of the siphon effect and the flow patterns, and we were unable to reproduce the bubble flow observed in the experiments.

In this report, with the aim of improving the accuracy of CFD analysis, we conducted additional investigations—including the reproduction of bubbles—focusing on changes to the computational scheme and mesh refinement to examine the effects of analysis and model conditions on the results. We report on these results.

Keywords

Building drainage systems; computational fluid dynamics; siphonic drainage systems

1 Introduction

The flow of water and air within sanitary fixtures and drain pipes is a multiphase flow, and because it is difficult to apply similarity laws, it has primarily been studied through full-scale experiments. However, further insights are needed for the optimal design of drainage systems, and in recent years there has been growing expectation of the use of computational fluid dynamics (CFD) analysis in addition to experiments.

In previous studies [1], CFD analysis successfully reproduced the drainage characteristics of siphonic drainage systems, confirming features of the siphon effect such as pressure fluctuations and increased flow rates. However, under conditions of low inflow rates and low outflow heads, discrepancies have been observed between the results and experimental data, and issues regarding analytical accuracy remain, such as the failure to reproduce the bubble flow confirmed in experiments.

In this study, we focus on computational schemes and mesh partitioning as factors affecting the accuracy of CFD analysis and investigate the impact has on the analysis results.

2 Methods

The analysis method in this study is fundamentally the same as that used in our previous study [1]. The CFD analysis was conducted using scFLOW. The volume-of-fluid method combined with the high-precision interface reconstruction method was applied to simulate multiphase flow. A low-Reynolds-number SST k-ω turbulence model was used for unsteady analysis.

The computational model was constructed based on previous studies [2]. Figure 1 shows the overall piping model, and Figure 2(a) shows the configuration of the inlet cylinder. Figure 2(b) indicates the boundary surfaces at the inlet.

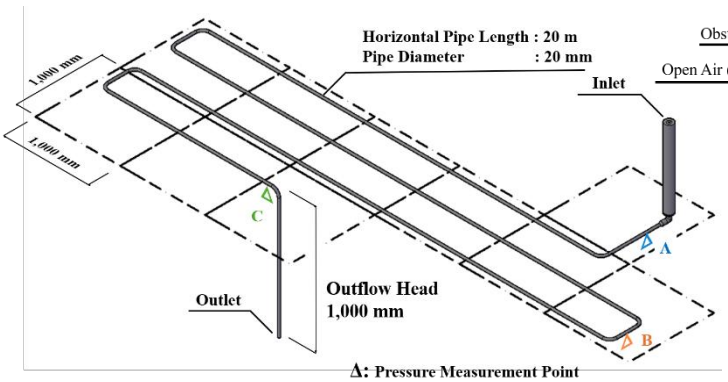

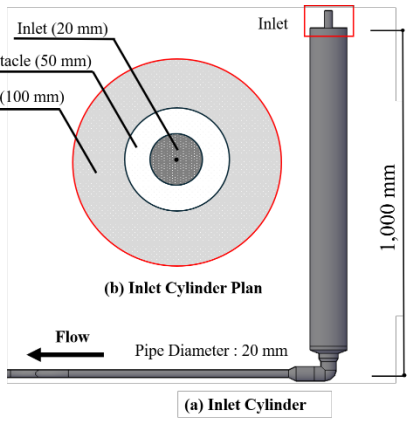

Figure 1 - Piping model **Figure 2 - Inlet cylinder configuration**

In this study, the following conditions were modified to investigate their effects on the reproduction of the siphon effect:

- Mesh resolution: a non-uniform mesh was used, with grid sizes of 3 and 4 mm. Boundary layer settings were applied with a thickness coefficient of 0.2 and five layers, resulting in minimum cell sizes of 0.6 and 0.8 mm, respectively.

- Boundary conditions: Based on the method proposed by Ichikawa et al.[3],total pressure (incompressible) with hydrostatic pressure ($-\rho gh$) was imposed at the open boundaries.

- Computational scheme: The previous scheme employed first-order temporal accuracy with the SMART scheme for the advection term, whereas the modified scheme employed second-order temporal accuracy with a blended advection scheme combining first-order upwind and second-order central differencing. The default blending setting provided in scFLOW was used.

Pipe pressure was measured at points A to C shown in Figure 1, corresponding to the inlet, midpoint and outlet, respectively. The flow rate was calculated from the discharge at the outlet.

Table 1 - Case definition

Case	Scheme	Grid size [mm]	Minimum cell size [mm]
Pre-4	Previous	4	0.8
Mod-4	Modified	4	0.8
Pre-3	Previous	3	0.6
Mod-3	Modified	3	0.6

Previous: First-order temporal accuracy, SMART scheme
Modified: Second-order temporal accuracy, Blended Upwind + Central differencing

3 Calculation results and discussion

Figure 3 shows the time history of pipe pressure, and Figure 4 shows the flow rate.

The siphon effect was observed only in the mod-3 case, whereas it was not observed in the other cases. In the mod-3 case, pressure fluctuations and an increase in flow rate were observed simultaneously, and the flow rate exceeded the inflow rate. Based on these behaviors, occurrence of the siphon effect was confirmed. In contrast, such behaviors were not observed in the other cases, and the siphon effect was not identified. These results indicate that reproducing the siphon effect requires not only mesh refinement but also an appropriate computational scheme.

This difference is considered to be related to the representation of the air–water interface at the outlet. In particular, near the elbow at the outlet, separation and re-mixing of air and water occur. Fluctuations of the water surface and bubble entrainment can interrupt the air path, resulting in a temporary blockage of the pipe. This temporary interruption of the air path is considered to contribute to initiation of the siphon effect.

When the mesh is relatively coarse or the computational scheme is not suitable, such small-scale interface fluctuations and bubble behavior cannot be adequately captured, and formation of the temporary blockage may be suppressed. In contrast, mesh refinement combined with an appropriate computational scheme enables the reproduction of such local flow phenomena.

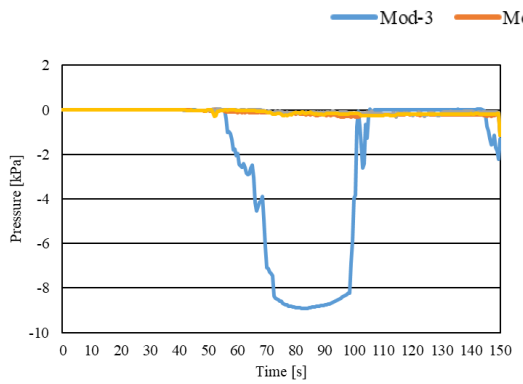

Figure 3 – Pressure (outlet)

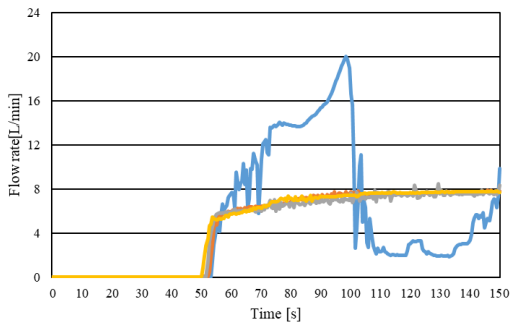

Figure 4 – Flow rate

4 Conclusion

In this study, the effects of minimum cell size and computational scheme on the reproduction of the siphon effect were investigated using CFD analysis.

The siphon effect was not reproduced with a grid size of 4 mm, whereas it was reproduced when the grid was reduced to 3 mm. It was also suggested that the behavior of the air–water interface at the outlet plays a significant role in the occurrence of the siphon effect, and that temporary interruption of the air path is a key factor.

These findings indicate that sufficiently small minimum cell size is essential for accurately reproducing the siphon effect in CFD analysis of drainage systems. Although the influence of the computational scheme was observed, its underlying mechanisms could not be clearly identified and remain a subject for future investigation.

5 References

[1] Yuki K et al. – Study on simulation of building drainage systems by CFD Part 4 Drainage characteristics of siphonic drainage systems, Proceedings of CIB-W062 Symposium, Aug. 2025.

[2] Inada T et al. – A study on characteristics of filled flow in siphonic drainage systems, Part 8 Experiments on flow characteristics of long piping, Technical papers of annual meeting, the Society of Heating, Air-Conditioning and Sanitary Engineers of Japan, Sep. 2011. (in Japanese)

[3] Ichikawa T et al. – Study on simulation of building drainage systems by CFD Part 3 Verification of seal water behavior and pressure fluctuations in S-trap pipes, Proceedings of CIB-W062 Symposium, Aug. 2025.

6 Presentation of Authors

Kazuki Yuki is a graduate student in the Department of Architecture, Graduate School of Engineering at Kanagawa University. His research focuses on building services, especially indoor siphonic drainage systems, using CFD analysis.

Integrating Head Loss Calculations into Network-Based Simulation of Water Supply Systems

D. Rich (1)*, T. Roberts (2)

(1) drew.rich@miami.edu, University of Miami, Department of Civil and Architectural Engineering, Miami, FL, USA, *Corresponding Author

(2) troberts@iccsafe.org, International Code Council, Canberra, ACT, Australia

Abstract

Traditional water supply design in the United States frequently relies on the "Equivalent Length" method to predict pressure drop. While established as a simplified manual calculation in the pre-computing era, this approach often oversimplifies complex hydraulic behaviors. To rectify these inaccuracies, this paper proposes the integration of automated pressure loss calculations into the Design toolkit for Robust International Plumbing Systems (DRIPS), a network-based simulation providing a novel, stochastic approach to estimate the expected simultaneous demand of components in plumbing systems.

The proposed methodology shifts away from broad approximations by implementing a comprehensive calculation suite that accounts for frictional, minor, and elevation head losses. By utilizing advanced K-value coefficients and the Darcy Weisbach formula, the model determines precise zonal pressure losses throughout the entire piping network. Unlike traditional methods that focus primarily on the most remote fixture, the DRIPS integration applies these rigorous calculations holistically. This granular approach provides engineers with accurate insights into localized areas of excess or deficient pressure that standard models might overlook. By transitioning from simplified "feet of head" estimates to high-fidelity, stochastic hydraulic modeling, the DRIPS toolkit offers a more realistic and robust framework for modern international plumbing design.

Keywords

Dynamic Pressure Loss, Static Pressure, Water Demand, Simulation

1. Introduction

Managing local pressure gradients within strict maximum and minimum limits is vital to ensure fixture functionality, prevent system fatigue, and maintain public health in premise plumbing. While global standards like the International Plumbing Code (IPC) [1] and DIN 1988 [2] dictate these boundary constraints, practical head loss estimation varies significantly. U.S. practices often rely on simplified "equivalent length" methods and conservative 50% safety factors focused solely on the hydraulically remote fixture, whereas DIN 1988 employs high-fidelity, computationally intensive Darcy-Weisbach equations and K-value minor loss coefficients. This research integrates these rigorous, scientifically accurate equations into a comprehensive, network-wide analysis. By evaluating the system across its full operational spectrum—from maximum continuous operating pressure (zero demand) to theoretical minimum operating pressure during peak loading—this methodology optimizes pressure gradients across all points of use simultaneously rather than relying on a single worst-case endpoint.

2. Methodology

To establish a foundational framework for network-wide hydraulic optimization, this research evaluates a system across its operational extremes: static pressure during period stagnation (maximum pressure) and peak simultaneous demand (minimum pressure). The proposed methodology was tested on a theoretical 5-story, 15-unit apartment building comprised of identical 2-bedroom, 2-bathroom units (Table 1), mapped sequentially via a 3D network topology from the street entry to individual apartment delivery endpoints. Distribution pipe sizing was established via the Design-toolkit for Robust International Plumbing Systems (DRIPS) as shown in Figure 1.

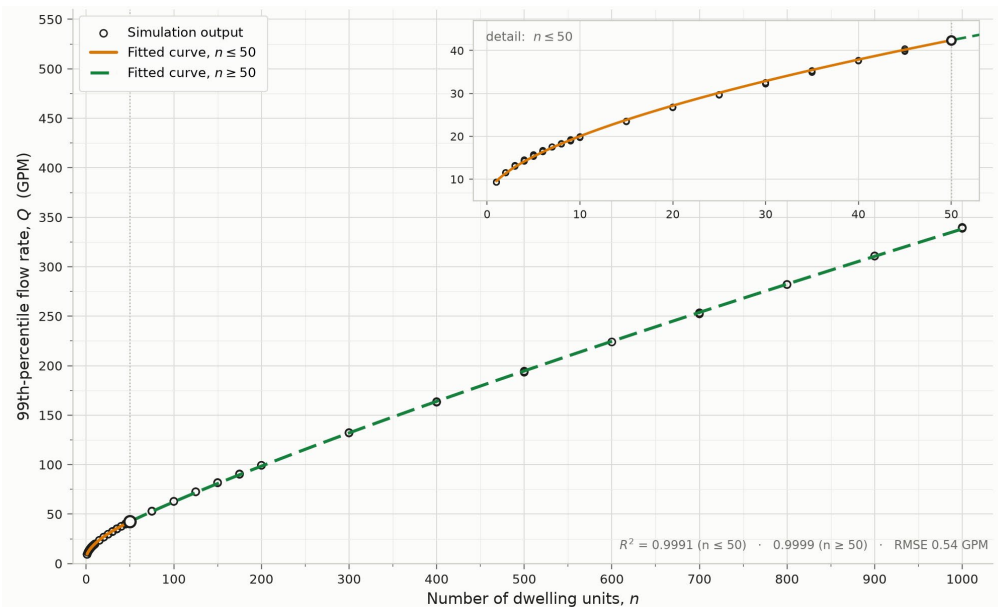

Figure 1. The Simulated 99th percentile demand as a function of the number of downstream dwelling units of a building comprised of solely 2-bedroom 2-bathroom units.

The curve shown in Figure 1 was generated through a series of simulations relating the design flow to the number of units in a building. The analysis was performed for a specific design case consisting of two-bedroom, two-bathroom apartments, with design occupancy determined using a standardized equation of two occupants per bedroom plus one additional occupant. The resulting curve was generated using two piecewise functions. Because the curve was developed for this specific test condition, its applicability is limited to the conditions evaluated and it should not be considered a standalone design tool. Rather, it is presented for demonstration purposes only. Utilizing these flow rates, pipe diameters were selected with a design velocity of 7 feet per second with pipes rounded to the nearest nominal size. The corresponding network is designed using Type L Copper pipe and fittings. The friction factor was calculated with the Colebrook White equation to ensure accurate computation of dynamic pressure losses. A standard value for the absolute pipe roughness ($\epsilon = 5 * 10^{-6}$ ft) was used for all calculations.

Table 1. Node Coordinates of 3-D Building Network

Node ID	**X*(ft)***	**Y *(ft)***	**Z *(ft)***	**Node ID**	**X *(ft)***	**Y *(ft)***	**Z *(ft)***
Bldg. Entry	-20	2	0	FX Apt A Branch	10	2	Typ. For Each Floor
Booster Pump	-10	2	0	FX Apt B Branch	30	2	
Riser Base	0	2	0	FX Apt C Branch	50	2	
F1 Branch	0	2	20	FX Apt. A Entry	10	10	
F2 Branch	0	2	30	FX Apt. B Entry	30	10	
F3 Branch	0	2	40	FX Apt. C Entry	50	10	
F4 Branch	0	2	50				
F5 Branch	0	2	60				

To demonstrate the high-fidelity modeling capabilities of the DRIPS toolkit, two distinct design failure scenarios were simulated:

1. **System Over-Pressurization:** Localized burst risks and fixture fatigue caused by excessive static and booster pump head.
2. **Critical Pressure Drop:** Insufficient operational head at peak loading due to cumulative friction and elevation losses.

Zonal hydraulic behaviors were computed across the network using the energy equation, integrating the Darcy-Weisbach formula [3] for explicit frictional losses and K-value minor loss coefficients for distribution fittings. This replaces traditional worst-case endpoint approximations with continuous, localized pressure gradient tracking. For simplicity this simulation utilized the design flow rate as the anticipated loading rate.

3. Results and Discussion

Two scenarios were generated using the proposed solution. Figure 2(a) shows the test building with a system inlet pressure at the distribution main of 40 PSI and no booster pump. Figure 2(b) shows the test building with the addition of a 55 PSI booster pump.

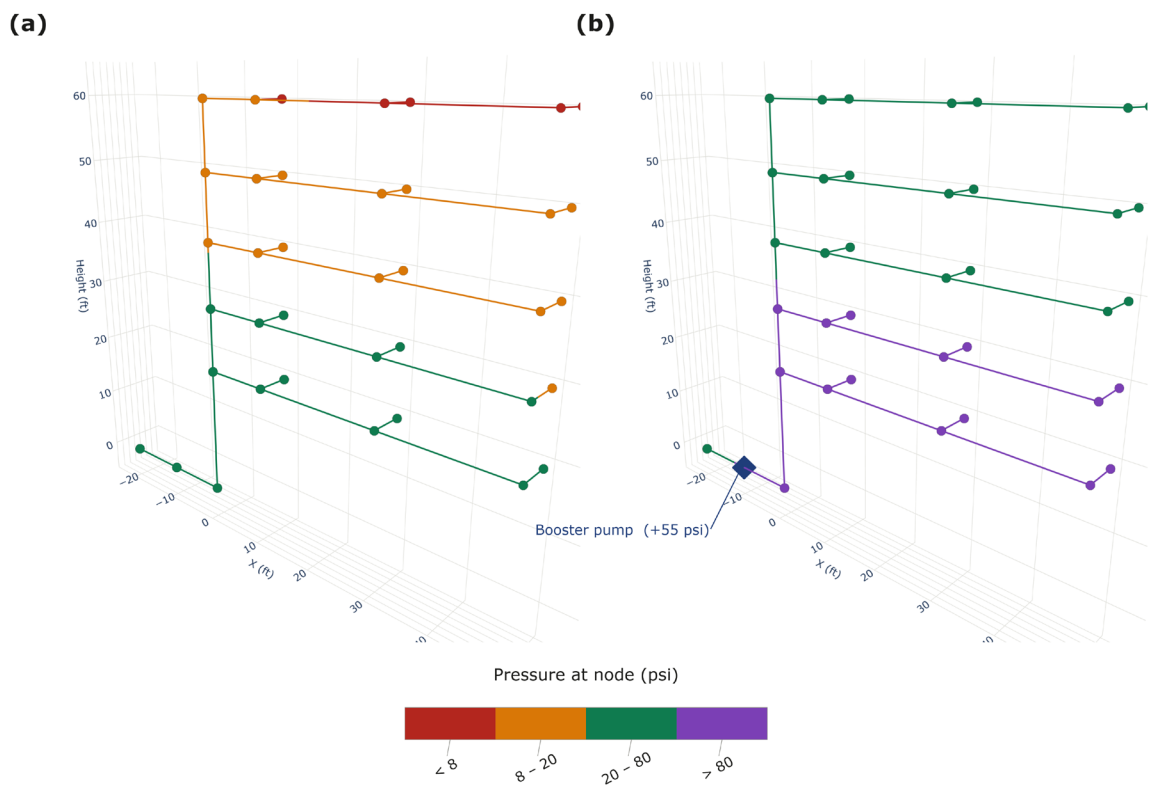

Figure 2. Test Case 1: 40 PSI at the building inlet with no added booster pump and dynamic pressure loss based on design flow (a) and Test Case 2: 40 PSI at the building inlet with a 55 PSI booster Pump with no flow (static condition) (b).

When considering Figure 2(a), it is visually apparent that a majority of the 5th floor drops entirely below the absolute 8 PSI minimum threshold, rendering all fixtures non-functional. Furthermore, major hydraulic deficiencies extend down to the third floor, where pressure drops below 20 PSI, causing high-pressure fixtures such as toilets and showers to experience operational failure. In the alternative situation, we see that adding a 55 PSI booster pump successfully elevates these upper-floor pressures, but it simultaneously drives the system past its maximum 80 PSI design parameters. This addition, although solving one problem introduces a challenge of its own.

When considering Figure 2(b), it is observed that incorporating the 55 PSI booster pump results in all the apartments located on the bottom two floors operating well above the proposed 80 PSI limit. This over-pressurization could lead to severe systemic issues, including the premature fatigue of sanitary fixtures or structural pipe bursts causing significant damage to the building. Ultimately, these results demonstrate that the simulation can easily adapt to the regional constraints enforced by a local Authority Having Jurisdiction, providing an invaluable pipe and equipment sizing tool that extends the DRIPS framework far beyond its primary role of stochastic demand estimation.

4. Conclusion

The successful integration of network-wide hydraulic calculations into the DRIPS 3D topological framework offers an advanced diagnostic tool for optimizing premise plumbing. By featuring fully customizable pressure-boundary constraints, the architecture dynamically adapts to localized international building codes. This advancement transitions the DRIPS toolkit from a standalone demand-estimation model into an integrated, comprehensive pipe-sizing system capable of rapidly simulating plumbing equipment modifications—such as booster pumps—to immediately evaluate varying manufacturer specifications on network performance.

5. References

[1] International Code Council, "International Plumbing Code," ICC, Washington, D.C., 2024.
[2] DIN 1988-300, "Codes of practice for drinking water installations - Part 300: Pipe sizing," Beuth Verlag, 2012.
[3] C. F. Colebrook, "Turbulent flow in pipes, with particular reference to the transition region," J. Inst. Civ. Eng., vol. 11, pp. 133-156, 1939.

6. Meet the Authors

Dr. Drew Rich is a Senior Research Associate and Adjunct Faculty at the University of Miami. His research focus is primarily focused on developing advanced computational modeling and simulation frameworks to accurately predict water demand in buildings. By capturing complex, stochastic water use behaviors, their work directly advances efficient infrastructure design, public health safety, and sustainability in the built environment.

Tom Roberts is the Global Director of Plumbing, Mechanical and Gas with the International Code Council. He chairs Standards Australia's WS-014 committee, overseeing the AS/NZS 3500 suite for water, plumbing, and drainage. Previously a Director with the Australian Building Codes Board, Tom was responsible for developing the Plumbing Code of Australia.

Compensating for Reduced Flush Volumes: Restoring Solid Transport in Sanitary Drainage Systems Through Increased Pipe Gradient

S. Wright (1), R. Sarukkalige (2)

(1) steven.wright@outlook.com.au

(2) p.sarukkalige@curtin.edu.au

(1), (2) Curtin University School of Civil and Mechanical Engineering: Perth, Western Australia

Abstract

The following research investigates the extent to which increasing pipe gradient can mitigate the reduction in solid transport caused by water-efficient 4.5L water closet (WC) flush volumes within 100 mm diameter horizontal sanitary drainage systems. Reduced flush volumes, introduced through water conservation measures in Australia and worldwide, have been shown to decrease the hydraulic energy available for effective solid transport, increasing the risk of blockages, surcharges and odour issues. The research aimed to determine an optimal gradient within these systems that restores the solid transport performance to levels comparable with those achieved under traditional 9L flush systems installed at the minimum required gradient for a DN 100mm pipe in accordance with AS/NZS 3500.2 of 1:60 (1.65%).

To achieve the goal of the research, a 17m long transparent uPVC sanitary drainage test rig was constructed, incorporating the ability to utilise various gradients and flush volumes. Controlled tests were conducted using a simulated solid waste media and a double ply conventional toilet paper brand available on the Australian market to measure the solids carry distance and velocity.

The results obtained in the research demonstrated that increasing pipe gradient effectively compensated for the lower hydraulic energy of modern 4.5L flushes. Quantitative analysis indicated that a gradient of approximately 1:31 (3.2%) was required for a 4.5L flush to achieve solid transport equivalent to that of a 9L flush at the baseline gradient of 1:60 (1.65%) for the test rig's pipework configuration.

The results support the potential inclusion of supplementary design guidance for standards or industry practice, enabling engineers and designers to better optimise pipe gradients for modern water efficient WCs.

Keywords

sanitary drainage, pipe gradient, pipe slope, low flush WCs, water closet.

1. Introduction

1.1. Overview

Over the past 3 decades, the drive to conserve water has led to the widespread adoption of WCs with the capacity of flush volume available reduced from traditional 9 – 13 litre cisterns to 4.5 litres in Australia and 6L in North America and the UK [1, 2]. While this has significantly reduced both household and commercial water consumption, it has also introduced unintended consequences within private property sanitary drainage systems, particularly those downstream of WCs, where the transport of solid waste relies heavily on the flush volume available to generate sufficient momentum and carry solids away and into the municipal sewerage system which yields higher volumes of base flow available to convey waste efficiently.

In gravity-fed conventional drainage systems, the effective transport of solid waste is highly dependent on the combination of flow rate, pipe slope, pipe configuration, toilet paper and the physical properties of the solid itself. Reduced flush volumes can result in decreased solid transport distances and greater confinement of solids that potentially accumulate and lead to blockages, flooding and increased maintenance requirements [3]. This issue becomes especially relevant in residential or commercial buildings where property sewers are installed with minimal gradient.

While there have been a multitude of past studies conducted in the last 30 years that have investigated the impact of low-flush volumes on these systems set up in laboratory-controlled conditions, few appear to have thoroughly investigated the mitigating effect of increasing pipe gradient to a level that negates the transport distance and solid velocity lost since the inception of water-efficient fixtures and toilets.

Within the plumbing and drainage community, it has also long been suggested by some and touched on in research [4] that steeper pipe gradients may be detrimental to solid conveyance and is based on the premise that water would outrun solid waste and cause it to deposit. While increased gradient does result in higher flow velocities, this view is generally based on simplified single phase flow assumptions regarding the transport behaviour of solids within sanitary drainage systems. The validity of this long-held belief is examined in this research, with particular focus on the relationship between pipe gradient and solid transport mechanics.

For the purposes of this research, steeper gradients refer to pipes slopes up to 1:25 (4%). While it is possible to install pipes steeper than this, when installing DN 100 mm pipes, whether in ceilings or in ground fill, pipe gradients over this threshold become difficult in excavation logistics, pipe fitting alignment and being able to physically connect to the municipal sewer connection point due to available depth limitations.

2. Methodology and experimental setup

2.1. Test rig design

Multiple different variations and additional parameters for the project's ultimate goal of determining optimal transport of solids were considered; however, a balance between what was physically achievable and what would yield practical and credible results was adopted.

The research utilised a 17 m long test rig supporting a single pipe size of 100 mm in diameter manufactured from translucent uPVC. The drain was connected to an upstream WC with a configuration representative of a typical residential plumbing installation.

Although improvements in the design and hydraulic efficiency of water-efficient WCs required over seven years of research and development in Australia prior to their introduction in 1993 [5], this study utilised a single modern 2025 model WC with a WELS 4-star rating for all flush volumes tested (4, 4.5, 6 and 9L). While advances in WC design have substantially improved fixture evacuation performance, the focus of this study was the subsequent transport of solid waste within the sanitary drainage system and enhancements from increased pipe gradient rather than the performance of the WC itself.

The experiment focused on two primary independent variables, namely flush volume and pipe gradient. During testing, both solid and water velocities were measured, and the total transport distance for each run was recorded. Where required, trends were plotted and interpolated or extrapolated based on fitted trendlines, with results validated using regression analysis, standard deviation, and confidence interval assessment.

The test rig configuration incorporated a 100 mm x 45º plain junction within the horizontal plane to connect the WC branch drain to the main pipe section. Many previous experimental studies using similar rigs have adopted straight pipe configurations without bends or junctions, likely to isolate key independent variables such as flow rate, pipe size, and gradient under near-ideal laboratory conditions. While this simplified approach was initially considered, it was ultimately deemed unrepresentative of real residential drainage layouts. Accordingly, a single change in direction was incorporated to better reflect actual installations typical of a residential property where a WC exits the side of the house, changes direction and extends to the municipal sewer connection at the rear of the lot.

In addition to the hydraulic equipment associated with the test rig, air pressure and airflow velocity sensors and an associated data acquisition system were also incorporated to quantify the air–water interaction within the pipe. This was considered particularly relevant given that increased pipe gradients can promote higher air entrainment and ventilation effects. The results of this air pressure/flow testing are outside the scope of this version of the research report; however, it should be noted that the effect of increased gradient on airflow within the system for the flow rates applicable to WC flushes was found to be negligible.

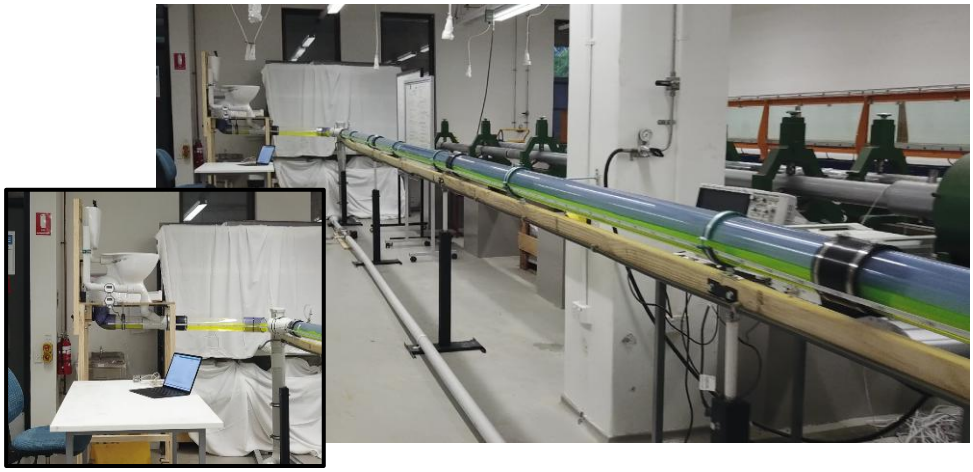

Figure 1 – Test rig setup

2.2. Simulated solid test media

To accurately simulate the behaviour of human waste through the system, the research adopted the use of uncased maximum performance testing media or 'MaP media' [6] rather than the water-filled cotton gauze test pieces stipulated in both Australian and European standards [7, 8], which pertain more to WC solids evacuation performance.

MaP test media is produced from a blend of miso paste and soy flour, which are ingredients commonly found in Japanese cooking. The size of the test solid used was based on the average physical characteristics of human waste reported in previous studies [5, 9].

The physical MaP test solid characteristics were as follows:

- Extruded cylinders of 32mm diameter, 130mm in length and mass of 130 grams
- Specific gravity of 1.15 g/mL $\pm$ 0.1 g/ml

In addition to the MaP media, each flush incorporated four balls of six sheets, double-ply toilet paper (24 sheets total), wet tensile strength of 1N/102g (avg) and dimensions of 114mm x 114mm rolled, crumpled up and placed into the WC.

Figure 2 – MaP test media

3. Results

3.1. Observed Solid Transport Mechanics

Experimental observations made in relation to the solids motion for each combination of flush and gradient reveal that transport was primarily governed by what was originally described in research conducted by Littlewood and Butler [10] as the 'sliding dam effect'. This phenomenon is initiated when the frictional resistance between the solid and the pipe wall attenuates its movement to a velocity slower than that of the surrounding water accompanying it. When the solid velocity drops to less than about 1 m/s, the trailing water and flush wave catch up to it, and a build-up of water accumulates behind the solid and toilet paper, effectively creating a temporary downstream moving dam that propelled the solid forward. Generally, leakage of water past the plug was low and was found to be dictated more by the permeability of the paper rather than solely on the hydrostatic head pressure differential.

Figure 3 – Sliding dam effect

After initiation of the sliding dam, and in most cases, the transport of the solid continued until the water height behind the solid dropped below a critical threshold, at which point the summation of the forces acting to move the solid was balanced by the frictional resistance between the solid and the pipe inner surface, causing the solid and toilet paper to deposit.

In rare circumstances where the solid and toilet paper became separated and prevented the sliding dam from forming, the solid transport distance was significantly affected. In these cases, the toilet paper still achieved complete clearance of the test rig; however, the solid became stranded at relatively short distances. To reinitiate meaningful movement of the solid *without subsequent flushes containing toilet paper* was difficult with consecutive flushes moving the solid little more than 100mm downstream per flush and thus, requiring up to 30 consecutive flushes to clear the solid from the test rig.

This finding contrasts with common recommendations that upstream fixtures aid transport and suggests that additional water alone is insufficient to effectively mobilise solids in the absence of toilet paper. This reinforces the importance of the blockage-induced head or sliding dam build-up as a key driver of solid transport, rather than flow rate alone.

3.2. 4.5L v 9L transport distances vs gradient

Figure 4 illustrates the relationship between pipe gradient and solid transport distance for the 4.5L and 9L flushes at gradients of 1.65%, 1.82%, 2%, 2.22%, 2.5%, 2.9% and 4%. Each gradient tested shows (as expected) a positive correlation between flush volume and transport distance. This is consistent with the trends observed by Gauley & Koeller [11]. It should be noted and as mentioned previously, that in some test runs, the solid test media and toilet paper became separated. This separation did not show any clear connection to the pipe gradient and was likely a result of the inherent variability in unsteady, partially full flows containing both liquid and solids. Separation clearly affected the solid carry distances and added some variability to the results. Had a greater number of tests been performed, the average distances in these cases would likely have been higher.

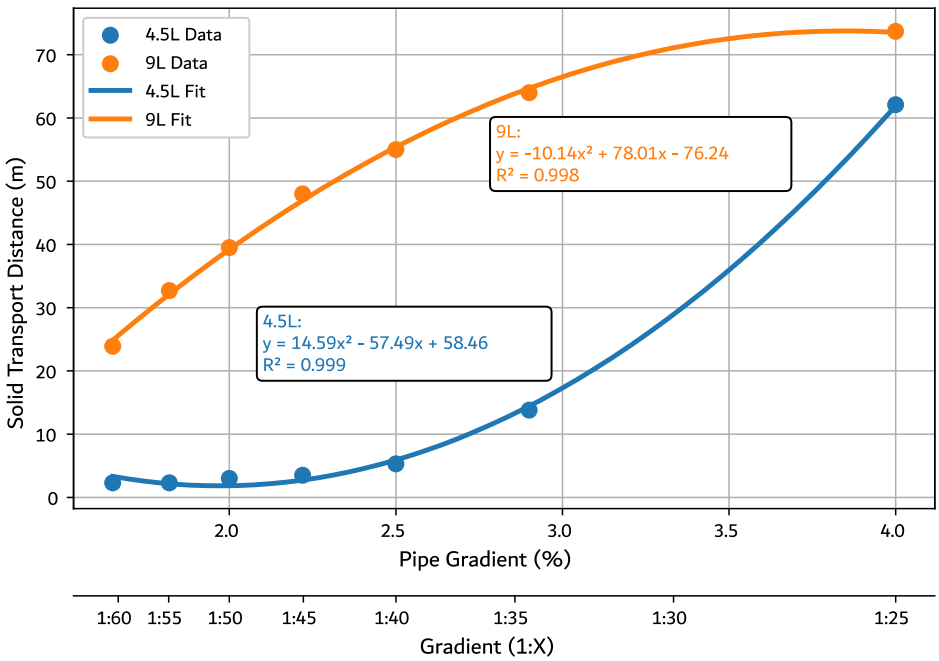

Figure 4 – 4.5L and 9L flush solid transport distances vs gradient

Of particular note, and worth emphasising, is the performance observed at a gradient of 1:60, which represents the minimum in accordance with AS/NZS 3500.2 for 100mm sanitary drains. When this minimum gradient is paired with the 4.5L flush volume required to achieve Water Efficiency Labelling Scheme (WELS) compliance, the results from the data raise concern about the effectiveness of this combination of design parameters.

Moreover, while an increase in transport distance is observed for the 4.5L flush between gradients of 1:60 and 1:40, the magnitude of this improvement is relatively minor. Although designers and contractors may expect a marked increase in performance over this range, the additional gravitational component is only about 0.0085g, despite the slope itself increasing by over 50%. When losses through bends and other fittings are also considered, it becomes more apparent and likely why meaningful gains in transport are not realised until gradients exceed 3%.

3.3. Direct comparison of 4.5L to 9L flush volumes

Given that this study is primarily concerned with performance at the baseline gradient of 1:60 (1.65%), the following comparison focuses specifically on this condition. A direct comparison between the 4.5L and 9L flush volumes provides the clearest demonstration of the disparity in transport distance performance, contrasting the current WELS-rated WC flush volume of 4.5L with the 9L flush used in Australian WCs prior to water-saving implementation measures. As evident in Figure 5, the 9L flush delivered more than a 900% increase in conveyance efficiency compared to the 4.5L flush.

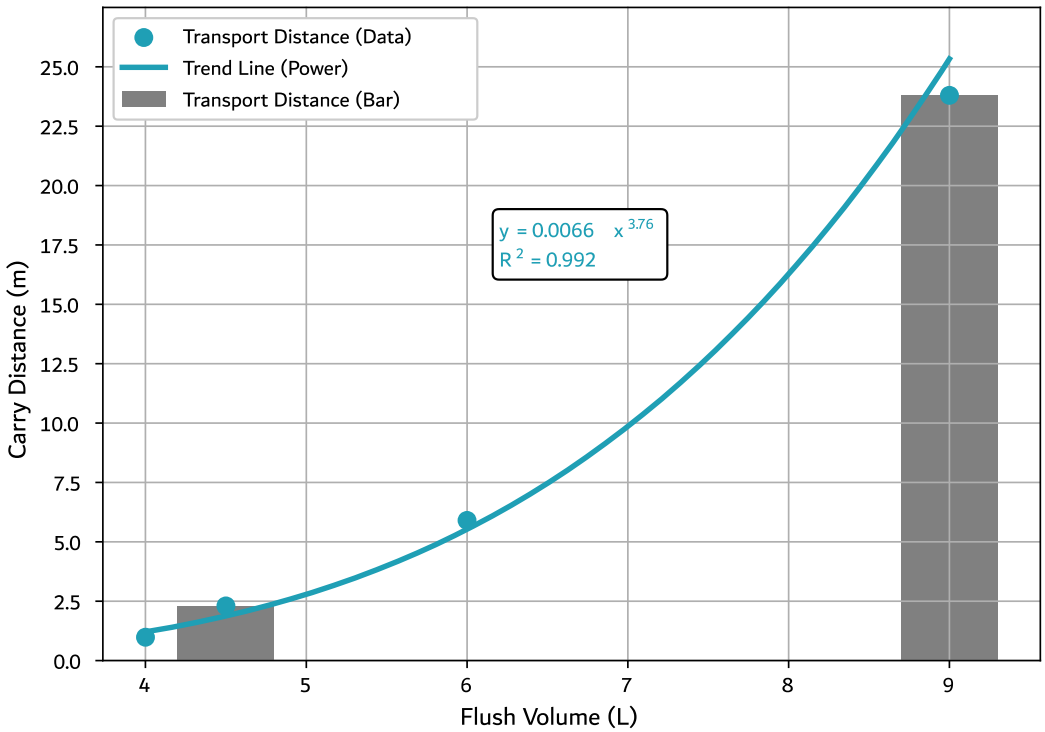

Figure 5 - 4.5L v 9L direct transport distance comparison

The velocity of the solid in each test was captured using a 60 FPS camera in conjunction with the longitudinal measurement markings along the test rig and frame-by-frame tracking used to derive the velocity-distance relationships. While the overall carry distance highlights the stark difference between the two, the velocity-distance profiles demonstrate that this disparity persists and amplifies throughout the transport process.

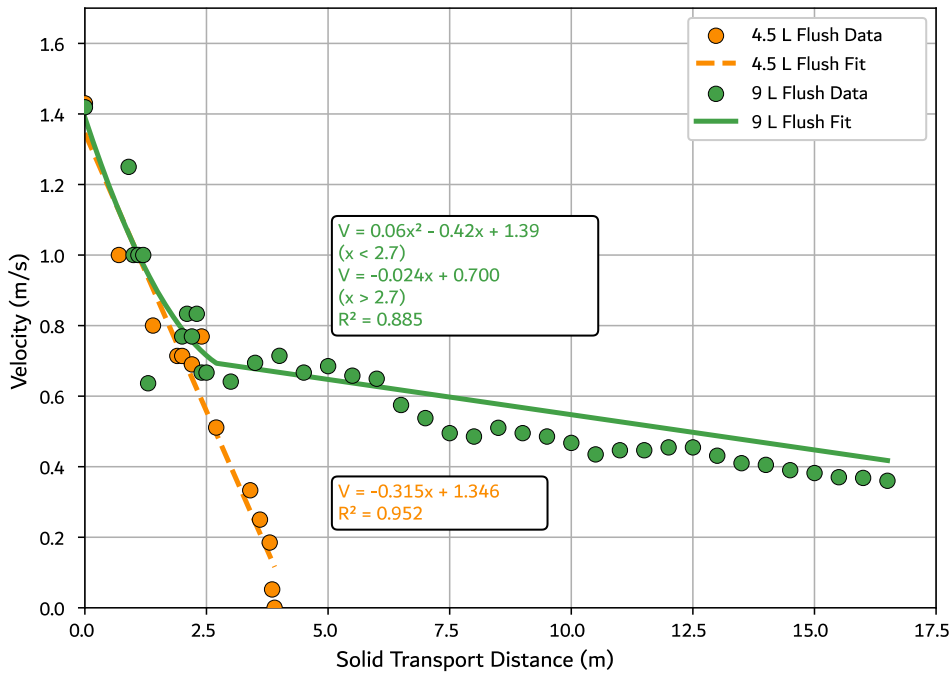

Figure 6 - 4.5L v 9L direct velocity comparison (1:60)

Using two of the higher performing 4.5L and 9L flushes, Figure 6 shows that both exhibit an initially high velocity that decays with distance, although the form of decay differs significantly. For the 4.5L flush, the velocity follows a sharp, near-linear decline, with the solid coming to rest within 2 - 3 m. This reflects the limited initial momentum and insufficient sustained water depth to maintain the sliding dam effect.

In contrast, the 9L flush displays a more complex, non-linear profile better represented by a piecewise function. An initial rapid velocity reduction occurs over approximately 2.5 m and is followed by a brief stabilisation and minor acceleration, before transitioning into a more gradual decay. This behaviour reflects the ability of the larger flush volume to maintain a backlog of water behind the solid, sustaining momentum via the sliding dam effect and enabling transport well beyond the test rig's length.

3.4. Results of increasing pipe gradient for the 4.5L flush

When the test rig's gradient was increased, particularly above 1:40 (2.5%), the velocity profile of the 4.5L flush began to change form. Rather than exhibiting a rapid linear decay and ceasing in transport beyond a few metres of the test rig, the higher slopes promoted a much more sustained velocity curve.

The velocity profile at the uppermost tested gradient achievable by the test rig of 1:25 (4%), shows the dramatic improvement in solid transport performance. The initial velocity is slightly higher than the other gradients; however, not by a noticeable difference. What is evidently different in the performance compared with the flatter gradients though, is upon transition from the vertical WC outlet to the horizontal pipe

section, the steeper gradient actually enables the solid to increase its velocity before suffering an abrupt loss of momentum due to the higher velocity impact that occurs against the 45º junction starting at about the 1.5m point in the test rig and continuing through the bend for just less than a metre or so of pipe.

Following on from this loss in energy, the motion of the solid begins to regain its speed to a local maximum velocity after the change in direction and then peaks before decaying linearly. This complex yet effective behaviour could not adequately be described by a single regression term, but instead a four-part piecewise function was used to capture the different stages of the solids motion and agrees with a similar observation made by Swaffield and Galowin [12] and Wise [13].

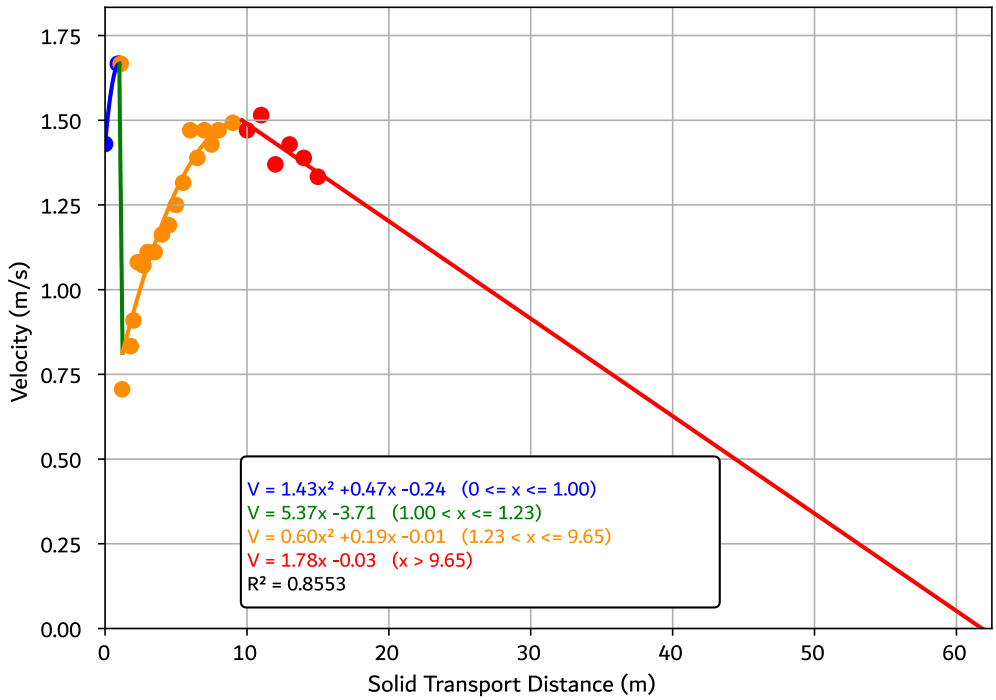

Figure 7 – 4.5L flush velocity profile 1:25 (4%)

3.5. Required gradient to mitigate the transport loss for 4.5L flush volumes

At the interpolated gradient of approximately 1:31 (3.2%) (Figure 8), the 4.5L flush achieved a transport distance equivalent to that of the 9L flush operating at the minimum gradient prescribed by AS/NZS 3500.2. This point represents a practical threshold at which the reduction in hydraulic energy associated with lower flush volumes is effectively offset by an increase in gravitational driving force. Importantly, the relationship is not linear; rather, the results indicate that relatively modest increases in gradient below this threshold yield limited improvement, whereas gradients beyond approximately 3% produce a far greater enhancement in transport performance.

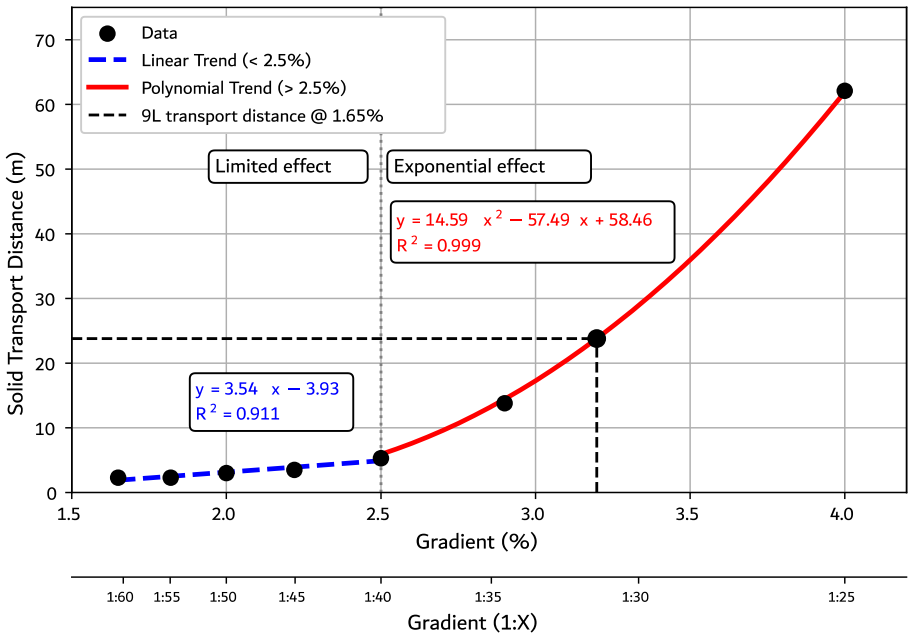

Figure 8 – 4.5L flush transport distance per gradient

In practical terms, this finding suggests (in this laboratory-installed setting and drain configuration) that the adverse effects associated with water-efficient flushing cisterns may be mitigated, provided the installation is made with steeper gradients than the nominal Australian code stipulates as a minimum requirement. Such a result highlights the relationship between the energy input from the flush volume and pipe gradient as two of, if not the most critical factors influencing solid transport effectiveness and reliability. Notably, the sliding dam effect counteracts the expected loss of water past the solid at higher gradients, preserving the upstream water head required for effective transport.

4. Conclusion

4.1. General

This study investigated the extent to which increasing pipe gradient can compensate for the reduced solid transport performance associated with modern 4.5L water-efficient WC flush volumes in 100 mm sanitary drainage systems. The results show that transport is governed not only by the initial momentum of the flush, but more critically by the sustained hydrostatic force generated through the sliding dam effect.

The findings confirmed that reduced flush volumes significantly diminish performance at standard minimum gradients, with the 4.5L flush achieving only a fraction of the transport distance observed for the traditional 9L flush at 1:60. Velocity profile analysis highlighted the inability of the lower flush volume to sustain motion, resulting in rapid decay and early deposition, whereas the 9L flush maintained a prolonged sliding dam effect and substantially greater transport distances.

Increasing pipe gradient was shown to be an effective means of restoring this lost performance. While incremental increases below approximately 2.5% produced only minor improvements, a clear transition in behaviour was observed beyond this range. At an interpolated gradient of approximately 3.2%, the 4.5L flush achieved transport distances equivalent to the 9L flush installed at the baseline gradient, demonstrating that the reduction in hydraulic energy can be offset through sufficiently increased slope, albeit beyond current minimum design standards.

4.2. Transport Metrics

A concluding remark in evaluating solid transport performance is the metric used to define successful conveyance. This study, like many others, adopts average transport distance as the primary indicator; however, this does not always reflect the operational reality of drainage systems. For instance, a solid that remains after a single flush will still (in most cases) be cleared by subsequent household water usage. The Plumbing Efficiency Research Coalition [14] used this broader perspective by assessing eventual clearance and the number of flushes required, rather than full transport in a single event.

This alludes to the evident question regarding performance expectations for modern low flush WCs. While temporary retention of solids may be acceptable where frequent upstream usage provides sufficient base flow, the results from this study indicate that additional flows not accompanied by toilet paper contribute little to further transport. This effect is likely exacerbated where flushes occur at longer intervals, allowing solids to lose moisture and likely result in an increased resistance to subsequent movement.

Accordingly, while delayed clearance may be tolerable in high-flow systems, a strong argument exists that effective sanitary drainage, at least in the shorter residential networks, should remove solids within the initial flush. This minimises the risk of blockage, odour buildup, and supports downstream transport where higher flows prevail. In this way, the findings align with what could be argued as the fundamental purpose of sanitary drainage design, which is to convey waste hygienically and at sufficient velocity, independent of uncertain upstream conditions.

5. References

[1] Snelling, C., Turner, A., Riedy, C., White, S., & Cummings, S. (2007). Where does the water go? Best practice stock modeling for water using appliances. *Water Practice and Technology, 2*(4).

[2] Pimentel-Rodrigues, C., Silva-Afonso, A., Gago, H., & Teles, J. (2025). Water efficiency in buildings: A review of the role of the flush cistern over time. In Proceedings of the CIB W062 Symposium.

[3] Valencio, I. P., & Goncalves, O. M. (2019). Drainage and sewage system performance – Consequences of reductions in toilet flush volume. *Building Services Engineering Research and Technology, 40*(5), 576–594.

[4] McDermott, R., Strong, A., & Griffiths, P. (2019). Solid transfer in low flow sewers: The distance travelled so far is not enough. *Journal of Environmental Protection, 2*, 164.

[5] Cummings, S., Wright, G., & Bonollo, E. (2001). Australian water closet developments and their role in sustainable sanitation. *Building Services Engineering Research & Technology, 22*(1), 47–57.

[6] MaP Testing. (2018). *Maximum performance (MaP) testing protocol – Ver 7*

[7] Standards Australia. (2014). *AS 1172.1:2014 water closet pans*.

[8] European Committee for Standardization. (2018). *EN 997: WC pans and WC suites with integral trap*.

[9] Wyman, J. B., Heaton, K. W., Manning, A. P., & Wicks, A. C. (1978). Variability of colonic function in healthy subjects. *Gut, 19*(2), 146.

[10] Littlewood, K., & Butler, D. (2003). Movement mechanisms of gross solids in intermittent flow. *Water Science and Technology, 47*(4), 45–50.

[11] Gauley, W., & Koeller, J. (2005). *Evaluation of water-efficient toilet technologies to carry waste in drainlines* (Final report). Canada Mortgage and Housing Corporation.

[12] Swaffield, J., & Galowin, L. (1992). *The engineered design of building drainage systems*. Routledge.

[13] Wise, A. F. E., & Swaffield, J. (2002). *Water, sanitary and waste services for buildings* (5th ed.). Butterworth-Heinemann.

[14] Plumbing Efficiency Research Coalition. (2012). *The drainline transport of solid waste in buildings*.

[15] Standards Australia. (2021). *AS/NZS 3500.2 Sanitary Plumbing & Drainage*.

6. Presentation of authors

Steve Wright is a hydraulic services engineer originally from Australia, currently consulting out of The Hague in the Netherlands. He holds a First-Class Honours degree in Civil and Construction Engineering and his work focuses on sanitary and roof drainage research and design, combining mathematical analysis and computational fluid dynamics to better understand, visualize and improve system performance.

Dr. Ranjan Sarukkalige is an Associate Professor of Civil Engineering at Curtin University, Australia. His research interests and experiences are in civil engineering hydraulics and hydrology with particular focus on urban hydrology, stormwater management, and groundwater systems. Dr. Sarukkalige has an outstanding academic record, having published over 100 peer-reviewed publications.

Performance Evaluation Method of Self-sealing Trap Part2. Characteristics of a Compact Umbrella-shaped Self-sealing Trap Applicable to Horizontal and Vertical Fixture Drainage Piping

Tsuyoshi Suruki (1), Takehiko Mitsunaga (2), Kyosuke Sakaue (3)
(1) suruki@marutrap-maruichi.co.jp
(2) mitsunaga@meiji.ac.jp
(3) sakaue@carrot.ocn.ne.jp
(1) Planning Manager, Maruichi Co., ltd., Japan
(2) Assoc. Prof., Dep. of Architecture, School of Science & Technology, Meiji University, Japan
(3) Emeritus professor, Meiji University, Japan

Abstract

A self-sealing trap is a mechanical trap that uses a silicone membrane that automatically opens and closes to prevent the backflow of wastewater gas into indoor spaces, and does not use any water seal. In the previous report, the characteristics and performance of a self-sealing trap developed as a countermeasure to seal water loss due to evaporation, which cannot be addressed by conventional drainage systems based on water-seal traps, were reported.

The device evaluated in that study was a cone-shaped self-sealing trap developed in 2012 by a Japanese manufacturer. The cone-shaped type was designed by shortening and compacting the membrane structure to accommodate Japanese plumbing design conditions. However, it was designed exclusively for vertical piping. Because its sealing mechanism requires uniform hydrostatic pressure to open the membrane, it cannot be applied to horizontal HVAC condensate piping.

To expand the range of applications, a newly developed umbrella-shaped self-sealing trap was developed. The umbrella-shaped self-sealing trap incorporates an innovative membrane structure and achieves a compact design while enabling application to horizontal HVAC condensate piping. The umbrella-shaped self-sealing trap obtained technical evaluation (BCJ evaluation) from the Building Center of Japan in 2021 and was subsequently included in the environmental standard AIJES-B0003-2025 published by the Architectural Institute of Japan.

This report presents the structural characteristics and principal performance evaluations of the umbrella-shaped self-sealing trap. The performance evaluation was conducted using the criteria established for the cone-shaped type.

Keywords

Self-sealing Trap; Performance Evaluation; Umbrella-shaped Membrane; Mechanical trap; HVAC condensate piping

1 Introduction

The self-sealing trap was developed in the UK in the 1990s as the 'Self-sealing Waste Valve'. Due to its structure, this self-sealing trap is referred to as the 'cylinder-shaped'. The cylinder-shaped subsequently obtained product certification in the UK, Australia and the US. In Japan, performance evaluations were conducted in connection with the acquisition of BCJ evaluation in 2009. [1] The structure of the cylinder-shaped self-sealing trap is shown in **Figure 1**. The structure prevents water ingress by overlapping the ends of cylindrical membranes.

In 2012, a smaller self-sealing trap adapted to Japanese drainage conditions was developed and obtained BCJ evaluation in 2015. This is referred to as the 'cone-shaped'. An evaluation of this product was detailed in a previous report [2]. The structure of the cone-shaped self-sealing trap is shown in **Figure 2**. It features a water-sealing mechanism based on the overlapping surfaces of the conically shaped membrane ends. However, the cone-shaped was designed exclusively for vertical piping, presenting the challenge that it could not be installed in horizontal piping.

Consequently, an 'umbrella-shaped' self-sealing trap featuring a new self-closing

membrane structure was developed. Designed not only for installation in the vertical piping of washbasins and HVAC condensate drainage systems, as with previous models, but also for use in horizontal branch pipes of HVAC condensate piping, it obtained BCJ evaluation in 2021 and was included in the Architectural Institute of Japan Environmental Standard 'AIJES-B0003-2025' [3]. Self-sealing traps have a cumulative sales record of over 800,000 units in Japan by 2025.

This report details the structure and performance evaluation tests of this umbrella-shaped self-sealing trap, as well as evaluation tests regarding its use for HVAC condensate piping.

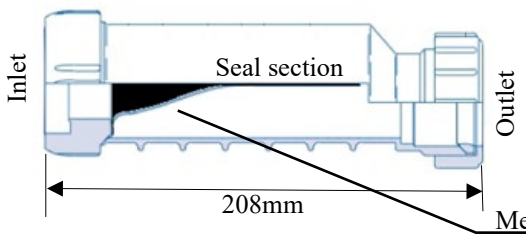

Figure 1 - Structure of Cylinder-shaped self-sealing trap

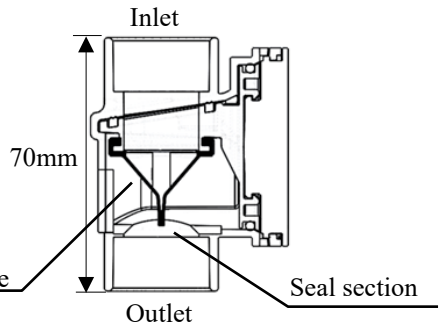

Figure 2 - Structure of Cone-shaped self-sealing trap

2 Issues with conventional self-sealing traps in Japan

The cylinder-shaped can be installed either vertically or horizontally and can be connected to a wide range of plumbing fixtures; however, due to the large surface area of the membrane's water-retaining surface, its overall length is 208 mm. In Japan, most washbasin drains are fitted with pipes rising from the floor; installing this model vertically leaves little room for adjusting the pipe position, which has posed a challenge in terms of installation.

Although the cone-shaped is a scaled-down version of the cylinder-shaped, it is designed exclusively for installation in vertical piping; to open the water-sealing section of the

If installed at a 1:50 gradient, water will remain within the area outlined in red on the upstream side when the membrane closes.

Figure 3 - Residual water level when a Cone-shaped self-sealing trap is installed horizontally

membrane, uniform hydraulic pressure must be applied to the sealing surface. **Figure 3** illustrates the appearance of the cone-shaped installed in a horizontal piping. However, as the membrane does not open unless the water depth reaches at least two-thirds of the pipe's internal diameter, and residual water remains in the upstream section of the pipe even after drainage, it has been difficult to apply this design to horizontal piping.

3 Characteristics and Functions of Umbrella-shaped self-sealing trap

An umbrella-shaped self-sealing trap with a membrane structure has been developed for use in horizontal piping; it is suitable for installation in vertical piping of hand-washing basins and in both vertical and horizontal piping of HVAC condensate. Its structure is shown in **Figure 4** and its characteristics in **Figure 5**. The unit can be connected using 20A-type pipes (with an adapter), 25A-type pipes or 30A-type sockets, in accordance with JIS K 6741[4]. It is therefore suitable for pipe diameters used in HVAC condensate piping and washbasin piping.

The membrane is an umbrella-shaped structure held in place by a central shaft; it blocks wastewater gas from the downstream side by sealing against the body via its peripheral edge (**Figure 5**, left). By adopting an umbrella-shaped design for the membrane, drainage is possible from the entire circumference of the valve, making it suitable for use in horizontal piping as well. When the flow rate is low, only a portion of the membrane

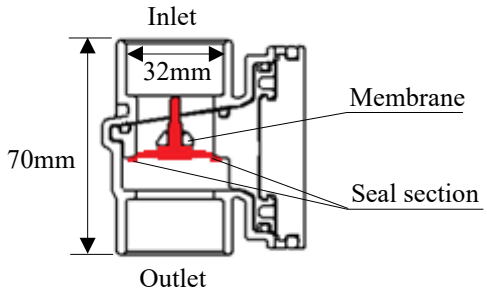

Figure 4 – Structure of Umbrella-shaped self-sealing trap

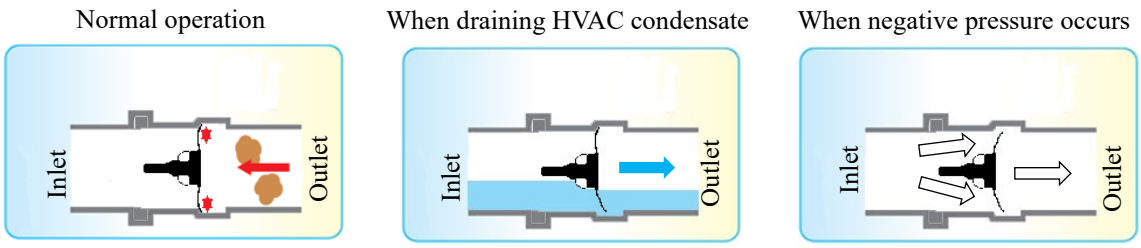

Figure 5 – Characteristics of Umbrella-shaped self-sealing trap

opens to allow drainage, thereby preventing the ingress of wastewater gas from the downstream side of the trap. Furthermore, the membrane offers low flow resistance (**Figure 5**, center). When there are no drainage flow and the downstream side of the trap is under negative pressure, the air intake function is activated, causing the membrane to open and draw air in from the appliance side (**Figure 5**, right).

The membrane is secured to the maintenance cap and can be easily removed for inspection and cleaning. However, when the maintenance cap is removed during horizontal piping, residual water may spill out depending on the installation orientation; therefore, the permissible installation orientation for actual use is limited to a 45° range to the left and right of the maintenance cap, as shown in **Figure 6**.

The main body is moulded from transparent material for indoor piping applications, to facilitate visual inspection of the interior during maintenance. When installing this in outdoor piping, weather-resistant resin must be used, as transparent resin is prone to accelerated degradation due to exposure to ultraviolet light (**Figure 7**).

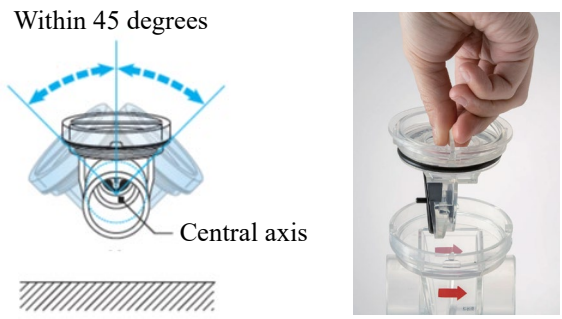

Figure 6 – Main unit installation angle

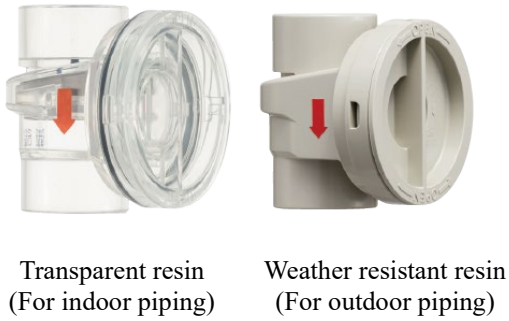

Figure 7 – Type of main unit

4 Performance Evaluation of Umbrella-shaped self-sealing trap

4.1 Test trap

The umbrella-shaped self-sealing trap shown in **Figure 7** was used as the test trap.

4.2 Performance evaluation test items

The performance evaluation test items were based on Reference [5], which incorporated evaluation criteria specific to horizontal installation of HVAC condensate piping, whilst drawing on the classification used in References [1] and [2] for cone-shaped self-sealing traps; this resulted in a total of 23 criteria covering basic performance, general performance, and characteristics. Typical tests for umbrella-shaped self-sealing traps are

shown in sections 4.3 to 4.6.

The basic performance consists of the following nine items;1) Drainage and low noise, 2) Minimum drainage passage, 3) Impurities discharge (self-cleaning function), 4) Hair draining, 5) Positive pressure resistance, 6) Small pressure resistance, 7) Minimum operational negative pressure, 8) Water flow performance, and 9) Adhesion performance.

The general performance consists of the following nine items; 10) Water tightness, 11) Heat resistance, 12) Heat-cycle resistance, 13) Thermal shock resistance -1, 14) Thermal shock resistance -2 (JIS), 15) Hot water resistance, 16) Freeze resistance, 17) Chemical resistance, 18) Chemical repetition resistance, 19) Operation resistance, and 20) Fall resistance.

The characteristics consist of the following three items; 21) Discharge characteristics, 22) Air intake characteristics, and 23) Backflow prevention.

4.3 Drainage and low-noise performance test

4.3.1 Test Overview

The aim was to verify the drainage performance of the test trap. An overview of the test apparatus is shown in **Figure 8**. Five litres of clean water were collected in the washbasin, and the drainage time (the time from the start of drainage to its completion) was measured. In addition, the noise level during drainage was measured, and the noise level L_{Aeq} [dB(A)] was calculated. The test was conducted three times.

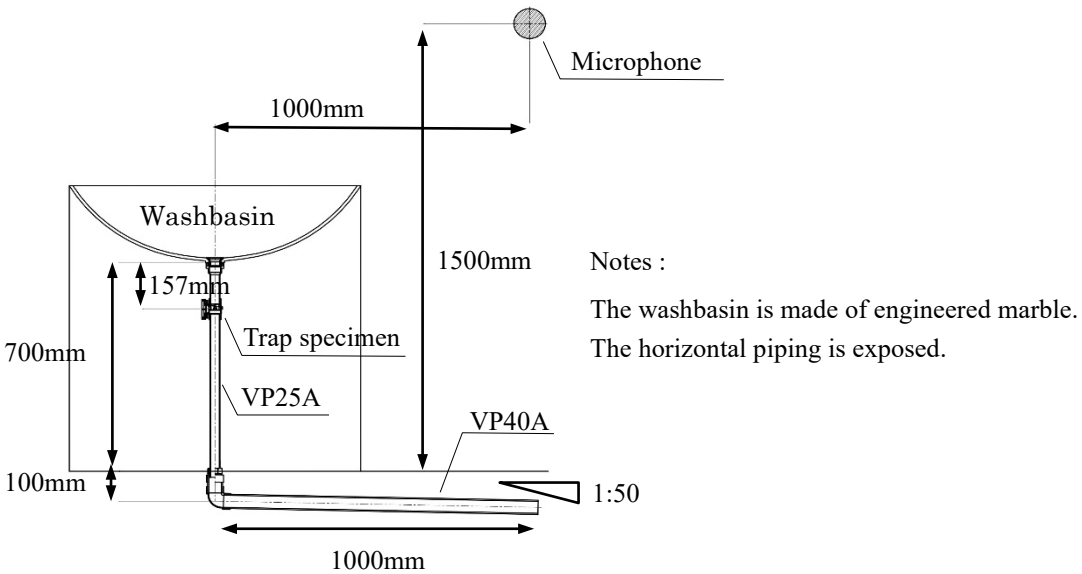

Figure 8 – Overview of the Drainage and low-noise performance test

4.3.2 Evaluation criteria

Drainage performance is measured by the drainage time T [s], and the assessment criteria are set out below.

$$T \leq 30s$$

Low-noise performance is assessed using the maximum equivalent noise level (L_{Aeq}) as an indicator, and the criteria for this assessment are set out below.

$$L_{Aeq} \leq 50dB(A)$$

4.3.3 Results and Discussion

The average result from the three tests showed a drainage time of 20.40 seconds, which met the assessment criteria; however, the equivalent noise level (L_{Aeq}) was 67.0 dB(A), exceeding the assessment criteria. This was because, whereas in the cone-shaped self-sealing trap used when the assessment criteria were established, the drainage water collects at the lower edge of the membrane before being discharged, in the test trap, the umbrella-shaped membrane vibrated during the initial few seconds of drainage, causing the water flow to be disrupted as it was discharged from the entire circumference of the valve. However, when a water-sealed trap was tested under the same conditions, the maximum equivalent noise level was 68 dB(A) during the suction phase due to the self-siphonage. As this result is almost equivalent to the above, it is judged that there are no issues in actual use.

4.4 Minimum drainage passage performance test

4.4.1 Test Overview

The aim is to verify the minimum drainage capacity of the test trap. The test method for the minimum drainage passage performance is shown in **Figure 9**. The test was conducted three times.

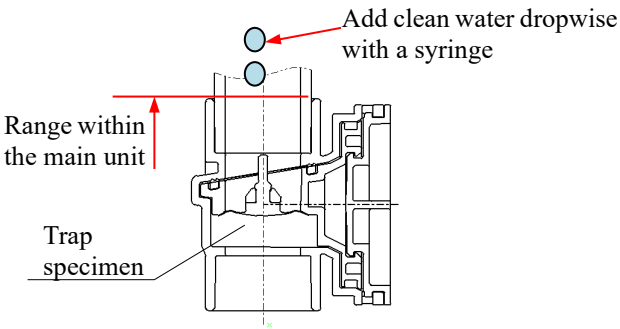

Figure 9 – Overview of the Minimum drainage passage performance test

4.4.2 Evaluation criteria

The minimum flow rate W [mL] required for passage (i.e. a state in which water does not

stagnate within the membrane) is shown below.

$$W \leq 2mL$$

4.4.3 Results and Discussion

The results of the three tests showed a minimum flow rate of 5.9–6.3 mL, with all test traps exceeding the assessment criteria. This is because, in the case of vertical piping, the umbrella-shaped membrane is designed to drain water from the entire outer circumference; consequently, the drainage is dispersed across the entire membrane, resulting in an increased volume of dripping water. Conversely, as shown in **Figure 2**, the cone-shaped self-sealing trap used when establishing the evaluation criteria concentrates drainage at the lower edge of the membrane. Due to this difference in membrane structure, the test traps exceeded the evaluation criteria. However, this value represents approximately 13% of the test trap's internal volume (49 mL), and it is judged that this does not pose a problem in actual use.

4.5 Water flow performance test

4.5.1 Test Overview

The aim is to verify the drainage performance of the HVAC condensate.

a) Test method: The reference water levels for the water flow performance test are shown in **Figure 10**. For vertical piping, the reference water level of 0 mm was set at the interface between the membrane and the main body; for horizontal piping, it was set at the downstream end face of the elbow. Water was supplied to maintain a constant flow rate at water levels of 0 mm and 50 mm. A VP25A (JIS K 6741) pipe was connected to the test trap.

b) Measurement Method: The drainage flow rates for both vertical and horizontal piping were measured at water levels of 0 mm and 50 mm.

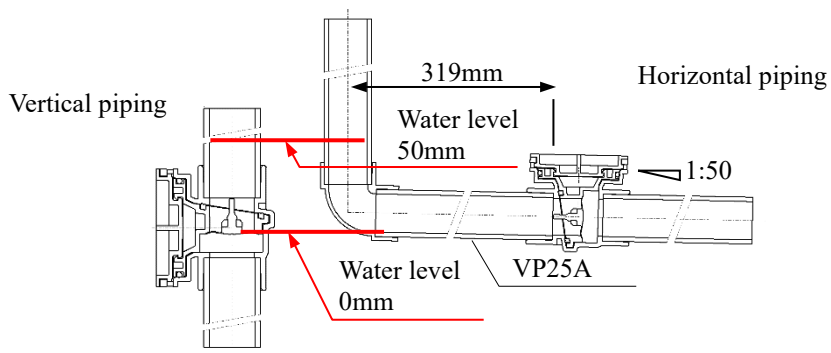

Figure 10 – Overview of the Water flow performance test

4.5.2 Evaluation criteria

The criteria were based on a typical office air conditioning unit with a maximum cooling capacity of 9.0 kW and an estimated drain flow rate of 84 mL/min. The criteria for the maximum flow rate q [mL/min] at a water level of 0 mm are shown below.

$$q \geq 84\text{mL/min}$$

4.5.3 Results and Discussion

The results of the water flow performance tests are shown in **Table－1**. All test traps met the assessment criteria.

Table – 1 Results of the Water flow performance test

Installation direction	Water level 0mm	Water level 50mm
Vertical piping	2,700mL/min	3,500mL/min
Horizontal piping	2,500mL/min	3,200mL/min
Assessment criteria	q ≥84mL/min	(Reference test)

4.6 Adhesion performance test

4.6.1 Test Overview

The drain pump draws not only the condensate from the air conditioning unit but also the scale that has accumulated in the drain pan, and discharges it. As the composition of the scale varies depending on the installation location, substitute scale materials were used to verify the anti-fouling performance of the test traps.

a) Test method: Dust, tar and oil were applied to the contact surfaces between the water-sealing section of the test trap and the trap pipe wall, respectively. After drying for 24 hours in an atmosphere at 40 °C, water was passed through the system. The quantities applied were 20 mg of dust, 20 mg of tar and 20 mg of oil.

b) Measurement method: The flow conditions at a reference water level of 0 mm, as shown in **Figure 11**, were verified.

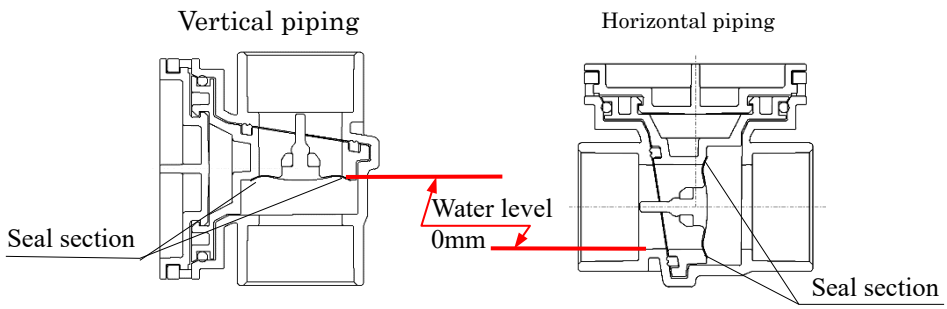

Figure 11 – Overview of the Adhesion performance test

4.6.2 Evaluation criteria

The criteria were based on the water-stopping section opening to allow water to flow smoothly.

4.6.3 Results and Discussion

The results of the water flow performance tests are shown in **Table－2**. All test traps met the assessment criteria.

Table – 2 Results of the Adhesion performance test

Installation direction	Dust：20mg	Tar：20mg	Oil：20mg
Vertical piping	Water flows through without stagnating	Water flows through without stagnating	Water flows through without stagnating
Horizontal piping	Water flows through without stagnating	Water flows through without stagnating	Water flows through without stagnating
Assessment criteria	Water flows through without stagnating		

4.7 Evaluation results of basic performance, general performance, and characteristics

In addition to the items covered in the preceding sections, evaluation tests were also conducted on the basic performance, general performance and characteristics reported in Reference [2]. **Table－3** summarises the assessment criteria and evaluation results for each of these items.

In all cases, the test trap met the required performance criteria and was deemed suitable for use in washbasins and HVAC condensate.

5 Conclusion

This report summarises the structure and performance evaluation of umbrella-shaped self-sealing traps. Regarding its application in washbasins, the trap failed to meet the evaluation criteria set out in Reference [2] for drainage and low noise performance and minimum drainage passage performance. However, as these criteria were established based on cone-shaped traps, and given that the results indicate no issues would arise in practical use, it was concluded that a review of the evaluation criteria for self-sealing trap performance testing methods is necessary. For all other items, the results met the evaluation criteria.

Regarding the application to HVAC condensate piping, we conducted experiments taking into account the use of horizontal piping—which was outside the scope of Reference [2]—and confirmed that there were no issues in any case.

In addition to being suitable for use in HVAC condensate piping and washbasin applications, the umbrella-shaped self-sealing trap can now be installed either vertically or horizontally in HVAC condensate piping, which is expected to improve planning and installation convenience.

Table – 3 Results of basic performance, general performance, and characteristics of Umbrella-shaped self-sealing trap

	Parameters		Assessment criteria	Suitability by application *1	
				Wash-basin	HVAC conde-nsate
Basic performance	1)	Drainage and low noise	Drainage time ≤ 30s Noise level L_{Aeq} ≤ 50dB(A)	△	—
	2)	Minimum drainage passage	Drain by minimum volume: 2mL	△	—
	3)	Impurities discharge (self-cleaning function)	No remains of impurities foreign substances	○	—
	4)	Hair draining	Pseudo hair should not be caught	○	—
	5)	Positive pressure resistance	Differential pressure between the open and closed states after 60 seconds under a pressure of 600 Pa: ≤ 30 Pa	○	○
	6)	Small pressure resistance	Differential pressure between the open and closed states after 60 seconds under a pressure of 10 Pa: ≤ 2 Pa	○	○
	7)	Minimum operational negative pressure	Operate negative pressure: ≤ -90Pa	○	○
	8)	Water flow performance *2	Maximum flow rate at a water level of 0 mm at the lower edge of the inlet side of the test trap: ≥ 84 mL/min	—	○
	9)	Adhesion performance *2	Water flows through without stagnating	—	○
General performance	10)	Water tightness	There should be no leakage	○	○
	11)	Heat resistance	There are no leakage and abnormalities	○	○
	12)	Heat-cycle resistance	There are no leakage and abnormalities	○	—
	13)	Thermal shock resistance -1	There are no leakage and abnormalities	○	○
	14)	Thermal shock resistance -2 (JIS)	There are no leakage and abnormalities	○	○
	15)	Hot water resistance	There are no abnormalities	○	—
	16)	Freeze resistance	There are no cracking, leakage and abnormalities	○	○
	17)	Chemical resistance	There are no cracking, leakage and abnormalities	○	○
	18)	Chemical repetition resistance	There are no cracking, leakage and abnormalities	○	—
	19)	Operation resistance	There are no leakage and abnormalities following exposure to a sinusoidal pressure (frequency 0.25 Hz, amplitude 0–3,200 Pa, duration 20,000 minutes)	○	○
	20)	Fall resistance	There are no abnormalities	○	○
Characteristics	21)	Discharge characteristics	Discharge-flow ratio of with trap to without trap: ≥ 0.6	○	—
	22)	Air intake characteristics	—	○	○
	23)	Backflow prevention	Water head of 9.8 kPa: Do no backflow	○	—

*1 ○ : No issues when applied
△ : Although outside the assessment criteria, there are no issues with application in practice
— : Not subject to evaluation
*2 Additional evaluation criteria based on the performance evaluation method described in Reference [2]

6 References

[1] Suka R, et al. - Evaluation on basic performance and characteristics of self-sealing trap, Technical papers of annual meeting, SHASE, pp.797-800, 2008 (In Japanese)

[2] Sakaue K, Ito Y - Performance evaluation method of self-sealing trap, Proceedings of the CIB/W062 International Symposium on Water Supply and Drainage for Buildings (Kosice), pp.189-197, 2016.
[3] Architectural Institute of Japan Environmental Standards AIJES-B0003-2025 Design Guidelines for Extra Drainage System (Mechanical and Siphonic Drainage System), Apr.,2025
[4] Japanese Industrial Standards JIS K 6741:2016 Unplasticized poly (vinyl chloride) (PVC-U) pipes, 2016
[5] Suruki T, et al. - Studies on Performance Evaluation Method of Self-sealing Trap Part 3: Performance Evaluation of Umbrella-shaped Self-sealing Trap, Technical papers of annual meeting, SHASE, pp.125-128, 2021 (In Japanese)

7 Presentation of Authors

Mr. Tsuyoshi Suruki is employed by Maruichi Co., Ltd., which is Japan's sole specialist manufacturer of drainage traps. He occupies the position of Head of the Planning Department, a role that entails the oversight of the entire process, from the inception of new products to their commercialisation.

Dr. Takehiko Mitsunaga is an associate professor at Department of Architecture, School of Science & Technology, Meiji University. His fields of specialization include water environment, building services engineering and plumbing system.

Dr. Kyosuke Sakaue is a professor emeritus of Meiji University. His fields of specialization include water environment, building services and plumbing system.

Pressure Resistance Performance and Allowable Drainage Capacity of Multi-Inlet Floor Gullies

Hibiki Hasemi (1), Masayuki Otsuka (2), Ayaka Kimura (3), and M. C. Jeffrey Lee (4)

(1) m25j3019@kanto-gakuin.ac.jp

(2) dmotsuka@kanto-gakuin.ac.jp

(3) d24j3002@kanto-gakuin.ac.jp

(4) MCJL@nutc.edu.tw

(1) Graduate School of Engineering, Kanto Gakuin University, Japan

(2) College of Architecture and Environmental Design, Kanto Gakuin University, Japan

(3) Doctoral Student in Architecture, Graduate School of Engineering at Kanto Gakuin University, Japan

(4) Department of Interior Design, National Taichung University of Science and Technology, Taichung 40401, Taiwan

Abstract

In Taiwan, gray water and sewage systems are separated for drainage within residential units. In apartment housing, wastewater from several fixtures is collected and then discharged through a single multi-inlet floor gully, instead of installing a trap for each fixture. Recent changes to the "Technical Code for Design of Building Water Supply and Drainage Systems"—which serves as the facility design standard for Taiwan—recommend a shift from underfloor drainage to same-floor drain. The code specifies installation standards for the multi-inlet floor gully. However, few studies focus on this trap; thus, its pressure resistance and allowable drainage flow rate have not been determined. If a multi-inlet floor gully is installed on upper floors, the large volume of wastewater from each dwelling may induce siphon action, suggesting a risk of trap seal break. A multi-inlet floor gully aggregates drainage; thus, simultaneous inflow of large amounts of drainage from multiple fixtures is expected. If drainage is not smooth, there is a possibility that backflow will occur into drainage system connected to other sanitary fixtures. These possibilities raise concerns that the indoor environment may become unsanitary. Therefore, in this study, we installed a representative multi-inlet floor gully

into a test drainage stack pipe system (9-story scale) using a top-venting method, and performed constant-flow drainage load experiments based on the drainage stack pipe system test method of the Society of Heating, Air-Conditioning, and Sanitary Engineers of Japan Standard 218-2021 (SHASE-S 218-2021) to evaluate its pressure resistance. We further investigated the allowable drainage capacity when wastewater flows into the test multi-inlet floor gully from a floor drain inlet, based on the drainage test method of JCW201-2012 floor drain trap standard of Japan.

Keywords

multi-inlet floor gully, pressure-resistance performance, allowable drainage capacity, Taiwan, drainage stack pipe system, trap seal break

1 Introduction

A drainage trap is installed in sanitary fixtures to block odors and pests from sewer pipes from entering living spaces. Standards in Japan and abroad generally require that each fixture be equipped with its own drainage trap. Regarding these traps, Mitsunaga[1)] and Ichikawa and Kiya[2)] investigated the effects of evaporation and capillary action on seal water loss in Japan. Research has also progressed over many years, including studies by Sakaue et al.[3)] on induced siphon action using simulation models. Chung et al.[4)] conducted surveys and case studies to investigate the structure, features, and advantages of multi-inlet floor gully units used in Taiwan. Lo[5)] carried out various tests and computational fluid dynamics (CFD) analyses using two multi-inlet floor gully types with different internal discharge shapes, showing that differences in shape affect self-cleaning ability and allowable drainage flow rate. Tests using pressurization equipment also reported no significant difference in pressure resistance between positive and negative pressure. However, there are few cases where a multi-inlet floor gully has been installed in a drainage stack pipe system and tested for pressure resistance. Therefore, in this study, we installed a trap in a standard top-venting drainage stack pipe system in Japan and evaluated its pressure-resistance performance based on the relationship between internal pipe pressure generated during drainage and trap seal loss. We also compared the results with those of commonly used drainage traps in Japan to assess the safety of the multi-inlet floor gully. Furthermore, the multi-inlet floor gully can connect to floor drain inlets and function as a floor drain trap; therefore, we examined its allowable drainage capacity with reference to drainage test methods used in Japan.

2. Pressure-resistance performance test

2.1 Experimental outline

2.1.1 Test drainage stack pipe system

This study used a 9-story high-rise simulation tower owned by Kanto Gakuin University to perform the constant-flow drainage load experiment to evaluate the pressure-resistance performance of the multi-inlet floor gully based on the Society of Heating, Air-Conditioning, and Sanitary Engineers of Japan Standard 218-2021[6)] (SHASE-S 218). The experiment was conducted using a test drainage stack pipe system with a top-venting method illustrated in Figure 2-1. A 100A vent cap was installed at the end of the top-venting. The drainage stack pipe was 100A, the horizontal branch pipe was 75A, and the slope was fixed at 1/100. The horizontal main drainage pipe was a straight pipe extending 11.5 m from the base of the drainage stack pipe to the drainage header, with a diameter of 125A and a slope of 1/150.

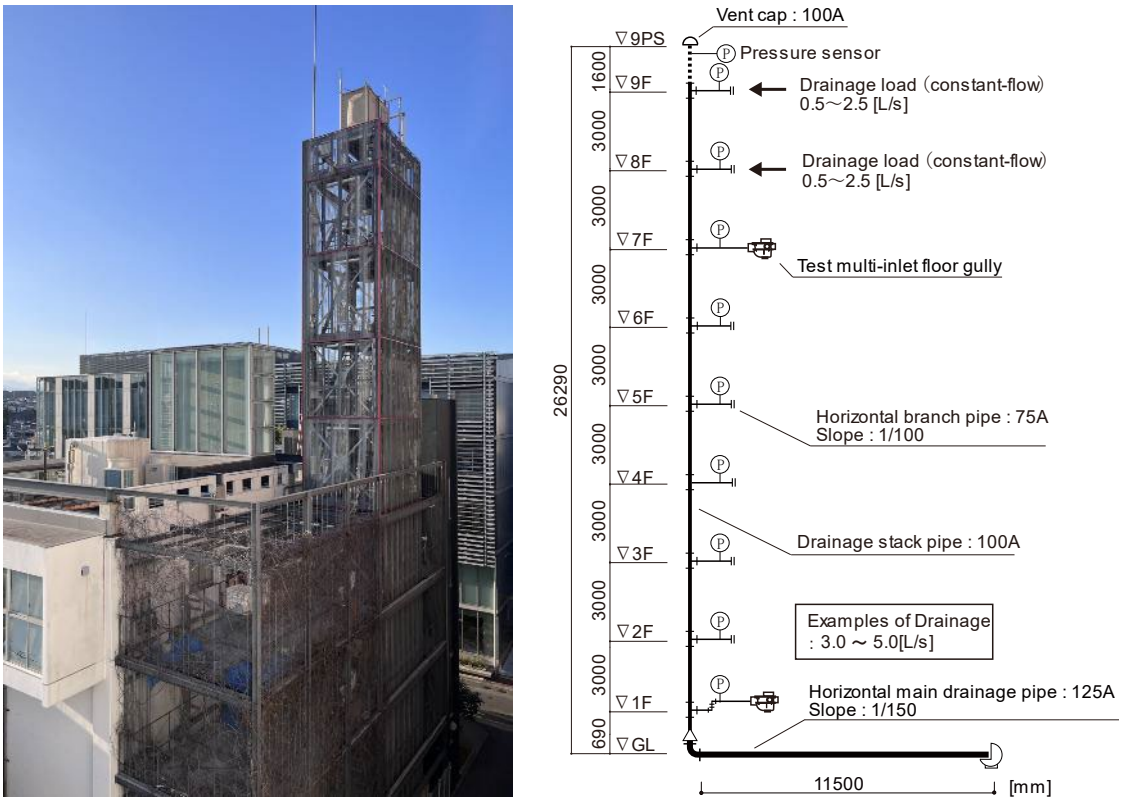

(a) **(b)**

Figure 2-1. (a) High-rise simulation tower and (b) test drainage stack pipe

Table 2-1 presents an outline of the test multi-inlet floor gully used in this study. The test multi-inlet floor gully was installed on the floor directly below the drainage floor and also on the first floor, which was the lowest level. We also compared the multi-inlet floor gully with a P-trap for washbasins and a waterproof pan trap for washing machines (Floor drain trap), both commonly used in Japan.

Table 2-1 Specifications of Each Trap Type

Various sizes		Multi-inlet floor gully	P-trap	Floor drain trap
Figure		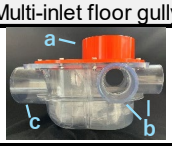	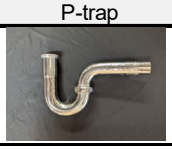	
Seal water depth [mm]		52	72	50.5
Ratio of leg's cross sectional area		0.50	1.00	0.87
Connection diameter	Floor drain (a)	100A	-	-
	Fixture drain(b)	50A	-	-
	Branch drain(c)	75A	-	-
Ratio of leg's cross sectional area ＝ mean sectional area of outlet leg / mean sectional area of inlet leg Ratio of leg's cross sectional area of the multi-inlet floor gully was calculated from the volume ratio.				

2.1.2 Measurement procedure and drainage load flow rate

Figure 2-2 illustrates the measurement procedure of this experiment. The total measurement duration was 90 s, where drainage began 10 s after the start and continued for 70 s. The analysis period was 40 s between 25 and 65 s, during which the drainage reached a steady flow condition. Drainage was carried out from the 9th and 8th floors, and the drainage load per floor followed SHASE-S 218 with a maximum of 2.5 L/s. The total drainage load flow rate ranged from 0.5 L/s to 5.0 L/s in increments of 0.5 L/s, as shown in Table 2-2, and measurements up to trap seal break were taken at smaller increments of 0.25 L/s to examine pipe pressure in more detail before and after trap seal break.

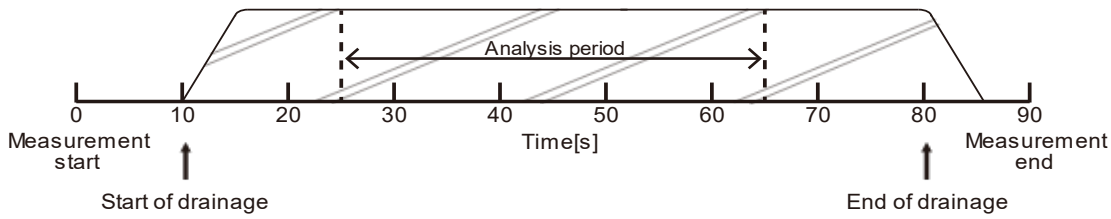

Figure 2-2. Measurement procedure

Table 2-2. Drainage load flow rate

Discharge Floor [F]	Drainage Load Flow Rate [L/s]									
9 F	0.5	1.0	1.5	2.0	2.5	2.5	2.5	2.5	2.5	2.5
8 F	-	-	-	-	-	0.5	1.0	1.5	2.0	2.5
Total	0.5	1.0	1.5	2.0	2.5	3.0	3.5	4.0	4.5	5.0

2.1.3 Measurement items and evaluation criteria

The measured parameters consisted of internal pipe pressure P [Pa] and trap seal loss Δh [mm]. The internal pipe pressure was measured using pressure sensors installed at the horizontal branch pipes on each floor and at the end of the top-venting pipe. The evaluation required that the maximum and minimum values (Pmax and Pmin) remain within ±400 Pa, according to the SHASE-S 218 standard criterion. The same standard applies to the trap seal loss, and the difference in seal water depth before and after drainage (seal loss value) must not exceed 25 mm.

2.2 Experimental results and discussion

2.2.1 Internal pipe pressure and drainage capacity of the drainage stack pipe system

Figure 2-3 shows an example of the internal pipe pressure distribution. When a drainage load of 2.0 L/s was applied as shown in Figure 2-3(1), the resulting internal pipe pressure values on all floors stayed within the acceptable limits. In contrast, when a drainage load of 2.5 L/s was applied as shown in Figure 2-3 (2), negative pressure exceeding the criterion value of −400 Pa appeared on floors 5–8.

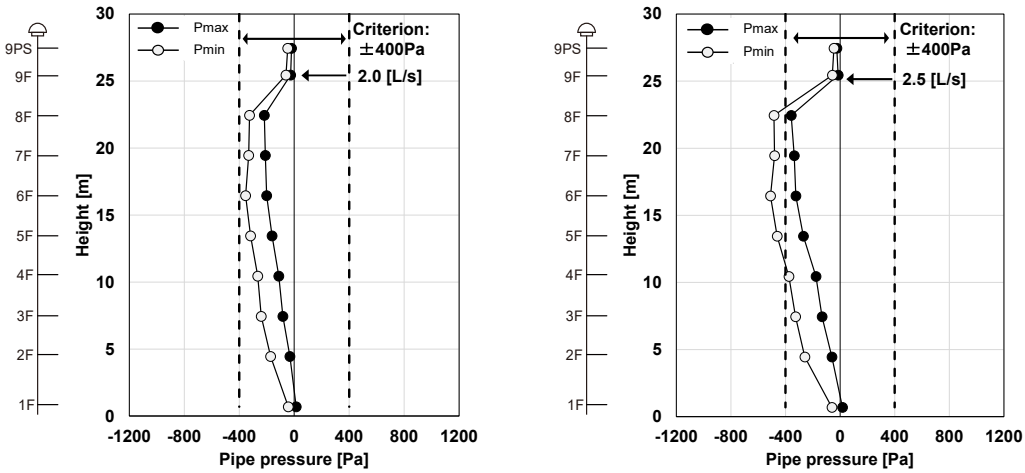

(1) Drainage load flow rate: 2.0 L/s **(2) Drainage load flow rate: 2.5 L/s**

Figure 2-3. Internal pipe pressure distribution

Figure 2-4 shows the minimum internal pipe pressure (Pmin) at the floor directly below the drainage floor and the maximum pressure (Pmax) at the lowest floor. As indicated, the negative pressure at the floor immediately below increased in proportion to the drainage load flow rate, and it surpassed the standard limit of −400 Pa at 2.5 L/s. Meanwhile, positive pressure remained nearly constant and did not exceed the specified limit. Figure 2-5 shows the trap seal loss for the multi-inlet floor gully installed at the floor directly below the drainage floor. The seal loss at that floor followed a trend similar to that of the internal pressure change, exceeding the standard value of 25 mm at 2.5 L/s, and the seal break caused by the induced siphon action was 3.0 L/s.

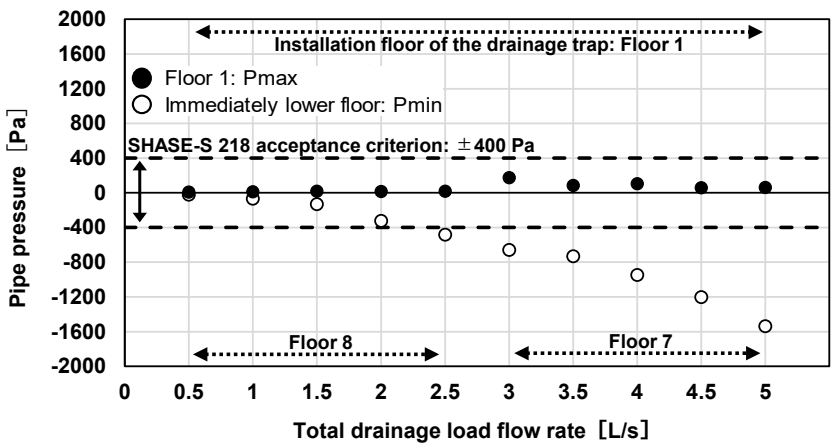

Figure 2-4. Transition of the total drainage load flow rate and pipe pressure

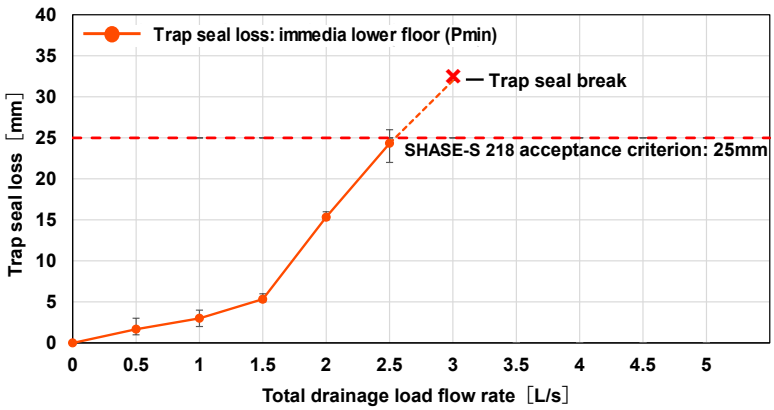

Figure 2-5 Trap seal loss of the multi-inlet floor gully

2.2.2 Pressure-resistance performance of the test multi-inlet floor gully

Figure 2-6 shows the pressure-resistance performance based on the relationship between the minimum pressure (Pmin) at the floor directly below and the seal loss in the test multi-inlet floor gully. The figure also includes the pressure-resistance performance of the two types of drainage traps commonly used in Japan. The results indicated that increasing negative pressure resulted in increased seal loss, and a strong correlation existed between the minimum pressure and the seal loss. Evaluating the resistance to negative pressure from the slope of the approximation line showed that the multi-inlet floor gully performed better than the floor drain trap, but it was inferior to the P-trap, which had the largest ratio of leg's sectional area. The minimum pressure at which seal break occurred had the same ranking, and a comparison between the multi-inlet floor gully and floor drain trap with similar seal depths showed that the higher-pressure resistance of the multi-inlet floor gully resulted in a lower likelihood of seal break.

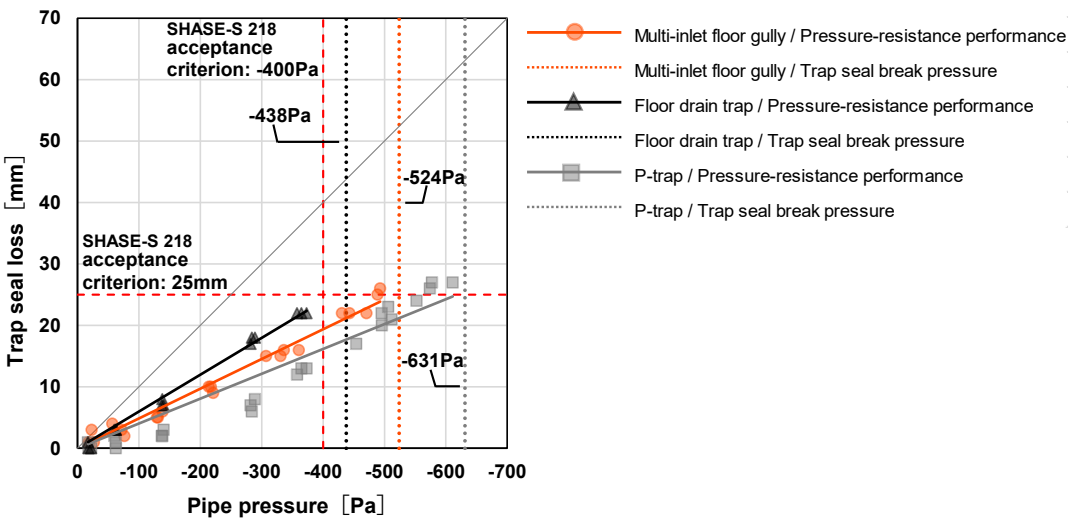

Figure 2-6. Pressure-resistance performance of the test multi-inlet floor gully

3. Allowable drainage flow rate test

3.1 Experimental outline

3.1.1 Test drainage system

This experiment aimed to determine the allowable flow rate when drainage enters the test multi-inlet floor gully by referring to the drainage test method specified in the Japan Cast Iron Cover & Waste Fitting Association Standard JCW201^{-2012} floor drain trap standard[7)]. Figure 3-1 shows the test drainage system. A 200 mm connecting pipe was installed between the multi-inlet floor gully and water tank. A drainage pipe with a diameter of 75A and length of 500 mm was installed at the connection of the horizontal branch pipe of the multi-inlet floor gully, and a 100A elbow enlarged by one size (25 mm up) was attached downstream to prevent drainage resistance.

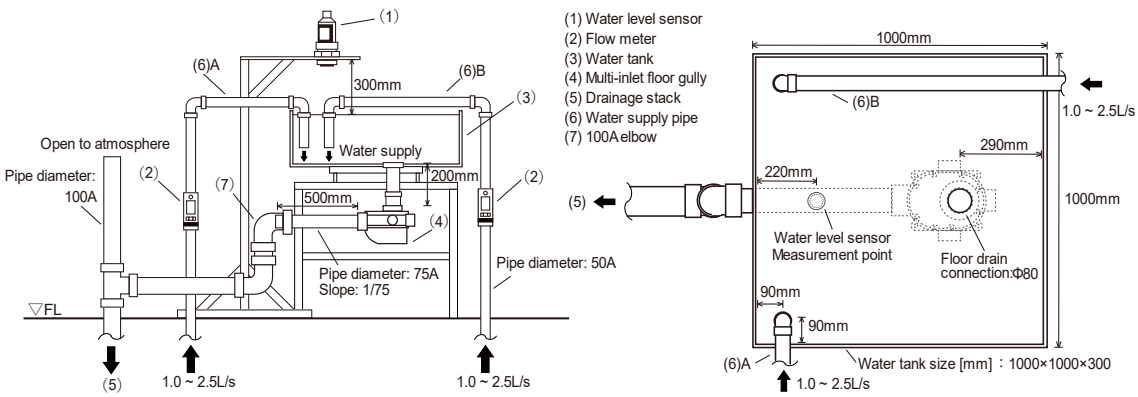

Elevation view **Plan view**

Figure 3-1. Test drainage system

3.1.2 Water supply flow rate

In this study, the flow entering the water tank from the supply pipe was defined as the water supply flow rate, and the flow discharged from the multi-inlet floor gully was defined as the drainage flow rate. The water supply flow rate was measured using a flow meter, and the total water supply flow rates applied in this experiment are shown in Table 3-1. Figure 3-2 presents the experimental procedure. The water level in the tank was initially set at 100 mm. After the measurement began, water supply started while simultaneously removing the stopper, which initiated drainage from the multi-inlet floor gully. The total measurement duration was 320 s, where the water supply began 10 s after the start and stopped after 300 s.

Table 3-1. The water supply flow rate

Water supply pipe	Water supply flow rate [L/s]							
A	1.0	1.0	1.5	1.5	2.0	2.0	2.5	2.5
B	—	1.0	1.0	1.5	1.5	2.0	2.0	2.5
Total	1.0	2.0	2.5	3.0	3.5	4.0	4.5	5.0

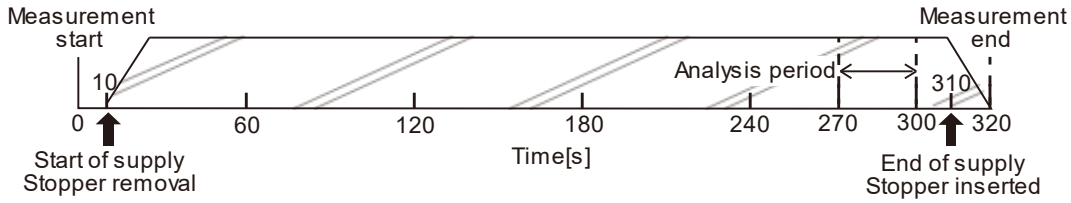

Figure 3-2. Measurement time and drainage details

3.1.3 Measurement items and evaluation criteria

The measured variables were the water supply flow rate [L/s] and the water level in the tank [mm]. The water level was recorded using a radar-type level sensor, and the analysis period was 30 s from 270 to 300 s when the water level in the tank remained nearly constant, with the average value over that interval being calculated. The evaluation criterion in this study required that the water level in the tank during supply be maintained at 100 mm, and the corresponding water supply flow rate at that condition was taken as the allowable drainage capacity of the gully. As indicated in Table 3-2, the JCW201^{-2012} standard specifies that the floor drain trap must allow drainage of 3.0 L/s or more for a nominal diameter of 80A. The multi-inlet floor gully of this experiment had a 75A horizontal branch pipe (nominal diameter 80A); therefore, one evaluation criterion was that its drainage capacity should be at least 3.0 L/s.

Table 3-2. Compliance standard defined by JCW201^{-2012}

Performance item	Pipe diameter	Perrformance
Drainage flow rate[L/s]	40A	1.0 or more
	50A	1.5 or more
	65A	2.0 or more
	80A	3.0 or more
	100A	4.0 or more

3.2 Experimental results and discussion

3.2.1 Drainage flow rate and water level variation

Figure 3-3 provides an example of water level fluctuation in the tank. As shown in Figure 3-3 (1), when supplying water at 4.0 L/s, the water level increased gradually at first, yet the drainage flow rate from the gully subsequently became approximately equal to the water supply flow rate, resulting in the water level staying at 100 mm within the analysis period. In contrast, as seen in Figure 3-3 (2), when supplying 4.5 L/s, the drainage flow rate failed to keep up with the water supply flow rate, causing the water level to rise sharply and continuously, and the average water level during the analysis period exceeded the evaluation criterion. Figure 3-4 shows the water level in the tank for each total water supply flow rate. The average tank water level within the analysis period increased as the water supply flow rate rose, and it exceeded the evaluation criterion when 4.5 L/s was supplied.

Based on these results, the allowable drainage flow rate of the multi-inlet floor gully was estimated to be approximately 4.0 L/s, which exceeded the Japanese standard requirement

of 3.0 L/s. Therefore, the multi-inlet floor gully has sufficient drainage capacity. Also, referring to the multi-inlet floor gully installation examples from Taiwanese commercial manufacturers, it was assumed that two washbasins, a bathtub, a shower drain outlet, and a floor drain outlet were connected to the gully. SHASE-S 206[8)] of Japan defines the average drainage flow rate from a fixture, q_d [L/s]. Using this information when calculating the average flow rate from a fixture entering gully during simultaneous discharge, the total becomes approximately 2.8 L/s if simply summed. Based on the allowable drainage capacity, the findings confirm that even when these fixtures are connected, drainage remains sufficient, and the system effectively handles inflow from fixtures.

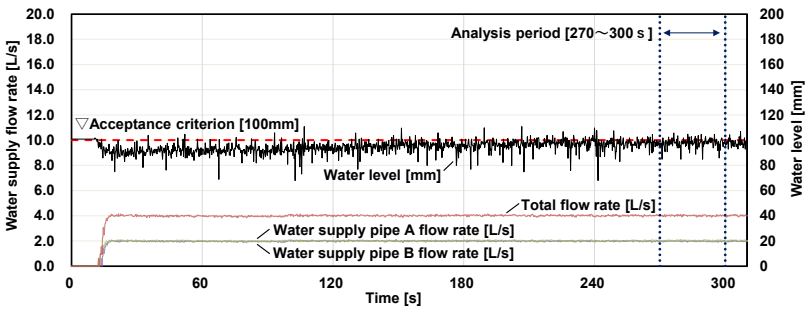

(1) At 4.0 L/s water supply

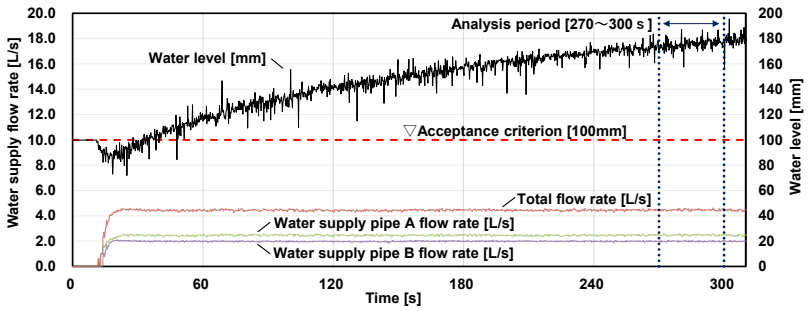

(2) At 4.5 L/s water supply

Figure 3-3. Water level variation in the tank

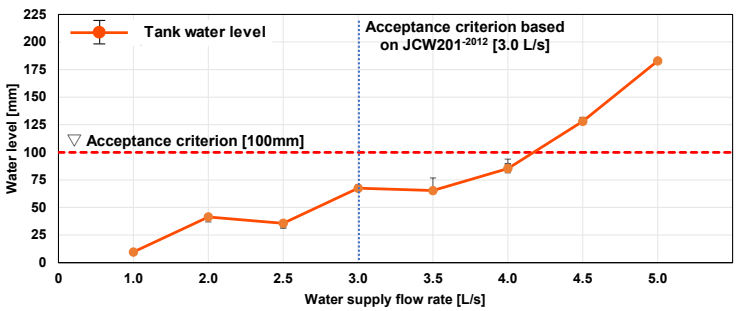

Figure 3-4. Total Water supply flow rate and average water level in the tank

Table 3-3. Average drainage flow rate from one fixture

Fixture	Washbasin	Bathtub	Shower drain	Floor drain
Average drainage flow rate from a fixture: q_d [L/s]	0.75	1.0	0.3	—
Assumed number of connected fixtures	2	1	1	1
Total	(0.75×2)+(1.0×1)+(0.3×1)= 2.8 [L/s]			

4. Conclusion

This study conducted two types of drainage tests on the multi-inlet floor gully and the following results were achieved.

1. Pressure-resistance performance: Seal loss in the multi-inlet floor gully showed a strong correlation with the generated internal pipe pressure (negative pressure), and it demonstrated resistance up to approximately −500 Pa without seal break. The pressure resistance of the multi-inlet floor gully was higher than that of the floor drain trap but lower than that of the P-trap.
2. Allowable drainage capacity: The allowable drainage capacity of the multi-inlet floor gully was approximately 4.0 L/s, and as a floor drain trap, it exceeded the requirements specified in JCW201^{-2012} of Japan. Also, fixtures were assumed to be installed. The comparison of the allowable drainage capacity with the total average flow rate from a fixture (calculated from each average flow rate from a fixture q_d defined in SHASE-S 206) revealed that sufficient drainage remained achievable even when fixtures were connected.

This study provides a basic examination of a single multi-inlet floor gully under a top-venting system, focusing on the pressure-resistance performance. Future work will evaluate the pressure-resistance performance of multiple multi-inlet floor gully types. In addition, the allowable drainage capacity will be further examined by including the effects of inflow from fixture drainage pipes.

Acknowledgments

We received support from the Osawa Memorial Institute of Architectural Environmental Engineering, Kanto Gakuin University and BOLIN Hydropower Material Co., Ltd. We would like to express our gratitude to both.

References

1) Takehiko Mitsunaga: Study on Evaporation Phenomenon of Trap Seal Water Part 2: Indoor and outdoor evaporation rates by regions: 48th International Symposium CIB W062, 2023

2) Noriyoshi Ichikawa and Fumitoshi Kiya, February 1986: A Study on the Water Seal Loss in the Trap of Sanitary Fixtures: Part 1-Influence of the Capillarity for S Trap: Transactions of the Society of Heating Air-Conditioning and Sanitary Engineers of Japan No. 30

3) K. Sakaue: Numerical Analysis of Induced Siphonage in P Trap, Proceedings of the 43rd International Symposium of CIB W062 on Water Supply and Drainage for Buildings, 2017

4) S.C. Chung: Study on New Style Trap and Application in Building Drainage System, Proceedings of the 38th international symposium CIB W062 on water supply and drainage for buildings, held on 27-30 August 2012 in Edinburgh, Scotland, 2012

5) Der-Chang Lo, Shyy Chang, Hsin-Feng Liu and Chao-Yan Chen, 2018: Experimental and Numerical Study of Hydrodynamic Characteristics of Gullies for Buildings: Water 10. 165

6) Society of Heating: Air-Conditioning and Sanitary Engineers of Japan: Society of Heating, Air-Conditioning and Sanitary Engineers of Japan Standard SHASE-S 218 2021 Test Method for Drainage Capacity of Drainage Stack Pipe Systems

7) Japan Cast Iron Cover & Waste Fitting Association Standard: JCW201-2012 Floor Drain Trap, established 1998, revised, 2012

8) Society of Heating: Air-Conditioning and Sanitary Engineers of Japan: Society of Heating, Air-Conditioning and Sanitary Engineers of Japan Standard SHASE-S 206-2019 Standards for Plumbing and Sanitary Systems

6. Authors

Hibiki Hasemi is a graduate student with the Otsuka Laboratory at Kanto Gakuin University and mainly researches multi-inlet floor gully units. Member of AIJ (Architectural Institute of Japan) and SHASE (Society of Heating, Air-Conditioning and Sanitary Engineers of Japan).

Masayuki Otsuka is a professor in the College of Architecture and Environmental Design at Kanto Gakuin University and conducts a wide range of research on plumbing and sanitary systems. Member of AIJ and has served as president of SHASE.

Ayaka Kimura is a second-year doctoral student in the Otsuka Laboratory at Kanto Gakuin University in Japan. During her studies, she was mainly involved in research on living space hygiene contributory to preventive measures against COVID-19. She also works at Tokyo Electric Power Company Holdings, Inc., where she is engaged in research on electricity demand and energy conservation.

Meng-Chieh, Jeffrey Lee is a PhD in Architecture. He is also the Professor at department of interior design and the Associate dean of design college in National Taichung University of Science and Technology. His major is water plumbing system, sanitary equipment safety and new technology development, interior environmental control, and energy saving.

Impact of kitchen food waste grinders on blockage risk and water use in high-rise drainage systems

T.W. Tsang (1), M.W. Chan (2), L.T. Wong (3), K.W. Mui (4)

(1) hayley.tsang@polyu.edu.hk

(2) rosie-mw.chan@polyu.edu.hk

(3) ling-time.wong@polyu.edu.hk

(4) horace.mui@polyu.edu.hk

(1), (2), (3), (4) Department of Building Environment and Energy Engineering, The Hong Kong Polytechnic University, Hong Kong

Abstract

Household food waste in Hong Kong is currently managed predominantly through manual separation and collection, a labour-intensive approach that offers limited incentives for careful sorting. Kitchen food waste grinders (disposers), a popular device used to collect food waste in North America and parts of Europe, is discouraged by the Authority over the concern of plumbing failures and blockages from solidified grease and oil inside pipes.

To address such concern, this study presents an experimental investigation of kitchen food waste grinders (FWGs) using a test rig representing a typical Hong Kong household kitchen drainage system. Repeated grinding and flushing cycles with representative household food waste mixtures were applied to simulate daily use and observe cumulative effects. System performance was examined in terms of transport of ground food waste, deposition patterns, blockage risk, and additional water usage. Particular attention was given to drainage design variables: trap type (U-trap vs. bottle trap) and pipe gradient (18, 54 and 90mm/m run). For each configuration, residence time and accumulation at key locations were measured, and the additional water required to avoid unacceptable residue build-up was quantified.

Processing the daily food waste of a typical household required an average of 77.2 s and 11.9 L of additional water per operation. Residue was concentrated mainly near the grinder outlet and within the trap, with negligible accumulation in the downstream pipe. Trap type was the dominant factor affecting transport performance: bottle traps retained significantly more residue than U-traps. Pipe gradient had a comparatively limited effect, and steeper slopes did not necessarily improve transport. The U-trap with a gradient of 54 mm/m showed the best overall performance. Long-term testing under the worst-case condition showed no substantial accumulation of bulk food waste, although bone chips and grease deposition were observed in the bottle trap system. The results suggest that FWGs can be used in residential buildings in Hong Kong, provided that appropriate drainage configurations are adopted.

Keywords

Food waste grinders (FWGs); High-rise residential buildings; Pipe blockage; Water usage

1 Introduction

Domestic food waste represents a significant challenge for high-density urban environments like Hong Kong. While regions such as Germany and the United Kingdom have implemented mandatory waste separation for composting or waste-to-energy conversion, Hong Kong lacks such regulations. Consequently, the city disposes of over 2,000 tons of domestic food waste daily, with only 2% being collected separately [Environmental Protection Department, 2024]. The remainder is treated as general municipal solid waste, leading to the burial of vast quantities of recyclable organic matter in landfills.

In parts of North America and Europe, household food waste grinders (FWGs) are a common solution. These devices reduce the volume of solid waste by grinding organic matter into fine particles, which are then transported through the sewage system for treatment at centralized facilities. Although these systems offer potential environmental and operational benefits [Bolzonella et al., 2003], their integration into existing infrastructure introduces technical complexities, particularly regarding drainage hydraulics.

The application of FWGs presents a unique challenge in cities characterized by high-rise residential architecture and aging sewer networks. In these settings, drainage systems are typically designed for liquid waste rather than particulate solids. Introducing ground organic matter into these networks may alter transport behavior, potentially leading to sedimentation, reduced flow efficiency, and an increased risk of blockages [Mattsson et al., 2014a]. In Hong Kong, where residential towers feature long vertical stacks and

shared risers, current guidelines discourage the use of FWGs to minimize the discharge of fats, oils, and solids into kitchen drains.

Despite the growing relevance of FWGs, empirical research into their performance under localized drainage conditions remains limited. Previous case studies in New York and Sweden focused primarily on city-scale impacts rather than the mechanics of localized system blockages [New York City Department of Environmental Protection, 1997; Mattsson et al., 2014b]. Specifically, the influence of trap configurations and pipe gradients on the transport and accumulation of ground solids has not been sufficiently examined.

Therefore, this study experimentally evaluates the performance of FWGs under controlled conditions representative of Hong Kong's residential infrastructure. Using a custom-built test rig comprising a standard kitchen sink, an FWG, and interchangeable traps and transparent pipe segments, this research investigates the movement of ground food waste and its impact on the drainage system. The study focuses on how trap design and pipe gradient influence waste transport, residue accumulation, and water consumption. The findings provide empirical evidence on whether retrofitting FWGs into high-rise systems increases hydraulic stress or blockage risks. Ultimately, this research identifies robust drainage configurations for FWG use and offers practical guidance for engineers, building managers, and policymakers involved in Hong Kong's circular economy and waste management strategies.

2 Method

2.1 Experimental set-up

2.1.1 Test rig configuration

A full-scale (1:1) drainage test rig was constructed to replicate a typical residential kitchen drainage system. The assembly consisted of a standard kitchen sink integrated with an under-sink food waste grinder (FWG) (Teka TR550; the U.S.), interchangeable trap components, and adjustable pipe segments to simulate varying vertical drops and gradients. Water consumption was monitored using a high-sensitivity calibrated flow meter with a measurement range of 0.2–1.2 m^3/h. The schematic layout and physical assembly of the test rig are illustrated in Figure 1.

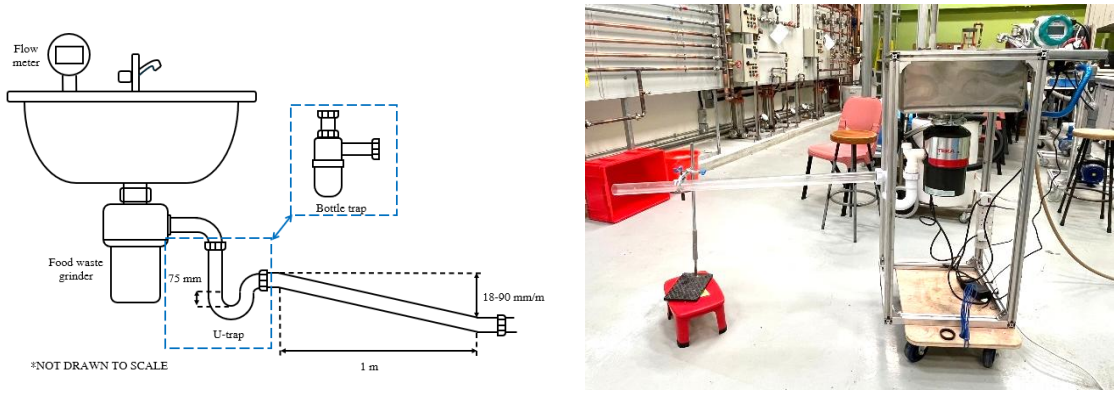

(a) (b)

Figure 1. (a) Schematic diagram; and (b) photograph of the experimental test rig.

2.1.2 Experimental matrix

The study investigated the impact of trap configuration and pipe gradient on food waste transport, residue accumulation, blockage risk, and water efficiency. Two common configurations—a bottle trap and a U-trap—were evaluated. Each trap was tested across three pipe gradients: 18 mm, 54 mm, and 90 mm (over a fixed length of 1 m), representing the minimum, mean, and maximum gradients permitted by the prevailing design standards [Institute of Plumbing, 2002]. This resulted in a total of six experimental cases. To ensure statistical reliability and repeatability, each case was conducted in triplicate.

2.1.3 Experimental procedure

In accordance with local waste audit data, a typical four-person household in Hong Kong generates approximately 0.73–0.78 kg of food waste daily [Environmental Protection Department, 2024]. Consequently, a standardized 755 g food waste sample was used for each trial. The sample, as shown in Figure 2, comprised a representative mixture of fruits, vegetables, starches, and meats, sourced daily from a local catering outlet to ensure freshness. The mixing proportions were based on established literature [Zan et al., 2018].

Figure 2. A sample of standardized food waste for experimental purpose.

The experimental protocol followed manufacturer recommendations:

1. Pre-flow: The cold-water tap was turned on for 5 seconds to stabilize the flow.
2. Grinding: The FWG was activated, and the food waste sample was introduced gradually. The device remained operational until a change in acoustic signature (a stable grinding sound) indicated that the matter had been fully processed.
3. Flushing: Post-grinding, water was allowed to flow for an additional 15 seconds to facilitate the transport of particles through the drainage network.

Following each trial, the sink inlet and pipe sections underwent visual inspection. Key junctions—including the FWG outlet, the trap, and pipe bends—were disassembled to identify and document any residue accumulation. The system was then thoroughly cleaned to remove all organic matter, oils, and grease before resetting for the next trial.

2.2 System performance indicators

2.2.1 Operation performance

Hydraulic behavior was assessed via qualitative observations during and after each trial, focusing on flow continuity, stagnation, and potential drainage delays. Quantitatively, the grinding completion time was recorded from the activation of the FWG to the stabilization of the grinding sound. Water consumption was measured across three distinct phases: pre-operation, grinding, and the final flushing stage.

2.2.2 Food waste residue analysis

System efficiency was evaluated by quantifying the organic matter retained within the pipes. In addition to visual documentation, any residue found at key locations was extracted using a spatula. The samples were drained of excess water and subsequently air-dried. To differentiate between total retained mass and actual solid accumulation, both the wet mass and the dry mass (following oven-drying in a laboratory) were recorded. The moisture content (MC) of the residue was calculated using the following equation:

$$\mathrm{MC} = \frac{\mathrm{W_{wet}} - \mathrm{W_{dry}}}{\mathrm{W_{wet}}} \times 100\%$$

2.3 Long-term operational testing

Following the initial parametric study, the configuration exhibiting the highest tendency for residue retention (the "worst-case scenario") was selected for long-term durability testing. This phase simulated prolonged residential use to identify cumulative system failures. The standard grinding-flushing cycle was repeated 30 times consecutively

without intermediate cleaning. Upon completion of the 30 cycles, the entire drainage system was disassembled, and the total accumulated residue was collected and measured to assess the long-term risk of sedimentation and blockage.

3 Results

3.1 Operational performance

Processing the daily food waste generated by a typical household in Hong Kong required an average of 77.2 s (range: 70.1–87.2 s; SD = 5.6 s). The additional water consumption associated with each operation averaged 11.9 L (range: 10.9–13.2 L; SD = 0.7 L), representing approximately 16% of the water used for cooking and other domestic purposes by an average household in Hong Kong [Water Supplies Department, 2025]. About 78% of the water was consumed during the grinding process, while the flushing stage required approximately 2 L.

No significant differences in grinding time or water consumption were observed among different trap types or pipe gradients ($p > 0.05$, t-test).

3.2 Food waste residue

3.2.1 Residue types and locations

During single-use operation, the food waste residue observed in the system mainly consisted of soft vegetable fragments (e.g., chopped onion and cabbage slices), which were flexible and less susceptible to grinding. Thin hard fibres (e.g., lotus leaf veins) were also difficult to grind and tended to become trapped within the system. The presence of fibrous material may have contributed to localized retention, particularly in configurations where flow continuity was disrupted. Figure 3 shows examples of food waste residue generated during a single operation.

Figure 3. Example of food waste residue during single-use operation.

Across all experimental conditions, residue accumulation was consistently concentrated near the FWG outlet and within the trap, while negligible residue was observed in the downstream pipe section. This suggests that once the food waste was ground sufficiently to pass through the trap, it was effectively transported along the downstream pipe, even at the smallest pipe gradient tested.

3.2.2 Trap types

Trap type played a critical role in determining food waste transport performance. The bottle trap tended to retain more food waste residue than the U-trap. As shown in Table 1, both the residue wet mass ($p < 0.05$, *t*-test) and dry mass ($p < 0.01$, *t*-test) were significantly higher in the bottle trap than in the U-trap.

Moisture content remained high across all configurations, generally ranging from 85% to 95%, indicating that the retained material predominantly consisted of water-rich slurry. However, the bottle trap tended to exhibit slightly lower moisture content than the U-trap, suggesting a greater proportion of solid material within the retained residue.

Table 1 – Food waste residue characteristics

Trap type	Pipe gradient (mm/m)	Residue wet mass (g)	Residue dry mass (g)	Moisture content (%)
Bottle trap	18	17.83	2.66	85%
	54	15.95	2.19	86%
	90	14.64	2.28	84%
U-trap	18	11.29	0.56	95%
	54	13.89	0.61	87%
	90	11.22	1.16	91%

3.2.3 Pipe gradient

Compared with trap type, pipe gradient had a less pronounced effect on food waste residue. No clear trend was observed with changing pipe gradient in the bottle trap configuration. For the U-trap, however, a slight increase in food waste residue was observed as pipe gradient increased. It is suspected that the angle formed between the steeper pipe and the U-trap may hinder smooth flow from the trap into the downstream pipe section.

Overall, the combined results indicate that optimal performance depends on the interaction between an appropriate trap type and a suitable pipe gradient. Among the tested configurations, the U-trap with an intermediate slope of 54 mm/m performed most effectively, whereas bottle trap systems consistently exhibited higher residue retention regardless of gradient.

3.3 Performance for long-term operation

Based on the initial tests, the bottle trap configuration with a pipe gradient of 18 mm/m was identified as the worst-case condition and was therefore selected for long-term operational testing. Over the course of the test, a total of 23.25 kg of food waste was processed, consuming 501.1 L of water.

After 30 repeated cycles of grinding and flushing, the system retained food waste residue with a wet mass of 6.54 g and a dry mass of 2.68 g. The retained residue was primarily composed of bone chips located at the bottom of the bottle trap, with a relatively low moisture content of 59%. No significant accumulation of fibrous or bulk food waste was observed within either the trap or the downstream pipe. However, visible oil deposition was found on the inner surfaces of both the bottle trap and the pipe section, indicating grease accumulation over prolonged operation.

(a) (b)

Figure 4. (a) Bone chips found at the bottom of the bottle trap; and (b) visible grease accumulation in the bottle trap and pipe.

4 Discussion

4.1 Experimental results

This study demonstrates that the feasibility of adopting FWGs in residential buildings depends less on the grinding process itself and more on the capacity of the drainage system to convey the resulting slurry. Under the tested conditions, daily household food waste could be processed in a short time with moderate additional water use, and neither trap type nor pipe gradient significantly affected operating time or water consumption.

The results clearly show that trap type is the dominant factor affecting food waste transport. Residue was consistently concentrated near the FWG outlet and within the trap,

while negligible accumulation was found in the downstream pipe. This indicates that the trap is the key control point in the system: once ground food waste passes through the trap, downstream transport is generally effective even at the lowest pipe gradient tested. Among the two trap types examined, the U-trap performed substantially better than the bottle trap, retaining significantly lower wet and dry residue masses. By contrast, bottle traps consistently promoted residue retention and therefore represent a less suitable configuration for systems fitted with FWGs.

The influence of pipe gradient was comparatively limited, and steeper slopes did not necessarily improve transport performance. The findings suggest that increasing pipe gradient alone is not an effective strategy for enhancing conveyance and may even reduce transport efficiency in some configurations. Instead, system performance appears to depend on the interaction between pipe slope and trap geometry. Of the tested arrangements, the U-trap with an intermediate pipe gradient of 54 mm/m provided the most favorable overall performance.

Long-term testing further suggests that solid food waste accumulation may not be the primary operational concern in FWG-equipped drainage systems. Even under the worst-case condition, repeated use did not result in substantial build-up of fibrous or bulk food waste. Residual material was mainly limited to bone chips settled at the bottom of the bottle trap. However, visible grease deposition was observed on the internal surfaces of both the trap and pipe, indicating that grease accumulation is likely to pose a greater long-term risk than solid residue. This finding is important because it shifts attention from blockage caused by food particles alone to the broader issue of fat, oil, and grease management in kitchen drainage systems.

4.2 Practical recommendations

From a practical perspective, the results support several recommendations for the implementation of FWGs in residential buildings:

1. U-traps should be preferred over bottle traps where FWGs are to be installed, as they provide better transport performance and lower residue retention.

2. Drainage design should not rely solely on steeper pipe gradients to improve performance; an appropriate gradient should be selected together with a compatible trap geometry.

3. Management of grease discharge should be emphasized in households with FWGs, since grease accumulation may become the main long-term maintenance concern.

4. System design guidelines and retrofit assessments should explicitly consider existing trap configurations before permitting or recommending FWG installation in residential buildings.

4.3 Limitations

Several limitations were identified in this experimental study. First, variability in the characteristics of the food waste samples, including the presence of harder components such as small bones or tougher fibres, may have influenced system behaviour. Second, the operation time and water consumption were highly dependent on the user's judgment of when a stable grinding sound had been reached, as indicated by changes in the acoustic signature. Finally, under normal kitchen drainage conditions, additional water and detergent would typically be discharged into the system, which may further flush food waste residue or grease. These conditions were not replicated in the present experiment.

Future studies involving the implementation of FWGs in real buildings could provide more representative information on their practical use, performance, and impacts on drainage systems.

5 Conclusion

This study showed that the performance of food waste grinders (FWGs) in building drainage systems is governed primarily by drainage configuration rather than by grinding operation itself. Although daily household food waste could be processed within a short time and with moderate additional water use, residue transport was strongly influenced by trap type. Residue accumulation was mainly confined to the FWG outlet and trap, with negligible deposition in the downstream pipe, indicating that once food waste passed through the trap, downstream conveyance was generally effective under all tested pipe gradients.

Among the tested configurations, the U-trap consistently outperformed the bottle trap by retaining significantly less residue, demonstrating superior transport performance. Pipe gradient had a comparatively limited effect, and steeper slopes did not necessarily improve residue conveyance. The U-trap with an intermediate pipe gradient of 54 mm/m provided the best overall performance.

Long-term testing under the worst-case condition showed no substantial accumulation of bulk food waste, although bone chips and visible grease deposition were observed in the bottle trap system. These findings suggest that trap design is a critical consideration for FWG implementation, while grease accumulation may present a more important long-term concern than solid food waste retention. Overall, the results support the feasibility of FWG application in residential buildings, provided that appropriate drainage configurations are adopted.

Acknowledgments

This work was jointly supported by the Start-up Fund for RAP (Strategic Hiring Scheme, project no. 1-BDWZ) and the Carbon Neutrality Funding Scheme (project no. 4-ZZW2), The Hong Kong Polytechnic University.

6 References

Bolzonella, D., Pavan, P., Battistoni, P., & Cecchi, F. (2003). The under-sink garbage grinder: A friendly technology for the environment. *Environmental Technology*, *24*(3), 349–359.

Environmental Protection Department. (2024). Monitoring of solid waste in Hong Kong: Waste statistics for 2023. Hong Kong SAR Government. Online: https://www.wastereduction.gov.hk/sites/default/files/resources_centre/waste_statistics/msw2023_eng.pdf

Institute of Plumbing. (2002). *Plumbing engineering services design guide* (2002 ed.). https://www.ciphe.org.uk/

Mattsson, J., Hedström, A., Viklander, M., & Blecken, G. T. (2014a). Fat, oil, and grease accumulation in sewer systems: comprehensive survey of experiences of Scandinavian municipalities. *Journal of environmental engineering*, *140*(3), 04014003.

Mattsson, J., Hedström, A., & Viklander, M. (2014b). Long-term impacts on sewers following food waste disposer installation in housing areas. *Environmental technology*, *35*(21), 2643-2651.

New York City Department of Environmental Protection. (1997). *The impact of food waste disposers in combined areas of New York City*. New York, NY: New York City Department of Environmental Protection.

Water Supplies Department (2025). Water and the Society – Value of Water. Online: https://www.waterconservation.gov.hk/en/at-school/secondary-school/water-and-society/value-of-water/index.html

Zan, F., Dai, J., Hong, Y., Wong, M., Jiang, F., & Chen, G. H. (2018). The characteristics of household food waste in Hong Kong and their implications for sewage quality and energy recovery. *Waste Management*, *74*, 63–73.

7 Presentation of Author(s)

Dr. T.W. Tsang is a Research Assistant Professor in the Department of Building Environment and Energy Engineering at The Hong Kong Polytechnic University. Her research interests are focused on the critical areas of airborne infection in the built environment, indoor environmental quality, building ventilation, carbon neutrality, and food waste.

Ms. M.W. Chan is an MPhil researcher in the Department of Building Environment and Energy Engineering at The Hong Kong Polytechnic University. Her research focuses on decentralised food waste management systems in high-density urban environments, with a particular focus on biological treatment methods and system integration. Her research interests include sustainable waste management, environmental monitoring, and carbon neutrality.

Rosie

Prof. L.T. Wong is an Associate Professor in the Department of Building Environment and Energy Engineering at The Hong Kong Polytechnic University. Prof. Wong is a Chartered Engineer and a member of HKIE an d CIBSE.

Prof. K.W. Mui is the Dean of Student and a Professor in the Department of Building Environment and Energy Engineering, and associate Head of the College of Undergraduate Researchers and Innovators (CURI) at The Hong Kong Polytechnic University. Prof. Mui is a Chartered Engineer, a Fellow of HKIE, and a member of ASHRAE(USA), HKSMI, CIBSE and ISIAQ.

Hydrodynamic Characteristics Analysis of the T-CORE Special Fitting Drainage and Venting System

Wan-Ju Liao (1), Hisanori Kojima (2), Shyy-Woei Chang (3)

(1) liaowj@nkust.edu.tw
(2) hkojima@kojima-core.co.jp
(3) swchang@mail.ncku.edu.tw
(1) Department of Construction Engineering, National Kaohsiung University of Science and Technology, No.1, University Rd., Yanchao Dist., Kaohsiung City 824, Taiwan (R.O.C)
(2) Chief Executive Officer, Kojima Seisakusho Co., Ltd.
(3) Department of Systems and Naval Mechatronic Engineering, National Cheng Kung University, No. 1, University Road, Tainan City 70101, Taiwan (R.O.C.)

Abstract

As demands for space efficiency and drainage performance in modern high-rise buildings intensify, single-stack drainage systems offer compelling advantages through simplified shaft configurations. Although Article 4.3.1 of Taiwan's Technical Code for Building Water Supply and Drainage Equipment acknowledges the pressure-suppression principle of special fittings, no full-scale empirical study has systematically quantified T-CORE system performance-with and without AAV-under SHASE-S 218. This knowledge gap impedes evidence-based design practice.

In light of these considerations, this study utilizes a nine-story full-scale drainage test tower to investigate the hydrodynamic characteristics of the T-CORE Special Fitting Single-Stack Drainage System under discharge loads ranging from 2.5 L/s to 6.5 L/s, in accordance with the SHASE-S 218 testing standards. Furthermore, comparative experiments were conducted by integrating the system with Air Admittance Valve to verify their effectiveness in mitigating pneumatic pressure fluctuations and maintaining pressure balance within the stack. The research findings serve as a technical basis for the selection of piping systems and construction planning in modern building drainage and venting systems, thereby enhancing the overall performance of building services and advancing the potential for technological innovation in engineering design.

Keywords

Single-stack drainage system, Special fittings, Hydrodynamic Characteristics, Air Admittance Valve

1 Introduction

Driven by rapid urbanization and the widespread adoption of multi-family high-rise housing, modern building drainage systems are evolving toward high efficiency, pipeline simplification, and the optimization of pipe shaft space. The fundamental purpose of planning drainage and vent systems is to ensure unimpeded flow dynamics, thereby safeguarding indoor environmental hygiene and the health and safety of occupants.

As architectural configurations grow increasingly complex, spatial constraints and traditional equipment thresholds struggle to meet contemporary drainage design demands. To overcome these limitations, the Taiwanese market has actively developed centralized water traps while concurrently adopting Air Admittance Valves (AAV)-a pivotal trend aimed at simplifying piping network layouts and reducing construction duration. Prior literature (Liao and Chang, 2023) indicates that the Japanese construction sector introduced AAV technology from Europe as early as 1983, establishing stringent mandates that AAV airflow capacity must be fully equivalent to conventional vent pipes, alongside mandatory implementation of robust positive pressure mitigation measures. Consequently, the "air admission rate" serves as the primary evaluation metric for AAV integration in drainage systems.

Pursuant to Taiwan's Technical Code for Building Water Supply and Drainage Equipment and relevant studies (Liao, Chang, and Guan, 2025), the sizing of vent pipe diameters is directly proportional to building height and fixture units (FU). When substituting with an AAV system, the air induction capacity must exhibit performance equivalent to the vent diameters prescribed by the regulatory code. For low-rise configurations or low-load environments, these capacity specifications may be appropriately scaled down. In short, the fundamental prerequisite for replacing conventional vent stacks with AAVs relies on a rigorous verification ensuring complete parity in air replenishment capacity compared to traditional venting systems.

In contemporary engineering practice, Taiwan’s architectural drainage and vent systems are undergoing a pronounced paradigm shift, transitioning from conventional four-pipe configurations-characterized by separate soil and waste vertical drainage paired with dedicated vent pipes (VP)-toward streamlined two-pipe systems integrated with AAV, as illustrated in Figures 1(a) and 1(b). Substituting conventional vent stacks with AAV, supplemented by comprehensive positive pressure relief measures, has become a widely adopted strategy to minimize stack counts and optimize spatial utilization within pipe shafts. Furthermore, field surveys indicate that some projects have pioneered the integration of special-fitting single-stack drainage systems or AAV-based single-stack alternatives, routing vertical stacks directly through service balconies to yield further spatial savings, as shown in Figures 1(c) and 1(d). Notably, the T-CORE special fitting single-stack drainage system has been extensively commercialized in Japan across

diverse building typologies, including high-rise residential complexes, hotels, and healthcare facilities, as demonstrated in Figure 1(e).

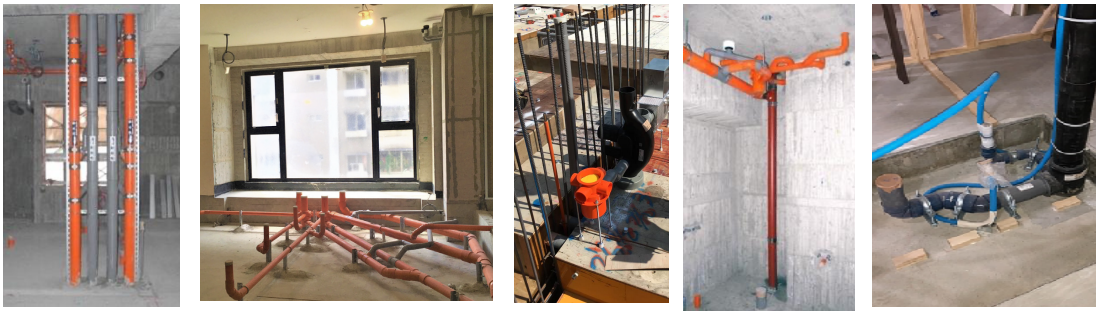

a. Conventional Four-Pipe System | b. Two-Pipe AAV System | c. Single-Stack Sovent System | d. Single-Stack AAV System | e. Single-Stack T-CORE System

Figure 1-Case Study of Building Drainage and Venting Systems [2]

With the continuous advancement of building water supply and drainage technologies and construction methods, special-fitting single-stack drainage and vent systems have gradually become an important development trend in high-rise building drainage design (Gormley et al., 2021), offering advantages such as reduced pipe shaft space requirements, lower construction complexity, and improved maintenance accessibility. Based on the practical application of combined trap systems and air admittance valves (AAVs) commonly adopted in Taiwanese multi-family residential buildings, this study establishes a T-CORE special-fitting single-stack drainage and vent system to investigate pressure variation and hydrodynamic characteristics under different drainage loading conditions, thereby providing a design reference for buildings constrained by limited space and cost considerations. To achieve this objective, full-scale comparative experiments were conducted on both T-CORE+AAV and T-CORE single-stack drainage systems based on the SHASE-S 218 testing framework. The objectives of this study are to: (1) measure the pressure distribution and fluctuation characteristics at measurement points A and B under drainage loading conditions ranging from 2.5 to 6.5 L/s; (2) evaluate the effectiveness of the AAV in mitigating negative pressure and improving pressure stability within the drainage system; and (3) analyze the hydrodynamic characteristics under different drainage loading conditions.

2. Development of Single-Stack Systems with Special Fittings

The technical evolution of single-stack drainage systems with special fittings is academically rooted in the dual pursuit of maximizing spatial efficiency in high-rise buildings and ensuring in-pipe pressure stability. Early foundational research is represented by the benchmark experiments conducted by Wyly and Eaton in 1952 at the National Bureau of Standards (NBS), which revealed that conventional single stacks generate severe pressure fluctuations under unvented conditions, thereby imposing physical limitations on the system's hydraulic carrying capacity. To surmount this bottleneck, Sommer developed a special fitting featuring air-water separation

capabilities (the Sovent System) in 1962, marking a major paradigm shift in single-stack technology from passive strategies-such as merely expanding pipe diameters-to the active control of the in-pipe flow field through structured geometric design.

Since the 1970s, in response to high-density urban development and the proliferation of multi-family residential complexes, the Japanese academic and industrial sectors shifted their research focus from early energy dissipation and buffering toward more precise swirling flow control technology. Empirical research by Motomura in 1987 further established that the design of internal guide structures within special fittings can force the downward fluid to adhere to the inner pipe wall, establishing a stable annular flow. This configuration preserves a continuous and stable air core within the central axis of the vertical stack, thereby significantly enhancing the system's overall drainage efficiency.

The hydrodynamic characteristics of single-stack systems are governed by the downward-flowing annular water film along the stack wall and its induced aerodynamic behavior. As the drainage load intensifies, the thickness of the liquid film expands and compresses the available core space for airflow, leading to drastic transient positive and negative pressure fluctuations within the network. Prior literature has indicated that such unstable pneumatic pressures jeopardize the trap seal stability of sanitary fixtures (Swaffield & Galowin, 1992; Jack & Swaffield, 2009). Pursuant to the technical criteria specified in the British Standard BS EN 12056-2 and the SHASE-S 218 standard promulgated by the Society of Heating, Air-Conditioning and Sanitary Engineers of Japan (SHASE), pressure fluctuations within drainage systems during operation must be rigorously maintained within ±400 Pa, which serves as a critical threshold for safeguarding building environmental hygiene and trap seal integrity.

3 Experimental details

3.1 Experimental method and facilities

The experiments in this study were conducted at the 9-story, full-scale drainage test tower of Kojima Seisakusho Co., Ltd., Japan, with the testing procedures strictly adhering to the Standard of the Society of Heating, Air-Conditioning and Sanitary Engineers of Japan (SHASE-S 218). The drainage hydraulic loading was introduced as a constant flow rate at each floor from the 9th to the 7th floor. Under varying total drainage flow rates of 2.5, 3.0, 4.0, 5.0, and 6.5 L/s, the transient internal pressure fluctuations and hydrodynamic performance of the T-CORE single-stack drainage system were investigated under two distinct configurations: with and without the installation of an Air Admittance Valve (AAV).

The configuration of the pressure monitoring points is illustrated in Figure 2. These points are strategically positioned at the drainage stack upstream of the specialized T-CORE fitting (Point A), the drainage stack downstream of the specialized fitting (Point

B), and the horizontal branch (Point C). Once the discharge flow field achieved a steady state at approximately 40 seconds, the maximum pressure (Pmax) and minimum pressure (Pmin) recorded within the 50-to-90-second interval were extracted to serve as the system performance evaluation indicators. To ensure reproducibility, each experimental condition was tested in duplicate, and the corresponding mean values were calculated for subsequent analysis. The experimental apparatus is shown in Figure 2.

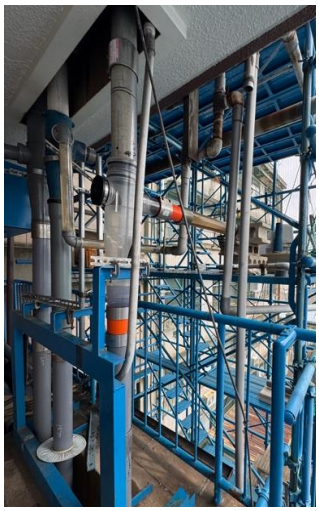

Drainage Experimental Tower

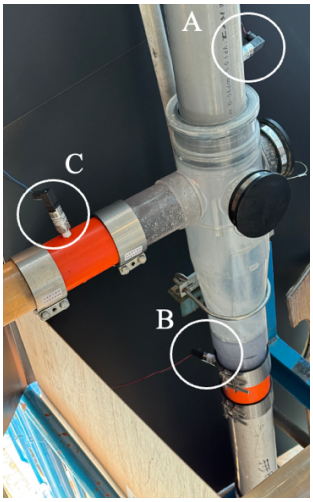

Pressure Measurement Location

Installation of an AAV on the horizontal branch

Airtightness Test - Electronic Air Tester

Figure 2-Experimental Setup

3.2 Airtightness Test

To ensure system integrity, an airtightness test was conducted prior to pressure measurements. According to the SHASE-S 206-2019 standards, if a drainage and venting system cannot undergo a water-filled test due to environmental or experimental constraints, an air pressure test can be performed as an alternative. The primary objective of this test is to prevent water leakage from the drainage pipes and odor emissions from the vent pipes. The specific procedure is as follows: an air compressor (electronic air tester) was connected to an appropriate measurement point on the drainage pipeline. After sealing all openings, the interior of the piping was pressurized to inspect for any air leakage. According to NPC regulations, the required pressure for the airtightness test must be a gauge pressure of 35 kPa or 250 mmHg, which must be maintained for a minimum duration of 15 minutes.

4 Results and Discussion

This study investigates the Japanese T-CORE single-stack drainage system. Its core mechanism utilizes built-in deceleration and swirling guide vanes within a special fitting to direct the drainage, generating a swirling flow that moves smoothly downward to form a stable annular flow. Under the influence of centrifugal force, the wastewater within the drainage stack is propelled against the pipe wall, creating a central air core

that serves as a ventilation pathway to regulate internal pressure fluctuations. Furthermore, at the transition from the vertical stack to the horizontal main line, the integration of a bottom transition fitting or an enlarged pipe diameter design smoothly guides the drainage into the horizontal main. This configuration effectively eliminates the positive drainage pressure induced by the hydraulic jump phenomenon, thereby providing a stable aerodynamic balance for high-rise single-stack drainage systems.

4.1 Stack Air Pressure Fluctuation and Hydrodynamic Characteristics

This study compares the T-CORE+AAV and T-CORE single-stack drainage systems under different drainage loading conditions through continuous discharge experiments. Air pressure variations within the drainage stack were measured using pressure sensors, and data collected during the steady drainage period (50-90 s) were extracted for analysis. The objective was to investigate system pressure fluctuation characteristics, pressure variation, and stability under different drainage loading conditions, as well as to evaluate the pressure regulation performance of the air admittance valve (AAV).

As shown in Figure 3, the T-CORE+AAV and T-CORE systems exhibited different pressure fluctuation characteristics during continuous drainage. Overall, the T-CORE+AAV system demonstrated more concentrated pressure fluctuations, smaller negative pressure amplitudes, and a more stable pressure variation trend. In contrast, the T-CORE system exhibited larger negative pressure amplitudes and more pronounced pressure fluctuations, indicating relatively lower pressure stability in the absence of an AAV.

Further examination of pressure variations during the steady drainage stage (approximately 50-90 s) revealed that both systems experienced a certain degree of transient pressure oscillation during continuous discharge. However, the T-CORE+AAV system exhibited a noticeably smaller fluctuation range, indicating that the AAV provided a pressure-regulating effect during drainage and effectively reduced the accumulation of negative pressure within the system. By comparison, the T-CORE system showed more severe pressure fluctuations and deeper negative pressure levels, which may suggest that the system's internal air compensation capability becomes more limited under higher drainage loading conditions.

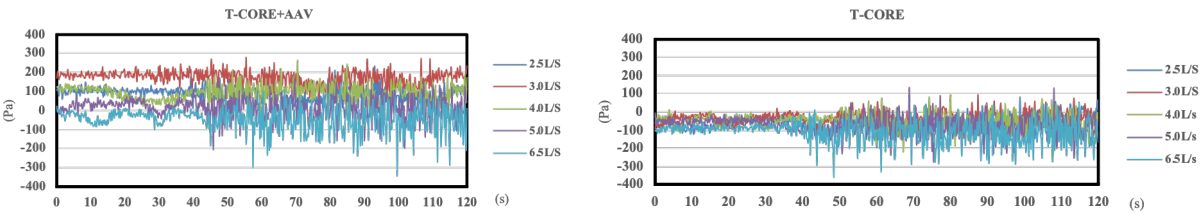

Figure 3-Characteristics of Stack Air Pressure Fluctuations under Varied Drainage Flow Rates

4.2 Pressure Extrema Under Different Drainage Flow Rate Conditions

This study focuses on two single-stack drainage configurations: T-CORE+AAV and a standalone T-CORE system. Under varying drainage hydraulic loading rates (2.5, 3.0, 4.0, 5.0, and 6.5 L/s), the maximum pressure (Pmax) and minimum pressure (Pmin) were extracted during the steady continuous discharge period from 50 to 90 seconds. Additionally, the pressure transmission behavior between monitoring points A and B along the drainage stack was investigated. The experimental results, as illustrated in Figure 4, demonstrate distinctly divergent pressure fluctuation characteristics between the two system configurations.

1. Impact of AAV Integration on Pressure Values at Stack Monitoring Points A and B

For monitoring point A, the integration of an AAV provides a highly pronounced mitigation effect on negative pressure. For instance, under a drainage flow rate of 2.5 L/s, the mean minimum pressure (Pmin) of the standalone T-CORE system was -288Pa, whereas that of the T-CORE+AAV system was substantially alleviated to -167Pa. Under a higher drainage load of 5.0 L/s, the mean minimum pressure (Pmin) of the standalone T-CORE system reached as deep as -383Pa, while the addition of the AAV suppressed this depression to -189Pa. These empirical results confirm that the AAV can effectively stabilize and balance the internal negative pressure within the stack.

Regarding monitoring point B, the experimental trends under the low drainage load were consistent with those observed at point A. Specifically, at a flow rate of 2.5 L/s, the mean minimum pressure (Pmin) for the standalone T-CORE and the T-CORE+AAV systems were -211Pa and -220Pa, respectively, showing no statistically significant discrepancy. This indicates that under lower hydraulic loading conditions, the air admittance valve possesses a relatively mild buffering effect on stack negative pressure.

However, when the drainage load increased to 5.0 L/s, the mean minimum pressure (Pmin) of the T-CORE system reached -253 Pa, whereas it was reduced to -204 Pa after the installation of the AAV. This indicates that the AAV can provide immediate air admission and achieve a certain degree of negative pressure mitigation. It is worth noting that, although the AAV reduced the negative pressure level, the system was also accompanied by more pronounced positive pressure fluctuations. The maximum positive pressure (Pmax) increased from 12 Pa in the T-CORE system to 133 Pa in the T-CORE+AAV system. These results indicate that, under higher drainage loading conditions, the air compensation provided by the AAV contributes to negative pressure mitigation; however, the lower stack section beneath the special fitting, where measurement point B is located, may still experience relatively large transient positive pressure responses. The underlying mechanism may be associated with flow reorganization within the special fitting, air–water interaction, and downstream pressure transmission behavior, which should be further discussed in conjunction with subsequent flow visualization and hydrodynamic characteristic analyses.

Overall, the experimental results indicate that the T-CORE+AAV system provides a clear benefit in suppressing negative pressure. In particular, at the upper stack measurement point A, the installation of the AAV effectively reduced the negative pressure level, thereby improving the pressure stability of the single-stack drainage system. However, under a higher drainage loading condition of 5.0 L/s, although the AAV improved the negative pressure condition within the system, measurement point B still exhibited more pronounced positive pressure fluctuations. This suggests that the pressure transmission behavior in the lower stack section beneath the special fitting requires further control. Therefore, in the application of single-stack drainage systems for high-rise buildings, attention should be given not only to negative pressure control in the upper stack but also to the flow-guiding and pressure-buffering design at the transition from the vertical stack to the horizontal main. Examples include the use of a T-LJ bend or an enlarged bottom pipe diameter configuration, which may help reduce downstream pressure fluctuations and improve overall system stability.

2. Impact of AAV Integration on Pressure Values at Horizontal Branch Monitoring Point C

Measurement point C on the horizontal branch is an important location for evaluating the protection of trap seal stability. The experimental results indicate that installing an air admittance valve (AAV) on the horizontal branch provides a noticeable negative pressure mitigation effect, with an average improvement of more than 50 Pa. This suggests that the AAV contributes to air compensation in the horizontal branch region and helps reduce the influence of negative pressure on trap seal stability.

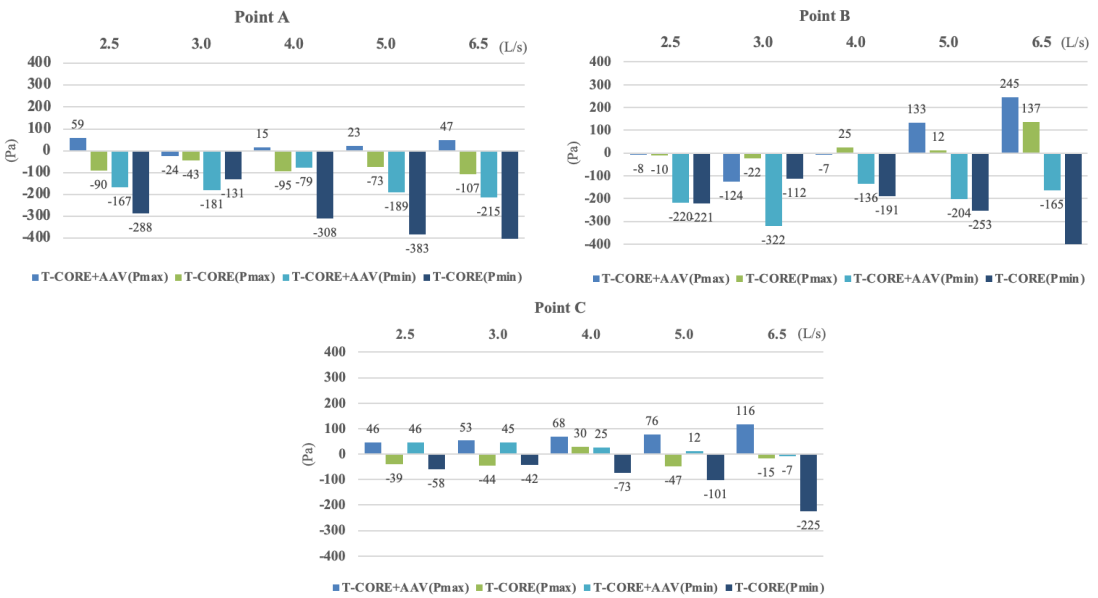

Figure 4-Comparison of maximum and minimum pressures between T-CORE + AAV system and T-CORE system under different drainage flow loads

4.3 Hydrodynamic Characteristics Analysis

This study compares the hydrodynamic characteristics of two single-stack drainage systems, T-CORE+AAV and T-CORE, under different drainage loading conditions of 2.5, 5.0, and 6.5 L/s. Pressure data during the steady drainage stage from 50 to 90 s were extracted to analyze the pressure response at measurement point A and the corresponding pressure variation at measurement point B when the discharge flow passed through the internal guide vane of the special fitting and induced a hydraulic jump. The objective was to investigate the hydrodynamic characteristics of the gas-liquid two-phase flow inside the special fitting. The results are shown in Figure5.

The results indicate that the pressure distributions at measurement points A and B exhibit different hydrodynamic characteristics depending on the drainage load. Since measurement point A is located near the upper region of the special fitting, its pressure variation can be regarded as the pressure response of the upper vertical stack to flow-field disturbances occurring inside the special fitting. In contrast, measurement point B reflects the pressure transmission behavior in the lower vertical stack section after the drainage flow passes through the special fitting. Therefore, P_A and P_B can serve as important indicators for evaluating the influence of internal flow-regime variations within the special fitting on the pressure behavior of the upper and lower stack sections.

Under the low drainage loading condition of 2.5 L/s, the T-CORE+AAV and T-CORE systems exhibited different pressure response characteristics between measurement points A and B. For the T-CORE+AAV system, the measured pressures were P_A = -68 Pa, P_B = -108 Pa, and P_A = 22 Pa, P_B = -168 Pa, indicating that the AAV effectively mitigated the negative pressure at point A, while point B still showed a certain degree of negative pressure response. In contrast, for the T-CORE system, the measured pressures were P_A = -212 Pa, P_B = -214 Pa, and P_A = -311 Pa, P_B = -319 Pa, showing that PA and PB remained at similar negative pressure levels. These results suggest that, under low-flow conditions, the local hydraulic jump and air–water interfacial disturbances induced by the discharge flow passing through the guide vane of the special fitting were still limited and insufficient to cause a significant difference in upstream and downstream pressure distribution. Therefore, the A and B points in the T-CORE system exhibited nearly synchronized pressure variations.

Under the higher drainage loading condition of 5.0 L/s, the T-CORE+AAV system recorded P_A =-18 Pa and P_B = -50 Pa, as well as P_A = -61 Pa and P_B = -100 Pa. The overall negative pressure magnitude was relatively small, indicating that the AAV maintained a certain degree of air compensation capability and contributed to a more stable pressure distribution within the system. In contrast, the T-CORE system recorded P_A = -286 Pa and P_B = -190 Pa, as well as P_A = -320 Pa and P_B = -167 Pa, showing that the negative pressure magnitude at P_B was clearly smaller than that at P_A. This result indicates that, as the drainage flow rate increased, local flow disturbances near the guide vane region of the special fitting became more pronounced, resulting in a stronger negative pressure response at measurement point A. After the discharge flow passed

through the special fitting, the water flow gradually redistributed along the pipe wall, and the central air core partially recovered, thereby reducing the negative pressure magnitude at downstream measurement point B and indicating a pressure recovery phenomenon. This suggests that, under high-flow conditions, the special fitting provides a certain degree of flow guidance and gas–liquid two-phase flow redistribution capability.

When the drainage flow increased to the critical high-loading condition of 6.5 L/s, both the T-CORE and T-CORE+AAV systems exhibited significant changes in internal pressure distribution, with the negative pressure magnitude at measurement point B being smaller than that at measurement point A. High-resolution flow visualization showed that severe turbulence and foaming occurred inside the special fitting under this high-loading condition, indicating that the flow regime had approached the limit at which the special fitting could maintain a stable annular swirling flow. Under this condition, the formation of a dense water curtain disturbed the continuity of the central air core, resulting in obstruction of the internal airflow passage. Even with the AAV installed, the air compensation effect was limited, causing both measurement points A and B to exhibit relatively large pressure fluctuations.

Overall, the results indicate that the T-CORE+AAV system demonstrated better overall pressure stability than the T-CORE system under different drainage loading conditions, suggesting that the AAV provides a certain degree of negative pressure regulation in the single-stack drainage system. However, as the drainage flow increased to high-loading conditions, internal flow disturbances and gas–liquid two-phase flow reorganization within the special fitting became more pronounced, and transient pressure fluctuations still occurred in the system. Future studies should further investigate the relationship among the flow-guiding structure of the special fitting, flow stability, and upstream–downstream pressure transmission, with the aim of reducing pressure fluctuations under high drainage loading conditions and improving overall system stability.

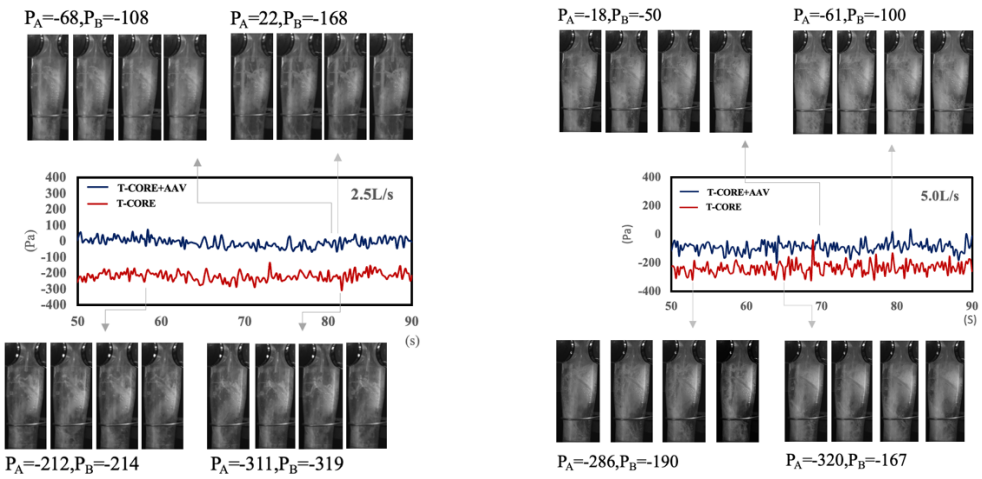

(a) 2.5L/s (b) 5.0L/s

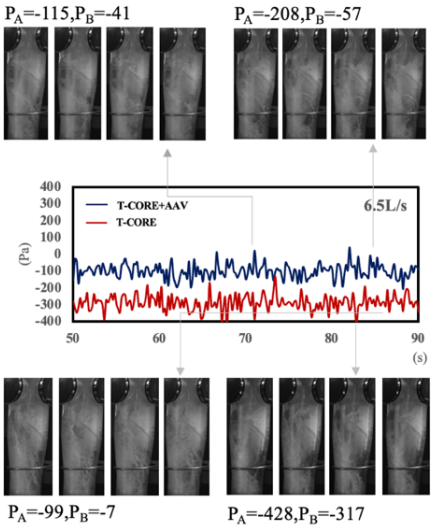

(c) 6.5 L/s

Figure 5-Hydrodynamic characteristics under different drainage flow rate conditions (2.5 L/s, 5.0 L/s, and 6.5 L/s)

5 Conclusions

With the increasing demands for spatial efficiency and drainage performance in modern high-rise buildings, single-stack drainage systems have demonstrated significant technical advantages due to their simplified pipe configuration and improved efficiency in the use of pipe-shaft space. The T-CORE special fitting promotes a stable swirling flow within the vertical stack through its internal deceleration and swirl guide vanes. In addition, its backflow-prevention wall is designed to reduce the risk of wastewater from the rotating stack flow and horizontal branch pipes flowing back into other horizontal branches.

The full-scale experimental results of this study confirm that the introduction of an air admittance valve (AAV) into the T-CORE special fitting single-stack drainage system can effectively mitigate instantaneous negative pressure fluctuations within the pipe under drainage flow rates of up to 5.0 L/s, thereby contributing to the stabilization of system pressure. Furthermore, the installation of a base transition fitting, such as a T-LJ fitting, together with an enlarged pipe diameter at the transition from the vertical stack to the horizontal main drain, can facilitate smoother discharge into the horizontal drainage main and reduce the positive pressure impact caused by hydraulic jump phenomena.

However, when the drainage flow rate approaches or exceeds the critical high-load condition of 6.5 L/s, the interaction between the stability of the internal swirling flow and the intensity of the hydraulic jump within the special fitting requires further investigation. Future research may further examine the effects of adjusting the geometric angle and flow-guiding configuration of the internal swirl guide vanes on hydraulic jump intensity, air-core continuity, and system pressure stability. These

findings may provide a basis for the subsequent optimization of single-stack drainage system design.

Acknowledgements

The authors gratefully acknowledge the financial support provided by the National Science and Technology Council under Grant Nos. NSTC 114-2221-E-992-006 and NSTC 113-2221-E-006-178-MY2.

6 References

Wan-Ju Liao, Chin-Wei Chang. Comparison of the maximum negative pressure value between the traditional drainage ventilation system and the suction valve ventilation system, Proceedings of the 35th Architectural Research Presentation, Architectural Institute of Taiwan, 2023, Kaohsiung, Taiwan,2023

Wan-Ju Liao, Yen- Ting Kuan. Study on the Technological Evolution of Same-Floor Drainage Methods and Ventilation Systems in Buildings, The 23rd Conference on Sustainable Development of the Construction Industry 2025, Taipei, Taiwan,2025

Wyly, R. B., & Eaton, H. N. Capacities of Stacks in Sanitary Drainage Systems. National Bureau of Standards (NBS),1952

Sommer, F. The Sovent System: Single-pipe drainage for multi-story buildings. Proceedings of the 3rd CIB Congress, Copenhagen, Denmark,1962

Motomura, K. Flow characteristics and pressure distribution in drainage stacks with special fittings. Journal of the Society of Heating, Air-Conditioning and Sanitary Engineers of Japan, 61(4), 311-318,1987

SHASE Testing methods for performance of drainage and vent piping systems in buildings (SHASE-S 218-2020). The Society of Heating, Air-Conditioning and Sanitary Engineers of Japan. https://www.shase.or.jp,2020

Swaffield, J. A. Transient airflow in building drainage systems. Routledge. https://doi.org/10.4324/9780203874448,2010

Gormley, M., Kelly, D., Campbell, D., Xue, Y., & Stewart, C. (2021). Building drainage system design for tall buildings: Current limitations and public health implications. Buildings, 11(2), 70. https://doi.org/10.3390/buildings11020070

Xue, Y., Stewart, C., Kelly, D., Campbell, D., & Gormley, M. Two-phase annular flow in vertical pipes: A critical review. Water, 14(21), 3496. https://doi.org/10.3390/w14213496,2020

Wong, L.-T., Mui, K.-W., Cheng, C.-L., & Leung, P. H.-M. Time-variant positive air pressure in drainage stacks as a pathogen transmission pathway. IJERPH, 18(11), 6068. https://doi.org/10.3390/ijerph18116068,2021

Improved Renovation Method for Drainage Stack Systems in High-Rise Residential Buildings

Tomoya Kono (1), Masayuki Otsuka (2), Koji Aizawa (3), Ryotaro Kikuchi (4), Kento Ishiwata (5), Ayaka Kimura (6)

(1) kouno@ns-net.jp

(2) dmotsuka@kanto-gakuin.ac.jp

(3) ko_ji.2525@i.softbank.jp

(4) m25J3006@kanto-gakuin.ac.jp

(5) m25J3003@kanto-gakuin.ac.jp

(6) d24J3002@kanto-gakuin.ac.jp

(1) Nihon Setsubi Kogyo Co., Ltd.

(2) Prof. Dr. Eng, Department of Architecture and Environmental Design, College of Architecture and Environmental Design, Kanto Gakuin University, Japan

(3) M. Eng., Former Graduate School of Engineering, Kanto Gakuin University, Japan

(4) Graduate Student, Graduate School of Engineering Kanto Gakuin University, Japan

(5) Graduate Student, Graduate School of Engineering Kanto Gakuin University, Japan

(6) Doctoral Student in Architecture, Graduate School of Engineering at Kanto Gakuin University, Japan

Abstract

As high-rise residential buildings age, their drainage systems continue to deteriorate; in Japan, for example, many such buildings have already exceeded 20 years of age. Cast iron pipes and ALFA steel pipes have been commonly used for drainage stack installations in these buildings, but these pipes have corroded and deteriorated over time, thereby necessitating renewal. This study focused on ALFA steel pipes installed in an existing high-rise residential building, proposed a drainage stack renewal method that uses lightweight and highly durable specialized resin drainage fittings, and verified its

effectiveness. Specifically, using an experimental high-rise drainage tower, the drainage capacity of a drainage stack system using the presented specialized resin drainage fittings was evaluated. Finally, in a high-rise residential building in which these fittings were applied, internal pipe pressure fluctuations were measured, and a comprehensive examination confirmed that the drainage capacity was sufficient to withstand them.

Keywords

high-rise residential building, drainage stack, renovation, steel pipe, internal pipe pressure fluctuation

1 Introduction

In 2024, the total stock of apartment buildings in Japan reached approximately 7,000,000 units, as illustrated in Figure 1, with many having been constructed from the 1960s through the early 2000s[1)]. Among these, as indicated in Figure 2, about 400,000 units are classified as high-rise residential building stock; this number has increased, mainly in urban areas, since 2000[2,3)]. Additionally, for drainage stack systems in high-rise residential building structures older than 20 years, cast iron pipes and ALFA (PVC[Polyvinyl Chloride]-coated steel pipe) steel pipes have been widely used, as illustrated in Photo 1. Leakage incidents caused by rust and pitting corrosion due to deterioration in these pipes have been reported. In the future, because an increase in drainage stack system renewal work is expected even in high-rise residential building structures, sophisticated and effective renovation methods must be developed and implemented to extend building service life. This study targeted a drainage stack system in a high-rise residential building that has been in use for approximately 20 years, aiming to propose a renewal method and to evaluate drainage performance before and after renewal.

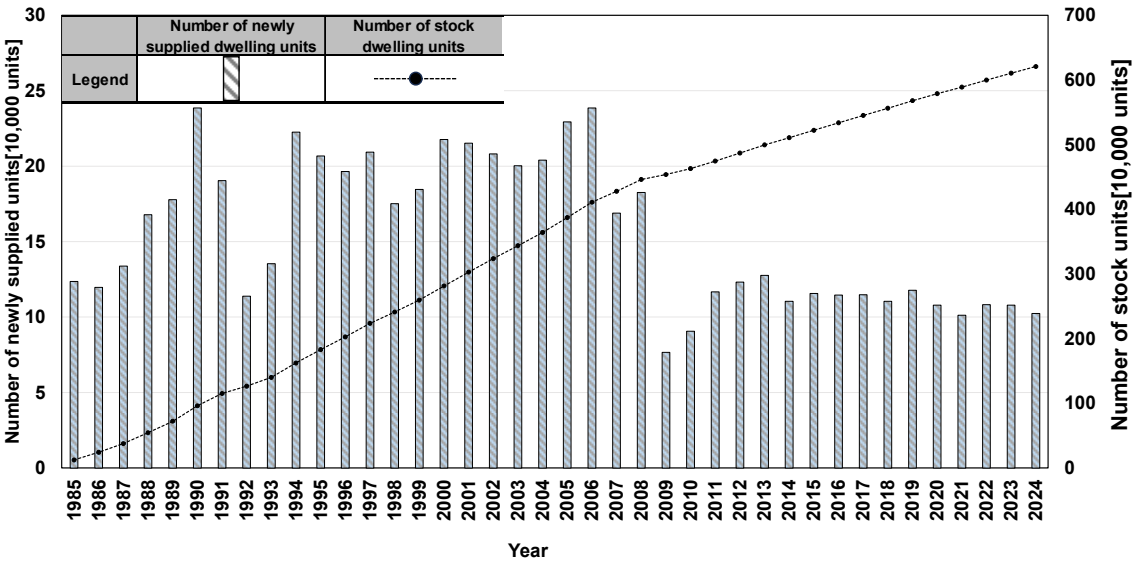

Figure 1 Trends in newly supplied and total stock apartment units

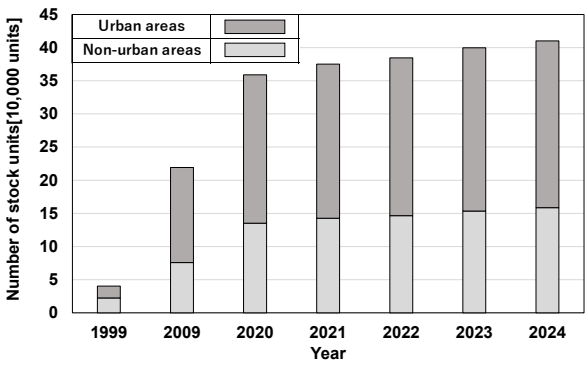

Figure 2 Number of high-rise residential building units

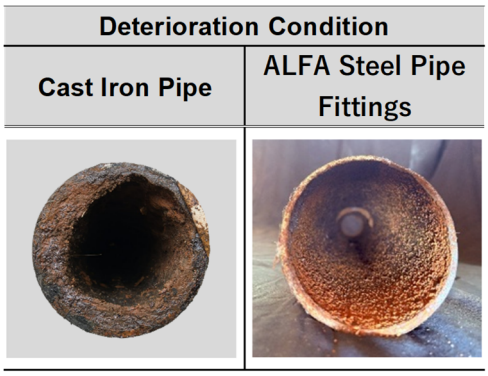

Photo 1 Pipe deterioration conditions

Figure 3 presents the standard floor plan of the target building. The drainage stack is installed in both shared and private areas. Therefore, because renovation work must be performed while residents remain at home, the impact on the living environment is a major consideration. Specifically, concerns arise regarding noise and dust generation during renewal work in occupied areas, and because restrictions on drainage times or usage are necessary during construction, disruptions to residents' daily lives are anticipated. Consequently, the construction period should be shortened and the drainage stack must be restored promptly. Furthermore, in conventional methods, it is common to construct one drainage stack system at a time, from the lowest floor to the top floor, which leads to daily drainage restrictions and imposes a significant burden on residents.

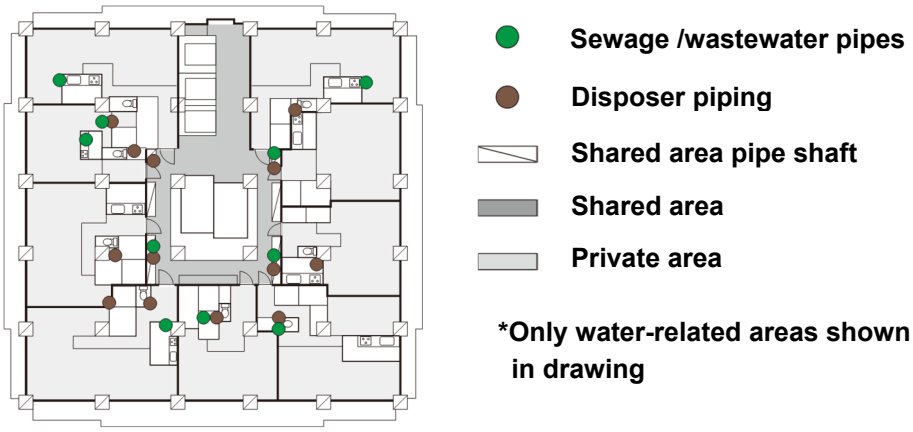

Figure 3 Locations of drainage pipes renovation work (plan view)

2. Renewal Methods That Take Residents into Consideration

This report addresses renewal work on drainage stack systems in a high-rise residential building located in the Tokyo waterfront area, constructed over 20 years ago. The newly applied method features two key aspects: dividing the same system into three blocks for staged construction, and adopting specialized tools that improve efficiency in drilling slab penetration openings.

2.1 Drainage stack renewal process

As shown in Figure 4, the structure is divided into low-rise, mid-rise, and high-rise blocks, considering differences in dwelling unit plans, and construction proceeds step by step. If the drainage stack were constructed all at once from the lowest floor to the top floor, the drainage system would become unusable for progressively longer periods at higher floors.

Renewal work is carried out sequentially in these stages: low-rise (1 to 5), mid-rise (6 to 10), and high-rise (11 to 15). Through this approach, drainage restriction periods are distributed, thereby reducing the burden on residents. In addition, to prevent disruptions regarding toilet use, temporary toilets for residents are installed in shared areas.

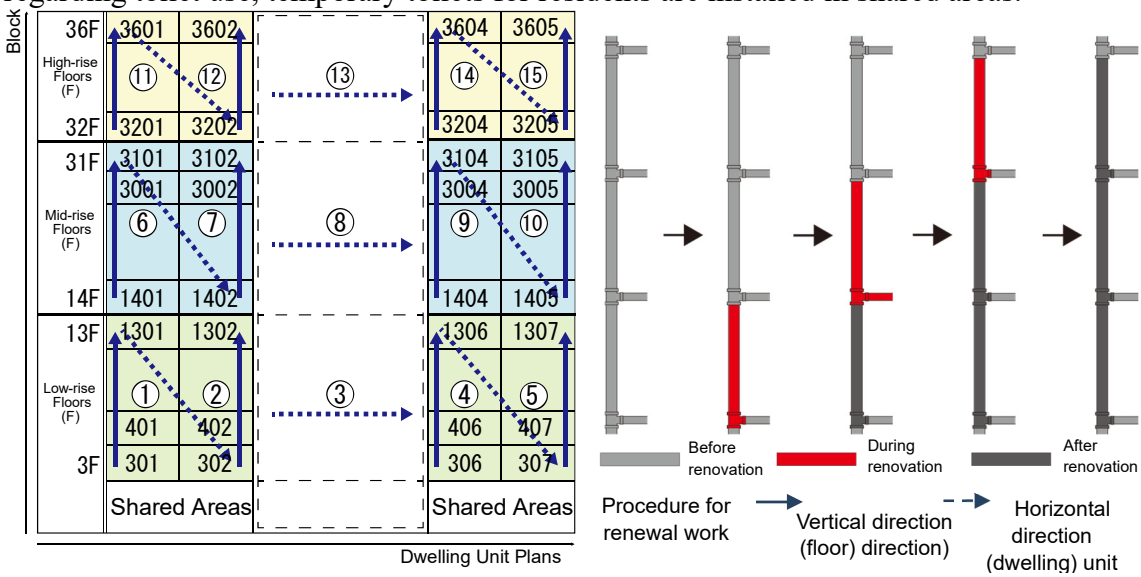

Figure 4 Process of pipe renewal based on three-block division (drainage stack system diagram)

2.2 Construction method using specialized resin drainage fittings

During drainage stack renewal, drilling must be performed at slab penetration sections to pass new pipes. However, pipes are densely concentrated inside the pipe shaft; this extremely confined space makes construction very difficult. Furthermore, as shown in Figure 5, when updating from the pre-renewal drainage stack system using ALFA steel pipe fittings with an outer diameter of 114.3 mm to the post-renewal system using specialized resin drainage fittings with an outer diameter of 190 mm, the existing penetration holes must be enlarged. Conventionally, chipping work at slab penetrations has been common; however, this approach generates significant amounts of noise and dust. Therefore, as indicated in Photo 2, a compact, space-saving specialized drilling tool designed for work inside narrow pipe shafts was developed in this study. As a result, chipping work time and overall construction duration are considerably reduced, while noise and dust are suppressed, reducing the burden on residents.

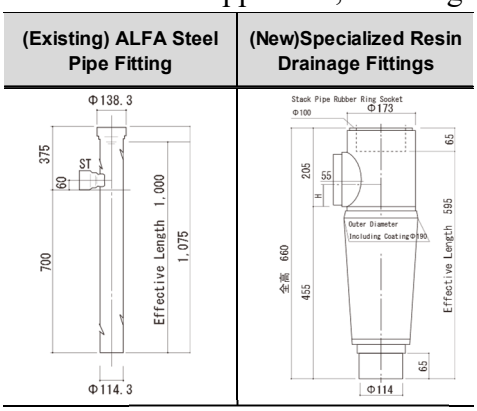

Figure 5 Details of the new and existing piping

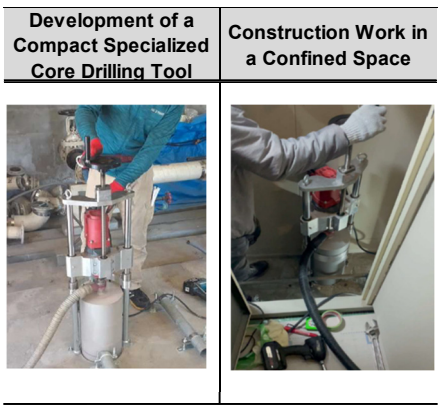

Photo 2 Specialized compact core Drilling tool

3 Verification of drainage performance in a drainage stack system using specialized resin drainage fittings

In this experiment, an experimental high-rise experimental tower located at Kanto Gakuin University (shown in Photo 3), consisting of a 9-level drainage stack system with an aboveground height of 26 m, was used to compare the drainage performance of systems using ALFA steel pipe fittings and specialized resin drainage fittings.

3.1 Test drainage stack system

Figure 6 shows the test drainage stack system used in this experiment, and Photo 4 presents the fittings before and after renewal. The drainage performance achieved using the pre-renewal drainage stack fittings with ALFA steel pipe fittings was compared with that obtained using the post-renewal drainage system with specialized resin drainage fittings, and the effectiveness of the latter was examined. The ventilation method in all cases followed the top vent system used in high-rise residential building structures. Pipe diameters and gradients were set as follows: drainage stack 100 mm, horizontal branch pipes 50 mm with a gradient of 1/100, and horizontal main drainage pipe 150 mm with a gradient of 1/100. The horizontal main drainage pipe configuration was a straight pipe with a total length of 11 m.

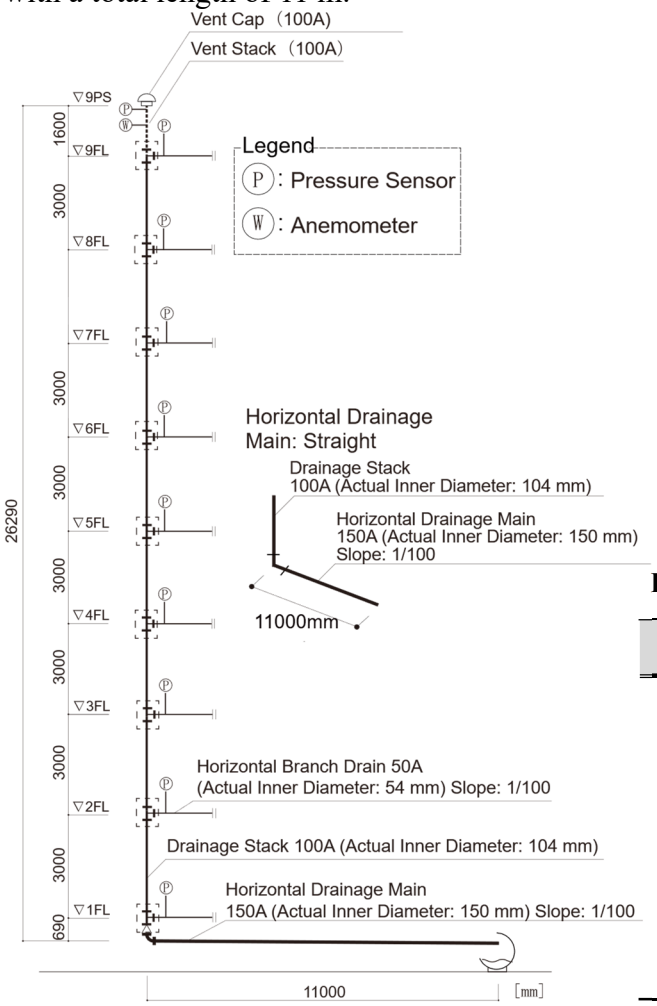

Figure 6 Test drainage stack system

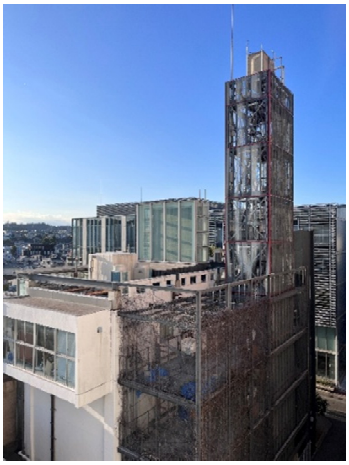

Photo 3 Osawa Memorial Institute of Architectural Environmental Engineering, Kanto Gakuin University

Photo 4 New and old piping

3.2 Measurement items and methods

Drainage load flow rates were applied in accordance with SHASE-S 218[4)](Society of Heating, Air-Conditioning and Sanitary Engineers of Japan standard: Test method for drainage capacity of drainage stack systems). Among the internal pipe pressure fluctuations measured at each floor, the maximum Psmax and minimum Psmin were determined, and the largest drainage load flow rate that remained within the range of ±400 Pa was defined as the allowable flow rate. Table 1 presents the load patterns of drainage flow rates. The drainage flow rate per floor was set up to a maximum of 2.5 L/s, and values were applied in increments of 0.5 L/s up to 7.5 L/s. For ALFA steel pipe fittings, the drainage load was applied up to a maximum of 5.0 L/s, whereas for resin drainage fittings, it was applied up to a maximum of 7.5 L/s.

Table 1 Drainage load flow rates

	Drainage Load [L/s]														
Drainage Floor	Level 1					Level 2					Level 3				
Applied Fitting	ALFA Steel Pipe														
	Specialized Resin Drainage Fittings														
9th Floor	0.5	1	1.5	2	2.5	2.5	2.5	2.5	2.5	2.5	2.5	2.5	2.5	2.5	2.5
8th Floor	-	-	-	-	-	0.5	1	1.5	2	2.5	2.5	2.5	2.5	2.5	2.5
7th Floor	-	-	-	-	-	-	-	-	-	-	0.5	1	1.5	2	2.5
Total	0.5	1	1.5	2	2.5	3	3.5	4	4.5	5	5.5	6	6.5	7	7.5

Figure 7 illustrates the method used to measure both drainage load and internal pipe pressure. As shown, the measurement duration was set to 90 seconds, with the drainage load applied 10 seconds after the start, maintained at a constant pressure, and then stopped at 80 seconds. The analysis interval was defined as the period from 25 seconds to 60 seconds after measurement began, during which stable pressure fluctuations were observed.

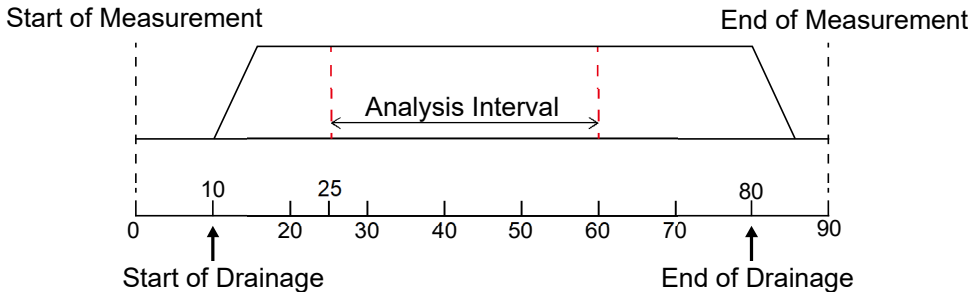

Figure 7 Measurement method

3.3 Comparison of internal pipe pressure at each floor

Figure 8 provides an example of internal pipe pressure distribution at each floor. When a drainage load flow rate of 3.5 L/s was applied as shown in Figure 8(1), Psmin in the ALFA steel pipe fittings reached approximately -480 Pa at the 6th floor, exceeding the limit criterion of ±400 Pa on the negative pressure side. In contrast, for the specialized resin drainage fittings, Psmin was approximately -70 Pa at the 7th floor, remaining within the acceptable range. Compared with ALFA steel pipe fittings, the internal pressure was reduced by roughly 90%. When a drainage load flow rate of 5.0 L/s was applied as shown in Figure 8(2), Psmin for the ALFA steel pipe fittings decreased to around -1100 Pa, greatly exceeding the limit criterion on the negative pressure side. In contrast, with specialized resin drainage fitting, Psmin was approximately -210 Pa; similar to the 3.5 L/s case, this value was within the acceptable range. These internal pipe pressure comparisons confirm that the specialized resin drainage fittings demonstrate drainage performance superior to that of ALFA steel pipe fittings.

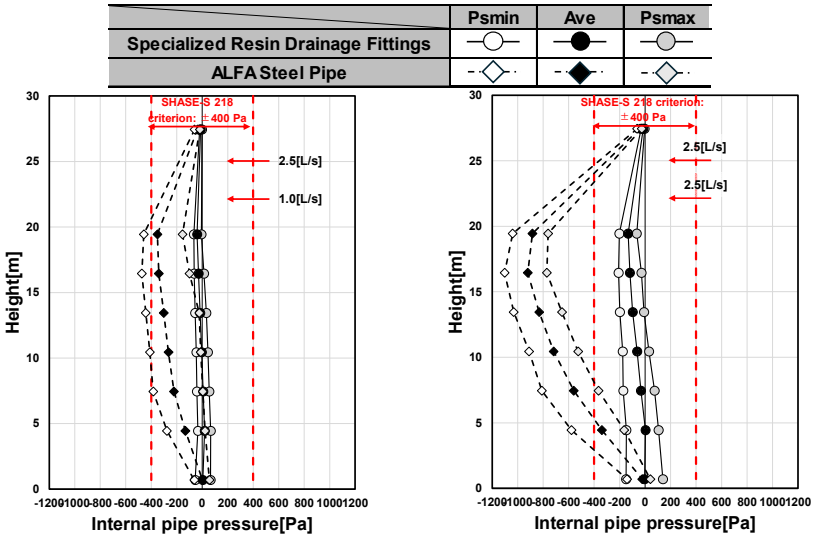

(1) Drainage load flow rate 3.5 L/s

(2) Drainage load flow rate 5.0 L/s

Figure 8 Example of internal pipe pressure distribution for each floor

3.4 Comparison of allowable drainage flow rates

Figure 9 presents the relationships between the total drainage load flow rate and Psmax and Psmin. For ALFA steel pipe fittings, because the criterion limit was exceeded on the negative pressure side at a drainage load flow rate of 3.5 L/s, the allowable drainage load flow rate was regarded as 3.0 L/s. In contrast, for the specialized resin drainage fittings, because the criterion limit was exceeded on the negative pressure side at 7.0 L/s, the allowable drainage load flow rate was taken as 6.5 L/s. These results confirm that the specialized resin drainage fittings provide more than double the drainage capacity compared with ALFA steel pipe fittings.

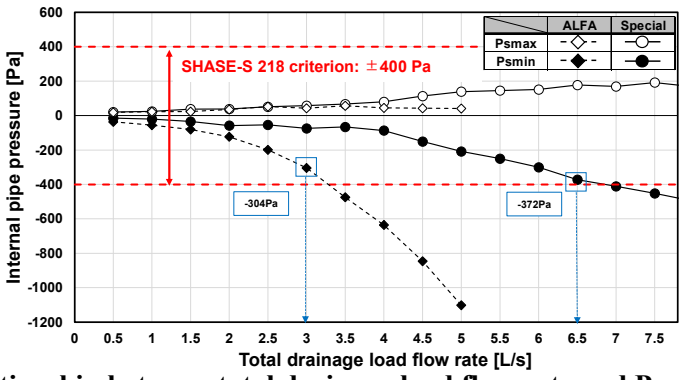

Figure 9 Relationship between total drainage load flow rate and Psmax and Psmin

3.5 Verification of applicable number of floors

The applicable number of floors was determined by comparing the drainage load flow rate calculated using the steady flow method in accordance with SHASE-S 206[5)] and the allowable drainage load flow rate obtained in Section 3.4. Figure 10 shows the relationship between number of floors and drainage load flow rate. This drainage load curve represents the combined wastewater discharge from toilets, bathtubs, washing machines, and washbasins. In the target building, the kitchen system is treated as a separate system because a disposer is used. The figure also shows changes in drainage capacity considering the reduction rate due to height, which was used for evaluation. When ALFA steel pipe fittings were used, the applicable number of floors was found to be approximately 10, whereas when specialized resin drainage fittings were used, it was

approximately 32. This result confirms that when specialized resin drainage fittings are applied, the building height requirements are generally satisfied.

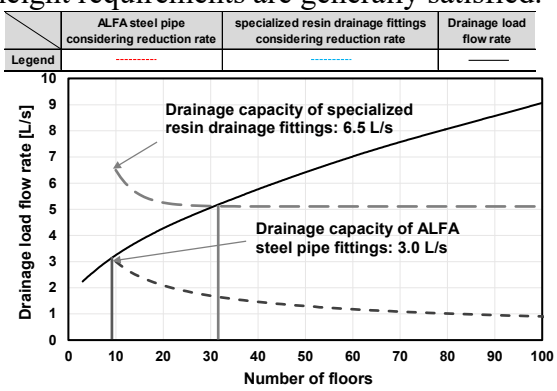

Figure 10 Relationship between number of applicable floors and allowable drainage flow rate QL [L/s] for each fitting, considering reduction rates

4. Performance evaluation in an actual building

Figure 11 shows the drainage stack system selected for investigation. Because six different dwelling unit types were connected to this system, Table 2 lists the number of sanitary fixtures connected to the drainage stack system used for measurement. As shown, the number of sanitary fixtures connected to the drainage pipes varies by floor. The measurement item is the internal pipe pressure P (in Pa) at each floor, and pressure data at one-second intervals before and after renovation are recorded at the point P shown in the figure. As shown in Table 3, measurement floors were selected from the high-rise, mid-rise, and low-rise levels (31st, 18th, and 4th floors), and measurements were conducted for approximately one week at each level. The results were evaluated following the approach described in Section 3.2.

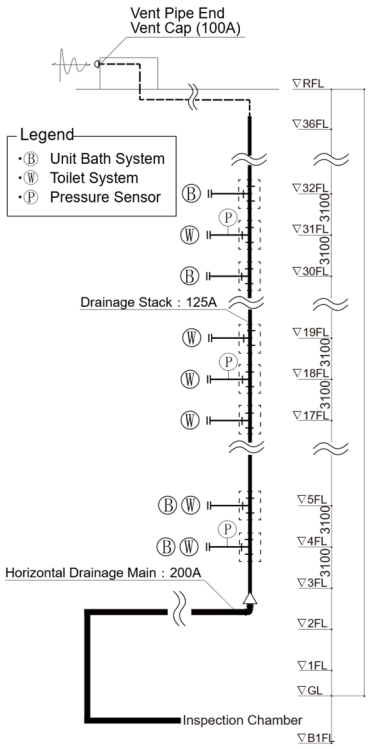

Figure 11 Drainage stack system diagram

Table 2 Number of sanitary fixtures connected to the drainage stack system

Calculation range	Number of dwelling units	Drainage fixtures				Total
		Bathroom Drainage System	Water Closet	Lavatory Closet	Washing Machine	
36F～32F	5	5		1	1	7
36F～19F	13	6	12			18
36F～5F	23	15	26			41

Table 3 Measurement periods before and after renovation in 2025

Measurement Floor	Pre-Renovation	Post-Renovation
	Steel Pipe Fitting	Specialized Resin Drainage Fittings
	Measurement Period	Measurement Period
31F	10/15～10/20	12/18～12/24
18F	10/15～10/20	12/18～12/24
4F	10/15～10/20	12/18～12/24

4.1 Daily variation of internal pipe pressure

Figure 12 illustrates an example of daily internal pipe pressure fluctuations before and after renovation. Using the measurement periods in Table 3, the 18th floor was selected as the location for evaluation, and holidays were selected as the times. In this case, the largest internal pressure fluctuation was observed when using ALFA steel pipe fittings before renovation, and a comparison between ALFA steel pipe fittings and specialized resin drainage fitting was conducted. As shown in Figure 12(1), when ALFA steel pipe fittings were used, the maximum positive pressure reached approximately 140 Pa, while the maximum negative pressure reached approximately -140 Pa. Additionally, pressure fluctuations of approximately ±100 Pa frequently occurred. In contrast, Figure 12(2) shows that when the specialized resin drainage fittings were used, the maximum positive pressure was approximately 140 Pa, similar to that of the ALFA steel pipe fittings, but the maximum negative pressure decreased to approximately -100 Pa, indicating a reduction of approximately 40 Pa. In addition, both the frequency and magnitude of pressure fluctuations were smaller, generally remaining within approximately ±50 Pa, which confirms that applying the specialized resin drainage fittings effectively suppresses internal pipe pressure fluctuations in an actual building.

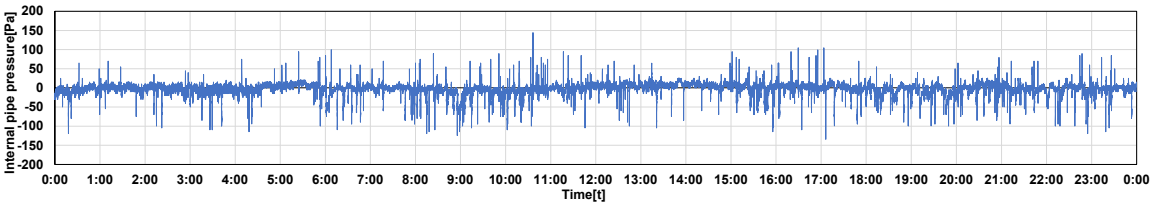

(1) Before renovation, with steel pipe fittings (Sunday, 10/20)

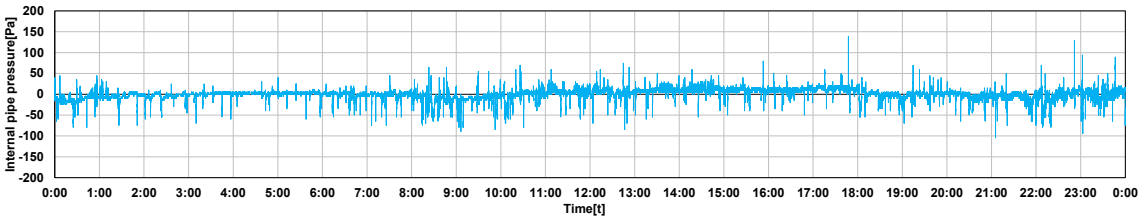

(2) After renovation, with specialized resin drainage fitting (Sunday, 12/21)

Figure 12 Example of internal pipe pressure variation over time for each drainage fitting type (measurement floor: 18th floor)

4.2 Evaluation of pressure distribution

Figure 13 shows the maximum value Psmax, minimum value Psmin, and average value Pave of internal pipe pressure measured at the 31st, 18th, and 4th floors. The figure includes examples from both weekdays and holidays. As shown in Figure 13(1), during weekdays after renovation, Psmin was reduced by an average of approximately 30 Pa across all floors compared with the values before renovation, indicating improved drainage performance. In contrast, for positive pressure, increases of approximately 40 to 90 Pa were observed at the 4th and 31st floors, though all values remained within +200 Pa. From Figure 13(2), during holidays after renovation, reductions in negative pressure similar to those seen on weekdays were confirmed. However, unlike the weekday values, the positive pressure at the 4th floor was approximately 50 Pa higher compared with that when using ALFA steel pipe fittings.

Note that throughout the measurement period, the criterion value of ±400 Pa was not

exceeded under any condition.

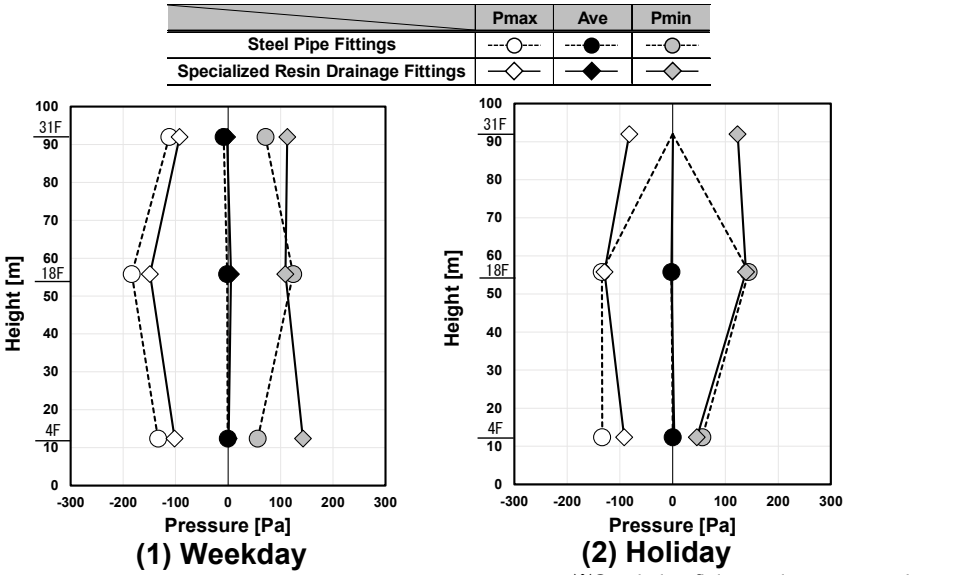

※Steel pipe fittings prior to renovation
: Measurements taken on the 31st floor

Figure 13 Example of internal pipe

5. Conclusion

This study proposed a new renewal method for drainage stack systems in a 36-story high-rise residential building exceeding 20 years of age, and verified the drainage performance achieved using specialized resin drainage fittings offering good constructability through both experiments and field measurements in an actual building. As a result, although construction was still in progress, it was found that the burden on residents could be reduced; additionally, introducing specialized tools can improve constructability within narrow pipe spaces and reduce the burden on residents. This renewal method, using the specialized resin drainage fittings, is demonstrated to be effective for drainage stack systems in high-rise residential building structures in terms of both constructability and drainage performance. However, this study focused on a limited number of drainage stack configurations and building conditions. Future work should examine the applicability of the proposed method to a wider range of high-rise residential buildings.

Acknowledgments

This research was supported by the Osawa Memorial Institute of Architectural and Building Services Engineering at Kanto Gakuin University.
We also received cooperation from the apartment complex homeowners' association and the technical staff at Toda Construction.

References

1) Current situation surrounding condominiums. Promotion of long service life: Ministry of Land, Infrastructure, Transport and Tourism, October 2024
2) Tokyo Kantei Co., Ltd.: Stock number of tower condominiums by prefecture, press release, October 2018.

3) Tokyo Kantei Co., Ltd.: Stock number of tower condominiums by prefecture in 2024, press release, January 2025.
4) Society of Heating, Air-Conditioning and Sanitary Engineers of Japan Standard: SHASE-S 218-2021 “Test method for drainage capacity of drainage stack systems”, October 2021.
5) Society of Heating, Air-Conditioning and Sanitary Engineers of Japan Standard: SHASE-S 206-2019 “Standards and commentary for plumbing and sanitary equipment”, July 2019.

6. Authors

Tomoya Kono works at Nihon Setsubi Kogyo Co., Ltd., where he is engaged in planning and construction related to apartment buildings. He is a member of the Architectural Institute of Japan (AIJ) and the Society of Heating, Air-Conditioning and Sanitary Engineers of Japan (SHASE).

Masayuki Otsuka serves as a professor in the College of Architecture and Environmental Design at Kanto Gakuin University and conducts extensive research on plumbing and sanitary systems. He is a member of the AIJ and has served as president of SHASE.

Koji Aizawa is a former graduate student who was affiliated with the Otsuka Laboratory at Kanto Gakuin University in Japan and is a member of the AIJ and SHASE.

Ryotaro Kikuchi is a graduate student affiliated with the Otsuka Laboratory at Kanto Gakuin University in Japan and is a member of the AIJ and SHASE.

Kento Ishiwata is a graduate student at the Otsuka Laboratory at Kanto Gakuin University in Japan, as well as a member of the AIJ and SHASE.

Ayaka Kimura is a second-year doctoral student in the Otsuka Laboratory at Kanto Gakuin University in Japan. During her studies, she was mainly involved in research on living space hygiene contributory to preventive measures against COVID-19.

Advances in benchmark HRB DWV system testing at the National Lift Tower: Recent updates to protocols and procedures, towards improved standards alignment

J. D. Cuellar S. (1) S. White (2) T. Hill (3) A. Horner (4)
(1) jose-david.cuellar@aliaxis.com
(2) swhite@aliaxis.com
(3) thill@aliaxis
(4) andrew.horner@aliaxis.com

Abstract

This report documents the updated protocols, procedures, and measurement methodologies for benchmark high-rise building (HRB) drainage-waste-vent (DWV) system testing at the National Lift Tower (NLT). The revised protocol synchronises fixture delays, trigger events, and flushes against a common master clock, to maximise transient superposition and momentary flow-rate congestion. Continuous-flow inputs are modulated from low to high rates, and extended acquisition windows capture the onset, peak, and recovery phases. The measurement suite combines multi-point pressure acquisition close to trap seals, synchronised video, and continuous ultrasonic trap-seal level measurement, resolving the dynamic seal displacement and the residual depth in a single time-stamped record, published per run through a private network with remote supervision. The procedures are designed to improve sensitivity, repeatability, and discrimination between venting strategies, and to strengthen traceability to regulatory expectations; no measured campaign results are presented.

Keywords

Building drainage; air-pressure transients; trap seals; high-rise buildings; performance testing.

1 Introduction

The integrity of the water-trap seal —the sole barrier between habitable space and the foul air of the drainage network— is threatened by the air-pressure transients that appliance discharges propagate through the drainage-waste-vent (DWV) system, depleting seals through induced siphonage and back-pressure [1]; the public-health consequences are established, from the 2003 SARS outbreak at Amoy Gardens [2] to COVID-19 transmission concerns [3] and experimental demonstration [4]. The challenge is most acute in high-rise buildings, where stack height amplifies pressure excursions into regimes that prescriptive codes, largely derived from low-rise work, do not adequately represent [5, 6]: BS EN 12056-2 [7] offers limited tall-stack guidance, and international codes diverge significantly for identical scenarios [8]. Full-scale testing is therefore essential, to characterise performance directly and to validate models such as AIRNET, revalidated for tall buildings against measured data from the National

Lift Tower (NLT), Northampton, UK [9]. CIBSE TM70 [10] marks a shift towards performance-based design, strengthening the case for repeatable, discriminating, traceable benchmark procedures.

This report documents recent updates to the NLT benchmark protocols, with three objectives: (i) a synchronised-discharge protocol for high-congested-system testing, with programmed fixture delays chosen to maximise transient superposition under modulated continuous flows; (ii) an expanded, master-clock-synchronised measurement suite in which measured seal response is cross-validated against its local pressure driver; and (iii) online publication and remote supervision of benchmark runs through the National Lift Tower website. The scope is procedural: no measured results are presented, and the trap-seal model underpinning the cross-validation is summarised only as far as the protocol requires (Section 5).

2 Benchmark testing at the National Lift Tower

The test rig is a full-scale drainage installation within the 127.5 m National Lift Tower, configured to represent a 34-storey building with a 76 m vertical stack [9, 10]. It simulates multiple venting configurations: a 110 mm primary ventilated (PV) single stack; a secondary ventilated (SV) modified one-pipe system with 50, 75, or 110 mm parallel vents; and a fully active (FA) system with air admittance valves and positive pressure relief devices. All of them remain equipped with cross-vent pipes valves for rapid reconfiguration; so venting strategies are compared on identical pipework under identical loading [10]. Discharge loading is provided by WCs and controllable continuous-flow inputs at multiple floors; distributed pressure transducers and ultrasonic instrumented trap seals record the pressure regime and the seal response directly.

Benchmark testing at the NLT is founded on a harmonised loading procedure: a prescribed sequence of discharges and continuous flows, applied identically across all venting configurations, on which measured differences are attributable to the venting strategy rather than to the load. Because trap-seal depletion is driven by the transient pressure regime [1, 5, 9], the procedure deliberately probes congested conditions in which transients superpose; operational experience from earlier campaigns [9] and the comparative assessments of the identified improvements addressed below.

3 Synchronised-discharge loading protocol

3.1 Transient superposition and programmed delays

The revised protocol replaces manually initiated discharges with centrally triggered events referenced to a common master clock connected to all the appliances. Each flush and valve actuation carries a programmed delay chosen so that discharges from different floors arrive coincidently at the stack base, to maximise momentary congestion within the prescribed load. Synchronisation is also designed for repeatability: successive runs impose nominally identical loads, with the achieved run-to-run variance itself a reported quantity (Table 2). Table 1 sets out a representative sequence; WC delays follow from the relationships of Section 6 and the as-built floor heights; values are illustrative.

Table 1 — Representative harmonised loading sequence (values illustrative; delays computed for coincident film arrival at the stack base)

#	Event / fixture: purpose	Floor	Delay (s)	Discharge
0	Acquisition start: per-run zero baseline	—	-120	None
1	Continuous-flow bank: envelope modulation	L14 + L13	-110 → -30	0.75 → 3.6 [l·s⁻¹] stepped
2	WC flush: reference discharge	L15	0.0	6 [l]: peak 1.8 [l·s⁻¹]
3	WC flushes: coincident arrival	L11 + L9	+5 / +8	6 [l] each
4	Pump and valves: continuous flow stop	L14 + L13	+60 → +120	None
5	Recovery: drain-down; last-state reading	—	+155 → +240	flows off at +240 s

3.2 Modulated flows and extended windows

Continuous-flow inputs are modulated from low to high rates within a single sequence. Stepped and ramped profiles carry the stack through its operating envelope, exposing threshold behaviours —the onset of appreciable seal oscillation, the approach of excursions to regulatory limits— that fixed-rate testing can straddle without detecting. Acquisition windows are extended to capture baseline, onset, peak, and recovery: residual depth is only meaningful once oscillation has ceased and appliance drain-back is complete, and the extended window yields onset and recovery time constants as discriminating metrics.

3.3 Application and derived metrics

The protocol is applied identically to the PV, SV, and FA configurations, with valve-selectable cross vents exchanging configurations without disturbing the instrumented pipework, so measurement geometry is constant across the comparison. The output is a like-for-like ranking of venting strategies under an identical, congestion-optimised load; configurations equivalent under light loading are expected to separate as flow approaches stack capacity. Table 2 defines the quantities reported for every run.

Table 2 — Reporting template: quantities derived from every benchmark run

Reported quantity	Derivation	Criterion / purpose
Peak pressure excursions (±)	extrema of near-trap and stack records	±375 Pa fluctuation limit
Maximum seal displacement	ultrasonic channel, per instrumented trap	splashover / induced siphonage
Residual seal depth (last state)	ultrasonic reading after oscillation and drain-back end	25 mm minimum retention
Stack-to-trap transmission	amplitude ratio and phase lag, stack vs near-trap records	venting comparison; Section 5
Entrained airflow Q_a	dp/dx friction-gradient inversion between stations	air-to-water ratio; model validation
Run-to-run repeatability	variance of peak pressures across repeat runs	protocol qualification

4 Measurement system and instrumentation practice

4.1 Multipoint pressure acquisition

Pressure measurement has been expanded from stack-mounted transducers to multi-point acquisition including sensors close to the trap seals: near-trap measurement records the excitation applied to the seal —attenuated and phase-shifted relative to the stack centreline. Differential transducers of low range and high natural frequency,

ranged at ±2.5 kPa against the ±375 Pa criterion [7, 10], are flush-mounted at wall tapings to avoid connecting-tube resonance, and are temperature-compensated; static calibration with zero checks at every pre-sequence baseline.

4.2 Ultrasonic trap-seal level measurement

Seal level is measured continuously by an ultrasonic sensor mounted above the appliance-side free surface of each instrumented trap, ranging on the time of flight of a 380 kHz pulse reflected at the air–water interface, an almost total reflector. The ±50 mm window accommodates the full excursion from splash over to depletion, with resolution ≤ 0.069 mm and repeat accuracy ±0.38 mm; the linear 0–10 V output is acquired on the master-clock system, so one time-resolved record captures the dynamic displacement and the residual depth. By design, the stand-off keeps splash over beyond the sensor's 20 mm blind zone with full depletion inside the window; sound-cone containment in the trap bore is verified at commissioning, excluding side-wall echoes; and, the speed of sound varying by about 0.17 % per °C, zero checks against the known quiescent level are taken at every baseline.

4.3 Synchronised video, timing, and data quality

Cameras trained on transparent trap sections and to the WC open surface, frame-locked to the master clock, resolve the mechanism of seal loss for each event —induced-siphonage draw-down, back-pressure displacement, oscillatory splash over, or bubble-through venting— and provide a visual audit trail for anomalous records. All channels are logged at 10 Hz, the rate at which the acquisition system guarantees synchronous, gap-free records; channel-to-channel coherence, on which the cross-validation of Section 5 rests. This is deliberately prioritised over per-channel bandwidth, so reported pressure extrema are band-limited values. Channels whose baseline drift exceeds tolerance are recalibrated before a run is accepted, and duplicate transducers at selected stations quantify repeatability.

5 Trap-seal response model and cross-validation

The near-trap pressure and ultrasonic displacement records measure the same event twice —the excitation applied to the seal, and its response— and the model exists to connect them: driven by the measured pressure record, it predicts the displacement the ultrasonic channel should observe, so agreement validates both channels simultaneously, a metrological cross-check neither could provide alone —a role that dictates a model small enough that every parameter is identifiable from the records the protocol already acquires. The seal is idealised as the trap boundary condition long established in the AIRNET solver [1, 12]: an incompressible liquid column of developed length L_w moving as a single slug in a rigid U-shaped conduit of uniform bore; the appliance side open to the atmosphere, and column mass constant while both surfaces remain free. Newton's second law then collects four forces — the measured gauge pressure $p_s(t)$ on the system-side surface, the hydrostatic restoring force of the level difference between the limbs, a laminar friction term derivable without free constants, and the remaining form losses lumped into one quadratic coefficient — and the displacement x(t) of either free surface from the instantaneous mean level obeys

$$\ddot{x} + 2\zeta_{lam}\,\omega_n\,\dot{x} + \frac{K_L}{2L_w}\,\dot{x}\,|\dot{x}| + \omega_n^2\,x = \frac{p_s(t)}{\rho_w L_w}, \quad \omega_n = \sqrt{2g/L_w} \qquad (1)$$

where ρ_w is the water density, ζ_{lam} the laminar damping ratio, and K_L the lumped loss coefficient; $\omega_n/2\pi$ lies between 1.6 and 2.2 Hz for typical geometries (L_w = 0.10–0.20 m), fixing the band the instrumentation must resolve. Each hypothesis bounds the validity of the comparison: the oscillatory boundary layer never fills the bore, so the laminar term is a strict lower bound on dissipation and K_L is an effective, calibrated coefficient rather than a geometric constant —hence parameters not fixed by geometry are identified per trap at commissioning and frozen, no per-run tuning, keeping the comparison a genuine prediction test. Equation (1) holds only within bounded excursions; beyond them, three irreversible retention-loss mechanisms —weir overflow, displacement into the appliance, and bubble-through venting— enter as explicit guard laws under which retained depth and column length become state variables, each expected to leave a distinct signature in the synchronised records. The branch air column is not modelled: the near-trap transducers measure the pressure applied to the seal, and the stack-to-trap path is characterised empirically as a transfer function (Table 2). Per-run agreement metrics —normalised error, peak-excursion error, phase lag, and net retention-loss error— tie the two channels to the ±375 Pa and -25 mm criteria [7, 10], with video arbitrating between measurement artefact and model deficiency.

The model's reach is bounded. A single-degree-of-freedom reduction. This is a metrological instrument analyse for cross-validating two channels, not a general design predictor; since it does not resolve surface breakup near depletion, sloshing, the bend curvature entered near complete loss, or pneumatic stiffening where the system-side air is confined, and its predictions hold within the amplitude and frequency range of that identification. Even within scope it brackets rather than fixes. For a seal just meeting the 25 mm minimum retention of BS EN 12056-2 [7], the static head resisting displacement is $\rho_w gh \approx 245$ Pa; whether the breaking pressure is that value or twice it depends on the appliance-side geometry, since a wide appliance leg holds its level while the seal is displaced, whereas an equal-bore leg rises by the same amount and doubles the differential to ≈ 490 Pa. The conservative bound, 245 Pa, falls inside the ±375 Pa fluctuation limit carried by the same criteria set [7, 10]: a system compliant with the pressure criterion may already have breached the depth criterion, so the two are not demonstrably consistent (Section 8) —an open question the test campaign is designed to settle. Challenges for future evaluation follow directly: whether commissioning-frozen parameters remain stationary over a campaign; whether the 10 Hz record remains sufficient as depletion raises the response frequency (Section 4); and validation of the guard thresholds against video. The full derivation, hypothesis audit, and numerical scheme are set out for further investigation in a complementary study phase; demonstration against measured data is beyond the scope of this report and will be treated separately.

6 Quantifying the imposed load: two-phase flow in the stack

Benchmark testing requires the imposed water load and the entrained air flow to be known. Stack flow is annular two-phase: the discharge falls as a film around a central air core, reaching terminal velocity typically within less than 10 m of fall [1, 10], and it is the entrained airflow —and the pressures where it is accelerated, retarded, or

stopped— that drives seal depletion. The film terminal velocity is TM70 equation B.1, first developed by Wyly [11]:

$$V_t = K\,(Q_w/D)^{0.4} \qquad (2)$$

with V_t in $m \cdot s^{-1}$, Q_w the water flow rate ($l \cdot s^{-1}$), D the stack diameter (mm), and $K \approx 12.4$ for smooth pipe [10]. Continuity yields the mean film thickness $t = Q_w/(\pi\, D\, V_t)$, the fill ratio $r = 1 - (1 - 2t/D)^2$, and the Wyly–Eaton capacity $Q_{max} = 3.15\times10^{-4}\, r^{5/3}\, D^{8/3}$, consistent with BS EN 12056-2 and TM70 capacity tables [7, 10, 11]. These relationships set the modulated flow rates as fractions of stack capacity and, inverted, check the imposed load from measured film thickness or timed film arrival; for the NLT reference case —a 6-litre flush at peak 1.8 $l \cdot s^{-1}$ over a 2.0 $l \cdot s^{-1}$ continuous load in the 110 mm stack— $V_t = 3.35\ m \cdot s^{-1}$, film thickness ≈ 3.6 mm, and fill ratio ≈ 0.14, in agreement with the published TM70 worked example [10]; these values fix the delays of Table 1.

The entrained air flow Q_a is a dependent variable, bounded by the core velocity and estimated by friction-gradient inversion between stations in single-phase air regions (Table 2) — the primary experimental estimate, and the validation data for transient air-phase solutions in AIRNET [1, 12]. The severity of the resulting transients is bounded by the Joukowsky relation $\Delta P = \rho_a\, c\, \Delta V$ [10]: arresting an air column moving at only 1 $m \cdot s^{-1}$ ($\rho_a \approx 1.2\ kg \cdot m^{-3}$, $c \approx 344\ m \cdot s^{-1}$) generates approximately 413 Pa, beyond the ±375 Pa criterion —hence measured air velocities, not only water flow rates, are reported.

7 Online publication and supervision: the nlt1.com platform

Each run produces a complete, synchronised record: multi-point pressure histories, the continuous ultrasonic displacement record with its last-state residual depth, and frame-locked video. The nlt1.com platform publishes and supervises these records: instrumented channels are streamed as time-stamped snapshots at approximately one-second cadence, with per-sensor quality flags, valve states, and run status for remote supervision; the archived per-run record is the template for the separate publication of campaign results.

8 Implications for standards alignment

Prescriptive sizing rules diverge for tall buildings [8], and TM70 argues for performance-oriented design supported by validated modelling and full-scale measurement [10]. The procedures described here support that transition: the harmonised, congestion-optimised sequence is a candidate template for standardised, facility-reproducible test prescriptions; the measured relation between imposed excursion and residual depth will give an empirical basis for reviewing acceptance criteria, including the ±375 Pa limit, historically resting on theoretical grounds [10]; and the data sets will extend the validation base for the models underpinning risk-based guidance [9]. Recording both the trap pressure history and the residual depth makes each run a documented test of the two criteria [7, 10] under a repeatable load —and puts directly a question not previously answerable: whether a depleted seal can be breached inside the acceptance band (Section 5), an outcome that would inform the review of both.

9 Conclusions

Recent updates to the benchmark HRB DWV test protocols at the National Lift Tower have been documented: master-clock synchronisation of fixture delays, trigger events, and flushes, to maximise transient superposition; continuous flows modulated across the operating envelope; and extended acquisition windows capturing onset, peak, and recovery. Measurement combines multi-point pressure acquisition close to trap seals, synchronised video, and continuous ultrasonic seal-level measurement; a compact trap-seal model links the pressure and displacement channels in per-run cross-validation, and each run is published and supervisable through nlt1.com. The resulting evidence base is intended to support standards development; the full measured data set across the PV, SV, and FA configurations will be reported separately.

References

1. Swaffield J – Transient Airflow in Building Drainage Systems, Routledge/Taylor & Francis, London, UK, 2010.
2. Hung HCK, Chan DWT, Law LKC, Chan EHW, Wong ESW – Industrial experience and research into the causes of SARS virus transmission in a high-rise residential housing estate in Hong Kong, Building Services Engineering Research and Technology, Vol 27, Nº2, pp 91–102, 2006.
3. Gormley M, Aspray TJ, Kelly DA – COVID-19: mitigating transmission via wastewater plumbing systems, The Lancet Global Health, Vol 8, Nº5, e643, 2020.
4. Gormley M, Swaffield JA, Sleigh PA, Noakes CJ – An assessment of, and response to, potential cross-contamination routes due to defective appliance water trap seals in building drainage systems, Building Services Engineering Research and Technology, Vol 33, Nº2, pp 203–222, 2012.
5. Gormley M, Kelly D, Campbell D, Xue Y, Stewart C – Building Drainage System Design for Tall Buildings: Current Limitations and Public Health Implications, Buildings, Vol 11, Nº2, 70, 2021.
6. Gormley M, Stewart C – Design Methodologies for Sizing of Drainage Stacks and Vent Lines in High-Rise Buildings, Buildings, Vol 13, Nº6, 1458, 2023.
7. CEN / BSI – European Standard BS EN 12056-2:2000 Gravity drainage systems inside buildings – Part 2: Sanitary pipework, layout and calculation. European Committee for Standardisation / British Standards Institution, 2000.
8. Mohammed SA, Gormley M, Stewart C, Kelly DA, Campbell DP – Comparison and Assessment of Building Drainage Design Codes for use in Tall Buildings, Proc. CIB W062 International Symposium on Water Supply and Drainage for Buildings, Leuven, Belgium, September 2023.
9. Gormley M, Mohammed S, Kelly DA, Campbell DP – Application and Validation of AIRNET in Simulating Building Drainage Systems for Tall Buildings, Buildings, Vol 15, Nº10, 1725, 2025.
10. CIBSE – TM70: Tall building drainage design, The Chartered Institution of Building Services Engineers, London, UK, 2025.
11. Wyly RS, Eaton HN – Capacities of Stacks in Sanitary Drainage Systems for Buildings, Monograph 31, National Bureau of Standards, Gaithersburg, MD, USA, 1961.
12. Jack LB – Developments in the definition of fluid traction forces within building drainage vent systems, Building Services Engineering Research and Technology, Vol 21, Nº4, pp 266–273, 2000.

Experimental quantification of evaporation rates in water trap seals within building drainage systems

D.A. Kelly (1) and M. Gormley (2)
(1) d.a.kelly@hw.ac.uk
(2) m.gormley@hw.ac.uk
(1, 2) Heriot-Watt University, Edinburgh, Scotland, UK.

Abstract

Water trap seals are essential components of building drainage systems, acting as a barrier to prevent the ingress of foul air and potentially contaminated aerosols into occupied spaces. Failure of these seals has been associated with airborne pathogen transmission. While pressure-induced seal depletion is well understood, evaporation remains a comparatively under-investigated mechanism of trap seal failure.

This study presents experimental measurements of evaporation-induced depletion in three common water trap seals: a 30 mm P-trap, a 35 mm P-trap, and a 30 mm bottle trap. Experiments were conducted within a benchtop environmental chamber maintained at a constant temperature of 25°C, representative of typical elevated indoor conditions. Each trap was monitored over a 10-day period, with continuous mass measurements recorded at two-hour intervals calibrated to determine water volume and trap seal depth.

The results demonstrate that evaporation can lead to significant reductions in both water volume and seal depth over relatively short timeframes. Substantial variation was observed between trap geometries. The P-traps exhibited rapid depletion, with average evaporation rates of approximately 11–18 ml/day (corresponding to seal depth reductions of 7–9 mm/day). In contrast, the bottle trap showed significantly lower evaporation rates (~5 ml/day and ~1.5 mm/day). These findings confirm that evaporation is a credible mechanism of trap seal degradation, particularly in intermittently used systems.

Keywords

Water trap seals, evaporation, trap depletion, aerosol transmission, public health

1 Introduction

Water trap seals are critical components of building drainage systems, providing a physical barrier that prevents foul air and sewer gases from entering occupied spaces (Swaffield and Galowin, 1992; Kelly and Gormley, 2013). Loss of this water barrier creates a direct pathway for the ingress of contaminated air, with potential implications for airborne disease transmission (Gormley et al., 2013). Even partial depletion of the seal depth has been shown to permit the migration of airborne pathogens from the drainage system into occupied spaces, increasing infection risk in densely occupied buildings (Gormley, 2010).

The 2003 SARS outbreak raised significant concerns regarding airborne transmission via faulty building drainage systems (Hung et al., 2006). More recently, the SARS-CoV-2 pandemic renewed focus on environmental transmission pathways, including those associated with wastewater and building drainage networks, particularly in high-density residential buildings and healthcare facilities (Gormley et al., 2020; Lyu et al., 2023). These events highlight building drainage systems as credible pathways for pathogen transmission, especially where system integrity is compromised.

Both laboratory and field investigations have demonstrated that trap seal depletion facilitates the transmission of aerosols from drainage systems into buildings. Gormley et al. (2017) conducted full-scale experimental studies and confirmed the movement of aerosolised pathogens through depleted trap seals between different floors. Subsequent work by Gormley et al. (2021) further characterised aerosol particle sizes generated during normal appliance discharge events, demonstrating their potential for long-distance transport within drainage networks and entry into occupied spaces.

While pressure transients are well-documented causes of trap seal depletion, evaporation represents a slower but equally important mechanism of failure, particularly during periods of fixture non-use. Despite its practical significance, evaporation has received relatively limited quantitative investigation. Existing literature suggests typical evaporation rates of approximately 2–3 mm per week under UK indoor conditions (Wise & Swaffield, 2002), with substantially higher rates expected at elevated temperatures. Observational evidence indicates that traps located in warm environments, such as plantrooms, may dry out completely on a daily basis (Kelly, 2009).

This paper presents controlled experimental measurements of evaporation rates for three common fixture trap seals. The aim is to provide robust quantitative data to inform risk assessment, maintenance strategies, and the identification of system vulnerabilities associated with evaporation-induced trap seal failure.

2 Methodology

2.1 Apparatus & test procedure

Three water trap seals were selected for assessment: (i) P-trap (30 mm); (ii) P-trap (35 mm); and (iii) Bottle-trap (30 mm), as shown in Figure 1. A benchtop environmental chamber was used to maintain a controlled ambient temperature of 25ºC, representative of typical summer conditions in Europe (Copernicus Climate Change Service, 2023).

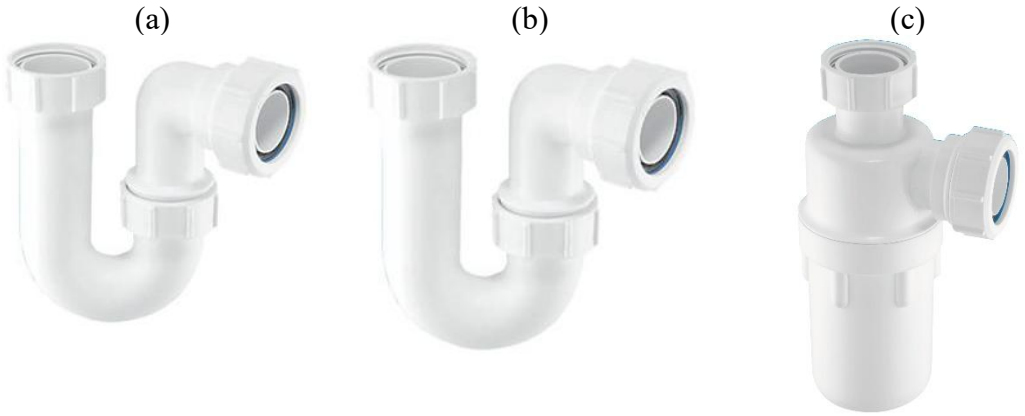

Figure 1: Water trap seals selected for assessment of water evaporation: (a) P-trap (30 mm), (b) P-trap (35 mm), and (c) Bottle-trap (30 mm)

Temperature within the chamber was monitored using a thermistor to ensure stability throughout the test period. Each trap was tested individually and monitored over a 10-day period. The trap was positioned centrally within the environmental chamber and suspended from digital scales mounted externally above the chamber. This configuration enabled continuous measurement of the mass of water contained within the trap, logged at 2 hour intervals. A diagram of the experimental setup is shown in Figure 2.

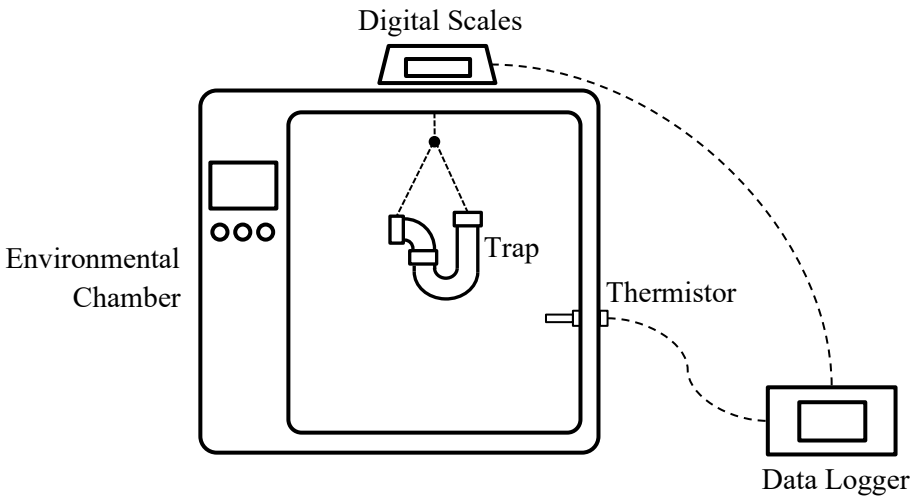

Figure 2: Experimental setup for assessing water trap seal evaporation rates

2.2 Calibration

Prior to testing, each water trap seal was calibrated to establish the relationship between the measured mass of water (recorded by the digital scales), the corresponding water volume, and the water seal depth. Calibration was performed incrementally from an empty condition to full trap capacity. At each increment, the combined mass of the trap and water was recorded, the seal depth (water column height) was measured, and the corresponding water volume was verified. A summary of the calibrated trap characteristics is presented in Table 1.

Table 1: Calibrated water trap seal characteristics

Trap Type	Trap Mass (g)			Water Volume (ml)	Water Depth (mm)
	Empty	Full	Difference	Full	Full
P-trap (30 mm)	143	307	164	162	105
P-trap (35 mm)	166	400	234	240	120
Bottle-trap (30 mm)	194	475	281	290	105

3 Results

3.1 Comparison of water volume and seal depth

The variation in water volume and seal depth over time for the three water trap seals is shown in Figure 3. All traps exhibited a continuous reduction in both water volume and seal depth due to evaporation, although the rate of depletion varied significantly with trap type and geometry.

The bottle trap (30 mm) demonstrated the slowest rate of evaporation, with water volume decreasing only marginally over the 240-hour test period (approximately 290 ml to 240 ml). Correspondingly, the reduction in seal depth was limited, decreasing from approximately 100 mm to 85 mm. In contrast, both P-trap configurations exhibited substantially greater reductions in volume and seal depth. The 35 mm P-trap decreased from approximately 240 ml to 60 ml, while the 30 mm P-trap reduced from approximately 160 ml to 50 ml over the same period.

For both P-traps, the rate of evaporation was initially higher, followed by a gradual reduction over time. This behaviour is attributed to changes in the exposed water surface area as the water level decreased. Despite differences in initial volume and seal depth, both P-traps converged towards similar residual seal depths of approximately 30 mm by the end of the test period.

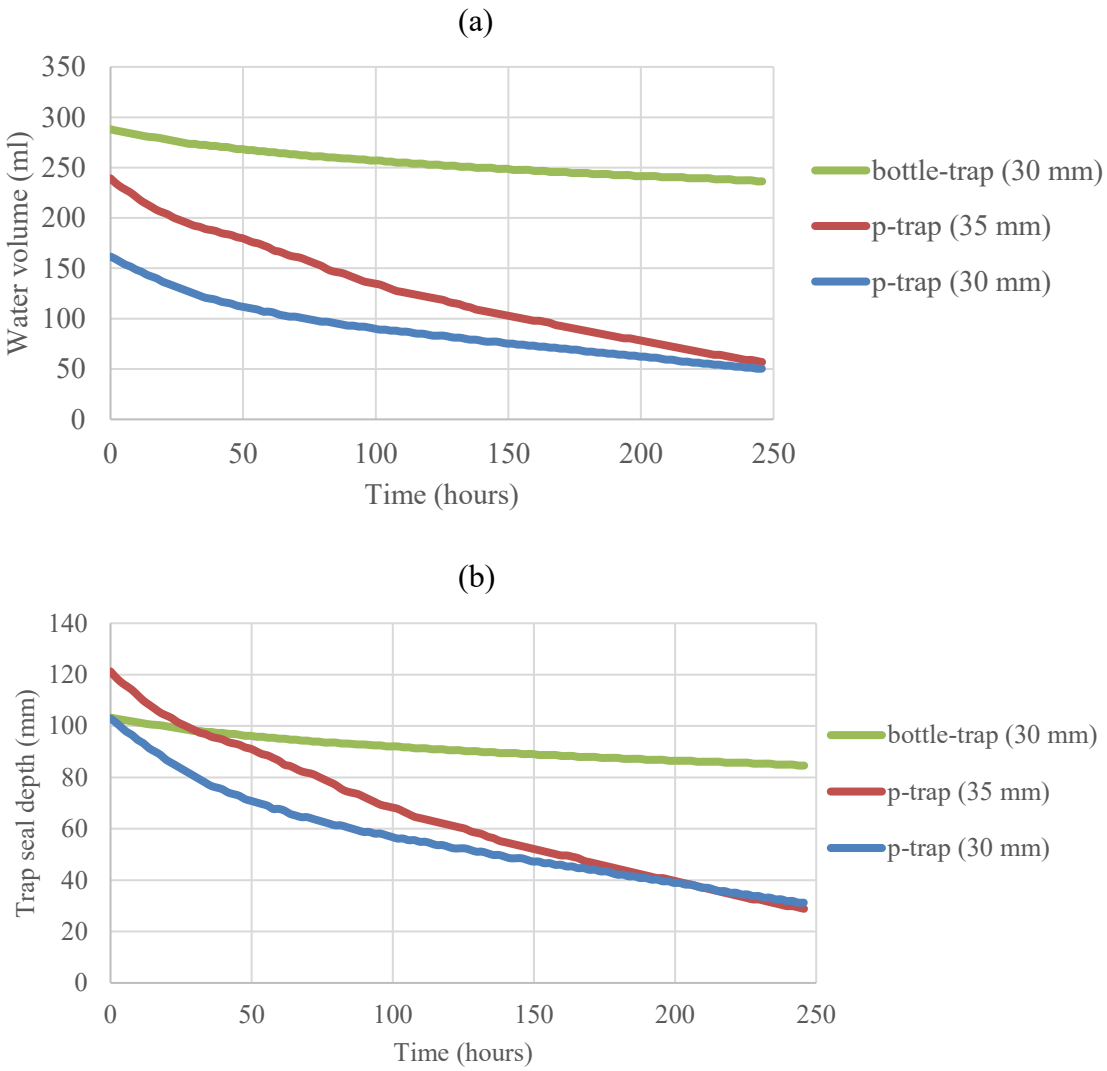

Figure 3: Variation due to evaporation for: (a) trap seal water volume, and (b) trap seal depth (water column height)

The results indicate that trap geometry plays a significant role in governing evaporation rates. The relatively stable behaviour of the bottle trap suggests that reduced exposure of the water surface can substantially limit evaporative losses. While increased initial seal depth (as in the 35 mm P-trap) provides additional storage capacity and delays depletion, it does not prevent significant loss over time. These findings highlight evaporation as a credible mechanism for trap seal degradation, particularly for P-trap configurations under conditions of prolonged non-use.

3.2 Evaporation rates

Evaporation rates were estimated from the measured reductions in both water volume and seal depth over the 240-hour test period. Figure 4 shows the daily rate of change in water column and trap seal depth for all three water trap seals. The results indicate significant variation between trap configurations.

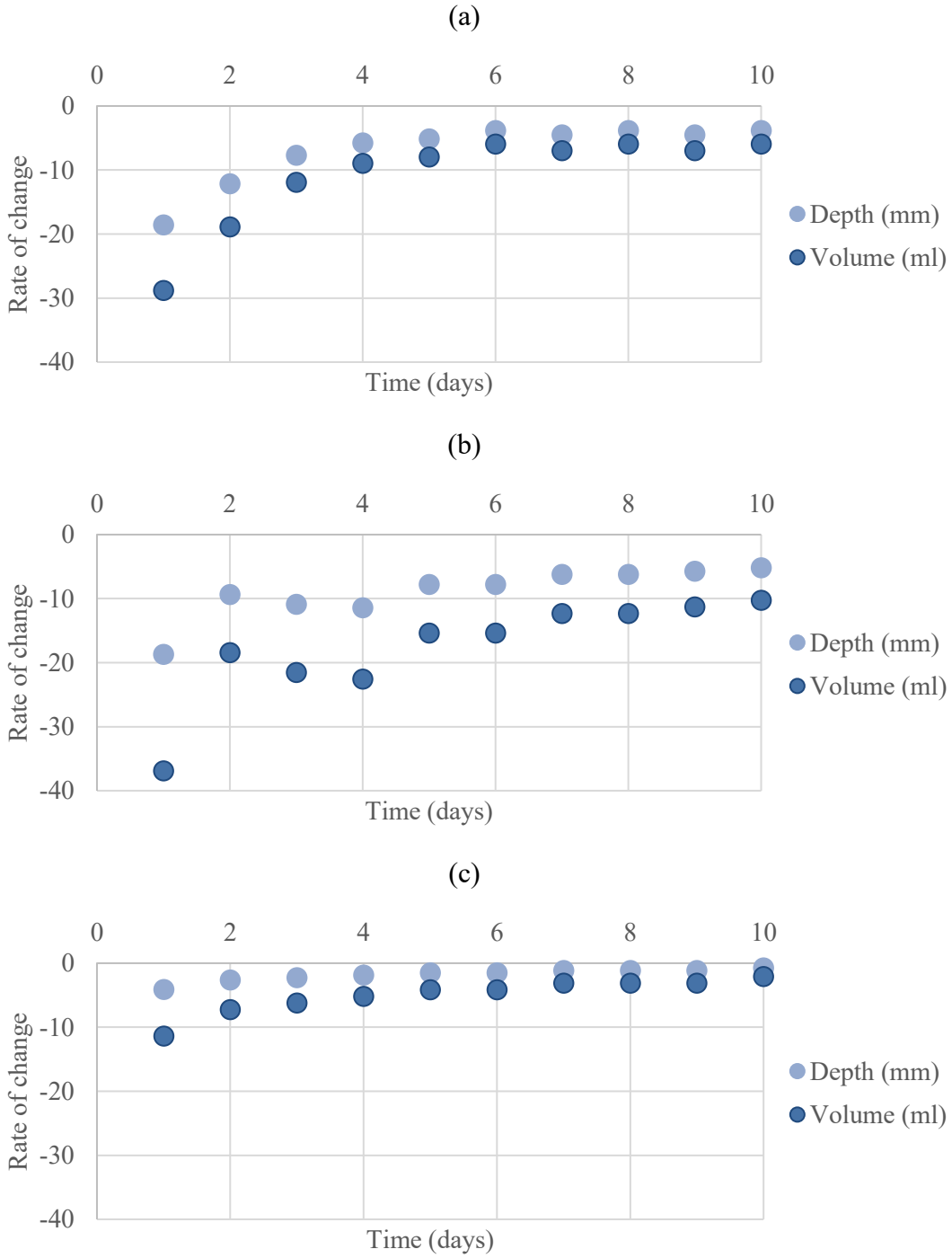

Figure 4: Daily rate of change in water volume and trap seal depth for: (a) P-trap (30 mm), (b) P-trap (35 mm), and (c) Bottle-trap (30 mm)

For the P-trap (35 mm), the average evaporation rate was approximately 18 ml/day, corresponding to a mean seal depth reduction of approximately 9 mm/day. The P-trap (30 mm) exhibited a lower but still substantial average evaporation rate of approximately 11 ml/day (~7 mm/day). In contrast, the bottle trap (30 mm) showed markedly reduced evaporation, with an average loss of approximately 5 ml/day, equivalent to a seal depth reduction of approximately 1.5 mm/day, see Table 2.

Table 2: Estimated evaporation rates (average, early, and late) for each water trap seal in terms of volume-based results and depth-based results

	Volume-based evaporation (ml/day)			Depth-based evaporation (mm/day)		
Trap	**Average**	**Early**	**Late**	**Average**	**Early**	**Late**
P-trap (35 mm)	~18	~25–30	~10–12	~9	~12–15	~5–6
P-trap (30 mm)	~11	~15–18	~6–8	~7	~10–12	~4–5
Bottle trap (30 mm)	~5	~6–7	~3–4	~1.5	~2–2.5	~1–1.5

In all cases, evaporation rates were highest during the initial phase of the experiment and decreased progressively over time. This behaviour is attributed to the reduction in exposed water surface area and evolving vapour conditions within the trap. Notably, both P-traps approached a residual seal depth of approximately 30 mm within 8–10 days, indicating a potential threshold for increased failure risk.

The measured evaporation rates significantly exceed those reported in the literature for typical indoor conditions in the UK (approximately 2–3 mm/week), particularly for P-traps. For context, the German standard, DIN EN 12056, states an admissible evaporation rate of just 1 mm per day for trap seals (DIN, 2000). A common industry rule of thumb in the US assumes that a standard 2-inch (51 mm) trap seal will evaporate completely in 30 to 60 days in a typical indoor environment if left unreplenished, corresponding to an evaporation rate of between 0.85-1.7 mm/day. In warmer conditions this is said to increase to a rate of 3-inches in 30 days, so 2.5 mm/day (Des Champs, ND). Our results suggest that evaporation may represent a more critical mechanism of trap seal depletion than previously assumed, particularly under elevated temperature conditions.

3.3 Model fitting

The temporal evolution of water volume and seal depth for each trap was further analysed using an exponential decay model of the form:

$$V(t) = V_\infty + (V_0 - V_\infty)e^{-kt}$$

$$H(t) = H_\infty + (H_0 - H_\infty)e^{-kt}$$

where V_0 and H_0 are the initial water volume and seal depth, V_∞ and H_∞ denote the equilibrium values, and k is the decay constant governing the rate of evaporation, see Figure 5.

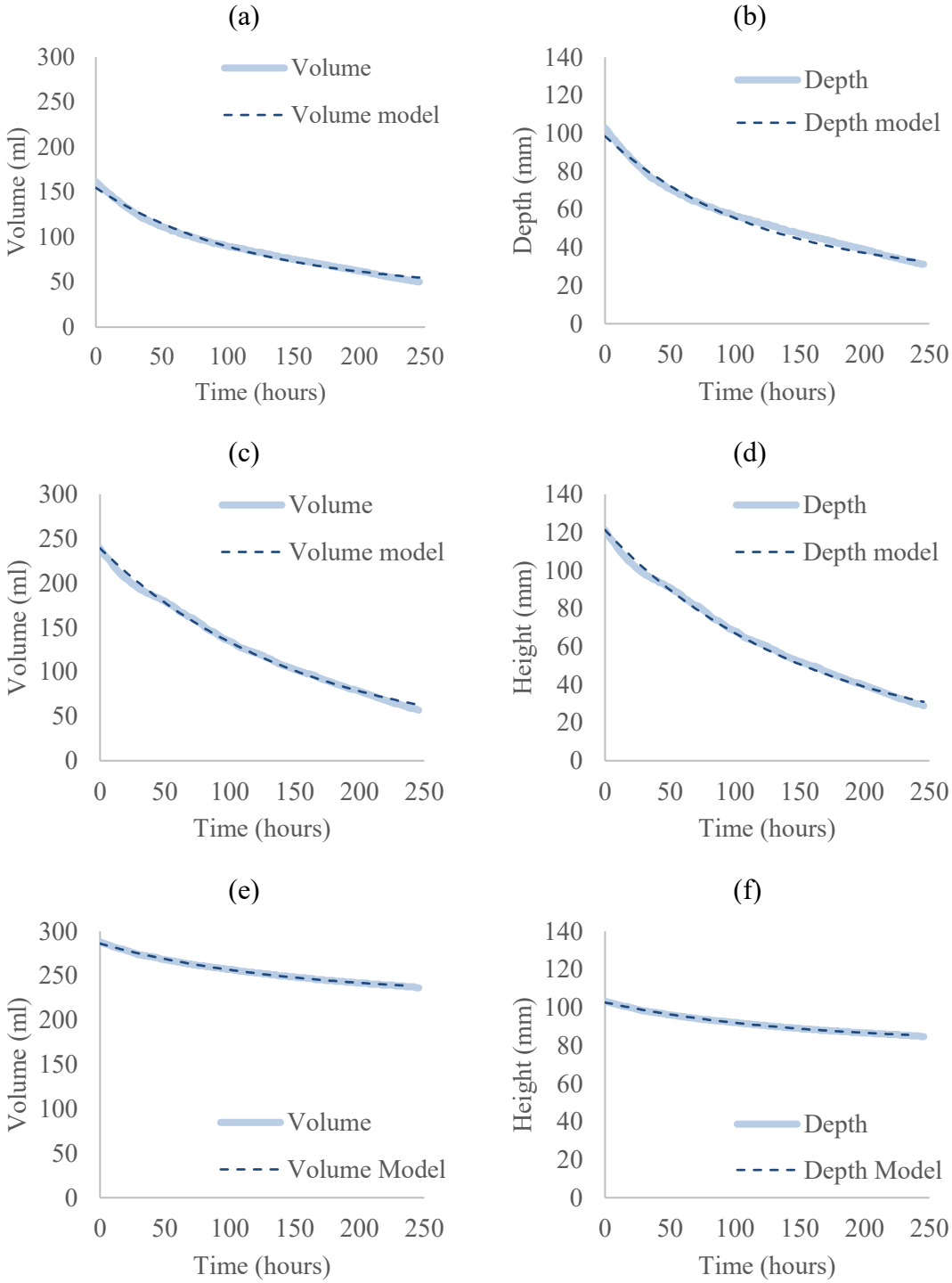

Figure 5: Comparison of experimental data with exponential model fits for trap seal evaporation: (a) P-trap (30 mm) volume, (b) P-trap (30 mm) seal depth, (c) P-trap (35 mm) volume, (d) P-trap (35 mm) seal depth, (e) Bottle-trap (30 mm) volume, and (f) Bottle-trap (30 mm) seal depth

The exponential form provides a good fit to the experimental data for all trap configurations, capturing both the rapid initial depletion and the progressive reduction in evaporation rate observed at later times.

The fitted parameter k provides a useful quantitative descriptor of evaporation dynamics, with higher values corresponding to more rapid depletion. Consistent with the direct observations, the P-trap configurations exhibited larger decay constants than the bottle trap, indicating a greater susceptibility to evaporation-driven seal loss. The equilibrium values, V_∞ and H_∞, converge towards finite non-zero values, reflecting the residual water volume retained within each trap and reflecting a limiting condition below which further evaporation is significantly reduced.

The close agreement between the fitted curves and the measured data indicates that a simple first-order exponential model is sufficient to characterise evaporation behaviour in trap seals under controlled conditions. This provides a useful framework for predicting depletion times and assessing the risk of seal failure in practical applications, particularly during extended periods of fixture non-use.

4 Conclusions

This study has provided experimental evidence of evaporation-induced depletion of water trap seals, addressing an important but relatively under-examined failure mechanism within building drainage systems. Three trap geometries (a 30 mm P-trap, a 35 mm P-trap, and a 30 mm bottle trap) were tested under controlled conditions at a temperature of 25°C. The results confirm that evaporation can significantly reduce both water volume and seal depth over relatively short timeframes under typical elevated indoor temperature conditions. The results clearly demonstrate that trap geometry is a critical factor governing evaporation behaviour.

The bottle-trap exhibited substantially greater resistance to evaporative loss, maintaining a relatively stable seal depth throughout the test period (with daily seal depth reductions of around 1.5 mm/day). In contrast, both P-trap configurations exhibited more rapid depletion, with daily seal depth reductions of up to 9 mm/day recorded. Despite differences in initial seal depth and water volume, both P-traps converged towards critically low seal depths within the 10-day test period, highlighting the limited benefit of increased initial seal depth.

From a building engineering perspective, this has important implications for system design, operation, and maintenance - particularly in intermittently occupied buildings, or during periods of low usage. Critically, evaporation-induced seal depletion may allow partial loss of the water barrier well before complete seal failure occurs. Given existing evidence linking even partial depletion to aerosol transmission pathways, this represents a concerning risk to indoor environmental quality and occupant health—one that may be further amplified by system pressure fluctuations that promote the movement of contaminated air through compromised seals.

The results presented here support the need for proactive mitigation strategies, including trap design optimisation, incorporation of evaporation-resistant solutions, and routine maintenance protocols to ensure seal integrity is maintained.

5 Limitations and Future Work

As a preliminary study we tested just one example of each of the three trap geometries. Future work will endeavour to test a wider range of trap geometries, types, and make/model, as well as the repeatability of results. Humidity and air movement within the environmental chamber will also be recorded.

Potential sources of error are mainly associated with the accuracy of the thermistor that recorded the air temperature and the digital scales that recorded the mass of the trap and water. Errors could also have been introduced during calibration of the water mass to water volume and trap depth. Care was taken to minimise sources of error when possible.

6 References

Copernicus Climate Change Service (2023). European summer 2023: a season of contrasting extremes. Implemented by ECMWF as part of The Copernicus Programme. https://climate.copernicus.eu/european-summer-2023-season-contrasting-extremes [accessed 07/05/2026]

Des Champs (N,D). Time to reconsider use of P-traps for condensate removal. Available at: https://inspectapedia.com/aircond/AC-Condensate-Check-Trap-hpac.pdf [accessed 17/07/2026].

DIN (2000) DIN EN 12056-2:2000-09. Gravity drainage systems inside buildings – Part 2: Sanitary pipework, layout and calculation. Berlin: Deutsches Institut für Normung (DIN).

Gormley M. (2010). “Water trap seal vulnerability monitoring: A case study of its application to a large hospital complex” CIB W062 36th International Symposium on Water Supply and Drainage for Buildings, Sydney, Australia, 8-10 November 2010.

Gormley M., Aspray T.J., Kelly D.A. (2020). "COVID-19: mitigating transmission via wastewater plumbing systems." The Lancet Global Health, Volume 8, Issue 5, May 2020, Page e643. https://doi.org/10.1016/S2214-109X(20)30112-1

Gormley, M., Aspray, T.J. and Kelly, D.A. (2021), Aerosol and bioaerosol particle size and dynamics from defective sanitary plumbing systems. Indoor Air, 31: 1427-1440. https://doi.org/10.1111/ina.12797

Gormley M, Aspray TJ, Kelly DA, Rodriguez-Gil C (2017) Pathogen cross-transmission via building sanitary plumbing systems in a full scale pilot test-rig. PLoS ONE 12(2): e0171556. https://doi.org/10.1371/journal.pone.0171556

Gormley M., Templeton K.E., Kelly D.A. and Hardie A. (2013). "Environmental conditions and the prevalence of norovirus in hospital building drainage system wastewater and airflows." Building Services Engineering Research & Technology, 35 (3), 244-253. https://doi.org/10.1177/0143624413485080

Hung H.C.K., Chan D.W.T., Law L.K.C., Chan E.H.W. and Wong E.S.W. (2006). "Industrial experience and research into the causes of SARS virus transmission in a high-rise residential housing estate in Hong Kong," Building Services Engineering Research and Technology, 27(2): 91-102. https://doi.org/10.1191/0143624406bt145oa

Kelly D.A. (2009). "Controlling the risk of cross-contamination from the building drainage system using the reflected wave technique to identify depleted water trap seals." PhD Thesis, Heriot-Watt University, Edinburgh, UK.

Kelly D.A. and Gormley M. (2013). "Automatic detection of depleted fixture trap seals using the reflected wave technique." Building Services Engineering Research & Technology, 35 (3), 254-267. https://doi.org/10.1177/0143624413485959

Lyu K., Wang Q., Li X., Zhang Z., Zhao X., Li Y., Tang Z., Li L., Deng F., Zhang X., Xu K., Zhao R. & Xu D. (2023). Neglected Aspects of SARS-CoV-2 Aerosol Transmission in Bathrooms of Multistory and High-Rise Buildings - Beijing Municipality, China, October 2022. China CDC weekly, 5(1), 1–4. https://doi.org/10.46234/ccdcw2023.001

Swaffield J.A. and Galowin L.S. (1992). The engineered design of building drainage systems. England: Ashgate Publishing Limited.

Wise A.F.E. and Swaffield J.S. (2002). Water, Sanitary and Waste Services for Buildings. 5th edn. Oxford: Butterworth-Heinemann.

7 Presentation of authors

Dr David A Kelly is Associate Professor of Architectural Engineering at Heriot-Watt University. His research interests cover: water conservation, minimisation of disease transmission from wastewater drainage systems, water systems in healthcare environments, and the use of nature-based solutions of stormwater management.

Prof. Michael Gormley is Professor of Public Health and Environmental Engineering at Heriot-Watt University. His research specialisms are: mathematical modelling of air and water flows in building drainage systems, infection spread via bioaerosols, water systems in healthcare environments, sanitation in developing countries, and product development.

Modelling approaches to produce design guidance- TM70: Tall building Drainage Design.

M. Gormley[1]

(1) m.gormley@hw.ac.uk

The School of Geoscience, Infrastructure and Society, Heriot-Watt University, Edinburgh, Scotland, UK

Abstract

TM 70: 2025 presents evidence-based recommendations for the design of drainage ventilation systems in tall buildings, based on research undertaken at Heriot-Watt University. Current design codes give limited consideration to the effects of building height on drainage system performance, restricting their applicability to high-rise buildings. The recommendations in TM 70 address this limitation and are supported by laboratory experiments, full-scale testing, and validated computational modelling using the AIRNET simulation tool, informed by more than 3,000 simulated system configurations. The research upon which the guidance is based, is grounded in empirical evidence and predictive modelling. Supporting material explains the technical rationale for the recommendations and documents the validation of the modelling approach. Designers must continue to comply with existing standards, which provide detailed guidance on pipe sizing and system configuration for both primary and secondary ventilation arrangements. As building height increases, drainage system behaviour changes markedly, particularly in terms of pressure fluctuations, airflow patterns, and water flow dynamics. These effects challenge conventional design approaches and can lead to underestimation of ventilation requirements. The guidance clarifies how system behaviour varies with height and defines associated levels of operational risk. Unique features of the guidance include; Control of positive and negative pressure transients, clear guidance on the treatment of offsets, introduction of a new term - effective height and a comprehensive commissioning test protocol. A risk-based assessment framework is introduced to evaluate system resilience, considering variables such as air and water flow rates, maximum pressures, pipe diameter, ventilation strategy, building height, and trap seal loss. Central to the methodology used to develop the guidance is the AIRNET model, which was used to simulate multiphase flows and transient pressures. Model predictions have been validated experimentally and used to develop risk curves and performance boundaries. The results demonstrate that system risk increases with height unless enhanced ventilation measures are adopted.

Keywords

Building Drainage Standards; modelling methodology and validation

1. Introduction

1.1 General

The development of modern building drainage systems can be traced with confidence to Edwin Chadwick's 1842 report, *The Sanitary Condition of the Labouring Population of Great Britain*. This influential work emphasised the essential role of sanitation in protecting public health and prompted sustained investigation over the following century into the safe conveyance of human waste from buildings to municipal sewer systems.

During this early period, design approaches focused largely on establishing water flow rates and, by extension, considering their effects on air pressure within drainage networks. However, the interaction between water movement, airflow and pressure was not well understood. As a result, design practice tended to prioritise pipe sizing for the efficient transport of wastewater, while giving limited attention to the control of air pressure. This was primarily to safeguard the water trap seal, which serves as the main defence against the ingress of contaminated sewer gases and is widely regarded as the most vulnerable component of the system.

A major step forward occurred in the early twentieth century, culminating in the work of Roy Hunter in the United States. In 1940, Hunter, building on earlier work by Whipple, (Whipple et al, 1923, Hunter, 1940) introduced a probabilistic design method that allocated dimensionless discharge units to plumbing fixtures and enabled the estimation of simultaneous flows. Although Hunter recognised the limitations of this approach, variations of his method continue to underpin many international drainage design codes.

Despite these advances, the importance of air supply and pressure equalisation has received relatively little formal consideration within drainage standards. Ventilation design has often been based on assumed pipe dimensions and an incomplete understanding of the governing fluid dynamics, particularly in tall buildings. The global increase in high rise and complex developments has renewed interest in the fundamental processes controlling air pressure behaviour in drainage systems.

In tall structures, the extended height of drainage stacks increases the distance through which air must move, leading to greater frictional losses and an elevated risk of detrimental pressure transients, both positive and negative. Such fluctuations can compromise the integrity of water trap seals. Existing design standards, which are largely founded on steady state assumptions, do not adequately capture the dynamic nature of airflow in these conditions.

Contemporary standards should incorporate transient analysis as an integral part of drainage system design, yet this is not routinely achieved. Advances in computational modelling, together with technologies such as Positive Pressure Relief Devices, now permit a more thorough evaluation of system performance under variable conditions. These developments align drainage engineering with other fields, including water supply, oil and gas transmission, and major civil infrastructure, where the analysis of transient behaviour has long been recognised as a fundamental design requirement.

1.2 Aims and objectives

The aim of this paper is to set out the methodology for the modelling and rationale for the assessment of a range of configurations as described in the CIBSE Technical Memorandum entitled 'Tall Building Drainage Design Guide' published in December 2025. (CIBSE, 2025)

The mechanisms of air pressure transient propagation in BDS are well understood. Numerical techniques suited to full bore fluid flow are used to model air pressure wave propagation in a bounded conduit (Swaffield, 2010).

The program simulates low amplitude air pressure transients using the fundamental St. Venant equations of momentum and continuity, solving these equations numerically via the method of characteristics. This method provides air pressure and velocity within a bounded duct system subjected to air pressure transient propagation. Figure 1 outlines the basic principles governing airflow and air pressure in a building drainage system. As water enters the stack from a branch as an annular flow, it entrains airflow into the network, creating suction pressure in the vertical stack. Pressure drops occur at the upper termination of the stack due to separation losses as airflow passes through the top stack termination. Frictional losses in the dry stack cause further pressure drops, which can be calculated using D'Arcy's equation. Additional pressure drops occur as the entrained airflow passes through the unsteady water curtain at the discharging branch. Figure 1 also shows positive pressure at the base of the stack as airflow is forced through the water curtain formed at the bend at the base of the stack. (Gormley et al 2025).

These pressure losses in the stack may be combined as:

$$\Delta P_{total} = \Delta P_{entry} + \Delta P_{dry\ pipe\ friction} + \Delta P_{branch\ junction} + \Delta P_{back\ pressure} \quad (1)$$

The 'motive force' that entrains this airflow and compensates for these pressure losses comes from the shear force between the annular terminal velocity water layer and the air in the wet portion of the stack. This can be seen as a 'negative' friction factor, generating an equal pressure rise, similar to a fan drawing air through the stack. Ongoing research has identified the form and relationships governing this shear force, allowing for the prediction of the transient response of the stack network to variations in applied water downflows.

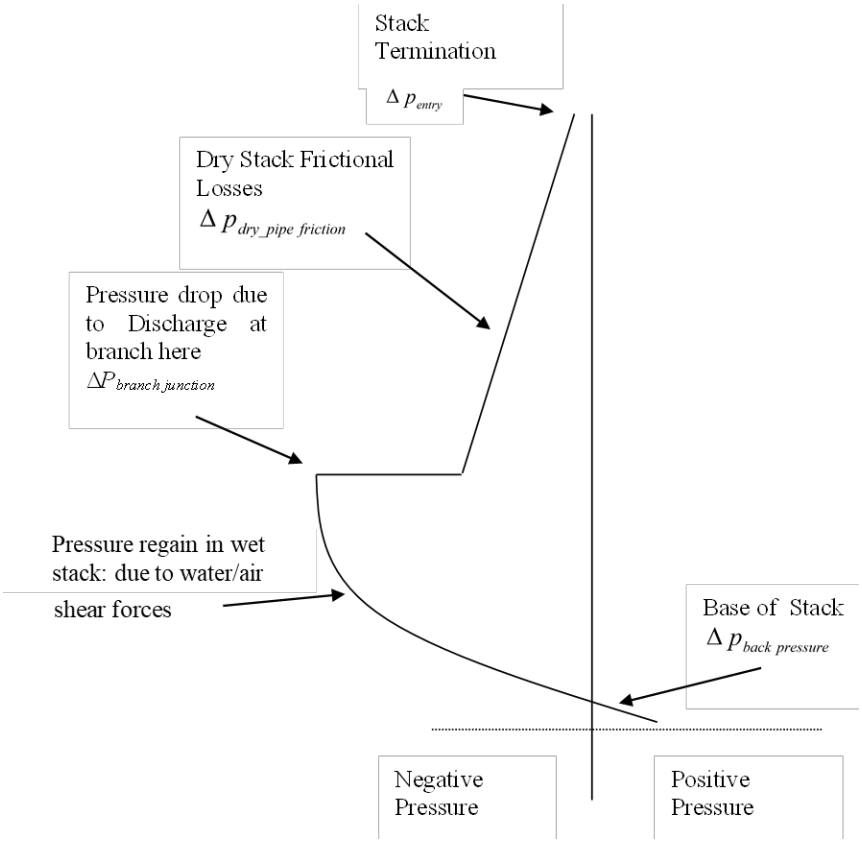

Figure 1. **Entrained airflow analysis for AIRNET model**

2.1. Mathematical Modelling of Air Pressure Transients

The method of characteristics offers a flexible mathematical model that effectively represents pressure transients in complex pipe and duct networks. It has become the standard solution technique for their analysis in the field.(Lister 1960)

Calculations progress through the system on a two-dimensional grid representing time (t) and distance (x). Conditions at one point in the grid are based on conditions at adjacent nodes upstream and downstream, one time step in the past, requiring a definition of the characteristic slope for calculation. In Figure 2, R and S represent points where conditions are known by interpolation between A and C, and B. The characteristic lines between R and P, and S and P, represent equations used to calculate the condition at point P. The characteristic slopes allow information regarding air velocity and wave speed, and hence pressure, to propagate throughout the network.

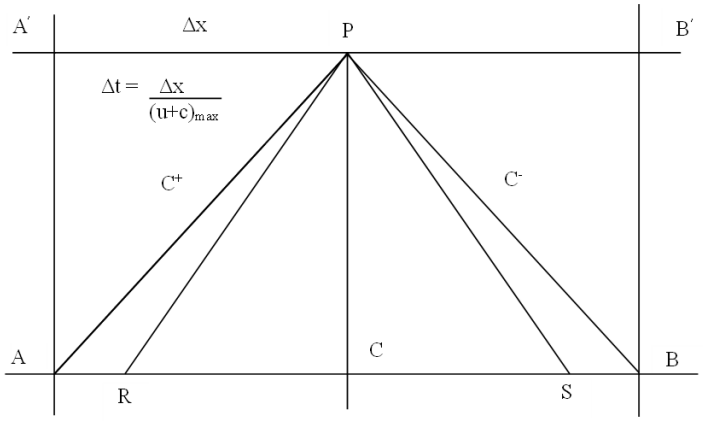

Figure 2. Grid showing characteristic lines as utilised in Method of Characteristics approach to air pressure transient modelling

The characteristic slopes, PR and PS, are given by 1/(u+c). If the fluid velocity is much less than the wave speed (u << c), the variation in the slope of the characteristic line may be assumed negligible, making AR and BS two points, removing the need to interpolate conditions at R and S.

The basic equations of transient propagation, the St. Venant equations of momentum and continuity, are quasi-linear hyperbolic partial differential equations. These can be transformed into a pair of total derivative equations via the method of characteristics, which can be solved using a finite difference scheme.

The transformation of the St. Venant equations of continuity and momentum into the total derivatives required by the method of characteristics are given below for a full description of the derivation please see (Swaffield, 2010). The total derivatives have been shown to be;

For C+ - Line PR.

$$u_P - u_R + \frac{2}{\gamma - 1}(c_P - c_R) + 4f_R\, u_R \mid u_R \mid \frac{\Delta t}{2D} = 0 \qquad (2)$$

When

And

$$\frac{dx}{dt} = u + c \qquad (3)$$

For C- - Line PS

$$u_P - u_S - \frac{2}{\gamma - 1}(c_P - c_S) + 4f_S\, u_S \mid u_S \mid \frac{\Delta t}{2D} = 0 \qquad (4)$$

When

$$\frac{dx}{dt} = u - c \tag{5}$$

In the case of a building drainage system fS and fR are functions of time, location and annular water downflow and hence act as drivers in the simulation by generating the entrained air flow within the wet stack, or as determinants of the frictional losses in the dry stack. The expression

$$\frac{dx}{dt} = u \pm c \tag{6}$$

is known as the Courant Criterion and must be adhered to, to ensure stability.

These equations may be reduced such that the resultant expressions are based around two simultaneous first order equations linking wave speed and flow velocity by letting:

$$u_p = K1 + K2\, c_p \tag{7}$$

for the C+ characteristic, and

$$u_p = K3 + K4\, c_p \tag{8}$$

for the C- characteristic, where

$$K1 = u_R + \frac{2}{\gamma - 1} c_R - 4 f_R u_R |u_R| \frac{\Delta t}{2D} \tag{9}$$

$$K2 = K4 = \frac{2}{\gamma - 1} \tag{10}$$

$$K3 = u_S - \left(\frac{2}{\gamma - 1}\right) c_S - 4 f u_s |u| \frac{\Delta t}{2D} \tag{11}$$

The pressure can then be calculated from the Gas Laws using the following expression

$$P_p = \left[\left(\frac{P_o}{\rho_o^{\gamma}}\right)\left(\frac{\gamma}{c^2}\right)^{\gamma}\right]^{\frac{1}{(1-\gamma)}} \tag{12}$$

The time steps between calculations is critical and depends upon the Courant Criterion. when used in this way

$$\Delta t \ \leq \frac{\Delta x}{(u+c)_{max}} = u \pm c \tag{13}$$

For the analysis of low amplitude air pressure transients in building drainage networks a typical time step would be less than –

$$\Delta t \ \leq \frac{\Delta x}{(u+c)_{max}} \approx \ \frac{1.0}{344+20} = 0.0027\ s \tag{14}$$

when Δx, the distance between calculation nodes, is 1m.

Although the time step will vary with wave speed, in this example the variations will be minimal, dependent only on variations in air pressure – itself minimal.

3. Boundary Conditions

Figure 3 shows how the method of characteristics can be applied to a drainage system. The example is stylised for clarity.

3.1 **Boundary condition for a water trap seal**

This paper will not seek to explain all the boundary conditions within a simple system as shown in Figure 3, rather the boundary condition for a water trap seal is shown to illustrate the process.

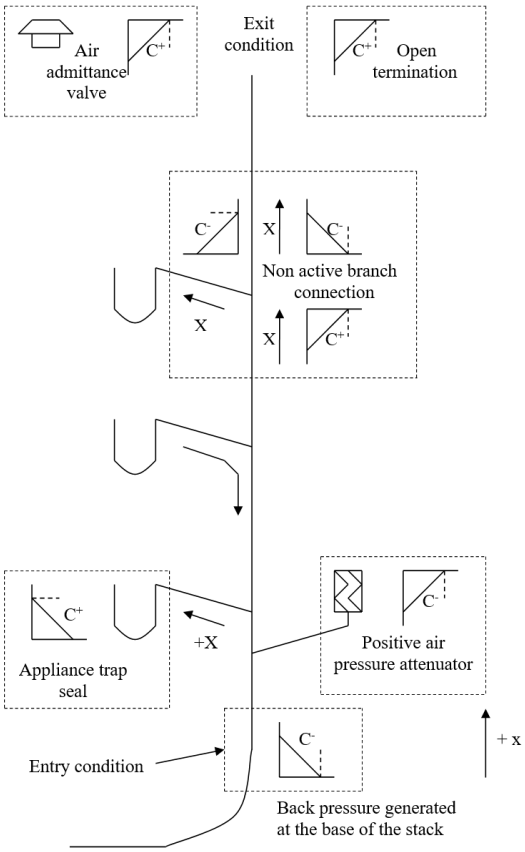

Figure 3. Method of characteristics boundary conditions for a single stack system.

The forces acting on the displaced water column may be defined as follows;

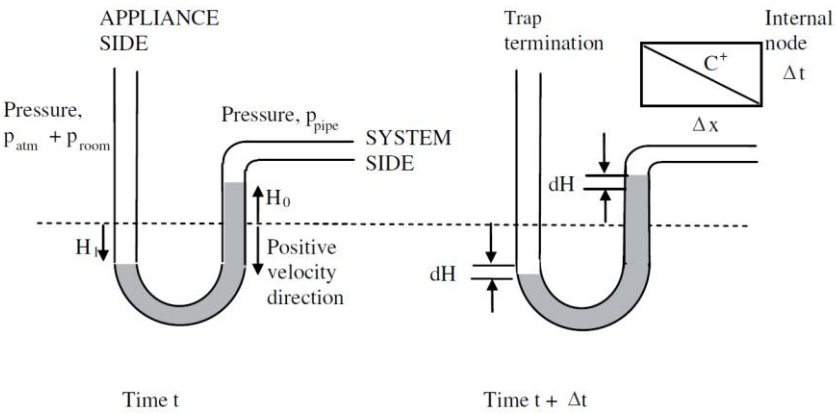

Note trap diameter, D and wetted perimeter P. The trap seal water length L may vary dependent upon the applied pressure transient regime as the trap seal is lost.

Figure 4 Definition of the trap seal termination illustrating trap deflection across a time step (Swaffield, 2010)

$$\text{Term T1} = A\left[0.5\left(p_{pipe,t+\Delta t} + p_{pipe,t}\right) - \left(p_{atm} + p_{room}\right)\right] \tag{15}$$

$$\text{Term T2} = \rho g A\left(H_0 - H_1 + 2dH\right) \tag{16}$$

$$\text{Term T3} = \tau LP = 0.5\rho f LPV_{trap}^2 \tag{17}$$

$$\text{Term T4} = \rho LA\frac{V_{trap,t+\Delta t} - V_{trap,t}}{\Delta t} \tag{18}$$

to yield a boundary condition expressed as

$$F = T1 + T2 - T3 - T4 = 0 \tag{19}$$

To be solved by the C^- characteristic expressed as

$$u_{trap,t+\Delta t} = K1 - K2c_{trap,t+\Delta t} \tag{20}$$

where the constants K1 and K2 are dependent on flow and frictional term values known at time *t* and, to allow for trap diameters smaller than the connected branch,

$$u_{trap,t+\Delta t} = \left(\frac{D_{trap}}{D_{branch}}\right)^2 V_{trap,t+\Delta t} \tag{21}$$

For a full derivation of equation 21, please see Swaffield, 2010.

From Equation (21) V is the trap water velocity. Solution may be achieved via the bisection method applied to the function F = T1 + T2 – T3 – T4 between suitable air pressure

limits. The C+ characteristic is included via Term 4 once the wave speed has been

determined from the assumed trial air pressure, pX as

$$c_{trap,t+\Delta t} = \sqrt{\frac{\gamma p_X}{\rho_{atm}\left(\frac{p_X}{p_{atm}}\right)^{\frac{1}{\gamma}}}} \tag{22}$$

The oscillations, while unsteady in nature can be represented by a laminar model within the trap itself. Thus friction can be derived from -

$$f = \frac{16}{\mathrm{Re}} = \frac{16\upsilon}{V_{trap} D_{trap}} \tag{23}$$

The Reynolds number being used for laminar flow is a constant when the viscosity is a constant and does not change with changes in velocity and density. As the flow is isothermal, as the temperature is constant the viscosity is constant and for a given transient flow the Reynolds number is the same at all points within the water trap.

Options for unsteady friction representations such as Carsten-Zilke formulation are available, however the extra computational cost does notjustify the small improvement in accuracy.

4. AIRNET Model validation

A full validation of the AIRNET model in relation to TM70 is given in Gormley et al (2025) and shows strong correlation between measured and predicted values for system pressures across the height of the building. The modelling approach covers steady and transient flows in building drainage systems and can be used for any configuration including single stacks and secondary vented systems, loop vents and any other possible arrangement. The system used was the National Lift Tower test system in Northampton UK and is operated by Aliaxis. The effective height of the installation (as per TM70 definition) is approximately 100 m. Figure 5 below shows the correlation between measured and predicted values for pressure.

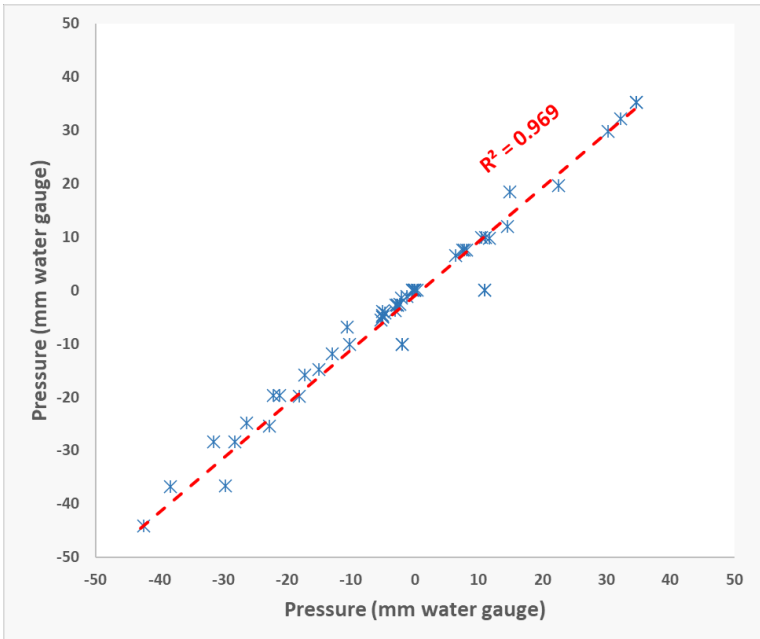

Figure 5. Correlation between simulated and measured pressure data

Overall, the correlations are good and as such the mechanisms developed upon which to represent the operation of a tall building drainage system can be properly represented by the output of the AIRNET model. By increasing the height of the vertical stacks involved it has been possible to incorporate height into the system in a way that underpins the mechanism and provides the basis for guidance to the designer.

5. Conclusions

This paper has outlined the development of a comprehensive methodology with which to create a design guide for tall building drainage systems, grounded in the use of the AIRNET simulation model. AIRNET is a one-dimensional, method-of-characteristics-based flow model, implemented through a finite difference scheme. The model has been validated against empirical data from a variety of buildings, including the 100 m tall test facility at the National Lift Tower in Northampton, United Kingdom.

The validation process demonstrated a strong correlation between measured and modelled air pressures, with a correlation coefficient of 0.969,. These results confirm the reliability and accuracy of the AIRNET model in predicting air pressure transients within tall building drainage systems. . The modelling approach covers steady and transient flows in building drainage systems and can be used for any configuration including single stacks and secondary vented systems, loop vents and any other possible arrangement.

The findings presented in this paper support the use of AIRNET as a robust and practical tool for the design and assessment of drainage systems in high-rise buildings. Its ability to model complex system behaviour with a high degree of accuracy provides designers with a valuable resource for addressing the growing demands of vertical urban development.

6. References

CIBSE, 2025 TM70:2025- Tall Building Drainage Design , CIBSE London, 2025

Gormley M, Mohammed S, Kelly DA, Campbell DP. Application and Validation of AIRNET in Simulating Building Drainage Systems for Tall Buildings. *Buildings*. 2025; 15(10):1725. https://doi.org/10.3390/buildings15101725

Hunter, R B. Plumbing Manual. In: National Bureau of Standards. Washington D C; 1940

Lister, M. (1960). The Numerical Solution of Hyperbolic Partial Differential Equations by the Method of Characteristics. In *Mathematical Methods for Digital Computers* (Chapter 15).

Swaffield, J. (2010). Transient Airflow in Building Drainage Systems. Tylor& Francis.

Whipple GC, Carson HY, Hanley TF, Groeninger WC, Gries JM, Cartwright FP, et al. Recommended minimum requirements for plumbing in dwellings and similar buildings :final report of subcommittee on plumbing of the building code committee July 3, 1923.

R H. Methods of Estimating Loads in Plumbing Systems. Natl Bur Stand USA. 1940; BMS65:17

7. Nomenclature

u Mean airflow velocity (m/s)
L Distance (m)
x Distance (m in MoC)
ρ Density (kg/m^3)
Re Reynolds number
γ Ratio of specific heats
D Pipe diameter (m)
K Loss or terminal velocity coefficient
N Number of pipe inter-nodal sections
p Pressure mm water gauge
t Time (s)
v Mean water velocity (m/s)
T1–T4 Terms used in MoC boundary for trap seal

8. Author

Michael Gormley is Professor of Public Health and Environmental Engineering at the School of Energy, Geoscience, Infrastructure and Society at Heriot-Watt University. His research specialisms are: mathematical modelling of air and water flows in building drainage systems, infection spread via bioaerosols and product development.

Drainage roof vent distance from fresh air ventilation inlet in the Netherlands

N. Post (1)
(1) nick.post@hydraloop.com
(1) Hydraloop Systems BV, Leeuwarden, the Netherlands

Abstract

Building drainage systems are a dynamic mixture of water and air, with constant pressure fluctuations which need to be attenuated to prevent traps to be siphoned or blown through. To do this, building drainage systems have open to air roof vents.

The location of the roof vents has to be of sufficient distance from any fresh air intake, be it a ventilation system or window to be opened, and accessible outdoor aeras. This to prevent sewer gas inside the building, or in direct contact with humans.

The measure of this distance is something of much debate.

In the Netherlands, NEN 3215 is the applicable Standard for Building Drainage systems, equivalent to EN-12056-2.

NEN 3215 states a roof vent termination point must be either 3 or 6 meters removed from a fresh air ventilation intake, or accessible outdoor area, depending on the configuration. Partly because roof spaces become 'busier', this distance has been widely scrutinised by the industry. After research by the Dutch Building Drainage Standards Committee, it has been their conclusion that the current distances are based on empirical data, without well documented scientific evidence for the effectiveness of such distances.

The Standards committee is accountable for this distance, which makes changing it without data challenging. There is however a need for more flexibility.

This industry paper describes the process and outcome of the Standards Committees' efforts on how to create a more flexible decision method on the determination of the distance of Building Drainage roof vent termination and fresh air supply intakes, and accessible roof space.

Keywords

Building drainage, roof vent, sewer gas, standardisation

1. Introduction

Building drainage systems are a dynamic mixture of water and air, with constant pressure fluctuations which need to be attenuated to prevent traps to be siphoned or blown through. To do this, building drainage systems require open to air roof vents.

Since venting via façades creates too great pressure differences due to wind influences and other external factors, the roof is the only suitable solution. Because of odour and health risks of sewer gas, drainage vents need to be of sufficient distance from any fresh air intake, be it a ventilation system, a window to be opened, as well as accessible outdoor aeras. This to prevent sewer gas inside the building, or in direct contact with humans.

2. Current situation

The current situation in the Netherlands is based on the NEN 3215 Standard on building drainage systems [1]. NEN 3215 states that, depending on the roof layout, a minimum distance of either 3 or 6 meter needs to be maintained.

In situations where the drainage vent and fresh air intake or accessible area are situated in the same roof space at the same height, or when a fresh air intake is above the drainage vent, a minimum distance of 6 m needs to be maintained, see Figure 1. Because of the direct contamination risk, and taking into account common wind influences, these configurations are deemed critical and are not being reviewed by the committee.

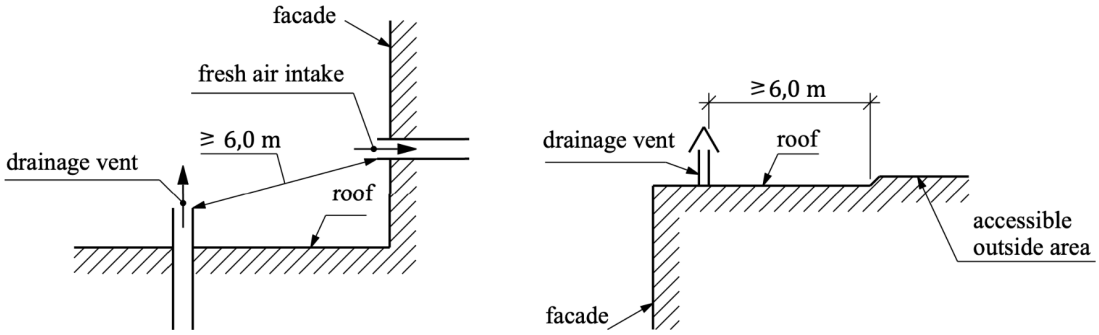

Figure 1 – Examples of configurations with 6 m distance between drainage vents and fresh air intake or accessible outdoor area [1]

Figure 2 shows examples from NEN 3215 in which the minimum horizontal distance maintained must be 3 m, with the additional requirement of the vent termination ≥ 1 m above the fresh air intake in either a roof or a façade, independent of the configuration. The situations where a minimum horizontal distance of 3 m applies have been reviewed by the committee.

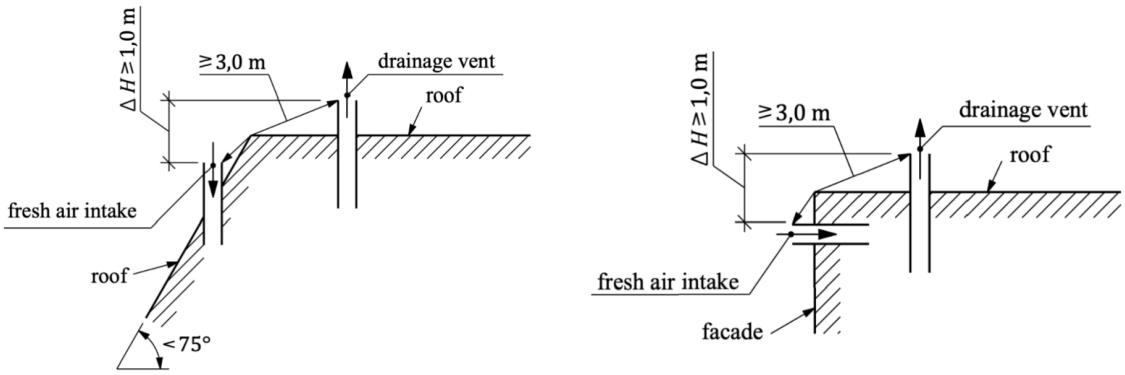

Figure 2 – Examples of configurations with 3 m distance between drainage vent and fresh air intake

2.1 Practical complaints

The current configurations with a minimum horizontal distance of 3 m have been leading to an increasing number of practical complaints. Not in the least because the requirements written in NEN 3215, are not always common knowledge to professionals outside the building drainage sector. Therefore, the installation company (predominantly plumbers) need to take responsibility of guarding the minimum distance. However, in the building process, the plumber is generally not the decision maker as to how a roof is laid out, where the fresh air intakes are, and even not where the drainage vents penetrate the roof. This often leads to conflict and unclarity during the construction process, and possibly mistakes.

Roof spaces also tend to become more crowded, with the roof space being more frequently occupied. The construction methods are also becoming more diversified. Where roofs historically were often either gabled or flat, we see an increase in more creative and different roof and façade configurations.

It's for these reasons that an increasing number of questions is coming from the industry about the why and how of the 3 m horizontal and 1 m vertical distance determination. These questions have been evaluated by the Standards committee with the conclusion that they were not able to give a satisfactory answer. Because of this conclusion, the committee has initiated the development for a more robust, adaptable and practically applicable method of determining the distances.

3. New methodology

The Dutch building drainage Standards committee has conducted desk research and consulted with various industry experts on the matter. Their conclusion was that in many countries and jurisdictions, a similar situation as in the Netherlands is present. Various Standards [2, 3] have minimum distances specified, seemingly based on empirical data without well documented scientific research, with distances varying from 2 to 6 m, whereas other have not specified any minimum distance requirements. [4]

The primary concern in developing a new methodology has been the protection of public health and odour control. For this, the committee has looked at the Dutch

building laws, which uses a specification of dilution parameters for ventilation performance requirements [5]. This specifies the Dutch NEN 1087 Standard on ventilation requirements [6] where the committee has looked at the calculation methods used for flue gas termination to fresh air intake distances. This has been the foundation of the new methodology. This Standard includes calculation methods on flue to fresh air intake, with a larger variety in roof/façade configurations and a calculation method to determine horizontal and vertical measurements.

The assumption has been made that a sufficient dilution of toxic flue can be seen as a sufficient distance with a low risk, also from building drainage vents. To ensure there will not be a too drastic change to the results, the strictest values from flue dilution, based on the mean value of dilution when using solid fuel at a capacity of 15 kW, has been used. This has led to the following formula:

$$L \geq (800 - 325 \times \Delta h) / 163 \qquad \text{(F-1)}$$

In which:

L = minimal distance (m);

Δh = height difference between drainage vent and fresh air intake (m).

The set values 800, 325 and 163 in formula F-1 are dilution coefficient values from table 3 in NEN 1087 [6]. These are the highest possible values, indicating a worst case scenario, to create the greatest safety margin in the dilution calculation method.

Figure 3 shows the many roof and façade configurations taken from NEN 1087 [6] that will be adopted in NEN 3215 [1]. The table on the left side in Figure 3 shows results based on formula F-1 with various horizontal and vertical distances.

L ≥ (800 - 325 x Δh) / 163

Δh	L	
-1	6.9	theoretical
-0.55	6.0	option in
-0.2	5.3	situation 8
0.1	4.7	
0.2	4.5	
0.3	4.3	
0.4	4.1	
0.5	3.9	
0.6	3.7	
0.7	3.5	
0.8	3.3	
0.9	3.1	
1	**2.9**	
1.1	2.7	
1.2	2.5	
1.3	2.3	
1.4	2.1	
1.5	1.9	
1.6	1.7	
~~1.7~~	~~1.518405~~	
~~1.8~~	~~1.319018~~	
~~1.9~~	~~1.119632~~	
~~2~~	~~0.920245~~	
~~2.1~~	~~0.720859~~	
~~2.2~~	~~0.521472~~	
~~2.3~~	~~0.322086~~	
~~2.4~~	~~0.122699~~	
~~2.5~~	~~-0.076687~~	
~~2.6~~	~~-0.276074~~	

red = not possible

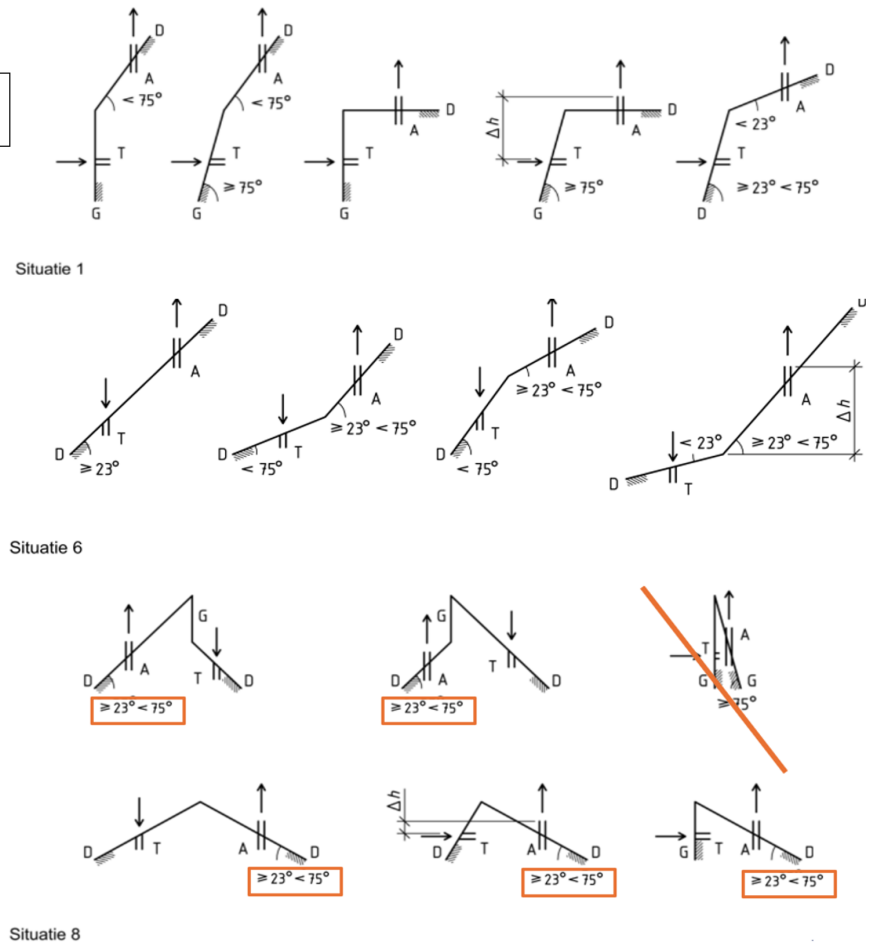

Situation 8.3 is a building vent oulet which is not allowed (façade outlet)

Figure 3 – Variety of configurations and calculation results with differentiation of vertical and horizontal distances, based on formula F-1

The current requirements are a horizontal distance of 3 m at a vertical distance of 1 m, this has been the basis for validating the calculation method. By using formula F-1 with 1 m as vertical control height, the result is 2.9 m horizontal difference which only varies 0.1 m from the current requirements, instilling confidence in the method.

There is a theoretical possibility of a negative height difference in the table in figure 3. This means that, given sufficient distance, the air intake could be located above the termination point of the drainage vent. Due to the configuration already covered in the 6 m horizontal distance rule, this will not be acceptable in this configuration.

The roof pitches in Figure 3 help distinguish between roof and façade. Between ≥ 23° <75° this is considered a gabled roof situation. When the pitch is >75° it is considered a façade, and a drainage vent is not allowed. A pitch <23° is considered a flat roof, and a minimum distance of 6 m applies.

The distance of 6 m in situations where both drainage vent and fresh air intake or accessible are in the same flat roof remains unchanged.

4. Conclusion

The problem of the static nature of the current requirements of 3 m horizontal and 1 m vertical distance in certain configurations has been addressed. Simultaneously, the apparent arbitrary distance requirement has been placed in an adaptable formula which can be used to assess more configurations to determine distance requirements.

On the basis that the distances following the newly proposed calculation method do not yield drastically different results in the control measure, we could conclude that the current presumed safe situation of drainage vent termination distances will not be compromised by a change in the Standard.

The main benefit for the industry will be in the flexibility and adaptability to a large variety of configurations. Where in the current method a minimum vertical distance of 1 m needs to be maintained at all times, lower height differences might be adopted. Or when larger height differences are present, shorter horizontal distances may be used.

Acknowledgements

I'd like to acknowledge the work of Hank Wes from Geberit (NL) for his major contribution to this topic.

5. References

[1] NEN 3215+C1:2014+A2:2022, Drainage system inside and outside buildings - Determination methods for drainage capacity, water and air tightness and distance for roof mounted outlets (2022)

[2] International Code Council (ICC). (2024). *International Plumbing Code (IPC)*. Country Club Hills, IL: International Code Council

[3] Standards Australia & Standards New Zealand. (2025). *AS/NZS 3500.2:2025, Plumbing and Drainage—Part 2: Sanitary Plumbing and Drainage*. Sydney, Australia: Standards Australia; Wellington, New Zealand: Standards New Zealand

[4] European Committee for Standardization. (2000). *EN 12056-2:2000: Gravity drainage systems inside buildings—Part 2: Sanitary pipework, layout and calculation*. Brussels: European Committee for Standardization (CEN)

[5] Besluit bouwwerken leefomgeving, art. 4.126 (luchtkwaliteit: plaats van de instroomopening en uitmonding), Stb. 2020, 400, zoals gewijzigd

[6] NEN 1087:2001, Ventilation in buildings – Determination methods for new estate, 2001

6. Presentation of Author

Nick Post is Head of Product Development at Hydraloop. He chairs the Building Drainage Standards committee (NL), is a member of the Water Supply Standard and active in European and international Standards development in the field of Water Supply and Building Drainage.

Measurement of Real Wastewater Flows in Building Drainage Systems

T. Waniganettige(1), M. Gormley (2), D. Kelly(3)

1. tw4009@hw.ac.uk

2. m.gormley@hw.ac.uk

3. d.a.kelly@hw.ac.uk

School of Energy, Geoscience, Infrastructure and Society, Heriot-Watt University, Edinburgh Campus, EH144AS, Scotland.

Abstract

Rapid population growth and climate change have influenced built environment systems, promoting the development of high-rise buildings as a solution to modern interrelated urban challenges. However, current design codes present methods for calculating wastewater flows based on experimental data and statistical analyses conducted several decades ago. There is a strong possibility that these fundamental studies are failing to represent the hydraulic conditions of contemporary building drainage systems (BDS). Sustainability drivers such as water-saving technologies and water scarcity concerns are reasons for potential changes in classical discharge characteristics compared with those of the mid-twentieth century and therefore require revisiting and further investigation.

This research begins to address the potential misalignment between code-generated wastewater flow rates and actual flow rates within a BDS. Wastewater flow in vertical stacks is fundamentally multiphase rather than single-phase and exhibits different flow regimes throughout, including bubbly, slug, churn, stratified and annular flow. A non-intrusive sensor system was built to measure water flow in vertical pipes using LabVIEW data acquisition and processing. The initial phase of the study related to calibration and preliminary validations is presented in this paper. The calibration curve for the sensor system were developed for different pipe materials PVC and HDPE and the corelations were strongly agreeing with 99% of R^2 value for each. The results demonstrate a strong correlation between steady-state supplied water flow rates and the measured flow rates within the vertical stack, with an R^2 of 98%. The proposed method has the potential to validate and verify discharge curves and flow characteristics in vertical BDS stacks.

Keywords

BDS Designs, Overdesign, Non-intrusive measuring system, Sensor Output, Calibration, Validation

1 Introduction

Building Drainage Systems (BDS) play a vital role in securing public health and sanitation by effectively directing wastewater away from occupied spaces. The impacts of emerging Greek civilisation led to the provision of reliable sanitation as a prerequisite of a developed society (Swaffield, 2010). This is the beginning of the development of BDS designed to transport fluids, faecal waste and other waste from appliances to sewer connections with zero possibility of cross-contamination, leakage or interruption to system availability. For thousands of years, the basic requirement of a BDS is as important as provisions of safe drinking water. However, at the beginning, the developments happened with some drawbacks. The Victorian development in the UK diverted attention to the prevention of odour ingress to habitable space, getting rid of unwanted water as soon as possible, hiding it in underground pipes and the innovation of a one-pipe system to combine sewer systems while neglecting the focus on impacts of heavy rainstorms (Sharif and Gormley, 2021).

Over time, codes and guidelines were introduced for the design of the BDS systems. The basis for these guides was experimental studies and theoretical development carried out between the 1920s and 1970s. There are various methods for calculation, but many have their origins in Hunter's fixture units, which follow a probabilistic approach to determine the simultaneous fixture discharge and to estimate peak water demand (Mangalekar and Gumaste, 2021). The fixture unit was decided for a given flow load which might be produced by different numbers of appliances depending on their characteristics (Wise and Swaffield, 2002). Although these studies were originally developed to estimate water demand in plumbing systems, the same fixture-use concept was used for BDS designs. The probability of a certain number of fixtures is taken into consideration in this process, and pipe sizing is conventionally based on a representation of simultaneous demand. The design flow, Probable Maximum Simultaneous Demand (PMSD) is calculated by using fixture-use probability as the basic entity. The probability distribution in use is binomial (Hunter, 1940). Other systems such as the square root method (German method) used in EN12056:2 200, approximate probability to an arbitrary square root function of the contribution of the discharge to peak flow in the system. Therefore, modern BDS designs still rely heavily on simplified probabilistic assumptions rather than actual wastewater flow behaviours.

Present designs based on guides established decades ago raise considerable uncertainty regarding their reliability, particularly given changes in contemporary buildings associated with population growth, water scarcity and climate change. Consequently, robust and proven engineering validations to build confidence in the building service dynamics will be beneficial. Conventional design approaches often limit potential to enhance performance, water consumption and pipework infrastructure cost. This is unsurprising given the basic premise underlying the analysis of steady-state flows in most globally adopted codes and guidelines (Jack and Swaffield, 2009). Hunter's curve was established based on older high-flow fixtures used in the 1940s with a very high confidence level around 99% (Mazumdar, Jaman and Das, 2014). This certainly does not align with modern low-water-consumption fixture characteristics, although it is

recognised that modifications have been made over the years; however, these have not kept pace with innovations in sanitaryware. Hence, even though Hunter's study provides a main entrance to the BDS designs, taking it as the main core of modern BDS design makes the outcome more susceptible to considerable misalignments.

The definition of the connection between tall buildings and drainage design is often misleading in current guides, codes and standards, and they end up leading the engineers to make certain assumptions which lead to inconsistency in design and lack of clarity in the industry when interpreting the requirements of guidelines (Gormley and Daureeawo, 2025). While local and international codes provide essential guidance for the design of drainage vent systems, there are limitations in applying current code practices for tall buildings to study how performance is influenced by observed variability and integrating these systems into the public network (Sharif and Gormley, 2021). According to Gormley and Stewart, 2023 there are a few main limitations associated with supertall buildings' BDS designs using seminal studies and contemporary design codes that become apparent. The experimental test systems were limited in height, often no more than eight floors; instrumentation was also limited at the time for measuring multiple flows. Practices like this reduce the confidence of design estimates used in any design guide. The height of the building introduces additional pressure losses due to friction, significant negative and positive air-pressure transients and higher air velocities and flow rates within drainage pipes, which emphasises the need for a separate design approach for tall buildings (Gormely and Daureeawo, 2025). There is a possibility of incorrect predictions of drainage flow values in current codes, which subsequently influence the decision of pipe sizing.

Water conservation is another widely held priority, as population growth and climate change threaten the balance of the environment. In the context of water conservation, a main concern in the current water-stressed world is that designers have moved to prioritise low-water-use fixtures (Mazumdar, Jaman and Das, 2014). Most modern buildings use water-efficient appliances, which do not give coded drainage flow rates, certainly even according to manufacturer details. The conventional coded view of water and air transport inside drainage systems is steady state (Sharif and Gormley, 2021) . However, in real-world scenarios with the effects of pressure transients, flow regimes and intermittent and random discharges, the combined water-air flow is not steady state. It points out that codes use simplified approximations in their design approaches, which is different from the actual case. Together, these reasons lead to over-designed drainage systems. When the industry has advocated sustainable use of water, ignoring the potential for the overdesign of sanitary plumbing systems is possible, and without good reason. (Mazumdar, Jaman and Das, 2014) . The same authors have modified traditional fixture-unit design values considering updated modern fixture characteristics. However, their focus was on modified predicted values rather than measuring actual wastewater flow, which creates a need for an experimental method to capture the real flow as a basis for present proof of flow behaviour. Salehi et al., 2017 have pointed out that non-intrusive measuring systems for two-phase flows are important, as traditional methods require phase separation, which is complex and have carried out experimental and numerical modelling for flow

measurements in oil-gas fluid. However, non-intrusive applications applied to BDS wastewater are very limited.

Accurate estimates and corrections of the existing flow rates associated with discharge units remain elusive. This study of a non-intrusive measurement system for monitoring wastewater flow rates within BDS represents a real step change in the understanding of discharge dynamics. The scope of the present study is narrowed to the laboratory-scale calibration and validation processes for the drainage flowmeter. Please note that since the device itself is subject to Intellectual Property (IP) confidentiality, it is not possible to give details of the mechanisms used for sensing flow rate at this stage, rather, the output of the device has been assessed and presented in this paper.

2 Methodology

Flow rates inside drainage pipes were measured using a laboratory-scale building drainage setup as shown in the schematic diagram in Figure 1. It represents the experimental setup used for controlled flow testing and data collection. Water was supplied from the supply tank to simulate drainage flow conditions, while the flow rate was controlled by the pump. The reference supply flow rate was measured using a factory-calibrated supply flow meter installed at the inlet of the drainage setup before it enters the drainage system. As indicated in the figure, the drainage flow meter is positioned closer to the outlet to record the sensor response associated with flow conditions within the pipe. The sensor output was transferred to the Data Acquisition System (DAQ) and recorded through LabVIEW, the graphical programming platform. Data were examined to build the relationship between the reference flow rate and sensor output.

The externally mounted non-intrusive sensing system is designed to detect flow behaviour within the vertical drains without obstructing the path of the flow. It has the sensitivity to capture the variations that happen in the simulated multiphase flow inside the stack. Non-intrusive flow-measuring systems can establish a relationship between sensor output and flow rate, which is influenced by several parameters related to the pipe system (Evans, Blotter and Stephens, 2004). The resulting sensor response demonstrates a combination of changes in flow regime and flow rate. Data analysis established the relationship between the sensor response and the reference flow rate.

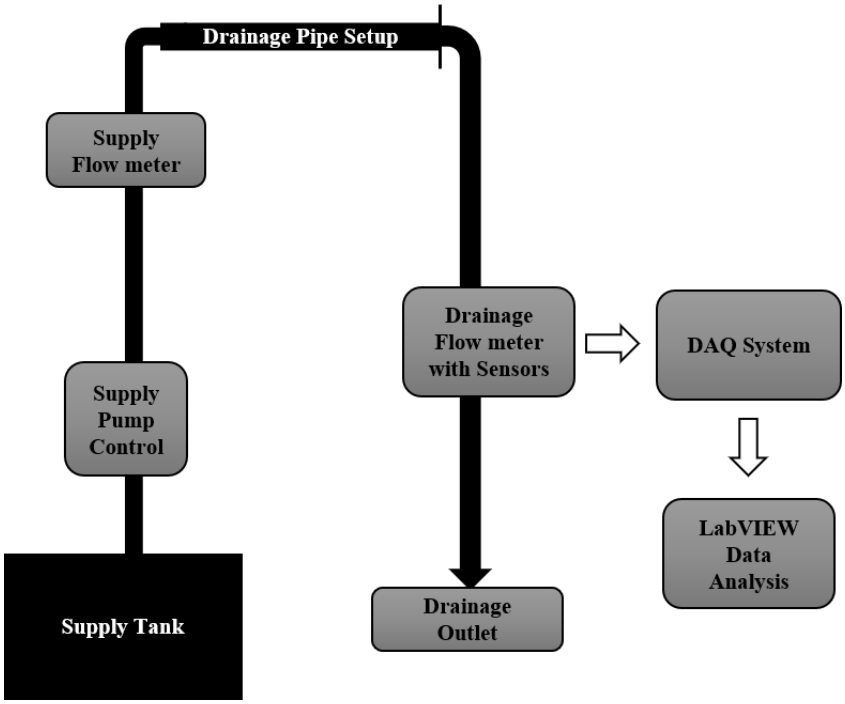

Figure 1: Schematic representation of the laboratory-scale experimental setup

Figure 2 illustrates the experimental and analytical procedure adopted in a summarised workflow. The work began with an initial assessment of the measuring instrument; a preliminary response examination was conducted on the sensor. Repeated flow-no flow cycles were passed through it continuously under controlled conditions. Each interval was approximately 30s to capture a more stable output. Between cycles, the system was allowed to return to zero flow, which was the baseline condition. This test was conducted to assess the sensor's response pattern and recovery behaviour, and the results were shown in Figure 3.

Different pipe materials were used for initial calibrations as the sensor output was expected to differ according to the pipe material on which the flowmeter was installed. Two different outputs for Polyvinyl Chloride (PVC) and High-Density Polyethylene (HDPE) pipes were observed. Following that, each flow scenario was carried out for each pipe type. Each flow was operated for 2 minutes, and the average sensor response was recorded to improve the data precision. Known flow rates were passed through the drains, and the measuring instrument's response was recorded for initial calibration purposes. The plots generated sensor output against flow rate as the basis of the calibration.

Following the calibration process, a preliminary validation was completed for the HDPE material. A series of known flow rates from 0 to 3.5 l/s was passed through the drainage setup, and the corresponding readings were recorded from the instrument. The flow rates

within the drainage system were estimated from recorded data and compared against the reference flow rates. The calibration results were incorporated to interpret subsequent flow measurements. A laboratory surge-event test was conducted to assess the response of the flowmeter to the unsteady flows expected within the pipe. Recorded instrument outputs were converted using developed equations, and the flow profile during flushes was plotted against time. The flow profiles were analysed by comparing peak flow responses, discharge volume and decay behaviour against the known supply flow profile. The generated graphs were subsequently analysed.

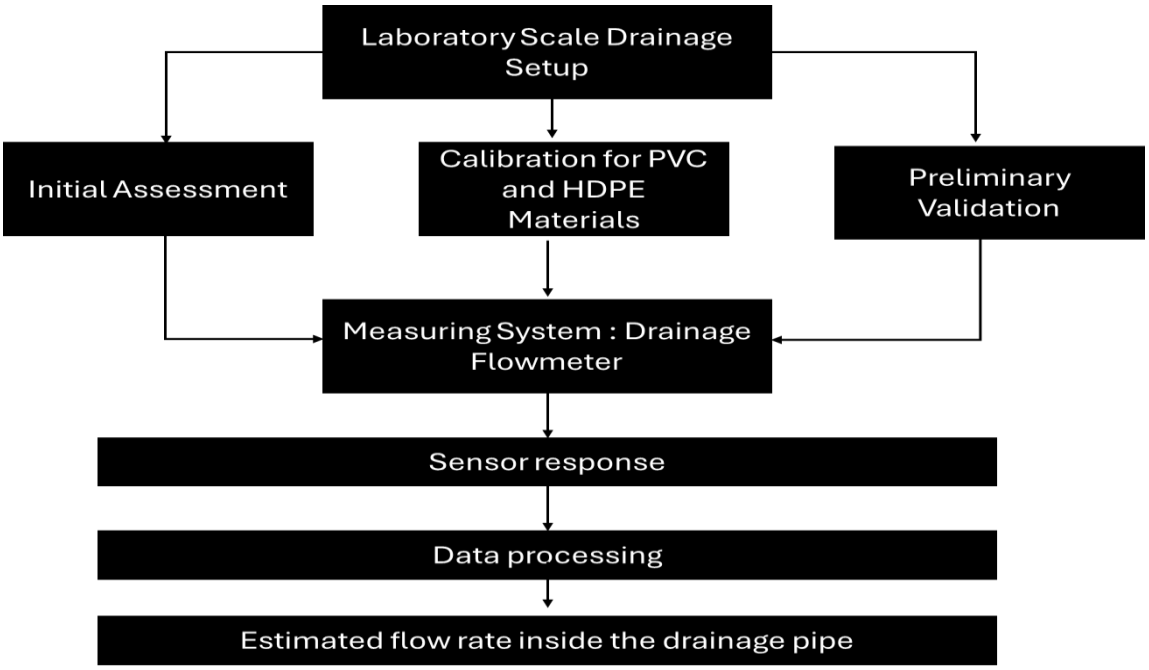

Figure 2: Experimental workflow for laboratory calibration and preliminary validation of the drainage flowmeter

3 Results

At the very beginning of the experimental trials, the measuring instrument was assessed for the response pattern under controlled flow conditions. Figure 2 expresses the sensor response under a sequence of no-flow and constant flow conditions in a PVC drainage system. As the test started with no flow inside the drainage system, the sensor output represents the zero-flow state. It indicates a stable reference to the baseline of the measuring instrument. Immediately after a flow was introduced to the system, the sensor reading decreased rapidly to a lower value and remained at that level for the duration of the flow. This step change in the response after a flow event demonstrates that the flowmeter can capture the flow transition within the pipes. The zero-flow condition was characterised by a relatively stable baseline response, whereas the sensor output during flow shows certain fluctuations. Any system that transports fluids will be subjected to local pressure increments caused by transient pressure surges resulting from inevitable

changes in the flow profile inside (Gormley and Kelly, 2019). A degree of noise in measurement is inevitable.

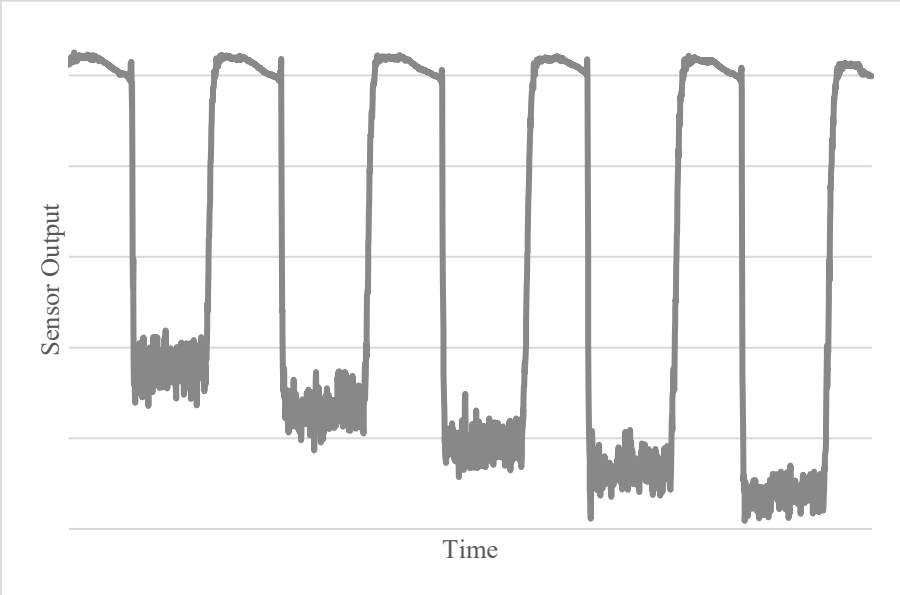

Figure 3 : Flowmeter response to controlled flow intervals

As shown in Figure 3, repeated one-minute flow-no-flow cycles were conducted to observe the sensor's response and recovery behaviour. The flow was stopped after each event to make it return towards its baseline state, as it allowed the flowmeter to show the performance for intermittent discharge events rather than continuous steady flow – in effect, this simulates a pseudo-unsteady flow within the system. The graph clearly shows a decrease in the sensor response as flow increases. The consistent inverse relationship between flow and the ability to recover after measurements is an important characteristic of the drainage flowmeter as observed during the initial stage. Meanwhile, this is quantitative evidence that the instrument can respond to classified flow scenarios.

As described in the methodology section, the flowmeter was initially set for two types of drainage pipes, which are HDPE (High-Density Polyethylene) and PVC (Polyvinyl Chloride) for calibration purposes. The following graphs refer to the calibration results for each pipe type. Figure 4 interprets the calibration curve for the PVC drainage system. The sensor response decreased systematically as flow increased. The consistency of this trend within the tested range verifies that the flowmeter was successfully able to detect the flow behaviour inside the pipe. Primarily, the calibration curve was evaluated using different trend lines, and the strongest agreement was observed with an R^2 value of 0.99. The curve in Figure 4 was selected as the empirical relationship between flow rate and sensor output for the PVC pipe. R^2 quantifies the proportion of variance described by a statistical model and is an important summary statistic tool (Nakagawa, Johnson and Schielzeth, 2017).

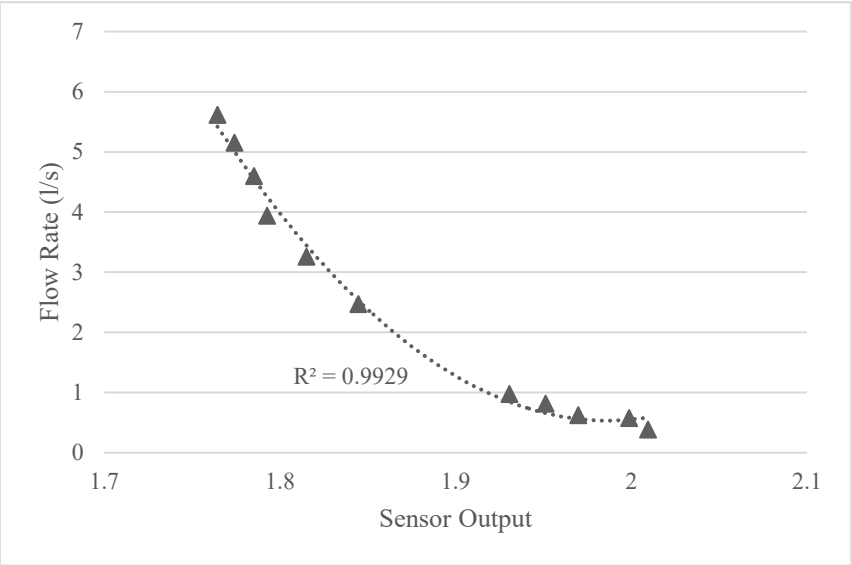

Figure 4: Calibration relationship of drainage flowmeter for the PVC pipe

Following the same procedure as in the PVC drainage system, the relationship indicated in Figure 4 was denoted as the calibration correlation between flow rate inside drains and sensor output for HDPE pipes. The pattern continued, and the results showed a decrease in sensor readings as flow increased. However, the sensor measurement fell within a different range than the PVC calibration, illustrating that the sensor output is impacted by the pipe material. A strong agreement was again obtained, with an R^2 value of 0.99 for HDPE material as well, as illustrated in Figure 5.

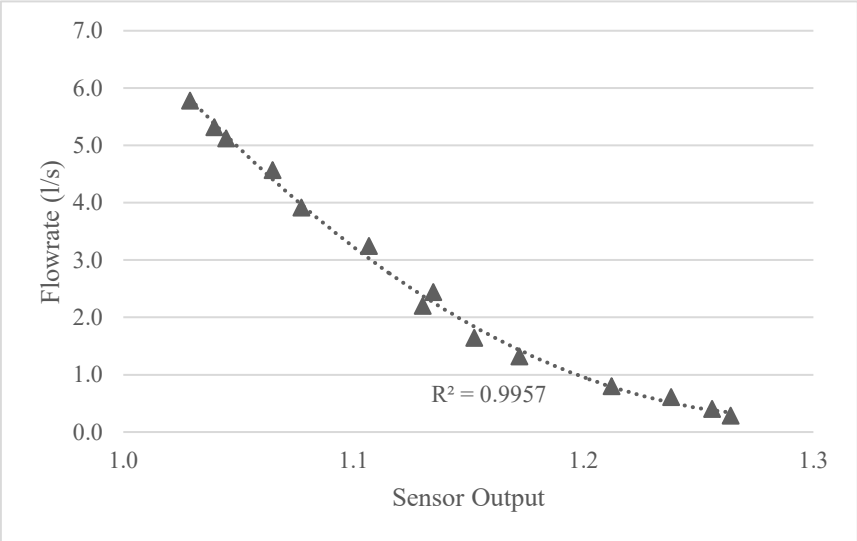

Figure 5: Calibration relationship of drainage flowmeter for the HDPE pipe

Comparison of the above calibration curves shows noticeable differences in sensor response ranges across different materials within the same flow range. PVC (1.75-2.0) generated higher range values while HDPE (1.0-1.3) gave comparably low values. However, the sensor output for the same flow rates inside the pipe differed depending on the pipe material. This confirms that pipe material influences the output of the flowmeter. Therefore, a single calibration relationship may not be suitable for any type of drainage system, with pipe material forming part of the input for any practical application Kim *et al*., 2008 also stated that similar studies which include an external sensor measurement system need careful calibration, as the output can be heavily dependent on pipe materials.

The calibration results for both pipe materials demonstrate that the flowmeter's measured response is consistent and inversely proportional to the flow. This confirms that the drainage flowmeter can capture changes in the flow profile inside the pipes, representing initial success of the study. The consistency of the sensor response with respect to flow is vital, as it provides the relationship to convert the sensor reading to an estimated flow for subsequent measurements. The relationship between the sensor output and flow rate being non-linear suggests that a simple linear model will not fully represent the response of the drainage flowmeter over the tested range.

An additional validation test was carried out for the HDPE drainage system using known supplied flow rates to evaluate whether the flowmeter could respond to the changes based on the selected calibration correlation. Figure 5 represents the results from validation of HDPE drainage pipe as estimated flowrate against the known flowrate. It shows a strong positive alignment between the actual and estimated flows. In an ideal case, the trend line should follow y = x, and according to the figure, the indicated line closely follows it, while the linear comparison shows an R^2 value of 0.98, indicating good agreement. This suggests that the calibrated instrument can reproduce changes in flow with good accuracy.

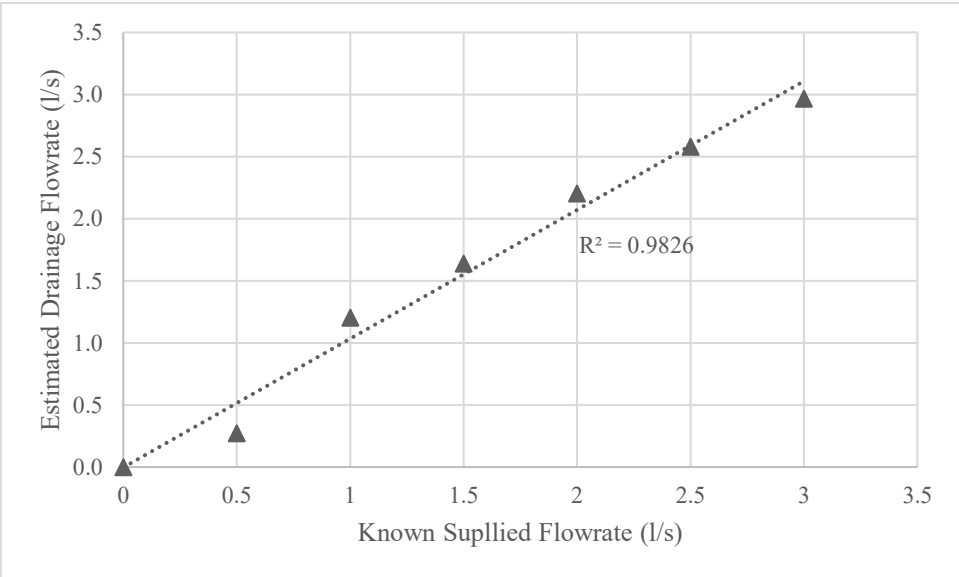

Figure 6: Comparison of known flowrates and estimated flowrates

4 Conclusion

This paper presented the initial calibration and preliminary validation of a measurement system for capturing flow-rate profiles in vertical BDS stacks. A laboratory-scale drainage system setup was used to establish a correlation between sensor output and drainage flow rates. As there are several pipe materials in use in modern BDS, initially the calibration relationships were assessed for PVC and HDPE materials within the flow rate range of 0-6 l/s. The dependency of sensor output on flow rate showed a consistent inverse pattern. However, the instrument's measurement range varied by material, indicating the need for material-specific calibration, as would be expected for such a measurement system. The functional relationship was selected based on the strongest agreement of trendlines. For both PVC and HDPE materials, the calibration curves showed strong agreement, with an R2 of 99%. A validation was performed for HDPE material on a laboratory scale by deriving the estimated flow rate against a reference flow, and the results showed considerable accuracy. The work continues with real-world setting measurements, and a full set of real water flows in BDS will be available soon.

5 Acknowledgements

The authors would like to acknowledge the technical support provided by the laboratory technical staff during the development of the experimental setup and early data collection stage.

6 References

Evans, R.P., Blotter, J.D. and Stephens, A.G. (2004) “Flow rate measurements using flow-induced pipe vibration,” *Journal of Fluids Engineering, Transactions of the ASME*, pp. 280–285. Available at: https://doi.org/10.1115/1.1667882.

Gormley, M. *et al.* (2021) “Building drainage system design for tall buildings: Current limitations and public health implications,” *Buildings*, 11(2), pp. 1–17. Available at: https://doi.org/10.3390/buildings11020070.

Gormley, M. and Daureeawo, J. (2025) *Tall Building Drainage Design TM70 2025,* 1st Edition, London, The Chartered Institution of Building Services Engineers.

Gormley, M. and Kelly, D.A. (2019) “Pressure transient suppression in drainage systems of tall buildings,” *Building Research and Information*, 47(4), pp. 421–436. Available at: https://doi.org/10.1080/09613218.2017.1412097.

Gormley, M. and Stewart, C. (2023) “Design Methodologies for Sizing of Drainage Stacks and Vent Lines in High-Rise Buildings.” Available at: https://doi.org/10.3390/buildings13061458.

Jack, L.B. and Swaffield, J.A. (2009) “Embedding sustainability in the design of water supply and drainage systems for buildings,” *Renewable Energy*, 34(9), pp. 2061–2066. Available at: https://doi.org/10.1016/j.renene.2009.02.009.

Mangalekar, R.D. and Gumaste, K.S. (2021) "Residential water demand modelling and hydraulic reliability in design of building water supply systems: A review," *Water Science and Technology: Water Supply*. IWA Publishing, pp. 1385–1397. Available at: https://doi.org/10.2166/WS.2021.021.

Mazumdar, A., Jaman, H. and Das, S. (2014) "Modification of Hunter's Curve in the Perspective of Water Conservation," *Journal of Pipeline Systems Engineering and Practice*, 5(1). Available at: https://doi.org/10.1061/(asce)ps.1949-1204.0000150.

Nakagawa, S., Johnson, P.C.D. and Schielzeth, H. (2017) "The coefficient of determination R2 and intra-class correlation coefficient from generalized linear mixed-effects models revisited and expanded," *Journal of the Royal Society Interface*, 14(134). Available at: https://doi.org/10.1098/rsif.2017.0213.

Salehi, S.M. *et al.* (2017) "Different configurations of capacitance sensor for gas/oil two phase flow measurement: An experimental and numerical study," *Experimental Thermal and Fluid Science*, 82, pp. 349–358. Available at: https://doi.org/10.1016/j.expthermflusci.2016.11.027.

Sharif, K. and Gormley, M. (2021) "Integrating the design of tall building, wastewater drainage systems into the public sewer network: A review of the current state of the art," *Water (Switzerland)*. MDPI. Available at: https://doi.org/10.3390/w13223242.

Swaffield, J. (2010) *Transient Airflow in Building Drainage Systems*, Oxon, Spon Press.

Wise, A.F.E. and Swaffield, J.A. (2002) *Water, Sanitary and Waste Services for Buildings*, 5th Edition, Butterworth, Heinemann, Elsevier Science.

7 Presentation of Authors

Thilini Waniganettige is a PhD student in Public Health and Environmental Engineering at the School of Energy, Geoscience, Infrastructure and Society, Heriot-Watt University. Her research interests are Wastewater flow measurements in building drainage systems and evaluating the performance of drainage systems in modern high-rise buildings.

Michael Gormley is Professor of Public Health and Environmental Engineering at the School of Energy, Geoscience, Infrastructure and Society at Heriot-Watt University. His research specialisms are: mathematical modelling of air and water flows in building drainage systems, infection spread via bioaerosols and product development.

Dr David Kelly is Associate Professor of Architectural Engineering and a member of the Public Health and Environmental Engineering group at Heriot-Watt University. His research interests include the monitoring and prevention of cross-contamination from building drainage systems.

An examination of the influence of 19th century disease theory on the design of sanitary drainage systems – Sewer intercepting traps

John Lansing

john.lansing@centerforbuilding.org

Center for Building in North America

Abstract

The Industrial Revolution produced unprecedented density in urban areas such as London, New York City, Berlin and Paris in the 19th century, creating widespread sanitation issues leading to the spread of disease. Water-based sanitation in buildings connecting to sewers became the dominant solution and the design and installation practices of sanitary drainage systems reflected predominant epidemiological theory of the time. Unsubstantiated empirical methods influenced by medical theory that was later abandoned were incorporated into building codes and regulations with prescriptive requirements for the design and installation of sanitary drainage systems. The sewer intercepting trap, designed to prevent sewer gases from entering sanitary drainage piping within buildings, is one example and will be examined by reviewing the historical context leading to its widespread requirement and prohibition.

Keywords

Sewer intercepting trap, building trap, sanitary drainage, 19th century, sanitation, miasma theory of disease

1 Introduction

Throughout the 19th century, design and installation practice related to sanitary drainage and building regulations were heavily influenced by the predominant miasma theory of disease. Exposure to 'bad air', air with foul odors, stagnant air, or air associated with feces and decomposing organic matter, was believed to be the primary cause of infectious disease. Diseases such as cholera, typhoid, diphtheria, classified as Zymotic diseases, were understood to spread through an organism known as a zyme, the Greek word for 'ferment'. While airborne disease spread caused by bacteria or viruses is known today as a transmission pathway, or in some cases aerosols from drains, the deadly diseases of the 19th century in rapidly urbanizing cities were being spread through other vectors such as physical contamination of food and water or through human-to-human transmission rather than sewer gases [1-4].

Miasma theory was promoted in leading medical journals until the end of the 1880s when scientific developments led to a broader acceptance of germ theory of disease. Miasma theory was influential

in early sanitation and plumbing practice, particularly relating to the installation of sanitary drainage piping. Ventilation was a foundational element of sanitary reform coupled with the promotion of cleanliness and safe disposal of human excreta [5-7].

The transition to germ theory of disease represented an epistemological break in the field of public health and sanitation and did not lead to an abrupt shift in building codes or the field of plumbing engineering. By the end of the 1870s, sanitary engineers had already published extensive literature outlining theories and solutions to preventing disease spread from sewer gas in buildings, and many disproven theories and practices were not readily dismissed [8-10].

2 Sewers and disease spread

Early plumbing fixtures in the late 18th and early 19th centuries discharged to cesspits either under or adjacent to the buildings they served. These cesspits leached water into the surrounding soil and required regular removal of solids and were a significant public health risk, regularly leading to outbreaks of cholera and typhoid fever. Before the 19th century, sewers in London were designed primarily for carrying storm drainage. It was illegal to connect sanitary drains from buildings to sewers in London until 1815 when the prohibition was relaxed. In 1844, buildings were required to connect sanitary drainage systems to the city sewer in London where the sewer was located within 15 m (50 ft) [5], [11-12].

Chief surveyor of London, John Phillips, advocated for traps at every fixture in buildings to prevent foul air from flowing out of the drainage piping. In an 1844 edition of the British construction journal *The Builder* [13], Phillips stated

> *Besides the insalubrity of the atmosphere, produced from the evaporation of the stagnant accumulation on the surface of badly drained localities, as well as the saturated ground from cesspools and drains, the malaria emitted from the decomposed animal matter retained within the cesspools, is of a poisonous and highly noxious character, very frequently producing typhus and other infectious fevers.*

While the traps at plumbing fixtures did provide a water seal preventing the passage of air from the sewer, this was not enough to satisfy the prevailing concerns of disease spread sewers. Sewer connections represented an interconnected network between buildings throughout the city, containing foul odors that were widely believed to be the cause of disease. As buildings began connecting directly to the sewer, the sanitary drains became a pathway for airflow, largely due to temperature differences between the sewer and outside air as well as drainage flow in the sewers [14]. Even if traps were present at fixtures, gaps or holes in the drainage piping often allowed air to pass through into indoor spaces. Chimney fires additionally created conditions where the draft brought indoor air pressure below that of atmospheric pressure, which further raised issues with air being drawn out of the drainage piping [15]. This air leakage was characteristic of the materials and methods used at the time for sanitary drains, which were often made with lead piping or lead

sealant between cast-iron piping segments that were vulnerable to defects and improper installation.

Edward VII, the Prince of Wales, became ill with typhoid fever in 1871 and The Lancet sent a team of investigators to Scarborough Lodge where the prince had been staying and the investigation concluded the cause was sewer gases. The report on the investigation blamed faulty plumbing, specifically noting the lack of a stack vent among other flaws, stating that "the faint and deadly influence might have pervaded the whole house, or burst out of the [water] closet". While the prince did recover the following year, his illness was described as a "national anxiety" by *The Times* and ushered in renewed panic [5] [16].

Osbourn Reynolds, primarily known for his foundational contributions to the field of fluid mechanics, suggested in 1872 that sanitary drains should have no direct connection to the sewer. The solution that Reynolds and others advocated for was the sewer intercepting trap, which consisted of a trap located on the drain connection to the sewer [17].

Egbert Viele, a civil engineer based in New York, insisted vent piping was necessary to relieve any sewer gas that managed to pass through the sewer intercepting trap, calling on the Department of Buildings to enforce this solution as a new requirement. In a New York Times article reporting on his recommendations at the annual American Public Health Association meeting in Baltimore from Dec. 20, 1875, the following conclusions were made [18]:

> *Indeed, the duty of protecting the public from sewer gas is even more imperative right now than that of preventing the building of houses without fire escapes; since, where one person perishes from fire, it is no exaggeration to say that a hundred are killed by sewer gas…It is now well understood that a very large proportion of the deaths from diphtheria, typhoid fever, and cerebro-spinal meningitis which occur annually in this and other cities, are due entirely to the poisonous effects of sewer-gas.*

3 Sewer intercepting traps

The sewer intercepting trap, also known as the house trap, building trap, or disconnecting trap (Figure 1), consists of a trap installed on the main horizontal drain connecting the building to the sewer. The trap may be located within an access chamber, buried underground, or located within the building it serves. An early variation of the sewer intercepting trap can be found in *The Builder* in 1844, which was used as an additional protection measure against air from sewers [19]. The sewer intercepting trap aimed to block air in the sewer from entering the drainage piping within the building, whereas the traps at the fixtures were a secondary barrier to protect against the air within the drains of the building. The Somerset trap, introduced in 1858 by Glasgow architect John Honeyman, featured a vented opening on each side of the trap to the air, later known as a fresh air inlet. Later variations such as one patented in 1875 by William Buchan in Glasgow, featured only one vent installed upstream of the trap [10]. The vent was intended to allow air to enter the sanitary

drain from the street level and circulate throughout the drainage piping installed in the building. Stevens Hellyer, a prominent sanitary engineer in London, promoted the use of vent piping at the lower and upper end of the drainage system to induce a current of air within the drain to 'render it wholesome' in his 1877 book [8].

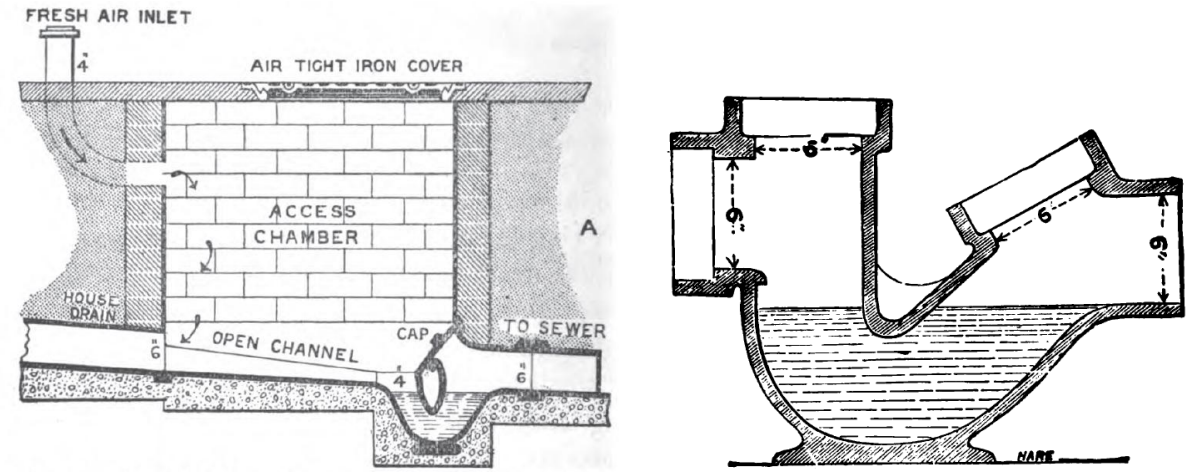

Figure 1 - Sewer intercepting trap within an access chamber and fresh air inlet (left) and intercepting trap without an access chamber (right) [20]

The sewer intercepting trap with a vent was incorporated into the 1877 Model Bylaws, a collection of public health ordinances developed by the Local Government Board[1] to be adopted and modified as deemed necessary by localities in England and Wales [21] [3]. The sewer intercepting trap became a requirement in local regulations such as Berlin in 1874 [22], New York City in 1881 [23], Boston in 1883 [24], and many other cities. Storm leaders from roof gutters often connected downstream of the intercepting trap, acting as a point of ventilation for the sewers [10].

[1] A British Government supervisory body

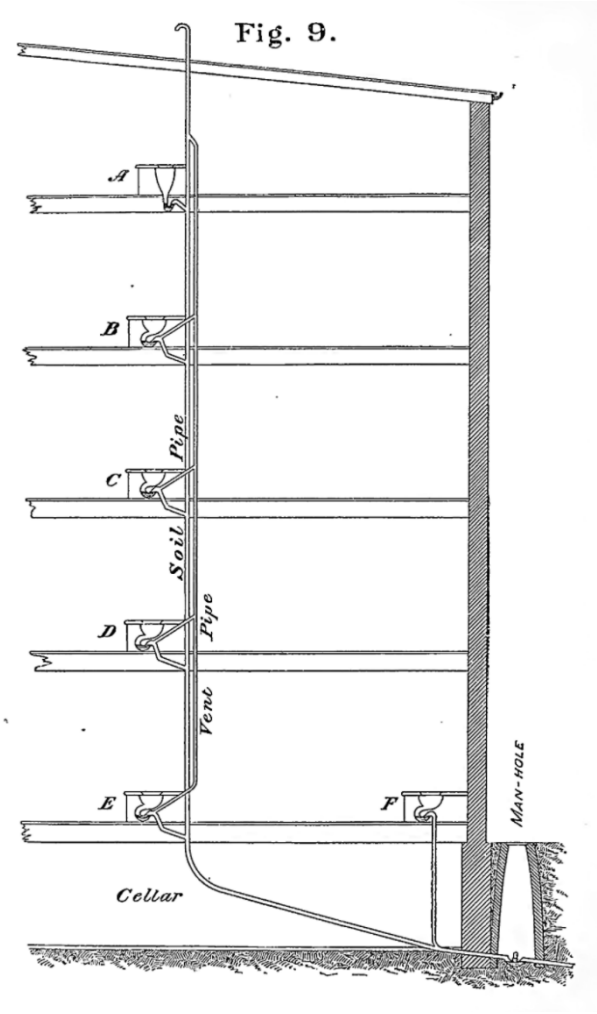

Figure 2 - Image from Philbrick's Massachusetts Board of Health report, with an unvented sewer intercepting trap [25]

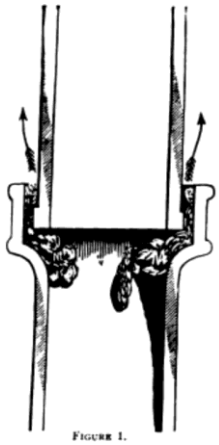

Figure 3 – Arrows depicting air escaping though joints [26]

Early variations of the sewer interceptor trap, particularly those in the US, were often unvented, which sealed off airflow at the lower end of the sanitary drain (Figure 2). With the vent through the roof being the only atmospheric opening for pressure equalization within the piping, pressure waves reflecting off the water seal of the sewer intercepting trap creates back-pressure conditions at the traps of fixtures on the lowest floor [10]. Osbourn Reynolds recommended installing the sewer interceptor trap and omitting traps at individual fixtures except water closets in an 1872 pamphlet, suggesting that enclosing a segment of air in the piping between the two traps would render 'otherwise harmless air will turn into poisonous gas', unless a vent was provided [17]

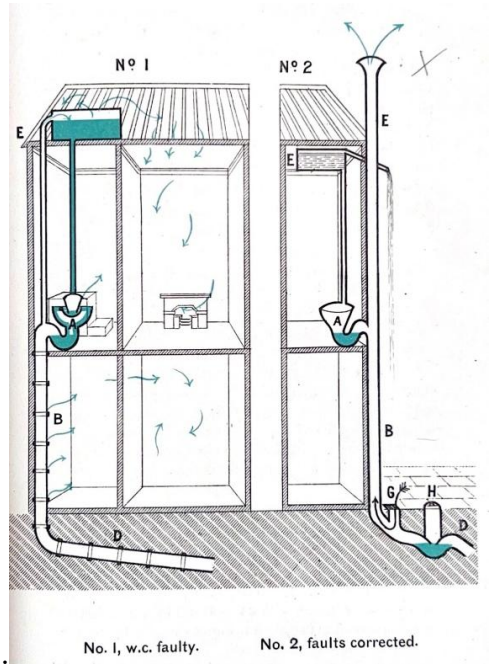

Figure 4 – (left) Sewer gases shown escaping from joints up soil piping installed inside, (right) sewer intercepting trap is preventing sewer gases from entering soil piping, which is installed on the exterior and vented [9]

4 Reform of requirements

The work at the Hygienic Institute of Munich was significantly influential reexamining the role of sewer gases in in the spread of disease. At the institute, the work of Max von Pettenkoffer, Isidor Soyka, and Friedrich Renk published between 1880 and 1882 provided evidence using epidemiological data from outbreaks showing sewer gas was not responsible for disease spread. Their investigations found that the air within the sewers contained less bacteria than that above ground. Their conclusions were controversial at the time and at odds with many influential figures in the sanitary reform movement in the UK and the US [27-28]. German engineer William Lindley advocated against the sewer intercepting trap since it prevents ventilation of the sewers. His influence led to many cities abandoning the use of sewer intercepting traps by the end of the 19th century, including Berlin, Frankfurt, Munich, Cologne, Vienna, Warsaw and others [28].

A later report [3] issued by the Local Government Board to reexamine the necessity for requiring sewer intercepting traps stated

> *The reason for [requiring sewer intercepting traps] arose from the belief, then almost universal among sanitarians, that sewer air was one of the most, if not the most direct and commonplace way of all, by which certain infectious diseases were disseminated.*

Similar justifications were given for requiring the sewer intercepting trap by the New York Board of Health as well, which was included in the 1881 ordinances, though some objected since this would restrict airflow from the sewers and accumulate debris [29]. A similar requirement for sewer intercepting traps was put in place in Boston [24]. The report issued by the Local Government Board also provided evidence suggesting that sewer intercepting traps do not prevent rodents from passing from the sewer to the building. It also noted the water seal of the trap, typically 25 mm (1 inch) to 75 mm (3 inches) could be displaced under scenarios where the sewer was subjected to high positive pressures under a surcharge event. Another examination by the National Bureau of Standards subcommittee on plumbing came to a similar conclusion on the sewer intercepting trap introducing performance issues both in terms of transient pressures from drainage flow and blockage risk [30]. The subcommittee also noted that sewer intercepting traps failed to prevent the passage of rodents but acted as a secondary barrier to insects. While a majority of subcommittee members were opposed to the usage of the sewer intercepting trap, some suggested advantages in the event of an individual trap failure.

Many plumbing codes and standards today prohibit the installation of building traps while others do not require them [30-34]. Some cities however still require sewer intercepting traps, including New York City [36], Philadelphia [37], and the City of London [38].

4 Conclusion

The development of early sanitary drainage methods and the regulations that followed were heavily influenced by miasma theory of disease, yet some practices incorporated into regulations were in many cases slow to be revised to reflect germ theory. Even as some cities removed requirements for sewer intercepting traps in the 1890s, other cities have maintained the requirement despite evidence invalidating the original justification for the requirement. As legacy requirements are carried forward into new codes and standards, reassessing the intent of original measures within the context of current objectives is necessary.

6 References

[1] "Zymotic Diseases," *Encyclopædia Britannica*, vol. 28. 1911.
[2] T. Crook and M. Esbester, *Governing Risks in Modern Britain - Sanger, Safety and Accidents, c 1800-2000*. Palgrave Macmillan, 2016.
[3] "Intercepting Traps in House Drains," His Majesty's Stationery Office, London, 1912.
[4] John Swaffield, *Transient Airflow in Building Drainage Systems*.
[5] Michelle Allen, "Cesspool to Sewer: Sanitary Reform and the Rhetoric of Resistance, 1848-1880," *Victorian Literature and Culture*, vol. 30, no. No 2, pp. 383–402, 2002.
[6] M. Stone, "The Plumbing Paradox: American Attitudes Toward Late Nineteenth-Century Domestic Sanitary Arrangements," *Winterthur Portfolio*, vol. 14, no. 3, pp. 283–309, Autumn 1979.
[7] S. Halliday, *The Great Stink of London*. The History Press.
[8] S. Stevens Hellyer, *The plumber and sanitary houses : A practical treatise on the principles of internal plumbing work*. T.B. Batsford 52 High Holborn, 1877.
[9] T. Pridgin Teale, *Dangers to Health*, 1st Edition. 1878.
[10] Baldwin Latham, *Sanitary Engineering*. 1878.
[11] Wood, Leslie B, *The restoration of the tidal Thames*. 1982.
[12] U.K. Parliament, *The Metropolitan Buildings Act. 7th & 8th. Vict. Cap. 84.* 1844.
[13] John Phillips, "On the Arrangement and Construction of House Drains," *The Builder*, no. 96, pp. 593–594, 606–608, Dec. 1844.
[14] Khanda Sharif, "Exploring the Impact of Sewer-Derived Airflows on the Air-Pressure Dynamics within Building Drainage Systems," Heriot-Watt University, Edinburgh, 2024.
[15] William Hosking, *A Guide for the Proper Regulation of the Buildings in Towns as a Means of Promoting the Securing the Health, Comfort, and Safety of the Inhabitants*. London: William Clowes and Sons, 1848.
[16] "Report on the Sanitary State of Londesborough Lodge," *The Lancet*, Dec. 09, 1871.
[17] Osbourne Reynolds, *Sewer Gas and How To Keep It Out of Houses*. London: Macmillan and Co, 1872.
[18] "Protection from Sewer Gas," *New York Times*, Dec. 20, 1875.
[19] Brecon, "Effluvia-trap for drains," *The Builder*, p. 99, 1844.
[20] W. Maguire, *Domestic Sanitary Drainage and Plumbing*, 2nd ed. London, 1896.
[21] "Model Byelaws." Local Government Board, 1877.
[22] *Kanalisation von Berlin Polizei - Verordnung*. 1874.
[23] New York CIty Department of Health, *Construction of Drains, Soil-Pipes and Plumbing of New Buildingds*, vol. Section 3, Chapter 450. 1881.
[24] "The Boston Plumbing Ordinance," *The Sanitary Engineer*, p. 367, Mar. 1883.
[25] Edward S. Philbrick, *American Sanitary Engineering*. The Sanitary Engineer, 1881.
[26] "Plumbing Practice," *The Sanitary Engineer*, vol. 4, no. 22, New York, p. 529, Oct. 15, 1881.
[27] H. Alfred Roechling, *Sewer Gas and Health*. London: Biggs and Co., 1898.
[28] A. Unna, "Die Ausführung der Hausentwässerung mit Rücksicht auf die hygienische Bedeutung der Kanalgase," *Gesundheits-Ingenieur*, vol. 18, no. 23, pp. 378–383, Dec. 1895.
[29] "Improving Tenement-Houses," *New York Times*, Jul. 09, 1880.
[30] G. C. Whipple *et al.*, "Recommended minimum requirements for plumbing in dwellings and similar buildings : final report of subcommittee on plumbing of the building code committee

July 3, 1923," National Bureau of Standards, Gaithersburg, MD, NBS BH 2, 1924. doi: 10.6028/NBS.BH.2.
[31] "Uniform Plumbing Code." International Association of Plumbing and Mechanical Officials, Ontario, CA, 2024.
[32] "International Plumbing Code." International Code Council, Country Club Hills, IL, 2024.
[33] "DIN 1986-100 Entwässerungsanlagen für Gebäude und Grundstücke - Teil 100: Bestimmungen in Verbindung mit DIN EN 752 und DIN EN 12056." DIN GmbH, Berlin, 2016.
[34] "GB 50015-2019 Standard for design of building water supply and drainage." China Planning Press, Beijing, 2019.
[35] "BS EN 12056-2 Gravity Drainage systems inside buildings." British Standards Institute, 2000.
[36] "New York City Plumbing Code." International Code Council, Country Club Hills, IL, 2022.
[37] "2018 Philadelphia Plumbing Code." International Code Council, Country Club Hills, IL.
[38] "Code of Practice for Deconstruction and Construction Sites." City of London, London, Jan. 2019.

Near Source Monitoring of pathogens in building drainage systems

J. Bavin (1), M. Gormley(2), and D.A. Kelly (3)

(1) jcb4003@hw.ac.uk
(2) m.gormley@hw.ac.uk
(3) d.a.kelly@hw.ac.uk
(1-3) Heriot-Watt University, Edinburgh, Scotland, UK.

Abstract

Wastewater-based epidemiology (WBE) has recently come to the forefront of research as a tool to accurately track SARS-CoV-2 and as a public health approach for assessing pharmaceutical use in a population. WBE has already been shown to be successful in small-scale monitoring efforts, including campuses, prisons, and hospitals. Hospital plumbing can also behave as a reservoir for deleterious microorganisms that may re-enter circulation, posing a particular threat to immunocompromised patients.

This study seeks to assess the feasibility and effectiveness of sampling for near-source WBE in a building drainage system. Results have been obtained for a range of timescales and implementation strategies. Samples were eluted from the sampler and analysed for the recovery of fluorescein and a plant virus - Pepper mild mottle virus (PMMoV). The results characterise the recovery of analyte within the building drainage system, enabling identification of trends in potentially dangerous pathogens and informing timely interventions. This research combines knowledge of building drainage system operation and aerosolisation processes to give a holistic record of ongoing monitoring of the system.

Keywords

Wastewater-based epidemiology, wastewater sampling, fluorescein, pepper mild mottle virus (PMMOV), building drainage systems

1 Introduction

1.1 Spread of infections in buildings

Infections are spread by a number of pathways and the understanding of those pathways is critical to preventing the spread of epidemics, such as the SARS-CoV-2 epidemic in December 2019 or other hospital-acquired infections.

The spread of infections happens by several methods; airborne transmission, direct contact between infected persons and via indirect contact with an intermediate surface contaminated by contact with the person or their expelled fomites[1]. Of these fomites, aerosolised droplets that contain the virus, bacteria or fungi are of particular interest within defective building plumbing systems.

1.2 Outbreak of SARS in Amoy Gardens

In March 21 2003 aerosol transmission via a buildings plumbing was responsible for the SARS outbreak in the Amoy Gardens complex in Kowloon Bay, China. Amoy Gardens consisted of 19 apartment towers, 33 stories high and with eight apartments on each floor. Each of these apartments connected their sanitary plumbing to a vertical drainage pipe, sometimes known as a stack pipe. To prevent the flow of sewer gases or aerosols into the apartments the sinks, bathing facilities, and toilets have a water trap seal installed. The traps utilise a small amount of water at the bottom of a bend of pipe. Due to the failure of these traps in Amoy gardens the aerosolised fomites from the faecal matter of a person infected with SARS was allowed to enter the apartments of other residents through failed p-traps causing an outbreak. Fomites expelled from the top of the vent stack entered windows also causing infection[2].

The outbreak is infamous for its rapid dissemination of SARS and in highlighting the ability of the building infrastructure to pose a health risk, but more importantly it highlights the ability of aerosols within a waste stack to be a vector, and thus diagnostic point of disease[3].

1.3 Aerosols spread up and down the stack

Airflows within building drainage systems has been recorded at $28ls^{-1}$ under normal operating conditions (and sometimes more). This can cause contaminated air to enter the interior of the building under defect conditions. Airflows are entrained from the flow of water down the soil stack and airflow movement occurred in both the up and down directions [4].

1.4 Hospital pathogens

It is known that hospital plumbing can be a reservoir of pathogens. and Low, et al. [5] identified that there was a positive correlation between droplet dispersion from sinks and the transmission of a model organism. Potential pathogens found in sinks such as carbapenemase-producing *Enterobacteriaceae* (CPE), *Pseudomonas aeruginosa*, *Acinetobacter baumanii* and *Stenotrophomonas maltophilia* could potentially be spread

from hospital sink by droplet to the surrounding area. Hospital plumbing can also be a reservoir of anti-microbial resistance (AMR) such as carbapenemase resistance [6], Beta-lactam resistance [7], which is further detectable in hospital wastewater further downstream. [7] where the AMR reflected the most prevalent antibiotic in use in the hospital [8].

Aerosolised droplets are known to be produced from a number of common practices in a bathroom such as showering, using tap water or use of the toilet flush. Previous work conducted by Gormley, et al. [9] on a waste stack test rig has demonstrated the ability of a normal 6 litre toilet flush to aerosolise enough of model organism *Pseudomonas putida* 10^6-10^9 cfu ml^{-1}, in 0.85% NaCl, to be subsequently culturable from air and surface samples surrounding the toilet. The typical sanitary plumbing system airflows generated by the study, 20-30 ls^{-1} were enough to aerosolise pathogens and enable the spread between different floors of the building via waste stack as demonstrated by the Authors.

1.5 Relevance to a Healthcare setting

Within hospital plumbing there are several pathogens of interest, although this list is not exhaustive as to what could be detected. Molecular and genomic methods that identify organisms by genetic material are sensitive enough that if the DNA or RNA persists in water long enough that we can detect it in a sample downstream.

Viruses such as SARS-CoV-2, Adenovirus, Rotavirus, Norovirus, or Astrovirus can be detected in hospital wastewater [10]. WBE is even able to specifically find genes encoding antibiotic resistance irrespective of the carrier organisms although viruses can also be determined by culture and immunofluorescence based assays.

WHO-listed highly infective and often antibiotically-resistant pathogens under an acronym ESKAPEE each of which can be detected in hospital wastewater where present using metagenomic, molecular and culture techniques: Enterococcus faecium, Staphylococcus aureus, Klebsiella pneumoniae, Acinetobacter baumannii, Pseudomonas aeruginosa, Enterobacter spp., and Escherichia coli [1112]

Examples of antibiotic resistance genes detected using WBE are carbapenemase encoding genes KPC, IMP, VIM, NDM, OXA-48-like[13] as well as resistance to animoglycosides, beta-lactams and Macrolide-Lincosamide-Streptogramin-class antibiotics [14].

2. Methodology

Samples were extracted non-intrusively from a waste stack such as in Figure 1 below. It is constructed out of PVC pipe to best match the conditions in a two-storey building and is built to current BS specifications.

Nitrile gloves and eye protection is worn throughout handling of fluorescein. Fluorescein is mixed into a 6-litre volume of water to simulate the standard flush and poured into the top of the stack to simulate a standard toilet flush.

The water is allowed to flow through the rig and would lead to droplets being collected by the sampler. An ultraviolet light is used to highlight any droplets and a photograph is taken of the plate. Percentage coverage is determined by use of Fiji[15]-image analysis software.. Fiji is an open-source software developed by the National institute of health for scientific image analysis, such as counting cells or droplets. A baseline conversion of pixels to distance was set to measure droplet coverage area. Selection of fluorescein was done by selecting a colour threshold, and using ROI (region of interest) manager to calculate the area selected.

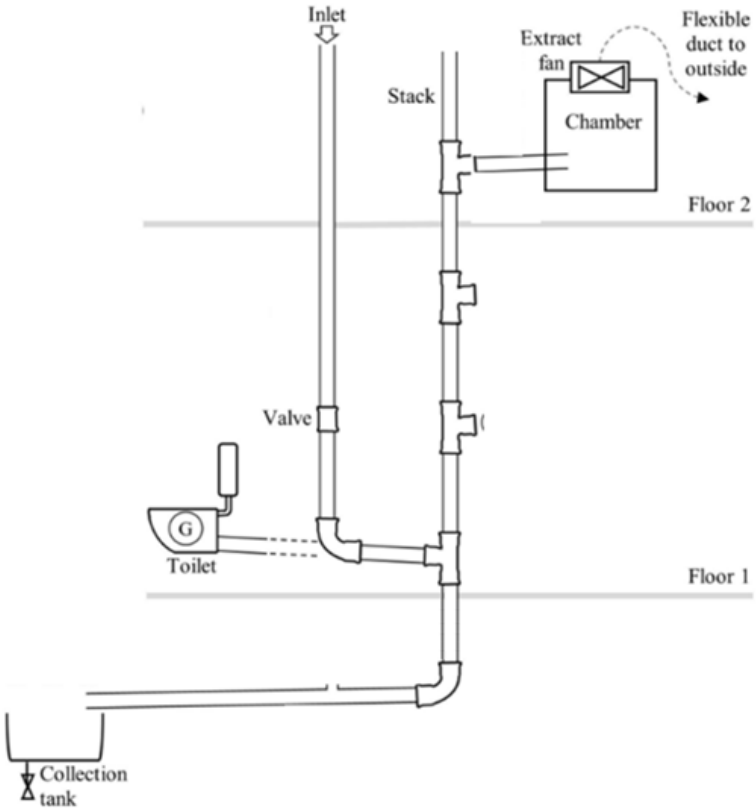

Figure 1. The test rig set up used to test sampler saturation with fluorescein, reproduced from Gormley, (2022) Note: the WC and the inlet pipe were interchangeable

A secondary experiment is performed using tabasco sauce – a known reservoir of PMMoV virus - diluted in 6L of water and flushed in the same manner. Droplets were eluted from the sampler and qPCR was required to find the concentration. Primers for PMMoV were as in Haramoto, et al. [16].

To test the sampler's ability to detect a waterborne virus, tabasco sauce was used as a safe surrogate as it contains PMMoV. Dilutions of the inoculum of 50ml, 100ml, 200ml, 400ml in 6 litres of cold tap water. 6 litres is used to represent the most common volume of toilet flush. The inoculum is entered into the top of a testing rig built to simulate a common flush in a 1st storey building. The sampler is affixed and the flush is released. After the passing of the water the sampler is unloaded and a sample taken for qPCR to enumerate the total gene copies per litre recovered.

3. RESULTS

3.1 Fluorescein

The water from the drain stack produced a number of large droplets that were able to be seen with the sampler. Using Fiji it was possible to determine the total coverage of Fluorescein. Total area of sampler is 5026.54mm^2. The coverage is 199mm^2 or 4%. It was also noted that the sampler on closer inspection contained much smaller aerosols that had settled on the surface of the sampler. Using a microscope the droplets were found to be as small as 1µm as shown in Figure 2.

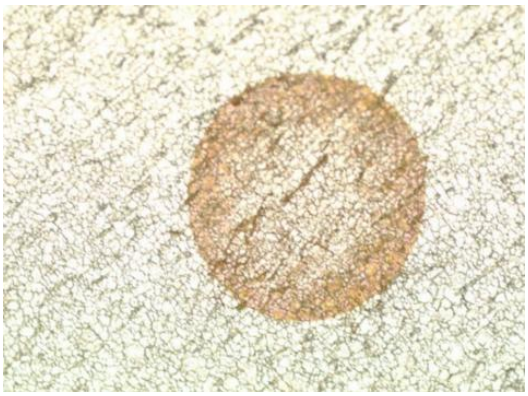

Figure 2. A dried droplet 1 µm diameter of fluorescein collected from the system

3.2 PMMoV

QPCR was performed on 100ml of tabasco sauce diluted in 6 litres of water. The total concentration measured of gc/L was 2.39 x 10^9 and the PCR cq was 27.03. Flushing the PMMoV inoculum at differing concentrations produced a measurable signal at the sampler. The gene copies per litre are shown in Figure 3, below.

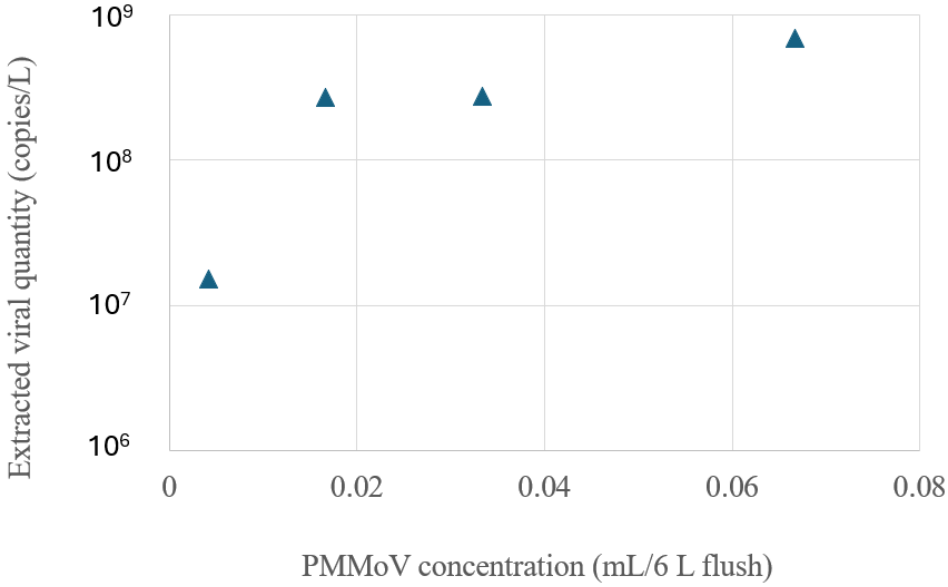

Figure 3. Gene copies per litre of PMMoV recovered from the sampler as the concentrations of PMMoV flushed through a test rig system is varied in magnitude

4. Discussion

4.1 Discussion

The approach to sampling a waste stack used in this experiment is a novel methodology. Although simple in its execution, the recovery of fluorescein does show the ability of a surface-based sampler to work effectively. It also highlights that it is possible to detect any type of aerosolised particle - chemical, bacteria and virus.

The results from the recovery of PMMoV were also successful. The relevance of this is that PMMoV is a small virus and biomarker for human faecal waste. Numerous studies have shown that it reflects the total number of humans using the sewer system and can be used to quantify that amount [17]. This represents a new possibility for passive waterborne viral collection.

What this experiment has shown is that cumulative surface sample of the wastewater system can be collected over time in the manner of passive samplers, such as the classic Moore swab. Many studies have easily demonstrated the applicability of the Moore swab to be used in wastewater monitoring. The classic Moore swab is a specific arrangement of cotton gauze shown in figure 4. The cotton provides a larger surface area for particles in flowing wastewater to adhere to. Examining the Moore swab as a benchmark passive sampling device to compare this sampler to reveals the same challenges in terms of saturation of the sampler.

Figure 4. Moore swab consisting of cotton gauze squares tied with nylon string

4.2 Moore swab – the existing gold standard

Sampler saturation

The well-known Moore swab reaches saturation equilibrium in around 6 hours[18,19]. The sampler that works here by droplet and aerosol deposition would be affected by a number of similar factors as it would approach saturation. Saturation here is defined as the point at which the amount of information being gained from sampling the plate is equal to the rate at which information is lost from the plate.

Environmental factors affecting saturation

Over time, air flow entrained by the passage of other flushes, the addition of wastewater on the sampler washing away previous sample, and a variable humidity affect the total amount of sample that can be retained as viable. Low Humidity or high air flow could kill some bacteria or hasten DNA degradation.

Biological considerations affecting saturation

A microbiologist who intends to later identify the wastewater biome from the sampler plate will want to be aware of the following variable factors that would influence the viability of the analytes and would represent a destruction of some information. Factors such as; DNA/RNA degradation over time, Bacterial viability over time, and Viral viability over time, this varies according to enveloped and non-enveloped viruses, where non-enveloped viruses are more viable in wastewater [20].

What these studies do confirm is that the use of a passive aerosol sampler connected to a wastewater stack would be a potential method of wastewater surveillance. The ability to recover aerosols and viruses (PMMoV) demonstrate a potential for clinical surveillance lending itself particularly to building level wastewater surveillance. The sampler also promises advances in the detection of small viruses that can be isolated in plumbing infrastructure such as the SARS outbreak at Amoy Gardens even referenced earlier [2].

5. Conclusion

It is possible to collect and sample the droplets and aerosols from within a wastewater stack of a building using a specialised passive sampler, similar but separate in design to existing passive samplers, such as the Moore swab. A successful dosing and reclamation of fluorescein and PMMoV has been demonstrated which infers that the recovery of viruses is also possible with this method. This sampler represents a step toward a new sampling technology that reclaims viable and condensed viral material from a wastewater stack. Further research is needed to calculate the recovery efficiency and saturation point of the method.

6. References

1. Morawska L. Droplet fate in indoor environments, or can we prevent the spread of infection? In: *Indoor Air*. Vol 16. Blackwell Munksgaard; 2006:335-347. doi:10.1111/j.1600-0668.2006.00432.x

2. Gormley M, Swaffield JA, Sleigh PA, Noakes CJ. An assessment of, and response to, potential cross-contamination routes due to defective appliance water trap seals in building drainage systems. *Building Services Engineering Research and Technology*. 2012;33(2):203-222. doi:10.1177/0143624411410619

3. Kelly R. McKinney, Yu Yang Gong, Thomas G. Lewis. Environmental Transmission of SARS at Amoy Gardens. *J Environ Health*. 2006;69(9):26-30.

4. Gormley M, Templeton KE, Kelly DA, Hardie A. Environmental conditions and the prevalence of norovirus in hospital building drainage system wastewater and airflows. *Building Services Engineering Research and Technology*. 2014;35(3):244-253. doi:10.1177/0143624413485080

5. Low JM, Chan M, Low JL, Chua MCW, Lee JH. The impact of sink removal and other water-free interventions in intensive care units on water-borne healthcare-associated infections: a systematic review. *J Hosp Infect*. 2024;150:61-71. doi:10.1016/j.jhin.2024.05.012

6. Hoffmann M, Fischer MA, Neumann B, et al. Carbapenemase-producing Gram-negative bacteria in hospital wastewater, wastewater treatment plants and surface waters in a metropolitan area in Germany, 2020. *Sci Total Environ*. 2023;890:164179. doi:10.1016/j.scitotenv.2023.164179

7. Kutilova I, Medvecky M, Leekitcharoenphon P, et al. Extended-spectrum beta-lactamase-producing Escherichia coli and antimicrobial resistance in municipal and hospital wastewaters in Czech Republic: Culture-based and metagenomic approaches. *Environ Res*. 2021;193:110487. doi:10.1016/j.envres.2020.110487

8. Siri Y, Bumyut A, Precha N, Sirikanchana K, Haramoto E, Makkaew P. Multidrug antibiotic resistance in hospital wastewater as a reflection of antibiotic prescription and infection cases. *Sci Total Environ*. 2024;908:168453. doi:10.1016/j.scitotenv.2023.168453

9. Gormley M, Aspray TJ, Kelly DA, Rodriguez-Gil C. Pathogen cross-transmission via building sanitary plumbing systems in a full scale pilot test-rig. *PLoS One*. 2017;12(2). doi:10.1371/journal.pone.0171556

10. Zhou X, Li Q, Shi Z, et al. Assessing the prevalence of human enteric viruses in hospital wastewater to evaluate the effectiveness of wastewater treatment systems. *Ecotoxicol Environ Saf*. 2025;289:117488. doi:10.1016/j.ecoenv.2024.117488

11. Hannah y. Mahmood, Shirin Jamshidi, J. Mark Sutton, Khondaker M. Rahman. Current Advances in Developing Inhibitors of Bacterial Multidrug Efflux Pumps.

Current Medical Chemistry. 2016;(23):1062-1081. doi:10.2174/0929867323666160304150522

12. Kotay SM, Donlan RM, Ganim C, Barry K, Christensen BE, Mathers AJ. Droplet- Rather than Aerosol-Mediated Dispersion Is the Primary Mechanism of Bacterial Transmission from Contaminated Hand-Washing Sink Traps. *Appl Environ Microbiol*. 2019;85(2). doi:10.1128/AEM.01997-18

13. Teban-Man A, Szekeres E, Fang P, et al. Municipal Wastewaters Carry Important Carbapenemase Genes Independent of Hospital Input and Can Mirror Clinical Resistance Patterns. *Microbiol Spectr*. 2022;10(2):e0271121. doi:10.1128/spectrum.02711-21

14. Silvester R, Webster G, Perry WB, et al. Genome-resolved metagenomics uncovers antimicrobial resistance gene carriers in hospital and municipal wastewater environments. *Sci Total Environ*. 2025;1002:180607. doi:10.1016/j.scitotenv.2025.180607

15. Schindelin J, Arganda-Carreras I, Frise E, et al. Fiji: An open-source platform for biological-image analysis. *Nat Methods*. 2012;9(7):676-682. doi:10.1038/nmeth.2019

16. Haramoto E, Kitajima M, Kishida N, et al. Occurrence of pepper mild mottle virus in drinking water sources in Japan. *Appl Environ Microbiol*. 2013;79(23):7413-7418. doi:10.1128/AEM.02354-13

17. Choi H, Coppin JD, Brackens E, et al. Utilities of PMMoV as an internal control for the building-level wastewater surveillance of SARS-CoV-2. *Microbiol Spectr*. 2025;13(10):1-3. doi:10.1128/spectrum.01418-25

18. Jones DL, Grimsley JMS, Kevill JL, et al. Critical Evaluation of Different Passive Sampler Materials and Approaches for the Recovery of SARS-CoV-2, Faecal-Indicator Viruses and Bacteria from Wastewater. *Water (Basel)*. 2022;14(21). doi:10.3390/w14213568

19. Cha G, Zhu KJ, Fischer JM, et al. Metagenomic evaluation of the performance of passive Moore swabs for sewage monitoring relative to composite sampling over time resolved deployments. *Water Res*. 2024;253:121269. doi:10.1016/j.watres.2024.121269

20. Ye Y, Ellenberg RM, Graham KE, Wigginton KR. Survivability, Partitioning, and Recovery of Enveloped Viruses in Untreated Municipal Wastewater. *Environ Sci Technol*. 2016;50(10):5077-5085. doi:10.1021/acs.est.6b00876

21. van Doremalen N, Bushmaker T, Morris DH, et al. Aerosol and Surface Stability of SARS-CoV-2 as Compared with SARS-CoV-1. *New England Journal of Medicine*. 2020;382(16):1564-1567. doi:10.1056/nejmc2004973

22. Solo-Gabriele HM, Kumar S, Abelson S, et al. Predicting COVID-19 cases using SARS-CoV-2 RNA in air, surface swab and wastewater samples. *Science of the Total Environment*. 2023;857. doi:10.1016/j.scitotenv.2022.159188

23. Kotwa JD, Jamal AJ, Mbareche H, et al. Surface and Air Contamination with Severe Acute Respiratory Syndrome Coronavirus 2 from Hospitalized Coronavirus Disease 2019 Patients in Toronto, Canada, March-May 2020. *Journal of Infectious Diseases*. 2022;225(5):768-776. doi:10.1093/INFDIS/JIAB578

24. Korajkic A, McMinn BR, Pemberton AC, Kelleher J, Ahmed W. The comparison of decay rates of infectious SARS-CoV-2 and viral RNA in environmental waters and wastewater. *Sci Total Environ*. 2024;946:174379. doi:10.1016/j.scitotenv.2024.174379

7. Presentation of Authors

Jake Bavin is a PhD student with a background in medical microbiology. He is studying Wastewater Based Epidemiology with the Public Health and Environmental Engineering research group at Heriot-Watt University.

Prof. Michael Gormley is Professor of Public Health and Environmental Engineering at Heriot-Watt University. His research specialisms are: mathematical modelling of air and water flows in building drainage systems, infection spread via bioaerosols, water systems in healthcare environments, sanitation in developing countries, and product development.

Dr David A Kelly is Associate Professor of Architectural Engineering at Heriot-Watt University. His research interests cover: water conservation, minimisation of disease transmission from wastewater drainage systems, water systems in healthcare environments, and the use of nature-based solutions of stormwater management.

Evaluating Urban Fire Water Supply Resilience with Hydrant Networks and Mobile Supply Strategies

Matjaž Nekrep Perc (1), Janja Kramer Stajnko (2)
(1) matjaz.nekrep@um.si
(2) janja.kramer@um.si

(1), (2) Faculty of Civil Engineering, Transportation Engineering and Architecture, University of Maribor, Slovenia

Abstract

Reliable fire water supply is essential for effective urban firefighting and constitutes a key component of community resilience. In many European countries, including Slovenia, firefighting operations primarily rely on municipal drinking water distribution systems, where public hydrant networks provide the principal source of extinguishing water. However, hydraulic limitations and operational deficiencies may reduce the availability of the water quantities required during emergency interventions.

This study evaluates the resilience of an urban fire water supply system through an integrated assessment of hydrant network performance and operational mobile water supply capacity. A case study was conducted in the Municipality of Slovenske Konjice (Slovenia) using hydraulic measurements obtained during routine inspections of 352 public fire hydrants, complemented by an assessment of the available firefighting water tanker fleet and operational response capacity. The results showed that approximately one-third of the inspected hydrants were classified as non-compliant, while only a limited number provided flow rates exceeding 10 L/s, highlighting the potential role of supplementary mobile water supply during high-demand firefighting operations.

Unlike conventional assessments based solely on hydraulic network performance, the proposed approach integrates infrastructure characteristics with operational firefighting capabilities, providing a more comprehensive evaluation of urban fire water supply resilience. The proposed framework supports the identification of vulnerable areas, improves decision-making for municipalities and water utilities, and contributes to the planning of more resilient urban fire protection systems.

Keywords

fire water supply; hydrant network; water distribution system; urban resilience; mobile water supply; tanker shuttle operations

1 Introduction

Reliable fire water supply is a fundamental prerequisite for effective firefighting and the protection of life, property, and critical infrastructure in urban environments (American Water Works Association, 2020; National Fire Protection Association, 2022). In most European countries, including Slovenia, municipal drinking water distribution systems provide the primary source of water for firefighting through public hydrant networks (European Committee for Standardization (CEN), 2021; Kozelj et al., 2004). Consequently, the hydraulic performance and spatial distribution of hydrants have a direct influence on the effectiveness of fire suppression operations (Lee et al., 2021; National Fire Protection Association, 2019).

The increasing complexity of urban water distribution systems, together with infrastructure aging, changing water demand, and climate-related stresses, has highlighted the importance of evaluating the resilience of fire water supply systems (United Nations Office for Disaster Risk Reduction, 2019). Although public water supply networks are primarily designed to satisfy domestic and industrial water demands, they must also provide sufficient flow rates and pressures during emergency firefighting operations (Rossman, 2000; Walski, 2003). Hydraulic deficiencies may reduce the available firefighting capacity, particularly in areas with high peak demand, inadequate network capacity, or limited hydrant coverage (American Water Works Association, 2020).

Previous research has primarily focused on hydraulic modelling of water distribution systems (Rossman, 2000), hydrant performance (National Fire Protection Association, 2019), and fire flow requirements, while only a limited number of studies have considered the operational capability of fire brigades to compensate for insufficient hydrant supply through mobile water transport (National Fire Protection Association, 2022). Consequently, assessments of fire water supply often overlook the combined contribution of fixed infrastructure and emergency response resources to the overall resilience of the system.

This study addresses this gap by evaluating urban fire water supply resilience through an integrated assessment of hydrant network performance and mobile water supply strategies. A case study conducted in the Municipality of Slovenske Konjice (Slovenia) combines an analysis of the existing hydrant network with an evaluation of tanker shuttle operations involving neighbouring fire brigades. The proposed approach enables the identification of hydraulically vulnerable areas and assesses the capacity of operational measures to maintain an adequate water supply during firefighting interventions. The

findings contribute to improved planning of resilient urban fire water supply systems and support decision-making for both water utilities and fire protection authorities.

2 Materials and Methods

2.1 Study Area

The study was conducted in the municipality of Slovenske Konjice, located in northeastern Slovenia within the Savinja Statistical Region. The municipality covers an area of approximately 98 km², comprises 58 settlements, and has a population of 15,515 inhabitants. Public water supply services are provided to 13,093 residents by the municipal utility company JKP Slovenske Konjice.

The investigated public water supply system is operated by JKP d.o.o. Slovenske Konjice, which manages five independent water supply systems: Slovenske Konjice, Spodnje Laže, Tolsti Vrh, Zeče, and Kamna Gora. Together, these systems provide potable water to urban and rural settlements within the municipality. The largest system, Slovenske Konjice, supplies the majority of consumers and includes 67.7 km of transmission and distribution pipelines with nominal diameters exceeding DN 80, 18 service reservoirs, 10 pumping stations, five drinking water treatment facilities, and an extensive telemetry system for operational monitoring. The layout of the municipal water distribution system is presented in Figure 1.

Figure 1 – Layout of the municipal water distribution system in the Municipality of Slovenske Konjice

The distribution network incorporates an extensive public fire hydrant system forming part of the municipal water infrastructure. The spatial distribution of public fire hydrants within the investigated water distribution system is shown in Figure 2. In accordance with Slovenian regulations, the hydrant network is subject to periodic inspection and hydraulic performance testing to verify its suitability for firefighting operations. The investigated database comprised 352 public fire hydrants distributed throughout the municipal water supply systems. For 276 hydrants (78.4%), complete hydraulic measurements—including static pressure, residual pressure under flow conditions, and discharge—were available, while the remaining hydrants were classified as non-operational or lacked complete measurement records due to damage, inaccessibility, absence, or other operational deficiencies.

The water utility maintains a comprehensive asset management system, including digital records of water infrastructure, hydrant inspections, pipeline failures, and telemetry-based monitoring of pressures and flows. Continuous monitoring is implemented at major water supply facilities through SCADA and telemetry systems, enabling real-time observation of hydraulic conditions and supporting efficient network management and maintenance.

The municipality was selected as a representative case study because it combines an urban distribution network with dispersed rural settlements served by multiple interconnected water supply systems. This diversity provides a suitable environment for evaluating the hydraulic performance and operational reliability of public fire hydrants under real operating conditions and for assessing the resilience of municipal fire water supply infrastructure.

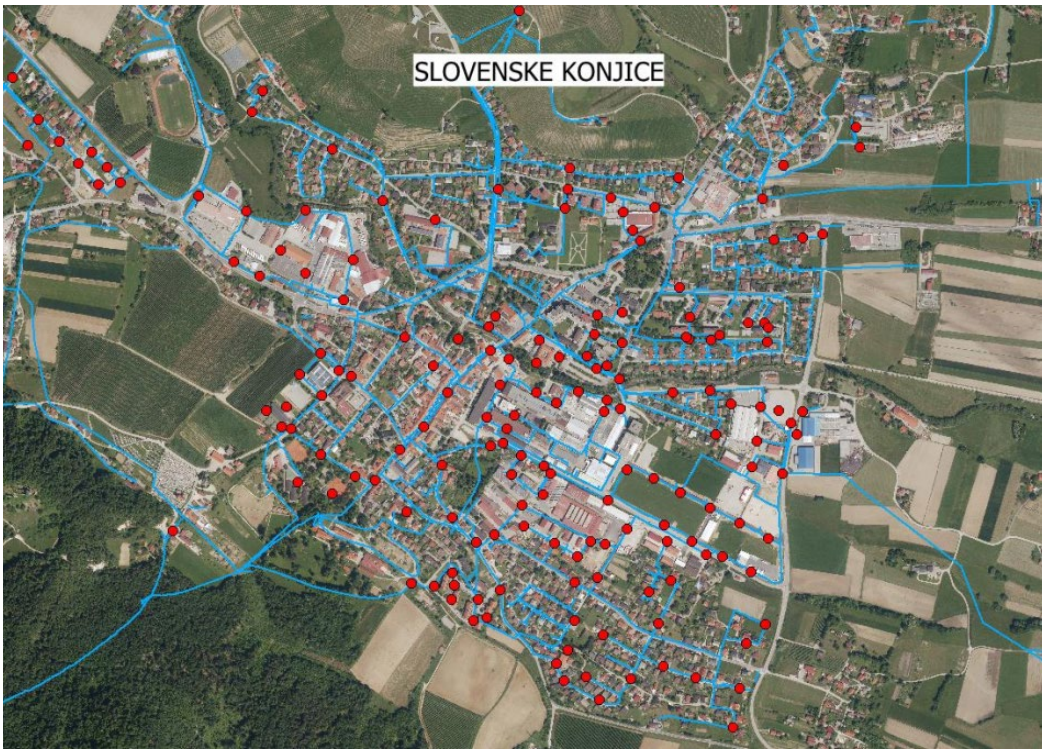

Figure 2 – Layout of the municipal water distribution system with the locations of public fire hydrants in the Municipality of Slovenske Konjice.

2.2 Hydrant Network Assessment

The performance of the public fire hydrant network was evaluated using hydraulic measurements obtained during routine inspections carried out by the municipal water utility. The assessment aimed to determine the operational condition of hydrants and to evaluate their ability to provide adequate water supply for firefighting purposes under normal operating conditions. The inspection database included 352 public fire hydrants distributed throughout the five municipal water supply systems. For each hydrant, the available records included its identification number, location, installation type (above-ground or underground), inspection status, static pressure, residual pressure during discharge, measured flow rate, and comments regarding operational deficiencies. Hydrants for which hydraulic measurements could not be performed because of physical damage, inaccessibility, missing components, or other technical reasons were classified as non-operational and were excluded from the hydraulic performance analysis.

Hydraulic performance was assessed using three principal indicators (National Fire Protection Association, 2019):

- Static pressure (bar), representing the network pressure before water discharge;
- Residual pressure (bar), measured during hydrant operation under flow conditions;
- Discharge (L s^{-1}), representing the available water flow delivered through the hydrant.

These parameters were selected because they directly determine the suitability of a hydrant for firefighting operations and are commonly used in the technical evaluation of municipal fire water supply systems (European Committee for Standardization (CEN), 2021; National Fire Protection Association, 2019). The assessment consisted of two stages. First, the operational status of all hydrants was evaluated by distinguishing functional and non-functional units. Second, statistical analyses were performed for hydrants with complete hydraulic measurements to characterize the overall hydraulic performance of the network. Descriptive statistics, including the mean, median, minimum, maximum, standard deviation, and selected percentiles, were calculated for each hydraulic parameter. In addition, the distributions of static pressure, residual pressure, and discharge were analysed to identify variability within the network and to detect potential hydraulic limitations. The resulting dataset provides a comprehensive overview of the hydraulic condition of the municipal hydrant network and forms the basis for subsequent evaluation of firefighting water availability and identification of sections of the distribution system requiring operational improvements.

Hydrants were classified as compliant when they successfully passed the routine inspection according to the requirements of the Slovenian fire protection regulations

2.3 Operational Fire Water Supply Capacity

To complement the assessment of the fixed hydrant network, the resilience of the fire water supply system was further evaluated by considering the operational capacity of the

local fire service to provide water through mobile transport. Mobile water supply represents an essential contingency measure in situations where hydrant flow rates are insufficient or where hydrants are unavailable due to hydraulic limitations, infrastructure failures, or remote incident locations (National Fire Protection Association, 2022).

The assessment was based on the operational resources of the Firefighting Association of Slovenske Konjice, which comprises seven operational fire brigades with a total of 207 operational firefighters. These brigades provide fire protection throughout the municipality and are equipped to establish alternative water supply during firefighting interventions. The principal operational resources considered in the assessment are summarized in Table 1.

Table 1 – Operational resources available for mobile fire water supply in the Municipality of Slovenske Konjice

Parameter	Value	Relevance for fire water supply
Operational fire brigades	7	Provides municipal coverage and enables coordinated response
Operational firefighters	207	Personnel available for firefighting and water shuttle operations
Firefighting vehicles with 3,000 L water tanks	≥ 4	Primary mobile water transport vehicles
Firefighting vehicles with 5,000 L water tanks	≥ 1	High-capacity mobile water transport
Minimum immediately available mobile water storage	≥ 17,000 L	Total initial water volume available for tanker operations
Water supply strategy	Tanker shuttle operation	Alternative water supply when hydrant capacity is insufficient
Mutual aid potential	Available	Additional water tankers can be requested from neighbouring fire brigades during large-scale incidents

As summarized in Table 1, the Firefighting Association of Slovenske Konjice has seven operational fire brigades comprising 207 operational firefighters and a tanker fleet with a minimum immediately available water storage capacity of 17,000 L. These resources form the basis for establishing tanker shuttle operations when hydrant capacity is insufficient.

The assessment assumed that mobile water supply would be deployed as a supplementary measure whenever the hydrant network alone could not provide the required firefighting flow. The evaluation therefore focused on the availability of water transport resources within the municipality and their potential contribution to maintaining a continuous water supply during firefighting operations. Particular consideration was given to the possibility

of simultaneous deployment of multiple tankers, enabling a shuttle operation between water sources and the fire scene.
Although the present assessment primarily considers the available transport capacity of the municipal firefighting fleet, the operational resilience of the system may be further enhanced through mutual aid agreements with neighbouring municipalities, allowing additional water tankers to be mobilised during large-scale or prolonged firefighting incidents. The integration of hydrant network performance with mobile water supply capability provides a more comprehensive assessment of urban fire water supply resilience than evaluation of the fixed infrastructure alone.

2.4 Integrated Resilience Evaluation

The resilience of the urban fire water supply system was evaluated by integrating the performance of the fixed hydrant network with the operational capacity for mobile water supply. The underlying assumption is that effective firefighting depends not only on the hydraulic capability of the water distribution system but also on the ability of the fire service to compensate for insufficient hydrant performance through alternative water supply strategies. The conceptual framework adopted for the integrated resilience evaluation is illustrated in Figure 3.

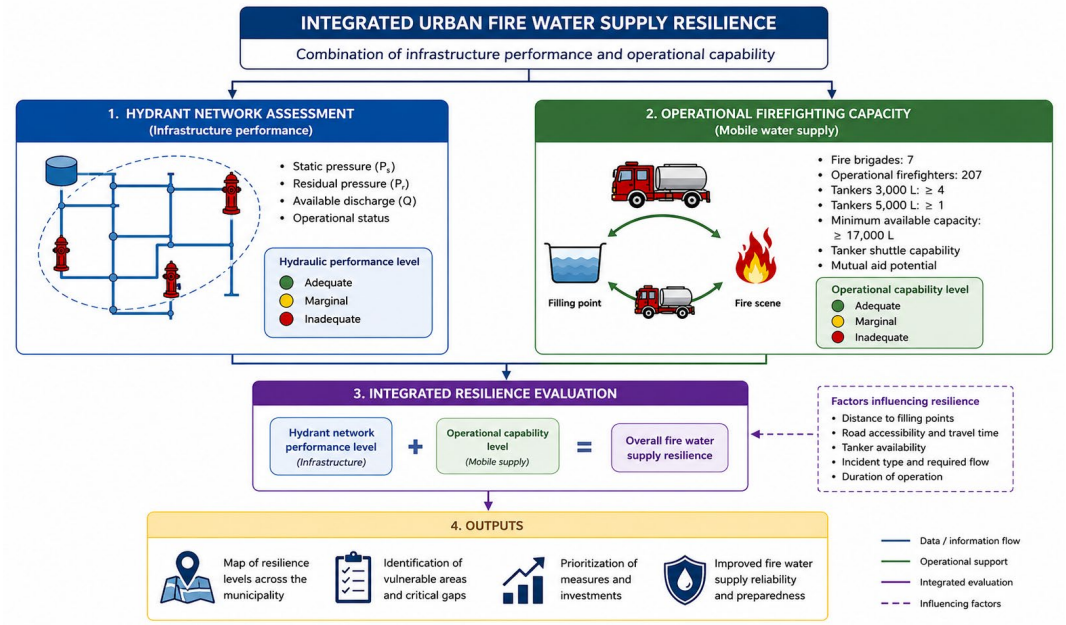

Figure 3 – Framework for the integrated evaluation of urban fire water supply resilience based on hydrant network performance and operational firefighting capacity

As illustrated in Figure 3, the integrated resilience evaluation was based on two complementary components. The first component assessed the hydraulic performance of the hydrant network using measured values of static pressure, residual pressure, and available discharge. These parameters describe the capacity of the public water distribution system to provide firefighting water directly at the incident location. The second component evaluated the operational capability of the municipal fire service to

establish a mobile water supply using firefighting water tankers and coordinated tanker shuttle operations (National Fire Protection Association, 2022).
The assessment framework assumes that the resilience of the fire water supply system increases when deficiencies in one component can be compensated by the other. Consequently, areas with limited hydrant performance may still achieve an acceptable level of firefighting water supply if sufficient mobile water transport resources can be deployed within an appropriate operational timeframe.
As shown in Figure 3, combining infrastructure performance with operational preparedness provides a more comprehensive evaluation than analyses based solely on hydraulic network performance. The methodology supports the identification of areas where existing hydrant infrastructure provides adequate fire water supply, as well as locations where additional operational measures or infrastructure improvements may be required to ensure reliable firefighting water availability.
The proposed framework is intended as a practical decision-support approach for municipalities, water utilities, and fire protection authorities. By combining engineering characteristics of the water distribution system with emergency response capabilities, it enables a more realistic assessment of urban fire water supply resilience and supports future planning of resilient fire protection systems.

3. Results and Discussion

3.1 Hydrant Network Performance

A total of 352 public fire hydrants were included in the assessment. Complete hydraulic measurements were available for 276 hydrants (78.4%), while the remaining 76 hydrants (21.6%) could not be hydraulically evaluated because they were inaccessible, damaged, dry, missing, or otherwise non-operational. The compliance status of the inspected hydrants is summarized in Figure 4.

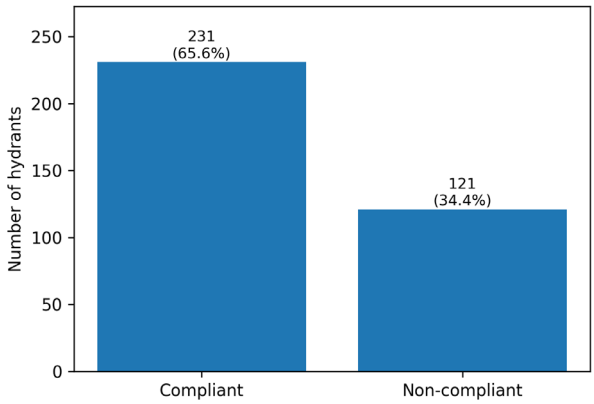

Figure 4 – Compliance status of the inspected public fire hydrants in the Municipality of Slovenske Konjice

As shown in Figure 4, 231 hydrants (65.6%) were classified as compliant, whereas 121 hydrants (34.4%) were identified as non-compliant, indicating that approximately one-third of the inspected hydrant network exhibited operational deficiencies.

Following the assessment of hydrant compliance, the hydraulic characteristics of the 276 hydrants with complete measurements were analysed. The corresponding descriptive statistics are presented in Table 2. The mean static pressure was 3.94 ± 1.55 bar, while the mean residual pressure decreased to 2.68 ± 1.30 bar during water discharge. The corresponding mean flow rate was 6.89 ± 2.06 L/s, with a median value of 7.54 L/s. Only nine hydrants (3.3%) achieved flow rates of 10 L/s or higher, whereas none exceeded 15 L/s, indicating limited discharge capacity for demanding firefighting scenarios.

Table 2 – Descriptive statistics of hydrants with complete hydraulic measurements.

Variable	n	Mean	SD	Median	Q1	Q3	Min	Max	95% CI
Static pressure (bar)	276	3.94	1.55	4.00	3.00	4.50	0.50	11.00	3.75-4.12
Residual pressure (bar)	276	2.68	1.30	2.90	2.00	3.30	0.10	9.50	2.52-2.83
Flow rate (L/s)	276	6.89	2.06	7.54	6.25	8.01	0.43	13.58	6.65-7.14

The distributions of the hydraulic variables deviated significantly from normality; therefore, non-parametric statistical methods were applied throughout the analysis. Residual pressure and reported flow rate exhibited a very strong positive correlation (Pearson $r = 0.953$, $p < 0.001$). However, as the flow values may have been derived from residual pressure during field testing, this relationship should be interpreted as an internal consistency check rather than as independent hydraulic validation.

A comparison between hydrant types revealed that above-ground hydrants achieved significantly higher residual pressures and flow rates than underground hydrants ($p = 0.037$). Furthermore, 74.2% of above-ground hydrants were classified as compliant compared with only 43.0% of underground hydrants, suggesting that underground hydrants may be more susceptible to operational deficiencies associated with accessibility, maintenance, or infrastructure age.

3.2 Operational Contribution of Mobile Water Supply

The available operational resources demonstrate that the Municipality of Slovenske Konjice possesses sufficient organisational capacity to establish alternative fire water supply when hydrant performance is inadequate. The seven operational fire brigades and the available tanker fleet provide a minimum immediately available mobile water storage capacity of 17,000 L, enabling the implementation of coordinated tanker shuttle operations during firefighting interventions.

From the perspective of urban fire water supply resilience, mobile water transport represents an important redundancy measure that compensates for hydraulic deficiencies within the fixed water distribution system. This capability is particularly important during

incidents requiring high fire flows, in peripheral areas with limited hydrant capacity, or in situations where hydrants are temporarily unavailable due to infrastructure failures.
Although the present study did not include a detailed simulation of tanker shuttle logistics, travel times, or sustained delivery rates, the available operational resources indicate that mobile water supply has the potential to improve the robustness of the municipal fire water supply system. However, this assessment is qualitative because tanker travel times and sustained delivery rates were not evaluated. Furthermore, the possibility of requesting additional water tankers through mutual aid agreements further increases operational resilience during large-scale or prolonged emergency incidents.

3.3 Overall Fire Water Supply Resilience

The integrated assessment demonstrates that urban fire water supply resilience depends on both the hydraulic performance of the public water distribution network and the operational capabilities of the local fire service.
From an infrastructure perspective, the results indicate several vulnerabilities. More than one-third of the hydrants were classified as non-compliant, and over one-fifth could not be hydraulically evaluated because they were inaccessible or non-operational. Moreover, only a small proportion of measured hydrants provided flow rates of 10 L/s or greater, suggesting that reliance on a single hydrant may be inadequate for incidents requiring high firefighting water demand.
However, these infrastructure limitations are partially mitigated by the municipality's operational firefighting capacity. The availability of multiple water tankers and trained personnel enables the implementation of tanker shuttle operations and alternative water supply strategies, thereby improving the overall resilience of the fire water supply system. Rather than relying solely on the hydraulic capacity of the distribution network, firefighting operations can combine hydrant supply with mobile water transport to maintain continuous water availability at the incident scene.
The findings demonstrate that resilience should not be evaluated solely on the basis of hydraulic parameters such as pressure and discharge. Operational factors—including hydrant accessibility, maintenance condition, availability of firefighting resources, and the capacity to establish alternative water supply—are equally important determinants of effective emergency response. Consequently, integrated assessments that combine infrastructure performance with operational preparedness provide a more realistic basis for planning resilient urban fire water supply systems. Of the 121 non-compliant hydrants, 76 were classified as non-operational because hydraulic measurements could not be completed, whereas the remaining non-compliant hydrants had complete measurements but failed to satisfy the inspection criteria.

4. Conclusions

This study evaluated the resilience of an urban fire water supply system through an integrated assessment of hydrant network performance and mobile water supply capacity. Using the Municipality of Slovenske Konjice as a case study, hydraulic measurements of

public fire hydrants were combined with an evaluation of the operational resources available for alternative water supply during firefighting interventions.

The results demonstrated that although the municipal water distribution network provides the primary source of firefighting water, its reliability is constrained by hydraulic and operational limitations. Approximately one-third of the inspected hydrants were classified as non-compliant, and only a small proportion of measured hydrants achieved flow rates exceeding 10 L/s, indicating that a single hydrant may not provide sufficient water for incidents with high firefighting demand. However, the municipality's operational resources, including dedicated water tankers and coordinated tanker shuttle operations, may enhance the resilience of the fire water supply system by helping compensate for local hydraulic deficiencies.

The principal contribution of this study is the demonstration that urban fire water supply resilience should be assessed through an integrated approach that combines infrastructure performance with emergency response capability. Such an approach provides municipalities, water utilities, and fire protection authorities with a more realistic basis for identifying vulnerabilities and planning resilient fire water supply systems.

Future research should integrate hydraulic network modelling, GIS-based hydrant accessibility analysis, and tanker shuttle simulations to further improve the assessment of urban fire water supply resilience.

6 References

American Water Works Association. (2020). *M31: Distribution System Requirements for Fire Protection*. American Water Works Association.

European Committee for Standardization (CEN). (2021). *EN 14384: Pillar Fire Hydrants*.

Kozelj, D., Steinman, F., Banovec, P., & Gosar, L. (2004). *Delovanje javnih vodovodnih omrežij kot hidrantnih omrežij*. https://doi.org/10.13140/RG.2.2.19177.39522

Lee, Y. H., Kim, M. S., & Lee, J. S. (2021). Firefighting in vulnerable areas based on the connection between fire hydrants and fire brigade. *Sustainability (Switzerland)*, *13*(1), 1–12. https://doi.org/10.3390/su13010098

National Fire Protection Association. (2019). *NFPA 291: Recommended Practice for Fire Flow Testing and Marking of Hydrants*.

National Fire Protection Association. (2022). *NFPA 1142: Standard on Water Supplies for Suburban and Rural Fire Fighting*.

Rossman, L. A. (2000). *EPANET 2: Users Manual*. U.S. Environmental Protection Agency.

United Nations Office for Disaster Risk Reduction. (2019). *Global Assessment Report on Disaster Risk Reduction 2019*.

7 Presentation of Authors

Matjaž Nekrep Perc is a Researcher and Senior Lecturer at the Faculty of Civil Engineering, Transportation Engineering and Architecture, University of Maribor, Slovenia

Janja Kramer Stajnko is a Researcher and Associate Professor at the Faculty of Civil Engineering, Transportation Engineering and Architecture, University of Maribor, Slovenia

Integrated Risk Assessment of Legionella Proliferation in Cold Drinking Water Systems: A Hospital Case Study

Z. Vranayova (1), D. Kosicanova (1) and D. Kaposztasova (1)

(1) zuzana.vranayova@tuke.sk, danica.kosicanova@tuke.sk, daniela.kaposztasova@tuke.sk

(1) Department of Building Services, Institute of Architectural Engineering, Faculty of Civil Engineering, Technical University of Kosice, Slovakia

Abstract

Legionella pneumophila is increasingly recognized as a microbiological hazard not only in hot water systems but also in cold drinking water networks, particularly in healthcare facilities exposed to elevated thermal stress. This study presents an integrated risk assessment of Legionella proliferation in the cold drinking water system of a continuously operated hospital in Košice, Slovakia. The assessment combined hydraulic analysis, simplified thermal modelling, and a semi-quantitative risk evaluation considering temperature, stagnation, hydraulic conditions, and biofilm formation.

The analysed DN80 steel pipeline, installed in a technical shaft with summer ambient temperatures of 25–30 °C, operated under fully turbulent flow conditions (1.5 m/s; Re > 10^5), providing rapid water exchange and limiting temperature increase during normal operation. Thermal analysis showed that the 19 mm insulation layer delayed the critical 20 °C threshold to approximately 10–12 hours of stagnation. Under typical hospital operating conditions, such stagnation periods were considered unlikely.

The results demonstrate that microbiological stability depends primarily on the combined effects of hydraulic performance, thermal exposure, stagnation duration, and biofilm development rather than on water temperature alone. The proposed methodology provides a practical engineering framework to support Water Safety Plans and the management of cold drinking water systems in healthcare facilities.

Keywords: *Legionella pneumophila*; cold drinking water systems; healthcare facilities; hydraulic performance; thermal exposure; risk assessment.

1 Introduction

Legionella pneumophila is one of the most significant microbiological hazards in building water systems, particularly in healthcare facilities where vulnerable occupants are continuously exposed (CDC, 2025; Ji et al., 2025). Although traditionally associated with hot water systems, cooling towers, and aerosol-generating devices, recent studies have demonstrated that cold drinking water systems may also support bacterial proliferation when water temperatures exceed 20 °C because of heat transfer, prolonged stagnation, and biofilm development (Bédard et al., 2025; Ji et al., 2025; Revetta et al., 2025).

Elevated ambient temperatures, climate change, and the increasing thermal insulation of modern buildings contribute to the warming of cold-water distribution systems, particularly in technical shafts where hot and cold pipelines are installed in close proximity (Arqué et al., 2026; Bédard et al., 2025). Additional factors such as low flow velocity, dead legs, oversized pipework, and irregular water consumption further increase the risk of biofilm formation and microbiological instability (Proctor et al., 2020; Revetta et al., 2025). Consequently, current engineering practice recommends integrated risk management based on hydraulic performance, thermal control, and operational measures within Water Safety Plans (WSP) and related guidelines (WHO, 2007; EN 806-2; VDI 6023).

This paper presents a hospital case study from Košice, Slovakia, evaluating the risk of *Legionella* proliferation in a cold drinking water distribution system. The proposed methodology integrates hydraulic analysis, simplified thermal assessment, and a semi-quantitative risk evaluation to identify operational risk factors and support practical mitigation strategies for healthcare facilities.

2 Literature Review

Recent studies have demonstrated that *Legionella pneumophila* may proliferate not only in hot water systems but also in cold drinking water networks when hydraulic and thermal conditions become unfavourable (CDC, 2025; Ji et al., 2025; Bédard et al., 2025). Heat transfer from adjacent hot-water pipelines, elevated ambient temperatures, and prolonged stagnation can increase cold-water temperatures above the recommended limit of 20 °C, creating conditions that support bacterial growth (WHO, 2007; Directive (EU) 2020/2184; EN 806-2; VDI 6023).

Hydraulic conditions strongly influence microbiological stability. Low flow velocities, extended residence times, oversized pipework, and dead legs promote biofilm formation, providing protection against disinfectants and creating favourable environments for *Legionella* colonization (Van der Kooij, 2003; Proctor et al., 2020; Revetta et al., 2025). Conversely, regular hydraulic exchange and turbulent flow reduce sediment deposition and limit biofilm development.

Thermal interaction between hot and cold pipelines installed in confined technical shafts has become an important issue in modern buildings, particularly during summer operation. Previous studies have shown that insufficient insulation and limited water demand may substantially increase cold-water temperatures, thereby increasing microbiological risk (Arqué et al., 2026; Bédard et al., 2025).

Current engineering practice recommends integrated risk management based on Water Safety Plans (WSP), combining hydraulic design, temperature monitoring, operational management, and preventive maintenance to ensure the hygienic safety of building water systems (BS 8680; CDC, 2025; VDI 6023). However, relatively few studies integrate hydraulic performance, thermal behaviour, and operational conditions into a practical engineering risk assessment for continuously operated healthcare facilities. This research addresses that gap through an integrated semi-quantitative assessment applied to a hospital cold drinking water system.

3 Aims and Methods

3.1 Research Aim

The aim of this study was to evaluate the risk of *Legionella pneumophila* proliferation in the cold drinking water distribution system of a continuously operated hospital in Košice, Slovakia. The assessment integrated hydraulic analysis, simplified thermal modelling, and a semi-quantitative risk evaluation to examine the influence of thermal exposure, hydraulic conditions, stagnation, and biofilm formation under realistic operating conditions.

Specifically, the study aimed to:

- quantify the thermal behaviour of a DN80 cold water pipeline exposed to elevated ambient temperatures (25–30 °C);
- evaluate the effect of thermal insulation on water temperature increase during stagnation;
- determine the stagnation period required to reach the critical temperature threshold of 20 °C; and
- assess the contribution of hydraulic flow conditions to microbiological stability and operational risk.

The research hypothesis was that continuous hydraulic exchange, turbulent flow, appropriate thermal insulation, and the elimination of dead legs significantly reduce the risk of *Legionella* proliferation in cold drinking water systems. It was further hypothesised that hydraulic performance and operational water exchange have a greater influence on microbiological stability than thermal insulation alone.

3.2 System Description

The analysed system comprises the cold drinking water distribution network of a continuously operated tertiary-care hospital in Košice, Slovakia. The facility has more than 500 beds and permanent occupancy, resulting in stable water demand and continuous hydraulic exchange. Owing to its operational characteristics and high hygiene requirements, the hospital provides a representative case study for evaluating the risk of *Legionella* proliferation in cold drinking water systems.

The distribution network includes a municipal cold-water supply, vertical risers, horizontal distribution pipelines, and terminal outlets serving hospital wards and sanitary facilities. The assessment focused on system components with an increased potential for microbiological risk, including thermally exposed technical shafts, terminal branches, low-use sections, and locations where hot and cold water pipelines are installed in close proximity.

The analysed pipeline section consisted of a 4 m long DN80 steel pipe installed in a technical shaft exposed to summer ambient temperatures of 25–30 °C. The pipe was insulated with a 19 mm polyethylene insulation layer (thermal conductivity $\lambda = 0.040$ $W \cdot m^{-1} \cdot K^{-1}$). The principal system parameters are summarized in Table 1.

The inlet cold-water temperature ranged from 10 to 15 °C, with 15 °C representing the summer design condition. Under normal operation, the pipeline operated at an average flow velocity of approximately 1.5 m/s, ensuring continuous water renewal and preventing prolonged stagnation.

Table 1 – The main system parameters

Parameter	Value
Pipe material	Steel
Nominal diameter	DN80
Internal diameter	76.1 mm
External diameter	89 mm
Pipe length	4.0 m
Water volume	20.1 L
Volume per meter	5.02 L/m
Insulation thickness	19 mm
Thermal conductivity	0.040 $W \cdot m^{-1} \cdot K^{-1}$
Cold water temperature	10–15 °C
Ambient temperature	25–30 °C
Flow velocity	1.5 m/s

3.3 Hydraulic Analysis

Hydraulic conditions were evaluated under normal operating and stagnation scenarios to assess their influence on water residence time and the potential risk of *Legionella pneumophila* proliferation. Under standard operating conditions, the residence time within the analysed DN80 pipeline was calculated as:

$$t = \frac{L}{v} = \frac{4}{1.5} = 2.67 \text{ s} \qquad (1)$$

where: t – residence time (s)

L – pipeline length (m)

v – mean flow velocity (m/s)

The calculated residence time of 2.67 s indicates rapid hydraulic renewal of the analysed pipeline section. The Reynolds number exceeded $Re > 10^5$, confirming fully turbulent flow conditions. Turbulent flow promotes continuous water exchange, limits sediment deposition, and reduces the potential for biofilm formation. The Reynolds

number was determined from the measured flow velocity, internal pipe diameter, and the kinematic viscosity of water at the operating temperature.

The hydraulic assessment also considered operational characteristics of the hospital water system, including continuous occupancy, regular water consumption, and the absence of dead legs exceeding 2 m. These conditions minimise prolonged stagnation under normal operation. To evaluate potential worst-case scenarios, additional analyses were performed assuming reduced water demand or temporary interruption of flow (Table 2).

Table 2 – Estimated water temperature under stagnation conditions

Stagnation duration	Estimated water temperature
10–12 h	20 °C
24–30 h	25–27 °C
>48 h	Flushing and disinfection required

Temperatures above 20 °C are generally considered to increase the potential for *Legionella* growth, whereas the range of 25–45 °C provides favourable conditions for bacterial proliferation. According to the Slovak Ministry of Health Regulation No. 91/2023 Coll., prolonged stagnation requires flushing and, where necessary, disinfection of the affected pipeline sections. However, owing to the continuous operation of the hospital and stable hydraulic conditions, stagnation periods exceeding 10 h were considered unlikely within the analysed DN80 pipeline under normal operating conditions.

3.4 Simplified Thermal Analysis

The thermal behaviour of the analysed cold drinking water system was evaluated using a simplified engineering heat-transfer model to estimate the temperature development of the pipeline under normal operating and stagnation conditions. The assessment considered conductive heat transfer through the insulation layer, thermal interaction with the surrounding environment and adjacent hot-water pipelines, as well as the thermal inertia of the water contained within the pipeline.

The analysis assumed one-dimensional radial heat transfer under steady summer ambient conditions representative of technical shafts (25–30 °C). The inlet cold-water temperature was taken as 15 °C, representing the worst-case seasonal condition supplied from the municipal distribution network. Thermal properties of the steel pipe and insulation material were assumed constant throughout the analysis, while short-term ambient temperature fluctuations, solar radiation, and internal heat sources were neglected. Consequently, the model provides a conservative engineering approximation suitable for comparative risk assessment rather than detailed transient thermal simulation.

The analysed DN80 pipeline was insulated with a 19 mm polyethylene insulation layer (thermal conductivity $\lambda = 0.040\ W \cdot m^{-1} \cdot K^{-1}$), which reduced heat transfer from the surrounding environment and delayed water temperature increase during stagnation

(Fig. 1). Owing to the relatively large water volume and the high specific heat capacity of water (4.18 $kJ \cdot kg^{-1} \cdot K^{-1}$), the system exhibited considerable thermal inertia, limiting rapid temperature changes.

Under normal operating conditions, the calculated residence time of 2.67 s ensured continuous hydraulic renewal of the pipeline. As a result, the estimated temperature increase during flow remained below 0.1 °C within the analysed section despite elevated ambient temperatures. This indicates that hydraulic renewal is the dominant factor maintaining thermal stability during normal operation, whereas thermal insulation primarily delays temperature increase during prolonged stagnation.

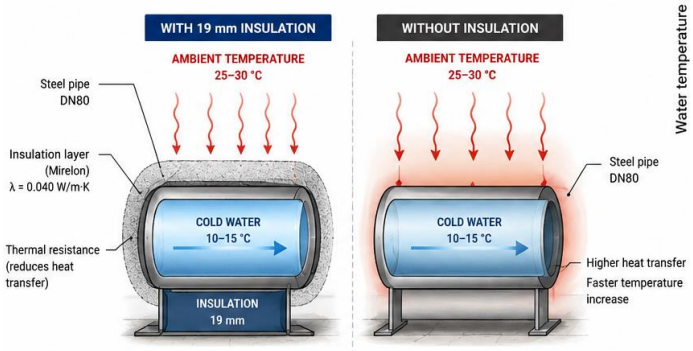

Figure 1. Thermal interactions affecting the analysed cold drinking water pipeline.

3.5 Risk Assessment and International Case Comparisons

The risk assessment framework integrated four principal parameters influencing the potential for *Legionella pneumophila* proliferation: water temperature, stagnation duration, hydraulic conditions, and biofilm development. These parameters were evaluated using a semi-quantitative approach derived from published microbiological evidence and engineering guidance for building water systems. The corresponding biological response of *Legionella* under different temperature conditions is summarized in Table 3.

Table 3 – Temperature-dependent biological response of *Legionella*

Water range	Biological response
<20 °C	Dormant state (viable but non-proliferative)
20–25 °C	Limited growth potential
25–45 °C	Favourable growth conditions
35–42 °C	Optimum proliferation range
>60 °C	Rapid thermal inactivation

The proposed methodology was benchmarked against documented international hospital case studies where *Legionella* proliferation was associated with inadequate hydraulic renewal, prolonged stagnation, or excessive thermal exposure (Table 4).

Table 4 – International studies

Case study	Main finding
Spain (Arqué et al., 2026)	Stagnation exceeding 12 h increased cold-water temperature above 22 °C, resulting in Legionella detection
Iran (Ji et al., 2025)	Seasonal cold-water temperatures above 20 °C were associated with an increased quantitative microbial infection risk.
United Kingdom (Legionella on Tap, 2025)	A hospital outbreak was linked to prolonged stagnation in a dead-leg section of a cold-water dispenser

To evaluate the operational performance of the analysed hospital, its hydraulic and thermal characteristics were compared with those reported in documented outbreak investigations (Table 5).

Table 5 – Comparison between the hospital and documented high-risk systems

Parameter	Košice hospital	Reported outbreak cases
Occupancy	Continuous	Seasonal/intermittent
Thermal insulation	19 mm	Insufficient or absent
Dead legs	Not identified	Frequently present
Hydraulic regime	Fully turbulent (1.5 m/s)	Low-flow conditions
Stagnation	Operationally unlikely	Frequent
Overall risk	Low	Documented outbreaks

The comparative assessment demonstrated that the analysed hospital operates under conditions that substantially reduce the likelihood of *Legionella* proliferation. Continuous occupancy ensures regular hydraulic renewal, while turbulent flow and appropriate thermal insulation limit both biofilm formation and water temperature increase during normal operation. The estimated stagnation period required to reach the critical temperature threshold of 20 °C (10–12 h) considerably exceeds expected residence times in the analysed pipeline.

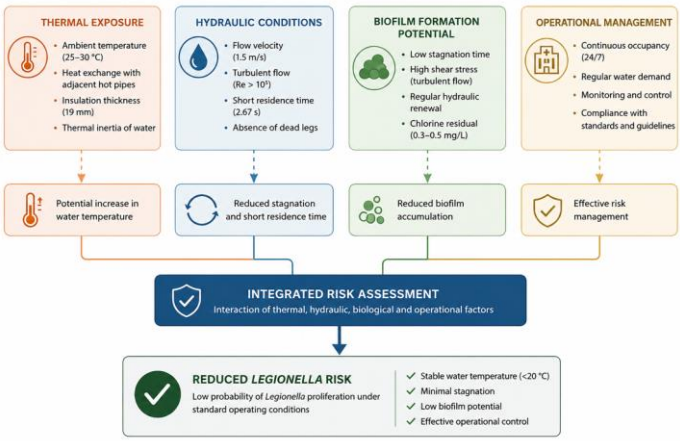

Figure 2. Interaction of thermal, hydraulic, biological, and operational factors influencing *Legionella* proliferation risk.

Overall, the proposed methodology combines hydraulic analysis, simplified thermal assessment, and operational evaluation into a practical engineering framework for

identifying potential *Legionella* risk in healthcare water systems. Although developed for a hospital environment, the methodology is applicable to other large public buildings with similar hydraulic and thermal operating conditions (Figure 2).

4 Results and Discussion

4.1 Thermal Behaviour of the Analysed System

The analysed DN80 cold drinking water branch maintained stable thermal and hydraulic conditions under normal hospital operation. Figure 3 illustrates the configuration of the investigated distribution system, highlighting thermally exposed technical shafts and hydraulically sensitive locations considered in the assessment.

Despite summer ambient temperatures of 25–30 °C, no significant increase in water temperature was observed during normal operation. Continuous water demand ensured rapid hydraulic renewal, resulting in a residence time of only 2.67 s and preventing prolonged thermal exposure of the transported water.

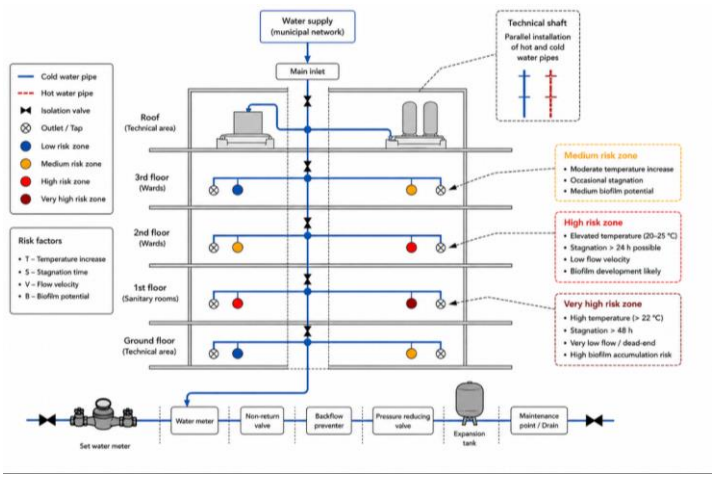

Figure 3. Schematic layout of the analysed hospital cold water distribution system with identified thermally exposed and hydraulically sensitive zones.

The results indicate that the combined effect of continuous hydraulic renewal and the high specific heat capacity of water effectively limited temperature increase within the analysed pipeline. Consequently, thermal conditions favourable for *Legionella* proliferation were not reached during normal operating conditions. These findings demonstrate that hydraulic performance plays a more significant role in maintaining thermal stability than ambient temperature alone, while thermal insulation primarily delays temperature increase during periods of stagnation.

The observed behaviour is consistent with previous studies reporting that continuous water renewal is one of the most effective measures for preventing microbiological deterioration in building water systems (Proctor et al., 2020; Bédard et al., 2025; Revetta et al., 2025).

4.2 Temperature Development under Stagnation Conditions

Under stagnation conditions, ambient thermal exposure became the dominant factor influencing water temperature. Figure 4 illustrates the simulated temperature evolution of the analysed DN80 pipeline for different insulation scenarios.

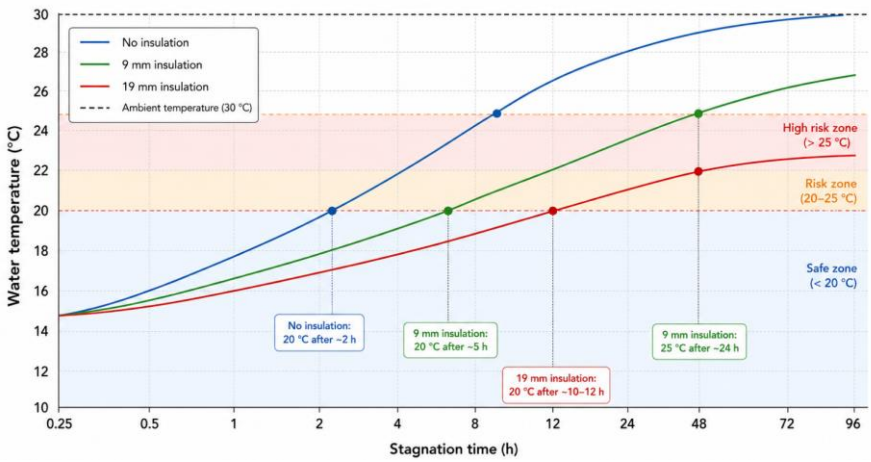

Figure 4. Simulated water temperature development within the DN80 cold drinking water pipeline under stagnation conditions for different insulation thicknesses.

The results demonstrate a substantial influence of thermal insulation on delaying water temperature increase. In the uninsulated pipeline, the critical temperature threshold of 20 °C was reached after approximately 1.5–2 h of stagnation. In contrast, the 19 mm insulation layer extended this period to approximately 10–12 h, significantly reducing the duration of exposure to temperatures favourable for *Legionella* growth.

Further temperature increase to 25–27 °C, representing conditions favourable for bacterial proliferation, occurred only after approximately 24–30 h without water renewal. These findings indicate that thermal insulation effectively delays heat transfer during stagnation; however, it cannot compensate for prolonged periods without water movement. Consequently, hydraulic renewal remains the primary mechanism controlling microbiological stability, while insulation provides an important secondary protective effect.

Under normal hospital operating conditions, characterised by continuous occupancy and regular water demand, stagnation periods exceeding 10 h were considered highly unlikely. Therefore, the analysed distribution system is expected to maintain cold-water temperatures below the critical threshold during standard operation. These findings are consistent with previous studies emphasising the combined importance of hydraulic performance and thermal control in preventing *Legionella* proliferation in building water systems (Proctor et al., 2020; Bédard et al., 2025).

Thermal insulation effectively delays heat transfer during stagnation; however, it cannot compensate for prolonged periods without water movement. From an engineering perspective, the results suggest that maintaining regular water renewal is more effective for controlling *Legionella* risk than increasing insulation thickness

alone. Therefore, hydraulic design and operational management should be considered the primary preventive measures, while thermal insulation should be regarded as a complementary mitigation strategy.

4.3 Integrated Legionella Risk Assessment

The semi-quantitative risk assessment integrated the combined effects of thermal exposure, stagnation duration, hydraulic performance, and biofilm development to classify the operational risk of *Legionella pneumophila* proliferation. Figure 5 presents the proposed risk matrix, which provides a practical engineering tool for evaluating microbiological risk under different operating conditions.

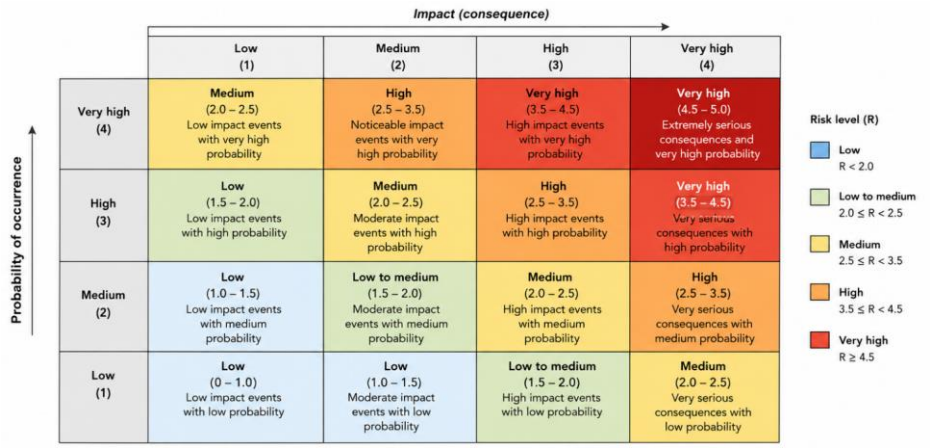

Figure 5. Semi-quantitative risk matrix illustrating the interaction between stagnation probability and microbiological impact in cold drinking water systems.

The assessment identified prolonged stagnation, elevated water temperatures (>22 °C), reduced hydraulic renewal, and increased biofilm development as the principal factors contributing to *Legionella* proliferation risk. These conditions correspond to high- and very high-risk zones within the proposed matrix and are consistent with previously reported hospital outbreak investigations.

In contrast, the analysed hospital distribution system exhibited favourable hydraulic and operational characteristics, including continuous occupancy, fully turbulent flow ($Re > 10^5$), adequate thermal insulation, and the absence of significant dead legs. These factors promoted regular water renewal and limited the duration of exposure to temperatures favourable for bacterial growth. Consequently, the analysed DN80 pipeline was classified as a **low-risk operational zone** under normal operating conditions.

Comparison with documented international case studies further supports this classification. Unlike reported outbreak systems characterised by intermittent occupancy, prolonged stagnation, and inadequate hydraulic performance, the investigated hospital maintained continuous water demand and stable operating conditions, substantially reducing the potential for microbiological instability.

Overall, the results demonstrate that *Legionella* proliferation is governed by the combined interaction of hydraulic, thermal, biological, and operational factors rather than by water temperature alone. The proposed semi-quantitative framework therefore provides a practical engineering approach for supporting Water Safety Plans and operational risk management in healthcare water systems. Unlike conventional approaches, the proposed framework integrates hydraulic, thermal, biological and operational factors into a single engineering risk assessment methodology.

4.4 Study Limitations

The proposed methodology represents a practical engineering approach for assessing *Legionella pneumophila* proliferation risk in cold drinking water systems. The thermal assessment was based on simplified heat-transfer assumptions and did not include computational fluid dynamics (CFD) or transient three-dimensional modelling. Likewise, the risk assessment was developed using hydraulic analysis, engineering calculations, and published microbiological evidence rather than direct microbiological sampling. Although these simplifications limit the quantitative prediction of bacterial proliferation, they enable a transparent and practical evaluation of operational risk suitable for engineering applications. Future research should combine advanced hydraulic modelling, continuous temperature monitoring, and microbiological analyses to further validate and refine the proposed risk assessment framework.

5 Conclusions

This study presented an integrated engineering assessment of *Legionella pneumophila* proliferation risk in the cold drinking water system of a continuously operated hospital in Košice, Slovakia. The results demonstrated that microbiological stability depends on the combined interaction of hydraulic performance, thermal conditions, operational water renewal, and biofilm development rather than on water temperature alone.

The analysed DN80 pipeline operated under favourable hydraulic and thermal conditions through continuous hydraulic renewal, fully turbulent flow ($Re > 10^5$), and appropriate thermal insulation. Under normal hospital operation, these factors prevented prolonged stagnation and limited water temperature increase, resulting in a low operational risk of *Legionella* proliferation. Thermal insulation significantly delayed temperature increase during stagnation; however, hydraulic renewal proved to be the dominant factor governing microbiological stability.

Comparison with documented international outbreak cases confirmed that continuous occupancy, adequate hydraulic design, and the elimination of dead legs substantially reduce the likelihood of conditions associated with *Legionella* growth. These findings emphasise the importance of integrating hydraulic performance into Water Safety Plans alongside conventional thermal and operational control measures.

The proposed semi-quantitative framework provides a practical engineering tool for identifying potential risk zones and supporting operational decision-making in healthcare facilities. Although developed for a hospital environment, the methodology is applicable to other large public buildings where hydraulic and thermal conditions influence drinking water safety.

7 Acknowledgements VEGA research project Nr. 1/0382/25.

8 References

Arqué, E., et al. (2026). *Impact of climate change on Legionnaires' disease incidence in Catalonia*. Environmental Health Perspectives.

Bédard, E., Laferrière, C., Déziel, E., et al. (2025). *Thermal contamination contributes to Legionella proliferation in building water systems*. Water Research.

CDC (2025). *Developing a Water Management Program to Reduce Legionella Growth and Spread in Buildings*. U.S. Department of Health and Human Services.

BS 8680:2020. *Water quality – Water Safety Plans – Code of practice*. British Standards Institution.

EN 806-2. (2021). *Specifications for installations inside buildings conveying water for human consumption – Part 2: Design*. European Committee for Standardization.

European Parliament and Council. (2020). *Directive (EU) 2020/2184 on the quality of water intended for human consumption*. Official Journal of the European Union.

Ji, P., et al. (2025). *Quantitative microbial risk assessment of Legionella in hospital cold water systems*. Journal of Water and Health.

Legionella on tap: Nosocomial pneumonia cluster linked to a hospital cold water dispenser. (2025). Infection Control & Hospital Epidemiology.

Proctor, C. R., et al. (2020). *Considerations for large building water quality after extended stagnation*. AWWA Water Science, 2(4), e1175. https://doi.org/10.1002/aws2.1175

Revetta, R. P., et al. (2025). *Legionella pneumophila response to shifts in biofilm structure mediated by hydrodynamics*. Applied and Environmental Microbiology.

Rhoads, W. J., et al. (2015). *Water heater temperature set point and water use patterns influence Legionella pneumophila and associated microorganisms in hot water plumbing systems*. Microbiome, 3, 67.

Van der Kooij, D. (2003). *Managing regrowth in drinking-water distribution systems*. Water Supply, 3(1–2), 119–125.

VDI 6023. (2023). *Hygiene in drinking water installations – Requirements for planning, execution, operation and maintenance*. Verein Deutscher Ingenieure.

World Health Organization. (2007). *Legionella and the Prevention of Legionellosis*. WHO Press.

Presentation of Author(s)

Prof. Ing. Zuzana Vranayova has been involved in scientific research and teaching activities at the Technical University of Košice, Faculty of Civil Engineering for a long time. Her professional interest is oriented toward the sustainable and safe water supply in buildings. She and her co-authors are internationally recognised experts in sustainable building water systems, green buildings, and urban water management, and actively participate in international research projects and conferences.

Comparison of Droplet Dispersal in Three Types of Hand Dryers

Ayaka Kimura (1), Masayuki Otsuka (2), Riki Tanaka (3)

(1) d24J3002@kanto-gakuin.ac.jp
(2) dmotsuka@kanto-gakuin.ac.jp
(3) ri-tanaka3019@outlook.jp

(1) Doctoral Student in Architecture, Graduate School of Engineering at Kanto Gakuin University, Japan
(2) Prof. Dr. Eng, Department of Architecture and Environmental Design, College of Architecture and Environmental Design, Kanto Gakuin University, Japan
(3) M. Eng., Former Graduate School of Engineering, Kanto Gakuin University, Japan

Abstract

In Japan, the use of hand dryers for drying hands after washing was temporarily restricted during the COVID-19 pandemic owing to concerns that they might induce droplet infection. Currently, the WHO emphasizes the importance of handwashing and hand drying after using the restroom. However, considering the earlier restriction on the use of hand dryers, it is necessary to enhance the knowledge on water droplet and aerosol dispersal during hand-dryer use. In addition, it is essential to examine the effectiveness of hand dryers and reconsider the prevailing hygiene and maintenance methods. The authors reported on the status of droplet dispersal during hand-dryer use at the 49th International Symposium CIB W062 (Northampton) held in 2023[1]. In this study, the dispersal of water droplets and aerosols during hand-dryer use was recorded for three types of hand dryers—single-sided blow-type and double-sided blow-type jet air dryers, and a suction-type dryer designed to suppress water-droplet dispersal—using particle counter measurements. Furthermore, the effectiveness of hand-dryer use was evaluated based on the bacterial count adhering to the hands. The findings showed

distinct differences in aerosol dispersal and bacterial adhesion among the three hand dryer types, indicating model-dependent variations in hygiene efficacy.

Keywords
Infectious diseases, Aerosol, Hand dryer

1 Introduction

The infection prevention guidelines formulated by the Japan Business Federation (Keidanren) in May 2020 includes a recommendation to suspend the use of hand dryers [2] [3]. Subsequently, since the designation of COVID-19 as a "Class 5 Infectious Disease" in Japan in 2023, that is, it is managed as an infectious disease subject to normal surveillance without requiring special behavioral restrictions, the Ministry of Health, Labour and Welfare issued guidelines that state that hand dryers in public restrooms can be used under the conditions of sufficient handwashing and appropriate cleaning and management. In addition, ISRAE (India) issued guidelines recommending handwashing with soap and alcohol disinfection [4], but REHVA (Europe) and IAPMO (USA) contain no recommendations for handwashing or restrictions on the use of hand dryers [5] [6]. The WHO recommends the use of both paper towels and hand dryers as suitable drying methods after handwashing [7].

A representative study regarding the dissemination of water droplets and aerosols during hand-dryer use was conducted by Takeuchi et al. [8] in Japan. The study clarified the differences in the amount of dispersed water droplets (particle sizes 0.5 to 2.0 mm) around double-sided hand dryers through visualization experiments using a laser light source and diffuse reflection camera. In other countries, reports from the ETS (European Tissue Paper Industry Association) [9] and studies by P.T. Kimmitt et al. [10] measured the dispersal status of bacteria (aerosols) for three types of hand-drying methods: paper towels, warm-air dryers, and jet air dryers. The results showed that warm-air dryers dispersed approximately five times more aerosols and jet air dryers approximately 24 times more aerosols than that dispersed by paper towels. It has also been pointed out that bacteria remain in the air near jet air dryers even after the 15 s hand-drying period has elapsed.

Regarding the dispersal of bacteria, bacterial growth, and disinfection effects during hand-dryer use, Kimura et al. [11] investigated bacterial contamination in hospital restrooms through swabbing tests. They pointed out that the detected amounts of bacteria on the entrance door handles and switches were tens to hundreds of CFU/mL, but the count inside hand dryers was much higher (1000 CFU/mL or more).

J.H. Taylor et al. [12] measured the number of microorganisms adhering to the hands by applying the contact plate method after handwashing with soap followed by hand drying. They pointed out that the number of bacteria adhering to the hands decreases as the hand-drying duration increases and the hands become visibly drier.

Based on the above background, this study had three objectives. The first was to clarify the dispersal status of water droplets and aerosols during the use of three commercially available hand-dryer models through particle measurements using a particle counter. The second was to evaluate the hygiene efficacy of hand dryers during use by measuring the changes in the residual water volume on the hands and bacterial count adhering to the hands. The third was to obtain basic knowledge for improving the cleaning and maintenance of hand dryers by measuring and evaluating the bacterial count inside each type of device.

2 Hand Dryers used in this Study

In this study, (1) aerosol dispersal, (2) bacterial count adhering to the hands, (3) residual water volume on the hands, and (4) bacterial count inside the device were measured for the three types of hand dryers shown in Figure 1 and described in Table 1. Hand dryers are commonly categorized as the conventional type (warm-air type) that evaporates water using warm air accompanied by rubbing of the hands, and the jet-type that blows away water droplets instantaneously by blowing jet air from nozzles fixed in the hand-drying chamber. In this study, the following jet-type hand dryers were examined: double-sided blow-type (Fig. 1(1)) used in previous studies, single-side blow-type (Fig. 1(2)), and suction-type (Fig. 1(3)).

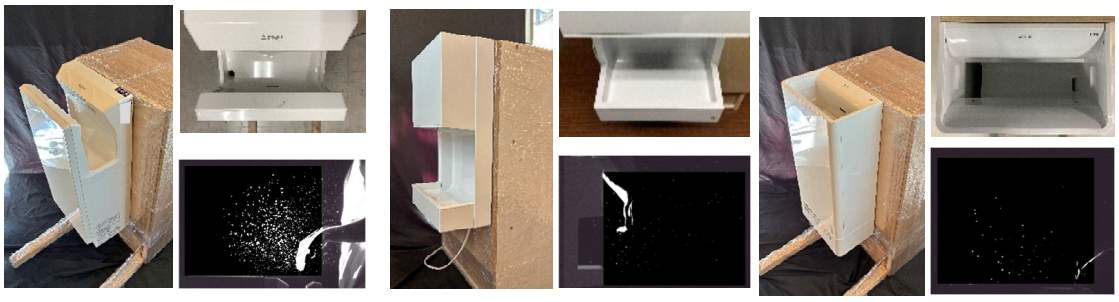

(1) Double-sided blow-type **(2) Single-sided blow-type** **(3) Suction-type**

Figure 1 External appearance of the tested hand dryers and illustration of water-droplet dispersal (image processing)

Table 1 Specifications of the tested hand dryers

	Double-sided blow-type	Single-sided blow-type	Suction-type
Blow nozzle wind speed [m/s]	98	110	90
Rated power [W]	1080	590	920

*In all cases, air volume setting: High, Heater: Off

3 Measurement of Aerosol Generation

In this experiment, a particle counter was used to measure the amount of aerosol generation in front of and above the various hand dryers during use, and the dispersal status was analyzed. The experiment was conducted in a clean room meeting ISO Class 5 standards.

3.1 Experimental overview

Figure 2 shows the measurement system. The hand dryers shown in Figure 1 and a particle counter were used for the measurements. The hand dryers were installed according to the height recommended by the manufacturers, and the particle counter was installed at five vertical points to measure the amount of aerosol generation during use. The blow nozzle position of each hand dryer was set as the reference measurement point, and particle counters were installed every 200 mm in the vertical direction from this point. The measurement point at a height of approximately 1400 mm from the floor was defined as the breathing zone height for a person in a standing position. The suction flow rate of the particle counter was 2.83 L/min, measured particle size d was 0.3 μm or more and less than 5.0 μm, and measured particle size categories were $0.3 \leq d < 0.5$, $0.5 \leq d < 0.7$, $0.7 \leq d < 1.0$, $1.0 \leq d < 2.0$, and $2.0 \leq d < 5.0$ μm.

In the measurement, sufficient ventilation was ensured using a fan filter unit in the clean room, and after stopping it, a 10 min stabilization period was observed. Next, the particle counter was started; the experiments inserted their hands into the hand-drying chamber after 30 s, and the measurements were obtained for 180 s. At this time, the measurement interval of the particle counter was set to one second. In addition, to eliminate the influence of dust generation from the human body, the experimenters wore dust-free clothing and vinyl gloves (powder-free) and entered the room after taking an air shower.

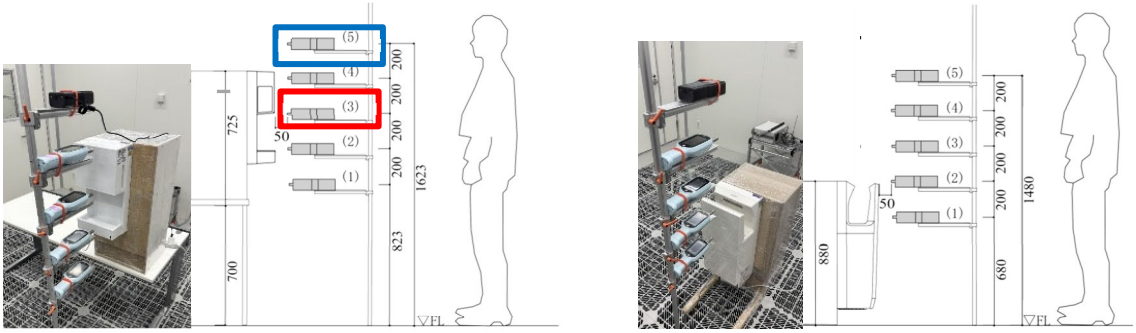

(1) Single-sided blow-type **(2) Double-sided blow-type, Suction-type**

*Parenthetical numbers indicate the measurement points.
**Red frames in the figure indicate the reference measurement points, and blue frames indicate the breathing zone height.

Figure 2 Aerosol measurement system [mm] (elevation view)

3.2 Experimental results and discussion

3.2.1 Time-course changes in number of aerosols

Figure 3 shows the representative waveforms of the number of aerosols for each hand dryer by particle size at the reference point and breathing zone for the following conditions: air volume set to High, drying time of 20 s, and hands are held steady without insertion/removal. The average waveform from five trials was calculated as the representative waveform, The root mean square error indicating the difference between each waveform and the average waveform was evaluated, and the one with the minimum error was selected.

First, at the reference measurement point for (1) the single-sided blow-type hand dryer, the number of aerosols generated increased from the start of use, then decreased to approximately 500 after 10 s, but increased subsequently until the end of use, reaching a maximum of approximately 1,000. The total number of aerosols generated over 180 s exceeded 20,000, which was approximately ten times that of the double-sided type described later. In the breathing zone, the number immediately after start of use was approximately 450, but it gradually increased similar to the trend at the reference point, reaching a maximum of approximately 700, and the total number of aerosols generated exceeded 12,000.

Next, for (2) the double-sided blow-type hand dryer, aerosols were generated from the start of use, as in the single-sided blow-type, but the maximum number of aerosols generated at the reference point was approximately 100, which decreased over time, and the total number was approximately 2,000. Furthermore, in the breathing zone, the maximum number of aerosols generated was approximately 30, a reduction of 85% when compared with the maximum value for the single-sided blow-type, and the total number was less than 1,000.

For (3) the suction-type hand dryer, the maximum number of aerosols generated at the

reference point was suppressed to approximately 40, and the dispersal of aerosols was considered to be suppressed by the drying air and surrounding air being sucked in through the suction port.

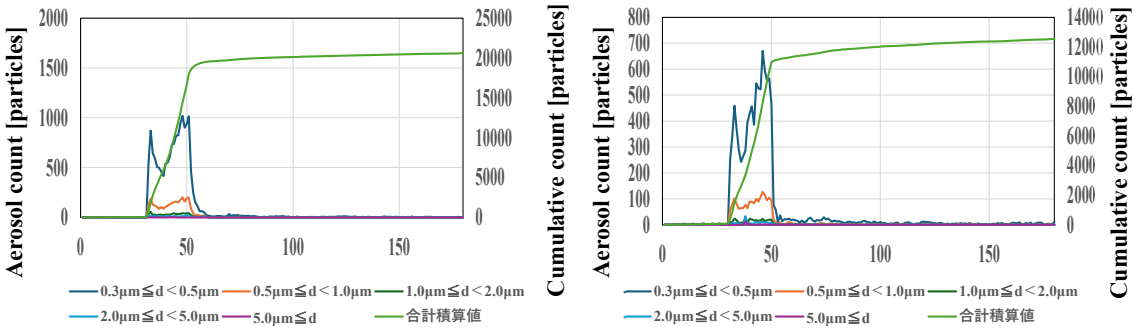

(a) Reference measurement point (Measurement point 3) (b) Breathing zone (Measurement point 4)

(1) Single-sided blow-type

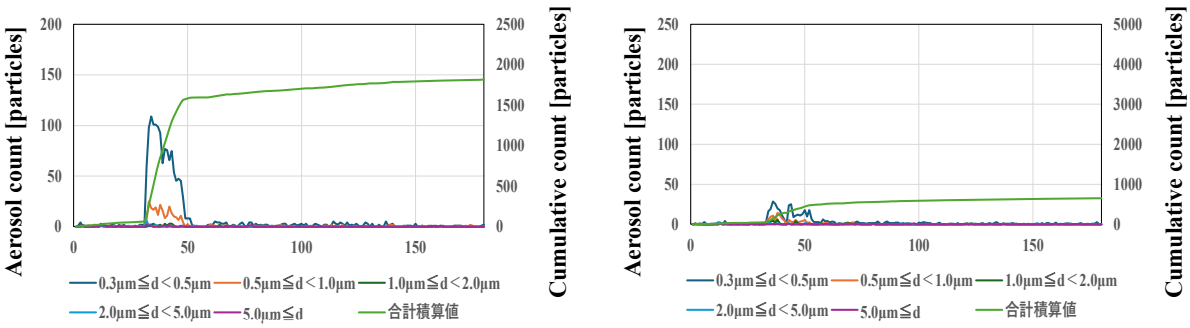

(a) Reference measurement point (Measurement point 2) (b) Breathing zone (Measurement point 5)

(2) Double-sided blow-type

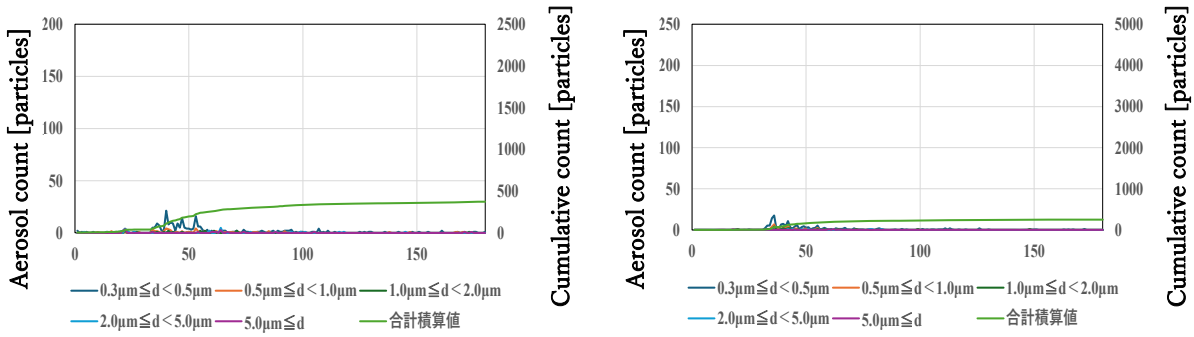

(a) Reference measurement point (Measurement point 2) (b) Breathing zone (Measurement point 5)

(3) Suction-type

Figure 3 Time-course changes in the number of generated aerosols and integrated values during the use of different types of hand dryers

3.2.2 Vertical distribution of aerosols

Figure 4 shows the vertical distribution of the total number of aerosols under the conditions of high air volume, drying time of 20 s, and hand held steady without

insertion/removal. The single-sided blow-type had the highest count of aerosols (approximately 19,000 aerosols were detected), whereas the count for the other two types of hand dryers were significantly lower—approximately 1,700 for the double-sided blow-type and approximately 1,800 for the suction-type; it was confirmed that the single-sided blow-type dispersed more than ten times as many particles. In addition, approximately 7,000 particles were measured in the vicinity of the breathing zone for the single-sided blow-type, which was greater than that in the other models. The possible reasons for this are the single-sided blow-type has a greater installation height and its blow nozzle is located near the breathing zone; although air blows downward from the nozzle, it was confirmed that the aerosols are additionally dispersed to the front and upper sides of the device.

In the suction-type, as mentioned in Section 3.2(1), the number of particles at the reference point decreased by approximately 82% when compared with that in the double-sided type. However, at measurement point 3, approximately 1,800 aerosols were dispersed, which is equivalent to the count at the reference measurement point (measurement point 2) of the double-sided blow-type. This is attributed to the difference in shape between the suction-type and double-sided blow-type models. In the double-sided blow-type, the sides of the hand-drying chamber are largely open, and air and aerosols blow out upward and to the left and right sides. In contrast, in the suction-type, aerosols are sucked into the device near the center of the blow-off port, but because the sides are closed, the air moving in the left and right directions is forced to escape upward along the sides, thus dispersing the aerosols.

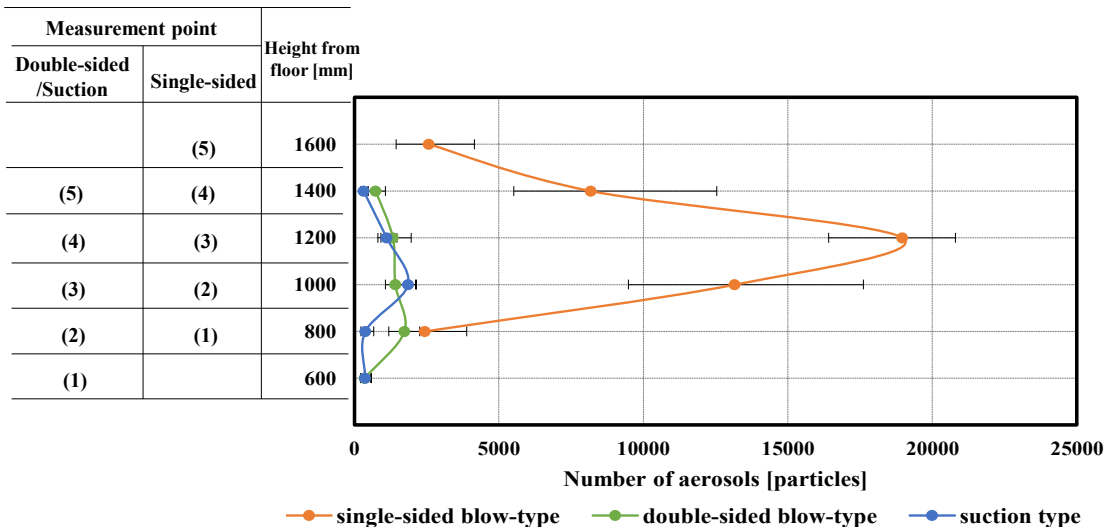

Figure 4Vertical distribution of total aerosol count

3. Measurement of Bacterial Count Adhering to Hands Before and After Hand-Dryer Use

3.1. Experimental overview

Bacteria adhering to hands were measured using the environmental microbial testing medium for general bacteria, shown in Photo 1. Figure 5 shows the measurement flow. The palm is pressed against the medium, which is then cultured for 48 h (2 days) in an incubator set at 35°C, after which a photograph of the medium is taken and the number of colonies is visually counted. Subsequently, the percent change [%] of the bacterial count is determined. In this experiment, three tests were conducted per participant: (1) before handwashing, (2) after handwashing, and (3) after drying. Before the palm stamp test, the palms were rubbed together to equalize the state of bacteria adhering to the left and right hands. Additionally, because bacteria may be transferred from the fingers to the medium during testing, leading to a decrease in the bacterial count, the samples for (1) and (2) were collected from the dominant hand, whereas that for (3) was collected from the non-dominant hand. Furthermore, handwashing was performed using the method recommended by the Ministry of Health, Labour and Welfare [13].

Photo 1 Medium for palm stamp testing

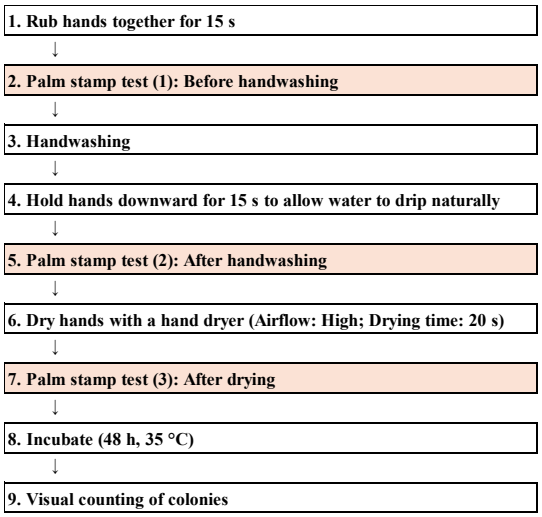

Figure 5 Measurement flow for bacteria adhering to hands

3.2. Experimental results

Figure 6 shows a comparison of the average values of the number of colonies converted to $\log_{10}(\mathrm{CFU} + 1)$ for bacteria adhering to the hands of each participant after hand cleaning (before drying) and after drying. In addition, Photo 2 shows examples of the medium after cultivation in each test.

The results of the t-test show that the number of colonies after handwashing is significantly higher than that before handwashing for all hand dryers. This is considered

to be caused by the emergence of indigenous skin bacteria. Although the number of colonies significantly decreases after drying when compared with that before drying, it tends to increase between the state before handwashing and after drying, and a significant difference is observed for the suction-type ($p = 0.0008$).

Figure 7 shows the percent change in the number of bacterial colonies from after handwashing (before drying) to after drying for each participant. For all devices, the number of colonies decreased after drying for most of the 20 participants, and the average change for each type of hand dryer was approximately −60%. Furthermore, for each type, one to two participants showed an increase in the number of colonies after drying, indicating individual differences.

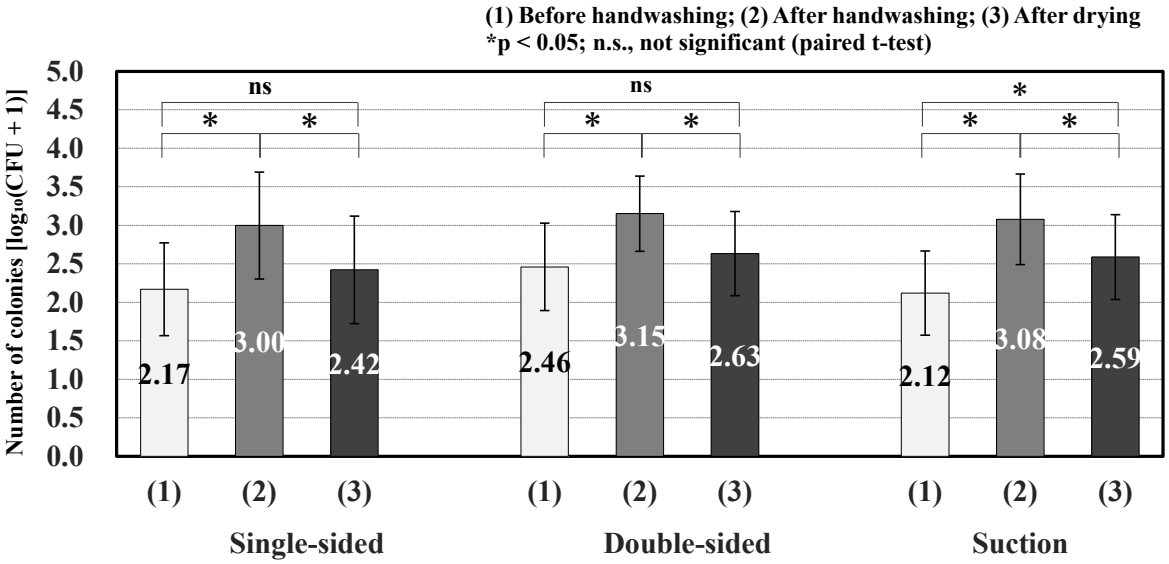

Figure 6 Comparison of average colony counts [$\log_{10}$(CFU + 1)]

(1) Before handwashing **(2) After handwashing** **(3) After drying**

Photo 2 Testing medium

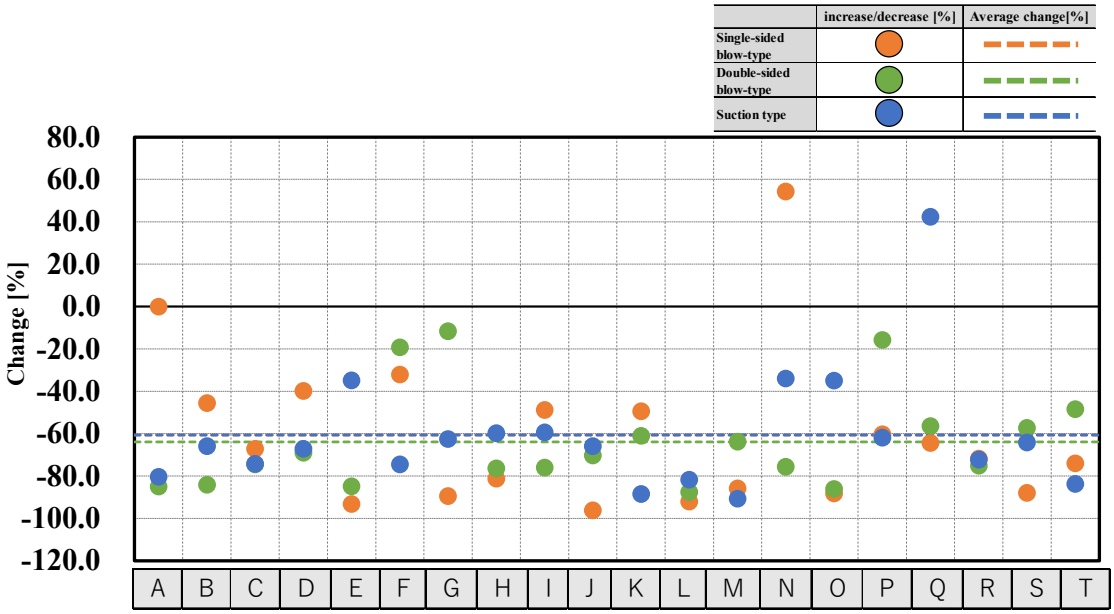

Figure 7 Comparison of percent changes in colony counts from after handwashing to after drying

4 Summary

In this study, the hygiene efficacies of three types of jet-type hand dryers were evaluated based on the following aspects: aerosol dispersal and the bacterial count adhering to the hands. The amount of aerosol dispersal differed significantly between the models, with the single-sided blow-type having the highest amount of aerosol dispersal, whereas the dispersal was significantly suppressed in the double-sided blow-type and suction-type. The number of bacteria adhering to the hands increased after handwashing and decreased after drying, but the variation in the drying performance was the smallest for the suction-type.

From the above, it was clarified that the hygiene efficacy of hand dryers is influenced by multiple factors, such as the blowing direction, housing shape, and drying performance. Intensive cleaning of the areas where water droplets tend to stagnate and use of the device based on the premise of appropriate handwashing are important. In the future, the effects of the blowing direction and housing shape will be clarified through computational fluid dynamics-based analysis.

Acknowledgement

This study was sponsored in part by Grants-in-Aid for Scientific Research from the Japan Society for the Promotion of Science (KAKENHI, 21H01497). We would like to express our gratitude to DAI-DAN Co., Ltd. For their cooperation in conducting the experiments

described in Chapter 2.

5 References

[1] Ayaka Kimura, Masayuki Otsuka: Dispersion of Droplets and Aerosols Generated by Use of Hand Dryer, Symposium CIB W 062,2024
[2] Japan Business Federation (Keidanren) (2020): Guidelines for Prevention of COVID-19 Infection in Offices, Japan Business Federation (Keidanren), p.4. 14 May 2020
[3] Japan Business Federation (Keidanren) (2021): Revised Guidelines for Prevention of COVID-19 Infection in Offices, Japan Business Federation (Keidanren), p.4. 13 April 2021
[4] Ministry of Health, Labour and Welfare (2025): Transition of COVID-19 to Category V Infectious Disease, Ministry of Health, Labour and Welfare, 25 December 2025.
[5] ISHRAE (2020): COVID-19 Guidance Document for Air Conditioning and Ventilation, Indian Society of Heating, Refrigerating and Air Conditioning Engineers (ISHRAE)（https://ishrae.in/mailer/ISHRAE_COVID-19_Guidelines.pdf)
[6] REHVA (2020): COVID-19 Guidance Version 4.0, Federation of European Heating, Ventilation and Air Conditioning Associations (REHVA), Europe, 7 November 2020.
[7] World Health Organization. Coronavirus disease (COVID-19) advice for the public: MythBusters – Hand dryers [Internet]. Geneva: WHO; 2020. https://www.who.int/emergencies/diseases/novel-coronavirus-2019/advice-for-public/myth-busters#hand-dryers,(2026-04-01)
[8] Shiro Takeuchi, Takuya Furuhashi, Masaki Uchida (2007): Behavior of water droplets during hand dryer use, Proceedings of the Annual Conference of the Society of Heating, Air-Conditioning and Sanitary Engineers of Japan, pp. 1,331–1,334.
[9] ETS (European Tissue Paper Industry Association); Contamination of air in toilet washroom after hand drying, 2014-11-18
[10] P.T. Kimmitt and K.F. Redway: Evaluation of the potential for virus dispersal during hand drying: a comparison of three methods, 120(2), 2016, pp. 478–486. https://ami-journals.onlinelibrary.wiley.com/doi/10.1111/jam.13014
[11] Satoshi Kimura, Hisako Aizawa, Tomoko Masuyama, Emiko Nakama (2004): Investigation of warm-air hand dryers and bacterial contamination in hospitals, Journal of Japanese Society for Infection Prevention and Control, pp. 21–26.
[12] J.H. Taylor, K.L. Brown, J. Toivenen, J.T. Holah: A microbiological evaluation of warm air hand driers with respect to hand hygiene and the washroom environment, 89(6), 2001-12-25, pp. 910–919. https://ami-journals.onlinelibrary.wiley.com/doi/full/10.1046/j.1365-2672.2000.01122.x?sid=nlm%3Apubmed,(2023-01-30)
[13] Ministry of Health, Labour and Welfare. (2020), General infection control measures, https://www.mhlw.go.jp/content/10900000/000593493.pdf

6 Presentations of Authors

Ayaka Kimura is a third-year doctoral student in the Otsuka Laboratory at Kanto gakuin University in Japan. During her studies, she was mainly involved in research on living space hygiene contributory to preventive measures against COVID-19. Currently She also works at Tokyo Electric Power Company Holdings, Inc., where she is engaged in research on electricity demand and energy conservation.

Masayuki Otsuka is a professor in the College of Architecture and Environmental Design at Kanto gakuin University and conducts a wide range of research on plumbing and sanitary systems. Member of AIJ and has served as president of SHASE

Riki Tanaka is a Master of Engineering from Kanto gakuin University. He is currently working in the field of housing management and maintenance. His graduate studies involved research on the hygienic characteristics and aerosol-related sanitary performance of hand dryers.

Investigation and Strategic Analysis of Odor Emissions and Biological Contamination Sources in Public Toilets

M. C. Jeffrey Lee(1)*, Yu-Chi Su(1), Jenn-Ann Tan(1), Shu-Han Liu(1), Chia-Yu Liao(1), Pi-Jan Chang(1)

(1) Email: MCJL@nutc.edu.tw

(1) Department of Interior Design, National Taichung University of Science and Technology, Taichung 40401, Taiwan

Abstract

With increasing governmental attention and the active promotion of 'toilet culture' by non-governmental organizations, such as the Taiwan Toilet Association, Taiwan has seen significant improvements in public sanitation facilities. However, critical issues in older public toilets remain overlooked. Factors such as poor cleanliness, persistent odors, aging equipment, and inadequate management continue to compromise environmental quality and user satisfaction. This study developed a scientific assessment mechanism and conducted systematic on-site inspections of 100 public toilets across Western Taiwan to analyze indoor environmental quality (IEQ), equipment maintenance, cleaning deficiencies, and user behavior.

The findings indicate that environmental quality is not only determined by spatial design but is also closely correlated with cleaning convenience, maintenance frequency, management systems, and user behavior. Inadequate management and poor ventilation were found to cause odor accumulation, elevated bacterial counts, and overall environmental degradation. Specific technical issues identified include urine scale buildup, the absence of P-traps, and high bacterial concentrations around sanitary fixtures. Finally, this study proposes recommendations, including comprehensive cleaning protocols, strengthened inspections, and ventilation optimization, serving as a critical reference for future policy-making.

Keywords
Public Toilets, Status Assessment, Environmental Quality, Cleaning and Maintenance, Management Strategies

1 Introduction

Public toilet quality is a critical urban hygiene indicator. In Taiwan's humid climate, odor and microbial growth accelerate rapidly; however, current evaluation systems (2017–2026) remain limited by a reliance on superficial visual scoring over biological or standardized odor monitoring. Consequently, even facilities rated as 'Excellent' often suffer from persistent malodors and substantial microbial contamination. [2],[3],[5],[9] While ventilation is known to reduce airborne pollutants, odors often persist due to under-researched factors like drainage infrastructure and 'cleaning dead zones'. This study integrates field diagnostics and microbial sampling to characterize contamination patterns, establishing a scientific model based on empirical data. By providing objective benchmarks for hygiene management, this research offers a robust framework for future policy improvements and targeted environmental interventions.

Table 1-Public Toilet Cleanliness Inspection Checklist (Adapted from Taiwan High Prosecutors Office, 2017)

Public Toilet Name / ID:		Inspection Date:		Public Restroom Inspection Grading Results	
No.	Category	Indicator Description	Check	Grade	Items Met
A	Maintenance Records	Cleaning frequency ≧ 4 times/day		Ordinary	1
		Update attendance sheet regularly			2
B	Cleaning Status	No stains on bowls, sinks, flush systems			3
		No stains on lighting and floors			4
C	Hardware Facilities	No damage to bowls, sinks, flush systems			5
		No damage to lighting and floors			6
		Use eco-friendly/energy-saving equipment			7
		Restroom greened/beautified; no stagnant water			8
		Floor dry or well-ventilated; no odor			9

D	Signage & Labeling	Labeled: M, F, Accessible, Mixed, Family	Excellent (10-13)	10
		Display grading, certification, and dates		11
		Display "Dispose paper in toilet" signs		12
		Vending machines within 10m sell toilet paper		13
		Lidded trash cans; sanitary disposal marked	Superior (14-16)	14
		Educational posters and etiquette		15
E	Value-Added Services	Provide at least one: paper, dryer, or sanitizer		16
Inspected Unit Signature		Inspection Unit	Inspector Signature/Seal	

2 Methodology

2.1 Research Design and Study Subjects

This cross-sectional field study investigated the indoor environmental quality (IEQ) of 100 public toilets in Taiwan. The assessment integrated onsite surveys, environmental monitoring, microbial sampling, and functional inspections to evaluate physical, chemical, biological, and infrastructural pollution characteristics.

2.2 Research Materials and Measurement Parameters

The study classified measurement indicators into physical (temperature, humidity, air velocity, noise, illuminance, water flow, and odor), chemical (CO2, NH3, HCHO, and TVOCs), biological, and functional parameters, selected in accordance with Taiwan's Indoor Air Quality Management Act and international standards. (Table 2)

2.3 Biological Indicators and Sampling Methods

Biological contamination was assessed using airborne and surface-contact sampling methods adapted from Lee & Tham [6]. Airborne bacteria and fungi were monitored to evaluate infection risks in poorly ventilated spaces, while surface sampling focused on high-touch, high-moisture areas such as toilets, urinals, sinks, and drains. Key microbial indicators included total bacterial count, *Escherichia coli* (*E. coli*), and *Staphylococcus aureus* (*S. aureus*).

2.4 Functional Inspection and Ventilation Assessment

Functional inspections focused on plumbing conditions, including pipe blockage, P-trap integrity, and uric scale accumulation. Endoscopic observations were conducted where necessary. Ventilation performance was evaluated using air velocity measurements obtained with a hot-wire anemometer to estimate airflow conditions and pollutant dilution efficiency.

Table 2: Measurement Indicators, Standard Values, and Reference Resources [4] [7] [8] [10]

Category	Measurement Item	Standard Value	Reference Resources
Physical	Temperature	Summer: 26~28℃ Winter: 18~20˚C	ASHRAE Standard 55
	Relative humidity	40~60％RH	ASHRAE Standard 55
	dBA	< 56 dBA	Noise Control Standards
	Wire anemometer	Air change rate: 10 ~15 times (Avg. wind speed0.5 m/s)	Sanitary Equipment Design Manual for Public Buildings
	Lux	100-300 lux	CNS12112 Lighting Standards
	Water flow rate	6~8 l/min	Executive Yuan Gazette: Standards for Water-Saving Labels
	Odor (Scale 1–5): The higher the number, the stronger the odor.		
Chemical	Ammonia	< 0.40 ppm	Empirical constants
	TVOC	< 0.56 ppm	
	CO_2	< 1000 ppm	Indoor Air Quality Standards
	HCHO	< 0.08 ppm	
Biological	Airborne Colony Count Standards:		
	Fungi	< 1000 CFU/m^3	Indoor Air Quality Standards
	Bacterial	< 1500 CFU/m^3	
	Contact Colony Count: Total bacteria, E. coli, Staphylococcus aureus		
Functional	Pipeline Status (Includes pipeline blockage, P-trap connection verification, and scale accumulation assessment.)		

2.5 Data Analysis

Environmental measurements, odor grades, and microbial concentrations were analyzed to explore the relationships between ventilation efficiency and pollutant accumulation. Comparative analyses were conducted across restroom types and contamination-prone locations to identify key odor sources and microbial hotspots.

2.6 Monitoring Equipment and Tools

Indoor environmental parameters and IAQ were measured using calibrated instruments according to Taiwan's standards, alongside noise and water flow rates. Biological assessments utilized active air sampling and swab/contact tests for surface contamination. Additionally, drainage systems were inspected via endoscopy to detect blockages and scale, as detailed in the field diagnostics protocol.

3 Field Investigation and Diagnostics

The scope of this investigation focuses on 100 public toilets in Taiwan that received a rating of two stars or lower in the 2024 Environmental Instant Messaging (EIM) system. These facilities were selected for rigorous field investigation, involving on-site inspections, quantitative logging, and photographic documentation to capture their current state.

3.1 Qualitative Assessment Protocol

The diagnostic process employs trained inspectors for systematic site mapping, data logging, and visual assessment. As shown in Figure 1, facilities are evaluated from exterior to interior, covering the surrounding area, washbasins, stalls, and urinals. Assessments focus on functionality, environmental comfort (dryness, odor, cleanliness, and lighting), and maintenance protocols, with all data recorded in a standardized form.

Site Mapping Point Logging Visual Assessment

Figure 1 Qualitative Assessment Process

3.2 Quantitative Assessment Protocol

The quantitative assessment encompasses physical parameters, chemical indicators, biological monitoring, and functional plumbing inspections. Advanced diagnostics, including hot-wire anemometry, gas detection tubes, active microbial impactors, and electronic endoscopes, are utilized to detect invisible failures such as dry P-traps, uric scale blockages, and airborne microbial accumulation across high-touch and drainage zones. The survey processes are shown as Figure 2.

Measurement of temp., RH, TVOC, HCHO, CO_2

Air velocity measurement

Illuminance measurement

Noise level measurement

Water flow rate measurement

Olfactory evaluation (odor assessment)

Ammonia detection

Contact microbial sampling

Airborne microbial sampling

Figure 2 Quantitative Assessment Process

4 Results and Discussion

4.1 Environmental Monitoring Results of Public Toilets

Surveyed public toilets show elevated temperature (27.5~29.7°C), high humidity (76%~80.5%), and excessive noise (73~77 dBA) exceeding recommended limits. Moreover, the persistently high indoor humidity creates an optimal environment for bacterial and fungal proliferation, while noise levels significantly exceeding the baseline standard highlight inadequate acoustic design and privacy concerns. While CO2 and TVOC levels are acceptable, formaldehyde in accessible restrooms (0.096 ppm) exceeds

the 0.08 ppm limit, likely due to poor local ventilation (air velocity < 0.11 m/s) or excessive chemical use. Additionally, spatial illuminance distribution is uneven; although overall levels appear compliant, individual cubicles record the lowest values, indicating insufficient lighting. Regarding water management, improper flow rates create distinct operational issues: insufficient water flow in urinals (55 ml/s) leads to incomplete rinsing and subsequent accumulation of urine scale, which becomes a primary source of persistent ammonia odors; conversely, excessive water flow in washbasins (80 ml/s) results in frequent splashing and standing water on the counter surfaces, as detailed in Figure 3.

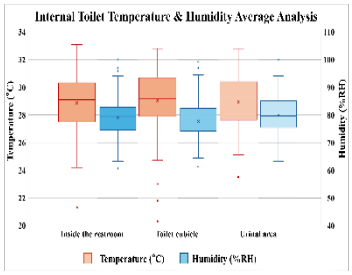

Internal Toilet Temp. & RH Average Analysis

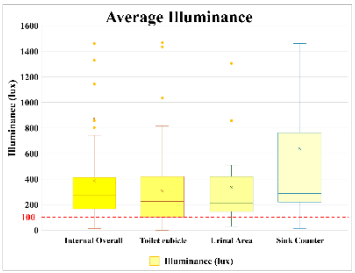

Average Illuminance

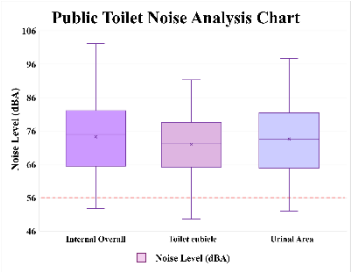

Public Toilet Noise Analysis Chart

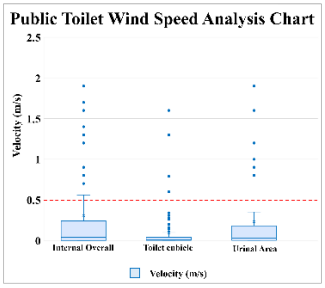

Public Toilet Wind Speed Analysis Chart

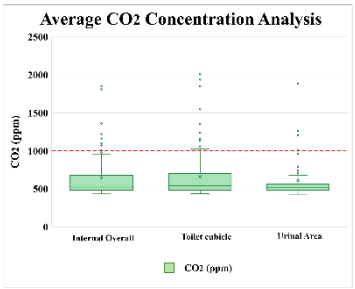

Average CO2 Concentration Analysis

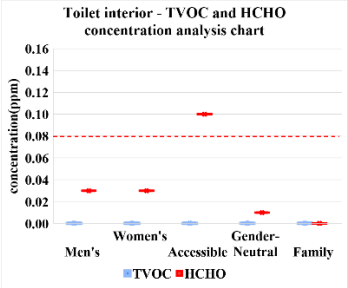

Toilet interior - TVOC and HCHO concentration analysis chart

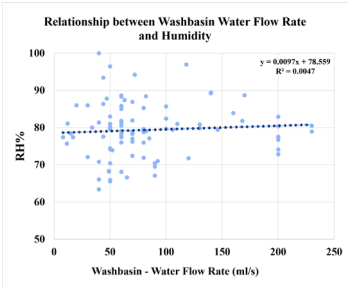

Relationship between Washbasin Water Flow Rate and Humidity

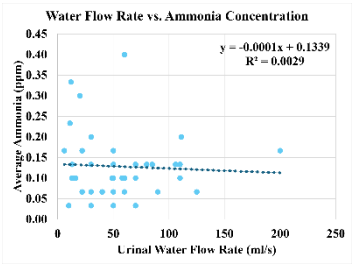

Water Flow Rate vs. Ammonia Concentration

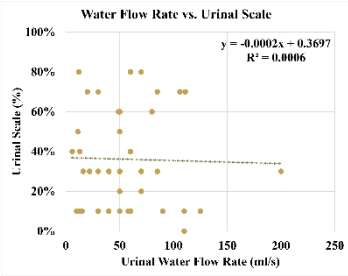

Water Flow Rate vs. Urinal Scale

Figure 3 The results of field survey in each part of field survey.

4.2 Relationship Between Ventilation, Odor, and Microbial Levels

The results indicate that odor and microbial levels are strongly linked to air velocity. While higher air velocity generally reduces these levels, persistent odors at speeds up to 2.4 m/s confirm that ventilation cannot replace source elimination. Fungal concentrations peak at ~2300 CFU/m³ below 0.2 m/s but stabilize below 400 CFU/m³ above 0.5 m/s. Bacterial levels follow a similar trend, reaching 3500 CFU/m³ under near-zero airflow. However, ventilation is less effective at reducing bacteria than fungi, as flushing and high-contact surfaces continuously generate new bio-aerosols.

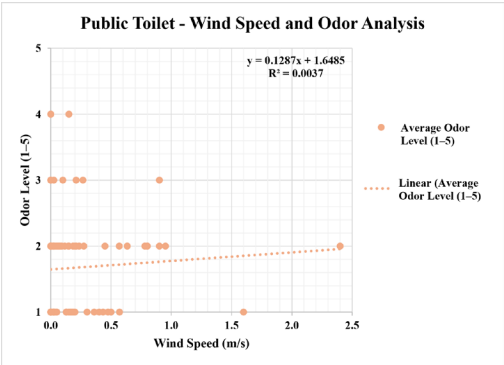

Public Toilet - Wind Speed and Odor Analysis

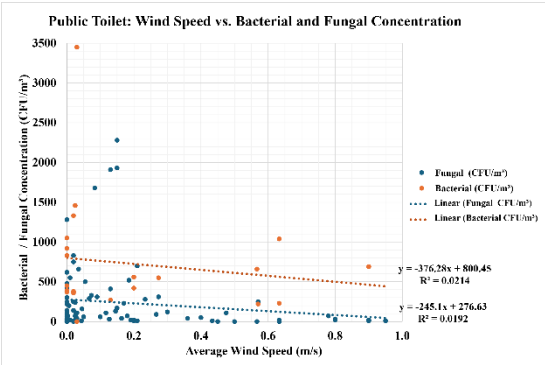

Public Toilet: Wind Speed vs. Bacterial and Fungal Concentration

Figure 4 The efficiency between ventilation, odor, micro-biological.

4.3 Key Odor Sources and Microbial Hotspots

Toilet types vary significantly in their odor profiles and microbial distribution, as summarized in Table 3. Male and all-gender toilets are primarily characterized by ammonia based urinary odors concentrated around urinals and drainage components, which also exhibit exceptionally high total bacterial counts. In contrast, female and accessible toilets present more complex odor profiles, a mix of fecal scents and residual chemical fragrances, particularly around high traffic stalls and waste bins, as shown in Figure 5. Additionally, elevated bacterial levels are heavily concentrated on both squatting and sitting toilet surfaces, as shown in Figure 6.

Table 3: Comprehensive Analysis of Odor Profiles and Bacterial Hotspots by Restroom Type

Restroom Type	Odor Profiles	Key Sources	Bacterial Hotspots
Men's Toilet	Putrid Urine	Urinals	Urinal drains, Grooves, Channels

Women's Toilet	Dry Fecal	Squat/Pedestal Toilets, Bins	Toilet grooves/floors, Bins, Sinks
All-Gender Toilet	Urine, Fecal	Urinals, Squat/Pedestal Toilets, Bins	Drains, Toilet-floor joints, Sinks
Accessible Toilet	Fecal	Pedestal Toilets, Bins	Toilet joints, Floor, Grab bars, Sinks
Family Toilet	Dry fecal odor	Pedestal Toilets, Bins	Bins, Sinks, Door handles, Toilet joints

Abbreviations & Notes: Microbial assessments target Total Plate Count, Escherichia coli, and Staphylococcus aureus across critical high-touch and drainage infrastructure.

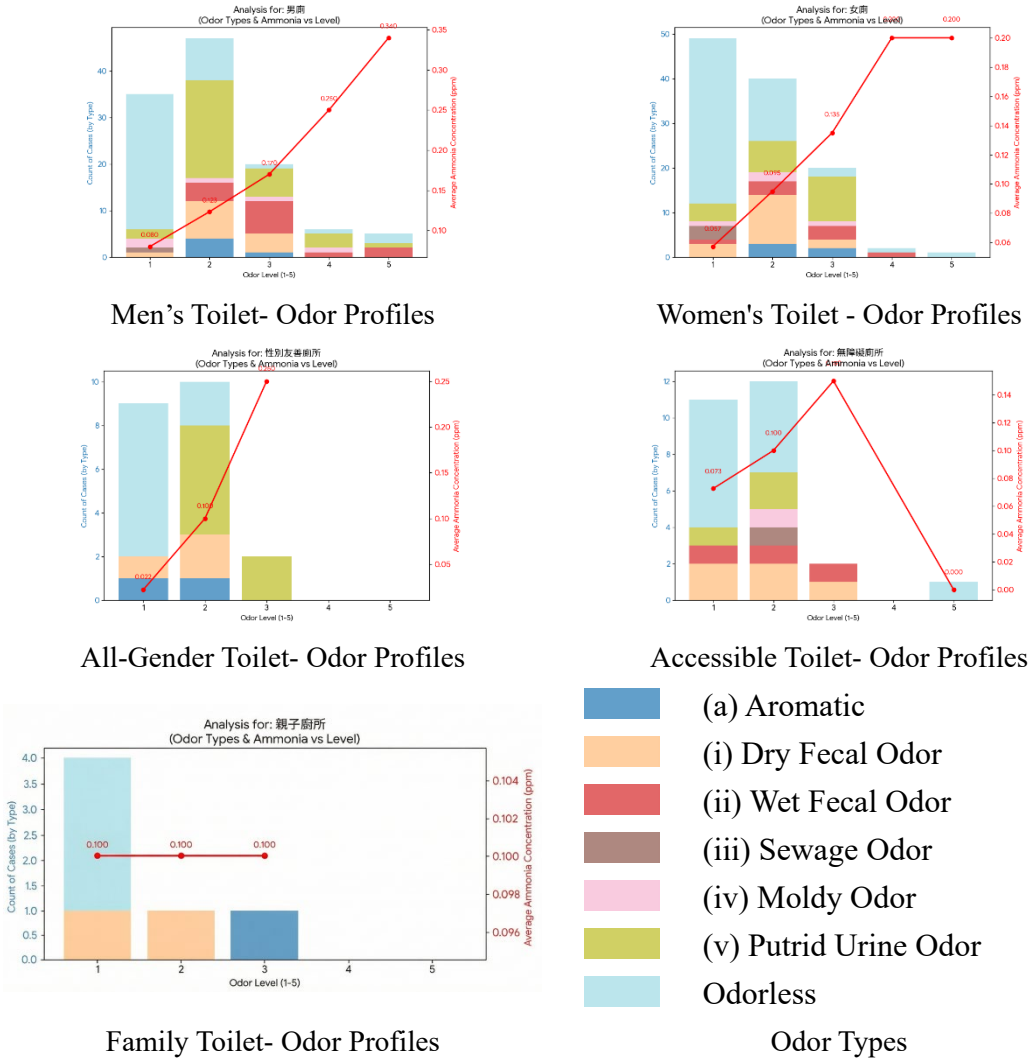

Figure 5 Public Toilet Odor Characteristics and Ammonia Concentration Analysis

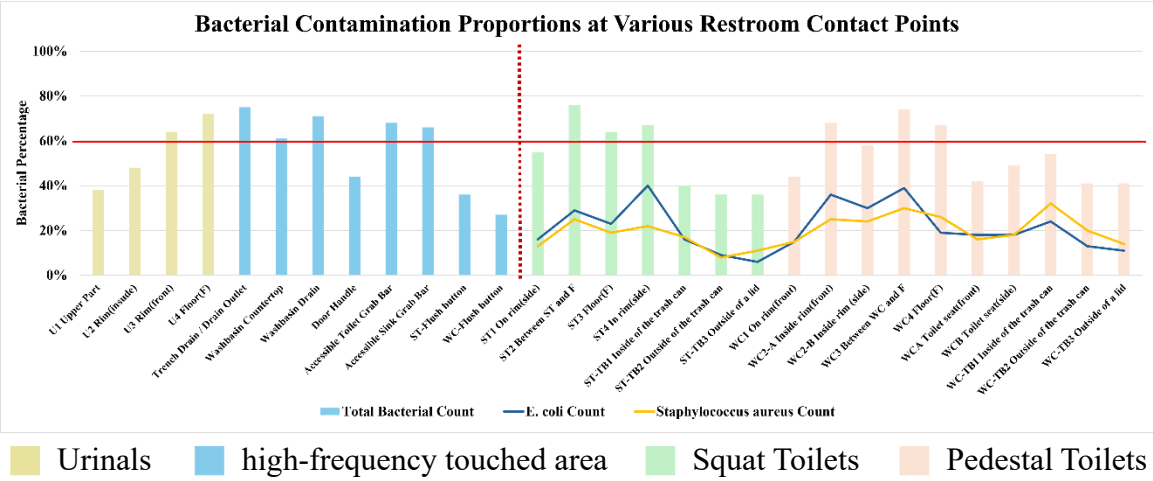

Figure 6 Mapping of High Bacterial Concentration Points in Public Toilets.

Microbial analysis identified toilet grooves, floor seams, and drainage outlets as primary contamination hotspots, where Escherichia coli and Staphylococcus aureus frequently co-occur with significantly higher bacterial loads observed on both squatting and sitting toilet surfaces. Notably, trash cans and door handles in family restrooms exhibited the highest total viable counts, highlighting the critical role of high-touch surfaces in cross-contamination and microbial transmission.

In contrast, urinals, handwashing stations, and drainage systems (including washbasins and grease/drainage traps) are primarily affected by a complex microbial community consisting of urine residues, environmental bacteria, aquatic bacteria, and biofilms. Because total viable count is a more suitable indicator for evaluating the overall hygiene status of such facilities given their contamination profile, this study did not proceed with further specific pathogen analysis (such as E. coli and S. aureus) for these equipment types.

5 Conclusions

This study evaluated facility maintenance, indoor air quality (IAQ), and pollutant distributions in 100 public toilets through visual assessments, environmental monitoring, and microbial sampling. By integrating usage patterns and management mechanisms, we provide the following conclusions and strategic recommendations:

(1) Multifaceted Interactions of Environmental Pollution

Public toilet pollution results from complex interactions between user behavior, facility design, and cleaning management. Poor hygiene habits, such as urine residue and water splashing, facilitate rapid microbial transmission. Furthermore, damaged facilities and inadequate ventilation create major hotspots for microbial growth, while insufficient cleaning or improper chemical agent use increases both odor levels and indoor chemical pollution risks.

(2) Correlation Between Odors and Ventilation Efficiency

High temperature and humidity accelerate urea decomposition into ammonia and the formation of stubborn uric scale, leading to persistent odor release. The joints of squat toilets and the flooring beneath urinals exhibit the highest odor and bacterial concentrations. While poor ventilation causes airflow stagnation and moisture accumulation, optimizing exhaust configurations effectively dilutes airborne chemical pollutants and inhibits microbial proliferation.

(3) Targeted Improvement Strategies

- **Hygiene Education and Behavioral Guidance:** Implement continuous public education via graphic signage, multimedia tools, and nudging environmental design to promote proper toilet usage and flushing protocols, minimizing pollution from splashes and residues.
- **Maintenance and Ventilation Optimization:** Strengthen cleaning protocols in high-risk zones using color-coded tools to prevent cross-contamination. Select low VOC, nonirritating cleaning agents, and optimize mechanical exhaust configurations and ventilation coverage to enhance air exchange efficiency.
- **Material and Spatial Circulation Design:** Utilize antimicrobial architectural materials and seamless flooring to inhibit dirt accumulation and microbial growth. Rationalize spatial circulation and accessibility layouts to reduce pedestrian cross flow and associated infection risks.

Acknowledgments

This study was funded by the Environmental Management Administration, Ministry of Environment, Taiwan. The authors express their sincere gratitude for the entire research team.

6 References

- ASHRAE. (2023). *ANSI/ASHRAE Standard 55: Thermal Environmental Conditions for Human Occupancy*. American Society of Heating, Refrigerating and Air-Conditioning Engineers.
- Environmental Protection Administration, Ministry of Environment. (2010). *Strengthening regulation of public toilets to improve toilet quality*. Ministry of Environment News.
- Environmental Management Administration, Ministry of Environment, Taiwan. (2024). *Guidelines for the supervision and maintenance management of public toilets*.
- Good Products Research Institute. (2026). *CNS 12112: National illumination standard of China*.
- Higham, C. A., López-García, M., Noakes, C. J., Tidswell, E., & Fletcher, L. (2024). A quantitative microbial risk assessment (QMRA) framework for exposure from toilet flushing using experimental aerosol concentration measurements. *Indoor Environments*, 2(1), 100069.
- Lee, M. C. J., & Tham, K. W. (2021). Public toilets with insufficient ventilation present high cross infection risk. *Scientific Reports*, 11, 20623.
- Ministry of Economic Affairs, Water Resources Agency. (2025). *Regulations for water-saving label management*.
- Ministry of Justice, National Laws and Regulations Database. (2012). *Indoor Air Quality Standards (Taiwan)*.
- Nantou County Environmental Protection Bureau. (2023). *Public Toilet Grading System*.
- U.S. Department of Labor, Occupational Safety and Health Administration. (2024). *Ammonia: OSHA Chemical Data (Chemical ID 623)*.

7 Presentation of Author(s)

Study on the Required Number of Sanitary Fixtures to Improve Conditions in Women's Restrooms

A. Koyama (1), H. Kose (2)

(1) 3B102600099@toyo.jp
(2) hkose@toyo.jp
(1) Master's students, Graduate School of Information Sciences and Arts, Toyo University, Japan
(2) Professor, Faculty of Information Sciences and Arts, Toyo University, Japan

Abstract

Long waiting lines at women's restrooms have become a visible social and planning issue in Japan. One possible reason is that the current standard for determining the number of sanitary fixtures, widely referred to in building design, is based on surveys conducted around 1980 and may not fully reflect recent changes in fixture occupancy time and restroom use. This study aims to obtain basic data for equalizing restroom waiting times between men and women by comparing the current SHASE standard with recalculated fixture requirements based on recent usage conditions.

The M/M/s queueing model was used for both free-use and concentrated-use facilities in order to provide a unified analytical framework. Updated mean occupancy times were assumed to be 300 s for male water closets, 40 s for urinals, and 120 s for female water closets. In addition, arrival-rate settings were examined so that the total male arrival rate (male water closets + urinals) was equal to the female arrival rate.

The results show that longer occupancy times increase the required number of fixtures for all fixture types, with the largest increase observed for female fixtures. Under the current SHASE assumptions, the required number of female fixtures is often smaller than the total number of male fixtures, which makes equal waiting times difficult to achieve. In contrast, when male and female total arrival rates are set equal, the required number of female fixtures often becomes equal to or greater than the total number of male fixtures. These findings suggest that revising fixture standards by incorporating recent occupancy times and gender-equitable arrival assumptions would contribute to reducing disparities in restroom waiting times.

Keywords

Sanitary fixtures, women's restrooms, queueing theory, M/M/s, waiting time, gender equity

1 Introduction

Long waiting lines at women's restrooms have recently attracted public attention in Japan [1]. Even in facilities where the numbers of male and female users are broadly comparable, women often experience longer queues than men. Men can use both water closets and urinals, whereas women generally rely only on cubicle-type fixtures. In addition, the occupancy time of women's fixtures tends to be longer.

In Japan, fixture planning has long relied on the SHASE standard, SHASE-S206-2019 [2]. However, its empirical basis largely derives from surveys conducted around 1980 [3–8]. Since then, restroom conditions and usage patterns have changed substantially. The replacement of squat toilets by western-style seated toilets, improvements in restroom amenity, and non-excretory use of cubicles have likely lengthened occupancy times, especially for female fixtures [9–13].

Previous studies have examined fixture requirements, user behavior, occupancy-time distributions, and queue conditions in specific building types [12–17]. Recent field studies have reported longer occupancy times than those assumed in the current standard [12,13]. International research has also shown that existing fixture standards do not necessarily provide gender-equitable restroom access [17]. However, few studies in Japan have compared current SHASE-based fixture requirements with recalculated values under updated occupancy-time assumptions within a unified queueing framework, while also examining gender balance in fixture numbers.

This study therefore aims to obtain basic data for improving gender equity in restroom waiting times by comparing the current SHASE standard with recalculated fixture requirements reflecting recent usage conditions. The M/M/s queueing model is used to evaluate the effect of longer occupancy times and to compare the required fixture numbers for male water closets, urinals, and female water closets.

2 Methods

2.1 Analytical framework

This study uses the M/M/s queueing model, which is also the basis of the SHASE method for free-use facilities [3–6]. Arrivals are assumed to follow a Poisson process and service times an exponential distribution. Users form a single queue and use the first available fixture.

For a queueing system with arrival rate λ [people/min], service rate μ [1/min], and number of fixtures s, the traffic intensity is given by:

$$\rho = \frac{\lambda}{s\mu}, \qquad \rho < 1 \qquad \text{---(1)}$$

where

$$\mu = \frac{1}{\tau} \qquad \text{---(2)}$$

and τ is the mean occupancy time [min]. Let

$$a = \frac{\lambda}{\mu} \qquad \text{---(3)}$$

Then the probability that an arriving user has to wait is given by the Erlang C formula:

$$P(\text{wait}) = \frac{\dfrac{a^s}{s!(1-\rho)}}{\sum_{n=0}^{s-1} \dfrac{a^n}{n!} + \dfrac{a^s}{s!(1-\rho)}} \quad \text{---(4)}$$

The probability that queue waiting time W_q exceeds a specified time t is:

$$P(W_q > t) = P(\text{wait}) \exp\{-(s\mu - \lambda)t\} \quad \text{---(5)}$$

For each condition, the minimum integer s satisfying the waiting-time criterion was defined as the required number of fixtures.

For concentrated-use facilities such as theaters, SHASE traditionally uses Monte Carlo simulation [7,8]. In this study, the M/M/s model was also applied to concentrated-use cases to establish a unified analytical framework.

2.2 Facility types and analytical conditions

Table 1 shows analytical conditions used in the calculation.

Three facility types were examined: department stores/shopping centers, office buildings, and theaters. Department stores/shopping centers and office buildings were treated as free-use facilities, whereas theaters were treated as concentrated-use facilities.

The fixture categories analyzed were:

- male water closets,
- urinals, and
- female water closets.

Washbasins, accessible toilets, and gender-neutral toilets were excluded.

Mean occupancy times were set at 300 s for male water closets, 40 s for urinals, and 120 s for female water closets, based on recent empirical studies and current academic discussions on revising fixture standards [9–13].

SHASE defines arrival conditions as fixture arrivals per minute per 100 building users. In this study, this was distinguished from arrival frequency [people/min], i.e., the actual number of restroom users arriving per minute. Two main arrival rate settings were examined: (1) the current SHASE assumptions, and (2) a revised condition in which the combined male arrival rate (male water closets + urinals) was set equal to the female arrival rate. The ratio between male water-closet arrivals and urinal arrivals was fixed at approximately 1:5 [15].

For free-use facilities, the gender comparison was conducted for a representative case of 300 building users. For department stores/shopping centers, an additional case assumed that women accounted for 60% of all users. Waiting-time thresholds of 10, 30, 60, 90, 120, 150, and 180 s were examined.

Table 1 - Analytical conditions used in the calculation

Fixture types		Building use	Male water closets	Urinals	Female water closets
Arrival rate [people/(min•100people)]	SHASE, Case 1	Department stores/shopping centers	0.080	0.300	0.300
		Offices	0.130	0.600	0.600
		Theaters *1)	0.333	2.000	2.000
	Case 2	Department stores/shopping centers	0.050	0.250	0.300
		Offices	0.100	0.500	0.600
		Theaters	0.333	1.667	2.000
Average occupancy time [s]	SHASE, Case A	Department stores/shopping centers	240	30	90
		Offices	300	30	90
		Theaters	250	30	75
	Case B		300	40	120
Waiting-time criterion [1] / Maximum waiting time [2]	SHASE Level 1	Department stores/shopping centers and Offices [1]	P(>10)<0.05	P(>0)<0.01	P(>10)<0.01
		Theaters [2]	120	15	40
	SHASE Level 2	Department stores/shopping centers and Offices [1]	P(>60)<0.05	P(>10)<0.01	P(>40)<0.01
		Theaters [2]	250	30	75
	SHASE Level 3	Department stores/shopping centers and Offices [1]	P(>120)<0.05	P(>30)<0.01	P(>90)<0.01
		Theaters [2]	400	60	150
	Level a		P(>10)<0.05	P(>10)<0.01	P(>10)<0.01
	Level b		P(>30)<0.05	P(>30)<0.01	P(>30)<0.01
	Level c		P(>60)<0.05	P(>60)<0.01	P(>60)<0.01
	Level d		P(>90)<0.05	P(>90)<0.01	P(>90)<0.01
	Level e		P(>120)<0.05	P(>120)<0.01	P(>120)<0.01
	Level f		P(>150)<0.05	P(>150)<0.01	P(>150)<0.01
	Level g		P(>180)<0.05	P(>180)<0.01	P(>180)<0.01

*1) Convert the calculation conditions in the Monte Carlo simulation in SHASE.
*2) "P(>x)<y" means that the probability of a queue waiting time exceeding x seconds is less than y.

3 Results

3.1 Effect of longer occupancy times on fixture requirements

Figure 1-3 show required number of each fixture as a function of the number of users in department stores/shopping centers and office buildings.

When mean occupancy times were increased to reflect recent restroom conditions, the required number of fixtures increased for all fixture types. Under the same arrival frequency in free-use facilities, the increase reached up to three fixtures for male water closets, three fixtures for urinals, and six fixtures for female water closets. The largest increase was observed for female water closets because their occupancy time was revised upward most substantially.

This result indicates that fixture planning based on older occupancy-time assumptions may underestimate demand, particularly for women’s restrooms.

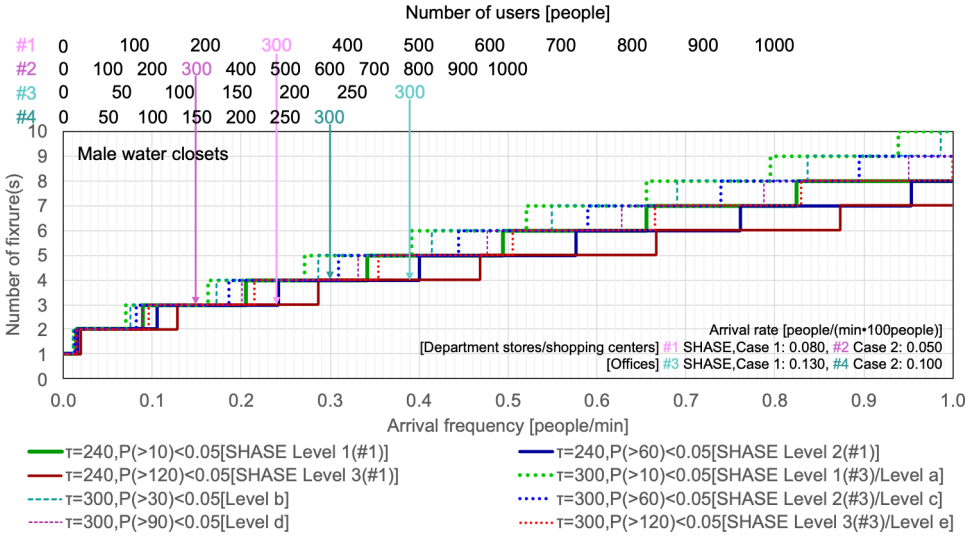

Figure 1 – Required number of male water closets as a function of the number of users in department stores/shopping centers and office buildings

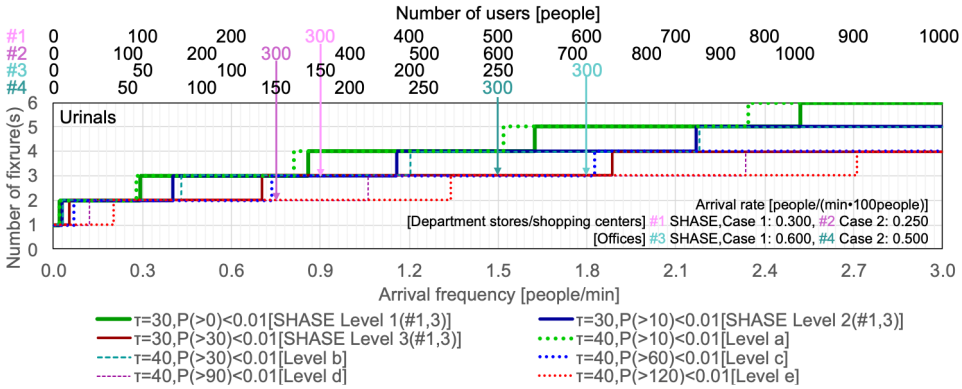

Figure 2 – Required number of urinals as a function of the number of users in department stores/shopping centers and office buildings

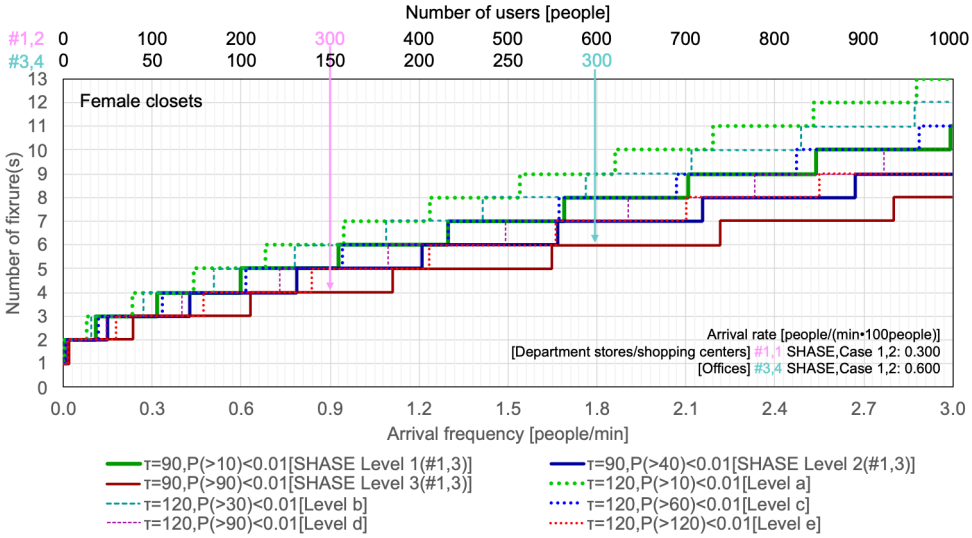

Figure 3 – Required number of female water closets as a function of the number of users in department stores/shopping centers and office buildings

3.2 Comparison with the current SHASE standard

Figure 4-6 show required number of each fixture as a function of the number of seats in theaters.

For a representative case of 300 building users in free-use facilities, revised arrival rate assumptions reduced some male fixture requirements. Male water closets decreased by one fixture in department stores/shopping centers and remained nearly unchanged in offices, while urinals decreased by one fixture in both facility types. In contrast, the required number of female water closets increased by one under representative waiting-time conditions because the female arrival rate was maintained while the occupancy time was increased.

The difference became more pronounced in theaters. Compared with the current SHASE-based results, the recalculated requirements for female water closets increased substantially, by as many as 13 fixtures under some conditions. This suggests that the current standard may significantly underestimate the number of women's fixtures required in highly congested facilities.

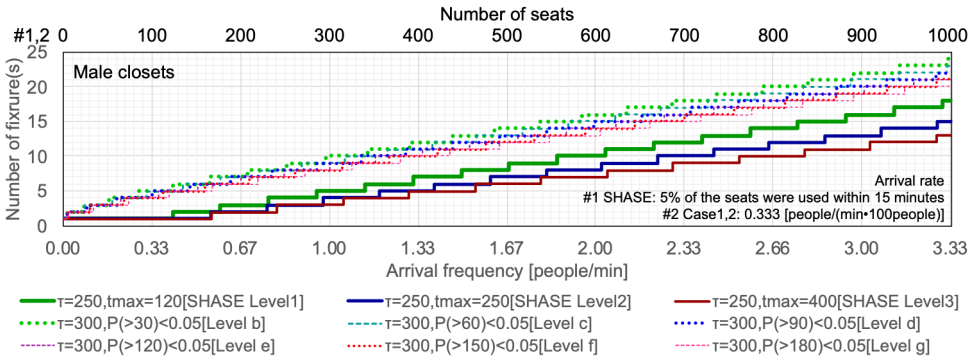

Figure 4 – Required number of male water closets as a function of the number of seats in theaters

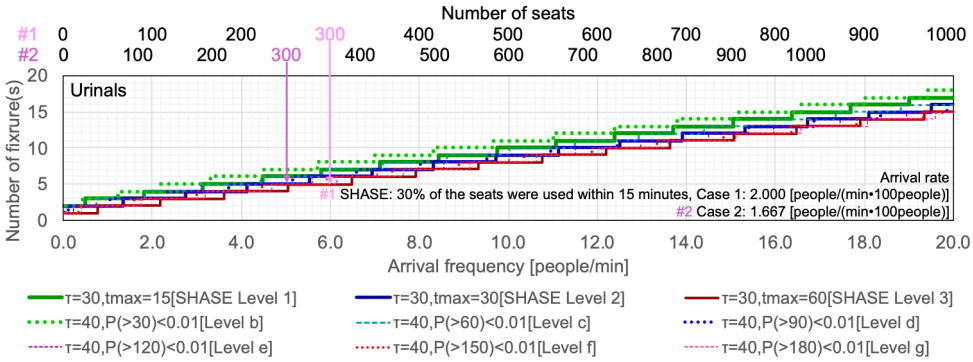

Figure 5 – Required number of urinals as a function of the number of seats in theaters

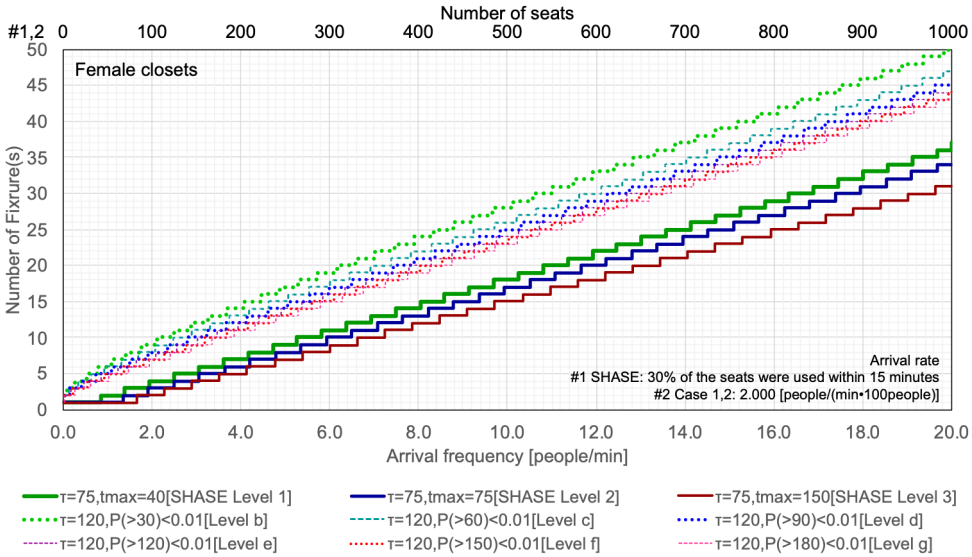

Figure 6 – Required number of female water closets as a function of the number of seats in theaters

3.3 Comparison between male and female fixture requirements

Table 2-3 show required numbers of sanitary fixtures for men and women and their ratio in each building use with 300 users.

To evaluate gender balance in fixture planning, the ratio of required female water closets to the total required male fixtures (male water closets + urinals) was examined. Under the current SHASE assumptions, this ratio ranged from 0.63 to 0.83 in department stores/shopping centers and from 0.80 to 0.88 in offices. Thus, the required number of female water closets was consistently smaller than the total number of male fixtures.

When the combined male arrival rate was set equal to the female arrival rate, the results changed markedly. In many cases, the required number of female water closets became equal to or greater than the total number of male fixtures. This tendency became more pronounced when the proportion of female users in department stores/shopping centers was assumed to be 60%.

Figure 7 shows comparison of required fixture numbers for men and women as a function of arrival frequency under representative waiting-time criteria.

These findings indicate that, if the goal is to provide comparable waiting times for men and women, fixture standards should be revised so that the required number of female water closets is at least equal to the total number of male fixtures in facilities where male and female demand is broadly similar.

Table 2 – Required numbers of sanitary fixtures for men and women and their ratio in department stores/shopping centers with 300 users

Department stores/shopping centers

Calculation 1: Assume the same conditions for arrival rate in SHASE and the calculation (Case 1-B)

300 people *1)	SHASE Level 1	SHASE Level 2	SHASE Level 3	Level a (10s)	Level b (30s)	Level c (60s)	Level d (90s)	Level e (120s)
Male closets (MC)	4	3	3	4	4	4	4	4
Urinals (U)	4	3	3	4	3	3	2	2
Female closets (FC)	5	5	4	6	6	5	5	5
FC/(MC+U)	0.63	0.83	0.67	0.75	0.86	0.71	0.83	0.83

Calculation 2: Making the arrival rate the same for male closets + urinals and female closets (Case 2-B)

300 people *1)	SHASE Level 1	SHASE Level 2	SHASE Level 3	Level a (10s)	Level b (30s)	Level c (60s)	Level d (90s)	Level e (120s)
Male closets (MC)	4	3	3	3	3	3	3	3
Urinals (U)	4	3	3	3	3	3	2	2
Female closets (FC)	5	5	4	6	6	5	5	5
FC/(MC+U)	0.63	0.83	0.67	1.00	1.00	0.83	1.00	1.00

Calculation 3: Setting the proportion of female users to a maximum of 60% in Calculation 2 (Case 2-B)

Maximum male ratio: 50%, Maximum female ratio: 60% *2)	SHASE Level 1	SHASE Level 2	SHASE Level 3	Level a (10s)	Level b (30s)	Level c (60s)	Level d (90s)	Level e (120s)
Male closets (MC)	4	3	3	3	3	3	3	3
Urinals (U)	4	3	3	3	3	3	2	2
Female closets (FC)	6	5	4	7	6	6	5	5
FC/(MC+U)	0.75	0.83	0.67	1.17	1.00	1.00	1.00	1.00

*1) In SHASE and Calculation 1, the arrival frequency for 300 people in department stores/shopping centers was calculated as follows: male closets 0.24[people/min], urinals 0.9[people/min], famale closets 0.9[people/min]. In Calculation 2, the usage frequencies for male closets + urinals and women's closets were assumed to be the same, resulting in calculations of famale closets 0.15[people/min], urinals 0.75[people/min], female closets 0.9[people/min].
*2) Calculated assuming a total of 600 people using restrooms in department stores/shopping centers, with a maximum of 50% male users (300 people, i.e., arrival frequency of 0.24[people/min] for male closets and 0.9[people/min] for urinals using SHASE; in Calculation 3, assuming the arrival frequency of male closets + urinals and female closets ware assumed to be the same, it is calculated as 0.15[people/min] for male closets and 0.75[people/min] for urinals), and a maximum of 60% female users (360 people, i.e., arrival frequency of 1.08[people/min] for female closets).
*3) Orange shading indicates the number of fixtures when the waiting time criteria are the same as for SHASE level 3, and green shading indicates when FC/(MC+U)>=1.

Table 3 – Required numbers of sanitary fixtures for men and women and their ratio in office buildings with 300 users

Offices

Calculation 1: Assume the same conditions for arrival rate in SHASE and the calculation (Case 1-B)

300 people *1)	SHASE Level 1	SHASE Level 2	SHASE Level 3	Level a (10s)	Level b (30s)	Level c (60s)	Level d (90s)	Level e (120s)
Male closets (MC)	5	4	4	5	5	5	5	5
Urinals (U)	5	4	3	5	4	3	3	3
Female closets (FC)	8	7	6	9	9	8	7	7
FC/(MC+U)	0.80	0.88	0.86	0.90	1.00	1.00	0.88	0.88

Calculation 2: Making the arrival rate the same for men's closets + urinals and women's closets (Case 2-

300 people *1)	SHASE Level 1	SHASE Level 2	SHASE Level 3	Level a (10s)	Level b (30s)	Level c (60s)	Level d (90s)	Level e (120s)
Male closets (MC)	5	4	4	5	5	4	4	4
Urinals (U)	5	4	3	4	4	3	3	3
Female closets (FC)	8	7	6	9	9	8	7	7
FC/(MC+U)	0.80	0.88	0.86	1.00	1.00	1.14	1.00	1.00

*1) In SHASE and Calculation 1, the arrival frequency for 300 people in offices was calculated as follows: male closets 0.39[people/min], urinals 1.8[people/min], famale closets 1.8[people/min]. In Calculation 2, the usage frequencies for male closets + urinals and women's closets were assumed to be the same, resulting in calculations of famale closets 0.3[people/min], urinals 1.5[people/min], female closets 1.8[people/min].

*2) Orange shading indicates the number of fixtures when the waiting time criteria are the same as for SHASE level 3, and green shading indicates when FC/(MC+U)>=1.

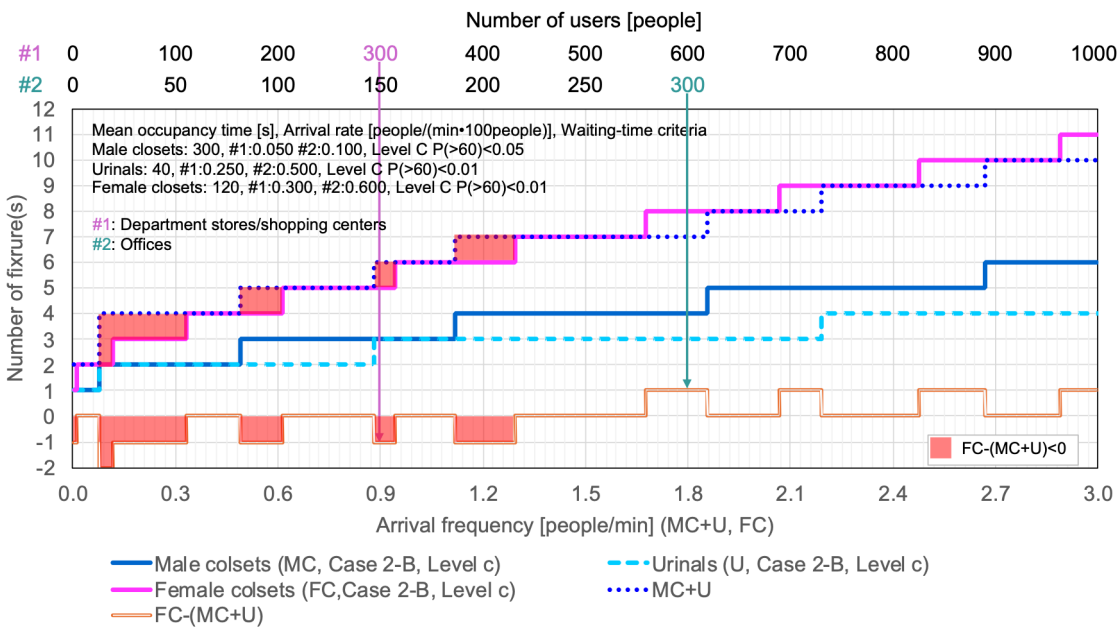

Figure 7 – Comparison of required fixture numbers for men and women as a function of arrival frequency under representative waiting-time criteria

4 Discussion

Longer occupancy times, especially for female fixtures, strongly affect fixture requirements. If planning continues to rely on outdated assumptions, long queues at women's restrooms are likely to persist, particularly in high-demand facilities. From the viewpoint of equalizing waiting times between men and women, it is reasonable to consider a planning rule under which the number of female fixtures should be at least equal to the combined number of male water closets and urinals when total male and female demand is similar. This is consistent with recent policy discussions in Japan [18,19].

Several limitations should be noted. First, the occupancy times used here are representative values and do not capture variation by building type, time of day, season, crowding level, or toilet-seat function [12,13]. Second, arrival rate assumptions remain uncertain because sufficiently rich observational data on restroom arrivals are limited. Third, concentrated-use situations such as theater intermissions were analyzed using the M/M/s model for consistency, although SHASE traditionally uses simulation [7,8]. Future work should incorporate richer data on both occupancy times and arrival rates and further examine practical methods for evaluating the waiting-time performance of a given fixture layout.

5 Conclusion

This study compared the current SHASE fixture requirements with recalculated requirements based on recent restroom occupancy conditions using a queueing-theoretic framework. The main findings are as follows.

1. Increasing mean occupancy times increases the required number of fixtures for all fixture types, with the largest increase observed for female water closets.
2. Under the current SHASE assumptions, the required number of female fixtures is often smaller than the total required number of male fixtures, making equal waiting times difficult to achieve.
3. When the combined male arrival rate is set equal to the female arrival rate, the required number of female fixtures often becomes equal to or greater than the total number of male fixtures, suggesting a feasible basis for gender-equitable fixture standards.

These findings suggest that revising sanitary fixture standards to reflect recent occupancy times and gender-equitable demand assumptions would contribute to reducing disparities in restroom waiting times.

6 Acknowledgements

This study was carried out as part of the activities of the SHASE Special Committee for Academic Recommendations on the Installation Numbers of Sanitary Fixtures. The authors gratefully acknowledge the valuable advice and support provided by the committee secretaries and members.

7 References

[1] K. Sekiguchi, T. Ogawa, and T. Yamashita, "Why are there lines only for women? A survey of 706 public restrooms found that in 90% of cases men had more fixtures than women," Asahi Shimbun, Morning Edition, p.22, 20 Feb. 2025. (in Japanese)

[2] The Society of Heating, Air-Conditioning and Sanitary Engineers of Japan (SHASE), "SHASE-S206-2019 Plumbing Code", 2020. (in Japanese)

[3] M. Okada, "Method for calculating the appropriate number of sanitary fixtures (1): Basic theory of the calculation method, Part 1," Journal of SHASE, Vol.58, No.6, pp.585–598, 1984. (in Japanese)

[4] M. Okada, "Method for calculating the appropriate number of sanitary fixtures (2): Basic theory of the calculation method, Part 2," Journal of SHASE, Vol.58, No.7, pp.697–709, 1984. (in Japanese)

[5] S. Murakawa, "Method for calculating the appropriate number of sanitary fixtures (3): Method for free-use buildings, Part 1," Journal of SHASE, Vol.58, No.8, pp.801–815, 1984. (in Japanese)

[6] S. Murakawa, "Method for calculating the appropriate number of sanitary fixtures (4): Method for free-use buildings, Part 2," Journal of SHASE, Vol.58, No.9, pp.919–930, 1984. (in Japanese)

[7] F. Kiya, "Method for calculating the appropriate number of sanitary fixtures (5): Method for concentrated-use buildings, Part 1," Journal of SHASE, Vol.58, No.10, pp.1007–1012, 1984. (in Japanese)

[8] F. Kiya, "Method for calculating the appropriate number of sanitary fixtures (6): Method for concentrated-use buildings, Part 2," Journal of SHASE, Vol.58, No.11, pp.1129–1138, 1984. (in Japanese)

[9] H. Kose, Y. Nagao, Y. Nakagawa, and S. Murakawa, "Present state and future challenge on installation number of the sanitary fixture," CIB W062 2007 33rd International Symposium, pp.369–378, 2007.

[10] H. Kose, "Consideration of revision for the method of calculating the installation number of a sanitary fixture," CIB W062 2014 40th International Symposium, pp.E1–15, 2014.

[11] H. Kose, "Current Status and Issues Regarding the Number of Sanitary Fixtures Installed in Japan," 49th International Symposium of CIB W062, pp.1–8, 2024.

[12] M. Takahashi, "A study on calculating method of fixture requirements for restrooms Part 1. A study on the use frequency of the restroom and time in the restroom at the office," Proceedings of the Annual Meeting of SHASE, pp.193–196, 2019. (in Japanese)

[13] M. Takahashi, Y. Kinoshita, A. Hikita, "A study on the calculating method of fixture requirements for restrooms Part2. Comparison of occupancy time by facility use and toilet seat function, and presumption of distribution by numerical formula," Proceedings of the Annual Meeting of SHASE, pp.117–120, 2020. (in Japanese)

[14] Y. Nakagawa, "Study on Fixture requirements based on factor and analysis of fixture usage of toilet in railway stations," Doctoral Dissertation, Hiroshima University, 2008.

[15] H. Kose, "Usage Behavior in the Restroom: Seen from the Questionnaire Investigation on Living Hours Examination on the Determination Method for Fixtures Requirement (Part3)," Proceedings of the Annual Meeting of SHASE, pp. 17–20, 2011. (in Japanese)

[16] A. Umayahara and K. Koyama, “Relationship Between Toilet Queueing Length and Time Occupancy at Expressway Rest Areas - Survey at New Tomei Expressway Shizuoka SA,” Summaries of Technical Papers of Annual Meeting, Architectural Institute of Japan, pp. 233–234, 2018. (in Japanese)
[17] Huh, W. T., Lee, J., Park, H., and Park, K. S., “The potty parity problem: Towards gender equality at restrooms in business facilities,” Socio-Economic Planning Sciences, Vol. 68, 100666, 2019.
[18] Cabinet Office, Government of Japan, Basic Policy on Economic and Fiscal Management and Reform 2025: Toward a Society in which People can Feel “Tomorrow will be Better than Today”, June 2025. Available at: https://www5.cao.go.jp/keizai-shimon/kaigi/cabinet/honebuto/2025/decision0613.html
[19] Ministry of Land, Infrastructure, Transport and Tourism, Guideline on Standards and Application of the Number of Toilet Fixtures (planned publication), 2026. (in Japanese)

8 Presentation of Author

Ao Koyama is the master’s students, Graduate School of Information Sciences and Arts, Toyo University from 2026. My research focuses on toilet waiting lines as a social issue, with particular interest in how queue length and waiting time differ by gender and facility design.

Hiroyuki Kose is the professor at Toyo University, Faculty of Information sciences and arts from 2009. Special fields of study are water supply and drainage for buildings, water environment, reproduction of the agricultural and forestry industries by collaboration of citizens and an organization and community design for regional vitalization.

Impact of Shower Drains on Infection, Prevention & Control Strategies through Design & Operation

L. Wilson (1), M. Gormley (2), and D.A. Kelly (3)
(1) leonie.wilson@hw.ac.uk
(2) m.gormley@hw.ac.uk
(3) d.a.kelly@hw.ac.uk
(1-3) Heriot-Watt University, Edinburgh, Scotland, UK.

Abstract

The hospital shower drain environment has been identified as a reservoir for microorganisms having features that exacerbate the spread of antimicrobial resistance genes. The transmission of multi-drug-resistant (MDR) pathogens leads to difficult, or impossible to treat infections. MDR hospital acquired infections pose a significant risk for patients who are immunocompromised such, for example, as those undergoing chemotherapy treatment.

The role of air pressure transients has been identified as a route in which MDR can spread from the sink-trap to contaminate the hand-wash basin via aerosols. This research utilises laboratory data using a full-scale test rig to model the hospital drainage system and shower trap arrangements. It highlights the role of air pressure transients within the drainage system in the contamination of shower trays and wet rooms in a hospital setting.

The driver for any transmission event is the connection to the building drainage system and the effect that air pressure transients can have on the movement of micro-organisms. The research shows that simple activities such as unblocking clogged toilets can lead to transmission events. Future research will focus on mitigation strategies including design guidance for building drainage systems in hospitals.

Keywords

Infection Control, Hospital-acquired infections, Hospital built environment, Building drainage systems, Antimicrobial resistance, Bioaerosols

1 Introduction

Hospital acquired infections (HAIs) are infections which patients develop after admission, or even after discharge from the hospital. They are of particular concern for immunocompromised patients, such as those undergoing chemotherapy, as the required number of microorganisms to cause infection is lower than that of the normal population, so the risk of infection is much greater [1]. Previous research has shown that these types of infections can be traced back to hospital environment such as high touch surfaces and sink drains [2]. This is of particular concern as HAIs have been found to have an increased likelihood of carrying antimicrobial resistance (AMR) [3].

AMR occurs naturally in microorganisms through genetic mechanisms but can be accelerated through human activity such as the overuse of antibiotics. This leads to difficult, or even impossible to treat infections as the medication becomes ineffective against these microorganisms. The consequences of not dealing with AMR from a societal point of view cannot be underestimated. The O'Neill report forecasts that the economic impact of the 'end of the antibiotic era' will coincide with other world economic factors to produce a crisis by 2050 [4]. This has often been misinterpreted as the date at which no antibiotics will work. For many people infected by AMR infections, the end of the antibiotic era is now [5].

Previous research has established water trap seals in hospitals as a concern for HAIs due to the growth of biofilms. These are complex layers of microorganisms which attach to surfaces and provide a protective environment to grow [6]. Water trap seals can act as a reservoir for microorganisms and biofilm growth as well as having features which can exacerbate the spread of antimicrobial resistance genes [7]. However, there are few studies which investigate the mechanisms in which AMR pathogens in the water trap seal can contaminate appliances.

One route of contamination that has been identified is air pressure transients. These are pressure waves which occur as part of normal use within the drainage system, causing pathogens within the system to be aerosolised and move into the building via the water trap seal [8]. However, little research has been carried out investigating this is hospital showers specifically.

Health building guidance documents recommend a wet room style design as best practice for hospital showers to allow accessibility for patients and staff [9]. These style of bathrooms include the shower drain in the floor of the wet room which can be prone to blockages. It is not uncommon for large numbers of blockages to be recorded in hospital buildings and increasingly, this is being linked to AMR infection outbreaks [10]. This puts pressure on staff resources as well as posing a transmission risk to patients as explored in this research. It has been shown that most sewer blockages are due to wipes flushed via WC [11]. Previous research and anecdotal evidence from hospital maintenance staff have suggested that major blockages occur predominantly due to incorrect disposal of wipes

[12]. As more hospitals move towards water-free care to combat AMR infections from the hospital environment [13], there is an increased chance of the incorrect disposal of cleaning wipes, leading to an increase in blockages in the hospital drainage system. Therefore, an increase in the risk of AMR pathogen transmission.

This research utilises an aerodynamic particle sizer and full-scale laboratory drainage system test-rig to investigate aerosol generation from the hospital drainage system. Specifically, from showers in the event of a blockage and subsequent manual unblocking to allow investigation into transmission mechanisms of AMR pathogens in the healthcare-built environment.

2 Methodology

2.1 Background aerosols

The laboratory drainage test-rig was set up as shown in figure 1, with a WC and 90mm shallow shower trap connected to the system via a 40mm waste pipe. A solution of 0.85% NaCl was used in the trap-seal to allow more accurate visualisation of particles.

The aerodynamic particle sizer (APS) 3321 spectrometer was connected to the system with the antistatic sampling tube 5mm above the trap drain plate. The APS provides real-time measurement of particles between 0.5-20µm with a resolution of 0.02µm at 1.0µm diameter and 0.03µm at 10µm diameter. This was used as per the manufacturer's instructions and was set to a sampling time of 1 second repeated for 99 cycles. These parameters were kept consistent throughout all testing. The operating temperature for the APS is between 10-40°C and relative humidity 10-90%. All tests were carried out within these parameters.

The APS was used to measure the particle count with no activity in the system to obtain the background level of aerosols for comparison in the remainder of the aerosol tests.

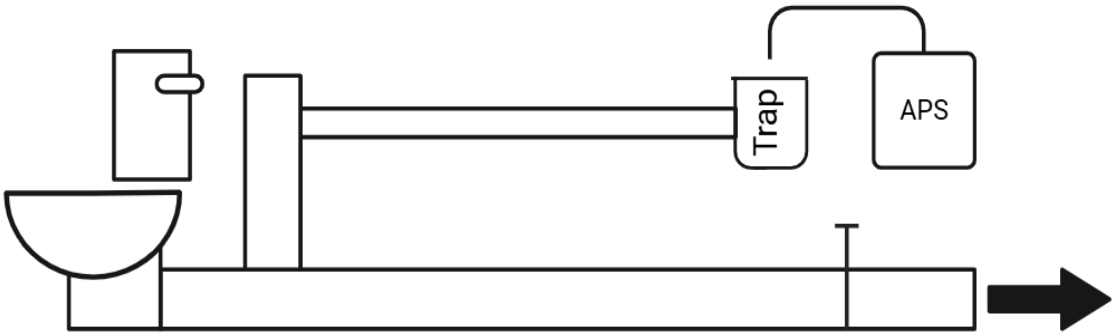

Figure 1 - Laboratory drainage test-rig with toilet, shower trap and simulated blockage to investigate aerosol generation with APS

2.2 Blockage event tests

The blockage tests were carried out with a simulated full blockage 3m from the WC in the drainage system test-rig. A 6L flush was discharged into the pipe. A toilet brush was used to simulate a manual unblocking action after 20 seconds. The APS was run for the remainder of the test time with no further activity in the system. Varying levels of intensity were used to simulate the manual unblocking over the course of several tests to more accurately demonstrate a range of real-life scenarios.

3 Results

3.1 Background aerosol levels

Figure 2 shows an average particle count of 84 from the laboratory drainage test-rig over time with no activity in the system to obtain the background aerosol level for comparison. This level of background detection of particulate is not uncommon. It is considered essential to get a background level regularly as this can change with variables like relative humidity, temperature and even atmospheric dust.

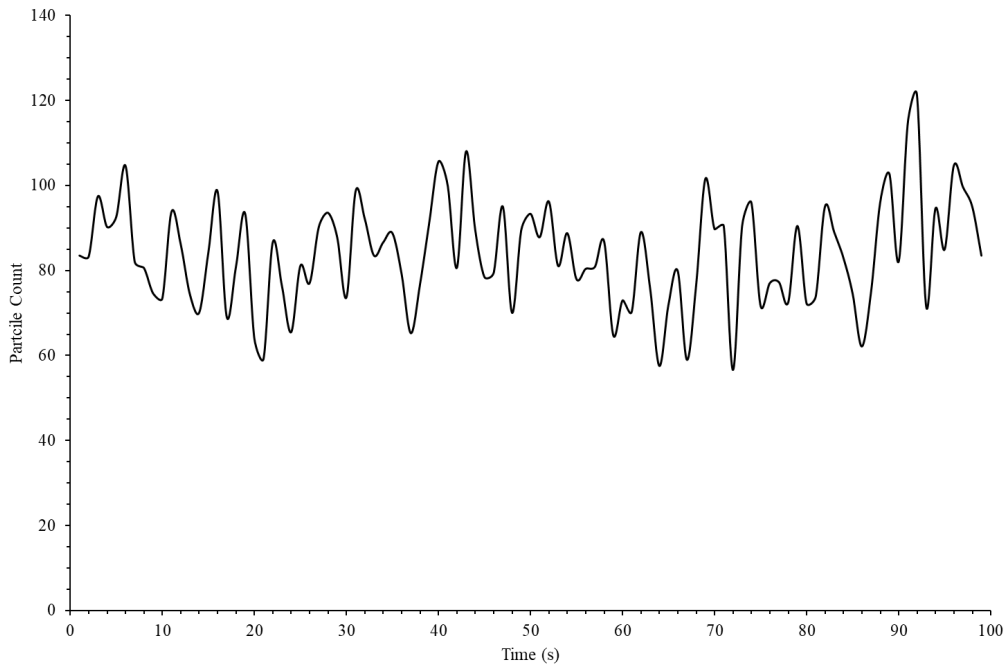

Figure 2 - Background aerosol particle count of particles 0.5-20µm from the laboratory drainage test-rig over time

3.2 Blockage event tests

Figure 3 shows the particle count from the laboratory drainage test-rig over time during an full bore blockage event. After 20 seconds there is an increase in particle count due to the manual unblocking action. This shows very high particle counts compared to the

background with the first peak at 1853 and the second peak, which is a result of reflecting waves inside the drainage test-rig. The second peak is higher than the first, peaking at 2193 particles. After 80 seconds the particle count starts to lower to similar levels as background particle count and the event is over.

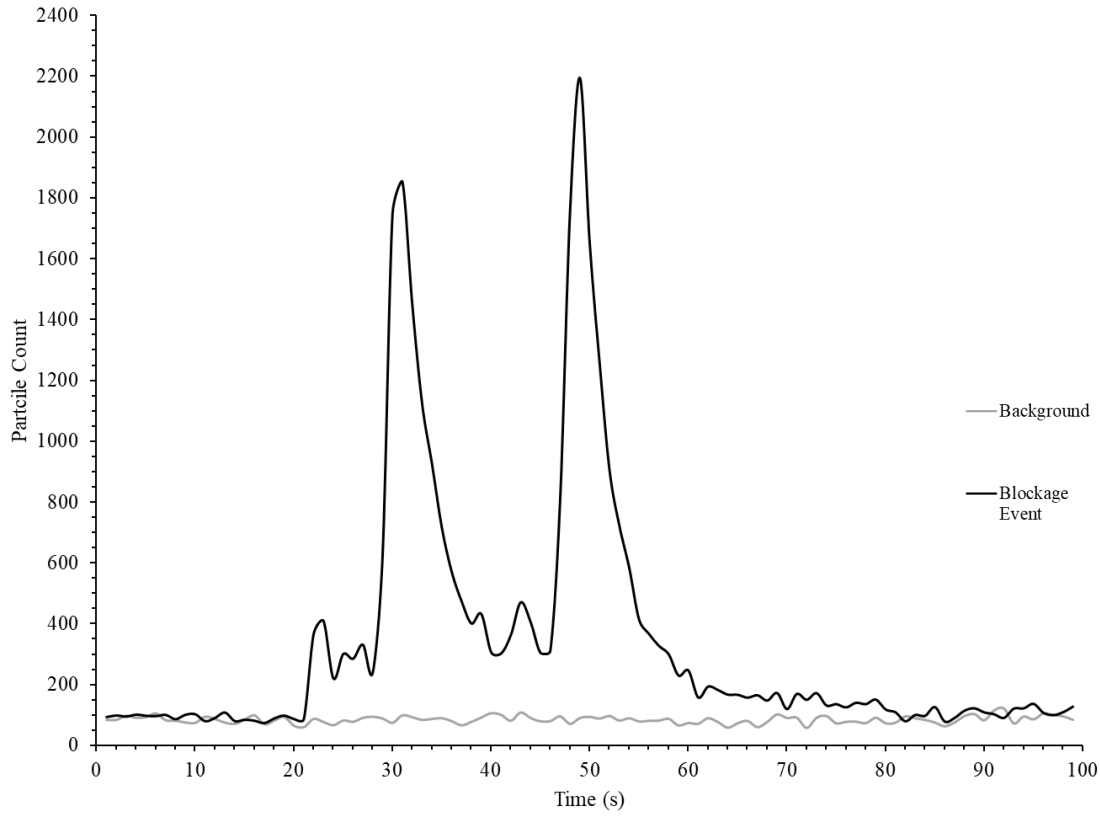

Figure 3 - Particle count over time of particles 0.5-20µm from drainage system test-rig during full bore blockage and manual unblocking event

Figure 4 shows the particle count from the laboratory drainage test-rig over time during three separate major blockage events with varying intensity of manual unblocking. Note this is a method that most plumbers would use initially to try to clear the toilet bowl and move the blockage.

All tests showed an increase in particle count from the drainage system after the unblocking event at 20 seconds. Blockage 1 showed the highest peak particle count of 1556, and reflection peak of 1302 which is consistent with this being the most intense unblocking event. Blockage 3 showed the lowest peak particle count of the three tests in figure 4 at 246, and reflection peak of 216 which is consistent with this being the least intense unblocking event.

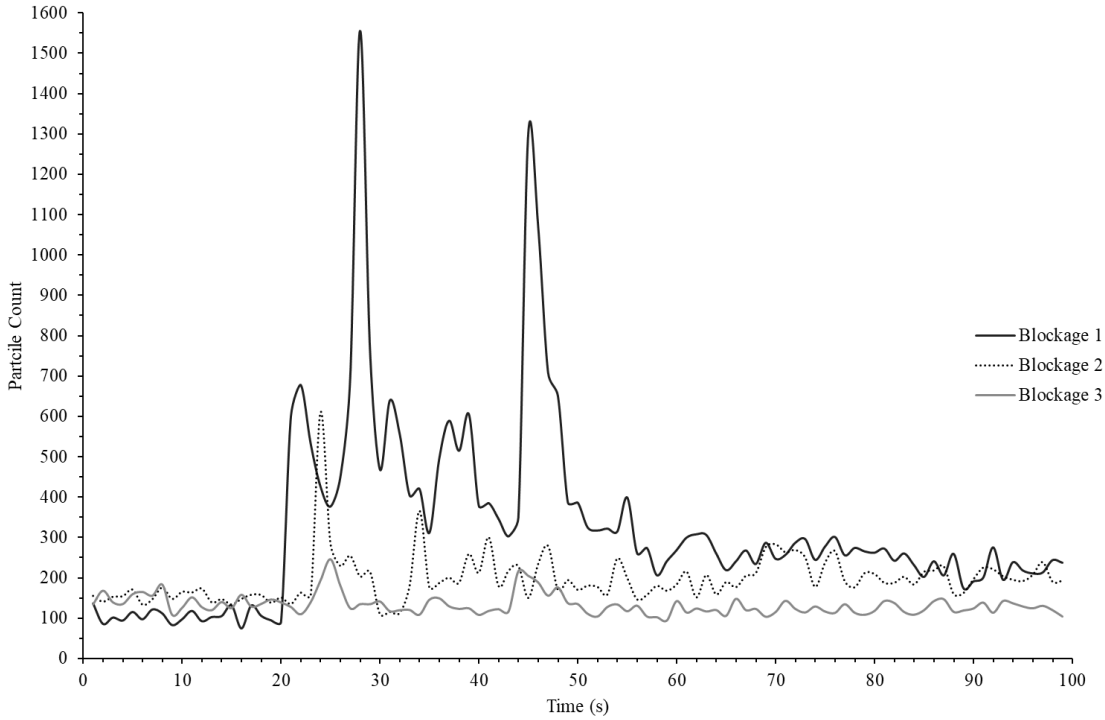

Figure 4 - Particle count over time of particles 0.5-20µm from drainage system test-rig during three separate major blockage events with varying intensities of manual unblocking events

4 Conclusions

The results from this research clearly show that in the event of a major blockage, which is common in a hospital environment, aerosols from the drainage system can enter the room via the shower trap during the manual unblocking process. This demonstrates the potential for bioaerosols to enter the room via the water trap seal from the drainage system.

During testing, water droplets from the trap were observed landing on the surface of the shower drain when manual unblocking was carried out. The water-trap seal is known to be a reservoir for AMR pathogens, especially in hospital settings. Therefore, in the event of a major blockage the act of unblocking the system could be enough to cause contamination of connected appliances with AMR pathogens, leading to transmission to vulnerable patients. This is consistent with previous research linking pressure transients with the ingress of bioaerosols to the interior of an en-suite bathroom in a hospital.

Further research is needed to investigate the extent of contamination that can occur in hospital showers during blockage events using model organisms. Additional experiments are required using a full-scale hospital shower connected to the laboratory drainage test-rig and through the comparison of aerosol production from different styles of shower trap

and other mitigation strategies. Finally, additional research into other causes of hospital shower contamination via the drainage system is also required, specifically further investigation into the role of air pressure transients.

This results of this research could help inform hospital maintenance strategies in the event of a blockage for infection prevention and control. For example, when a blockage has occurred, showers connected to the same line could be cleaned after the blockage has been cleared. This research could also inform improvements to hospital bathroom and drainage system designs to reduce HAIs. Overall, this will help improve patient outcomes and contribute to combatting AMR infections.

5 Acknowledgements

We acknowledge NHS Scotland Assure for funding this research and the team at Heriot-Watt University for assisting in data collection and providing expertise for this research.

6 References

1. Kramer A, Assadian O. Survival of Microorganisms on Inanimate Surfaces. Use of Biocidal Surfaces for Reduction of Healthcare Acquired Infections. 2014; 7–26.

2. Nieto-Rosado M, Sands K, Portal EAR, Thomson KM, Carvalho MJ, Mathias J, et al. Colonisation of hospital surfaces from low- and middle-income countries by extended spectrum β-lactamase- and carbapenemase-producing bacteria. Nature Communications. 2024;15(1):2758.

3. Mustafa M, Salih Q, Hidayat N, None Wafa A. Hamadameen, None Suhaib H. Kakamad, Abdullah NF, et al. Evolution of Antimicrobial Resistance in Community vs. Hospital-Acquired Infections. Barw Medical Journal. 2024.

4. O'Neill J. Tackling drug-resistant infections globally: Final report and recommendations. Archives of Pharmacy Practice. 2016.

5. Weinbren M, Meda M, Inkster T, Gormley M, Sunder W, Fucini G, et al. Built Environment Stewardship (BESt)- the missing pillar of antimicrobial resistance (AMR) action plans. The Journal of hospital infection. 2026; S0195-6701(26)000976.

6. Department of Health. Health Technical Memorandum 04-01: Safe water in healthcare premises Part A: Design, installation and commissioning, 2016

7. McCallum GE, Hall JPJ. The hospital sink drain microbiome as a melting pot for AMR transmission to nosocomial pathogens. npj Antimicrobials and Resistance. 2025; 3(1).

8. Gormley M, Kelly DA, Campbell DP, Aspray TJ, Dight T. The role of air pressure transients on the spread of bacteria from wash-hand basin sink traps in hospital en-suite bathrooms: a laboratory-based pilot study. Journal of Hospital Infection. 2025; 165:32–40.

9. Department of Health. Health Building Note 00-02 Core elements: Sanitary spaces, 2016

10. Meda M, Weinbren M, Nagy C, Gentry V, Gormley M. Polymicrobial outbreak of carbapenemase producing Enterobacterales managed using universal admission and discharge screening and water-safe built environment. Journal of Hospital Infection. 2024; 156:1–12.

11. Drinkwater A, Moy F. Wipes in sewer blockage study final report. 2017.

12. Breathnach AS, Cubbon MD, Karunaharan RN, Pope CF, Planche TD. Multidrug-resistant Pseudomonas aeruginosa outbreaks in two hospitals: association with contaminated hospital waste-water systems. Journal of Hospital Infection. 2012; 82(1):19–24.

13. Inkster T, Walker J, Weinbren M. Water-free patient care: a narrative review of the literature and discussion of the pressing need for a way forward. The Journal of hospital infection. 2024; 152:36–41.

7 Presentation of Authors

Leonie Wilson is a PhD researcher and Research Assistant at the School of Energy, Geoscience, Infrastructure and Society at Heriot-Watt University. Her PhD research project focusses on the role of air pressure transients in the spread of microorganisms from water trap seals in hospital showers.

Prof. Michael Gormley is Professor of Public Health and Environmental Engineering at Heriot-Watt University. His research specialisms are: mathematical modelling of air and water flows in building drainage systems, infection spread via bioaerosols, water systems in healthcare environments, sanitation in developing countries, and product development.

Dr David A Kelly is Associate Professor of Architectural Engineering at Heriot-Watt University. His research interests cover: water conservation, minimisation of disease transmission from wastewater drainage systems, water systems in healthcare environments, and the use of nature-based solutions of stormwater management.